ФІЗИКО-ТЕХНІЧНИЙ ІНСТИТУТ НИЗЬКИХ ТЕМПЕРАТУР
ІМ. Б.І. ВЄРКІНА НАЦІОНАЛЬНОЇ АКАДЕМІЇ НАУК УКРАЇНИ
ХАРКІВСЬКИЙ НАЦІОНАЛЬНИЙ УНІВЕРСИТЕТ ІМ. В.Н. КАРАЗІНА
МІНІСТЕРСТВО ОСВІТИ І НАУКИ УКРАЇНИ

Кваліфікаційна наукова праця

оформлена для наукової доповіді

ПАШИНСЬКА ВЛАДА АНАТОЛІЇВНА

УДК 577.32+543.51

ДИСЕРТАЦІЯ

МАС-СПЕКТОМЕТРИЧНІ МАРКЕРИ ТА МОЛЕКУЛЯРНО-ФІЗИЧНІ МЕХАНІЗМИ ДІЇ БІОЛОГІЧНО АКТИВНИХ РЕЧОВИН

Спеціальність 03.00.02 – біофізика (фізико-математичні науки)

Подається на здобуття ступеня доктора фізико-математичних наук

Дисертація містить результати власних досліджень. Використання ідей, результатів і текстів інших авторів мають посилання на відповідне джерело

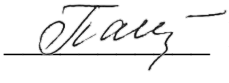
В.А. Пашинська

Харків – 2023

АНОТАЦІЯ

Пашинська В.А. Мас-спектрометричні маркери та молекулярно-фізичні механізми дії біологічно активних речовин. – Кваліфікаційна наукова праця, оформлена для наукової доповіді.

Дисертація на здобуття наукового ступеня доктора фізико-математичних наук за спеціальністю 03.00.02 «Біофізика» (фізико-математичні науки). – Фізико-технічний інститут низьких температур ім. Б.І. Вєркіна НАН України, Харківський національний університет ім. В.Н. Каразіна Міністерства освіти і науки України, Харків, 2023.

Дисертація присвячена біофізичній проблемі встановлення молекулярно-фізичних механізмів процесів, які визначають функціональну дію біологічно активних речовин, зокрема сполук лікарського призначення та антропогенних або біогенних за походженням компонентів довкілля, на біологічні системи різного рівня організації. Актуальність досліджень у цьому напрямку зумовлена тим, що знання молекулярно-фізичних основ дії біологічно активних агентів відкривають значні перспективи для спрямованого пошуку нових ефективних ліків та дозволяють прогнозувати та регулювати вплив компонентів довкілля на здоров’я людей та кліматичні і біологічні процеси в біосфері. Виходячи з важливості вказаної біофізичної проблеми, та у зв'язку з необхідністю модернізації методів природничих досліджень в дисертації розвинуто один з перспективних методологічних підходів, що полягає у визначенні маркерів (індикаторів) біофізичних процесів на молекулярному рівні, зокрема, сучасними мас-спектрометричними методиками.

Метою дисертаційної роботи стало встановлення молекулярно-фізичних механізмів та мас-спектрометричних маркерів біологічно значущих процесів за участі ряду біологічно активних речовин (представників груп протималярійних, протибактеріальних, противірусних та кардіопротекторних ліків, а також полярних органічних сполук із довкілля), які базуються на невалентних міжмолекулярних взаємодіях цих речовин із потенційними біомолекулами-мішенями та з компонентами оточуючого середовища. Основними фізичними

методами експериментальних досліджень, що використовувалися та вдосконалювалися в роботі, стали мас-спектрометрія з м'якими методами іонізації, а саме: з іонізацією електророзпиленням (ІЕР); з матрично-активованою лазерною десорбцією/іонізацією (МАЛДІ); а також комбінований метод, що поєднує газову хроматографію і мас-спектрометрію (ГХ/МС). Для пояснення експериментальних даних та встановлення структурно-енергетичних характеристик нековалентних асоціатів біологічно активних агентів між собою та з біомолекулами було застосовано сучасні методи квантово-механічних розрахунків: DFT (DFT/B3LYP/6-31^{++}G**, B3LYP/aug-cc-pVDZ); MP2 (MP2/6-31^{++}G**); PCM; AM1.

Завдяки отриманим результатам у дисертації було вирішено зазначену вище проблему молекулярної біофізики для вибраних об'єктів дослідження, а саме, визначено молекулярно-фізичні механізми, що пов'язані з функціональною дією низки біологічно активних речовин лікарського призначення: протималярійних агентів артемізинінового ряду, протиінфекційних бісчетвертинних амонієвих сполук та рамноліпідів, протитуберкульозного антибіотика циклосерин, противірусного агенту тилорон, кардіопротекторного препарату флокалін; а також встановлено мас-спектрометричні маркери біологічно важливих молекулярно-фізичних процесів, що відбуваються за участю біологічно активних органічних компонентів атмосферних аерозолів (зокрема моносахаридних ангідридів, поліолів).

Для групи протималярійних ліків, у роботі вперше на основі визначення мас-спектрометричних маркерів (характеристичних мас-спектральних ліній/піків) формування *in vitro* нековалентних комплексів молекул широковживаних препаратів артемізинінового ряду з їхньою потенційною молекулярною мішенню в клітинах – Fe(III)-гемом – запропоновано молекулярно-фізичний механізм, пов'язаний із протималярійною активністю цих агентів. Цей механізм розглядає утворення стабільних міжмолекулярних асоціатів артемізинінових ліків із гемом як етап, необхідний для активації

подальших процесів, що зумовлюють протималярійну дію артемізинінових агентів. У дисертації також проаналізовано залежність «структура-активність» для ряду похідних артемізиніну. У рамках встановлення молекулярно-фізичних основ показаної в ряді клінічних досліджень протипухлинної активності препаратів артемізинінового ряду, вперше експериментально доведено нековалентне комплексоутворення молекул артемізиніну та дигідроартемізиніну з азотистими основами нуклеїнових кислот: аденіном, цитозином та метилтиміном у полярному середовищі. Запропоновано ідею, що формування таких стабільних нековалентних асоціатів між артемізиніновими агентами та цими азотистими основами може блокувати функціональну активність ДНК та РНК пухлинних клітин, які активно розмножуються, та зумовлювати протиракову дію артемізиніну та його похідних. Завдяки застосуванню комплексного підходу, що поєднує експериментальний метод мас-спектрометрії з IEP та метод квантово-механічних розрахунків B3LYP/aug-cc-pVDZ, встановлено явище міжмолекулярної конкуренції між артемізиніновими агентами та молекулами препаратів, які належать до класу органічних кислот – аспірин (ацетилсаліцилова кислота) та вітамін С (аскорбінова кислота) – за нековалентне зв’язування з мембранними фосфоліпідами на прикладі дипальмітоїлфосфатидилхоліну. Така конкуренція між молекулами ліків, що належать до різних груп, при їхній взаємодії з фосфоліпідами біомембран є важливою з точки зору модифікації (зміни) функціональної дії препаратів при одночасному введенні вже на етапі їх трансмембранного проникнення в клітину. Поряд із взаємодією з фосфоліпідами, експериментально виявлено формування стабільних парних асоціатів між молекулами самих лікарських агентів різних груп та методом DFT визначено структурно-енергетичні характеристики таких комплексів. Встановлені конкурентні процеси нековалентного комплексоутворення вперше запропоновано в якості молекулярно-фізичних механізмів модифікації біологічної активності артемізинінових препаратів та аспірину або вітаміну С при їхньому одночасному застосуванні в медичній практиці. Отримані дані

мають суттєве практичне значення для розробки ефективних схем комбінованої терапії малярії та інших захворювань, що передбачає вживання комбінації лікарських агентів.

У рамках дослідження молекулярно-фізичних аспектів дії представників низки груп протиінфекційних ліків удосконалено метод мас-спектрометрії з ІЕР з метою ефективної реєстрації мас-спектрометричних маркерів мембранотропної активності антисептичних бісчетвертинних амонієвих сполук та рамноліпідів. В якості таких маркерів обрано мас-спектральні піки стабільних нековалентних комплексів молекул та іонів цих протиінфекційних агентів із фосфоліпідними компонентами біомембран. Завдяки оптимізації експериментального методу, вдалося зареєструвати в спектрі маркери формування супрамолекулярних комплексів дикатіонів декаметоксину та етонію з великорозмірними (до дев'яти молекул) кластерами дипальмітоїлфосфатидилхоліну, що моделюють взаємодію препаратів із фосфоліпідними доменами біомембран. Удосконалена ІЕР мас-спектрометрична методика рекомендується для практичного швидкого скринінгу бісчетвертинних амонієвих сполук із потенційною протиінфекційною активністю, зумовленою їхнім мембранотропним ефектом, який чинить дестабілізуючий вплив на мембранні структури клітин бактерій. При вивченні молекулярних механізмів модифікації активності цих препаратів, уперше виявлено формування стабільних комплексів дикатіонів бісчетвертинних амонієвих солей (декаметоксин, етоній та тіоній) з аспірином та конкуренцію лікарських сполук різних груп за нековалентне зв'язування з молекулами дипальмітоїлфосфатидилхоліну в полярному розчиннику. Ці міжмолекулярні конкурентні процеси комплексоутворення визначено як молекулярно-фізичні основи ймовірної зміни активності протиінфекційних амонієвих агентів та аспірину при одночасному введенні. Для об'єкту дослідження з групи протитуберкульозних ліків – циклосерину, ідентифіковано мас-спектрометричні маркери формування міжмолекулярних асоціатів цього антибіотика з його потенційною біомолекулою-мішенню в клітинній стінці

бактерій – компонентом пептидоглікану N-ацетил-D-глюкозаміном. Утворення таких нековалентних асоціатів запропоновано в якості молекулярно-фізичної складової процесу пригнічення формування бактеріальної клітинної стінки, що забезпечує протиінфекційну дію циклосерину. Для групи противірусних препаратів, уперше встановлено специфічне нековалентне зв'язування між молекулами агенту тилорон та нуклеозидом уридином у полярному середовищі при відсутності формування стабільних комплексів тилорону з аденозином та тимідином. Таке комплексоутворення пропонується в якості молекулярно-фізичного механізму, пов'язаного з противірусною активністю тилорону та дозволяє розглядати саме РНК, у склад якої входить уридин, як найбільш ймовірну біомолекулу-мішень противірусної дії агенту серед нуклеїнових кислот, а уридин - як потенційний центр специфічного зв'язування тилорону з молекулами РНК.

У напрямку дослідження серцево-судинних ліків, вперше визначено мас-спектрометричні маркери (референтні мас-спектральні піки) винайденого в Україні кардіопротекторного агенту флокалін. Базуючись на результатах вивчення міжмолекулярної взаємодії флокаліну з рядом амінокислот, запропоновано молекулярно-фізичний механізм взаємодії препарату з АТФ-чутливим калієвим мембранним каналом, пов'язаний із кардіопротекторним ефектом флокаліну. Цей механізм полягає в селективному формуванні нековалентних комплексів молекул флокаліну з амінокислотними залишками лізину та треоніну в складі регуляторних доменів АТФ-чутливих калієвих мембранних каналів.

Застосування комплексу мас-спектрометричних методик з ІЕР, МАЛДІ та розрахункового методу АМ1 для дослідження модельних систем, що містили бісчетвертинні амонієві сполуки (декаметоксин, етоній) у сольватному оточенні (вода, спирти, кислотні розчини), дозволило визначити мас-спектрометричні маркери структурної стабільності цих протиінфекційних агентів в умовах міжмолекулярної взаємодії з гідратним або іншим сольватним оточенням та в умовах мас-спектрометричного експерименту під впливом ряду фізичних

факторів (електричне поле, зіткнення з високоенергетичними частинками та ін.). Показано, що взаємодія дикатіонів бісчетвертинних амонієвих солей із компонентами оточення, зокрема з аніонами органічних кислот, значно впливає на їхню структурну стабільність та функціональну активність.

Вагома частина дисертаційної роботи присвячена розробці та валідації методики на основі методу ГХ/МС для визначення в складі нековалентних частинок атмосферних аерозолів біологічно активних органічних речовин, зокрема левоглюкозану та ряду інших моносахаридних ангідридів, що є продуктами горіння біомаси в довкіллі. Ці сполуки завдяки їхній активній міжмолекулярній взаємодії з молекулами води та інших компонентів довкілля відіграють значну роль у молекулярно-фізичних процесах в атмосфері, зокрема у формуванні вторинних органічних аерозолів, які мають біологічну активність. Для кількісного аналізу вмісту левоглюкозану визначено його мас-спектрометричний маркер та застосовано підхід внутрішнього стандартного калібрування. Завдяки використанню цієї ГХ/МС методики вперше в зразках атмосферних аерозолів ідентифіковано раніше неописані складові – полярні органічні сполуки 2-метилтреїтол та 2-метилеритритол та встановлено молекулярний механізм утворення цих поліолів. Ефективність та практична цінність розробленої ГХ/МС методики доведені в масштабному міжнародному біосферному дослідженні зразків атмосферних аерозолів з Амазонії, в ході якого визначено органічні компоненти аерозольних частинок та їхню роль у біологічно важливих молекулярно-фізичних процесах у довкіллі з метою прогнозування впливу атмосферних аерозолів на здоров’я людей та стан біосфери в цілому.

Ключові слова: біологічно активні речовини, ліки, органічні складові атмосферних аерозолів, міжмолекулярна взаємодія, біомолекули-мішені, нековалентні комплекси, молекулярно-фізичні механізми біологічної дії, модуляція активності ліків, сольватація, м’якоіонізаційна мас-спектрометрія, газова хроматографія/мас-спектрометрія, мас-спектрометричні маркери, квантово-механічні розрахунки структурно-енергетичних характеристик.

ABSTRACT

Pashynska V. A. Mass spectrometric markers and molecular physical mechanisms of action of biologically active substances. – Qualification scientific work for a scientific report.

Thesis for the scientific degree Doctor of science in physics and mathematics, specialty 03.00.02 "Biophysics". – B.I. Verkin Institute for Low Temperature Physics and Engineering of the NAS of Ukraine, V.N. Karazin National University of the Ministry of Education and Science of Ukraine, Kharkiv, 2023

The current dissertation is devoted to the biophysical problem of disclosure of molecular physical mechanisms of processes which determine the functional action of biologically active substances (in particular, compounds of medicinal application and anthropogenic or biogenic components of the environment) on biological systems of various levels of organizing. The topicality of research in this area is determined by the fact that knowledge of the physical basis of the action of biologically active agents opens up significant prospects for the directed search for new effective medicines. It also allows to predict and regulate the impact of environmental components on peoples health, climatic and biological processes in the biosphere. Based on the urgency of the specified biophysical problem, and the necessity of modernization of the methods of natural sciences research, a promising methodological approach has been developed in the disseration. This approach is related to the determination of markers (indicators) of biophysical processes at the molecular level using modern mass spectrometry techniques.

The aim of the work is to determine the molecular physical mechanisms and mass spectrometric markers of biologically significant processes which involve biologically active substances - representatives of antimalarial, antibacterial, antiviral and cardioprotective drugs groups, as well as polar organic compounds from the environment. The considered processes are based on intermolecular interactions of these biologically active agents with potential target biomolecules and components of the surrounding environment. The main experimental research methods used and

advanced in the dissertation are soft ionization mass spectrometry techniques, in particular: electrospray ionization (ESI); matrix-activated laser desorption/ionization (MALDI); as well as a method combining gas chromatography and mass spectrometry (GC/MS). To establish the structural and energetic characteristics of noncovalent associates of biologically active agents between themselves and with biomolecules, which are registered in the mass spectrometric experiments, the following methods of quantum mechanical calculations have been used in the work: DFT (DFT/B3LYP/6-31++G**, B3LYP/aug-cc-pVDZ); MP2 (MP2/6-31++G**); PCM; AM1.

Based on the obtained experimental and theoretical results, the above-mentioned problem of molecular biophysics has been solved in the dissertation for the selected research objects. Namely, the molecular physical mechanisms causing the functional action of a number of medicines with different action spectrum (antimalarial agents of artemisinin type, anti-infective bisquaternary ammonium compounds and rhamnolipids, antituberculosis antibiotic cycloserine, antiviral drug tyloron, cardioprotective agent flocalin) have been proposed. Moreover, the mass spectrometric markers of biologically and climatically important molecular physical processes that occur with the participation of biologically active organic components of atmospheric aerosols (in particular, levoglucosan, polyols) have been determined.

For the group of antimalarial agents the molecular physical mechanism, which determines the antimalarial activity of widely used of the artemisinin type drugs, has been proposed on the basis of the initially determined mass spectrometric markers (characteristic mass spectral lines/peaks) of *in vitro* formation of stable noncovalent complexes of molecules of these drugs with their potential molecular target in cells – Fe(III)-heme. This mechanism considers the formation of stable intermolecular associates of artemisinin drugs with heme as the first basic step, which is necessary for the activation of further processes, which cause the antimalarial effect of artemisinin agents. The structure-activity relationship for a number of artemisinin derivatives has been analyzed in the work. In the framework of revealing the molecular physical basis of the antitumor activity of artemisinin type drugs shown in

a number of clinical studies, noncovalent complexation of artemisinin and dihydroartemisinin molecules with the nucleobases of nucleic acids: adenine, cytosine, and methylthymine; in a polar environment has been experimentally established for the first time. The idea has been proposed that formation of such stable noncovalent associates between artemisinin type agents and the nucleobases can block the functional activity of DNA and RNA of fast proliferating tumor cells that provides the anticancer effect of artemisinin and its derivatives. Due to application of the complex approach, which combines the experimental method of ESI mass spectrometry and the theoretical method of quantum mechanical calculations B3LYP/aug-cc-pVDZ, the phenomenon of intermolecular competition between artemisinin antimalarial agents and molecules of medicines belonging to the class of organic acids – namely, anti-inflammatory agent aspirin (acetylsalicylic acid) and vitamin C (ascorbic acid) – for noncovalent binding with membrane phospholipids (e.g. dipalmitoylphosphatidylcholine) has been revealed. Such competition between the molecules of drugs of different groups during their interaction with phospholipids of biomembranes is biologically significant from the point of view of modulating the functional action of the drugs already at the stage of their transmembrane transfer into the cell. Along with the interaction with phospholipids, the formation of stable pair associates between the molecules of medicinal agents of different groups has been experimentally proved, and structural and energetic characteristics of the complexes have been determined by the DFT method. The revealed competitive processes of noncovalent complexation are proposed for the first time as molecular physical mechanisms of the process of modulating the biological activity of artemisinin type drugs and aspirin or vitamin C when they are used simultaneously in medical practice. The data obtained are of significant practical importance for the development of effective schemes of combined therapy of malaria and other diseases, which involves the use of a combination of medicinal agents.

As part of a comprehensive study of molecular aspects of action of representatives of some anti-infective drugs, the ESI mass spectrometry method has

been refined in order to effectively register mass spectrometric markers of the membranotropic activity of antiseptic biquaternary ammonium compounds and rhamnolipids. Mass spectral peaks of the stable noncovalent complexes of molecules and ions of these anti-infective agents with phospholipid components of biomembranes have been chosen as such markers. Owing to the optimization of the ESI experimental method, it became possible to register markers of the formation of supramolecular complexes of decamethoxinum and ethonium dications with large (up to nine molecules) clusters of dipalmitoylphosphatidylcholine, which simulates the interaction of the drugs with the phospholipid domains of biomembranes. This optimized ESI mass spectrometry method is proposed firstly for effective rapid screening of biquaternary ammonium compounds with potential anti-infective activity, which is due to the membranotropic effect of these agents providing destabilizing action on the membrane structures of bacterial cells. Under study of the molecular mechanisms of modulation of the drugs action, the formation of stable complexes of dications of bisquaternary ammonium salts (decamethoxinum, ethonium and thionium) with aspirin has been shown for the first time. At the same time the competition between these medicinal compounds of different groups for binding to molecules of dipalmitoylphosphatidylcholine in a polar solvent has been revealed. These intermolecular competitive processes of the noncovalent complexes formation are defined as the molecular physical basis of modulation of the activity of anti-infective ammonium agents and aspirin when they are used simultaneously in medical practice. For the object of research from the group of antituberculosis drugs – cycloserine, mass spectrometric markers of the formation of intermolecular associates of this antibiotic with its potential target biomolecule in the cell wall of bacteria, a component of peptidoglycan – N-acetyl-D-glucosamine, have been identified. The formation of such noncovalent associates is proposed as a molecular physical stage of the process of inhibiting the formation of the bacterial cell wall, which ensures the anti-infective effect of cycloserine. For the group of antiviral drugs, the specific noncovalent complexation of the molecule of antiviral agent tilorone with uridine nucleoside in a polar medium in the absence of the formation of stable complexes of

tilorone with adenosine and thymidine has been revealed for the first time. Such complexation is proposed as a molecular physical mechanism of the antiviral activity of tilorone and allows us to consider RNA itself (which includes uridine) as the most likely target biomolecule of antiviral action of tilorone among nucleic acids. Uridine is considered as a potential center of specific binding of tilorone to the RNA molecules.

In the framework of cardiovascular drugs research, the mass spectrometric markers (characteristic peaks in the mass spectrum) of the cardioprotective agent flokalin recently invented in Ukraine have been determined for the first time. Based on the results of the study of intermolecular interactions of flokalin with a number of amino acids, a molecular physical mechanism of the interaction of the drug with cardiac-specific ATP-sensitive membrane channel have been proposed. This mechanism is associated with the selective formation of non-covalent complexes of flokalin molecules with the amino acid residues of lysine and threonine in the regulatory domains of the membrane proteins of potassium channels.

A complex of mass spectrometric techniques with ESI, MALDI, FAB ionization and the semi-empirical calculation method AM1 were applied to study the model systems containing biquaternary ammonium compounds (decamethoxine, ethonium) in a solvate environment (water, alcohols, acidic environment). The obtained results allowed us to determine mass spectrometric markers of the molecular stability of the studied agents at intermolecular interactions with hydrate or other solvate surrounding and under the mass spectrometric experiment conditions – i.e. under the influence of a number of physical factors (electric field, collision with high-energy particles, etc.). It was shown that interactions of the dications of biquaternary ammonium salts with the components of the environment, notably with the anions of organic acads, can seriously effect on the agents functional activity.

A significant part of the dissertation is devoted to the development and validation of a technique based on the GC/MS method for the determination of biologically active substances in atmospheric aerosols particles, namely levoglucosan and a number of other monosaccharide anhydrides, which are products of biomass

burning in the environment. Due to their active intermolecular interaction with water and other surrounding molecules, these compounds play an important role in the molecular physical processes in the atmosphere, in particular in the formation of secondary organic aerosols that are characterized by biological activity. For the quantitative analysis of levoglucosan content in aerosols, its mass spectrometric marker was determined, and an internal standard calibration approach was applied using the structurally related compound methyl-b-L-arabinopyranoside. Due to the application of the developed GC/MS technique, the previously undescribed components of atmospheric aerosols – polar organic compounds 2-methylthritol and 2-methylerythritol have been identified for the first time in aerosol samples, and the molecular mechanism of the formation of these polyols during the photooxidation of atmospheric isoprene has been established. The effectiveness and practical value of this GC/MS technique has been proven in a large-scale international biospheric study of the molecular composition of atmospheric aerosols in the Amazon. In this study the molecular components of the aerosol particles have been determined and their role in molecular physical processes of biological significance have been revealed with the purpose to predict the effect of atmospheric aerosols on the human health and state of the biosphere.

Key words: biologically active substances, drugs, organic components of atmospheric aerosols, intermolecular interactions, target biomolecules, noncovalent complexes, molecular physical mechanisms of biological action, modulation of drugs activity, solvation, soft ionization mass spectrometry, gas chromatography/mass spectrometry, mass spectrometric markers, quantum mechanical calculations of structural and energetic characteristics.

СПИСОК ПУБЛІКАЦІЙ ЗДОБУВАЧА ЗА ТЕМОЮ ДИСЕРТАЦІЇ

Основні наукові результати дисертації опубліковано в 22 статтях у провідних фахових наукових виданнях [1-22], включаючи видання, що віднесені до першого і другого квартилів (Q1 і Q2) - 12 статей, до третього квартилю (Q3) - 4 статті відповідно до класифікації SCImago Journal & Country Rank, у наукових періодичних виданнях, включених до Переліку наукових фахових видань України - 5 статей, та у закордонних фахових наукових виданнях - 1 стаття.

Статті, в яких опубліковані основні наукові результати дисертації

1. Pashynska V. A., Kosevich M. V., Van den Heuvel H., Claeys M. Characterization of noncovalent complexes of antimalarial agents of the artemisinin type and Fe(III)-heme by electrospray ionization mass spectrometry and collisional activation tandem mass spectrometry. *J. Am. Soc. Mass Spectrom.* 2004. Vol. 15. P. 1181-1190. DOI: https://doi.org/10.1016/j.jasms.2004.04.030 [Q1]

(Особистий внесок здобувача: визначення основних завдань дослідження спільно з співавторами, безпосереднє отримання експериментальних даних методом мас-спектрометрії ІЕР, інтерпретація та аналіз отриманих даних спільно з співавторами, написання статті у співпраці з співавторами.)

2. Pashynska V. A. Mass spectrometric study of intermolecular interactions between the artemisinin-type agents and nucleobases. *Біофізичний вісник*. 2009. Т. 22(1). С. 20-28.

(Особистий внесок здобувача: Стаття - без співавторів, тому визначення основної ідеї роботи, формулювання завдань, планування та виконання експериментів, аналіз отриманих даних та написання статті виконано автором особисто.)

3. Pashynska V. A., Kosevich M. V., Van den Heuvel H., Cuyckens F., Claeys M. Study of non-covalent complexes formation between the bisquaternary

ammonium antimicrobial agent decamethoxinum and membrane phospholipids by elecrtospray ionization and collision-induced dissociation mass spectrometry. *Вісник харківського національного університету ім. Каразіна №637. Біофізичний вісник*. 2004. Т. 1-2 (14). С. 123-130.

(Особистий внесок здобувача: визначення основної ідеї та завдань дослідження, планування експерименту, безпосереднє отримання експериментальних даних, інтерпретація, аналіз за узагальнення отриманих результатів, їх обговорення з співавторами (включаючи комунікацію з закордонними співавторами), написання статті та редагування тексту згідно з зауваженнями співавторів та рецензентів.)

4. Pashynska V., Kosevich M., Stepanian S., Adamowicz L. Noncovalent complexes of tetramethylammonium with chlorine anion and 2,5-dihydroxybenzoic acid as models of the interaction of quaternary ammonium biologically active compounds with their molecular targets. A theoretical study. *Journal of Molecular Structure: THEOCHEM*[*]. 2007. Vol. 815. P.55-62. DOI: https://doi.org/10.1016/j.theochem.2007.03.019 [Q2]

   [*]З 2011 року назву журналу змінено на *Computational and Theoretical Chemistry*

(Особистий внесок здобувача: формування основної ідеї та завдань роботи спільно з співавторами, планування розрахунків, участь в отриманні розрахункових даних, їх інтерпретація, аналіз та узагальнення результатів спільно з співавторами, написання статті та редагування тексту згідно з зауваженнями співавторів та рецензентів.)

5. Pashynska V., Boryak O., Kosevich M., Stepanian S., Adamowicz L. Competition between counterions and active protein sites to bind bisquaternary ammonium groups. A combined mass spectrometry and quantum chemistry model study. *Eur. Phys. J. D.* 2010. Vol. 58. P.287-296. DOI: https://doi.org/10.1140/epjd/e2010-00125-5 [Q2]

(Особистий внесок здобувача: визначення основної ідеї та завдань дослідження спільно з співавторами, участь у плануванні експерименту та планування розрахунків спільно з співавторами, участь в отриманні експериментальних та розрахункових результатів, аналіз отриманих результатів, включаючи порівняння даних експерименту та розрахунків, написання статті та редагування тексту згідно із зауваженнями співавторів.)

6. Pashynska V. A. Mass spectrometric study of rhamnolipid biosurfactants and their interactions with cell membrane phospholipids. *Biopolymers and Cell.* 2009. Vol. 25, N 6. P. 504-508. DOI: http://dx.doi.org/10.7124/bc.0007FE [Q3]

(Особистий внесок здобувача: Стаття – без співавторів, тому визначення основної ідеї роботи, формулювання завдань, планування та виконання експериментів, аналіз отриманих даних та написання статті виконано автором особисто.)

7. Pashynska V. A.,. Zholobak N. M, Kosevich M. V., Gomory A., Holubiev P. K., Marynin A. I. Study of intermolecular interactions of antiviral agent tilorone with RNA and nucleosides. *Біофізичний вісник.* 2018. Т. 39(1). С. 15-26. DOI: https://doi.org/10.26565/2075-3810-2018-39-02

(Особистий внесок здобувача: формування основної ідеї та завдань дослідження спільно з співавторами, особисте планування мас-спектрометричного експерименту та отримання експериментальних результатів методом мас-спектрометрії, їхня інтерпретація та підготовка до публікації, аналіз та узагальнення результатів дослідження спільно з співавторами, написання статті спільно з співавторами.)

8. Pashynska V., Stepanian S., Gomory A., Vekey K., Adamowicz L. New cardioprotective agent flokalin and its supramolecular complexes with target amino acids: An integrated mass-spectrometry and quantum-chemical study. *J.*

Mol. Struc. 2017. Vol. 1146. P. 441-449. DOI: https://doi.org/10.1016/j.molstruc.2017.06.007 [Q3]

(Особистий внесок здобувача: визначення основної ідеї та завдань дослідження, планування експерименту та розрахунків, безпосереднє отримання експериментальних даних та участь в отриманні розрахункових даних, інтерпретація, аналіз та узагальнення отриманих результатів та їх обговорення з співавторами (включаючи комунікацію із закордонними співавторами), написання статті та редагування тексту згідно з зауваженнями співавторів та рецензентів.)

9. Pashynska V., Stepanian S., Gomory A., Vekey K., Adamowicz L. Competing intermolecular interactions of artemisinin-type agents and aspirin with membrane phospholipids: Combined model mass spectrometry and quantum-chemical study. *Chem. Phys.* 2015. Vol. 455. P. 81-87. DOI: https://doi.org/10.1016/j.chemphys.2015.04.014 [Q2]

(Особистий внесок здобувача: визначення основної ідеї та завдань дослідження, планування експерименту та розрахунків, безпосереднє отримання експериментальних даних та участь в отриманні розрахункових даних, аналіз та узагальнення отриманих результатів, комунікація з закордонними співавторами, написання статті та редагування тексту згідно із зауваженнями співавторів та рецензентів.)

10. Pashynska V., Stepanian S., Gömöry Á., Adamowicz L. What are molecular effects of co-administering vitamin C with artemisinin-type antimalarials? A model mass spectrometry and quantum chemical study. *J. Mol. Struc.* 2021. Vol. 1232. P. 130039. DOI: https://doi.org/10.1016/j.molstruc.2021.130039 [Q2]

(Особистий внесок здобувача: визначення основної ідеї та завдань дослідження, планування експерименту та розрахунків, безпосереднє отримання експериментальних даних та участь в отриманні розрахункових даних, інтерпретація, аналіз та узагальнення отриманих результатів та їх

обговорення з співавторами (включаючи комунікацію із закордонними співавторами), написання статті та редагування тексту згідно із зауваженнями співавторів та рецензентів.)

11. Pashynska V. A., Kosevich M. V., Gomory A., Vekey K. Model mass spectrometric study of competitive interactions of antimicrobial bisquaternary ammonium drugs and aspirin with membrane phospholipids. *Biopolymers and Cell.* 2013. Vol. 29(2). P. 157-162. DOI: http://dx.doi.org/10.7124/bc.000814 [Q3]

(Особистий внесок здобувача: визначення основної ідеї та завдань дослідження, планування експерименту, безпосереднє отримання експериментальних даних, інтерпретація, аналіз та узагальнення отриманих результатів, їх обговорення з співавторами (включаючи комунікацію із закордонними співавторами), написання статті та редагування тексту згідно із зауваженнями співавторів та рецензентів.)

12. Kasian N. A., Pashynska V. A., Vashchenko O. V., Krasnikova A. O., Gomory A., Kosevich M. V., Lisetski L. N. Probing of the combined effect of bisquaternary ammonium antimicrobial agents and acetylsalicylic acid on model phospholipid membranes: differential scanning calorimetry and mass spectrometry studies. *Molecular BioSystems.* 2014. Vol.10. P. 3155-3162. DOI: 10.1039/c4mb00420e [Q1]

(Особистий внесок здобувача: участь у формуванні основної ідеї та завдань дослідження спільно з співавторами, особисте планування мас-спектрометричного експерименту та отримання експериментальних результатів методом мас-спектрометрії, їх інтерпретація та підготовка до публікації, участь в аналізі та узагальненні результатів дослідження спільно з співавторами, участь в написанні статті спільно з співавторами.)

13. Pashynska V. A., Kosevich M. V., Gomory A. Mass spectrometry study of noncovalent complexes formation of antibiotic cycloserine with N-acetyl-D-glucosamine and ascorbic acid. *Біофізичний вісник.* 2020. Vol. 43. P. 103-110. DOI: https://doi.org/10.26565/2075-3810-2020-43-11

(Особистий внесок здобувача: визначення основної ідеї та завдань дослідження, планування експерименту, безпосереднє отримання експериментальних даних, інтерпретація, аналіз та узагальнення отриманих результатів, їх обговорення з співавторами (включаючи комунікацію із закордонними співавторами), написання статті та редагування тексту згідно із зауваженнями співавторів та рецензентів.)

14. Pashynska V. A., Kosevich M. V., Van den Heuvel H., Claeys M. The effect of cone voltage on electrospray mass spectra of the bisquaternary ammonium salt decamethoxinum. *Rapid Commun. Mass Spectrom.* 2006. Vol. 20(5). P. 755-763. [Q1]

(Особистий внесок здобувача: визначення основної ідеї та завдань дослідження, планування експерименту спільно з співавторами, безпосереднє отримання експериментальних даних, інтерпретація, аналіз та узагальнення отриманих результатів, комунікація із закордонними співавторами, написання статті спільно з співавторами.)

15. Пашинская В. А., Косевич М. В., Степаньян С. Г. Квантовомеханическое исследование структуры гидратированного бисчетвертичного аммониевого соединения декаметоксина. *Вісн. Харк. Ун-ту N 49. Біофізичний вісник*. 2000. Т. 2(7). С. 29-34.

(Особистий внесок здобувача: формування основної ідеї та завдань роботи спільно з співавторами, планування розрахунків, участь в отриманні розрахункових даних, їх інтерпретація, аналіз та узагальнення результатів спільно з співавторами, написання статті та редагування тексту згідно із зауваженнями співавторів та рецензентів.)

16. Pashynska V. A., Kosevich M. V., Gomory A., Vekey K., Claeys M., Chagovets V. V., Pokrovskiy V. A. Variable Electrospray Ionization and Matrix-Assisted Laser Desorption/Ionization Mass Spectra of the Bisquaternery Ammonium Salt Ethonium. *Mass Spectrometry & Purification Techniques*. 2015. Vol. 1:103. P. 1-9. DOI: 10.4172/2469-9861.1000103

(Особистий внесок здобувача: визначення основних завдань дослідження спільно з співавторами, безпосереднє отримання експериментальних даних методом мас-спектрометрії з іонізацією електрозпиленням, інтерпретація та аналіз отриманих даних спільно з співавторами, участь у написанні статті спільно з співавторами.)

17. Kosevich M. V., Boryak O. A., Chagovets V. V., Pashynska V. A., Orlov V. V., Stepanian S. G., Shelkovsky V. S. "Wet chemistry" and crystallochemistry reasons for acidic matrix suppression by quaternary ammonium salts under matrix-assisted laser desorption/ionization conditions. *Rapid Commun. Mass Spectrom.* 2007. Vol. 21(11). P. 1813-1819. DOI: https://doi.org/10.1002/rcm.3020 [Q1]

(Особистий внесок здобувача: участь у формуванні основної ідеї та завдань дослідження, у плануванні експериментів та розрахунків спільно з співавторами, участь в отриманні експериментальних мас-спектрометричних та розрахункових даних, в аналізі та узагальненні результатів, участь в написанні статті спільно з співавторами.)

18. Vashchenko O. V., Pashynska V. A., Kosevich M. V., Panikarskaya V. D., Lisetski L. N. Modulation of bisquaternary ammonium agents affect on model biomembranes by complex formation with an organic anion. *Biopolymers and Cell*. 2010. Vol. 26, N 6. P. 472-477. DOI: http://dx.doi.org/10.7124/bc.000176 [Q3]

(Особистий внесок здобувача: участь у визначенні завдань дослідження спільно з співавторами, участь в отриманні експериментальних мас-спектрометричних даних, в аналізі та узагальненні результатів, участь в написанні статті спільно з співавторами.)

19. Pashynska V., Vermeylen R., Vas G., Maenhaut W., Claeys M. Development of a gas chromatography/ion trap mass spectrometry method for determination of levoglucosan and saccharidic compounds in atmospheric aerosols. Application to urban aerosols. *J. Mass Spectrom.* 2002. Vol. 37. P.1249-1257. DOI: https://doi.org/10.1002/jms.391 [Q1]

(Особистий внесок здобувача: участь у визначенні основних завдань дослідження та в розробці експериментальної методики спільно з співавторами, особисте отримання експериментальних результатів методом газової хроматографії/мас-спектрометрії (ГХ/МС), їхня інтерпретація та аналіз отриманих даних спільно з співавторами, участь у написанні статті.)

20. Claeys M., Graham B., Vas G., Wang W., Vermeylen R., Pashynska V., Cafmeyer J., Guyon P., Andreae M., Artaxo P., Maenhaut W. Formation of secondary organic aerosols through photooxidation of isoprene. *Science*. 2004. Vol. 303. P. 1173-1176. DOI: 10.1126/science.1092805 [Q1]

(Особистий внесок здобувача: участь у плануванні мас-спектрометричного експерименту та в розробці ГХ/МС експериментальної методики, безпосереднє отримання частини експериментальних результатів роботи, зокрема методом ГХ/МС, участь в інтерпретації та аналізі результатів спільно з співавторами, участь у написанні статті.)

21. Decesari S., Fuzzi S., Facchini M.C., Mircea M., Emblico L., Cavalli F., Maenhaut W., Chi X., Schkolnik G., Falkovich A., Rudich Y., Claeys M., Pashynska V., Vas G., Kourtchev I., Vermeylen R., Hoffer A., Andreae M.O., Tagliavini E., Moretti F., Artaxo P. Characterization of the organic composition

of aerosols from Rondônia, Brazil, during the LBA-SMOCC 2002 experiment and its representation through model compounds. *Atmos. Chem. Phys.* 2006. Vol. 6. P. 375-402. DOI: https://doi.org/10.5194/acp-6-375-2006 [Q1]

(Особистий внесок здобувача: участь у визначенні основних завдань та плануванні мас-спектрометричного експерименту в рамках дослідження, участь у розробці ГХ/МС експериментальної методики, безпосереднє отримання частини експериментальних результатів роботи, зокрема методом ГХ/МС, участь в їхній інтерпретації та аналізі спільно з співавторами, участь у написанні статті.)

22. Claeys M., Kourtchev I., Pashynska V., Vas G., Vermeylen R., Wang W., Cafmeyer J., Chi X., Artaxo P., Andreao M.O., Maenhaut W. Polar organic marker compounds in atmospheric aerosols during the LBA-SMOCC 2002 biomass burning experiment in Rondônia, Brasil: sources and source processes, time series, diel variations and size distributions. *Atmos. Chem.Phys.* 2010. Vol.10. P. 9319-9331. DOI: https://doi.org/10.5194/acp-10-9319-2010 [Q1]

(Особистий внесок здобувача: участь у визначенні основних завдань та плануванні мас-спектрометричного експерименту в рамках дослідження, участь у розробці ГХ/МС експериментальної методики, безпосереднє отримання частини експериментальних результатів роботи, зокрема методом ГХ/МС, участь в їхній інтерпретації та аналізі спільно з співавторами, участь у написанні статті.)

Наукові праці, які засвідчують апробацію матеріалів дисертації: тези наукових доповідей

(Особистий внесок здобувача у наведених нижче публікаціях [23-45] полягає у визначенні основної ідеї та завдань наукової праці спільно з співавторами або особисто, безпосередньому отриманні експериментальних результатів методом мас-спектрометрії, участі в квантово-механічних розрахунках, аналізі отриманих даних, особистому або з співавторами написанні тез

наукових доповідей, підготовці презентацій усних доповідей або постерних доповідей, особистому представленні результатів дослідження на міжнародних наукових конференціях).

23. Pashynska V. A. Mass spectrometric markers of modulation effects on molecular level under drugs co-administering: development of mass spectrometry approach to nanobiocomplexes study. *7-th International Conference Nanobiophysics: Fundamental and Applied Aspects*: Conference Program and Book of Abstracts, Kharkiv, Ukraine, October 4-8, 2021. Kharkiv, 2021. P. 75.

24. Pashynska V., Stepanian S., Kosevich M., Gomory A. Nanobiocomplexes of ascorbic acid with antimalarial or antituberculosis drugs molecules: study of molecular mechanisms of the drugs activity modulation. *6-th International Conference Nanobiophysics: Fundamental and Applied Aspects*: Book of Abstracts, Kyiv, Ukraine, October 1-4, 2019. Kyiv, 2019. P. 69.

25. Pashynska V., Kosevich M., Gomory A. Mass spectrometry study of nanobiocomplexes formation between antibiotic cycloserine and N-acetylglucosamine. *XV-th International Conference on Molecular Spectroscopy: "From molecules to molecular materials, biological molecular systems and nanostructures"*: Programme. Abstracts. List of authors, Wroclaw-Wojanow, Poland, September 15-19, 2019. Wroclaw-Wojanow, 2019. P. 128.

26. Pashynska V., Stepanian S., Kosevich M., Gomory A., Vekey K. Model mass spectrometry and quantum chemical study of antimalarial artemisinin-type agents interactions with ascorbic acid and membrane phospholipids. *37-th Informal Meeting on Mass Spectrometry*: Book of abstracts and program, Fiera di Primiero, Italy, 5-8 May 2019. Fiera di Primiero, 2019. P. 96-97.

27. Pashynska V., Kosevich M., Gomory A., Vekey K. Mechanistic study of noncovalent complexes of antiviral and antibacterial agents with targeting biomolecules by electrospray ionization mass spectrometry. *36-th Informal Meeting on Mass Spectrometry*: Book of abstracts and program, Koszeg, Hungary, 6-9 May, 2018. Koszeg, 2018. P. 75.

28. Pashynska V. A., Kosevich M. V., Gomory A., Vekey K., Zholobak N. M. Mechanistic study of nanobiocomplexes of antiviral agent tilorone with nucleosides by electrospray ionization mass spectrometry. *5-th International Conference Nanobiophysics: Fundamental and Applied Aspects*: Book of Abstracts, Kharkiv, Ukraine, October 2-5, 2017. Kharkiv, 2017. P. 90.

29. Pashynska V., Kosevich M., Stepanian S., Gomory A., Vekey K. Mechanistic model study of intermolecular interactions of cardioprotector flokalin and amino acids by electrospray ionization mass spectrometry and quantum chemical calculations. *34-th Informal Meeting on Mass Spectrometry*: Book of Abstracts, Fiera di Primiera, Italy, 15-18 May, 2016. Fiera di Primiera, 2016. P. 130.

30. Pashynska V., Stepanian S., Kosevich M., Gomory A., Vekey K. Combined model mass spectrometric and quantum chemical study of arthemisinin-type agents and aspirin interactions with membrane phospholipids. *33-rd Informal Meeting on Mass Spectrometry*: Book of Abstracts, Szczyrk, Poland, 10-13 May, 2015. Szczyrk, 2015. P. 76.

31. Пашинська В. А., Косевич М. В., Гоморі А. Мас-спектрометричне дослідження формування нековалентних комплексів антибіотика циклосерина з N-ацетил-D-глюкозаміном та аскорбіновою кислотою. *VIII з'їзд Українського біофізичного товариства:* Матеріали VIII з'їзду Українського біофізичного товариства, Київ-Луцьк, 12-15 листопада 2019. Київ, 2019. Стор.27.

32. Pashynska V. A., Kosevich M. V., Gomory A., Vekey K. Mass spectrometry based approach in the study of nanobiocomplexes of chemotherapeutical drugs with the targeting biological molecules. *3-rd International Conference Nanobiophysics: Fundamental and applied Aspects*: Book of Abstracts, Kharkov, Ukraine, October 7-10, 2013. Kharkov, 2013. P. 89.

33. Pashynska V., Kosevich M., Vashchenko O., Lisetski L., Gomory A., Vekey K. Mass spectrometry as an efficient method of revealing the membranotropic antimicrobial drugs activity modulation by organic acids. *30-th Informal meeting on mass spectrometry*: Book of abstracts, Olomouc, Czech Republic, 29 April-3 May 2012. Olomouc, 2012. P. 118.

34. Pashynska V. A., Kosevich M. V., Gomory A. Mass spectrometry sensing of nanoclusters composed of membrane phospholipids and antimicrobial agents . *2-nd Intern. Conf. "Nanobiophysics: Fundamental and Applied Aspects"*: Book of Abstracts, Kyiv, Ukraine, 6-9 October 2011. Kyiv, 2011. P. 105.

35. Pashynska V. Electrospray Mass Spectrometry Study of Rhamnolipid Biosurfactants and Their Interactions with Membrane Phospholipids. *27-th Informal Meeting on mass spectrometry*: Book of Abstracts, Retz, Austria, 3-6 May, 2009. Retz, 2009.P. 36.

36. Pashynska V. A., Kosevich M. V., Boryak O. A., Stepanian S. G. Stability of multi-component complexes of tetramethylammonium with biologically significant counterions by the FAB mass spectrometry and quantum chemical data. *26-th Informal Meeting on Mass Spectrometry*: Book of abstracts, Fiera di Primiero, Italy, 4 -8 May 2008. Fiera di Primiero, 2008. P. 123-124.

37. Pashynska V. A., Kosevich M. V., Boryak O. A., Stepanian S. G. Model mass spectrometry and quantum chemical study of competition between counterions and active protein sites for a binding of quaternary ammonium groups. *25-th Informal Meeting on Mass Spectrometry*: Book of abstracts, Nyiregyhaza-Sosto, Hungary, 6-10 May 2007. Nyiregyhaza-Sosto, 2007. P. 97.

38. Pashynska V. A., Kosevich M. V., Stepanian S. G., Chagovets V. V., Pokrovsky V. A., Osaulenko V. L. Modelling of noncovalent interactions of bisquaternary antimicrobial agents with protein active groups by combined MALDI mass spectrometry and quantum-chemical study. *IV з'їзд Українського біофізичного товариства:* Тези доповідей, Донецьк, Україна, 19-21 грудня 2006. Донецьк, 2006. С. 126-128.

39. Pashynska V. A., Kosevich M. V., Van den Heuvel H., Claeys M. Comparative analysis of in-source CID and MS/MS CID under ESI mass spectrometry by the example of the bisquaternary ammonium agent decamethoxinum. *24-th Informal Meeting on Mass Spectrometry*: Book of Abstracts, Uston, Poland, 14-18 May 2006. Uston, 2006. P. 98

40. Pashynska V. A., Kosevich M. V., Chagovets V. V., Shelkovsky V. S., Osaulenko V. L., Porkovskiy V. L. Combined MALDI mass spectrometric and quantum chemical study of antimicrobial agent decamethoxinum in 2,5-dihydroxybenzoic acid. *23-rd Informal Meeting on Mass Spectrometry:* Book of Abstracts, Fiera di Primiero, Italy, 15-19 May 2005. Fiera di Primiero, 2005. P. 114-115.

41. Kosevich M., Pashynska V., Heuvel H., Claeys M. Electrospray mass spectrometry study of the bisquaternary ammonium compound decamethoxinum at different skimmer-nozzle potentials. *21-st Informal Meeting on Mass*

Spectrometry: Book of Abstracts, Antwerp, Belgium, 11-15 May, 2003. Antwerp, 2003. P. 107.

42. Pashynska V., Kosevich M., Heuvel H., Claeys M. Study of formation and characteristics of non-covalent complexes between heme and antimalarial agents of the artemisinin type by electrospray ionization mass spectrometry. *21-st Informal Meeting on Mass Spectrometry*: Book of Abstracts, Antwerp, Belgium, 11-15 May, 2003. Antwerp, 2003. P. 148.

43. Pashynska V. A., Vashchenko O. V., Kosevich M. V., Boryak O. A., Kasian N. A., Lisetski L. N. Model investigation on combined effect of quaternary ammonium compounds and an organic acid on phospholipids membranes. *V з'їзд Українського біофізичного товариства*: Тези доповідей, Луцьк, 22-25 червня 2011. Луцьк, 2011. Стор.14.

44. Pashynska V., Vermeylen R., Vas G., Claeys M., Maenhaut W. Development of a gas chromatography/ion trap mass spectrometry method for determination of levoglucosan and related saccharidic compounds in atmospheric aerosols. *20-th Informal Meeting on Mass Spectrometry*: Proceedings of the conference, Primiero, Italy, 12-14 May, 2002, P.103-104.

45. Pashynska V. ESI and CID mass spectrometry study of non-covalent complexes of a bisquaternary ammonium antimicrobial agent decamethoxinum with a phospholipids dipalmitoylphosphatidylcholine, related to the molecular mechanism of the drug action. *Molecules of Biological Interest in the Gas Phase. Optical Spectroscopy, Mass Spectrometry and Computational Chemistry*: Book of Abstracts, Exeter, United Kingdom, 13-18 April 2004. Exeter, 2004. P.53.

ЗМІСТ

spectrometry. *Біофізичний вісник*, N 1-2 (14), 123-130 (2004)

1.4. Нековалентні комплекси тетраметиламонію з аніоном хлору та 2,5-дигідроксібензойною кислотою як модель взаємодії бісчетвертинних амонієвих біологічно активних сполук з їх молекулами-мішенями. Теоретичне дослідження: Pashynska V., Kosevich M., Stepanian S. and Adamowicz L. Noncovalent complexes of tetramethylammonium with chlorine anion and 2,5-dihydroxybenzoic acid as models of the interaction of quaternary ammonium biologically active compounds with their molecular targets. A theoretical study. *Journal of Molecular Structure: THEOCHEM*, 815, 55-62 (2007) **84**

1.5. Конкуренція між протиіонами та активними центрами протеїнів за зв'язування бісчетвертинних амонієвих груп. Комбіноване модельне дослідження методами мас-спектрометрії та квантово-механічного моделювання: Pashynska V., Boryak O., Kosevich M., Stepanian S. and Adamowicz L. Competition between counterions and active protein sites to bind bisquaternary ammonium groups. A combined mass spectrometry and quantum chemistry model study. *Eur. Phys. J. D*, 58, 287-296 (2010) **92**

1.6. Мас-спектрометричне вивчення рамноліпідних біосурфактантів та їх взаємодії з фосфоліпідами клітинних мембран: Pashynska V.A. Mass spectrometric study of rhamnolipid biosurfactants and their interactions with cell membrane phospholipids. *Biopolymers and Cell,* 25 (6), 504-508 (2009) **102**

1.7. Вивчення міжмолекулярної взаємодії антивірусного агенту тілорон з РНК та нуклеотидами: Pashynska V.A.,. Zholobak N.M, Kosevich M.V., Gomory A., Holubiev P.K., Marynin A.I. Study of intermolecular interactions of antiviral agent tilorone with **107**

ПЕРЕЛІК УМОВНИХ ПОЗНАЧЕНЬ

ІЕР – іонізація електророзпиленням (ESI – electrospray ionization);

МАЛДІ – матрично-активована лазерна десорбція/іонізація (MALDI – matrix-assisted laser desorption/ionization);

БША – бомбардування швидкими атомами (FAB – fast atom bombardment);

ДІЗ – дисоціація, індукована зіткненнями (CID – collision induced dissociation);

ГХ/МС – газова хроматографія/мас-спектрометрія (GC/MS – gas chromatography/mass spectrometry);

CV - електричний потенціал на конусному електроді (cone voltage);

DFT – теорія функціоналу щільності (density functional theory);

MP2 – теорія збурень Меллера-Плессета другого порядку (second order Møller-Plesset perturbation theory);

AM1 – модель Аустіна (Austin model);

PCM – модель континууму, що поляризується (polarizable continuum model);

ДНК – дезоксирибонуклеїнова кислота;

РНК – рибонуклеїнова кислота;

АТФ – аденозинтрифосфат;

NAG – N-ацетил-D-глюкозамін (N-Acetyl-D-glucosamine);

Ade – аденін;

Cyt – цитозин;

mThy – метилтимін;

TMA^+ – іон тетраметиламонію;

DPPC – дипальмітоїлфосфатидилхолін;

PCn – фосфатидилхолін;

Til – тилорон;

Ado – аденозин;

Urd – уридин;

Thd –тимідин;

Lys – лізин;

Thr – треонін;

Gly – гліцин;

An – артемізинін;

DHAn – дигідроартемізинін;

Fl – флокалін;

CYS – циклосерин;

ASP – ацетилсаліцилова кислота, аспірин;

ASC – аскорбінова кислота, вітамін С;

DHB – дигідроксибензойна кислота;

LBA-CLAIRE – Cooperative Large- Scale Biospere-Atmosphere Experiment in Amazonia Airbone Regional Experiment;

LBA-SMOCC – Large-Scale Biosphere Atmosphere Experiment in Amazonia – Smoke Aerosols, Clouds, Rainfall, and Climate: Aerosols From Biomass Burning Perturb Global and Regional Climate;

WSOC – водорозчинні органічні сполуки (water-soluble organic compounds).

ВСТУП

Обґрунтування вибору теми дослідження

Однією з найактуальніших проблем сучасної молекулярної біофізики та пов'язаних із нею новітніх наукових галузей, зокрема, нанобіофізики, молекулярної медицини та ін., є проблема встановлення молекулярно-фізичних механізмів, що визначають функціональну дію біологічно активних речовин, включаючи речовини лікарського призначення та/або антропогенні й біогенні компоненти довкілля, на біологічні системи різного рівня організації - від комплексів біомолекул до клітин, організмів та біосфери в цілому. Молекулярно-фізичний підхід до розгляду біологічно значущих явищ передбачає встановлення фізичних основ процесів у біологічних системах на молекулярному рівні, результати яких спостерігаються на надмолекулярних рівнях. Базовими молекулярно-фізичними процесами, що мають значний вплив на різноманітні біологічні явища, є міжмолекулярні фізичні взаємодії біомолекул між собою та з біологічно активними лігандами, включаючи ліки та речовини з навколишнього середовища. Зокрема, проникнення лікарського агенту через клітинну мембрану значною мірою визначається фізико-хімічними параметрами взаємодії молекули лікарської сполуки з молекулярними фосфоліпідними та/або білковими компонентами біомембран [46], а, наприклад, формування стабільних міжмолекулярних нековалентних комплексів протималярійних препаратів хінін та хлорохін із гемом забезпечує пригнічення процесу детоксикації токсичного для збудника малярії вільного гему шляхом його полімеризації [47]. Зазначимо, що міжмолекулярні взаємодії з нековалентним комплексоутворенням між рецептор-зв'язуючим доменом S білків (receptor binding domain of the S protein) вірусів та антитілами складають фізичну основу процесу блокування зв'язування вірусів із клітинами хазяїна, що активно досліджується сьогодні у зв'язку з розробкою вакцин та препаратів моноклональних антитіл у рамках боротьби з пандемією SARS-CoV-2 [48]. Міжмолекулярні взаємодії за участі біомолекул та біологічно активних сполук важливі не тільки для процесів, що безпосередньо відбуваються в клітинах

окремих живих організмів, вони також грають значну роль в атмосферних явищах, що опосередковано впливають на живі організми через стан навколишнього середовища. Зокрема, нековалентні взаємодії за участі біологічно активних органічних сполук у довкіллі забезпечують формування та стабілізацію нано- та мікророзмірних частинок атмосферних аерозолів, включаючи вторинні органічні аерозолі, що приймають участь у кліматично важливих процесах у біосфері, а також впливають (часто негативно) на якість повітря та здоров'я людей та тварин [49-52]. Встановлення закономірностей взаємодій лікарських агентів із біомолекулами-мішенями дає підґрунтя для спрямованого пошуку нових ефективних ліків, в той час як знання про міжмолекулярні взаємодії біологічно активних агентів довкілля є важливими для прогнозування впливу цих агентів на здоров'я людей і тварин та на біосферу в цілому.

Незважаючи на вже досягнуті успіхи у визначенні фізичних основ багатьох важливих біологічних процесів, дослідження молекулярно-фізичних механізмів дії біологічно активних агентів не втрачають актуальності, бо від їхніх фундаментальних результатів очікується нагальний практичний відгук на такі сучасні глобальні виклики, як:

- формування антибіотикорезистентності та інших видів резистентності у патогенних мікроорганізмів до існуючих ліків;
- виникнення епідемій та пандемій, викликаних раніше невідомими збудниками хвороб;
- висока смертність та погіршення якості життя людей, пов'язані з давно відомими захворюваннями, що ще неподолані, серед яких малярія, інфекційні, онкологічні та кардіологічні захворювання;
- а також біологічно важливі кліматичні зміни та стрімке погіршення стану довкілля, зумовлене техногенною та антропогенною діяльністю.

Необхідність вельми швидкого реагування на нові виклики сучасності потребує розвитку та осучаснення методологічної та методичної бази наукових досліджень природничого напрямку. У даній роботі розвивається один із

перспективних методологічних підходів до отримання та використання знань щодо молекулярних механізмів біологічно значущих процесів, спрямований на пошук за допомогою сучасних фізичних методів маркерів (індикаторів) фізичних процесів за участю біологічно активних сполук на молекулярному рівні. Актуальною задачею в цьому напрямку є визначення маркерів процесів нековалентного комплексоутворення між молекулами ряду протиінфекційних (або інших) ліків та потенційними біомолекулами-мішенями, процесів зміни активності цих протиінфекційних агентів завдяки взаємодії з молекулами лікарських сполук інших груп при їхньому одночасному застосуванні, а також процесів взаємодії біологічно активних молекул із молекулами води та іншими молекулами та частинками сольватного оточення, що впливають на функціональність цих агентів у різних середовищах, включаючи організм людини або довкілля.

Розвиток сучасних методологічних підходів, включаючи визначення фізичними методами маркерів біологічно важливих процесів на молекулярному рівні, а також підвищення ефективності біофізичних досліджень, значною мірою може бути досягнуто за рахунок оновлення та вдосконалення методичної бази, яка сьогодні мусить поєднувати експериментальні та теоретичні методи досліджень. Серед широковживаних та результативних для вирішення біофізичних проблем експериментальних фізичних методів, таких як методи оптичної спектроскопії, ЯМР, калориметрія, електронна мікроскопія, які активно використовуються для вивчення біофізичних процесів на молекулярному рівні, особливе місце посідають сучасні м’якоіонізаційні мас-спектрометричні методи. Мас-спектрометрія дозволяє за фізичним параметром відношення маси іону до його заряду точно ідентифікувати молекулярні та супрамолекулярні маркери процесів, що відбуваються в досліджуваних системах, зокрема в таких, які включають біомолекули та біологічно активні речовини. Розвиток м’яких методів іонізації в мас-спектрометрії, таких як іонізація електророзпиленням (IEP, ESI) та матрично-активована лазерна десорбція/іонізація (МАЛДІ, MALDI), відкриття яких відзначено Нобелівською

премією з хімії у 2002 році, зумовив значний стрибок у використанні мас-спектрометрії в медико-біологічних дослідженнях, як у наукових, так і в клінічно-діагностичних галузях. Мас-спектрометрія з ІЕР, яка дозволяє реєструвати інтактні молекулярні іони термічно лабільних біологічних молекул та іони нековалентних комплексів цих молекул [53], зробила вагомий внесок у розвиток новітніх молекулярно-біологічних наукових напрямків, включаючи протеоміку, геноміку, ліпідоміку, метаболоміку [54-57]. Накопичення значного експериментального досвіду дозволяє сьогодні використовувати найсучаснішу мас-спектрометричну техніку в біомедичних дослідженнях для ідентифікації молекулярних маркерів патологічних процесів в організмі людини, включаючи діагностику онкологічних новоутворень на ранніх стадіях [58] та вивчення процесів молекулярного розпізнавання і взаємодії лікарських сполук із біомолекулами-мішенями [59], а також визначати молекулярні маркери кліматично, екологічно та біологічно важливих процесів, що відбуваються в довкіллі [19-22]. Водночас використання сучасних методів квантово-механічних розрахунків для встановлення структурно-енергетичних характеристик молекулярних нековалентних комплексів, зокрема й комплексів біомолекул з лігандами, також дає потужний інструмент у вирішенні завдань встановлення молекулярних механізмів біологічно важливих процесів за участю біологічно активних речовин і ліків [60-62] та вказує на перспективність використання саме комбінованого експериментально-теоретичного підходу в біофізичних дослідженнях.

Усе вищезазначене свідчить про актуальність теми даної дисертаційної роботи, яка спрямована на вирішення біофізичної проблеми встановлення молекулярно-фізичних основ та механізмів біологічно значущих процесів за участю біологічно активних речовин. При цьому нагальним методичним аспектом дисертаційної роботи став розвиток мас-спектрометричних методик як потужного інструменту вирішення зазначеної біофізичної проблеми через визначення мас-спектрометричних маркерів процесів міжмолекулярної взаємодії біологічно активних молекул із потенційними біомолекулами-

мішенями та молекулами оточуючого середовища. Під мас-спектрометричними маркерами (подібно до спектроскопічних маркерів, що також вивчаються в сучасних біофізичних дослідженнях [63-67]) у дисертаційній роботі розуміють характеристичні лінії/піки в мас-спектрі (з урахуванням співвідношення інтенсивності цих ліній та можливої динамічної зміни параметрів мас-спектру), що служать індикаторами молекулярно-фізичних процесів у системах або характеризують склад та/або стан систем, що досліджуються.

Мета і завдання дослідження

Метою роботи є визначення молекулярно-фізичних механізмів та мас-спектрометричних маркерів біологічно значущих процесів за участю біологічно активних речовин (представників груп протималярійних, протибактеріальних, противірусних та кардіопротекторних ліків, а також полярних органічних сполук з довкілля), які базуються на міжмолекулярних взаємодіях цих біологічно активних агентів із потенційними біомолекулами-мішенями та з компонентами оточуючого середовища.

Для досягнення поставленої мети в роботі вирішувалися наступні ***завдання***:

1. Провести систематичне дослідження міжмолекулярних взаємодій представників лікарських речовин різних груп (протималярійних артемізинінових ліків, протиінфекційних мембранотропних агентів, противірусного препарату тилорон, антибіотика циклосерин та кардіопротекторного агенту флокалін) з їхніми потенційними молекулами-мішенями шляхом пошуку та визначення методами м’якоіонізаційної мас-спектрометрії маркерів формування стабільних нековалентних комплексів цих ліків із біомолекулами та їхніми компонентами в системах *in vitro*.
2. Встановити структурно-енергетичні характеристики ідентифікованих у мас-спектрометричних експериментах нековалентних асоціатів молекул зазначених лікарських речовин із біомолекулами та іншими агентами за результатами квантово-механічних розрахунків.

3. Запропонувати молекулярно-фізичні механізми біологічної дії досліджуваних лікарських агентів, спираючись на аналіз даних мас-спектрометрії та квантово-механічних розрахунків.
4. Визначити молекулярно-фізичні механізми ймовірної зміни активності протималярійних агентів артемізинінового ряду та протиінфекційних бісчетвертинних амонієвих сполук при одночасному застосуванні з представниками протизапальних або антиоксидантних агентів шляхом встановлення мас-спектрометричних маркерів конкурентних процесів міжмолекулярної взаємодії цих лікарських агентів різних груп.
5. Ідентифікувати мас-спектрометричні маркери структурної стабільності протиінфекційних бісчетвертинних амонієвих агентів в умовах сольватного оточення методами мас-спектрометрії з іонізацією електророзпиленням (ІЕР) та матрично-активованою лазерною десорбцією/іонізацією (МАЛДІ) та проаналізувати вплив гідратації на структурні параметри декаметоксину за даними квантово-механічних розрахунків.
6. Запропонувати методику для швидкого скринінгу нових потенційних лікарських сполук серед четвертинних амонієвих агентів та інших речовин, функціональна дія яких пов’язана з мембранотропним ефектом, базуючись на оптимізації методики на основі мас-спектрометрії з ІЕР.
7. Розробити та апробувати методику на основі газової хроматографії/мас-спектрометрії (ГХ/МС) для визначення біологічно активних органічних речовин (левоглюкозан, сахариди антропогенного та біогенного походження, та ін.) у складі нековалентних частинок атмосферних аерозолів.
8. Шляхом аналізу отриманих експериментальних даних ГХ/МС досліджень зразків атмосферних аерозолів встановити присутність ряду біологічно активних органічних сполук та їхні міжмолекулярні взаємодії в аерозольних частинках з метою прогнозування їхнього впливу на молекулярно-фізичні процеси в довкіллі та на здоров’я людей і тварин.

Об’єкт дослідження- міжмолекулярні фізичні взаємодії молекул біологічно активних речовин із біомолекулами та молекулами або іонами оточуючого

середовища, що зумовлюють молекулярно-фізичні механізми біологічної дії цих речовин.

Предмет дослідження- мас-спектрометричні маркери біологічно значущих молекулярно-фізичних процесів за участю біологічно активних речовин лікарського призначення (представників різних груп протиінфекційних і кардіопротекторних ліків) та органічних полярних сполук, що є біологічно та екологічно важливими компонентами довкілля.

Методи дослідження

Об'єктивність та обґрунтованість висновків, що отримані в ході виконання дисертаційної роботи, зумовлені використанням комплексного підходу в дослідженнях, що поєднував спектр експериментальних методик на базі фізичного методу мас-спектрометрії з теоретичними методами квантово-механічних розрахунків із застосуванням сучасної комп'ютерної техніки та програмного забезпечення.

Основними експериментальними методами, що було використано та оптимізовано в роботі для визначення маркерів молекулярно-фізичних процесів за участю біологічно активних сполук, стали мас-спектрометричні методики з м'якими методами іонізації, а саме:

- з іонізацією електророзпиленням (IEP, electrospray ionization (ESI));
- з матрично-активованою лазерною десорбцією/іонізацією (МАЛДІ, matrix assisted laser desorption ionization (MALDI));
- з бомбардуванням швидкими атомами (БША, fast atom bombardment (FAB));
- метод тандемної мас-спектрометрії з дисоціацією, індукованою зіткненнями (ДІЗ, collision induced dissociation (CID)).

У дисертаційній роботі активно застосовувався метод, що поєднує газову хроматографію і мас-спектрометрію (ГХ/МС, gas chromatography/mass spectrometry (GC/MS)) з іонною пасткою, на базі якого вдалося розробити нову методику ідентифікації мас-спектрометричних маркерів ряду важливих

органічних біологічно активних компонентів атмосферних аерозолів та молекулярно-фізичних процесів за їх участю.

Для пояснення результатів, отриманих експериментальним шляхом, та встановлення структурно-енергетичних характеристик нековалентних міжмолекулярних комплексів біологічно-активних агентів із біомолекулами, між собою, а також із молекулами оточуючого середовища (води та інших полярних розчинників), що були зареєстровані в мас-спектрометричних експериментах, у роботі використовувалися наступні методи квантово-механічних розрахунків:

- *ab initio* метод теорії функціонала щільності DFT (DFT/B3LYP/6-31^{++}G**, B3LYP/aug-cc-pVDZ);
- *ab initio* метод теорії збурень Меллера-Плессета другого порядку MP2 (MP2/6-31^{++}G**);
- напівемпіричний метод AM1 (Austin Model 1)*;*
- метод PCM (polarizable continuum model, модель континууму, що полярізується).

Наукова новизна отриманих результатів

Основні наукові результати, які отримані в рамках дисертаційної роботи, є оригінальними і новими. У дисертації було вирішено важливу проблему молекулярної біофізики для обраних біологічно активних речовин різних груп, а саме: визначено молекулярно-фізичні механізми, що пов’язані з функціональною активність ряду лікарських сполук - представників груп протималярійних ліків, протибактеріальних та противірусних препаратів, кардіопротекторних агентів та ряду органічних компонентів частинок атмосферних аерозолів шляхом встановлення мас-спектрометричних маркерів біологічно важливих фізичних процесів за їх участю.

Новизна основних результатів роботи полягає в наступному:

- Уперше шляхом визначення мас-спектрометричних маркерів формування в умовах *in vitro* стабільних нековалентних комплексів молекул

протималярійних агентів артемізинінового ряду з їхньою потенційною молекулярною мішенню в клітинах – Fe(III)-гемом – запропоновано молекулярно-фізичний механізм, пов'язаний із протималярійною дією цих широковживаних препаратів. Проаналізовано залежність «структура-активність» для досліджених похідних артемізиніну.

- У рамках встановлення молекулярних механізмів показаної в ряді клінічних досліджень протипухлинної активності препаратів артемізинінового ряду, вперше експериментально доведено формування стабільних нековалентних комплексів артемізиніну та дигідроартемізиніну з азотистими основами нуклеїнових кислот: аденіном, цитозином та метилтиміном у полярному середовищі. Формування таких нековалентних асоціатів між артемізиніновими агентами та азотистими основами в складі нуклеїнових кислот розглядається як ймовірний фактор пригнічення функціональної активності ДНК та РНК пухлинних клітин, пов'язаний із протипухлинною дією цих агентів.
- Уперше, завдяки застосуванню комплексного підходу, що поєднує експериментальний метод мас-спектрометрії з IEP та розрахунковий метод DFT, *in vitro* встановлено явище міжмолекулярної конкуренції між протималярійними артемізиніновими агентами та молекулами препаратів, що належать до класу органічних кислот: протизапальним засобом аспірин або антиоксидантним агентом вітамін С, за нековалентне зв'язування з мембранними фосфоліпідами. Також доведено формування стабільних парних асоціатів між молекулами цих лікарських агентів різних груп у полярному середовищі. Базуючись на отриманих результатах, уперше запропоновані молекулярно-фізичні механізми ймовірної зміни функціональної активності досліджених лікарських агентів при їхньому одночасному застосуванні.
- Оптимізовано методику мас-спектрометричного експерименту з IEP задля покращення можливостей реєстрації мас-спектрометричних маркерів мембранотропної активності протиінфекційних бісчетвертинних амонієвих

агентів. Уперше рекомендовано використовувати оптимізовану IEP методику для ефективного швидкого скринінгу бісчетвертинних амонієвих сполук із потенційною протибактеріальною активністю, яка зумовлена їхнім мембранотропним ефектом.

- Уперше в системах *in vitro* експериментально визначені міжмолекулярні конкурентні процеси нековалентного комплексоутворення за участю протиінфекційних бісчетвертинних амонієвих агентів, протизапального препарату аспірин та молекул мембранного фосфоліпіду дипальмітоїлфосфатидилхолін, які запропоновані в якості молекулярних механізмів зміни активності цих ліків при одночасному введенні.
- В експериментах методом мас-спектрометрії з IEP уперше встановлено специфічне комплексоутворення молекули противірусного агенту тилорон із нуклеозидом уридином у полярному середовищі, що запропоновано в якості молекулярно-фізичного механізму, пов'язаного з противірусною активністю тилорону та вказує саме на РНК (у склад яких входить уридин) як найбільш ймовірні біомолекули-мішені біологічної дії тилорону серед нуклеїнових кислот.
- Уперше ідентифіковано мас-спектрометричні маркери формування *in vitro* супрамолекулярних комплексів антибіотика циклосерин із його ймовірною молекулою-мішенню в складі клітинної стінки бактерій – N-ацетил-D-глюкозаміном (NAG). Утворення таких нековалентних комплексів між молекулами циклосерину та NAG-компонентами пептидоглікану клітинної стінки розглядається в якості молекулярно-фізичної складової процесу пригнічення формування клітинної стінки бактерій, пов'язаного з протиінфекційною дією препарату.
- Уперше визначено мас-спектрометричні маркери (референтні піки в мас-спектрах) винайденого в Україні кардіопротекторного агенту флокалін. Базуючись на результатах комплексного експериментально-теоретичного дослідження, запропоновано молекулярно-фізичний механізм взаємодії флокаліну з АТФ-чутливим калієвим мембранним каналом, що включає

формування нековалентних комплексів молекул препарату з амінокислотними залишками лізину та треоніну в складі регуляторних субодиниць цього мембранного каналу.

- Уперше визначено мас- спектрометричні маркери для ідентифікації в біологічних та технологічних зразках двох біогенних мембранотропних рамноліпідів, що спродуковані бактеріями штаму *Pseudomonas* sp. PS-17 та характеризуються протиінфекційною активністю. *In vitro* встановлено, що в результаті міжмолекулярної взаємодії молекул цих рамноліпідів та дипальмітоїлфосфатидилхоліну формуються стабільні нековалентні комплекси, які можуть впливати на функціональну активність мембранних фосфоліпідів бактеріальних клітин, визначаючи антимікробну дію цих агентів.
- Розроблено та валідовано методику на основі методу ГХ/МС для визначення полярних біологічно активних речовин (органічної сполуки левоглюкозан та ряду інших моносахаридних ангідридів) у складі нековалентних частинок атмосферних аерозолів, які завдяки їхній міжмолекулярній взаємодії з молекулами води та іншими органічними сполуками відіграють значну роль у біологічно важливих молекулярно-фізичних процесах у довкіллі.
- Застосування ГХ/МС методики дозволило вперше виявити в складі частинок атмосферних аерозолів органічні сполуки 2-метилтреїтол та 2-метилеритритол, що належать до класу поліолів та, завдячуючи їхній активній гідратації та взаємодії з іншими полярними компонентами довкілля, вносять значний вклад у формування нековалентних частинок біологічно активних вторинних органічних атмосферних аерозолів.

Практичне значення отриманих результатів

Отримані в дисертаційній роботі результати вносять вагомий вклад як у фундаментальні знання про фізичні основи процесів у біологічних системах, так і в прикладні наукові напрямки, пов’язані зі здоров’ям людей та станом довкілля.

Визначені в роботі молекулярно-фізичні механізми, що пов’язані з біологічною дією представників ряду груп лікарських речовин (протималярійних ліків, протибактеріальних та противірусних агентів та ін.), відкривають перспективи для спрямованого пошуку нових лікарських агентів серед сполук, споріднених за молекулярною структурою до досліджених ліків. Методологія цього пошуку може ґрунтуватися на отриманих в роботі даних щодо структурно-енергетичних характеристик нековалентних комплексів, що формують досліджені лікарські агенти з біомолекулами-мішенями. Якщо біологічна та функціональна дія лікарських сполук пов’язана з формуванням нековалентних асоціатів із біомолекулами або їх компонентами, то більш потенційно ефективними серед споріднених за структурою сполук можна вважати агенти, що формують більш стабільні комплекси з молекулами-мішенями та мають у своєму складі функціональні групи, що забезпечують більш активну взаємодію з функціональними групами цих біомолекул. Застосований у роботі комбінований експериментально-теоретичний підхід на базі поєднання мас-спектрометрії та квантово-механічних розрахунків, а також оптимізована IEP мас-спектрометрична методика рекомендуються для практичного використання в рамках скринінгу потенційних лікарських агентів, що належать до класів біологічно активних сполук, функціональна дія яких пов’язана з формуванням нековалентних комплексів із біомолекулами.

Суттєве практичне значення для медичної практики можуть мати отримані в роботі дані щодо молекулярно-фізичних механізмів ймовірної зміни активності ряду протиінфекційних ліків при одночасному застосуванні з протизапальними або вітамінними агентами, що належать до класу органічних кислот (аспірин та вітамін С) та часто використовуються як додаткові лікарські речовини при лікуванні інфекційних захворювань. При цьому, визначені в роботі мас-спектрометричні маркери такої взаємно-модифікуючої дії лікарських сполук різних груп дають підстави рекомендувати оптимізовану методику мас-спектрометрії з IEP як практичний експрес-метод для

попереднього *in vitro* тестування сумісності лікарських агентів для одночасного введення.

Розроблена в роботі ГХ/МС методика визначення біологічно активних органічних речовин та їхніх взаємодій у складі частинок атмосферних аерозолів вже в рамках цієї роботі довела свою практичну цінність. ГХ/МС методика була успішно застосована в рамках масштабних міжнародних біосферних експериментів LBA-CLAIRE (Cooperative Large-Scale Biospere-Atmosphere Experiment in Amazonia Airbone Regional Experiment) та LBA-SMOCC (Large-Scale Biosphere Atmosphere Experiment in Amazonia – Smoke Aerosols, Clouds, Rainfall, and Climate) із дослідження зразків атмосферних аерозолів з метою встановлення впливу молекулярно-фізичних атмосферних процесів за участі органічних сполук антропогенного та біогенного походження на стан довкілля, здоров'я людей та тварин, кліматичні зміни та стан біосфери в цілому [20-22]. Важливо, що в рамках цих досліджень уперше вдалося виявити в складі частинок атмосферних аерозолів органічні сполуки класу поліолів, що раніше не були ідентифіковані, та визначити їхній вплив на біологічно значущі процеси в довкіллі [20].

Зв'язок роботи з науковими програмами, планами, темами

Дисертаційна робота виконана у відповідності з планами наукової діяльності відділу молекулярної біофізики Фізико-технічного інституту низьких температур (ФТІНТ) ім. Б.І. Вєркіна НАН України в рамках наступних відомчих тематичних програм Національної академії наук України: "Дослідження взаємодії біоактивних металокомплексів та хромофорів з біомолекулами та вуглецевими нанотрубками" (номер державної реєстрації 0102U003100, 2002-2006 рр.); "Дослідження міжмолекулярних взаємодій та конформаційних переходів в комплексах біологічно активних речовин з нуклеїновими кислотами різного рівня структурної організації та їх компонентами" (номер державної реєстрації 0103U000312, 2003-2005 рр.); "Дослідження взаємодії між біополімерами, біологічно активними речовинами

та вуглецевими нанотрубками як складовими біосенсорів" (номер державної реєстрації 0106U002560, 2006-2010 рр.); "Дослідження структури і визначення енергетичних характеристик нанобіогібридів, сформованих біополімерами та їх компонентами з вуглецевими нанотрубками, хромофорами та іонами металів" (номер державної реєстрації 0110U007895, 2011-2013 рр.); "Біофізичні властивості складних нанобіоструктур, сформованих вуглецевими нанотрубками, біополімерами та біоактивними лігандами" (номер державної реєстрації 0114U001070, 2014-2016 рр.);"Нанобіоструктури вуглецевих нанотрубок, оксиду графену з біомолекулами: створення, дослідження фізичних властивостей та можливості їх практичного застосування" (номер державної реєстрації 0117U002287, 2017-2019 рр.); «Створення та дослідження фізичних властивостей наногібридів біологічних молекул з 1-D, 2-D та 3-D наноматеріалами» (номер державної реєстрації 0120U100157, 2020-2022 рр.);

та в рамках міжнародних проєктів: Спільні українсько-угорські дослідницькі проєкти, що виконувалися в рамках Протоколу про наукове співробітництво між Угорською академією наук і Національною академією наук України - «Мас-спектрометричне та теоретичне дослідження структурної організації комплексів органічних полімерів з іонами та наночастинками» (2010 – 2012 рр); «Мас-спектрометричне дослідження та комп'ютерне моделювання модуляції активності фармакологічних сполук на рівні їх супрамолекулярних комплексів» (2013 – 2015 рр.); «Розкриття молекулярних механізмів взаємодії фармакологічних сполук з їх молекулярними мішенями у біонаноструктурах засобами мас-спектрометрії та комп'ютерного моделювання» (2016 – 2018 рр.); «Молекулярні основи функціонування агентів для доставки ліків: розвиток мас-спектрометричного підходу» (2019 – 2021рр.);

а також в рамках роботи Пашинської В.А. в якості запрошеного дослідника (за рекомендацією ФТІНТ ім. Б.І. Вєркіна НАН України) в університеті міста Антверпен (Бельгія) в період з 01.10.2001 по 30.09.2003 рр. за грантової підтримки «Belgium Office for Scientific, Technical and Cultural Affairs».

Особистий внесок здобувача

Основні наукові результати дисертації опубліковано в 22 статтях [1-22] у провідних наукових фахових виданнях: у віднесених до першого і другого квартилів (Q1 і Q2) – 12 статей, до третього квартилю (Q3) – 4 статті відповідно до класифікації SCImago Journal & Country Rank; у наукових періодичних виданнях, включених до Переліку наукових фахових видань України – 5 статей та у закордонних наукових фахових виданнях – 1 стаття. 2 статті [2, 6] опубліковано без співавторів. Результати також представлено у 23 публікаціях [23-45], що видані за матеріалами наукових конференцій, із них 3 [23, 35, 45] – без співавторів.

В опублікованих зі співавторами наукових працях за темою дисертаційної роботи особистий внесок здобувача полягає в наступному:

- у роботах [3, 11, 13, 14, 24, 25, 27, 31, 32, 34, 39, 41] – визначення основної ідеї та завдань дослідження, планування експерименту, безпосереднє отримання експериментальних даних методом мас-спектрометрії, аналіз та узагальнення отриманих результатів, їхнє обговорення зі співавторами (включаючи комунікацію із закордонними співавторами), написання статті (або тез наукової доповіді) та редагування тексту згідно із зауваженнями співавторів та рецензентів, для доповідей – особиста підготовка та представлення усної/стендової доповіді на науковій конференції;
- у роботах [8, 9, 10, 26, 29, 30, 37] – визначення основної ідеї та завдань дослідження, планування експерименту та розрахунків, безпосереднє отримання експериментальних даних та участь в отриманні розрахункових даних, аналіз та узагальнення отриманих результатів та їхнє обговорення зі співавторами (включаючи комунікацію із закордонними співавторами), написання статті (або тез наукової доповіді) та редагування тексту згідно із зауваженнями співавторів та рецензентів, для доповідей – особиста підготовка та представлення усної/стендової доповіді на науковій конференції;

- у роботах [4, 15] – визначення основної ідеї та завдань роботи спільно зі співавторами, планування розрахунків, участь в отриманні розрахункових даних, їхня інтерпретація, аналіз та узагальнення результатів спільно із співавторами, написання статті та редагування тексту згідно із зауваженнями співавторів та рецензентів;
- у роботах [1, 16, 42] – визначення основних завдань дослідження спільно зі співавторами, безпосереднє отримання експериментальних даних методом мас-спектрометрії з ІЕР, інтерпретація та аналіз отриманих даних спільно зі співавторами, участь у написанні статті (або тез доповіді) спільно з співавторами;
- у роботах [19, 20, 21, 22, 44] – участь у визначенні основних завдань дослідження та в розробці ГХ/МС експериментальної методики спільно зі співавторами, безпосереднє отримання частини експериментальних результатів роботи, зокрема методом ГХ/МС, їхня інтерпретація та аналіз спільно зі співавторами, участь у написанні статті (або тез наукової доповіді), підготовка стендової доповіді та представлення на науковій конференції;
- у роботах [5, 17, 18, 36, 38, 40, 43] – участь у формуванні основної ідеї та завдань дослідження, участь в отриманні експериментальних мас-спектрометричних та розрахункових даних, в аналізі та узагальненні результатів, участь у написанні статті (або тез доповідей) спільно зі співавторами, підготовка стендової доповіді та представлення на науковій конференції;
- у роботах [7, 12, 28, 33] – участь у визначенні основної ідеї та завдань дослідження спільно зі співавторами, особисте планування мас-спектрометричного експерименту та отримання експериментальних результатів методом мас-спектрометрії, їхня інтерпретація та підготовка до публікації, участь в аналізі та узагальненні результатів дослідження спільно зі співавторами, участь у написанні статті (або тез наукової доповіді) спільно зі співавторами.

Частина результатів спільних публікацій [12, 18 (статті), 33 (тези доповіді)], що стосується сукупної дії бісчетвертинних амонієвих сполук та ацетилсаліцилової кислоти (або дигідробензойної кислоти) на модельні ліпідні мембрани, яка отримана співавторами з Інституту сцинтиляційних матеріалів НАН України методом диференціальної скануючої калориметрії, була використана в дисертаційній роботі Ващенко О.В. «Індивідуальні та спільні взаємодії компонентів лікарських препаратів з модельними ліпідними мембранами» [68]. У своїй дисертаційній роботі здобувач Пашинська В.А. виносить на захист положення, які базуються на інших результатах цих спільних робіт, отриманих здобувачем методом мас-спектрометрії. Ці положення стосуються запропонованого молекулярно-фізичного механізму (що базується на нековалентному конкурентному комплексоутворенні) зміни активності протиінфекційних бісчетвертинних амонієвих сполук при одночасному застосуванні з іншими препаратами, що належать до органічних кислот, зокрема і з протизапальним агентом аспірин. Отримані здобувачем мас-спектрометричні дані на молекулярному рівні щодо конкурентного формування нековалентних асоціатів досліджених лікарських агентів різних груп між собою та з молекулами мембранних фосфоліпідів дозволяють пояснити ефекти, що спостерігалися колегами-співавторами на модельних ліпідних мембранах, тобто на надмолекулярному рівні, що описано в спільних наукових публікаціях [12, 33].

Окремо слід зазначити, що вимірювання методом мас-спектрометрії в дослідженнях, що проводились у рамках міжнародних проєктів [1, 3, 6, 7, 8, 9, 10, 11, 12, 13, 14, 16, 19–22, 24–30, 32–34, 39, 41–45], виконувалися Пашинською В.А. особисто під час закордонних відряджень в Інститут органічної хімії Дослідницького Центру природничих наук Угорської академії наук (Угорщина) та під час роботи в якості запрошеного дослідника в Університеті м. Антверпен (Бельгія).

Апробація результатів дисертації

Результати роботи були представлені на багатьох міжнародних і вітчизняних наукових конференціях, у тому числі:

- 20-th Informal Meeting on Mass Spectrometry (Primiero, Italy, 12-14 May, 2002)
- 21-st Informal Meeting on Mass Spectrometry (Antwerp, Belgium, 11-15 May, 2003)
- EURESCO conferences: Molecules of Biological Interest in the Gas Phase. Optical Spectroscopy, Mass Spectrometry and Computational Chemistry (Exeter, United Kingdom, 13-18 April 2004)
- 23-rd Informal Meeting on Mass Spectrometry (Primiero, Italy, 15-19 May 2005)
- 24-th Informal Meeting on Mass Spectrometry (Uston, Poland, 14-18 May 2006)
- IV з'їзд Українського біофізичного товариства (Донецьк, Україна, 19-21 грудня 2006)
- 25-th Informal Meeting on Mass Spectrometry (Nyiregyhaza-Sosto, Hungary, 6-10 May 2007)
- 26-th Informal Meeting on Mass Spectrometry (Fiera di Primiero, Italy, 4 -8 May 2008)
- 27-th Informal Meeting on Mass Spectrometry (Retz, Austria, 3-6 May, 2009. Retz, 2009)
- V з'їзд Українського біофізичного товариства (Луцьк, 22-25 червня 2011)
- 2-nd Intern. Conf. "Nanobiophysics: Fundamental and Applied Aspects" (Kyiv, Ukraine, 6-9 October 2011)
- 30-th Informal meeting on mass spectrometry (Olomouc, Czech Republic, 29 April-3 May 2012)
- 3-rd International Conference Nanobiophysics: Fundamental and applied Aspects (Kharkov, Ukraine, October 7-10, 2013)

- 33-rd Informal Meeting on Mass Spectrometry (Szczyrk, Poland, 10-13 May, 2015)
- 34-th Informal Meeting on Mass Spectrometry (Fiera di Primiera, Italy, 15-18 May, 2016)
- 5-th International Conference Nanobiophysics: Fundamental and Applied Aspects (Kharkiv, Ukraine, October 2-5, 2017)
- 36-th Informal Meeting on Mass Spectrometry *(*Koszeg, Hungary, 6-9 May, 2018)
- 37-th Informal Meeting on Mass Spectrometry (Fiera di Primiero, Italy, 5-8 May 2019)
- XV-th International Conference on Molecular Spectroscopy: "From molecules to molecular materials, biological molecular systems and nanostructures (Wroclaw-Wojanow, Poland, September 15-19, 2019)
- 6-th International Conference Nanobiophysics: Fundamental and Applied Aspects (Kyiv, Ukraine, October 1-4, 2019)
- VIII з'їзд Українського біофізичного товариства (Київ-Луцьк, 12-15 листопада 2019)
- 7-th International Conference Nanobiophysics: Fundamental and Applied Aspects (Kharkiv, Ukraine, October 4-8, 2021)

Результати, викладені в дисертації, доповідались і обговорювались на наукових семінарах ФТІНТ ім. Б.І. Вєркіна НАН України, на міжнародних наукових семінарах в Інституті органічної хімії Дослідницького центру природничих наук Угорської академії наук (м. Будапешт, Угорщина) під час наукових відряджень у рамках спільних україно-угорських проєктів та на семінарах лабораторії мас-спектрометрії Університету м. Антверпен (м. Антверпен, Бельгія) під час наукового стажування здобувача.

Публікації

Основні результати дисертації опубліковано у 45 роботах, в тому числі у 22 статтях у провідних фахових наукових виданнях: з них 16 статей

опубліковано у виданнях, що проіндексовані у базах даних Web of Science Core Collection та Scopus (з них 12 робіт - у виданнях, що віднесені до перших двох квартилів (Q1/Q2), а 4 - у виданнях, що віднесені до третього квартилю (Q3) за класифікацією SCImago Journal and Country Rank); 5 статей – у наукових періодичних виданнях, включених до Переліку наукових фахових видань України; 1 стаття – в закордонному фаховому науковому виданні. 23 роботи видані за матеріалами наукових конференцій.

Структура і обсяг дисертації

Дисертацією є кваліфікаційна наукова праця, оформлена для наукової доповіді, тобто розділами дисертації є сукупність публікацій здобувача за науковою тематикою роботи. Дисертація складається зі Вступу, чотирьох Розділів, підрозділами яких є наукові публікації здобувача (включаючи публікаціїї у виданнях, віднесених до перших двох квартилів (Q1/Q2) та до третього квартилю (Q3) за класифікацією SCImago Journal and Country Rank), Висновків, Переліку використаних джерел та Додатку. Обсяг дисертації становить 303 сторінки. Дисертація містить 108 рисунків, 13 схем та 35 таблиць. Список використаних джерел включає 669 посилань. Додаток займає 9 сторінок.

РОЗДІЛ 1

Міжмолекулярні взаємодії лікарських агентів із потенційними біомолекулами-мішенями: визначення мас-спектрометричних маркерів та молекулярно-фізичних механізмів, пов'язаних із біологічною дією лікарських речовин

У рамках вирішення актуальної проблеми сучасної молекулярної біофізики щодо встановлення фізичних основ та молекулярних механізмів дії біологічно активних агентів (включаючи лікарські речовини) на біологічні системи досліджено модельні системи, до складу яких входили молекули лікарських сполук, що належать до різних груп ліків (включаючи протималярійні, антисептичні та протибактеріальні, противірусні, а також кардіопротекторні агенти) та їхні потенційні біомолекули-мішені. Системи *in vitro* вивчалися із застосуванням комплексного методичного підходу, що поєднував експериментальний метод мас-спектрометрії з IEP та *ab initio* методи квантово-механічних розрахунків DFT та MP2. В представлених у цьому розділі роботах проаналізовано мас-спектрометричні маркери формування стабільних нековалентних комплексів ряду досліджених лікарських агентів з їхніми потенційними молекулярними мішенями з числа біомолекул, що пов'язане з реалізацію біологічної (зокрема й лікувальної) активності цих ліків.

Characterization of Noncovalent Complexes of Antimalarial Agents of the Artemisinin-Type and FE(III)-Heme by Electrospray Mass Spectrometry and Collisional Activation Tandem Mass Spectrometry

Vlada A. Pashynska,* Hilde Van den Heuvel, and Magda Claeys
Department of Pharmaceutical Sciences, University of Antwerp, Antwerp, Belgium

Marina V. Kosevich
Verkin Institute for Low Temperature Physics and Engineering, National Academy of Sciences of Ukraine, Kharkov, Ukraine

In this study, we demonstrate, using electrospray ionization mass spectrometry (ESI-MS) and collision-induced dissociation tandem mass spectrometry (ESI-MS/CID/MS), that stable noncovalent complexes can be formed between Fe(III)-heme and antimalarial agents, i.e., quinine, artemisinin, and the artemisinin derivatives, dihydroartemisinin, α- and β-artemether, and β-arteether. Differences in the binding behavior of the examined drugs with Fe(III)-heme and the stability of the drug-heme complexes are demonstrated. The results show that all tested antimalarial agents form a drug-heme complex with a 1:1 stoichiometry but that quinine also results in a second complex with the heme dimer. ESI-MS performed on mixtures of pairs of various antimalarial agents with heme indicate that quinine binds preferentially to Fe(III)-heme, while ESI-MS/CID/MS shows that the quinine-heme complex is nearly two times more stable than the complexes formed between heme and artemisinin or its derivatives. Moreover, it is found that dihydroartemisinin, the active metabolite of the artemisinin-type drugs in vivo, results in a Na^+-containing heme-drug complex, which is as stable as the heme-quinine complex. The efficiency of drug-heme binding of artemisinin derivatives is generally lower and the decomposition under CID higher compared with quinine, but these parameters are within the same order of magnitude. These results suggest that the efficiency of antimalarial agents of the artemisinin-type to form noncovalent complexes with Fe(III)-heme is comparable with that of the traditional antimalarial agent, quinine. Our study illustrates that electrospray ionization mass spectrometry and collision-induced dissociation tandem mass spectrometry are suitable tools to probe noncovalent interactions between heme and antimalarial agents. The results obtained provide insights into the underlying molecular modes of action of the traditional antimalarial agent quinine and of the antimalarials of the artemisinin-type which are currently used to treat severe or multidrug-resistant malaria. (J Am Soc Mass Spectrom 2004, 15, 1181–1190) © 2004 American Society for Mass Spectrometry

The major problem in the treatment of malaria is the increasing resistance of the malarial parasites, e.g., *Plasmodium falciparum*, to the commonly used antimalarial drugs, i.e., quinolines [1–3]. The quinolines, particularly quinine, chloroquine, and mefloquine, have been the basic drugs for treatment of malaria during the past 50 years and are still widely used in clinical practice. The antimalarial effect of the quinolines is due to inhibition of the polymerization pathway of free heme, which is released inside the food vacuole of the parasite after hemoglobin proteolysis and is toxic to the parasite owing to its oxidative damage to cell membranes and other biomolecules [4]. It has been demonstrated that the underlying molecular mechanism of the quinolines is based on association of the drugs with Fe(III)-heme and heme polymer, i.e., noncovalent binding, which can interfere with the heme polymerization pathway [5–7]. The polymerized heme accumulates in the form of an insoluble, microcrystalline black-brown pigment called hemozoin or the ma-

Published online June 19, 2004

Address reprint requests to Dr. M. M. Claeys, Department of Pharmaceutical Sciences, University of Antwerp, Universiteitsplein 1, B-2610 Antwerp, Belgium. E-mail: magda.claeys@ua.ac.be

*On leave from Verkin Institute for Low Temperature Physics and Engineering, National Academy of Sciences of Ukraine, Kharkov 61103, Ukraine.

1044-0305/04/$30.00
doi:10.1016/j.jasms.2004.04.030

Received August 28, 2003
Revised January 16, 2004
Accepted April 14, 2004

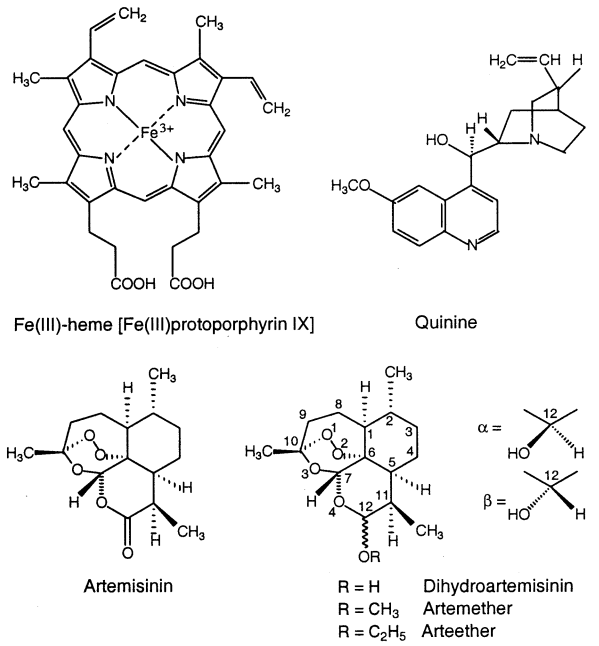

Scheme 1. Structures of Fe(III)-heme, quinine and the artemisinin-type drugs examined in the present study.

laria pigment, which is identical to synthetic β-hematin and is not a polymer as previously thought but a repeating array of coordinated dimers, bound through reciprocal iron(III)-carboxylate bonds to one of the propionic side chains of each porphyrin and held together in a crystalline matrix by hydrogen bonding interactions [8]. Because the polymerization pathway is unique to the malarial parasite, it offers an attractive target for the design of new antimalarials.

The first antimalarial compound to be discovered, which also served as the lead compound for synthetic antimalarials of the quinoline-type, was the alkaloid quinine isolated from *Chinchona* bark (for a historical account, see [9]). Many other leads for potential new antimalarials have been characterized since then, and several of them have been isolated from medicinal plants. One of these plants is *Artemisia annua*, which has been used in Chinese traditional medicine (Quinghaosu) for more than two thousand years as a herbal anti-fever remedy [1, 10]. In 1969, a promising lead compound, artemisinin, was isolated from *Artemisia annua* by the Chinese scientist Zhenxing Wei [10], and since then a number of artemisinin derivatives have been synthesized and tested. Artemisinin and its derivatives are currently successfully used to treat severe or multidrug-resistant *Plasmodium falciparum* malaria, including cerebral malaria [1, 11]. However, the exact molecular mechanisms of drugs of the artemisinin-type are still not properly understood and are, therefore, a current topic of active investigation [12]. Artemisinin is a sesquiterpene lactone bearing an endoperoxide function (Scheme **1**), which was shown to be crucial for antimalarial activity. The heme-catalyzed cleavage of the endoperoxide bridge of artemisinin and formation of toxic free radicals have received considerable attention as a likely molecular mechanism for the antimalarial activity of artemisinin and its derivatives [13]. Formation of non-polymerizable alkylated heme derivatives has been demonstrated in vitro and evidence has been provided that C-centered radicals derived from artemisinin act as alkylating agents [14, 15]. Furthermore, it has been shown that covalent artemisinin-heme adducts mimick heme in binding to the enzyme histidine-rich protein II and as such have the ability to inhibit heme polymerization [16]. Recently, evidence has been obtained that iron-activated artemisinin-type drugs act by alkylating an essential enzyme of *Plasmodium falciparum*, i.e., a sarco/endoplasmic reticulum Ca^{2+}-ATPase ortholog [17].

Formation of a relatively stable noncovalent complex between antimalarial drugs of the artemisinin-type and Fe(II)-heme can be regarded as the first step in covalent interaction, since Fe^{2+} is required for activation of artemisinin derivatives, i.e., generation of alkyl radicals [17, 18]. Experimental evidence using spectrophotometry has demonstrated that noncovalent interaction indeed occurs prior to covalent association in in vitro experiments [19]. A theoretical model based on a combination of molecular docking and a three-dimensional quantitative structure-activity study, developed by Cheng et al. [20], revealed a good correlation between antimalarial activity and the binding energy of artemisinin derivatives with Fe(II)-heme. The global energy-minimum configuration of the artemisinin type drug-heme complex indicates that the endoperoxide bridge of the drug molecule exactly points towards the Fe ion of heme and the two carboxyl ethyl groups in heme are perpendicular to the porphyrin ring, their carboxyl groups interacting with the hydrogens attached to the C1 and C9 carbons (Scheme **1**) of the artemisinin derivatives (Figure 3 in [20]). The latter study showed that the electrostatic energy comprises about two thirds of the total binding energy, which includes also steric and hydrophobic components. Since the electrostatic component revealed the same trend of variation (increase or decrease) as the total stabilization energy with variation of the structure of the artemisinin-type drugs, it was suggested that the electrostatic component alone permits evaluation of the stability of the complexes.

The present study deals with the characterization of noncovalent complexes formed in vitro between Fe(III)-heme and artemisinin-type drugs as a model system for the interaction between the latter drugs and Fe(III)-heme, Fe(II)-heme or Fe(II)-heme-containing proteins, which may occur in vivo. In order to evaluate the potential of the drugs to form noncovalent complexes with Fe(III)-heme and their relative binding strengths, we resorted to electrospray ionization mass spectrometry (ESI-MS) and collision-induced dissociation tandem mass spectrometry (ESI-MS/CID/MS). Electrospray ionization mass spectrometry provides a rapid, sensitive and highly selective tool for probing noncova-

lent interactions [21–24]. Most studies that are based on this approach rely on the ability of ESI to transfer noncovalent solution-phase assemblies intact into the gas phase. The validity of this strategy has been supported in numerous studies, especially for experiments on protein-protein and protein-ligand interactions (for a review, see [25]), including studies on heme-containing proteins [26]. The relative binding strengths between the drugs and Fe(III)-heme was assessed using low-energy collision-induced dissociation. This approach has previously been shown to be useful in determining the structure-activity relationship of antimalarial agents, namely, terpene isonitriles [27] and neocryptolepine derivatives [28]. We demonstrate in the present work that artemisinin-type drugs form a noncovalent complex with Fe(III)-heme in vitro, which is weaker than that with quinine. However, in contrast to quinine a complex with the dimeric form of Fe(III)-heme or β-hematin could not be detected. Dihydroartemisinin, the active metabolite of artemisinin derivatives in vivo [1], is shown to form a second more stable complex in which a hydrogen is replaced by a sodium atom, which has a binding strength comparable with that of the quinine-heme complex.

Experimental

Materials

Hemin (i.e., Fe(III)protoporphyrin IX chloride, purity >98%) was obtained from Fluka (Buchs, Switzerland), and quinine sulfate salt (purity, 90%) was purchased from Sigma (St. Louis, MO). Artemisinin and its derivatives, dihydroartemisinin, α- and β-artemether, and β-arteether, were a gift from Dafra Pharma (Oud-Turnhout, Belgium). The tested artemisinin-type drugs had a purity >99%. The structures of Fe(III)-heme (hereafter, referred to as heme), quinine and the artemisinin-type drugs investigated in this study are presented in Scheme **1**. Methanol (super grade) was purchased from Lab-Scan (Dublin, Ireland).

Abbreviations: FP^+, heme or Fe(III)protoporphyrin IX (cationic mass, 616 Da); An, artemisinin (MW 282); DHAn, dihydroartemisinin (MW 284); α- and β-Am, α- and β-isomers of artemether, respectively (MW 298); Ae, β-arteether (MW 312); Qn, quinine (MW 324).

Sample Preparation

Stock solutions of heme were prepared using hemin and contained 5 mM in MeOH (plus a drop of NH_4OH to solubilize heme), while those of quinine, artemisinin, and its derivatives, dihydroartemisinin, artemether, and arteether, contained 5 mM of the drug in MeOH:CH_2Cl_2 (19:1; vol/vol). Mixtures of the drugs with heme were prepared in MeOH with different drug:heme concentration ratios starting from the stock solutions. In the final solutions, water was added in order to ensure the stabilization of the ESI process. The final pH of the solutions was about 7, at which the iron atom in the heme molecule is known to be in the Fe(III) state [27]. Drug-heme mixtures with a molar concentration ratio 1:1 contained 250 μM drug and 250 μM heme in MeOH:H_2O (3:1; vol/vol); for the drug-heme mixtures with a concentration ratio 1:2 the concentration of the drug was 125 μM, while that of heme was 250 μM in MeOH:H_2O (3:1; vol/vol). For the three-component mixtures (drug 1/drug 2/heme), mixtures were prepared with several concentration molar ratios, i.e., 1:1:1 (125 μM of drug 1, 125 μM of drug 2, 125 μM heme in MeOH:H_2O (3:1; vol/vol)), 1:1:2 (125 μM of drug 1, 125 μM of drug 2250 μM heme in MeOH:H_2O (3:1; vol/vol)) and 1:1:4 (125 μM of drug 1, 125 μM of drug 2500 μM heme in MeOH:H_2O (3:1; vol/vol)). The final mixtures were subjected to electrospray ionization mass spectrometry or to collision-induced dissociation tandem mass spectrometry.

Mass Spectrometry

The mass spectral data were obtained in the positive ion mode on an Autospec-oa-TOF mass spectrometer (Micromass, Manchester, UK), which was equipped with an electrospray ionization source. The electrospray ionization source was operated at 4 kV, while the electrospray needle was operated at a maximum voltage of 3 kV (i.e., relative to the pepper pot counter electrode which is at 5 kV). Nitrogen was used both as bath gas (100 °C; 250 L/h) and as nebulizing gas (15 L/h). First-order ESI mass spectra were recorded in the mass range *m/z* 100–1600. The drug-heme solutions were introduced into the mass spectrometer by a syringe pump (Harvard Apparatus, South Natick, MA), employing a 100 μL syringe, at a constant flow rate of 5 μL/min. The effect of the cone voltage on the intensity of the signal of the drug-heme complexes was examined. Low- and high-energy collision-induced dissociation (CID) spectra were acquired at a collision energy (E_{lab}) of 400 eV using He and Xe, respectively, as collision gas. Helium or xenon was introduced into the collision cell until the signal of the very weak $[FP:CH_3OH]^+$ complex (*m/z* 648) reached about 80% of its original value. In order to ensure reproducible results the setting of the collision cell gas pressure was not changed during our experiments. Data acquisition and processing were performed using OPUS V3.1X software. All scans were acquired in the continuum mode.

Results and Discussion

Optimization of ESI Conditions for Detection of Noncovalent Complexes Between Artemisinin-Type Drugs and Heme

In a first series of experiments, we recorded first-order ESI mass spectra of heme, the drugs and binary drug-heme mixtures and optimized the ESI conditions. In particular, we noted that the potential on the first

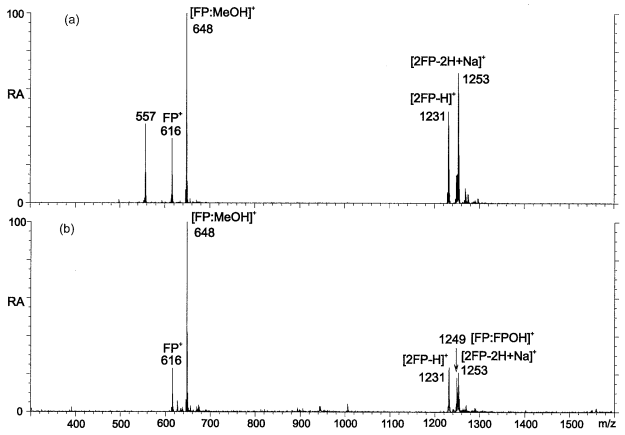

Figure 1. ESI mass spectra obtained for Fe(III)-heme in MeOH: H_2O (3:1, vol/vol) at (**a**) non-optimal cone voltage, 150 V, and (**b**) optimal cone voltage, 75 V. The needle voltage was 2.3 kV.

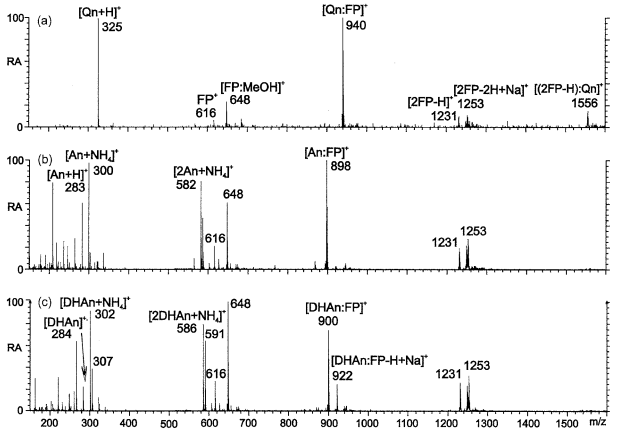

Figure 2. ESI mass spectra of two-component mixtures: (**a**) quinine-heme (1:2), (**b**) artemisinin-heme (1:2), and (**c**) dihydroartemisinin-heme (1:2).

skimmer (cone voltage) had to be adjusted in order to reduce in-source fragmentation of heme (*m/z* 616), which was evident from the formation of an ion at *m/z* 557 due to loss of the ethylcarboxyl side chain (Figure 1). The loss of a $^{\cdot}CH_2$-COOH radical (59 u) is consistent with the structure of Fe(III)-heme, shown in Scheme 1. The same procedure was performed for the binary drug-heme mixtures. Gradual variation of the cone voltage allowed the establishment of an optimal value of 75 V at which the signals of the drug-heme complexes were the highest and fragmentation was the lowest. Optimization of the needle voltage was also performed because it was found that the dihydroartemisinin-heme complex is susceptible to reduction. Oxidation-reduction processes are known to occur during electrospray ionization and have been well documented (for a review, see [29]). At high needle voltage (>2.5 kV), the isotopic cluster of the dihydroartemisinin-heme complex ($[DHAn:FP]^+$ *m/z* 900) was severely distorted by a hydrogenated species, which corresponds to $[DHAn:FP + H]^+$ (*m/z* 901) containing protonated Fe(II)-heme. It is worth mentioning that protonated Fe(II)-heme (*m/z* 617) has also been reported for electrospray ionization of the complex between heme and cytochrome *c* [26]. Gradual variation of the needle voltage, employing a dihydroartemisinin-quinine-heme mixture (1:1:1), allowed the establishment of an optimal value of 2.3 kV for the signal intensity of the dihydroartemisinin-heme complex without affecting the isotopic pattern as well as for the signal intensity of the quinine-heme complex.

Using these optimized conditions, first-order ESI mass spectra were obtained for drug-heme binary mixtures (1:2). In order to allow the detailed interpretation of the spectra, we also recorded the spectrum of heme. Figure 1a and b show the ESI spectra obtained for heme under non-optimal and optimal conditions, respectively. Under optimal conditions, the following ions can be noted in the spectrum of heme: FP^+ (*m/z* 616), $[FP:MeOH]^+$ (*m/z* 648), $[2FP - H]^+$ (*m/z* 1231), $[FP:FPOH]^+$ (*m/z* 1249) and $[2FP - 2H + Na]^+$ (*m/z* 1253). The formation of heme dimer-related ions (i.e., $[2FP - H]^+$ and $[2FP - 2H + Na]^+$) is worth noting. Their basic structures likely correspond to that of the dimer units of β-hematin or hemozoin. The ion at *m/z* 1249, corresponding to $[FP:FPOH]^+$, can be regarded as a noncovalent complex between heme and hematin (i.e., Fe(III)protoporphyrin IX hydroxide).

Quinine-heme mixture. Before examining the artemisinin-type drugs, we first examined quinine which is known to bind to heme [5–7]. Figure 2a illustrates the ESI mass spectrum obtained for the quinine-heme (1:2) mixture. Formation of a quinine-heme noncovalent complex is evident from the intense peak $[Qn:FP]^+$ (*m/z* 940, RA 97%). In addition, a complex of quinine with the heme dimer $[(2FP - H):Qn]^+$ (*m/z* 1556, RA 10%) can be noted. Formation of a noncovalent complex with heme dimer or β-hematin has been detected previously for neocryptolepine [28]. Peaks related to heme, namely, $[FP]^+$ (*m/z* 616, RA 6%), $[FP:MeOH]^+$ (*m/z* 648, RA 18%), $[2FP - H]^+$ (*m/z* 1231, RA 7%), $[2FP - 2H + Na]^+$ (*m/z* 1253, RA 11%), and quinine $[QnH]^+$ (*m/z* 325, RA 100%) are also present.

Artemisinin-heme mixture. The ESI mass spectrum obtained for the artemisinin-heme (1:2) mixture is shown in Figure 2b. The artemisinin-heme noncovalent complex $[An:FP]^+$ (*m/z* 898) is the most abundant ion in the spectrum. It is interesting to note that the artemisinin-heme complex is stable upon electrospray ionization. One could expect that artemisinin which contains a labile endoperoxide bridge would give rise to radical formation in electrospray ionization, but apparently this is not the case. In contrast to quinine, a complex of artemisinin with the heme dimer could not be detected. The other peaks in the spectrum could easily be attributed to ions characteristic of the individual components of the mixture, i.e., $[An + H]^+$ (*m/z* 283, RA 61%), $[An + NH_4]^+$ (*m/z* 300, RA 98%), $[2An + NH_4]^+$ (*m/z* 582,

Table 1. Major peaks in the ESI mass spectrum of a dihydroartemisinin-heme (1:2) mixture

m/z	Peak identification	RA (%)
284	$[DHAn]^{+\cdot}$	22
302	$[DHAn + NH_4]^+$	92
307	$[DHAn + Na]^+$	38
586	$[2DHAn + NH_4]^+$	80
591	$[2DHAn + Na]^+$	65
616	$[FP]^+$	28
648	$[FP:MeOH]^+$	100
900	$[DHAn:FP]^+$	75
922	$[DHAn:FP - H + Na]^+$	25
1231	$[2F] - H]^+$	28
1253	$[2FP - 2H + Na]^+$	33

RA 80%), FP^+ (*m/z* 616, RA 22%), $[FP:MeOH]^+$ (*m/z* 648, RA 62%), $[2FP - H]^+$ (*m/z* 1231, RA 20%), $[2FP - 2H + Na]^+$ (*m/z* 1253, RA 30%). These data provide experimental evidence that artemisinin just as quinine can form a noncovalent complex with heme in solution. It is worth noting that the solution consisted of MeOH:H_2O in a molar ratio of 3:1 and that even in the presence of a relatively high concentration of the organic solvent methanol an intense peak for the drug-heme complex could be generated, consistent with the strong electrostatic nature of the drug-heme complex. However, it is pointed out that there is a distinct difference between quinine and artemisinin in that quinine also forms a noncovalent complex with dimeric heme, which is relevant to its underlying molecular mechanism of action. It has namely been suggested that quinoline-type drugs such as chloroquinine and quinidine interact with both the heme monomer and dimer [6], which is in agreement with our mass spectrometric observations.

Dihydroartemisinin-heme mixture. Dihydroartemisinin is of particular interest because it is the active metabolite of semi-synthetic derivatives of artemisinin in vivo [1, 30]. The major peaks of the ESI mass spectrum obtained for the binary mixture of dihydroartemisinin with heme (1:2) (Figure 2c) are summarized in Table 1. The formation of a radicalar molecular ion species for dihydroartemisinin (i.e. $[DHAn]^{+\cdot}$, *m/z* 284) is worth noting. This $[DHAn]^{+\cdot}$ ion can be explained by electrochemical oxidation in the electrospray needle [29]. Taking into account that molecular radical formation is not observed for artemisinin, artemether and arteether, it can be suggested that an intact 12-hydroxyl group facilitates radical formation.

The data obtained for dihydroartemisinin (Figure 2c and Table 1) demonstrate that dihydroartemisinin just as artemisinin forms a noncovalent complex with heme $[DHAn:FP]^+$ (*m/z* 900). The formation of a noncovalent dihydroartemisinin-heme complex with 1:1 stoichiometry is in agreement with the study by Messori et al. [19] which used spectrophotometric determinations. In addition, dihydroartemisinin also results in a complex with heme in which a hydrogen is replaced by a sodium atom $[DHAn:FP - H + Na]^+$ (*m/z* 922), which was not detected for either quinine or artemisinin. As sodium ions are ubiquitous in physiological conditions, it is logical to assume that this complex may be relevant to in vivo conditions.

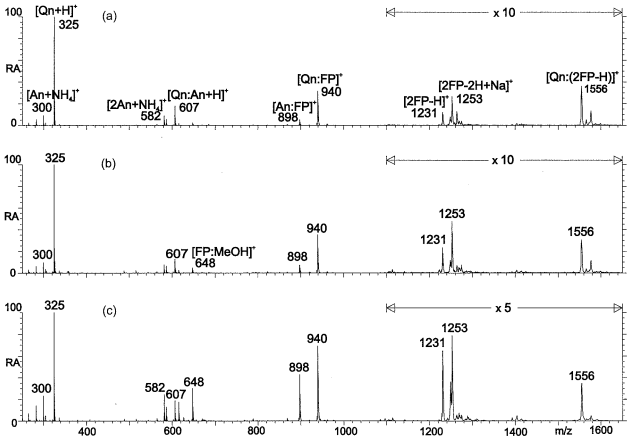

Figure 3. ESI mass spectra of three-component quinine-artemisinin-heme mixtures with molar ratios of (**a**) 1:1:1, (**b**) 1:1:2, and (**c**) 1:1:4.

Estimation of the Relative Efficiency of Drugs to Form Drug-Heme Complexes

For estimation of the relative efficiency of the drugs to form noncovalent complexes with heme, we examined three-component mixtures containing a reference drug, the drug to be tested, and heme. In these mixtures two drugs, the drug to be tested and the reference drug, competed for heme. Two drugs were selected as reference drugs, namely, quinine as a well-known and highly efficient antimalarial drug and artemisinin as the lead compound of the artemisinin-type series.

Quinine-artemisinin-hememixture. Quinine-artemisinin-heme three-component mixtures in different molar concentration ratio, 1:1:1, 1:1:2 and 1:1:4, were tested (Figure 3).

In the ESI mass spectra obtained for all these mixtures, peaks related to the individual components were present, i.e., $[Qn + H]^+$ (*m/z* 325), $[An + H]^+$ (*m/z* 283), $[An + NH_4]^+$ (*m/z* 300), $[2An + NH_4]^+$ (*m/z* 582), $[FP:MeOH]^+$ (*m/z* 648), and $[2FP - 2H + Na]^+$ (*m/z* 1253). For the three-component mixtures, the same types of noncovalent drug-heme complexes were detected as in the experiments with binary mixtures, i.e., $[Qn:FP]^+$ (*m/z* 940), $[(2FP - H):Qn]^+$ (*m/z* 1556) and $[An:FP]^+$ (*m/z* 898).

The general analysis of the spectra allows us to suggest that quinine binds more efficiently with heme in comparison with artemisinin, since the abundance of the quinine-heme complex is higher than the artemisinin-heme complex for all molar ratios tested. At the same time, certain concentration dependences were

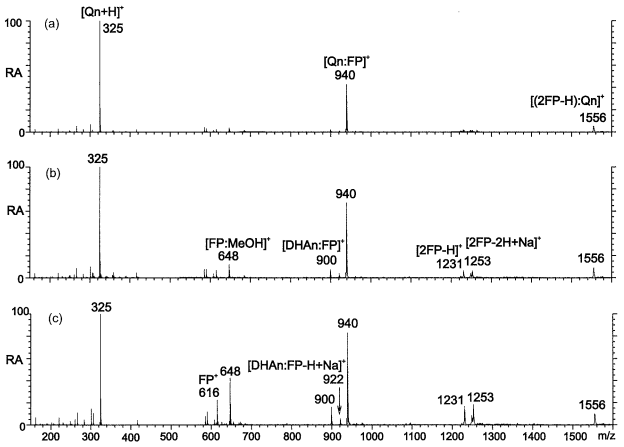

Figure 4. ESI mass spectra of three-component quinine-dihydroartemisinin-heme mixtures with molar ratios of (**a**) 1:1:1, (**b**) 1:1:2, and (**c**) 1:1:4.

observed. The relative abundances (RAs) of the drug-heme noncovalent complexes increased with the heme concentration, for the $[Qn:FP]^+$ complex, starting at a RA of 32% and increasing to 40 and 70% (Figure 3a, b, c), and, for the $[An:FP]^+$ complex, starting at a RA of 6% and increasing to 10 and 40% . Along with this, the relative abundance of the $[An:FP]^+$ complex in relation to that of the $[Qn:FP]^+$ complex increased from 19 to 25 and 57% with an increase of the heme concentration in the mixtures. These results indicate that there is a competition between the two drugs for binding with heme in solution: under the conditions of a heme deficit, quinine binds preferentially, while at a heme molar excess more intense binding of artemisinin becomes possible. The efficiency of artemisinin to bind noncovalently with heme, however, remains lower than that of quinine even at a four-fold molar excess of heme in relation to both drugs.

Quinine-dihydroartemisinin-heme mixture. The same experiment as described above was performed with quinine-dihydroartemisinin-heme mixtures (Figure 4). Noncovalent drug-heme complexes were detected for $[Qn:FP]^+$ (*m/z* 940) with a relatively high abundance and for $[(2FP - H):Qn]^+$ (*m/z* 1556) and $[DHAn:FP]^+$ (*m/z* 900) with a low RA. With the growth of the concentration of heme in the mixtures (molar ratios 1:1:2 and 1:1:4), the relative intensities of complex peaks also increased. For the 1:1:2 mixture (Figure 4b) the ions, corresponding to the quinine complexes with heme, $[Qn:FP]^+$ (*m/z* 940) and $[(2FP - H):Qn]^+$ (*m/z* 1556), had a RA of 68 and 11%, respectively, while the RA of $[DHAn:FP]^+$ (*m/z* 900) increased to 8%. A peak of the sodium-containing complex $[DHAn:FP - H + Na]^+$ (*m/z* 922), discussed above for the binary DHAn-heme system (see Figure 2c), appears here with a RA of 3%. The results obtained for the 1:1:4 mixture (Figure 4c) show that the intensity of the DHAn complexes with heme further increased, i.e., $[DHAn:FP]^+$ (*m/z* 900, RA 17%) and $[DHAn:FP - H + Na]^+$ (*m/z* 922, RA 5%).

Table 2. Relative abundances of drug-heme complexes in relation to artemisinin-heme observed in the ESI mass spectra of three-component mixtures (1:1:2)

Noncovalent complex drug:heme	*m/z*	TA (%) (N = 3)
$[An:FP]^+$	898	100
$[DHAn:FP]^+$	900	63 ± 1.5%
$[DHAn:F] - H + Na]^+$	922	29 ± 2.5%
$[\alpha$-Am:FP$]^+$	914	36 ± 2.6%
$[\beta$-Am:FP$]^+$	914	22 ± 1.3%
$[AE:FP]^+$	928	22 ± 3.5%

The results obtained for the quinine-dihydroartemisinin-heme mixtures demonstrate that quinine is the most efficient in forming a noncovalent complex with heme in equimolar mixtures but that with increase of the heme concentration dihydroartemisinin-heme complex formation also increases. From the comparison of the results obtained for the three-component mixtures discussed above, it follows that artemisinin is slightly more effective than dihydroartemisinin in binding with heme. In subsequent experiments aimed at evaluating more in detail the relative efficiency of the various artemisinin derivatives, we have, therefore, selected artemisinin as a reference compound.

Artemisinin-dihydroartemesinin-heme, artemisinin-β-arteether-heme, artemisinin-α-artemether-heme and artemisinin-β-artemether-heme mixtures. Mixtures with a molar ratio of 1:1:2 were examined, and for all the three-component mixtures tested, drug-heme complexes were detected with the artemisinin-heme complex (*m/z* 898) dominating the spectrum. In Table 2 the comparison is shown of the RAs of the drug-heme complexes in relation to that of artemisinin-heme.

The data obtained for the three-component mixtures containing artemisinin as a reference compound suggest that artemisinin is favored compared with its derivatives for complex formation with heme. Dihydroartemisinin, the active metabolite formed from artemisinin derivatives in vivo, is distinguished in the set of the artemisinin derivatives in that it is the only compound which forms two types of complexes with heme, i.e., the expected one ($[DHAn:FP]^+$) and the corresponding Na-containing complex (see Table 2). Similar results were obtained for the three-component mixtures containing quinine as a reference compound, discussed above. Furthermore, our data reveal that the stereoisomers of artemether have a different efficiency to form a noncovalent complex with heme, the α-isomer being about a 1.5 times more efficient than the β-isomer. This experimental observation is in agreement with that derived by a theoretical model based on a combination of molecular docking and a three-dimensional quantitative structure-activity study [20], which illustrates that α-isomers of artemisinin derivatives are, in general, more active than the corresponding β-isomers.

Although the ESI technique is widely used in studies

of noncovalent complexes of biomolecules [21–26], the correspondence between the specific noncovalent complexes formed in solution and gas-phase cluster ions produced by the ESI technique may be questioned [31–33]. Concern has been expressed that single molecules present in the solute can be randomly distributed in the sprayed droplets and can form any possible type of associate upon desolvation of the droplets. The patterns of the ESI mass spectra of the drug-heme mixtures recorded in the present work (Figures 2, 3, and 4) show, that there is a distinct selectivity in complex formation which must proceed in the initial solution. In particular, the association with the heme dimer is characteristic of quinine and is not observed for artemisinin derivatives. Among the artemisinin derivatives that have slight structural differences, only dihydroartemisinin forms a complex with heme with inclusion of a sodium atom. Since dihydroartemisinin is the active metabolite of artemisinin derivatives [1, 30], it can be suggested that interaction of dihydroartemisinin with heme in vivo may involve association with Na^+, which is present in all subcellular liquids. This feature is to be accounted for in the development of models of molecular mechanisms of action of artemisinin-type antimalarial agents.

Estimation of the Relative Binding Strength of Drug-Heme Complexes by Low-Energy Collision-Induced Dissociation

The relative binding strength between the drugs and heme in the noncovalent complexes was assessed using low-energy CID. First, metastable decomposition spectra of the drug-heme complexes (not shown) were obtained, which revealed no elimination of the drug and indicated that the drug-heme complexes are stable in the gas phase. Subsequently, CID spectra were obtained at low and high collision energy using He and Xe, respectively, as collision gas. The reproducibility of the CID conditions was evaluated by monitoring the decomposition of the weakly bound associate of heme with the solvent molecule methanol, i.e., $[FP:MeOH]^+$ (*m/z* 648):

$$[FP;MeOH]^+ \rightarrow FP^+MeOH \quad (1)$$

The RA of the FP^+ product ion in the CID mass spectra obtained at low collision energy (E_{com} = 1.8 eV) with He was about 42 ± 2% (N = 20) of that of the precursor $[FP:MeOH]^+$ selected from any of the studied systems (Figure 5c). Taking into account that the cone voltage affects the signal intensity of the $[FP:MeOH]^+$ complex, it was also confirmed that it does not decay spontaneously via Pathway 1. All studied $[M:FP]^+$ complexes (where M denotes the drug molecule) decomposed under CID through the neutral loss of the noncovalently bound drug molecule:

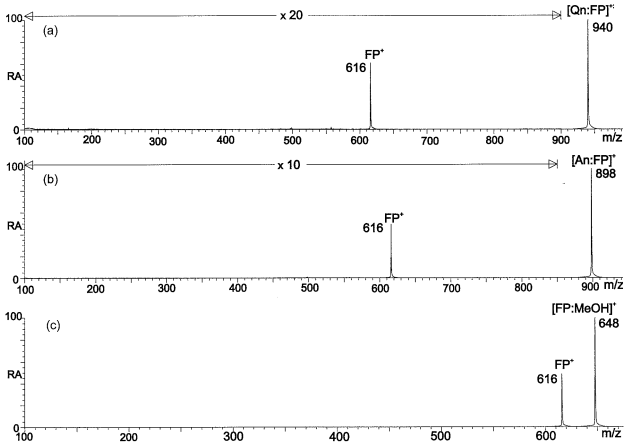

Figure 5. Low-energy CID spectra of heme complexes with (**a**) quinine, (**b**) artemisinin, and (**c**) of the non-specific associate of heme with methanol. The spectra were obtained with helium as collision gas at an E_{lab} of 400 eV.

$$[M:FP]^+ \rightarrow FP^+ + M \quad (2)$$

The CID efficiency of the drug-heme complexes did not depend on the source of a particular complex in that it was practically the same for $[M:FP]^+$ ions selected in experiments using mixtures with different number and ratio of the interacting components. As could be expected, a dependence on the collision gas was observed. Figures 5 and 6 illustrate the CID mass spectra obtained with He and Xe, respectively, as collision gas, for two complexes $[Qn:FP]^+$ (a) and $[An:FP]^+$ (b). It can be noted that the RA of the product ion FP^+ is higher for high-energy CID with Xe. Furthermore, product ions at lower *m/z* such as the ion at *m/z* 557, due to fragmentation of FP^+, were generated, as could be expected for high-energy CID. In contrast, low-energy CID with He only resulted in the elimination of the noncovalently bound drug molecule and was, therefore, selected in further experiments aimed at determining the relative binding strengths of the drug-heme complexes.

Taking into account that DHAn is the only compound among the evaluated artimisinin-type drugs which forms two types of complexes with heme (Table 2), the CID mass spectrum (Figure 7) was obtained for

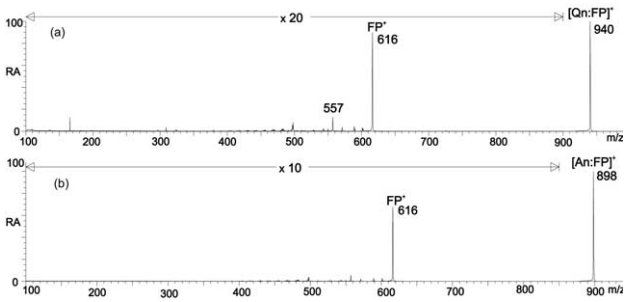

Figure 6. High-energy CID spectra of heme complexes with (**a**) quinine and (**b**) artemisinin. The spectra were obtained with xenon as collision gas at an E_{lab} of 400 eV.

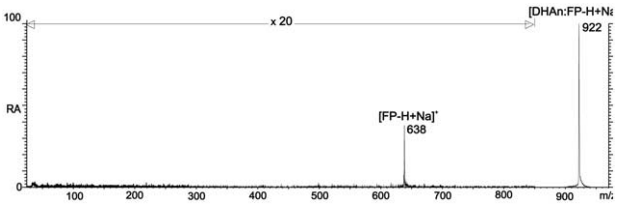

Figure 7. Low-energy CID spectra of the Na^+-containing heme complex with dihydroartemisinin. The spectrum was obtained with helium as collision gas at an E_{lab} of 400 eV.

$[DHAn:FP - H + Na]^+$ (*m/z* 922) complex, for which the following decomposition was observed:

$$[DHAn:FP - H + Na]^+ \rightarrow [FP - H + Na]^+ + DHAn \quad (3)$$

This low-energy CID experiment thus reveals that the Na-containing dihydroartemisinin:heme complex (*m/z* 922) results in Na-containing heme (*m/z* 638), in which the Na atom can be located in one of the two ethylcarboxyl side chains. It is suggested that during complex formation the Na atom is transferred from the sodiated dihydroartemisinin molecule (detected at *m/z* 307; Table 1), most likely from the 12-hydroxyl group which is part of a hemiketal function and has acidic properties.

The relative abundances of the product ions FP^+ or $[FP - H + Na]^+$, obtained in low-energy CID of different drug-heme complexes, averaged using the data of three to eight independent measurements, are summarized in Table 3.

The analysis of these data reveals a nearly two-fold lower CID efficiency of the $[Qn:FP]^+$ complex in comparison with that of all other complexes $[M:FP]^+$, indicating a higher stability of the quinine-heme complex. The relative stabilities of all complexes of heme with the artemisinin-type drugs as determined by CID of the $[M:FP]^+$ complexes are comparable within the experimental error. It is interesting to note that the stability of the $[DHAn:FP - H + Na]^+$ complex is as high as that of the $[Qn:FP]^+$ complex. The increase of the stability of the drug-heme complex containing a Na^+ ion can be explained by an increased electrostatic interaction, which has been reported as the main component of noncovalent interaction in the complex [20]. Since DHAn is known to be the active metabolite of artemisinin derivatives, it can be suggested that the DHAn-heme interaction in vivo may also involve sodium ions. We have stated in the introduction that formation of a relatively stable noncovalent complex between heme and drugs of the artemisinin-type can be regarded as the first step in covalent interaction between the ligand and heme, since Fe^{2+} is required for activation of artemisinin derivatives, i.e., generation of alkyl radicals. In this respect, it has been found experimentally in in vitro experiments by Messori et al. [19] that the covalent association is slightly faster for dihydroartemisinin compared with other artemisinin derivatives, a feature that could be explained by the initial formation of a more stable noncovalent heme-dihydroartemisinin complex.

Table 3. Relative abundances and relative standard deviations of product ions obtained in low-energy CID (He) of different drug-heme complexes

	RA of product ion, %
Complex	FP^+ *m/z* 616
$[Qn:FP]^+$	2.78 ± 0.22 (N=5)
$[An:FP]^+$	5.6 ± 0.25 (N=8)
$[DHAn:FP]^+$	5.86 ± 0.35 (N=4)
$[\alpha Am:FP]^+$	5.13 ± 0.26 (N=4)
$[\beta Am:FP]^+$	4.98 ± 0.44 (N=4)
$[AE:FP]^+$	5.33 ± 0.31 (N=3)
	$[FP - H + Na]^+$ *m/z* 638
$[DHAn:FP - H + Na]^+$	1.93 ± 0.16 (N=3)

The comparison of the CID behavior of all drug-heme complexes with that of $[FP:MeOH]^+$ (Figure 5c) shows, that the binding between the components of this non-specific associate of heme with the solvent molecule methanol is about 10 times weaker than between the components of specific drug-heme complexes. In contrast to the ESI-MS data obtained for the α- and β-isomers of artemether, indicating that the α-isomer is about 1.5 times more efficient than the β-isomer in binding with heme, the CID data reveal that their binding strengths are comparable within the experimental error. The reason for this discrepancy may be due to the fact that solvent effects play a role in noncovalent complex formation in the bulk solution.

Conclusions

In this study, we have demonstrated, using ESI-MS and ESI-MS/CID/MS, that stable noncovalent complexes can be formed between Fe(III)-heme and antimalarial agents, i.e., quinine, artemisinin, and the artemisinin derivatives, dihydroartemisinin, α- and β-artemether, and β-arteether. Differences in the binding behavior of the examined drugs with Fe(III)-heme and the stability of the drug-heme complexes were demonstrated. The results show that all tested antimalarial agents form a drug-heme complex with a 1:1 stoichiometry but that quinine also results in a second complex with the heme dimer or β-hematin. ESI-MS experiments performed on mixtures of the various antimalarial agents with heme indicate that quinine binds preferentially to Fe(III)-heme, while ESI-MS/CID/MS shows that the quinine-heme complex is nearly two times more stable than the complexes formed between heme and artemisinin and its derivatives. Moreover, it was found that dihydroartemisinin, the active metabolite of the artemisinin-type drugs in vivo, results in a Na^+-containing heme-drug complex, which is as stable as the heme-quinine complex. The efficiency of drug-heme binding of artemisinin derivatives is generally lower and the decomposi-

tion under CID higher compared with quinine, but these parameters are within the same order of magnitude. These results suggest that the efficiency of antimalarial agents of the artemisinin-type to form noncovalent complexes with Fe(III)-heme is comparable with that of the traditional antimalarial agent quinine. While the noncovalent complexes between Fe(III)-heme and artemisinin, artemether or arteether, were stable in electrospray ionization conditions, electrochemical reactions were observed for the dihydroartemisinin-heme complex.

Our study illustrates that electrospray ionization mass spectrometry and collision-induced dissociation tandem mass spectrometry are suitable tools to probe noncovalent interactions between heme and antimalarial agents. The results obtained provide insights into the underlying molecular modes of action of the traditional antimalarial agent quinine and of the antimalarials of the artemisinin-type which are currently used to treat severe or multidrug-resistant malaria.

Acknowledgments

This work has been supported by the Special Research Fund of the University of Antwerp through a BOF concerted action (grant no. 99/3/34) and a visiting postdoctoral fellowship to VP. The authors are grateful to Dr. F. H. Janssen (Dafra Pharma, Oud-Turnhout, Belgium) for the generous gift of artimisinin derivatives and for stimulating discussions.

References

1. Jansen, F. H. *Artesunate and Artemether. Towards the Eradication of Malaria?* Dafra Pharma Ltd: Oud-Turnhout, 2002; p 1.
2. Guterl, F. Battle Against the Bugs. *Sci. Technol.* **2002,** *14,* 51–53.
3. Warthurt, D. C.; Craig, J. C.; Adagu, I. S. Lysosomes and Drug Resistance in Malaria. *Lancet* **2002,** *360,* 1527–1529.
4. Padmanaban, G.; Rangarajan, P. N. Heme Metabolism of Plasmodium is a Major Antimalarial Target. *Biochem. Biophys. Res. Commun.* **2000,** *268,* 665–668.
5. Slater, A. F. Chloroquine: Mechanism of Drug Action and Resistance in Plasmodium Falciparum. *Pharmacol. Ther.* **1993,** *57,* 203–235.
6. Sullivan, D. J.; Matile, H.; Ridley, R. G.; Goldberg, D. E. A Common Mechanism for Blockade of Heme Polymerization by Antimalarial Quinolines. *J. Biol. Chem.* **1998,** *273,* 31103–31107.
7. Loria, P.; Miller, S.; Foley, M.; Tilley, L. Inhibition of the Peroxidative Degradation of Haem as the Basis of Action of Chloroquine and Other Quinoline Antimalarials. *Biochem. J.* **1999,** *339,* 363–370.
8. Pagola, S.; Stephens, P. W.; Bohle, D. S.; Kosar, A. D.; Madesn, S. K. The Structure of Malaria Pigment β-Haematin. *Nature* **2000,** *404,* 307–310.
9. Mann, R. D. Modern *Drug Use: An Enquiry on Historical Principles*; MTP Press, Ltd.: Lancaster, UK, 1984; p 268.
10. Jansen, F. H.; Yin, Z. Who Discovered Artemisinin? In *Artesunate and Artemether. Towards the Eradication of Malaria*? Jansen, F. H., Ed.; Dafra Pharma Ltd: Oud-Turnhout, Belgium, **2002;** p 25.
11. Benoit-Vical, F.; Robert, A.; Meunier, B. In Vivo and in Vitro Potentiation of Artemisinin and Synthetic Endoperoxide Antimalarial Drugs by Metalloporphyrins. *Antimicrob. Agents Chemother.* **2000,** *44,* 2836–2841.
12. Olliaro, P. L.; Haynes, R. K.; Meunier, B.; Yuthavong, Y. Possible Modes of Action of the Artemisinin-Type Compounds. *Trends Parasitol.* **2001,** *17,* 122–126.
13. Meshnick, S. R.; Taylor, T. E.; Kamchonwongpaisan, S. Artemisinin and the Antimalarial Endoperoxides: From Herbal Remedy to Targeted Chemotherapy. *Microbiol. Rev.* **1996,** *60,* 301–315.
14. RobertA.CoppelY.MeunierB. Alkylation of Heme by the Antimalarial Drug Artemisinin. *J. Chem. Soc. Chem. Commun.* **2002,** 414–415.
15. WangD.-Y.WuY.-L.WuY.LiangJ.LiY. Further Evidence for Participation of Primary Carbon-Centered Free Radicals in the Antimalarial Action of the Qinghaosu (Artemisinin) Series of Compounds. *J. Chem. Soc. Perkin Trans.* **2002,** 65–609.
16. Kannan, R.; Sahal, D.; Chauhan, V. S. Heme-Artemisinin Adducts are Crucial Mediators of the Ability of Artemisinin to Inhibit Heme Polymerization. *Chem. Biol.* **2002,** *9,* 321–332.
17. Eckstein-Ludwig, U.; Webb, R. J.; van Goethem, I. D. A.; East, J. M.; Lee, A. G.; Kimura, M.; O'Neill, P. M.; Bray, P. G.; Ward, S. A.; Krishna, S. Artemisinins Target the SERCA of *Plasmodium falciparum*. *Nature* **2003,** *424,* 957–961.
18. Paitayatat, S.; Tarnchompoo, B.; Thebtaranonth, Y.; Yuthavong, Y. Correlation of Antimalarial Activity of Artemisinin Derivatives with Binding Affinity with Ferroprotoporphyrin IX. *J. Med. Chem.* **1997,** *40,* 633–638.
19. Messori, L.; Piccioli, F.; Eitler, B.; Bergonzi, M. C.; Bilia, A. R.; Vincieri, F. F. Spectrophotometric and ESI-MS/HPLC Studies Reveal a Common Mechanism for the Reaction of Various Artemisinin Analogues with Hemin. *Bioorg. Med. Chem.* **2003,** *13,* 4055–4057.
20. Cheng, F.; Shen, J.; Luo, X.; Zhu, W.; Gu, J.; Ji, R.; Jiang, H.; Chen, K. Molecular Docking and 3-D-QSAR Studies on the Possible Antimalarial Mechanism of Artemisinin Analogues. *Bioorg. Med. Chem.* **2002,** *10,* 2883–2891.
21. Cole, R. B. *Electrospray Ionization Mass Spectrometry. Fundamentals, Instrumentation and Applications*; John Wiley and Sons: New York, 1997; p 578.
22. Przybylski, M.; Glocker, M. O. Electrospray Mass Spectrometry of Biomacromolecular Complexes with Noncovalent Interactions—New Analytical Perspectives for Supramolecular Chemistry and Molecular Recognition Processes. *Angew. Chem. Int. Ed.* **1996,** *108,* 878–899.
23. Veenstra, T. D. Electrospray Ionization Mass Spectrometry in the Study of Biomolecular Noncovalent Interactions. *Biophys. Chem.* **1999,** *79,* 63–79.
24. Skribanek, Z.; Balaspiri, L.; Mák, M. Interaction Between Synthetic Amyloid-β-Peptide (1-40) and its Aggregation Inhibitors Studied by Electrospray Ionization Mass Spectrometry. *J. Mass Spectrom.* **2001,** *36,* 1226–1229.
25. Loo, J. A. Studying Noncovalent Protein Complexes by Electrospray Ionization Mass Spectrometry. *Mass Spectrom. Rev.* **1997,** *16,* 1–23.
26. Li, Y.-T.; Hsieh, Y.-L.; Henion, J. D. Studies on Heme Binding in Myoglobin, Hemoglobin, and Cytochrome*c* by Ion Spray Mass Spectrometry. *J. Am. Soc. Mass Spectrom.* **1993,** *4,* 631–637.
27. Wright, A. D.; Wang, H.; Gurrath, M.; König, G. M.; Kocak, G.; Neumann, G.; Loria, P.; Foley, M.; Tilley, L. Inhibition of Heme Detoxification Processes Underlies the Antimalarial Activity of Terpene Isonitrile Compounds from Marine Sponges. *J. Med. Chem.* **2001,** *44,* 873–885.
28. Jonckers, T. H. M.; Van Miert, S.; Cimanga, K.; Bailly, C.; Colson, P.; De Pauw-Gillet, M.-C.; Van den Heuvel, H.; Claeys, M.; Lemière, F.; Esmans, E. L.; Rozenski, J.; Quirijnen, L.; Maes, L.; Dommisse, R.; Lemière, G. L. F.; Vlietinck, A.; Pieters, L. Synthesis, Cytotoxicity, and Antiplasmodial and Antitrypanosomal Activity of New Neocryptolepine Derivatives. *J. Med. Chem.* **2002,** *45,* 3497–3508.

29. Cech, N. B.; Enke, C. G. Practical Implications of Some Recent Studies in Electrospray Ionization Fundamentals. *Mass Spectrom. Rev.* **2001,** *20,* 362–387.
30. Grace, J. M.; Aguilar, A. J.; Trotman, K. M.; Brewer, T. G. Metabolism of β-Arteether to Dihydroginhaosu by Human Liver Microsomes and Recombinant Cytochrome P450. *Drug Metab. Dispos.* **1998,** *26,* 313–317.
31. Aplin, R. T.; Robinson, C. V.; Schofield, C. J.; Westwood, N. J. Does the Observation of Noncovalent Complexes between Biomolecules by Electrospray Ionization Mass Spectrometry Necessarily Reflect Specific Solution Interactions? *J. Chem. Soc. Chem. Commun.* **1994,** 2415–2417.
32. Kebarle, P. A Brief Overview of the Present Status of the Mechanisms Involved in Electrospray Mass Spectrometry. *J. Mass Spectrom.* **2000,** *35,* 804–817.
33. Loo, J. A. Electrospray Ionization Mass Spectrometry: A Technology for Studying Noncovalent Macromolecular Complexes. *Int. J. Mass Spectrom.* **2000,** *200,* 175–186.

УДК: 577.32:615.28

MASS SPECTROMETRIC STUDY OF INTERMOLECULAR INTERACTIONS BETWEEN THE ARTEMISININ-TYPE AGENTS AND NUCLEOBASES

V. A. Pashynska

B. Verkin Institute for Low Temperature Physics and Engineering of the National Academy of Sciences of Ukraine, Lenin Avenue 47, 61103 Kharkov, Ukraine, vlada@vl.kharkov.ua

Submitted March 10, 2009

Accepted April 2, 2009

Artemisinin-type agents are well known as effective antimalarial medicines and recently their anticancer activity was reported, however there is lack of investigations on the molecular mechanisms of antitumor activity of artemisinin and its derivatives. This study is aimed at the examining of mechanisms of artemisinin-type agents anticancer activity. DNA as carrier of genetic information is one of the major targets for antitumor drugs effect and nucleic acids are also suggested as molecular targets of artemisinin action in cancer cells. Biologically significant intermolecular interactions of artemisinin and dihydroartemisinin with some purine and pyrimidine nucleobases were studied by means of testing the drug-nitrogen base mixtures by electrospray ionization mass spectrometry. The peaks of stable noncovalent complexes of the artemisinin-type drug with Ade, Cyt, and mThy were registered in the mass spectra. Comparison of the relative abundances of the peaks of the drug-nucleobase complexes for purine and pyrimidine nitrogen bases was performed. The spectra analysis allowed us to conclude that an effectiveness of the complexation process depends on the structural peculiarities of the drugs and nucleobases molecules. The experimental data and features of the molecular structure of the drugs and nucleobases testify to the suggestion that noncovalent complexes of the artemisinin-type agents and nitrogen bases are stabilized by van der Waals forces and hydrogen bonds between the functional groups of the interacting molecules. Formation of the supramolecular complexes of the artemisinin-type drugs and nucleobases is considered as a possible molecular mechanism of anticancer activity of the studied antimalarial agents. The obtained results demonstrate the great potential of electrospray ionization mass spectrometry method in the study of the artemisinin-type agents and their intermolecular interactions related to the mechanisms of the drugs biological activity.

KEY WORDS: antimalarial agents, artemisinin, dihydroartemisinin, nucleobases, noncovalent complexes, anticancer activity, electrospray ionization mass spectrometry.

Antimalarial agent artemisinin and its derivatives, which have been used in Chinese traditional medicine since ancient times, are currently successfully used to treat severe or multidrug-resistant *Plasmodium falciparum* malaria [1, 2]. The molecular mechanisms of their action, however are still not properly understood and are the subjects of a number of investigations [3-7]. Our previous mass spectrometry study related to the molecular mechanisms of the artemisinin-type agents antimalarial activity have revealed the noncovalent complexes formation between the drugs and their suggested molecular target – heme - *in vitro* [8]. Recently in scientific literature it was also reported about anticancer activity of artemisinin and some its derivatives. In 1995 researchers H. Lai and S. Narenda of the University of Washington published paper in Cancer Letters journal [9] concerning the use of artemisinin against numerous cancer cell lines in vitro. In a subsequent article [10] of these scientists pointed out the selective toxicity of artemisinin and holotrasferrin towards human breast cancer cells. In that article, quite rapid and complete distruction of a radiation-resistant breast cancer cell line was achieved when the in vitro cell system was supported in iron uptake with holotrasferrin. In a paper by Efferth et al, published in Oncology journal in 2001 [11], it was stated that the antimalarial artesunate was also active against cancer. That article described dramatic cytotoxic activity of this artemisinin derivative against a wide variety of cancers including drug resistant cell lines of leukelia and colon cancer, melanomas, breast,

ovarian, prostate and renal cancer cell lines. In the review [12] it was also reported that artemisinin has been used for about 30 years in Vietnam and China for cancer treatment and the experience with artemisinin for this purpose is increasing.

While the molecular mechanisms of artemisinin-type antimalarial action are actively investigating by a number of scientific groups there is lack of investigations on the mechanisms of anticancer activity of artemisinin and its derivatives. This study is aimed at the understanding of possible molecular mechanisms of artemisinin-type agents anticancer activity. DNA as carrier of genetic information is one of the main targets for antitumor drugs effect because of the ability to interfere with transcription, gene expression, protein synthesis and DNA replication, major steps in cell growth and division. The latter is central for tumorgenesis and pathogenesis. Taking into account this known property shared by cancer cells related to their active growth and proliferation we decided to examine the interaction of artemisinin and its active metabolite dihydroartemisinin with some nucleobases in the current study. We consider that formation of noncovalent complexes of the drugs with the nitrogen bases in malignant cells can affect the functioning of their nucleic acids on the stages of transcription and DNA replication and selectively suppress the growth of the tumor cells as compared to non growing or slowly growing healthy tissue. Such effect can explain artemisinin-type drugs citotoxisity towards malignant cells.

MATERIALS AND METHODS

Materials

Artemisinin (MW 282) and dihydroartemisisnin (MW 284) were provided by Dafra Pharma Company (Oud-Tunhout, Belgium) for investigations. The structures of Artemisinin and Dihydroartemisinin are presented on the Scheme 1a and 1b, respectively. The nucleobases Adenine (MW 135), Cytosine (MW 111), and Methylthymine (MW 140) were purchased from Aldrich Company. Nitrogen base Guanine was not tested in our experiments because its weak solubility. Methanol (super grade) was purchased from Lab-Scan (Dublin, Ireland). Stock solutions of artemisinin (5 mM), dihydroartemisinin (5 mM) and nucleobases (5 mM) were prepared in methanol. The analyte solutions of the compounds studied in methanol had final molar concentration of 250μM. Mixtures of the drugs with the nitrogen bases were also prepared in MeOH. The final analyte solutions of the drug-nucleobase mixtures had molar ratios of 1:1and molar concentration of 250 μM of drug and 250μM of the nucleobase.

Abbreviations: An, artemisinin; DHAn, dihydroartemisinin; Ade, adenine; Cyt, cytosine; mThy, methylthymine.

a) b)

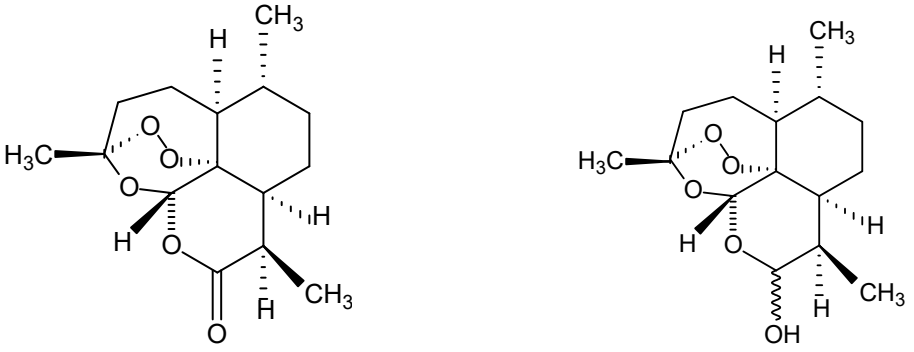

Scheme 1. Structure of a) artemisinin and b) dihydroartemisinin.

Instrumentation

The mass spectral data were obtained in the positive ion mode, using an Atmospheric Pressure Ionization (API) Triple Quadrupole mass spectrometer API 2000 triple quadrupole HPLC-MS/MS (Perkin Elmer Sciex, Toronto, Canada) which was equipped with a Turbo IonSpray source. This source was operated in a standard electrospray ionization (ESI) mode. The analyte solutions (20 μL) were infused into the mass spectrometer by glass syringe at a constant flow rate of 0.2 mL/min of methanol solvent.

The electrospray ionization source temperature was set to 200^0C. Curtain gas (N_2) back pressure of 0.14 MPa (20 units), nebulizer gas (N_2) of 0.42 MPa (60 units) and turbo gas (N_2) of 0.21 MPa (30 units) were applied. Ion source capillary voltage was set to 4 kV. Typical declustering potential (also called skimmer potential) value was 35 V, focusing potential value was 200 V and entrance potential - 10 V.

ESI spectra were recorded in the mass range of *m/z* 100-4000.

Data acquisition and processing were performed using Analyst 1.4.1 software. All scans were acquired in the continuum mode.

RESULTS AND DISCUSSION

ESI mass spectrometry investigation of the individual components of the systems studied

In the first series of experiments the ESI mass spectra of individual components of the systems studied – artemisinin-type drugs and nucleobases - were recorded and the experimental conditions were optimized. In the spectrum of artemisinin (Fig. 1) characteristic molecular and quasimolecular ions can be noted: An•H^+(m/z 283, relative abundance (RA) 27%), An•Na^+ (m/z 305, RA 58%), An•K^+ (m/z 321, RA 10%), 2An•H^+(m/z 565,RA 6%), 2An•Na^+ (m/z 587, RA 100%), 2An•K^+ (m/z 603, RA 17%), 3An•Na^+ (m/z 869, RA 27%), 3An•K^+ (m/z 885, RA 2%). The most intensive quasimolecular peaks in the spectra are the peaks of artemisinin molecules cationized by Na^+ and K^+. Cationization as a way of ion formation is characteristic for the electrospray method of ionization [13] and peaks of cationized molecules of the artemisinin-type drugs were also registered in our previous ESI mass spectrometry study [8] of these agents. The high intensity of the protonation and cationization of artemisinin is obviously conditioned on the peculiarities of artemisinin structure (see Scheme 1) in particular the presence of endoperoxide bridge and carbonyl group in the drug structure provides the centers to connect protons and more heavy cations.

In the following experiment the artemisinin derivative dihydroartemisinin was examined. While in the ESI mass spectra of DHAn the ions of protonated drug molecules were not registered, the cationized adducts of DHAn drug monomer, dimer and trimer were recorded (Fig. 2): DHAn•Na^+ (m/z 307, RA 35%), DHAn•K^+ (m/z 323, RA 15%), 2DHAn•Na^+ (m/z 591, RA 30%), 2DHAn•K^+ (m/z 607, RA 3%), 3DHAn•Na^+ (m/z 875, RA 4%). The most intensive peak in the spectra is peak at m/z 261, which can be considered as a fragment adduct of DHAn molecule. The analysis of the spectra of An and DHAn also pointed to the fact that dihydroartemisinin as well as artemisinin tends to form ions of dimers and trimers under the ESI experimental conditions. Apparently the chemical structure of the artemisinin-type agents and in particular presence of the polar functional groups (CO, OH, endoperoxide bridge) in the structures can provide the dimmer and trimer noncovalent complexes formation by van

der Waals interactions, hydrogen bonds and other types of noncovalent interactions. Stacking interactions of An and DHAn molecules are less probable because of an absence of π-electron system in the heterocyclic structure of artemisini-type drugs and because of nonplanarity of the artemisinin-type molecules reported in [14]. Moreover the electrospray ion formation process including solvent drops spray with the following solvent evaporation also promotes the formation of ions of dimers and trimers of analyzed molecules.

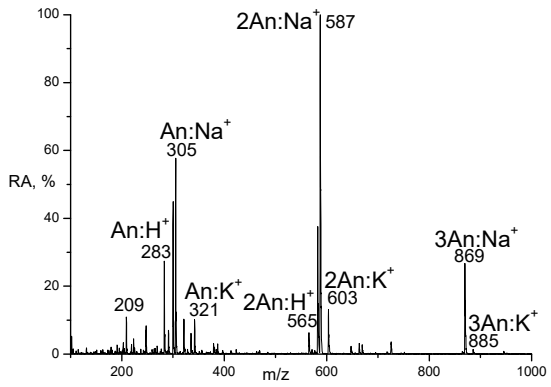

Fig. 1. Artemisinin ESI mass spectrum.

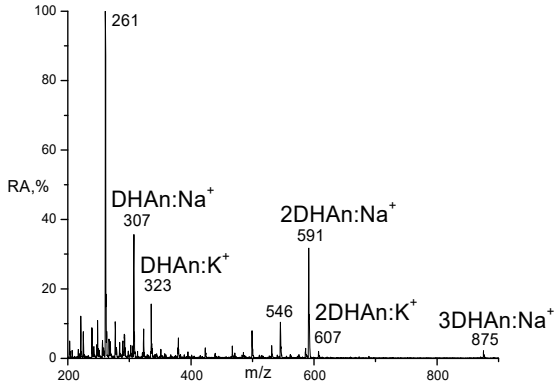

Fig. 2. Dihydroartemisinin ESI mass spectrum.

The peaks characteristic for An and DHAn observed in the present work are in a good agreement with the peaks registered for the drugs in our previous ESI investigation of these antimalarial agents [8] and can be used for the further analysis of the mixtures of the drugs with nucleobases.

Figure 3 (a,b,c) shows the individual ESI mass spectra of each studied nucleobase, Ade, Cyt and mThy , respectively. In these mass spectra the peaks of protonated nitrogen bases are the most intensive: Ade•H^+ (m/z 136, RA 100%), Fig. 3a; Cyt•H^+ (m/z 112, RA 100%), Fig. 3b; and mThy•H^+ (m/z 141, RA 100%), Fig.3c. At the same time the peaks of cationized monomers, dimers and trimers of Ade, Cyt and mThy were registered too (Fig.3), however their intensity were lower than intensities of the protonated peaks: Ade•Na^+ (m/z 158, RA 43%), Ade•K^+ (m/z 174, RA 4%), 2Ade•Na^+ (m/z 293, RA 18%), 3Ade•Na^+ (m/z 428, RA 7 %), Fig.3a; Cyt •Na^+ (m/z 134, RA 25%), 2Cyt •Na^+ (m/z 245, RA 24%), 3Cyt •Na^+ (m/z 356, RA 10%), Fig. 3b; mThy•Na^+ (m/z 163, RA 53%), mThy•K^+ (m/z 179, RA 14%), 2mThy •Na^+ (m/z 303, RA 24%), 2mThy•K^+ (m/z 319, RA 10%), 3mThy•Na^+ (m/z 443, RA 4%), 3mThy•K^+ (m/z 459, RA 6%), Fig. 3c.

Some interesting peculiarities of ion formation process for studied compounds under ESI conditions can be revealed from the spectra (Fig. 1- 3) analysis. In particular, we can see that for the artemisinin-type drugs the ions of cationized molecules are prevailed over the protonated ones, while for the nucleobases a protonation of the bases molecules is more favorable process. Such peculiarities are obviously determined by the chemical structures of the molecules studied. The endoperoxide bridge is in existence in the artemisinin-type compounds structures (Scheme 1) and it is considered as a center with high density of negative charge in the molecules. Such center can provide more strong interaction of the drug molecules with cations Na^+ and K^+ in comparison with the interaction of nitrogen bases with these cations.

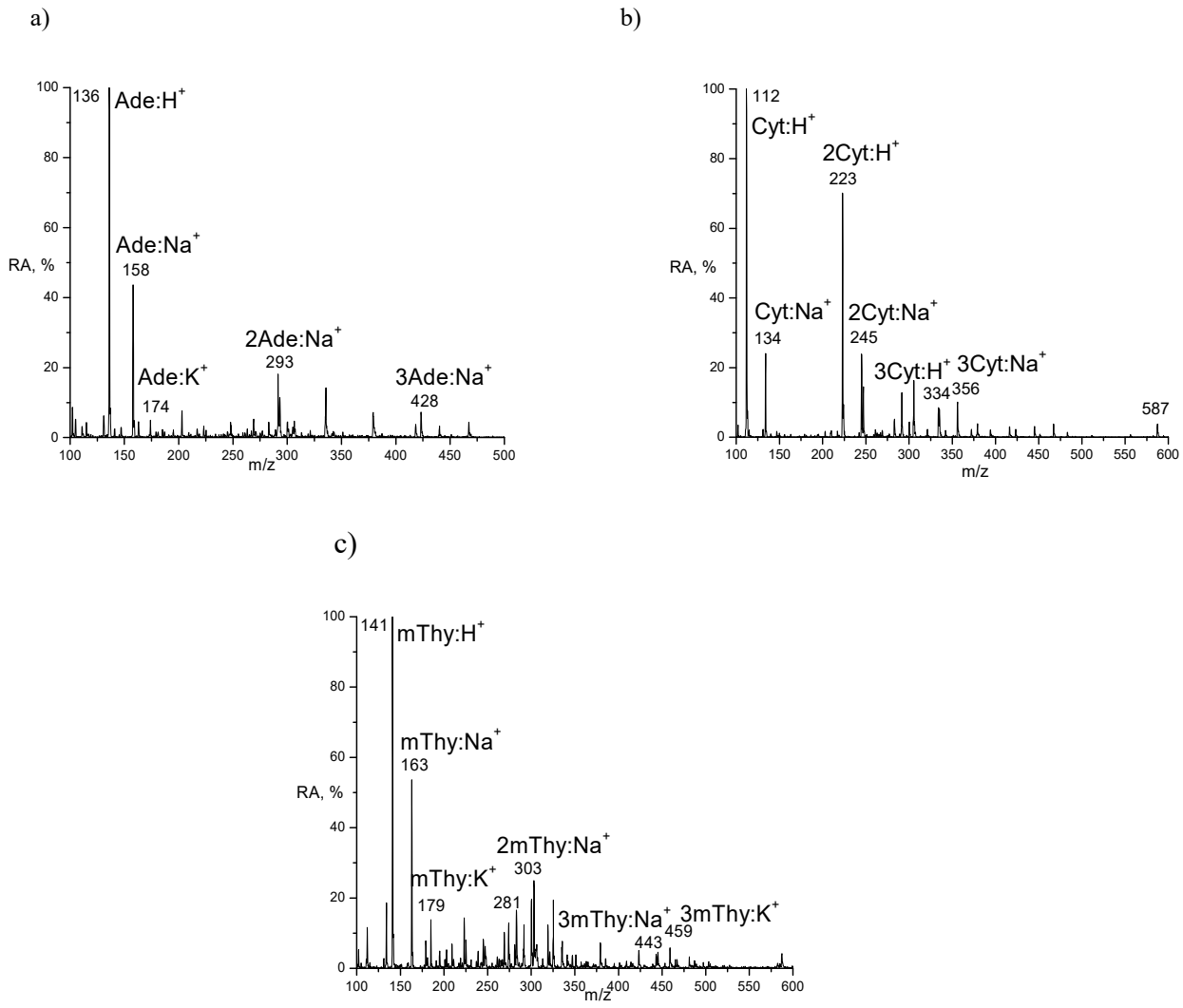

Fig.3. ESI mass spectra of nitrogen bases: a) adenine, b) cytosine, c) methylthymine.

ESI mass spectrometry study of the drug-nitrogen base systems

Artemisinin-Ade Mixture

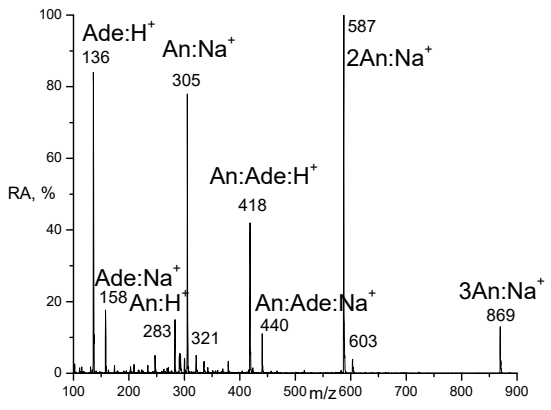

The ESI mass spectrum obtained for the artemisinin-adenine (1:1) mixture is shown in Figure 4. There are peaks related to individual components of the mixture in the spectrum: An•H^+(m/z 283, RA 15%), An•Na^+ (m/z 305, RA 78%), An•K^+ (m/z 321, RA 5%), 2An•Na^+ (m/z 587, RA 100%), 2An•K^+ (m/z 603, RA 4%), 3An•Na^+ (m/z 869, RA 13%); Ade•H^+ (m/z 136, RA 84%), Ade•Na^+ (m/z 158, RA 17%). The most interesting result of this

Fig.4. ESI spectrum of artemisinin-adenine system.

experiment is that the formation of a artemisinin-adenine noncovalent complex in the mixture is evident from the intensive peaks $[An•Ade•H]^+$ (m/z 418, RA 42%) and $[An•Ade•Na]^+$ (m/z 440, RA 11%). Registration of quite intensive peaks of the cationized noncovalent complexes under ESI mass spectrometry conditions is nontrivial phenomenon and testifies to the high stability of such complexes. Analysis of the chemical structures of artemisinin (Scheme 1) and adenine allowed us to suggest that complex stability can be provided by van der Waals forces and hydrogen bonds between the endoperoxide bridge or CO groups of artemisinin and NH groups of adenine. Such interactions can supply with quit high stability of the supramolecular complexes and their survival under the mass spectrometry registration process. Stacking interactions between the heterocyclic systems of artemisinin and nitrogen base are less probable because mentioned above absence of the π-system in artemisinin structure and the drug molecule nonplanarity [14].

Artemisinin-Cyt System

The major peaks of the ESI mass spectrum of the artemisinin-cytosine system (1:1) were also related to the individual components of the mixture studied, artemisinin and cytosine (Fig. 5): $An•H^+$(m/z 283, RA 19%), $An•Na^+$ (m/z 305, RA 100%), $An•K^+$ (m/z 321, RA 16%), $2An•Na^+$ (m/z 587, RA 83%), $2An•K^+$ (m/z 603, RA 16%), $3An•Na^+$ (m/z 869, RA 6%), $Cyt•H^+$ (m/z 112, RA 72%), Cyt $•Na^+$ (m/z 134, RA 25%), 2Cyt $•H^+$ (m/z 223, RA 54 %), 2Cyt $•Na^+$ (m/z 245, RA 24%). The group of peaks of nonocovalent complexes of artemisinin with cytosine (Fig. 5) can be registered in the spectrum too: $[An•Cyt•H]^+$ (m/z 394, RA 10%) and $[An•Cyt•Na]^+$ (m/z 416, RA 19%). The data obtained for this system demonstrate that cytosine just as adenine forms stable noncovalent complexes with artemisin in solution. Such complexes can also be provided by van der Waals interactions and hydrogen bonds between –O-O-, CO groups of artemisinin and NH groups of cytosine.

Artemisinin-mThy System

The same experiment as described above was performed with artemisinin-methylthymine mixture (Fig.6). Peaks of cationized noncovalent artemisinin-methylthymine complexes were detected in the spectrum (Fig.6) $[An•mThy•H]^+$ at m/z 423 with RA of 8% and $[An•mThy•Na]^+$ at m/z 445 with RA of 9.5%.The other intensive peaks in the spectrum could be attributed to the mixture components: $An•H^+$(m/z 283, RA 42%), $An•Na^+$ (m/z 305, RA 95%), $An•K^+$ (m/z 321, RA 23%), $2An•Na^+$ (m/z 587, RA 100%), $2An•K^+$ (m/z 603, RA 18%), $3An•Na^+$ (m/z 869, RA 12%), $mThy•H^+$ (m/z 141, RA 39%), $mThy•Na^+$ (m/z 163, RA 25%), 2mThy $•H^+$ (m/z 283, RA 42%). It is interesting to note that relative abundency of the peaks of noncovalent complexes of artemisinin with mThy in the spectrum (Fig. 6) are smaller than RA of the peaks for complexes artemisinin with Cyt (Fig. 5). This fact is probably connected with methylation of one of nitrogens in the mThy that results in decreasing the amount of polar NH groups in pyrimidine nucleobase and with presence in mThy one more carbonyl group in comparison with Cyt that can lead to less stability of noncovalent complexes of An-mThy comparing with An-Cyt.

The comparative analysis of the RA of the peaks of the complexes of artemisinin with purine base adenine (Fig.4) and the peaks related to the complexes of the drug with pyrimidine bases (Cyt and mThy) (Fig. 5 and 6) shows that artemisinin-base complexes with purine base are more relatively stable. Such result probably connected with the structural

compliance of artemisinin and adenine molecules to form complexes with several H-bonds. Moreover the bigger size of pyrine base molecule in comparison with pyrimidine one provides more strong van der Waals interactions with artemisinin molecule.

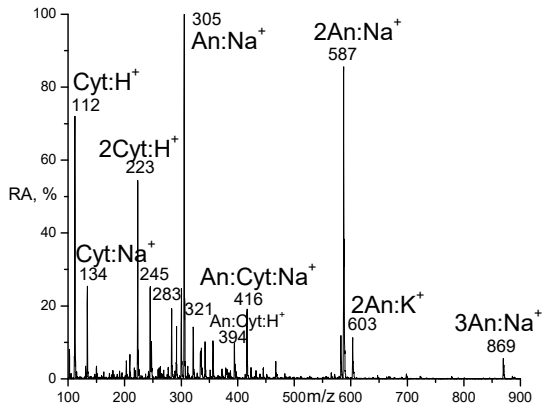

Fig.5. ESI mass spectrum of artemisinin-cytosine mixture.

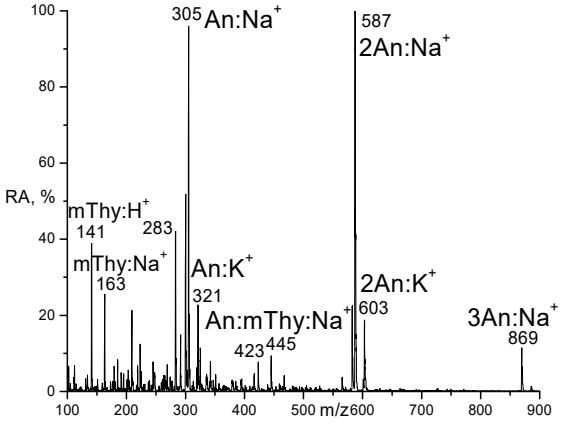

Fig.6. ESI mass spectrum of artemisinin-methylthymine system.

Dihydroartemisinin-Ade Mixture

Dihydroartemisinin is of particular interest for the understanding of artemisinin-type drugs action because DHAn is known as active metabolite of some derivatives of artemisinin in vivo [1, 15]. The mixtures of dihydroartemisinin with the nucleobases were studied at the same ESI mass spectrometry conditions. The ESI mass spectrum dihydroartemisinin –adenine system (1:1) is presented on the Figure 7.

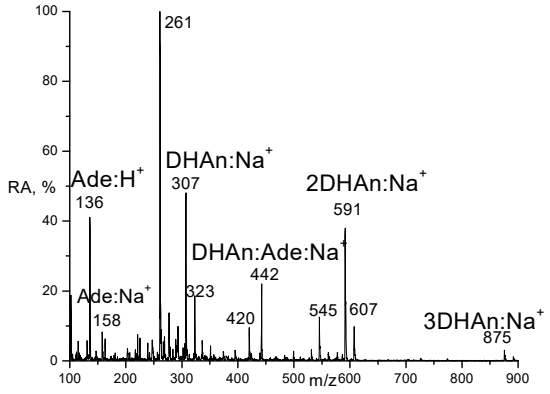

The spectrum contains ions characteristic of the individual components of the mixtures, namely, DHAn•Na^+ (m/z 307, RA 49%), DHAn•K^+ (m/z 323, RA 19%), 2DHAn•Na^+ (m/z 591, RA 38%), 2DHAn•K^+ (m/z 607, RA 9%); Ade•H^+ (m/z 136, RA 42%), Ade•Na^+ (m/z 158, RA 8%). Registration in the spectrum the peaks of [DHAn•Ade•H]$^+$ (m/z 420, RA 10%) and [DHAn•Ade•Na]$^+$ (m/z 424, RA 22%) demonstrates that dihydroartemisinin like artemisinin forms a noncovalent complexes with adenine in the solution.

Fig.7. ESI mass spectrum of dihydroartemisinin-adenine system.

Dihydroartemisinin-Cyt System

Interaction of dihydroartemisinin with pyrimidine nitrogen bases was tested in the ESI experiment on the DHAn-Cyt mixture (1:1). In the Fig. 8 presenting the mass spectrum of this system we can find just one peak which can be related to the noncovalent complex of the drug with Cyt, namely [DHAn•Cyt•Na]$^+$ peak at m/z 418 with RA 6%. In contrast to the spectrum of An-Cyt system in the case of DHAn the protonated peak of the noncovalent complex of the

drug with the nucleobase was not registered. The intensive peaks of the spectrum of DHAn-Cyt mixture can be attributed to the individual components of the mixture: DHAn•Na^+ (m/z 307, RA 41%), 2DHAn•Na^+ (m/z 591, RA 4%), Cyt•H^+ (m/z 112, RA 87%), Cyt •Na^+ (m/z 134, RA 48%), 2Cyt •H^+ (m/z 223, RA 46 %), 2Cyt •Na^+ (m/z 245, RA 40%). RA of the peak of DHAn-Cyt complex (Fig.8) is smaller than that for An-Cyt (Fig. 5) that can be explained by the peculiarity of DHAn structure in which hydroxyl group is situated on the place of carbonyl group in An.

Dihydroartemisinin-mThy System

The mixture of dihydroartemisinin with other pyrimidine base methylthymine was also studied in the experiment. In the spectrum of this system (Fig.9) the ions originated from DHAn are more intensive than the ions from the nucleobase: peak at m/z 261 (RA 100%) from DHAn, DHAn•Na^+ (m/z 307, RA 70%), DHAn•K^+ (m/z 323, RA 13%), 2DHAn•Na^+ (m/z 591, RA 58%), 2DHAn•K^+ (m/z 607, RA 9%); m Thy•H^+ (m/z 141, RA14.5%), mThy•Na^+ (m/z 163, RA 45%), mThy•K^+ (m/z 179, RA 3%), 2mThy •Na^+ (m/z 303, RA 16%). The peak of ion [DHAn•mThy•Na]$^+$ at m/z 447 with RA 17 % was registered in the spectrum that testify to the formation of stable supramolecular complex DHAn with mThy in the solution. RA of DHAn-mThy complex is higher than the RA of DHAn-Cyt complex. This fact is probably connected with the structural peculiarities of the nucleobases: in Cyt there is one CO group (which can interact with OH group of DHAn forming H bond) in comparison with two groups in mThy.

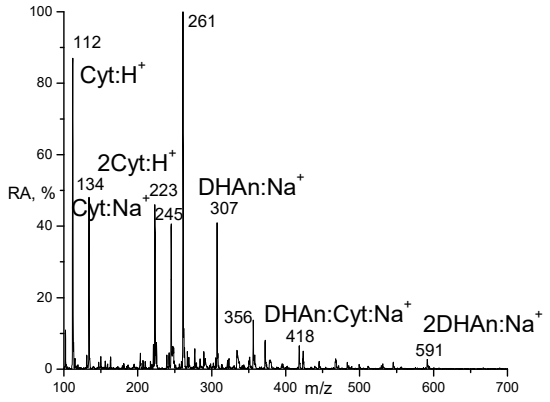

Fig.8. ESI mass spectrum of dihydroartemisinin-cytosine system.

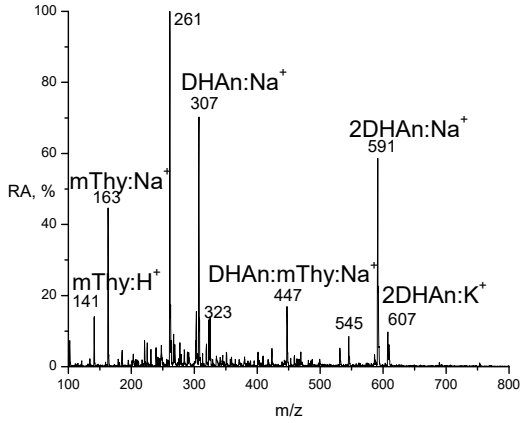

Fig.9. ESI mass spectrum of dihydroartemisinin-methylthymine system.

Analysis of the spectra of systems containing the artemisinin-type drugs and nucleobases confirms the formation of stable supramolecular complexes of the drugs and nitrogen bases in solution and shows that the RA of the peaks related to the noncovalent complexes of An and DHAn with purine nucleabase Ade is higher than that for the peaks of the complexes of the drugs with pyrimidine nucleabases Cyt and mThy.

CONCLUSIONS

Cationized noncovalent complexes of artemisinin and dihydroartemisinin with nucleobases Ade, Cyt and mThy, which model drug-DNA interaction in biological systems, were registered by ESI mass spectrometry. The spectra analysis allowed us to conclude that an effectiveness of the complexation process depends on the structural peculiarities of the drugs and nucleobases molecules: the relative abundances of the peaks of the complexes of artemisinin and dihydroartemisinin with purine base are higher than those for the peaks corresponding to the drug-pyrimidine base complexes. The experimental data and structural features of the drugs and nucleobases testify to the suggestion that noncovalent complexes of the artemisinin-type agents and nitrogen bases are stabilized by van der Waals forces and hydrogen bonds between the polar functional groups of the molecules, such as endoperoxide bridge or CO groups of the drugs and NH groups of the bases. Formation of the drug-nucleobase surpamolecular complexes in cells is suggested as a possible molecular mechanism of anticancer activity of the artemisinin-type drugs. The present investigation also demonstrates the great potential of electrospray ionization mass spectrometry method in the study of the artemisinin-type agents and their biologically significant intermolecular interactions related to the mechanisms of the drugs biological activity.

Acknowledgements

The experiments of the present study were performed in the Mass Spectrometry Department of the Chemical Research Center of the Hungarian Academy of Sciences during Dr. Pashynska visit to the Institute within the framework of the program of cooperation between Ukrainian and Hungarian Academies of Sciences. Author acknowledges the Head of the Department Prof. Karoly Vekey, M.Sc. Agnes Gomory and Dr. Ferenc Pollreisz for significant experimental support. Author also expresses ones thanks to Dr. Marina Kosevich for support this work and long-term effective cooperation.

REFERENCES

1. Jansen F. Artesunate and Artemether. Towards the Eradication of Malaria? Dafra Pharma Ltd: Oud-Turnhout. 2002, 63 p.
2. Benoit-Vical F., Robert A., Meunier B. // Antimicrob. Agents Chemother. 2000 . V.44. P. 2836-2841.
3. Olliaro P., Haynes R., Meunier B., Yuthavong Y. // Trends Parasitol. 2001. V. 17. P. 122-126.
4. Meshnick S., Taylor T., Kamchonwongpaisan S. // Microbiol. Rev. 1996. V. 60. P. 301-315.
5. Robert A., Coppel Y., Meunier B. // J. Chem. Soc. Chem. Commun. 2002. P. 414-415.
6. Wang D.-Y., Wu Y.-L., Liang J., Li Y. // J. Chem. Soc. Perkin Trans. 2002. P. 65-69.
7. Eckstein-Ludwig U., Webb R., Van Goethem I., East J., Lee A., Kimura M., O'Neill P., Bray P., Ward S., Krishna S. // Nature. 2003. V. 424. P. 957-961.
8. Pashynska V., Van den Heuvel H., Claeys M., Kosevich M. // J. Am. Soc. Mass Spectrom. 2004. V.15. P. 1181-1190.
9. Lai H., Singh N. // Cancer letters. 1995. V. 91. P. 41-46.
10. Singh N., Lai H. // Life Sci. 2001. V. 70(1). P. 49-56.
11. Efferth T., Dunstan H., Sauerbrey A., Miyachi H., Chitambar C. // Oncol. 2001. V.18(4). P. 767-773.
12. Robert J. R. Artemisinin: From malaria to Cancer Treatment. // Townsend Letter. 2002. V.10. P.1-8.
13. Principles of Mass Spectrometry Applied to Biomolecules. Ed. By Laskin. J. and Lifshitz C. John Wiley & Sons, Inc.: Hoboken. 2006. 678 p.
14. Cheng F., Shen J., Luo X., Zhu W., Gu J., Ji R., Jiang H., Chen K. // Bioorg. Med. Chem. 2002. V.10. P. 2883-2891.
15. Grace J., Aguilar A., Trotman K., Brewer T. // Drug Metab. Dispos. 1998. V. 26. P. 313-317.

УДК: 577.352:615.281

STUDY OF NON-COVALENT COMPLEXES FORMATION BETWEEN THE BISQUATERNARY AMMONIUM ANTIMICROBIAL AGENT DECAMETHOXINUM AND MEMBRANE PHOSPHOLIPIDS BY ELECTROSPRAY IONIZATION AND COLLISION-INDUCED DISSOCIATION MASS SPECTROMETRY

V. A. Pashynska[1,2*], M. V. Kosevich[1], H. Van den Heuvel[2], F. Cuyckens [2], M. Claeys[2]

[1] *B. Verkin Institute for Low Temperature Physics and Engineering of the National Academy of Sciences of Ukraine, Lenin Avenue 47, 61103 Kharkov, Ukraine, pashynska@ilt.kharkov.ua*
[2] *University of Antwerp, Department of Pharmaceutical Sciences, Universiteitsplein, 1, B-2610 Antwerp, Belgium*
7 September 2004

The non-covalent complex formation between the membrane phospholipid, dipalmitoylphosphatidylcholine, and the bisquaternary ammonium antimicrobial agent, decamethoxinum, which is related to its biological activity, was studied by electrospray ionization (ESI) mass spectrometry and collision-induced dissociation (CID) tandem mass spectrometry. Stable doubly-charged complexes of the drug dication with phospholipid molecule assemblies containing up to nine phospholipid molecules, which model drug-phospholipid interactions in biological membrane systems, were registered. For examination of the structure and the stability characteristics of the drug-phospholipid non-covalent complexes, their CID spectra were examined. The developed ESI mass spectrometry methodology is proposed for fast screening of bisquaternary ammonium compounds with antimicrobial activity.

KEY WORDS: non-covalent complexes, bisquaternary ammonium compounds, decamethoxinum, dipalmitoylphosphatidylcholine, electrospray ionization mass spectrometry, collision-induced dissociation.

Non-covalent interactions play a significant role in the structure organization and the functioning of biological membranes and are responsible for important biological processes, e.g. the cellular reflex response, immunological reactions, some enzymatic processes, etc. [1]. Examination of the effects of biologically active membranothropic substances on the functional state of a cell membrane by non-covalent binding can be considered as a promising strategy in drug development. Among membranothropic biologically active compounds, the class of bisquaternary ammonium salts is well known to have antimicrobial, anticancer or antimalarial activity, while some of these substances are used as medicines [2-7]. The biophysical study of molecular mechanisms underlying the activity of these compounds, which can lead to the development of new drugs, has become increasingly popular in recent years. Meaningful results have been obtained in mechanistic investigations of drug-biological target interactions by means of soft ionization mass spectrometry techniques which are powerful modern physical tools that are suited to the study of supramolecular complexes [8-10].

In our previous work [11], the non-covalent complex formation of the bisquaternary ammonium antimicrobial agent, decamethoxinum, which is produced in Ukraine, with phospholipid molecules, was demonstrated by liquid secondary ion mass spectrometry (LSIMS), while interaction of the drug with a model phospholipid membrane was revealed by differential scanning calorimetry. This interaction is responsible for a change of the liquid-crystalline properties of the lipid bilayer in a model and real bacterial membrane and allows to explain the antimicrobial activity of decamethoxinum. However, because of limitations of the LSIMS technique, we could not observe large drug-phospholipid complexes, only paired complexes of the phospholipid molecule with the decamethoxinum dication were registered. The more recently developed electrospray ionization (ESI) technique, which is based on electrospray of the analyte solution and subsequent solvent evaporation from the charged droplets, has been successfully used for probing non-covalent interactions of biomolecules and ligands, and very large molecular assemblies were registered [12-16]. In the present study, we have resorted to ESI mass spectrometry to examine the interaction of the antimicrobial agent, decamethoxinum, with the membrane phospholipid component, dipalmitoylphosphatidylcholine. Complexes of the drug dication with phospholipid assemblies (up to nine phospholipid molecules under optimal experimental conditions) were observed that could serve as a model system for drug-phospholipid interaction in a real cellular environment.

MATERIALS AND METHODS

Materials

Decamethoxinum ($C_{38}H_{74}N_2O_4Cl_2$, monoisotopic molecular mass 692.5 Da) was synthesized at the Institute of Organic Chemistry of the National Academy of Sciences of Ukraine (Kiev, Ukraine). The synthetic phospholipid dipalmitoylphosphatidylcholine ($C_{40}H_{50}NO_8P$, monoisotopic molecular mass 733.5 Da) was produced by Biolek (Kharkov, Ukraine). Methanol (Super grade) was purchased from Lab-Scan (Dublin, Ireland). Stock solutions of decamethoxinum (5 mM) and phospholipid (2.5 mM) were prepared in methanol. The final analyte solutions of the drug-phospholipid mixtures had molar ratios 1:5 and 1:10; the final concentrations of decamethoxinum were 40 µM/L and of phospholipid were 200 and 400 µM/L, respectively.

Instrumentation

The mass spectral data were obtained in the positive ion mode, using an Autospec-oa-TOF mass spectrometer (Micromass, Manchester, UK) which was equipped with an ESI ion source. The instrument is comprised of a double-focusing stage of *EBE* configuration coupled to an orthogonal acceleration time-of flight (oaTOF) analyzer for MS/MS experiments. The electrospray ionization source was operated at 4 kV. Nitrogen was used both as bath gas (100∞C; 250 L/h) and as nebulizing gas (15 L/h). ESI spectra were recorded in the mass range *m/z* 100-4000. The analyte solutions were infused into the mass spectrometer by a syringe pump (Harvard Apparatus, South Natick, MA, USA), employing a 500 µL syringe, at a constant flow rate of 5 µL/min.

The effects of the nozzle-skimmer, cone voltage (CV) in the ion source on the spectra of drug-phospholipid system and the fragmentation were examined. The CV was varied from 50 to 200 V in steps of 25 V. The value of the needle voltage was 7200 V. Collision-induced dissociation (CID) spectra were obtained at a laboratory frame energy (E_{lab}) of 400 eV using He and Xe as collision gases. Data acquisition and processing were performed using OPUS V3.1X software. All scans were acquired in the continuum mode.

RESULTS AND DISCUSSION

ESI mass spectrometry study of the drug-phospholipid system

The structure of the bisquaternary ammonium salt, decamethoxinum, is presented in Scheme 1; it can be described as $[R_1(CH_3)_2\tilde{n}N\tilde{n}R_2\tilde{n}N\tilde{n}(CH_3)_2R_1]^{2+}\ddot{i}2Cl^{\tilde{n}}$ or $Cat^{2+}\ddot{i}2Cl^{\tilde{n}}$ where R_2 is a rather long polymethylene chain $(CH_2)_{10}$ and the two R_1 substituents are menthyl rings attached by ester linkages ($R_m\tilde{n}$menthyl ring). The phospholipid molecule is denoted in the text and spectra as M.

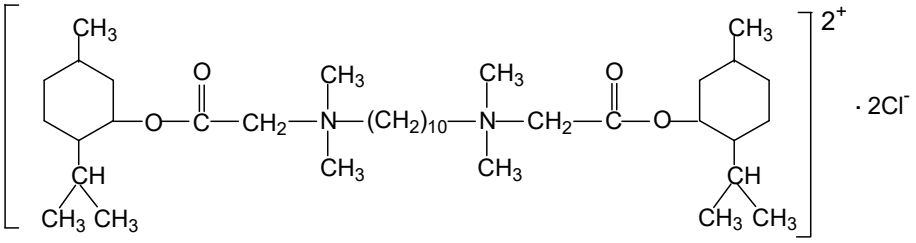

Scheme 1. Structure of the bisquaternqry ammonium salt decamethoxinum.

Positive ESI mass spectra were obtained for two different molar ratios of the drug-phospholipid mixtures in order to evaluate their concentration dependence. Figures 1 and 2 show the ESI mass spectra obtained under the same mass spectrometric conditions (cone voltage of 75 V) for the mixtures with a 1:5 and 1:10 drug:phospholipid molar ratio, respectively. The spectra contain ions characteristic of the individual components of the mixtures, namely, decamethoxinum: $Cat^{2+}\cdot Cl^{\tilde{n}}$ (m/z 657.5); Cat^{2+} (m/z 311.3); $[Cat^{2+}\tilde{n}R_m+H]^{2+}$ (m/z 242.2); $[Cat^{2+}\tilde{n}\ 2R_m+2H]^{2+}$ (m/z 173.2); the phospholipid: MNa^+ (m/z 756.5), and ions of the $nM\cdot Na^+$ phospholipid complexes (n=2-4), m/z 1490.1, m/z 2223.5, and m/z 2957.3. The most significant result from the biophysical point of view relates to the observation of abundant ions of doubly-charged complexes of the decamethoxinum dication with phospholipid molecules: $M\cdot Cat^{2+}$ (m/z 678.1); $2M\cdot Cat^{2+}$ (m/z 1044.8); $3M\cdot Cat^{2+}$ (m/z 1411.6) (Figs. 1 and 2); $4M\cdot Cat^{2+}$ (m/z 1778.4); $5M\cdot Cat^{2+}$ (m/z 2145.2); and $6M\cdot Cat^{2+}$ (m/z 2512.0) (Fig. 2). The abundance of these ions decreases with the number of phospholipid molecules in the complex, namely, from a relative abundance of 40% for the $M\cdot Cat^{2+}$ paired complex to a value of about 1% for the $6M\cdot Cat^{2+}$ complex (Fig. 2). Comparison of the mass spectra obtained for the drug:phospholipid mixtures with a 1:10 and

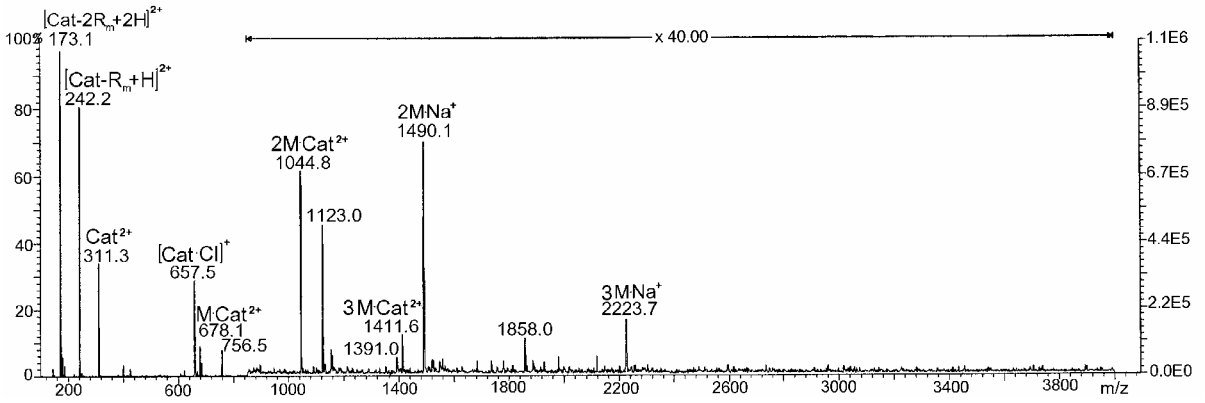

Fig. 1. Positive ion ESI mass spectrum of the drug:phospholipid system with a molar ratio of 1:5.

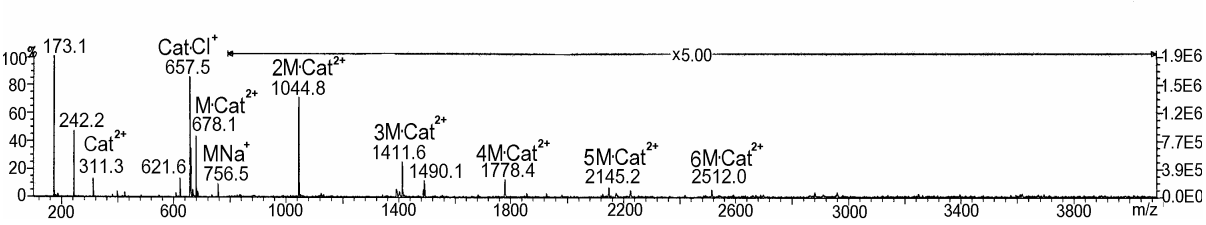

Fig. 2. Positive ion ESI mass spectrum of the drug:phospholipid system with a molar ratio of 1:10.

1:5 molar ratio (Figs. 1 and 2) shows that a drug:phospholipid molar ratio of 1:10 is more suitable than 1:5 for observing drug-phospholipid complexes, because complexes with a larger number of phospholipid molecules in the assemblies could be observed under a ten times molar predominance of phospholipid over decamethoxinum. Consequently, we selected a molar ratio of 1:10 in following experiments.

The registration of doubly-charged ions of the large non-covalent complexes by the ESI technique testifies the high stability of the drug:phospholipid complexes that are preserved upon their transfer from the solution to the gas phase. It is worth mentioning that the existence of non-covalent interactions between decamethoxonium and phospholipid molecules in solution was demonstrated in our previous study by differential scanning calorimetry [11]. The mass spectrometric detection of large molecular assemblies of drug and phospholipid molecules in the present study demonstrates that the ESI technique, which is based on the ability to transfer non-covalent solution-phase assemblies intact into the gas phase, is a suitable technique to study non-covalent interactions between a drug and phospholipid molecules. The validity of this strategy has been supported in numerous studies, especially for experiments on protein-protein and protein-ligand interactions [12-16]. The results obtained in the present study strongly support this approach because the gas phase formation of multicomponent complexes is unlikely under ESI conditions where ions are influenced by the accelerating potential and neutral molecules are removed by the pumping system of the mass spectrometer.

Effect of the cone voltage on ESI mass spectra of the drug-phospolipid system

The conditions of a mass spectrometric experiment significantly affect the appearance of ESI mass spectra. One of the crucial factors that determine the appearance of ESI mass spectra is the potential between the nozzle and skimmer lenses (cone voltage, CV) in the ion source [17-19]. Hence, the effect of the CV on the appearance of ESI mass spectra of the drug-phospholipid system was examined. The CV was varied from 50 to 200 V in steps of 25 V (Figs. 3a-g). Analysis of these spectra reveals that the CV affects both the pattern of the non-covalent complex peaks and the level of fragmentation of the drug and phospholipid molecules. At a CV of 50 V (Fig. 3a), drug-phospholipid complexes nM·Cat^{2+} (n=1-5) are observed, while cationized homocomplexes of phospholipid molecules are absent. With an increase of the CV (75 ñ 125 V), the intensities of peaks of the drug-phospholipid complexes grow (Fig. 3b-d) and heterocomplexes containing a larger number of phospholipid molecules appear. Large nM·Cat^{2+} complexes with n up to nine could be detected at a CV of 125 V, while the abundances of the nM·Na$^+$ cationized homocomplexes of phospholipid molecules increase too. In the interval of

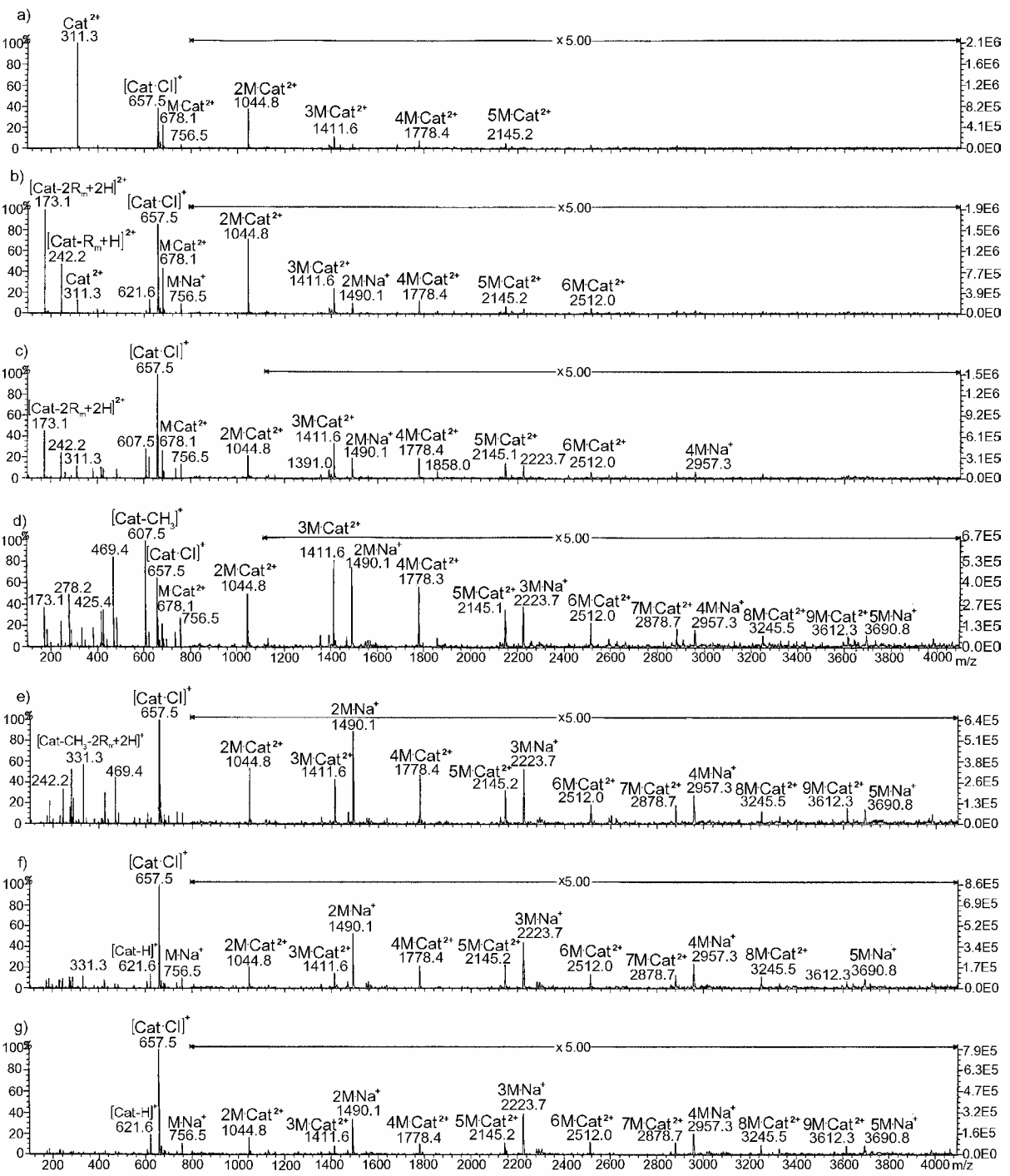

Fig. 3. Positive ion ESI mass spectra of the drug-phospholipid system at different cone voltage values: (a) 50 V, (b) 75 V, (c) 100 V, (d) 125 V, (e) 150 V, (f) 175 V, and (g) 200 V.

the CV from 50 to 150 V, a redistribution of the relative intensities of the drug-phospholipid complex peaks in comparison with the phospholipid homocomplexes is revealed: while at a CV of 75 V the ion intensity ratio $[2M{\cdot}Na^+]/[\ 2M{\cdot}Cat^{2+}]$ is about 0.125, it is about 1.6 at a CV of 150 V. Upon an increase of the CV from 150 to 200V, the relative intensities of the complexes containing decamethoxinum decrease and the tendency of homocomplexes of phospholipid molecules to dominate over heterocomplexes is preserved (Figs. 3e-g). Based on these experimental results, the optimal CV interval for registration of drug-phospholipid non-covalent complexes was determined to be in the range of 100 ñ 125 V: in this range, we could observe complexes with a maximal number of up to nine phospholipid molecules and the relative abundances (RA) of all these complexes were maximal too (Fig. 3d).

The fragmentation behavior of pure decamethoxinum at different CV values (which is described below) shows that the degree of fragmentation of the bisquaternary ammonium salt has a bell distribution that is dependent on the nozzle-skimmer potential with a maximum at a CV of 150 V and which approaches zero at low (0 ñ 50 V) and high (200 ñ 225) CV values.

At the lowest CV (50 V), the doubly-charged Cat^{2+} ion (m/z 311.3; RA=100%) and an abundant singly-charged complex of the dication with the counter ion $Cl^{ñ}$, $Cat^{2+}\cdot Cl^{ñ}$ (m/z 657.5), are detected in the spectrum (Fig. 3a). In our previous study, we established that there are three main fragmentation pathways for decamethoxinum: dequaternization via dealkylation of one of the quaternary groups, loss of the methyl ring substituents R_m and charge separation. At a CV of 75 V, the characteristic fragment ions of the decamethoxinum dication appear (Fig. 3b): decomposition of the molecular dication Cat^{2+} through loss of one or two methyl ring substituents occurs and the resulting fragment ions at m/z 242.2 and m/z 173.2 are abundant in the spectrum:

$$Cat^{2+} \rightarrow \underset{m/z\ 242.2}{[Cat\ ñ\ R_m + H]^{2+}} + (R_m\ ñ\ H) \quad (1)$$

$$\rightarrow \underset{m/z\ 173.2}{[Cat\ ñ\ 2R_m + 2H]^{2+}} + 2(R_m\ ñ\ H) \quad (2)$$

The fragment ion of $Cat^{2+}\cdot Cl^{ñ}$ (m/z 657.5) at m/z 621.6 formed by loss of a molecule of HCl is also seen in the spectrum:

$$Cat^{2+}\cdot Cl^{ñ} \rightarrow \underset{m/z\ 621.6}{[Cat\ ñ\ H]^{+}} + HCl \quad (3)$$

Analysis of the ESI mass spectrum obtained at a CV of 100 V (Fig. 3c) shows the appearance of a fragment ion formed through another pathway, dequaternization, namely, the ion $[Cat\ ñ\ CH_3]^+$ (m/z 607.5):

$$Cat^{2+}\cdot Cl^{ñ} \rightarrow \underset{m/z\ 607.5}{[Cat\ ñ\ CH_3]^{+}} + CH_3Cl \quad (4)$$

It is noted that the most abundant ion in this spectrum is still the quasimolecular ion $Cat^{2+}\cdot Cl^{ñ}$ (m/z 657.5).

At a CV of 125 V (Fig. 3d), the fragment ions of decamethoxinum become dominant: the most abundant ion is $[Cat\ ñ\ CH_3]^+$ (m/z 607.5; RA=100%). Other abundant fragment ions are also present at m/z 469.4 (RA=85%) and m/z 425.4 (RA=35%), while the quasimolecular ion $Cat^{2+}\cdot Cl^{ñ}$ (m/z 657.5) has a RA of 65%.

At a CV of 150 V (Fig. 3e), the decamethoxinum ion $Cat^{2+}\cdot Cl^{ñ}$ (m/z 657.5; RA=100%) is again the base peak and ions at m/z 621.6 $[Cat\ ñ\ H]^+$, m/z 607.5 $[Cat\ ñ\ CH_3]^+$, m/z 469.4 $[Cat\ ñ\ CH_3\ ñ\ R_m + H]^+$, m/z 425.4 $[Cat\ ñ\ R_1]^+$, m/z 242.2 $[Cat^{2+}ñ\ R_m + H]^{2+}$, and m/z 331.3 are observed in the spectrum. The new abundant fragment ion at m/z 331.3 can be characterized as a ìthird orderì fragment of the intact decamethoxinum dication and can be explained through a two step fragmentation process of the $[Cat\ ñ\ CH_3]^+$ ion:

$$[Cat\ ñ\ CH_3]^+ \rightarrow [Cat\ ñ\ CH_3\ ñ\ R_m + H]^+ + (R_m\ ñ\ H) \rightarrow \underset{m/z\ 331.3}{[Cat\ ñ\ CH_3\ ñ\ 2R_m + 2H]^+} + 2(R_m\ ñ\ H) \quad (5)$$

In the spectrum obtained at a CV of 175 V, the abundances of the decamethoxinum fragment ions become weaker (Fig. 3f), and, at a CV of 200 V, the fragment ions almost disappear (Fig. 1g), while the intact $Cat^{2+}\cdot Cl^{ñ}$ complex (m/z 657.5) is the base peak.

The fragmentation behavior of phospholipid molecules at different CV values is as follows. In the spectra obtained at a CV of 50 V and 75 V, only a weak molecular species of the sodiated phospholipid molecule $M\cdot Na^+$ (m/z 756.5; RA about 5%) is noted and no fragment ions or phospholipid complexes are observed (Figs. 3a,b). At a CV of 100 V (Fig. 3c), the phospholipid ions $M\cdot H^+$ (m/z 734.6), $M\cdot Na^+$ (m/z 756.5), the phosphocholine head group-containing fragment ion $[N(CH_3)_3ñ(CH_2)_2ñOñP(O)_2OH]^+$ (m/z 184) (diagnostic of this class of phospholipids [20, 21]), and ions of phospholipid complexes $nM\cdot Na^+$(n=2-4) appear. In the spectrum obtained at a CV of 125 V, the $M\cdot Na^+$ and $[N(CH_3)_3ñ(CH_2)_2ñOñP(O)_2OH]^+$ ions have relative abundances comparable to those seen in the spectrum obtained at a CV of 100 V, while ions of the phospholipid complexes $nM\cdot Na^+$(n=2-5) increase in abundance. At a CV of 150 V (Fig. 3e), the molecular and fragment ions of the phospholipid decrease in comparison with those obtained at a CV of 125 V, but the ions corresponding to sodiated phospholipid complexes still have a significant relative abundance. At the highest CV values of 175 and 200 V, the fragment ion of the phospholipid at m/z 184 virtually disappears and only ions due to sodiated phospholipid and its assemblies with the drug are seen.

The above experiments in which the CV values were varied allow us to establish optimal ESI-MS conditions in the range between 100 and 125 V for registration of decamethoxinum-phospholipid non-covalent complexes. These conditions can be recommended for screening of new potential antimicrobial agents of the bisquaternary ammonium salt class. The intensity of the non-covalent complex with phospholipid molecules reflects the activity of the latter antimicrobial agents and as such allows to select potential active members of this class of drugs.

CID mass spectra of drug-phospholipids complexes

To obtain information on the structure and stability of drug-phospholipid non-covalent complexes, collision-induced dissociation (CID) experiments were performed using He or Xe as collision gas. Figures 4 a,b show the CID spectra of the M·Cat^{2+} ion (m/z 678.1) obtained by using He and Xe, respectively, as collision gas. The high-energy CID spectrum registered with Xe is characterized by product ions that are about five times more abundant than those seen in the low-energy CID experiment with He, indicating that CID processes induced by Xe are more efficient, consistent with the higher energy imparted to the M·Cat^{2+} ion during the collision process. Consequently, we have performed CID with Xe as collision gas in subsequent experiments.

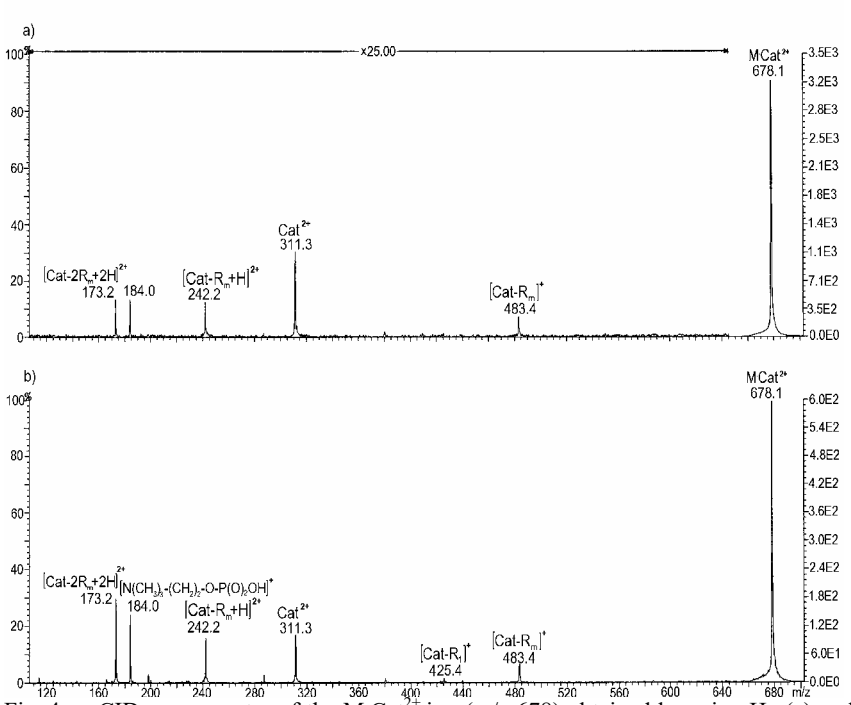

Fig. 4. CID mass spectra of the M.Cat^{2+} ion (m/z 678) obtained by using He (a) and Xe (b) as collision gas.

The CID spectra of complexes of decamethoxinum containing 1 to 6 phospholipid molecules are presented in Figures 5a-f. It is noted that product ions of intact decamethoxinum or phospholipid in the CID spectra correspond to fragment ions previously discussed for the ESI mass spectra of the system (Fig. 3a-g), suggesting that CID pathways are similar to the general ESI fragmentation pathways. In the CID spectrum of the M·Cat^{2+} ion (Fig. 5a), the product ions of decamethoxinum Cat^{2+} (m/z 311.3), [Cat^{2+}ñR$_m$+H]$^{2+}$ (m/z 242.2), [Cat^{2+}ñ2R$_m$+2H]$^{2+}$ (m/z 173.2), m/z 483.4 and the phosphocholine head group-containing product ion of phospholipid [N(CH$_3$)$_3$ ñ (CH$_2$)$_2$ñOñP(O)$_2$OH]$^+$ (m/z 184) are seen. It is worth noting that the CID spectrum of the 2M·Cat^{2+} precursor ion (m/z 1044.8) (Fig. 5b), contains, in addition to product ions due to dissociation of decamethoxinum and phospholipid, product ions corresponding to the paired complex M·Cat^{2+} and the MH$^+$ ion, while the relative abundances of the product ions of the Cat^{2+} ion are maximal in comparison with those observed in the CID spectra examined for complexes containing a higher number of phospholipid molecules. The CID spectra obtained for 3M·Cat^{2+} (m/z 1411.6), 4M·Cat^{2+} (m/z 1778.4), 5M·Cat^{2+} (m/z 2145.2) and 6M·Cat^{2+} (m/z 2512.0) reveal product ions of decamethoxinum and phospholipid, which were described above, as well as product ions of drug-phospholipid complexes of a lower order (Fig. 5c-f). For example, the CID spectrum of the 3M·Cat^{2+} ion contains product ions corresponding to the complexes M·Cat^{2+} and 2M·Cat^{2+} (Fig. 5c). The CID mass spectral data thus allow us to observe the stepwise decomposition process of drug-phospholipid assemblies that can be useful in the structural investigation of unknown complexes and in testing new active membranothropic compounds.

It should be mentioned that the absolute intensity (digital counts) of the CID spectra decreased from $6.0 \cdot 10^2$ for the spectra of the paired complex M·Cat^{2+} to $6.9 \cdot 10^0$ for the 6M·Cat^{2+} complex. However, analysis of the CID spectra of 3M·Cat^{2+}, 4M·Cat^{2+}, 5M·Cat^{2+} and 6M·Cat^{2+} shows that the 2M·Cat^{2+} product ion (m/z 1044.8) has a higher relative abundance in comparison with other product complexes (Fig. 5 c-f), which suggests that the stability of the 2M·Cat^{2+} complex is higher than that of complexes of other stoichiometry.

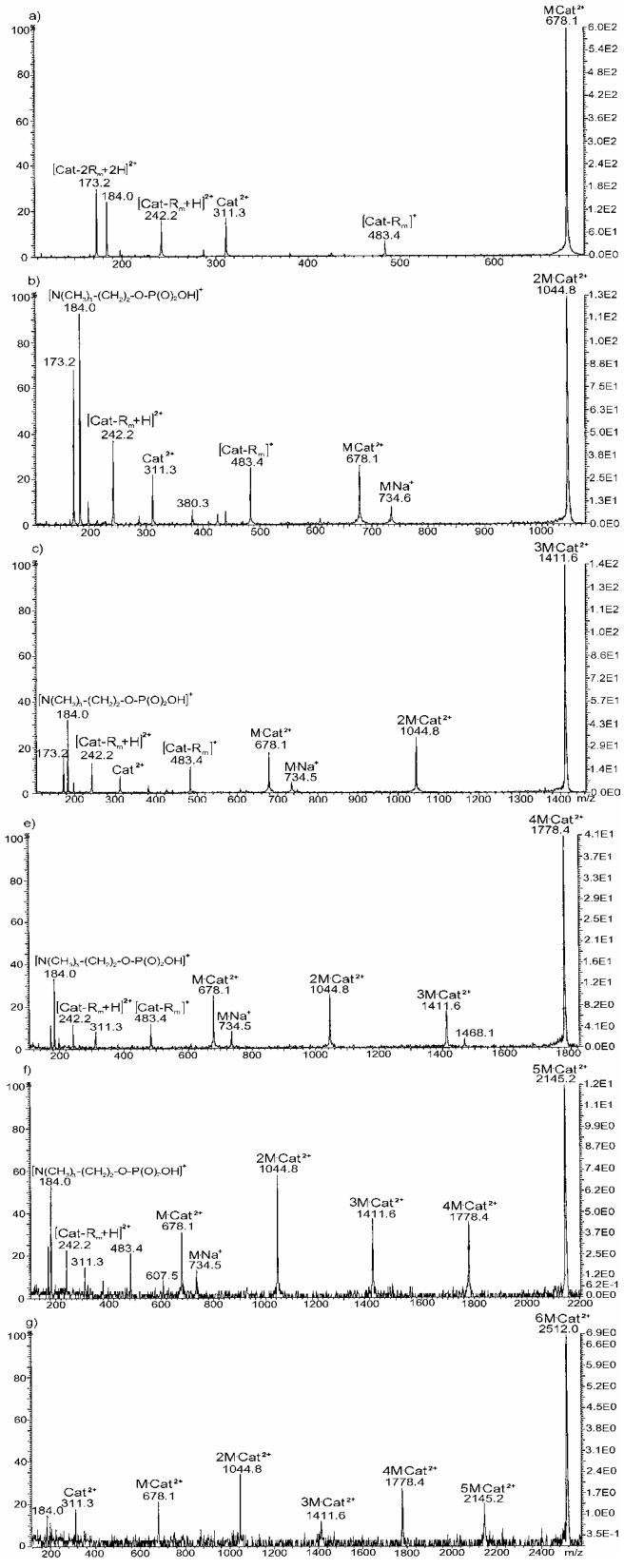

Fig. 5. CID spectra of nM·Cat^{2+} (n=1-6) complexes.

This observation is consistent with previously reported quantum-chemical data obtained for the interaction of the decamethoxinum dication with phospholipid molecules by the semi-empirical AM1 method [22]. These theoretical calculations showed a favourable steric and electronic compliance of the decamethoxinum dication and the polar head groups of two dipalmitoylphosphatidylcholine molecules.

Furthermore, the extent of fragmentation of the intact dication of decamethoxinum Cat^{2+} upon collision activation of drug-phospholipid complexes containing a different number of phospholipids molecules was examined. The CID spectra (Figs. 5b-f) show that the relative abundances of the product ions at m/z 173.2, 242.2 and 483.4 decrease in comparison with that of the Cat^{2+} ion with an increase of the number of phospholipid molecules from 2 to 6 in the nM·Cat^{2+} non-covalent complexes. The product ions of the intact dication are absent from the CID spectra of the 6M·Cat^{2+} complex (Fig. 5f), which suggests that the dication is located inside the complex with the 6 phospholipid molecules and that its fragmentation is hampered. This behaviour suggests that the structure of this complex is similar to that of a micelle consisting of the surface active phospholipid molecules with the dication inside.

CONCLUSIONS

Non-covalent complexes of bisquaternary ammonium compound decamethoxinum with dipalmitoylphosphatidylcholine molecule assemblies (up to 9 molecules), which model drug-phospholipid interaction in a biological membrane, were registered by ESI mass spectrometry. The conditions optimal for the detection of these complexes were established. The optimal value of the cone voltage for detection of the drug-phospholipid non-covalent complexes was between 100 and 125 V; in this range, complexes with a maximal number of up to nine phospholipid molecules and the highest relative abundances were observed. The decomposition of nM·Cat^{2+} drug-phospholipid complexes (n=1-6) was examined by collision-induced dissociation with xenon as collision gas. This CID study indicated that the complex of decamethoxinum with two phospholipid molecules has the highest relative stability.

The present investigation demonstrates the potential of ESI mass spectrometry alone or in combination with CID to study complexes of a bisquaternary ammonium compound with a phospholipid molecule or multicomponent phospholipid assemblies. Since the non-covalent interaction of bisquaternary antimicrobial agents with membrane phospholipids underlies the molecular

mechanism of their antimicrobial action, the ESI-MS methodology developed in the present study can be proposed as a sensitive and robust approach for the fast screening of bisquaternary ammonium compounds with potential antimicrobial activity.

Acknowledgements

We acknowledge the financial support by the special research fund of the University of Antwerp (UA-BOF) through a concerted research action (grant no. 99/3/34) and a visiting postdoctoral fellowship to V. Pashynska.

REFERENCES

1. Alberts B., Lewis J., Raff M., Roberts K., Walter P. Molecular Biology in the Cell 4th. ed. Garland Science Taylor & Francis Group: New York. 2002, 1463 p.
2. ThorsteinssonT., Masson M., Kristinsson K.G., Hjalmarsdottir M.A., Hilmarsson H., Loftsson T.// J. Med. Chem. 2003 . V.46. N 19. P. 4173-4181.
3. Vievsky A.N. Mechanisms of Biological Action of Cationic Surface-Active Compounds (Russ.). Moscow Univ.: Moscow. 1990. 250 p.
4. Pavlikova-Moricka M., Lacko I., Devinsky F., Masarova L., Milynarcik D. // Folia Microbiol. (Praha). 1994. 39(3): 176-180.
5. Majtan V., Majtanova L. Microbios. 1996. V. 87. N 351. P. 89-96.
6. Ancelin M.L., Calas M., Bonhoure A., Herbute S., Vial H.J. Antimicrob. Agents Chemother. 2003. V. 47. N. 8. P. 2598-2605.
7. Calas, M., Ancelin, M.L., Cordina, G., Portefaix, P., Piquet, G., Vidal-Sailhan, V., Vial, H. Antimalarial activity of compounds interfering with Plasmodium falciparum phospholipid metabolism: comparison between mono- and bisquaternary ammonium salts. J. Med. Chem. 2000 Feb 10; 43(3): 505-516.
8. Suizdak G. Mass Spectrometry for Biotechnology. Academic Press: San Diego. 1996. 162 p.
9. Millar A.L, Jackson N.A.C., Dalton H., Jennings K.R., Levi M., Wahren B., Dimmock N.J. // Eur. J. Biochem. 1998. V. 258. P. 164 - 169.
10. Pashynska V.A., Kosevich M.V., Van den Heuvel H., Claeys M. // J. Am. Soc. Mass Spectrom. 2004 V.15. P. 1181-1190.
11. Pashynskaya V.A., Kosevich M.V., Gomory A., Vashchenko O.V., Lisetski L.N. // Rapid Comm. Mass Spectrom. 2002. V. 16. P. 1706-1713.
12. Cole R.B. Electrospray Ionization Mass Spectrometry. Fundamentals, Instrumentation and Applications. John Wiley and Sons: New York. 1997. 578 p.
13. Przybylski M., Glocker M.O. // Angew. Chem. Int. Ed. 1996. V. 108. P. 878-899.
14. Veenstra T.D. // Biophys. Chem. 1999. V. 79. P. 63-79.
15. Skribanek Z., Balaspiri L., M·k M.// J. Mass Spectrom. 2001. V. 36. P. 1226-1229.
16. Loo J.A. // Mass Spectrom. Rev. 1997. V. 16. P. 1-23.
17. Collette C., Drahos L., De Pauw E., Vekey K. // Rapid Comm. Mass Spectrom. 1998. V. 12. P. 1673-1678.
18. Butcher C.P.G., Dyson P.J., Johnson B.F.G., Langridge-Smith P.R.R., Mclndoe J.S., Whyte C. // Rapid Comm. Mass Spectrom. 2002. V. 16. P. 1595-1598.
19. Milman B.L. // Rapid Comm. Mass Spectrom. 2003. V. 17. P. 1344-1349.
20. Ekroos K., Chernushevich I.V., Simons K., Shevchenko A. // Anal. Chem. 2002. V. 74. P. 941-949.
21. Ekroos K., Ejsing C.S., Bahr U., Karas M., Simons K., Shevchenko A. // J. Lipid Research. 2003. V. 44. P. 2181-2192.
22. Pashynska V., Kosevich M., Gomory A.,Vekey K., Korzovskaya O., Lisetsky L., Blagoy Yu. // *Visnyk V.N. Karazin Kharkiv National University N 450, Biophys. Bullet.* 1999. V. 2. P. 59-62.

ВИВЧЕННЯ ФОРМУВАННЯ НЕКОВАЛЕНТНИХ КОМПЛЕКСІВ МІЖ БІСЧЕТВЕРТИННИМ АМОНІЙОВИМ АНТИМІКРОБНИМ АГЕНТОМ ДЕКАМЕТОКСИНОМ ТА МЕМБРАННИМИ ФОСФОЛІПІДАМИ ЗА ДОПОМОГОЮ МЕТОДУ МАС-СПЕКТРОМЕТРІЇ З ІОНІЗАЦІЄЮ ЕЛЕКТРОСПРЕЄМ ТА ДИСОЦІАЦІЄЮ ІНДУКОВАНОЮ ЗІТКНЕННЯМИ

В.А. Пашинська[1,2*], М.В. Косевич[1], Х. Ван ден Хювел[2], Ф. Кекенс [2], М. Клаєс[2]

[1] *Фізико-технічний інститут низьких температур ім. Б.І. Вєркіна НАН України, пр. Леніна 47, 61103 Харків*
[2] *University of Antwerp, Department of Pharmaceutical Sciences, Universiteitsplein, 1, B-2610 Antwerp, Belgium*

В роботі методами мас-спектрометрії з іонізацією електроспреєм (ІЕС) та тандемної мас-спектрометрії з дисоціацією індукованою зіткненнями (ДІЗ) вивчено формування нековалентних комплексів між мембранним фосфоліпідом діпальмітоілфосфатиділхоліном та бісчетвертинним амонійовим антимікробним агентом декаметоксином, що звíязано з молекулярним механізмом біологічної активності цього лікарського засобу. Було зареєстровано стабільні двозаряджені комплекси дікатіону декаметоксину з молекулами фосфоліпіду (до девíяти молекул), що моделюють взаємодію препарату з фосфоліпідами у біологічних мембранах. Для вивчення структури та стабільності декаметоксин-фосфоліпідних комплексів отримано їх ДІЗ мас-спектри. ІЕС мас-спектрометрична методика, що була використана та оптимізована в роботі, пропонується для швидкого скринінгу бісчетвертинних амонійових сполук з потенційною антимікробною активністю.

КЛЮЧОВІ СЛОВА: нековалентні комплекси, бісчетвертинні амонійові сполуки, декаметоксин, діпальмітоілфосфатиділхолін, мас-спектрометрія з іонізацією електроспреєм, дисоціація індукована зіткненнями.

ELSEVIER

Journal of Molecular Structure: THEOCHEM 815 (2007) 55–62

THEO CHEM

www.elsevier.com/locate/theochem

Noncovalent complexes of tetramethylammonium with chlorine anion and 2,5-dihydroxybenzoic acid as models of the interaction of quaternary ammonium biologically active compounds with their molecular targets: A theoretical study

Vlada Pashynska [a,*], Marina Kosevich [a], Stepan Stepanian [a], Ludwik Adamowicz [b]

[a] *B.Verkin Institute for Low Temperature Physics and Engineering of the National Academy of Sciences of Ukraine, Lenin Ave., 47, 61103 Kharkiv, Ukraine*
[b] *Department of Chemistry, University of Arizona, Tucson, AZ 85721, USA*

Received 25 December 2006; received in revised form 6 March 2007; accepted 16 March 2007
Available online 25 March 2007

Abstract

A theoretical study of the interaction of tetramethylammonium cation with chlorine anion and 2,5-dihydroxybenzoic acid modeling a carboxylic group and an aromatic ring of side radicals of proteins has been performed by the DFT/B3LYP/6-31++G** and MP2/6-31++G** theoretical methods. To evaluate how the solvation affects the interaction, the Polarizable Continuum Models method has been employed. The calculated interaction energies of the noncovalent complexes were compared with the experimental data describing the stability of some noncovalent complexes of a dication of bisquaternary ammonium salt decamethoximun with Cl^- and 2,5-dihydroxybenzoic acid obtained with the mass-spectrometric technique.

Keywords: Tetramethylammonium; Bisquaternary ammonium agent decamethoxinum; Chlorine anion; 2,5-Dihydroxybenzoic acid; Noncovalent complexes; *Ab initio*; DFT/B3LYP/6-31++G**; MP2/6-31++G**; Mass spectrometry

1. Introduction

Study of molecular mechanisms of the action of biologically active quaternary ammonium compounds represents one of the topical tasks of molecular biology and medicine. Identification of general features in the molecular recognition of proteins and/or other molecular targets by quaternary ammonium groups can contribute to a better understanding of the mechanisms of a number of processes occurring in the human organism and may lead to new drugs design. The interaction of antimicrobial quaternary ammonium compounds with bacterial membrane structures is considered as the most important effect related to their biological functions [1]. In view of the continuous search for new effective bisquaternary ammonium antimicrobial agents, the modeling of interactions of the active groups of these compounds with possible molecular targets in biological systems attracts considerable interest. A process of this kind was modeled in our experimental studies [2–4] on the bisquaternary ammonium agent decamethoxinum (Scheme 1) developed in Ukraine. Decamethoxinum possesses antimicrobial and fungicidal properties [1,5], and it is a basic constituent in a number of medicinal products being produced and marketed in Ukraine. These products include "Septefrilum" for sore throat relief, "Aurisanum"[R] and "Oftadecum"[R] for curing eye and ear inflammations, and some others. Decamethoxinum is a membranothropic agent [2], and a believable molecular mechanism of its action involves affecting the lipid and the protein constituents of the membranes of bacterial cells. In our previous works, the interaction of decamethoxinum

* Corresponding author. Tel.: +38 057 340 4906; fax: +38 057 340 4905.
E-mail address: vlada@vl.kharkov.ua (V. Pashynska).

0166-1280/$ - see front matter © 2007 Elsevier B.V. All rights reserved.
doi:10.1016/j.theochem.2007.03.019

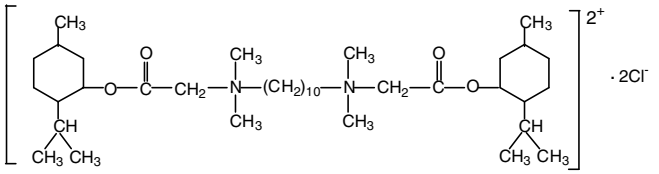

Scheme 1. Structure of bisquaternary ammonium salt decamethoxinum, $C_{38}H_{74}Cl_2N_2O_4$.

with phospholipids was investigated using soft ionization mass spectrometry techniques, the differential scanning calorimety, and quantum chemical calculations. The formation of stable supramolecular complexes of the drug with phospholipids was demonstrated in those works [2,3]. These complexes affect the liquid-crystalline state of the membrane lipid matrix of microorganisms that can result in the disturbance of some membrane processes. It was also suggested that the drug binding to some membrane proteins engaged in the breathing chain of bacteria, in particular some Cytochromes, disturbs their functioning and facilitates the drug's antimicrobial action [6]. Noncovalent binding of the quaternary compounds to their molecular targets in the membrane can occur by different means depending on the chemical structure of the active groups of the membrane proteins. These include ionic interactions, hydrogen bonding, Van der Waals, or cation–π interactions.

Considering the interaction of quaternary compounds with proteins as one of the most probable molecular mechanisms of their action, a model study of decamethoxinum in 2,5-dihydroxybenzoic acid (DHB) (Scheme 2) matrix has been performed by the matrix-assisted laser desorption/ionization (MALDI) mass spectrometry method [4]. In the mass spectra obtained this way, the most intensive peak was that of a noncovalent complex of decamethoxinum with DHB. Furthermore, it was revealed that the abundance of the complex of decamethoxinum dication with DHB was much higher than that of its complex with the Cl^- counterion.

In these experiments, DHB was considered as a model compound whose components mimic two types of recognition sites present in proteins, namely the carboxylic group or the carboxylate anion in the ionic deprotonated state the group and the aromatic ring, which can provide a cation–π interaction. In amino acids, the carboxylic group is a part of side chains of aspartic and glutamic acids, and aromatic residues are parts of tryptophan, tyrosine, phenylalanine and histidine. Salt bridges in the form of ammonium-carboxylate salts are believed to stabilize the proteins [7].

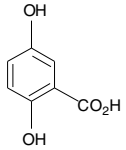

Scheme 2. Structure of 2,5-dihydroxybenzoic acid.

As for the drugs, it is known that quaternary ammonium groups participate in the molecular recognition processes involving these compounds. They serve as inorganic and organic anion receptors [8–10] and thus can actively interact with the carboxylate anion formed in the deprotonation process of the DHB molecule, which can mimic an electronegative site located on the protein surface. The interaction of the quaternary group with the neutral but polarized carbonyl moiety, C=O, can also be rather strong, as it was shown in the recent theoretical study of the properties of the $R_3{-}N^{(+)}{-}H_2C{-}H{\cdots}O{=}C{-}$ hydrogen bond [11]. It should be of interest that the results of our earlier quantum chemical calculations on the decamethoxinum dication [12] have shown that the intramolecular interactions of carbonyl oxygens of the side radicals with alkylammonium groups (see Scheme 1) contribute to the stabilization of the dication. On the other hand, the role of the cation–π bonding (that is, the interaction with the conjugated π-system of the aromatic moieties) presently attracts considerable attention in structural biology research [13–19]. This type of interactions involving amino acids side chains appeared to be quite common in the protein folding [13,16,17], in binding of some ligands to proteins, and in drug-receptor recognition [14,15]. For example, it was shown that the domains of bonding of quaternary ammonium agents in some proteins incorporate tryptophan and tyrosine amino acids that provide cation–π interactions [19,20]. Thus, the interaction of quaternary ammonium groups of decamethoxinum with the DHB aromatic ring involving a cation–π bonding is also possible. Realizing that DHB can be considered just as approximate model of some side radicals of amino acids we focused present investigation on the evaluation of the strength of the drug attachment to the carboxylic group or a π-system of DHB, since it was shown that these two types of interactions can affect each other if simultaneously present in the system [7].

With the above discussion in mind, we can describe the main purpose of the present work as the modeling of the noncovalent interactions of quaternary ammonium compounds with their potential molecular targets in living systems. Since the *ab initio* calculations of larger intact biologically active molecules such as decamethoxinum are still beyond the reach of present-day computers, we have selected the noncovalent complexes of the tetramethylammonium cation (TMA) with a chlorine anion and DHB in its neutral and anionic forms as the objects of our model investigations. TMA as a model of the active group of quaternary ammonium compounds, Cl^- as a counterion in quaternary salts, and DHB as a compound modeling carboxylic and aromatic groups of side radicals of membrane proteins are the building blocks of the complexes, which were registered under MALDI mass-spectrometric experiments [4].

To justify the selection of the TMA as an adequate model compound one needs to verify the TMA–DHB complex can be formed in an experiment. A TMA–DHB mixture in glycerol matrix has been studied by the fast atom bombardment (FAB) mass-spectrometric technique. A complex of a single

TMA cation with chlorine or DHB anion is neutral and cannot be registered in the mass spectrum. However, peaks of charged complexes of two TMA cations with a single anion, $[2TMA:Cl]^+$ and $[2TMA:(DHB–H)]^+$, were recorded in the FAB mass spectra. The abundance of the noncovalent TMA complex with the organic anion was several times higher than the complex with the inorganic one. The peak of the complex TMA with a neutral DHB molecule was absent in the spectrum. It should be noted that in the living organisms, quaternary salts dissociate and a competition between active groups of molecular targets and the salt counterions of the quaternary ammonium ions plays a significant role in the biological recognition processes involving quaternary ammonium compounds. Thus, model calculation of the TMA ion and its competitive interaction with inorganic and organic counterions is a biophysical problem that needs to be addressed.

Ab initio molecular orbital calculations of the electron distribution in TMA cation and the interaction of the cation with the fluoride anion have been carried out in the work [21]. The Van der Waals surface of the TMA ion was found to be characterized by the "patched" positive charge distribution associated with the methyl groups. Similar positive charge delocalization over the quaternary group was found for decamethoxinum in our *ab initio* study of electron and structural features of the dication [22]. As for the TMA interaction with a fluoride anion, the lowest-energy geometry was found to be one in which the anion approaches the "face" of the tetrahedral cation (between three methyl groups opposite to a C—N bond direction) [21]. In this geometry of the complex, the anion is fairly close to all three methyl groups and their associated "patches" of the positive charge and it can approach relatively close the central nitrogen.

The objectives of our model study on the noncovalent complexes of TMA cation with a chlorine anion and with DHB that have been addressed in the calculations are:

(1) to obtain the equilibrium geometries of the model noncovalent complexes;
(2) to determine the contributions of different interaction effects to the complex stabilization; and
(3) to explain the results of the MALDI mass-spectrometric study of decamethoxinum–DHB complexes [4].

2. Methods of investigation

A theoretical study for noncovalent complexes $TMA^+:Cl^-$, $TMA^+:DHB^0$ and $TMA^+:[DHB–H]^-$ was performed. For the TMA cation complex with a chlorine anion a single configuration of the complex exists while for the TMA cation complexes with DHB and deprotonated DHB several different configurations of the complexes were selected as starting. In these starting configurations TMA cation interacts with different oxygen atoms of DHB or with the π-system of the DHB aromatic ring. The geometries of the selected starting structures were first fully optimized at the DFT level of theory. The calculations converged to the only structure of the $TMA^+:[DHB–H]^-$ complex while for the $TMA^+:DHB^0$ complex we found two possible complex configurations. The DFT calculations were carried out with the three-parameter density functional usually abbreviated as B3LYP, which includes Becke's gradient exchange correction [23], the Lee, Yang, Parr correlation functional [24], and the Vosko, Wilk, and Nusair correlation functional [25]. Next, harmonic frequency calculations were carried out for the equilibrium DFT geometries, and the frequencies were used to determine the zero-point vibrational energy (ZPVE) corrections. Additionally, single point energy calculations were performed at the MP2 level of theory for the DFT geometries. In the calculations we used the standard 6-31++G** basis set. To evaluate the ability of the DFT method to predict correct equilibrium geometries of the studied systems we also performed geometry optimization of the $TMA^+:[DHB–H]^-$ complex at the MP2 level of theory. To account for the BSSE influence on the resulting geometry we performed BSSE-free optimization of the $TMA^+:[DHB–H]^-$ complex at the MP2/6-31++G** level of theory, i.e., with accounting for the BSSE correction energy during optimization.

To account for the solvation effects, we have employed the PCM (Polarizable Continuum Models (PCM)) method [26–29]. All interaction-energy calculations were performed with taking into account the BSSE correction using the standard counterpoise correction method [30]. All calculations were performed using the Gaussian 03 quantum chemistry package [31].

3. Results and discussion

3.1. Calculation of the TMA^+ complex with the chlorine counterion in the vacuum

At the first stage of the investigation we calculated the structure of the $TMA^+:Cl^-$ complex, which is our simplest model of the active group of an alkylammonium chloride salt. The optimized geometry of the complex in the vacuum conditions is shown in Fig. 1. The interaction energies in this complex calculated using different methods are shown in Table 1 and comprise the values −385.33 and −378.86 kJ/mol calculated by the DFT/B3LYP/6-31++G** and MP2/6-31++G** methods, respectively.

The main structural features of the $TMA^+:Cl^-$ complex obtained in the present calculations appear to be similar to those reported in [21] and discussed in Section 1. Smearing of the positive charge of TMA^+ ion over the hydrogen atoms of the methyl groups creates areas of higher concentration of the positive charge between each three methyl groups (in the middle of the "faces" of the tetrahedron). The Cl^- anion is attracted to one of these areas by a Coulomb force. The attractive interaction is confirmed by the negative value of the interaction energy (Table 1). In the equilibrium geometry of the complex (Fig. 1) the TMA^+

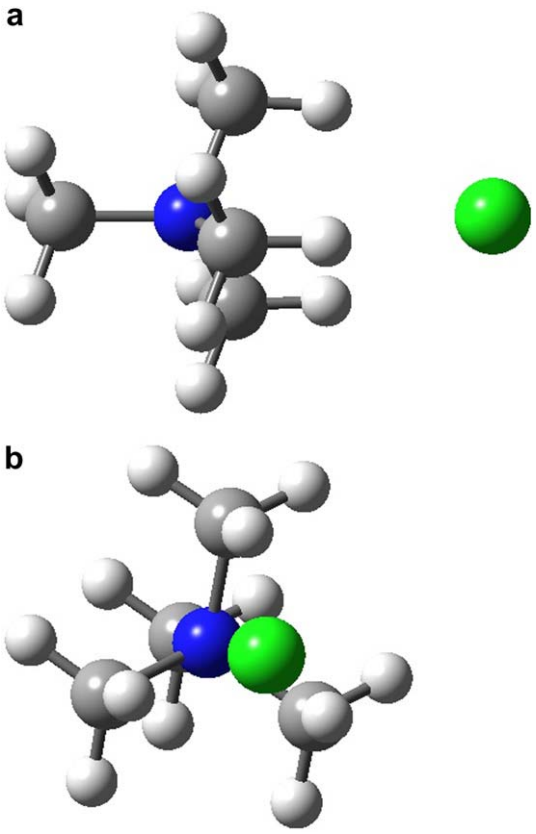

Fig. 1. Optimized geometry of TMA^+:Cl^- noncovalent complex obtained in the DFT/B3LYP/6-31++G** calculations in two projections (a and b).

Table 1
ZPVE and BSSE corrected interaction energies (IE, kJ/mol) in complexes of TMA^+ with Cl^- and DHB (neutral and deprotonated) calculated by different methods in the vacuum approach

Complex	IE (kJ/mol)	
	DFT/B3LYP/6-31++G**	MP2/6-31++G**
TMA^+:Cl^-	−385.33	−378.86
TMA^+:DHB^0	−36.51	−43.61
TMA^+:$[DHB–H]^-$	−349.51	−351.66

cation and the Cl^- anion are in close contact leading to a high stability of the TMA^+:Cl^- complex in the vacuum conditions.

3.2. Modeling of the complexes of TMA^+ with DHB in the vacuum

Two types of complexes of TMA^+ with DHB, which can be formed under the experimental mass spectrometry conditions, were studied theoretically: a complex of TMA^+ with a neutral DHB molecule and a complex of TMA^+ with a deprotonated DHB ($[DHB–H]^-$ anion). In the calculations a number of starting configurations of the two systems were tested. They included those with TMA^+ located in the plane of DHB near the COOH or COO^- groups and above the plane of the DHB ring.

The optimized geometries of the noncovalent complexes, TMA^+:$[DHB–H]^-$ and TMA^+:DHB^0, calculated with the DFT/B3LYP/6-31++G** method are presented in Figs. 2 and 3, respectively. The interaction energies of TMA^+ with a DHB molecule and with a deprotonated DHB are shown in Table 1. It should be noted that the DFT/B3LYP/6-31++G** and MP2/6-31++G** methods predict different interaction energies of the complexes, however the general trends in the calculated stabilities of the complexes obtained by the two methods are similar (Table 1).

As it is shown in Fig. 2, in the most favorable configuration of the complex TMA^+:$[DHB–H]^-$, the TMA^+ cation interacts by its three CH_3 groups with the COO^- group of the $[DHB–H]^-$ ion. In such geometry, the ionic forces play the crucial role in the stabilization of the noncovalent complex because the majority of the negative charge is concentrated at the COO^- group of $[DHB–H]^-$. The ionic nature of the interaction is confirmed by the calculated value of the interaction energy of −385.33 kJ/mol (see Table 1), which corresponds to the values characteristic of Coulomb interaction. The interaction of the cation with the π-system of $[DHB–H]^-$ contributes less to the complex stabilization than the ionic forces. To confirm this, a DFT calculation of the TMA^+:$[DHB–H]^-$ complex was performed starting with a geometry in which TMA^+ was situated directly above the DHB benzyl ring (Fig. 4). In the course of the calculation the TMA^+ cation gradually shifted towards the COO^- group of $[DHB–H]^-$ and the final optimal geometry of the complex was very similar as that shown in Fig. 2. The energy of the complex corresponding to the optimal geometry was −785.1014885 a.u., which is very close to the energy (−785.1030334 a.u.) of the complex obtained in the calculation where, in

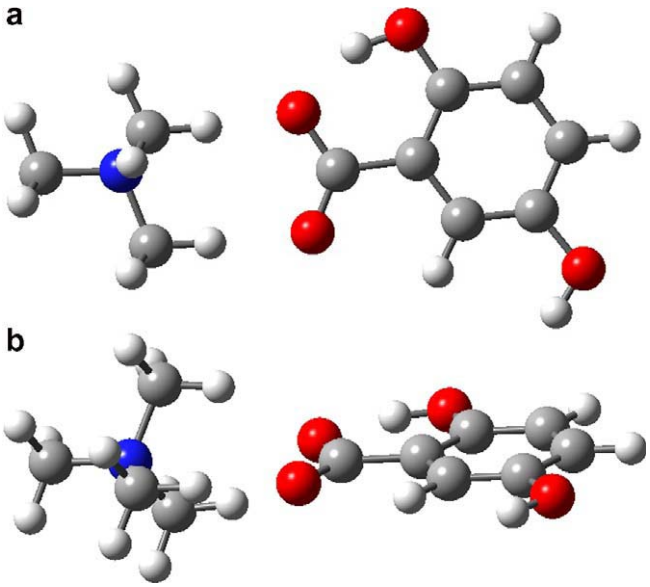

Fig. 2. Optimized geometry of TMA^+:$[DHB-H]^-$ noncovalent complex obtained in the DFT/B3LYP/6-31++G** calculations in two projections (a and b).

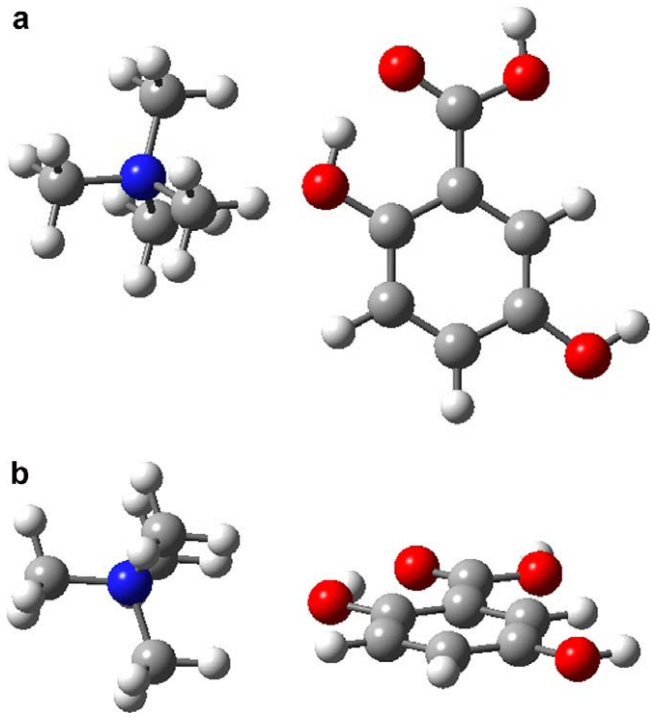

Fig. 3. Optimized geometry of TMA^+:DHB^0 noncovalent complex obtained in the DFT/B3LYP/6-31++G** calculations in two (a and b) projections (geometry 1).

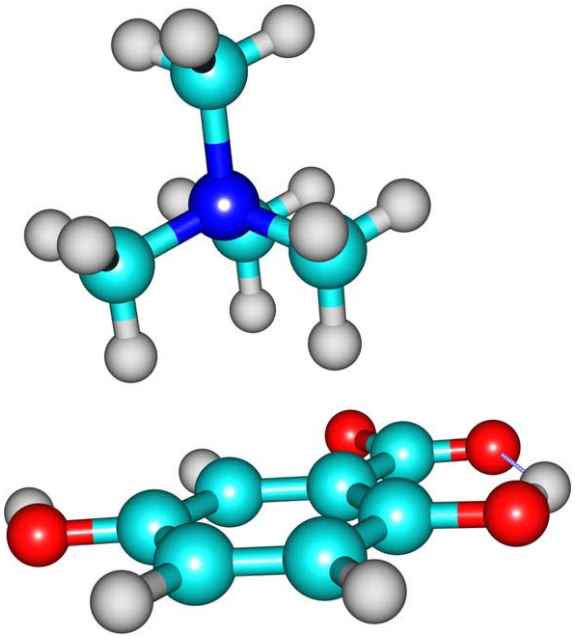

Fig. 4. Starting configuration of TMA^+:[DHB-H]$^-$ complex in which TMA^+ was placed directly above the DHB benzyl ring.

the starting geometry, TMA^+ was situated near the COO^- group in the plane of the [DHB–H]$^-$ anion (Fig. 2). To verify if the DFT method is adequate to calculate the geometries of such complexes, we performed a full geometry optimization of the TMA^+:[DHB–H]$^-$ complex at the MP2 level of theory starting from the structure where TMA^+ was placed directly above the DHB benzyl ring (Fig. 4). Again, optimization converged to the structure where TMA^+ was situated near the COO^- group in the plane of the [DHB–H]$^-$ anion (Fig. 2). The interaction energy of the complex obtained in that calculation was −352.28 kJ/mol. This value is very close to the value of the MP2 interaction energy (−351.66 kJ/mol) of the TMA^+:[DHB–H]$^-$ complex calculated using its DFT geometry. This agreement shows that the DFT method is adequate for calculating the geometries of the complexes studied in this work. One may argue that the neglecting of the BSSE during geometry optimization can affect the resulting geometry. To answer the question we performed BSSE-free optimization of TMA^+:[DHB–H]$^-$ complex at the MP2/6-31++G** level of theory, i.e., with accounting for the BSSE correction energy during optimization starting from the structure shown in Fig. 4. This optimization also converged to the planar configuration of the complex which is almost identical to the structure shown in Fig. 2. Interaction energy found in this calculation (−351.39 kJ/mol) is very close to the energy obtained in the calculation with accounting for the BSSE correction after optimization (−352.28 kJ/mol).

In the optimized geometry of the complex of TMA^+ with a neutral DHB molecule (Fig. 3), TMA^+ is connected with the oxygen of the COH group of DHB through a hydrogen of one of its methyl radicals. The stabilizing force in this case is a weak hydrogen **—C—H···O** bond. The interaction energy calculated with the DFT method is −36.5 kJ/mol (Table 1).

The calculation of the TMA^+:DHB^0 complex initiated with the TMA^+ cation positioned directly above the ring of the DHB molecule (like in Fig. 4) converged to a structure shown in Fig. 5. Here TMA^+ is shifted towards the nearest hydroxyl group of DHB but it is still situated under the plane of the DHB ring. The interaction energy in a complex with such geometry (geometry 2) is −29.83 kJ/mol (calculated by MP2 method). This is much smaller interaction energy than for the complex (geometry 1, Fig. 3) whose structure was obtained starting the geometry optimization with TMA^+ in the plane of the DHB molecule (for that complex the interaction energy is −43.61 kJ/mol). This shows that the TMA^+:DHB^0 complex in geometry 1 is more stable than in geometry 2 in vacuum conditions. In geometry 1, TMA^+ is connected to the DHB molecule with an ionic bond involving the oxygen of the COH group (Fig. 3) and axis of the TMA tetrahedral cation lies in the plane of DHB ring. In the other possible complex configuration (geometry 2), TMA^+ is situated above the DHB ring and the cation–π interaction plays a more significant role (Fig. 5). The results presented here show that the interaction energy of TMA^+ with deprotonated DHB is about ten times higher than the TMA^+ interaction with a neutral DHB molecule. This confirms the difference of the nature of the stabilizing forces in these two different complexes.

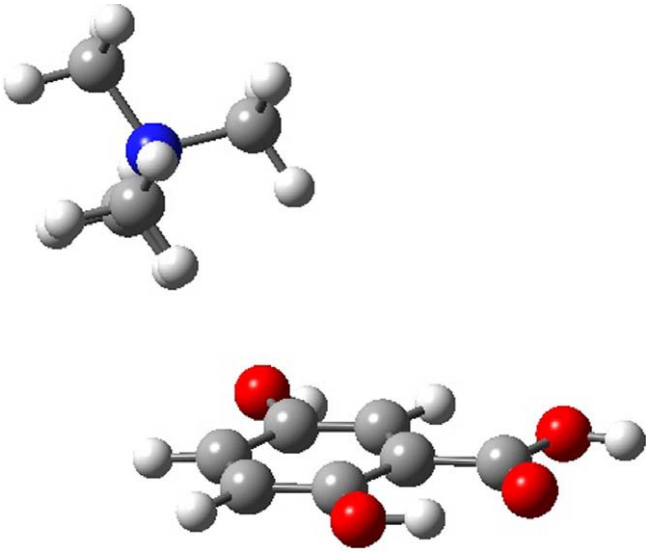

Fig. 5. Optimized geometry of TMA^+:DHB^0 noncovalent complex obtained in the DFT/B3LYP/6-31++G** calculations initiated with the TMA ion located above the DHB ring (geometry 2).

A comparison of the interaction energies of TMA^+ with a neutral DHB molecule and a deprotonated DHB anion shows that the latter is predictably higher (Table 1). In the relation to the molecular recognition of the proteins aromatic side groups by the quaternary ammonium agents, this finding means that the electrostatic interaction with charged groups is, surely, more favorable in the vacuum conditions than other types of noncovalent interactions. However, under certain favorable steric conditions quaternary ammonium groups may get in close contact with neutral aromatic side chains of the protein and the cation–π interaction may become strong.

3.3. Modeling of complexes of TMA^+ with Cl^- and DHB in the water environment

To elucidate the solvation effects, we employed the PCM method to calculate the interaction energies in the TMA^+:Cl^-, TMA^+:DHB^0 (in two different geometries), and TMA^+:$[DHB–H]^-$ complexes in water environment. The calculated interaction energies of the complexes are presented in Table 2.

The energies of the complexes calculated in the polar solvent surrounding presented in Table 2 differ significantly from the data obtained for the same complexes in the vacuum (Table 1). While in the vacuum conditions the complex of tetramethylammonium with a chlorine counterion, TMA^+: Cl^-, is the most stable among the calculated systems (IE = −378.84 kJ/mol), in a polar medium (water) this complex is unstable (IE = +11.55 kJ/mol). Similar conclusions are obtained for the TMA^+:$[DHB–H]^-$ complex. The calculations shows high stability of this complex in vacuum (Table 1; IE = −351.66 kJ/mol) while in water such a complex should dissociate (Table 2; the interaction energy is positive IE = +4.34 kJ/mol). However, the formation of the TMA^+:$[DHB–H]^-$ complex in water is more probable than the formation of the TMA^+:Cl^- complex.

Table 2
ZPVE and BSSE corrected interaction energies (IE, kJ/mol) in complexes of TMA^+ with DHB (neutral and deprotonated) and Cl^- in water media calculated by the PCM method

Complex	IE (kJ/mol)
	MP2/6-31^{++}G** PCM
TMA^+:Cl^-	+11.55
TMA^+:DHB^0 (geometry 1)	−3.24
TMA^+:DHB^0 (geometry 2)	−4.27
TMA^+:$[DHB–H]^-$	+4.34

The interaction energy of TMA^+ with a neutral DHB molecule obtained from the PCM calculation is negative. This indicates a possibility of the formation of stable noncovalent complexes of DHB^0 with quaternary compounds in polar solvents, although the interaction energy calculated in solution (about −4 kJ/mol) is ten times smaller than in vacuum (IE = −43.61 kJ/mol).

Significant differences between the interaction energies obtained from the PCM calculations and in vacuum are expected in accordance with the theory of salts dissociation in polar solutions since the complexes of TMA^+ with the Cl^- and $[DHB–H]^-$ anions are not stable in polar solvents and dissociate into ions. On the other hand, the formation of the TMA^+ complex with a neutral DHB molecule in such conditions is possible. Moreover, in solution the TMA^+:DHB^0 complex with geometry 2 (cation–π interaction) is more stable than with geometry 1, in which TMA^+ interacts with the carboxyl group of the DHB molecule. This indicates that for biological systems in the aqua environment the cation–π interaction of TMA^+ with its molecular recognition targets can be more favorable than TMA^+ coordination with a negatively charged group of a biomolecule. Such an interaction is nonspecific contrary to the specific cation–π interaction. The distinction between specific and nonspecific interactions is important because the specific interactions facilitate high fidelity of the molecular recognition processes and the reproducibility of complex biological reactions.

3.4. Comparison of experimental mass-spectrometric and theoretical data on the noncovalent stability of molecular complexes

To verify the data obtained from the modeling of the processes related to the biological recognition of quaternary compounds, a comparative analysis of MALDI mass spectrometry experimental data and the results obtained in the calculations was performed. One of the aims of the present quantum chemical modeling was to obtain data useful for an analysis and interpretation of the results of our MALDI mass-spectrometric experiments.

In those experiments, bisquaternary ammonium salt decamethoxinum deposited in the DHB matrix was studied [4]. On the basis of our previous experiments on the same compound using other mass-spectrometric techniques (such as the secondary-ion mass spectrometry [22] and the electrospray ionization [32]) we anticipated that the main peak in the mass spectrum should correspond to a cluster of the doubly charged dication of the salt with a chlorine counterion (Cat^{2+}:Cl^-). Indeed, a peak corresponding to this cluster was recorded in the MALDI spectra, but it showed relative low abundance of the species. The peak appeared against the background of an unexpectedly intense peak of the dication cluster with a deprotonated DHB molecule, Cat^{2+}:$[DHB–H]^-$. (This species can also be interpreted as due to a cluster of a partially dequaternized dication $[Cat^{2+}–H]^+$ with a neutral DHB^0 molecule). The relative abundance of $[Cat^{2+}:Cl^-]^+$ was about 40% of that of the Cat^{2+}:$[DHB–H]^-$ ion in the positive ion MALDI mass spectra of decamethoxinum in the DHB matrix obtained in the linear mode [4]. The collected data seems to indicate a competition between reactions involving the inorganic Cl^- anion and the organic $[DHB–H]^-$ anion in binding to the bisquaternary ammonium dication or to the quaternary cation. As the analysis of the MALDI experiment shows, the complex of the decamethoxinum dication with the deprotonated DHB ion prevails over the dication complex with the Cl^- counterion.

Furthermore, in our controlled mass spectrometry measurements of the TMA^+ Cl^-–DHB system in the glycerol matrix by the FAB mass spectrometry technique, the intensity of the $[2TMA:Cl]^+$ peak in the spectrum was found to be several times smaller than the intensity of the $[2TMA:(DHB–H)]^+$ ion. It should also be noted that clusters of the decamethoxinum dication with the matrix or with solvent organic molecules (such as glycerol or nitrobenzyl alcohol in FAB and methanol or ethanol in electrospray) have never been recorded before. That points to the selectivity of the interactions involving alkylammonium cations.

The results of the present calculations on model associates of the TMA^+ cation with the Cl^- and $[DHB–H]^-$ anions show that TMA^+ binding to Cl^- in the gas phase (vacuum) is energetically more favorable than the binding to $[DHB–H]^-$ (see Table 1). The difference in binding energies is, however, not too large. It should be mentioned that, while the absolute values of the interaction energy in the complexes are different for the two different methods of the calculations, DFT/B3LYP/6-31++G** and MP2/6-31++G**, both methods agree on the Cl^- preference. Two explanations of the discrepancy between the experimental and theoretical results for the vacuum approach can be suggested.

On one hand, it is expected that the binding of the anions to tetramethylammonium and ammonium derivatives with other types of alkyl substituents (as in decamethoxinum) can differ.

Both steric factors and a presence of two quaternary groups in the structure of decamethoxinum dication may contribute to these differences. One of the quaternary groups can interact with DHB ion as shown in Fig. 2 for the interaction of TMA^+ with $[DNB–H]^-$, while the second one can interact with the π-system of the DHB ring or with one of the DHB hydroxyl groups. The presence of the second quaternary active group in the dication structure can play a crucial role in the stabilization of the noncovalent Cat^{2+}:$[DHB–H]^-$ complex and add to a higher stability of this complex in comparison to the Cat^{2+}:Cl^- complex as shown in the MALDI mass spectrometry experiment.

There is another way the difference between the experimental and theoretical data for vacuum conditions can be interpreted. From the experimental point of view, it is important to know whether the different molecular associates detected in the MALDI spectra were initially present in the sample or were formed in gas-phase reactions in the plume created by a laser shot. The analysis of the theoretical data on complexes studied stability in vacuum approach and in polar surrounding may indicate the Cat^{2+}:$[DHB–H]^-$ complexes formation directly in the sample. In liquid polar media, as we have seen in the PCM calculations, the complex of TMA^+ with DHB is more energetically favorable than the TMA^+ complex with the chlorine counterion, which is energetically unfavorable in water because of the interaction energy (Table 2). Further, an anion exchange may take place in solution; that is, the Cl^- anion can be substituted by the organic anion $[DHB–H]^-$ formed by the deprotonation of the DHB acid. Due to these effects, crystals of the decamethoxinum dication with $[DHB–H]^-$ anion or complexes $[Cat^{2+}–H]^+$:DHB^0 can be formed on drying of the mixture of decamethoxinum and DHB water solution. Sputtering of a sample formed this way may, in the MALDI experiment, contribute to the enhanced abundance of the $[Cat^{2+}:(DHB–H)^-]^+$/$[[Cat–H]^+:DHB^0]^+$ ions as registered at m/z 775 in the MALDI mass spectra.

4. Conclusions

The model complexes of the tetramethylammonium ion with the chlorine anion and the 2,5-dihydroxybenzoic acid (neutral and deprotonated) have been studied using DFT/B3LYP/6-31++G** and MP2/6-31++G** calculations in vacuum. The equilibrium geometries and the interaction energies of the complexes have been determined. The interaction energies of TMA^+ with the $[DHB–H]^-$ anion and Cl^- are similar; however the complex of TMA^+ with the Cl^- counterion is more energetically favorable in vacuum than the other complex. The complex of the TMA^+ ion with a neutral DHB molecule has ten times smaller interaction energy in vacuum than the complex of TMA^+ with the $[DHB–H]^-$ anion. This results from the fact that in the equilibrium geometry the TMA^+ ion interacts with the hydroxile group of DHB molecule only by a weak hydrogen bond.

To evaluate the solvation effects on the stability of the complexes, PCM calculations have been performed. The calculated interaction energies in the noncovalent complexes in a polar medium (water surrounding) differ significantly from those obtained in vacuum. The interaction energies in the complexes of TMA^+ with the Cl^- and $[DHB–H]^-$ anions were found to be positive showing that these complexes are not stable in polar solutions. On the other hand, the complex of a TMA^+ ion with a neutral DHB molecule can form in water. The calculations of the TMA^+:DHB^0 complex showed that in the water environment the specific cation–π interactions of TMA^+ and its molecular recognition targets can be more favorable than the TMA^+ interaction with a negatively charged group of the biomolecule.

The theoretical results have allowed us to explain the MALDI mass-spectrometric experimental data showing the dominance of the ions of the complexes of the bisquaternary ammonium cation decamethoxinum with DHB in the spectra. They also allowed us to elucidate the interactions of quaternary compounds with active groups of molecular protein targets, which occur under competition between these groups and the counterions of quaternary salts.

Acknowledgment

The authors acknowledge Oleg Boryak for his help with the FAB mass spectrometry measurements of the tetramethylammonium chloride and DHB systems.

References

[1] A.N. Vievskiy, Mechanisms of Biological Activity of Cationic Surface Active Compounds (Russian), Moscow, 1991.
[2] V.A. Pashynskaya, M.V. Kosevich, A. Gomory, O.V. Vashchenko, L.N. Lisetski, Rapid Commun. Mass Spectrom. 16 (2002) 1706.
[3] V.A. Pashynska, M.V. Kosevich, H. Van den Heuvel, F. Cuyckens, M. Claeys, Visnyk of Karazin Kharkov National University, Biophys. Bull., 14 (2004) 123.
[4] V.A. Pokrovsky, M.V. Kosevich, V.L. Osaulenko, V.V. Chagovets, V.A. Pashynska, V.S. Shelkovsky, V.A. Karachevtsev, A.Yu. Naumov, Mass-Spectrometria 2 (2) (2005) 1.
[5] M.D. Mashkovskiy, Medicinal Remedies (Russian), Medicina, Moscow, 1978.
[6] V.A. Pashynska, M.V. Kosevich, S.G. Stepanian, Visnyk problem biology i medicine (Russian) 9 (1999) 118.
[7] P.-O. Norrby, T. Liljefors, J. Am. Chem. Soc. 121 (1999) 2303.
[8] J.M. Llinares, D. Powell, K. Bowman-James, Coordination Chem. Rev. 240 (2003) 57.
[9] J. de Mendoza, V. Alcfizar, E. Botana, A. Galln, G. Lu, J.O. Magrans, M.M. Portugub, P. Prados, A. Salmerdn, J. Shchez-Quesada, C. See1, M. Segura, Pure Appl. Chem. 69 (1997) 577.
[10] C.A. Hunter, Angew. Chem. Int. Ed. Engl. 40 (2004) 5310.
[11] C.E. Cannizzaro, K.N. Houk, J. Am. Chem. Soc. 124 (2002) 7163.
[12] M.V. Kosevich, V.A. Pashinskaya, S.G. Stepanian, V.S. Shelkovsky, V.V. Orlov, Yu. P. Blagoy, Visnyk of Karazin Kharkov National University, Biophys. Bull., 1 (1999) 22.
[13] J.P. Gallivan, D.A. Dougherty, Proc. Nat. Acad. Sci. USA 96 (1999) 9459.
[14] N. Zacharias, D.A. Dougherty, Trends Pharmacol. Sci. 23 (2002) 281.
[15] N.S. Scrutton, A.R. Raine, Biochem. J. 319 (1996) 1.
[16] A.R. Raine, C.C. Yang, L.C. Packman, S.A. White, F.S. Mathews, N.S. Scrutton, Protein Sci. 4 (1995) 2625.
[17] M.M. Gromiha, Biophys. Chem. 103 (2003) 251.
[18] S. Bartoli, S. Roelens, J. Am. Chem. Soc. 124 (2002) 8307.
[19] D.A. Dougherty, Science 271 (1996) 163.
[20] F. Nachon, L. Ehret-Sabatier, D. Loew, C. Colas, A. Dorsselaer, M. Goeldner, Biochemistry 37 (1998) 10507.
[21] A.N. Barrett, G.C.K. Roberts, A.S.V. Burgen, G.M. Clore, Mol. Pharmacol. 24 (1983) 443.
[22] V.A. Pashynska, M.V. Kosevich, A. Gomory, Z. Szilagyi, K. Vekey, S.G. Stepanian, Rapid Commun. Mass Spectrom. 19 (2005) 785.
[23] A.D. Becke, Phys. Rev. B 38 (1988) 3098.
[24] C. Lee, W. Yang, R.G. Parr, Phys. Rev. B 37 (1988) 785.
[25] S.H. Vosko, L. Wilk, M. Nusair, Can. J. Phys. 58 (1980) 1200.
[26] M. Cossi, N. Rega, G. Scalmani, V. Barone, J. Comput. Chem. 24 (2003) 669.
[27] M. Cossi, G. Scalmani, N. Rega, V. Barone, J. Chem. Phys. 117 (2002) 43.
[28] R. Cammi, B. Mennucci, J. Tomasi, J. Phys. Chem. A 103 (1999) 9100.
[29] B. Mennucci, E. Cances, J. Tomasi, J. Phys. Chem. B 101 (1997) 10506.
[30] S.F. Boys, F. Bernardi, Mol. Phys. 19 (1970) 553.
[31] M.J. Frisch, G.W. Trucks, H.B. Schlegel, G.E. Scuseria, M.A. Robb, J.R. Cheeseman, J.A. Montgomery, Jr., T. Vreven, K.N. Kudin, J.C. Burant, J.M. Millam, S.S. Iyengar, J. Tomasi, V. Barone, B. Mennucci, M. Cossi, G. Scalmani, N. Rega, G.A. Petersson, H. Nakatsuji, M. Hada, M. Ehara, K. Toyota, R. Fukuda, J. Hasegawa, M. Ishida, T. Nakajima, Y. Honda, O. Kitao, H. Nakai, M. Klene, X. Li, J.E. Knox, H.P. Hratchian, J.B. Cross, V. Bakken, C. Adamo, J. Jaramillo, R. Gomperts, R.E. Stratmann, O. Yazyev, A.J. Austin, R. Cammi, C. Pomelli, J.W. Ochterski, P.Y. Ayala, K. Morokuma, G.A. Voth, P. Salvador, J.J. Dannenberg, V.G. Zakrzewski, S. Dapprich, A.D. Daniels, M.C. Strain, O. Farkas, D.K. Malick, A.D. Rabuck, K. Raghavachari, J.B. Foresman, J.V. Ortiz, Q. Cui, A.G. Baboul, S. Clifford, J. Cioslowski, B.B. Stefanov, G. Liu, A. Liashenko, P. Piskorz, I. Komaromi, R.L. Martin, D.J. Fox, T. Keith, M.A. Al-Laham, C.Y. Peng, A. Nanayakkara, M. Challacombe, P.M.W. Gill, B. Johnson, W. Chen, M.W. Wong, C. Gonzalez, J.A.Pople, Gaussian 0, Revision B.05, Gaussian, Inc., Pittsburgh PA, 2003.
[32] V.A. Pashynska, M.V. Kosevich, H. Van den Heuvel, M. Claeys, Rapid Commun. Mass Spectrom. 20 (2006) 755.

Eur. Phys. J. D **58**, 287–296 (2010)
DOI: 10.1140/epjd/e2010-00125-5

THE EUROPEAN PHYSICAL JOURNAL D

Regular Article

Competition between counterions and active protein sites to bind bisquaternary ammonium groups. A combined mass spectrometry and quantum chemistry model study

V. Pashynska[1,a], O. Boryak[1], M.V. Kosevich[1], S. Stepanian[1], and L. Adamowicz[2]

[1] B. Verkin Institute for Low Temperature Physics and Engineering of the National Academy of Sciences of Ukraine, Lenin Ave. 47, 61103 Kharkov, Ukraine
[2] University of Arizona, Department of Chemistry, Tucson, 85721 Arizona, USA

Received 15 January 2010 / Received in final form 2 April 2010
Published online 12 May 2010 –

Abstract. A model study of the interaction between biologically active bisquaternary ammonium salts and their molecular targets in living systems is urgently needed to elucidate the molecular mechanisms involved in the interactions between these compounds. To address this need a combined experimental-computational study of the interaction of two tetramethylammonium cations (modeling two quaternary groups) with the chlorine anion and with the deprotonated 2,5-dihydroxybenzoic acid (modeling a carboxylic group and an aromatic ring of side radicals of proteins) has been performed. Fast atom bombardment mass spectrometry method and DFT/B3LYP/6-31++G** and MP2/6-31++G** calculations have been employed in the study. Stable noncovalent complexes with different ratios of the tetramethylammonium cations and chlorine anions or deprotonated 2,5-dihydroxybenzoic acid anions were registered in the mass spectra of tetramethylammonium chloride and 2,5-dihydroxybenzoic acid mixture. This finding shows that the organic and inorganic anions compete to bind tetramethylammonium in the studied system. The theoretically determined stabilities of the noncovalent complexes were compared with the relative stabilities evaluated from the mass spectrometric measurements. The results of the study allow us to elucidate the competing interactions that exist between quaternary groups with inorganic counterions or with active groups of molecular protein targets.

1 Introduction

In view of the continuous search for new effective bisquaternary ammonium antimicrobial agents, the modeling of the interactions of the active groups of these compounds with assumed molecular targets in biological systems attracts considerable interest. In living organisms quaternary salts dissociate. A competition between the active groups of molecular targets and the salt inorganic counterions of the quaternary ammonium ions produced in this dissociation plays an important role in biological recognition processes. Thus, the competing interaction of the quaternary ammonium group with inorganic and organic counterions is a property of biophysical significance that needs to be addressed in a model study.

The interaction of antimicrobial quaternary ammonium compounds with components of the bacterial membrane (phospholipids and proteins) is considered to be the most important factor which is related to their biological functions [1]. This importance has been confirmed by the results of our systematic mechanistic investigations of the bisquaternary ammonium antimicrobial agent decamethoxinum developed in Ukraine [2–5]. Decamethoxinum is a membranothropic agent [1] and a likely molecular mechanism of its action involves its interaction with lipids and protein constituents of the cell membranes. In our prior works, the interaction of decamethoxinum with phospholipids was investigated using soft ionization mass spectrometry techniques, the differential scanning calorimetry, and quantum chemical calculations. The formation of stable supramolecular complexes of the compound with membrane phospholipids was demonstrated in those works [2,3]. The results of differential scanning calorimetry experiments on some model phospholipid membranes showed that complexes of the decamethoxinum dication with phospoholipid can affect the liquid-crystalline state of the membrane lipid matrix of the microorganism and disturb some membrane processes [2]. It was also suggested that the drug binding to some membrane proteins involved in the breathing chain of bacteria, in particular to some cytochromes, disturbs their functioning and facilitates decamethoxinum antimicrobial action [6].

In view of the above it is reasonable to consider the interaction of quaternary agents with bacterial membrane proteins as the important element of the likely

[a] e-mail: vlada@vl.kharkov.ua

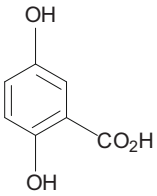

Fig. 1. Structure of 2,5-dihydroxybenzoic acid.

molecular mechanisms of biological action of the agents. This has motivated us to undertake a model study concerning decamethoxinum in the 2,5-dihydroxybenzoic acid (DHB) matrix (Fig. 1) by matrix-assisted laser desorption/ionization (MALDI) mass spectrometry (MS) technique [5]. In the mass spectra obtained this way, the most prominent peak was the one corresponding to a noncovalent complex of decamethoxinum dication with $[DHB–H]^-$ anion. Furthermore, the experiments revealed that the abundance of the complex of decamethoxinum dication with $[DHB–H]^-$ was much higher than that of its complex with the Cl^- counterion. An additional study of the decamethoxinum-DHB mixture in a glycerol liquid matrix was performed by the fast atom bombardment (FAB) MS method [7]. In the mass spectra obtained in that study, comparable abundances of the $Cat^{2+}•Cl^-$ and $Cat^{2+}•[DHB–H]^-$ clusters were recorded. That finding showed that anion exchange takes place in the solution.

In those MS experiments [5,7], DHB (usually used as a matrix in the MALDI MS technique) was used as a model of two types of recognition sites present in proteins, namely the carboxylic group or the carboxylate anion in the ionic deprotonated state and the aromatic ring, which can be involved in a cation-π-electron interaction. In amino acids, carboxylic groups are parts of side chains in the aspartic and glutamic acids and aromatic residues are parts of tryptophan, tyrosine, phenylalanine, and histidine. As for the drugs, it is known that quaternary ammonium groups participate in the molecular recognition processes involved in some drug actions [8–10]. The quaternary groups serve as receptors of inorganic and organic anions [8–10] and thus can actively interact with the carboxylate anion formed in the deprotonation process of the DHB molecule. DHB can mimic an electronegative sites located on the protein surface.

Motivated by the above-raised points, we have initiated a systematic study on modelling the noncovalent interactions of quaternary ammonium compounds with their potential molecular targets in living systems by the mass spectrometry and quantum chemical calculations. Since ab initio calculations of large intact biologically active molecules such as decamethoxinum are still beyond the reach of present-day computers, we have selected the noncovalent complexes of the tetramethylammonium cation $N^+(CH_3)_4$ (TMA) with a chlorine anion and with DHB in the anionic form as the subject of the investigation. In these complexes TMA is a model of the active group common to all quaternary ammonium compounds, Cl^- is a counterion in quaternary salts, and DHB is the compound modelling the carboxylic and aromatic groups of side radicals of membrane proteins. The mentioned complexes were observed in the mass spectrometric experiments [5,7].

Our previous computational investigation [11] performed at the MP2/6-31++G** level of theory demonstrated that the interaction energies (IE) of TMA^+ with the $(DHB–H)^-$ anion and Cl^- are −351.66 and −378.86 kJ/mol, respectively, and the latter complex is more energetically stable in vacuum than the former one [11]. The complex of the TMA^+ ion with a neutral DHB molecule has IE ten times smaller in vacuum than the complex of TMA^+ with the $[DHB–H]^-$ anion. The IEs of the double noncovalent complexes in water calculated with the polarizable continuum model (PCM) method differed significantly from the IEs obtained in vacuum. The IEs of the complexes of TMA^+ with the Cl^- and $[DHB–H]^-$ anions in water were found to be positive showing that these complexes are likely unstable in polar liquid environments. However, the results of the previous computational study [11] could not be directly compared with the mass spectrometric data obtained by the MALDI and FAB techniques for the systems containing decamethoximun with DHB [5,7], because for the decamethoxinum only singly charged noncovalent complexes of bisquaternary dication with anion were detected. The complexes containing two TMA^+ ions with anions (Cl^- or $[DHB–H]^-$) better model the competition of organic and inorganic counterions to attach to the active bisquaternary groups. Such a competition takes place both in the experiment and in the living systems.

The aims of our current model study on the noncovalent complexes of two TMA^+ cations with a chlorine anion and deprotonated DHB anion are:

1. an experimental investigation of the formation of supramolecular complexes of $2TMA^+$ with chlorine anion or deprotonated DHB under the FAB mass spectrometry conditions;
2. determination of the equilibrium geometries of the model triple noncovalent complexes by quantum chemical methods;
3. calculation of the IEs of the complexes of bisquaternary groups with organic and inorganic anions;
4. correlation of the results of computational study with the mass spectrometry data concerning the relative stability of the complexes.

2 Experimental

Mass spectrometry experiments in this work have been performed by the fast atom bombardment (FAB) method using the MI-1201E magnetic sector mass spectrometer ("SELMI" Works, Sumy, Ukraine) equipped with commercial FAB units. Argon was used as the bombarding gas. The energy of the primary argon beam was 4.5 keV. Glycerol was used as the matrix for the FAB MS experiments. In the first step of the experiment tetramethylammonium (TMA) chloride and 2,5-dihydroxybenzoic acid (DHB) solutions with different relative concentrations were prepared. Deionized water was used in the solution

preparation. Equal volumes of water solutions and glycerol matrix were mixed to assure that the initial concentration of TMA and DHB remain intact upon evaporation of water in the fore vacuum system of the instrument. The FAB mass spectra were recorded during the first five minutes of the experiments following the exposure of the samples to the bombarding beam. TMA chloride and DHB used in the experiments were purchased from "Sigma Aldrich", and glycerol was purchased from "Reanal", Hungary.

The theoretical study of the noncovalent $2TMA^+ \bullet Cl^-$, and $2TMA^+ \bullet [DHB–H]^-$ complexes in this work has been performed using ab initio quantum chemical calculations. The geometries of the selected starting structures were first fully-optimized at the DFT level of theory. The DFT calculations were carried out with the three-parameter density functional usually abbreviated as B3LYP, which includes Becke's gradient exchange correction [12], the Lee, Yang, Parr correlation functional [13], and the Vosko, Wilk, and Nusair correlation functional [14]. Next, harmonic frequency calculations were carried out for the equilibrium DFT geometries, and the frequencies were used to determine the zero-point vibrational energy (ZPVE) corrections. Additionally, single point energy calculations were performed at the MP2 level of theory using the geometries of the systems obtained at the DFT level. In the calculations we used the standard 6-31++G** basis set. All interaction-energy calculations were performed taking into account the BSSE correction using the standard counterpoise correction method [15]. To test whether the DFT method can correctly predict equilibrium geometries of the studied systems we performed geometry optimization of the $2TMA^+ \bullet [DHB–H]^-$ complex at the MP2 level of theory. We also tested the effect of the BSSE on the calculated geometries. The test involved BSSE-free MP2/6-31++G** geometry optimization of the $2TMA^+ \bullet [DHB–H]^-$ complex. All calculations have been performed using the Gaussian 03 quantum chemistry package [16].

3 Results and discussion

3.1 FAB mass spectrometry study of tetramethylammonium chloride – DHB system

In the first step FAB mass spectra of the individual components of the studied system were recorded and checked for consistency. The FAB mass spectra of DHB in glycerol solvent contain peaks corresponding to the following DHB-related ions: $DHB^{+\bullet}$ (m/z 154), $DHB \bullet H^+$ (m/z 155), and their fragments at m/z 136, 137. In the background there are peaks originated from the glycerol matrix with the general formula $G_n \bullet H^+$ (m/z 93 for $n = 1$, m/z 185 for $n = 2$, m/z 277 for $n = 3$). Positive ion mass spectra of concentrated solution of TMA chloride in glycerol contain a prominent peak of TMA^+ cation (m/z 74) and a set of less prominent peaks corresponding to $[TMA^+_n \bullet Cl^-_{n-1}]^+$, $n = 1–4$, cluster ions. These peaks appeared in groups and the ratios of the relative intensities of the peaks in the groups agree with the abundance ratio of the chlorine isotopes in a natural sample (the natural ratio of ^{35}Cl and ^{37}Cl isotopes is about 3 to 1). The abundance of the cluster ions decreased with dilution of the solution and fell practically to the background level at the TMA^+ concentration of less than 10^{-2} M.

In the next step, solutions of the TMA chloride salt and the DHB acid mixed in varied ratios in glycerol matrix were studied. Dissociation, association, and ion exchange reactions are expected to occur in such systems leading to a variety of neutral and charged products whose yields must depend on the concentration and the initial ratio of the components of the mixture. The reactions can be schematically described as:

$$\begin{aligned} &TMA^+ \bullet Cl^- + DHB \rightarrow \text{mixture} \rightarrow TMA^+ \bullet Cl^- + DHB \\ &+ TMA^+ + Cl^- + [DHB{-}H]^- + [DHB + H]^+ \\ &+ [TMA^+]_n \bullet Cl^-_n + [TMA^+]_m \bullet [DHB{-}H]^-_m \\ &+ [TMA^+]_n \bullet Cl^-_{(n-1)} + [TMA^+]_m \bullet [DHB{-}H]^-_{(m-1)} \\ &+ [TMA^+]_n \bullet Cl^-_m \bullet [DHB{-}H]^-_k . \end{aligned} \quad (1)$$

It should be noted that TMA chloride and DHB have different dissociation constants $pKw = 13.93$ for $N(CH_3)_4Cl$ and $pKw = 2.97$ for DHB, and these constants affect the concentrations of the various dissociation products in solution. The distribution of the individual cations, the anions, and the neutrals among the large variety of clusters makes it difficult to directly estimate and quantitatively describe the stability of the complexes based on the intensities of their peaks in the mass spectrum. Only qualitative analysis of the relative stabilities can be performed.

We will now present some examples of the mass spectra typical to certain concentration ratios in the mixture. In the first example equal volumes of the 10^{-1} M water solution of the TMA chloride and DHB were placed into a double volume of glycerol matrix. The final concentration of each component was 5×10^{-2} M after water evaporation (see Sect. 2). The positive ion FAB mass spectrum of the sample (Fig. 2) contains peaks characteristic of the DHB and TMA^+ cations. Positively charged associates of two TMA^+ cations with a single anion of either chlorine – $2TMA^{2+} \bullet Cl^-$ (m/z 183/185) – or the deprotonated DHB – $2TMA^{2+} \bullet [DHB–H]^-$ (m/z 301) – are also present. (It should be noted that the peak of the ^{37}Cl-containing isotopomer of $2TMA^{2+} \bullet Cl^-$ overlaps with the peak of $2G \bullet H^+$ due to the same mass of 185 a.u.) The absolute intensity of the most prominent peak corresponding to $2TMA^{2+} \bullet Cl^-$ (m/z 183) exceeds more than three times the intensity of the $2TMA^{2+} \bullet [DHB–H]^-$ (m/z 301) peak. No larger associates are found in the mass spectrum of the sample.

The experimental detection of stable noncovalent complexes of TMA^+ with Cl^- and TMA^+ with $[DHB–H]^-$ in the mass spectra of the mixture is a nontrivial result which confirms the existence of a competition between the organic and inorganic anions to bind TMA^+ in the studied systems. The result suggests that a similar competition in the counterions binding to quaternary groups can also occur in real biological processes.

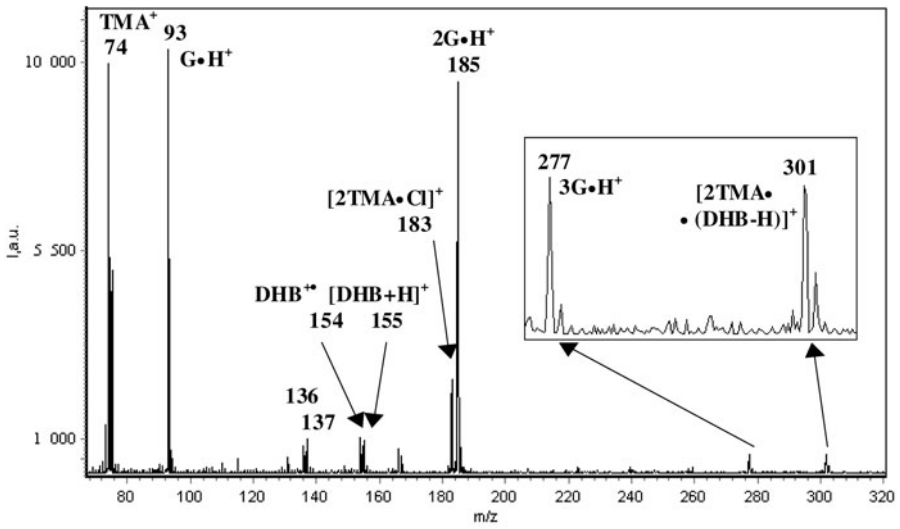

Fig. 2. FAB mass spectrum of 5×10^{-2} M TMA chloride and 5×10^{-2} M DHB mixture in glycerol matrix.

The next example concerns a system with a higher concentration of the components and with some excess TMA chloride (2×10^{-1} M TMA chloride and 10^{-1} M DHB). The mass spectrum of this system is shown in Figure 3. As one notices, the increase of the net concentration of the sample results in the appearance of multicomponent complexes containing TMA^+, Cl^-, and $(DHB–H)^-$, such as, for example, $[(TMA)_n^+ \bullet Cl_{(n-1)}^-]^+$ $(n = 1–4)$, and $[TMA_x^+ \bullet (DHB–H)_y^- \bullet Cl_z^-]^+$. The intensity ratio of the peaks of $2TMA^{2+} \bullet Cl^-$ to $2TMA^{2+} \bullet [DHB–H]^-$ $(m/z$ 301) is about 4:1 in the FAB mass spectrum of the system (Fig. 3).

To investigate the system behavior under the concentration predominance of DHB over TMA•Cl, a mixture of a saturated solution of DHB (to obtain such solution we gathered supernatant liquid over the DHB sediment) and 10^{-1} molar solution of TMA•Cl in glycerol was tested in the experiment. In the FAB spectra the intensity ratio of the peaks corresponding to the TMA^+ ions and the peaks related to DHB ($DHB^{+\bullet}$, $DHB \bullet H^+$) clearly shows the domination of the DHB components in the mixture. In the spectra, the peaks due to the three-component complexes, $2TMA^{2+} \bullet Cl^-$ $(m/z$ 183) and $2TMA^{2+} \bullet [DHB–H]^-$ $(m/z$ 301), have low intensities and the peaks of multicomponent complexes are completely absent. Such a result can be explained by the fact that, under low relative concentration of TMA•Cl in the sample, only two-component noncovalent complexes (e.g. TMA $^+ \bullet Cl^-$, $(TMA)^+ \bullet [DHB–H]^-$, etc.) can be formed as there are not enough TMA^+ ions to form the triple complexes and complexes containing larger number of quaternary cations. However, we should add that the two-component complexes are neutral and cannot be detected in the FAB MS experiment.

It should also be noted that we have not noticed any complexes of TMA^+, which is a hydrophobic cation, with glycerol solvent molecules in the FAB spectra. It testifies to the specificity of the interaction of quaternary ions with the deprotonated DHB molecules. It also confirms our conclusion that in both the laboratory studies and in real living systems, the competition between the native counterion Cl^- and the organic anion (the deprotonated DHB anion in the present case) for the TMA^+ binding takes place. This competition is essential to the processes governing the specific interaction of the quaternary group with the recognizing centers of proteins.

The present mass spectrometry investigation confirms the high stability of the supramolecular complexes containing two tetramethylammonium cations and $Cl^-/[DHB–H]^-$ anions under the mass-spectrometry conditions of the current experiments. Furthermore, the results conclusively point to the different stability of the triple complexes of two TMA^+ ions with Cl^- and a deprotonated DHB anion under the present experimental conditions. In the equimolar system of TMA•Cl and DHB the survival (relative stability) of triple complex of two TMA^+ with inorganic counterion Cl^- dominates over the $2TMA^+$ complex with the $[DHB–H]^-$ anion under mass spectrometric conditions. In next section, we describe quantum chemical calculations of the geometries and energetic parameters of the complexes detected in the mass spectrometry experiment performed to elucidate the interplay between the ions involved in the above-described complexes formation.

3.2 Computation of the $2TMA^+$ complex with the chlorine counterion in vacuum

In the first step of the computational study, we calculated the equilibrium structure of the $2TMA^+ \bullet Cl^-$ complex, which is our simplest model of the active group of the bisquaternary ammonium chloride salt. The optimized geometry of the complex in vacuum conditions is shown in Figure 4 (the Cartesian coordinates

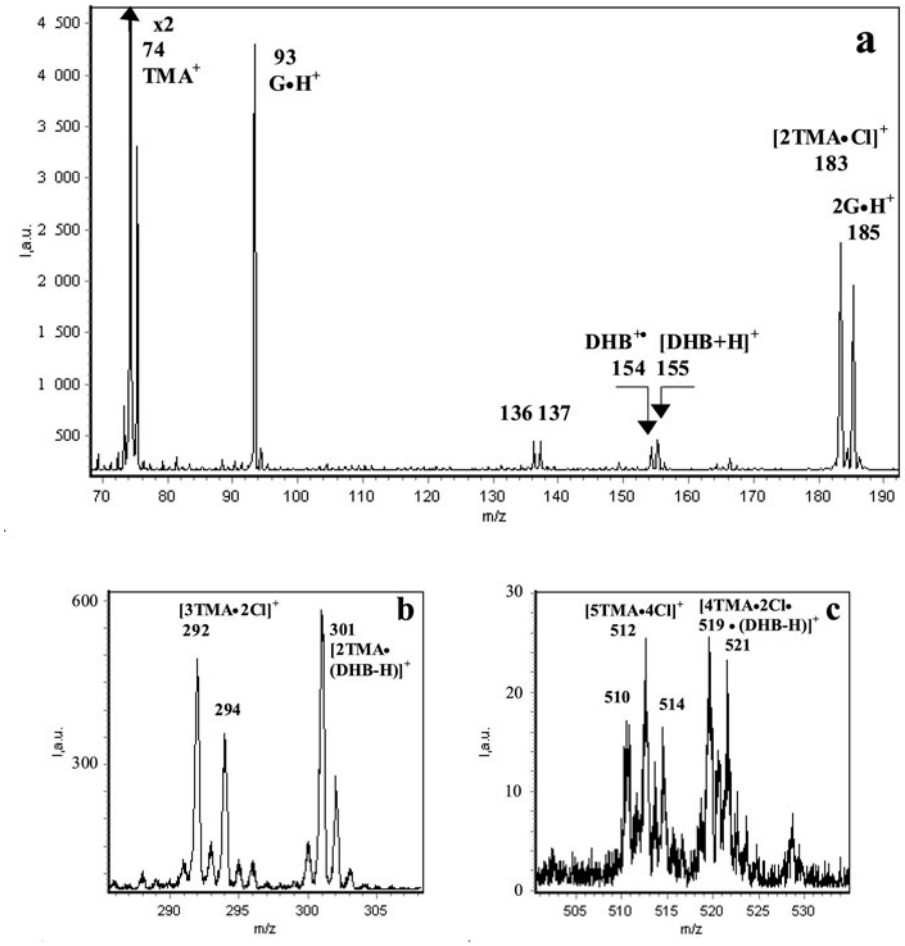

Fig. 3. FAB mass spectrum of 2×10^{-1} M TMA chloride and 10^{-1} M DHB mixture in glycerol matrix.

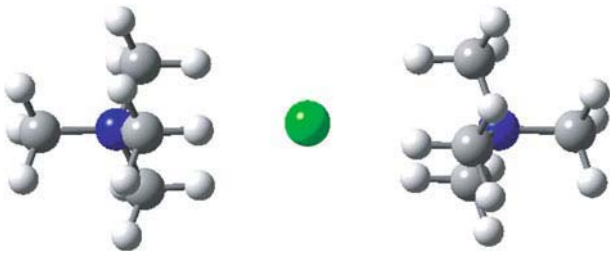

Fig. 4. (Color online) Equilibrium geometry of the $2TMA^+ \bullet Cl^-$ noncovalent complex obtained in the DFT/B3LYP/6-31++G** calculations.

of the complex are provided in Appendix). The interaction energies in this complex calculated using different methods are shown in Table 1. These values include the energy of −521.41 kJ/mol obtained at the DFT/B3LYP/6-31++G** level of theory and the energy of −521.24 kJ/mol obtained at the MP2/6-31++G** level. As the aim of this work is to obtain biologically relevant information concerning the interactions in the systems investigated in the FAB mass spectrometry experiments and these experiments have been carried out at room temperature, we have also calculated the IE of the complex based on the Gibbs free energies of the complex and its components (Tab. 2). The IE calculated this way is −491.68 kJ/mol. The Gibbs free energies were calculated at the temperature of 298.14 K and pressure of 1 atm.

The main structural features of the $2TMA^+ \bullet Cl^-$ complex obtained in the present calculations appear to be similar to those reported in our previous theoretical investigation [11] of the $TMA^+ \bullet Cl^-$ and those reported by others [17] for the $TMA^+ \bullet F^-$ complex. The likely localization of the positive charge of TMA^+ ion at the hydrogen atoms of the methyl groups creates areas of higher concentration of the positive charge between each of the three methyl groups (in the middle of the tetrahedron "faces"). In the $2TMA^+ \bullet Cl^-$ complex the Cl^- anion is situated between the areas of the positive charge of two TMA^+ ions and attracted to them by a Coulomb force. The attractive interaction results in the negative value of the interaction energy (Tab. 1). The sandwich-like geometrical configuration of the complex with the Cl^- ion in the middle (Fig. 4) provides a close contact of both TMA^+ cations with the Cl^- anion. This spatial arrangement leads to the high stability of the $2TMA^+ \bullet Cl^-$ complex under the vacuum condition.

Table 1. ZPVE and BSSE corrected interaction energies (IE, kJ/mol) in complexes of $2TMA^+$ with Cl^- and deprotonated DHB calculated at the DFT/B3LYP/6-31++G** and MP2/6-31++G** levels of theory in vacuum[a].

Complex	IE, kJ/mol	
	DFT/B3LYP/6-31++G**	MP2/6-31++G**
$2TMA^+ \bullet Cl^-$	−521.41	−521.24
$2TMA^+ \bullet [DHB–H]^-$	−443.14	−462.73

[a] The interaction energy for each complex was calculated as a difference between the energy of the complex and the energies of the ions forming the complex, because the separation of each complex into ions is the lowest energy decomposition path in vacuum. This was confirmed by MP2/6-31++G** calculations which showed that the sum of the energies of the ions forming the complexes $TMA^+ \bullet [DHB–H]^-$ and $TMA^+ \bullet Cl^-$ ($IE_{TMA+} + IE_{[DHB-H]-}$) and ($IE_{TMA+} + IE_{Cl-}$) are lower by −14.3 kcal/mol and −23.7 kcal/mol, respectively, than the sum of the energies of the corresponding neutral species, ($IE_{TMA0} + IE_{DHB0}$) and ($IE_{TMA0} + IE_{Cl0}$).

Table 2. Interaction energies (IE, kJ/mol) determined based on Gibbs free energies calculations for complexes of $2TMA^+$ with Cl^- and deprotonated DHB obtained at the DFT/B3LYP/6-31++G level of theory.

Complex	IE, kJ/mol
$2TMA^+ \bullet Cl^-$	–491.68
$2TMA^+ \bullet [DHB–H]^-$	–355.15

3.3 Modeling of complexes of $2TMA^+$ with the deprotonated DHB anion in vacuum

In our earlier work, double complexes of one TMA^+ cation with the $[DHB–H]^-$ anion, which can be formed under the experimental mass spectrometry conditions, were theoretically studied in two possible starting configurations. In the first configuration TMA^+ was located in the plane of DHB near the COO^- group and in the second one TMA^+ was located above the plane of the DHB ring [11]. In that investigation it was shown that in the most favorable configuration of the complex $TMA^+ \bullet [DHB–H]^-$, the TMA^+ cation directly interacts by its three CH_3 groups with the COO^- group of the $[DHB–H]^-$ ion. In such a configuration, the Coulombic forces play the crucial role in the stabilization of the complex because the majority of the negative charge in $[DHB–H]^-$ is concentrated at the COO^- group. In a DFT structure optimization of the $TMA^+ \bullet [DHB–H]^-$ complex performed starting with a geometry in which TMA^+ was situated directly above the DHB benzyl ring, the TMA^+ cation gradually shifted towards the COO^- group of $[DHB–H]^-$ and the final optimal geometry of the complex was very similar to that of the most favorable configuration [11].

Considering the above, the present calculation of the triple $2TMA^+ \bullet [DHB–H]^-$ complex was started from a geometry where one of the quaternary ions interacted with the COO^- group and the other ion was located near the oxygen of the OH group of DHB. This OH group is the closest to the carboxyl group.

The optimized geometry of the noncovalent complexes $2TMA^+ \bullet [DHB–H]^-$ calculated at the DFT/B3LYP/6-31++G** level of theory is presented in Figure 5 (the Cartesian coordinates of the complex are provided in Appendix). In this configuration one of the TMA^+ cations

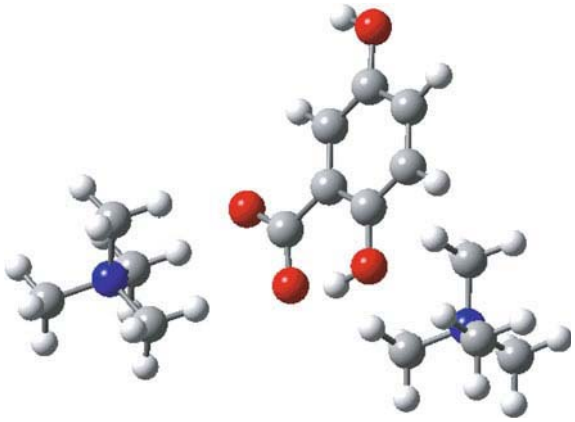

Fig. 5. (Color online) Equilibrium geometry of the $2TMA^+ \bullet [DHB–H]^-$ noncovalent complex obtained in the DFT/B3LYP/6-31++G** calculations.

interacts by its three methyl groups ("face of tetrahedron") with the COO^- group of the deprotonated DHB. This geometrical arrangement is consistent with the equilibrium geometries of the double complexes describe before [11]. Another TMA^+ cation forms a weak hydrogen bond of the C–H...O type with the hydroxyl group of DHB (Fig. 5).

The IE values of the complex of two TMA^+ ions with a deprotonated DHB are shown in Table 1 and include the IE of −443.14 kJ/mol obtained with the DFT method and the IE of −462.73 kJ/mol obtained in the MP2 calculations. The comparison of the IE values of $2TMA^+ \bullet Cl^-$ and $2TMA^+ \bullet [DHB–H]^-$ complexes demonstrate that the triple complexes of quaternary ions with inorganic counterion are more stable than the complexes containing the deprotonated DHB. It should be noted that the DFT/B3LYP/6-31++G** and MP2/6-31++G** methods predict somewhat different interaction energies of the complexes. However the relative stabilities predicted for the two complexes are similar.

The ionic nature of the complex is confirmed by the calculated value of the interaction energy of −462.73 kJ/mol (by MP2 method) (see Tab. 1) which is typical to a Coulomb interaction. The IE in the $2TMA^+ \bullet [DHB–H]^-$ complex has also been calculated at normal conditions using the Gibbs free energies of the

complex and its components. This IE is −355.15 kJ/mol (Tab. 2). The comparison of the IEs calculated using the Gibbs free energies (Tab. 2) for the $2TMA^+ \bullet Cl^-$ and $2TMA^+ \bullet [DHB–H]^-$ complexes also show higher stability of the complexes of quaternary ions with a chlorine anion than the complexes containing the $[DHB–H]^-$ anion. This result is in a good agreement with the relative stabilities calculated at 0 K (Tab. 1).

3.4 Comparison of the experimental mass spectrometric and computational data on the stability of the studied supramolecular complexes

One of the aims of the present computational modeling study was to obtain data useful for analysis and comparison with the results of our FAB mass spectrometric experiments. The earlier studies of the stability of bisquaternary ions of the antimicrobial agents decamethoxinum and aethonium under the FAB MS conditions showed that, while the decamethoxinum doubly charged cation and the quasimolecular complex of this dication with a chlorine anion were present in the FAB spectra, the quasimolecular ions of aethonium were not [18,19]. This behavior was explained by our previous quantum chemical calculations of the bisquaternary compounds and it was attributed to strong correlation between certain structural features (in particular, the distance between the quaternary groups) of the dications and their stabilities [20]. While the calculated distance between centers of quaternary groups (atoms of nitrogen) in the decamethoxinum dication is about 14 Å, the distance in the aethonium dication is only about 4 Å. Such a difference in the distance between the centers where the positive charges are localized in the two dications leads to a significant difference in the stabilities of the decamethoxinum and aethonium quasimolecular ions under the MS conditions. In the aethonium dication, where the distance is 4 Å, the Coulomb repulsion between the two positively charged groups in the bisquaternary dication is high and results in the lack of stability of both the noncovalent complex of the dication with Cl^- counterion and the intact aethonium dication.

The same approach based on the quantum chemical calculations of the distance between the quaternary groups can also be used to analyze the relative stability of the $2TMA^+ \bullet Cl^-$ and $2TMA^+ \bullet [DHB–H]^-$ complexes under the FAB MS conditions. The present calculations show that, while the distance between nitrogens of the quaternary groups in the $2TMA^+ \bullet Cl^-$ complex is 7.5 Å, the distance between N atoms in the $2TMA^+ \bullet [DHB–H]^-$ complex is about 8 Å. Both distances are long enough not to destabilize the complexes. This is confirmed by the FAB spectra where both complexes are present (Figs. 3, 4). Clearly, the attraction of the cations to the anion located between them in the two complexes outweighs the repulsion between the cations. This agrees with our previous results on the stability of the bisquaternary complex ions [18–20].

Regarding the relative stability of the $2TMA^+ \bullet Cl^-$ and $2TMA^+ \bullet [DHB–H]^-$ complexes we can summarize the experimental and theoretical results obtained in this work as follows. The FAB MS results show that under the FAB conditions the $2TMA^+ \bullet Cl^-$ complex is more stable than the $2TMA^+ \bullet [DHB–H]^-$ complex. This finding agrees with the results of our calculations in vacuum (Tabs. 1, 2) that show that the IE of the complex of two TMA^+ cations with a chlorine counterion is more negative than the IE of the complex of two TMA^+ with a deprotonated DHB. It should be mentioned that, while the IE values of the complexes are somewhat different for DFT/B3LYP/6-31++G**, MP2/6-31++G**, and that obtained from the Gibbs free energies, all methods agree on the preference of Cl^- over the deprotonated DHB in binding TMA^+ in the gas phase.

Our present modeling study demonstrates that the FAB mass spectrometry data on the relative stabilities of the $2TMA^+ \bullet Cl^-$ and $2TMA^+ \bullet [DHB–H]^-$ supramolecular complexes agree with the stabilities obtained by the quantum chemical calculations performed in vacuum. This shows that the thermodynamic stability is an important feature of gas-phase processes providing the survival of ions of supramolecular complexes under the FAB mass spectrometry conditions.

4 Conclusions

The interaction of TMA^+ cations with an inorganic chlorine anion and an organic 2,5-dihydroxybenzoic acid anion have been studied by FAB mass spectrometry and by quantum chemical calculations. Stable ions of several supramolecular complexes formed by TMA^+ cations and Cl^- and $[DHB–H]^-$ counterions have been registered in the FAB mass spectra of the tetramethylammonium chrolide/DHB mixture. The coexistence of the ions indicates that the organic and inorganic anions compete to bind TMA^+ in the studied samples. The much higher intensity of the peak due to the $2TMA^{2+} \bullet Cl^-$ complex ion than that of the peak due to the $2TMA^{2+} \bullet [DHB–H]^-$ ion in equimolar mixture of TMA chloride and DHB testifies to the higher stability of the former complex under the experimental mass spectrometry conditions.

The equilibrium geometries and the interaction energies of the most stable complexes registered in the experiment (these triple complexes were formed by two TMA^+ ions with the chlorine anion and the deprotonated DHB) have been studied using DFT/B3LYP/6-31++G** and MP2/6-31++G** methods in vacuum. Comparing the IE values of the $2TMA^+ \bullet Cl^-$ and $2TMA^+ \bullet [DHB–H]^-$ complexes obtained in the calculations demonstrates that the triple complexes of the quaternary ions with the inorganic counterion are more stable in vacuum than the complexes containing the deprotonated DHB. This finding agrees with the relative stability of the complexes found in the FAB experiment.

The results of this study allow us to elucidate the intermolecular interactions between quaternary compounds and active target groups of proteins. These interactions occur under the competition between these groups and the inorganic counterions to bind the quaternary agent.

Appendix

Table A.1. Cartesian coordinates of the optimized geometry of the $2TMA^{+}\bullet CL^{-}$ complex obtained at DFT/B3LYP/6-31++G level of theory.

Center number	Atomic number	Atomic type	Coordinates (Å)		
			X	Y	Z
1	6	0	–5.256639	–0.067838	0.003905
2	7	0	–3.756150	–0.019271	0.000396
3	6	0	–3.284261	1.265872	–0.638378
4	6	0	–3.235685	–0.084370	1.417765
5	1	0	–5.638443	0.784201	0.568040
6	1	0	–5.616087	–0.023676	–1.025039
7	1	0	–5.581112	–0.998427	0.471523
8	1	0	–2.191223	1.263668	–0.624767
9	1	0	–3.680246	2.103602	–0.062477
10	1	0	–3.662392	1.302137	–1.661139
11	1	0	–2.144171	–0.039910	1.374521
12	1	0	–3.571783	–1.019824	1.867428
13	1	0	–3.639332	0.763708	1.972930
14	6	0	–3.206027	–1.188937	–0.782126
15	1	0	–3.546934	–2.111466	–0.309900
16	1	0	–3.585070	–1.129402	–1.803539
17	1	0	–2.114798	–1.120174	–0.765044
18	17	0	0.000058	0.095927	–0.001296
19	7	0	3.756043	–0.019379	0.000489
20	6	0	3.239328	–0.348061	1.381440
21	1	0	2.146848	–0.313299	1.348661
22	1	0	3.589312	–1.344795	1.654691
23	1	0	3.631204	0.390567	2.082316
24	6	0	5.257152	–0.059887	–0.006617
25	1	0	5.587627	–1.061961	0.269997
26	1	0	5.614249	0.186010	–1.007589
27	1	0	5.636106	0.668016	0.712012
28	6	0	3.209060	–1.027097	–0.983375
29	1	0	3.581286	–0.775790	–1.977621
30	1	0	2.117887	–0.968046	–0.948063
31	1	0	3.557302	–2.019238	–0.692590
32	6	0	3.277206	1.359060	–0.390863
33	1	0	2.184152	1.350470	–0.373078
34	1	0	3.674673	2.079260	0.325734
35	1	0	3.649902	1.581696	–1.391670

Table A.2. Cartesian coordinates of the optimized geometry of the $2TMA^{+}\bullet[DHB–H]^{-}$ complex obtained at DFT/B3LYP/6-31++G level of theory.

Center number	Atomic number	Atomic type	Coordinates (Å)		
			X	Y	Z
1	6	0	2.387738	2.081861	1.375623
2	6	0	1.396264	1.110498	1.171266
3	6	0	0.447081	1.285273	0.139855
4	6	0	0.515771	2.435711	–0.665505
5	6	0	1.508892	3.389449	–0.463838
6	6	0	2.446709	3.210461	0.564490
7	1	0	3.094398	1.947077	2.188781
8	1	0	–0.231649	2.551906	–1.446138
9	1	0	3.206242	3.969537	0.721870
10	6	0	–0.641362	0.266728	–0.089954
11	8	0	–0.571313	–0.819513	0.606739
12	8	0	–1.550557	0.513983	–0.917576
13	8	0	1.376640	0.003676	1.970251
14	8	0	1.629556	4.524514	–1.227805
15	1	0	0.910535	4.570528	–1.871416
16	7	0	–4.664086	–0.613236	0.005120
17	6	0	–4.297587	–0.917934	–1.428486
18	1	0	–4.455119	–1.983226	–1.604409
19	1	0	–4.945733	–0.332216	–2.082378
20	1	0	–3.249405	–0.637943	–1.564448
21	6	0	–4.438980	0.857695	0.265360
22	1	0	–5.114140	1.428108	–0.374487
23	1	0	–4.657361	1.061967	1.314517
24	1	0	–3.398770	1.083594	0.022060
25	6	0	–6.104530	–0.956542	0.252672
26	1	0	–6.350873	–0.730784	1.291177
27	1	0	–6.255633	–2.019155	0.058390
28	1	0	–6.731776	–0.364169	–0.414738
29	6	0	–3.780676	–1.426922	0.921869
30	1	0	–3.980001	–2.483748	0.735596
31	1	0	–2.730560	–1.195050	0.717337
32	1	0	–4.035425	–1.179266	1.953612
33	1	0	0.561801	–0.505892	1.650788
34	7	0	3.193343	–2.389124	–0.395935
35	6	0	4.133258	–3.381634	–1.023207
36	1	0	4.052745	–4.330397	–0.491478
37	1	0	3.860534	–3.517542	–2.070469
38	1	0	5.152536	–3.000402	–0.950369
39	6	0	3.293375	–1.072506	–1.126618
40	1	0	3.024692	–1.231569	–2.171716
41	1	0	2.611242	–0.358084	–0.666064
42	1	0	4.319351	–0.709578	–1.054184
43	6	0	1.776710	–2.906994	–0.487253
44	1	0	1.085710	–2.178205	–0.054029
45	1	0	1.721697	–3.852347	0.054422
46	1	0	1.537574	–3.066897	–1.539732
47	6	0	3.566118	–2.187159	1.054974
48	1	0	3.479995	–3.145697	1.568659
49	1	0	4.597021	–1.832959	1.099291
50	1	0	2.888270	–1.450259	1.494903

References

1. A. Vievskiy, *Mechanisms of biological activity of cationic surface active compounds (in Russian)* (Moscow University, Moscow, 1991)
2. V.A. Pashynskaya, M.V. Kosevich, A. Gomory, O.V. Vashchenko, L.N. Lisetski, Rapid Commun. Mass Spectrom. **16**, 1706 (2002)
3. V.A. Pashynska, M.V. Kosevich, H. Van den Heuvel, F. Cuyckens, M. Claeys, Biophysical Bulletin **14**, 123 (2004)
4. V.A. Pashynska, M.V. Kosevich, A. Gomory, Z. Szilagyi, K. Vekey, S.G. Stepanian, Rapid Commun. Mass Spectrom. **19**, 785 (2005)
5. V.A. Pokrovsky, M.V. Kosevich, V.L. Osaulenko, V.V. Chagovets, V.A. Pashynska, V.S. Shelkovsky, V.A. Karachevtsev, A.Yu. Naumov, Mass-Spectrometria **2**, 1 (2005)
6. V.A. Pashynska, M.V. Kosevich, S.G. Stepanian, Visnyk Problem Biology i Medicine **9**, 118 (1999) (in Russian)
7. M.V. Kosevich, O.A. Boryak, V.V. Chagovets, V.A. Pashynska, V.V. Orlov, S.G. Stepanian, V.S. Shelkovsky, Rapid Commun. Mass Spectrom. **21**, 1813 (2007)
8. J.M. Llinares, D. Powell, K. Bowman-James, Coord. Chem. Rev. **240**, 57 (2003)
9. J. De Mendoza, V. Alcázar, E. Botana, A. Galán, G. Lu, J.O. Magrans, M. Martín-Portugués, P. Prados, A. Salmerón, J. Sánchez-Quesada, C. Seel, M. Segura, Pure Appl. Chem. **69**, 577 (1997)
10. C.A. Hunter, Angew. Chem. Int. Ed. Engl. **40**, 5310 (2004)
11. V. Pashynska, M. Kosevich, S. Stepanian, L. Adamowicz, J. Mol. Struct. Theochem **815**, 55 (2007)
12. A.D. Becke, Phys. Rev. B **38**, 3098 (1988)
13. C. Lee, W. Yang, R.G. Parr, Phys. Rev. B **37**, 785 (1988)
14. S.H. Vosko, L. Wilk, M. Nusair, Can. J. Phys. **58**, 1200 (1980)
15. S.F. Boys, F. Bernardi, Molec. Phys. **19**, 553 (1970)
16. M.J. Frisch, G.W. Trucks, H.B. Schlegel, G.E. Scuseria, M.A. Robb, J.R. Cheeseman, J.A. Montgomery, J.T. Vreven, K.N. Kudin, J.C. Burant, J.M. Millam, S.S. Iyengar, J. Tomasi, V. Barone, B. Mennucci, M. Cossi, G. Scalmani, N. Rega, G.A. Petersson, H. Nakatsuji, M. Hada, M. Ehara, K. Toyota, R. Fukuda, J. Hasegawa, M. Ishida, T. Nakajima, Y. Honda, O. Kitao, H. Nakai, M. Klene, X. Li, J.E. Knox, H.P. Hratchian, J.B. Cross, V. Bakken, C. Adamo, J. Jaramillo, R. Gomperts, R.E. Stratmann, O. Yazyev, A.J. Austin, R. Cammi, C. Pomelli, J.W. Ochterski, P.Y. Ayala, K. Morokuma, G.A. Voth, P. Salvador, J.J. Dannenberg, V.G. Zakrzewski, S. Dapprich, A.D. Daniels, M.C. Strain, O. Farkas, D.K. Malick, A.D. Rabuck, K. Raghavachari, J.B. Foresman, J.V. Ortiz, Q. Cui, A.G. Baboul, S. Clifford, J. Cioslowski, B.B. Stefanov, G. Liu, A. Liashenko, P. Piskorz, I. Komaromi, R.L. Martin, D.J. Fox, T. Keith, M.A. Al-Laham, C.Y. Peng, A. Nanayakkara, M. Challacombe, P.M.W. Gill, B. Johnson, W. Chen, M.W. Wong, C. Gonzalez, J.A. Pople, *Gaussian 03, Revision E.01.* (Gaussian Inc., Pittsburgh PA, 2003)
17. A.N. Barrett, G.C.K. Roberts, A.S.V. Burgen, G.M. Clore, Mol. Pharm. **24**, 443 (1983)
18. L.F. Sukhodub, M.V. Kosevich, V.S. Shelkovsky, Yu.L. Volyansky, Antibiotiki i Chimiotherapia **34**, 823 (1989) (in Russian)
19. L.F. Sukhodub, M.V. Kosevich, V.S. Shelkovsky, O.A. Boryak, Yu.L. Volyansky, V.I. Moleva, T.A. Chumachenko, Antibiotiki and Chimiotherapia **35**, 10 (1989) (in Russian)
20. M.V. Kosevich, V.A. Pashinskaya, S.G. Stepanian, V.S. Shelkovsky, V.V. Orlov, Yu.P. Blagoy, Biophysical Bulletin **1**, 22 (1999)

ISSN 0233-7657. Biopolymers and Cell. 2009. Vol. 25. N 6

Mass spectrometric study of rhamnolipid biosurfactants and their interactions with cell membrane phospholipids

V. A. Pashynska

B. Verkin Institute for Low Temperature Physics and Engineering of the National Academy of Sciences of Ukraine
47, Lenin Ave., Kharkiv, Ukraine, 61103

vlada@vl.kharkov.ua

Aim. *To examine the formation of supramolecular complexes of biogenous rhamnolipids with membrane phospholipids that is considered as a molecular mechanism of the biosurfactants antimicrobial action.* ***Method***. *In the present work rhamnolipid biosurfactant samples produced by Pseudomonas sp.* PS-17 *strain have been investigated by electrospray ionization mass spectrometry for the first time.* ***Results***. *As a result of the study, characteristic mass spectra of the rhamnolipid samples were obtained, that can be used as reference spectra for mass spectrometric identification of the compounds in any biological or industrial samples. At the next stage of the experiments the pair systems, containing the biosurfactants and a membrane phospholipid dipalmitoylphosphatidylcholine, have been tested. The cationized noncovalent complexes of the rhamnolipids with the phospholipid were observed in the spectra.* ***Conclusions***. *The results obtained testify to the consideration that rhamnolipids (similar to other membranotropic agents) can form stable supramolecular complexes with membrane phospholipids that are able to evoke the biosurfactants antimicrobial action. A great potential of electrospray ionization mass spectrometry for the biosurfactants identification and study has been demonstrated in the work.*

Keywords: rhamnolipids, phospholipids, mass spectrometry, electrospray ionization (ESI), noncovalent complexes.

Introduction. Surface active compounds of natural or biotechnological origins including rhamnolipids, being widely investigated in a number of studies [1–8], are perspective antimicrobial agents for application in modern technologies in pharmacology, cosmetology, food industry and agriculture. The biogenic surfactants are produced by special strains of microorganisms or plants [1–3, 7]. The advantages of these surfactants as compared with synthetic ones are non-toxicity, biodegradability and ecological safety. Biosurfactants belong to the class of amphiphilic compounds the molecules of which contain hydrophobic and hydrophilic parts. Owing to the unique physicochemical properties, these compounds reveal membranotropic activity [4, 8], and, therefore, the considered molecular mechanism of the surfactants antimicrobial action is their interaction with bacterial membrane structures [6]. In the present work the samples of rhamnolipid biosurfactants produced by *Pseudomonas* sp. PS-17 have been investigated by electrospray ionization (ESI) mass spectrometry (MS) for the first time.

Materials and Methods. The samples of biosurfactants studied – mono- (RL1) and di- (RL2) rhamnolipids – were obtained from the Department of Physical Chemistry of Combustive Minerals, Institute of Physical-Organic Chemistry, NAS of Ukraine, Lviv. The rhamnolipid biosurfactants were produced naturally by a bacterial strain *Pseudomonas* sp. PS-17 and obtained by the method described in [9]. The extracted mixture of di- and monorhamnolipids was separated by thin layer chromatography. However the final sample of RL1 contained an admixture of RL2 and vice versa that

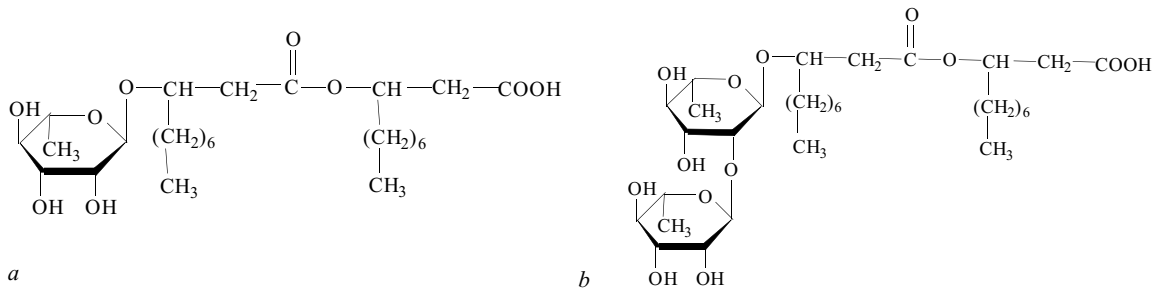

Scheme. Rhamnolipid RL1 (*a*) and Rhamnolipid RL2 (*b*)

was shown in the MS spectra. The structures of mono- and dirhamnolopids, L-Rhamnosyl-β-hydroxydecanoyl-β-hydroxydecanoate (RL1, M_r = 504 Da) and L-Rhamnosyl-L-rhamnosyl-β-hydroxydecanoyl-β-hydroxydecanoate (RL2, M_r = 650 Da), are presented in the Scheme *a* and *b*, respectively.

Methanol (Super grade), being used as a solvent, was purchased from Lab-Scan (Ireland).

The synthetic phospholipid dipalmitoylphosphatidylcholine ($C_{40}H_{80}NO_8P$, M_r = 734 Da) was purchased from ALSI, the company distributing the SIGMA-ALDRICH products in Ukraine (Kyiv, Ukraine).

MS data were obtained in the positive ion mode, using a mass spectrometer API 2000 quadrupole HPLC-MS/MS (Perkin Elmer Sciex, Canada) equipped with the Turbo IonSpray source. This source was operated in the standard ESI mode. The ESI source temperature was set to 200 °C. Curtain gas (N2) back pressure of 0.14 MPa (20 units), nebulizer gas (N2) of 0.42 MPa (60 units) and turbo gas (N2) of 0.21 MPa (30 units) were applied. Ion source capillary voltage was set to 4 kV. The typical declustering potential value was 35 V, focusing potential value –200 V and entrance potential –10 V. ESI spectra were recorded in the mass range of *m/z* 100–4000. Data acquisition and processing were performed using Analyst 1.4.1 software.

Results and Discussion. At the first stage of the study solutions of the samples of RL1 and RL2 in methanol with the final concentration of 250 μM were investigated by ESI MS and characteristic spectra of the biosurfactants were obtained. The spectra registered are in a good agreement with the MS spectra of rhamnolipid samples produced by another strains of microorganisms and investigated in [10, 11]. The peaks of cationized molecules of rhamnolipids were registered in our spectra: $[RL1:Na]^+$ at *m/z* 527, relative abundance (RA) 100 %, $[RL1:K]^+$ at *m/z* 543, RA 19 % for the monorhamnolipid (Fig. 1, *A*); $[RL2:Na]^+$ at *m/z* 673, RA 100 %, $[RL2:K]^+$ at *m/z* 689, RA 39 % for the dirhamnolipid (Fig. 1, *B*). Cationization as a way of ion formation is characteristic for the electrospray method of ionization [10, 12]. These peaks of the compounds can be used as reference peaks to reveal rhamnolopids in any biological samples or biotechnological products by ESI MS method and to study the compounds interactions with target biological molecules.

At the next stage of the experiments the interaction of these biosurfactants with membrane phospholipid dipalmitoylphosphatidylcholine (PL) was examined. The spectra of the systems RL1 + PL (1:1) (Fig. 2, *A*) and RL2 + PL (1:1) (Fig. 2, *B*) contain ions related to the individual components of the mixtures, namely the peaks of the above cationized rhamnolipid molecules and the peaks originated from PL: $[PL:H]^+$ at *m/z* 735, $[PL:Na]^+$ at *m/z* 757, $[PL:K]^+$ at *m/z* 773.

However, the most interesting result from the biophysical point of view relates to the observation in the spectra of the ions of noncovalent complexes of the rhamnolipids with the phospholipid molecules: $[RL1:PL:Na]^+$ at *m/z* 1261, RA 8 %; $[RL1:PL:K]^+$ at *m/z* 1277 with RA 4 % for RL1 (Fig. 2, *A*) and $[RL2:PL:Na]^+$, *m/z* 1407, RA 12 %; $[RL2:PL:K]^+$, *m/z* 1423, RA 4 % for RL2 (Fig. 2, *B*). The experimental detection of the stable cationized supramolecular complexes of rhamnolipid and phospholopid molecules in the mass spectra is a nontrivial result which confirms a high stability of the complexes being sprayed from the solution under high ion source capillary voltage (4 kV).

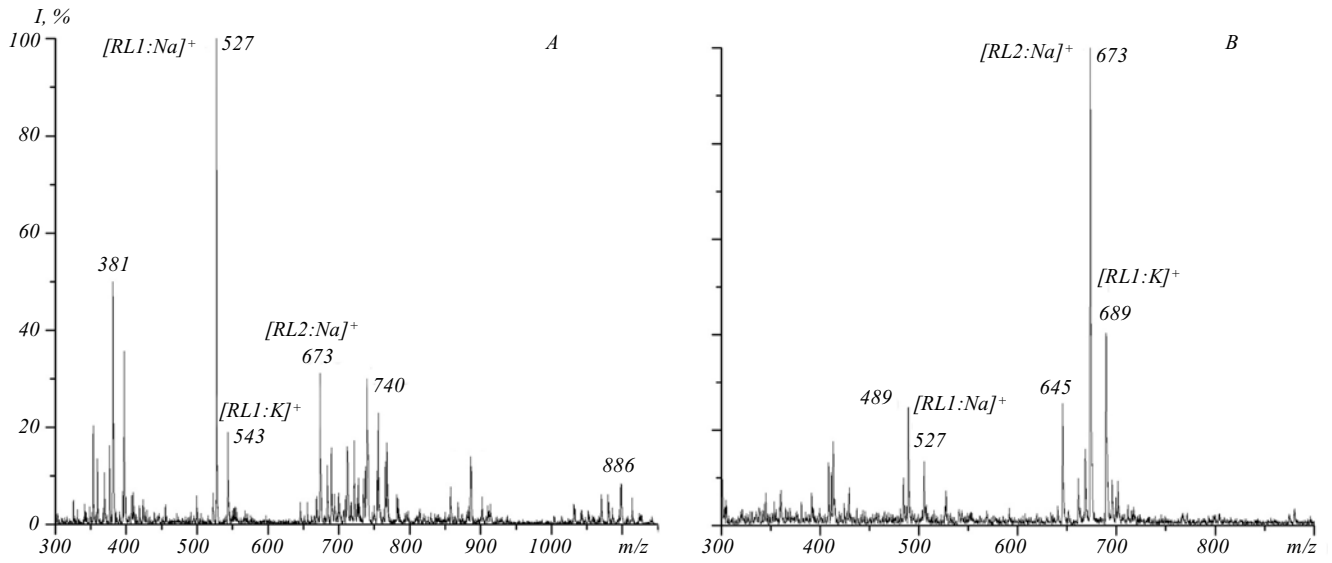

Fig. 1. ESI mass spectra of RL1 (*A*) and RL2 (*B*) sample

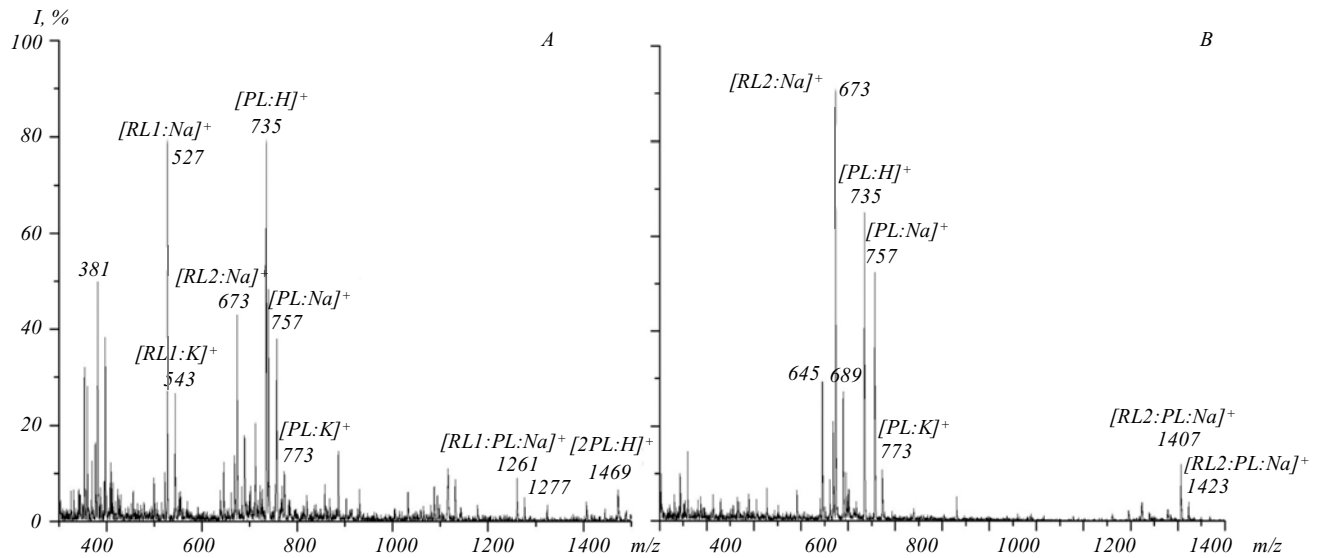

Fig. 2. ESI mass spectra of the RL1 + PL (*A*) and RL2 + PL (*B*) mixture in MeOH

In ESI MS, which is widely used for investigating noncovalent complexes, it is assumed that the ions of supramolecular complexes registered in the spectra reflect the composition of the liquid sample and can be used to characterize the complexation processes occurring in the solution [12]. The formation of the noncovalent complexes of membranotropic rhamnolipids with membrane phospholipids is considered as a possible molecular mechanism of antimicrobial activity of the biosurfactant studied. The supramolecular complexes of the rhamnolipids with phospholipids can affect the liquid-crystalline state of the membrane lipid matrix of microorganisms and disturb some membrane processes, including cells transport and breathing, like it was reported for another membranothropic agent, bisquaternary ammonium compound decamethoxinum, having been studied in our previous investigations [13].

Conclusions. In the present study the biogenic rhamnolopid biosurfactants produced by *Pseudomonas* sp. PS-17 have been investigated by the ESI MS for the first time. In the spectra of rhamnolipid samples solutions in MeOH the intensive peaks of cationized molecules of the compounds were registered that demonstrates the great potential of ESI MS method for the identification of biosurfactants in different samples. As a result of the ESI MS investigation of the mixtures of rhamnolipids and dipalmitoylphosphatidylcholine (1:1), the cationized noncovalent complexes of the biosurfactant and phospholipid molecules were observed. The formation of stable supramolecular complexes of the membrane phospholipids with the biosurfactants revealed in the experiments is considered as the molecular mechanism of their antimicrobial activity.

Acknowledgements. The author acknowledges the Program of Cooperation between Ukrainian and Hungarian Academies of Sciences for the financial support of the visit to the Chemical Research Center in Budapest, where the experiments were done. The author is also grateful to Dr. O. Karpenko from the Department of Physical Chemistry of Combustive Minerals, Institute of Physical-Organic Institute, NAS of Ukraine, Lviv, for the rhamnolipid samples provided for the investigation.

В. А. Пашинська

Мас-спектрометричне дослідження рамноліпідних біосурфактантів та їхньої взаємодії з фосфоліпідами клітинних мембран

Резюме

***Мета**. Перевірити можливість формування супрамолекулярних комплексів біогенних рамноліпідів та мембранних фосфоліпідів, що розглядається як молекулярний механізм антимікробної дії цих біосурфактантів. **Методи**. У представленій роботі зразки рамноліпідних біосурфактантів, продуковані штамом Pseudomonas sp.* PS-17*, вперше досліджено за допомогою методу мас-спектрометрії з іонізацією електроспреєм. **Результати**. Отримано характеристичні мас-спектри рамноліпідів, які можна використовувати як референтні спектри для мас-спектрометричної ідентифікації цих сполук у різних біологічних та технологічних зразках. На наступному етапі експериментів вивчали парні системи зазначених біосурфактантів з мембранним фосфоліпідом дипальмітоїлфосфатидилхоліном. У спектрах зареєстровано катіонізовані нековалентні комплекси рамноліпідів з фосфоліпідом. **Висновки**. Одержані результати підтверджують можливість формування стабільних супрамолекулярних комплексів мембранних фосфоліпідів з рамноліпідами (так само, як і з іншими мембранотропними агентами), що пов'язують з антимікробною дією цих біосурфактантів. Показано перспективність використання методу мас-спектрометрії з іонізацією електроспреєм для ідентифікації та вивчення біосурфактантів.*

Ключові слова: рамноліпіди, фосфоліпіди, мас-спектрометрія, іонізація електроспреєм (ESI), нековалентні комплекси.

В. А. Пашинская

Масс-спектрометрическое исследование рамнолипидных биосурфактантов и их взаимодействия с фосфолипидами клеточных мембран

Резюме

***Цель**. Проверить возможность формирования супрамолекулярных комплексов биогенных рамнолипидов и мембранных фосфолипидов, что рассматривается как молекулярный механизм антимикробной активности этих биосурфактантов. **Метод**. В настоящей работе образцы рамнолипидных биосурфактантов, продуцируемые штаммом Pseudomonas sp.* PS-17*, впервые изучены методом масс-спектрометрии с ионизацией электроспреем. **Результаты**. Получены характеристические масс-спектры рамнолипидов, которые можно использовать как референтные спектры для масс-спектрометрической идентификации этих соединений в различных биологических или технологических образцах. На следующем этапе экспериментов анализировали парные системы рамнолипидов и мембранного фосфолипида дипальмитоилфосфатидилхолина. В спектрах зарегистрированы катионизированные нековалентные комплексы рамнолипидов с фосфолипидом. **Выводы**. Полученные результаты подтверждают возможность образования стабильных супрамолекулярных комплексов мембранных фосфолипидов и рамнолипидов (подобно другим мембранотропным агентам), что связывают с антимикробным действием этих биосурфактантов. Показана перспективность использования метода масс-спектрометрии с ионизацией электроспреем для идентификации и изучения биосурфактантов.*

Ключевые слова: рамнолипиды, фосфолипиды, масс-спектрометрия, ионизация электроспреем (ESI), нековалентные комплексы.

REFERENCES

1. *Gautam K. K., Tyagi V. K.* Microbial surfactants: a review // J. Oleo Sci.–2006.–**55**, N 4.–P. 155–166.
2. *Rodrigues L., Banat I. M., Teixeira J., Oliveira R.* Biosurfactants: potential applications in medicine // J. Antimicrob. Chemother.–2006.–**57**, N 4.–P. 609–618.
3. *Nitschke M., Costa S. G., Contiero J.* Rhamnolipid surfactants: An update on the general aspects of these remarkable biomolecules // Biotechnol. Progr.–2005.–**21**, N 6.–P. 1593–1600.
4. *Vasileva-Tonkova E., Galabova D., Karpenko E., Shulga A.* Biosurfactant-rhamnolipid effects on yeast cells // Lett. Appl. Microbiol.–2001.–**33**, N 4.–P. 280–284.
5. *Karpenko E., Lisova N., Scheglova N., Vildanova R., Pokynbroda T., Hamkalo Z.* The perspectives of using ecologically safe biosurfactants for agriculture // Development in production and use of new agrochemicals.–Jesenik: «Czech-Pol Trade», 2003.–P. 1–7.

6. *Eliseev S. A., Kucher R. V.* Surface-active compounds and biotechnology.–Kiev: Nauk. dumka, 2001.–60 p.
7. *Pat*. of Ukraine N 10467 A, 1996. Strain *Pseudomonas* sp. PS-17-producer of extracellular biosurfactants and biopolymers / O. V. Karpenko, O. M. Shulga, S. A. Eliseev, N. S. Shcheglova, R. I. Vildanova-Martsishin // Bull. N 4, 1996.
8. *Solitova A., Spasova D., Galabova D., Karpenko E., Shulga A*. Rhamnolipid-biosurfactant permeabilizing effects on Gram-positive and Gram-negative bacterial strains // Curr. Microbiol.–2008.–**56**, N 6.–P. 639–644.
9. *Pat*. of Ukraine N 71792 A, 2004. Surface active biopreparation / E. V. Karpenko, N. B. Martynyuk, A. N. Shulga // Bull. N 12, 2004.
10. *Deziel E., Lepine F., Dennie D., Boismenu D., Mamer O. A., Villemur R.* Liquid chromatography/mass spectrometry analysis of mixtures of rhamnolipids produced by *Pseudomonas aeruginosa* strain 57 RP grown on mannitol or naphthalene // BBA-Molecular and Cell Biology of Lipids.–1999.–**1440**, N 2–3.–P. 244–252.
11. *Price N. P. J., Ray K. J., Vermillion K., Kuo T.-M.* MALDI-TOF mass spectrometry of naturally occurring mixtures of monorhamnolipids and dirhamnolipids // Carbohydrate Res.–2009.–**344**, N 2.–P. 204–209.
12. *Principles* mass spectrometry applied to biomolecules / Eds J. Laskin, C. Lifshitz.–New York: John Wiley and Sons, 2006.–687 p.
13. *Pashinskaya V. A., Kosevich M. V., Gomory A., Vashchenko O. V., Lisetski L. N.* Mechanistic investigation of the interaction between bisquaternary antimicrobial agents and phospholipids by liquid secondary ion mass spectrometry and differential scanning calorimetry // Rapid Commun. Mass Spectrom.–2002.–**16**, N 18.–P. 1706–1713.

УДК 577.32:615.28
Надійшла до редакції 13.08.09

https://doi.org/10.26565/2075-3810-2018-39-02
UDC 577.32:615.28:544.173

STUDY OF INTERMOLECULAR INTERACTIONS OF ANTIVIRAL AGENT TILORONE WITH RNA AND NUCLEOSIDES

V.A. Pashynska [1], N.M. Zholobak [2], M.V. Kosevich [1], A. Gomory [3], P.K. Holubiev [4], A.I. Marynin [4]

[1] *B. Verkin Institute for Low Temperature Physics and Engineering of the National Academy of Sciences of Ukraine, 47, Nauky Ave., Kharkov, 61103, Ukraine*
e-mail: pashynska@ilt.kharkov.ua
[2] *D.K. Zabolotny Institute of Microbiology and Virology of the National Academy of Sciences of Ukraine, 154, Acad. Zabolotnoho str., 03680, Kyiv, Ukraine*
e-mail: n.zholobak@gmail.com
[3] *Institute of Organic Chemistry of Research Centre for Natural Sciences of the Hungarian Academy of Sciences, Magyar tudosok korutja, 2, Budapest, H-1117, Hungary;*
[4] *National University of Food Technologies, 68, Volodymyrska str., 01601, Kyiv, Ukraine*
Submitted January 29, 2017
Accepted February 23, 2018

Background: While antiviral and interferon-inducing agent tilorone is used as a reactant of a number of popular pharmacological preparations, the molecular mechanisms of its biological antiviral activity are under discussions among the specialists. That is why the molecular level model studies of interactions of tilorone with targeting biomolecules and their components are considered to be urgent and useful for understanding the molecular mechanisms of the agent biological activity.
Objectives: The current model study is devoted to mechanistic examining of the intermolecular interactions of tilorone with its possible biomolecular targets which are believed to be nucleic acids and such their components as nucleosides containing purine or pyrimidine nitrogen bases.
Materials and methods: The objects of the study are model systems composed of tilorone dihydrochloride (Til•2HCl) and its potential targeting biomolecules: single-stranded RNA (ssRNA) obtained from *Saccharomyces cerevisiae* yeast or nucleosides - adenosine (Ado), thymidine (Thd), or uridine (Urd). Dynamic light scattering (DLS) measurements aimed at observation of drug-biomolecules aggregation is applied to the system (tilorone+ssRNA) (1:10 molar ratio) in RNA-free phosphate buffered saline solution (with 10% fetal bovine serum). Electrospray ionization (ESI) mass spectrometry is used to examine the intermolecular interactions in the binary (tilorone + nucleoside) (Ado, or Thd, or Urd in 1:10 molar ratio) and triple (tilorone + Ado + Urd) (1:10:10 molar ratio) systems dissolved in polar solvent methanol.
Results: The obtained DSL data demonstrate that under conditions similar to the physiological ones, introduction of tilorone into the ssRNA solution results in formation of tilorone+ssRNA aggregates which more than 10 times exceed in size the particles observed in the ssRNA solution itself. The ESI mass spectrometry experiments reveal that while the mass spectra of all studied (tilorone + nucleoside) model systems contain ions characteristic of the individual components of the mixtures, in the spectra of (tilorone + Urd) system the ions of stable ion-molecular clusters of uridine with tilorone dication Urd•Til•$2H^{2+}$ are recorded. The examining of the three-component model system (tilorone + Ado + Urd) testifies to the selectivity of tilorone binding: while the peak of noncovalent complex of Urd•Til•$2H^{2+}$ is detected, any peaks of the complexes of Ado with tilorone are not found in the mass spectrum.
Conclusions: Formation of large-scale molecular aggregates of tilorone with ssRNA in the solutions which are similar to the physiological solution in physical and chemical characteristics is revealed in the performed DLS investigation. Creation of stable Urd•Til•$2H^{2+}$ noncovalent complexes in (tilorone + nucleoside) model systems was demonstrated by ESI mass spectrometry, while the complexes of tilorone with Ado and Thd are not detected in the experiments. It testifies to the possibility of formation of stable noncovalent complexes of tilorone with ssRNA and their components in biological systems, and pointed at Urd as one of the potential centers of specific binding of RNA molecules with tilorone.
KEY WORDS: tilorone; RNA; nucleosides; intermolecular interactions; dynamic light scattering; mass spectrometry.

ВИВЧЕННЯ МІЖМОЛЕКУЛЯРНОЇ ВЗАЄМОДІЇ АНТИВІРУСНОГО АГЕНТУ ТИЛОРОНУ З РНК ТА НУКЛЕОЗИДАМИ

Пашинська В.А.[1], Жолобак Н.М.[2], Косевич М.В.[1], Гоморі А.[3], Голубєв П.К.[4], Маринін А. І.[4]

[1]Фізико-технічний інститут низьких температур ім. Б.І. Вєркіна Національної академії наук України, 47, пр. Науки, Харків, 61103, Україна

e-mail: pashynska@ilt.kharkov.ua

[2]Інститут мікробіології і вірусології ім. Д.К. Заболотного Національної академії наук України, 154, вул. Академіка Заболотного, Київ, 03680, Україна

e-mail: n.zholobak@gmail.com

[3] Інститут органічної хімії Наукового центру природничих наук Угорської академії наук, Magyar tudosok korutja, 2, Budapest, H-1117, Hungary;

[4] Національний університет харчових технологій, 68, вул. Володимирська, Київ, 0160, Україна

Актуальність. Незважаючи на застосування антивірусного та інтерферон-індукуючого агенту тилорону в якості діючої речовини ряду сучасних фармакологічних препаратів, молекулярні механізми його антивірусної дії залишаються предметом наукової дискусії. Тому дослідження на молекулярному рівні взаємодії тилорону з біомолекулами-мішенями та їх компонентами є актуальними та важливими з точки зору встановлення молекулярних механізмів його біологічної активності.

Мета роботи. Метою роботи стало вивчення міжмолекулярних взаємодій тилорону з потенційними біомолекулами-мішенями: нуклеїновими кислотами та їх компонентами – нуклеозидами, що можуть містити, як пуринові, так і піримідинові азотисті основи.

Матеріали і методи. Об'єктами дослідження було обрано модельні системи, що містили тилорону дигідрохлорид та потенційні молекули-мішені одноланцюгові РНК (ssRNA), які було отримано з дріжджів *Saccharomyces cerevisiae*, або нуклеозиди: аденозин (Ado), тимідин (Thd), чи уридин (Urd). Маючи за мету вивчення можливої агрегації тилорону з біомолекулами, методом динамічного розсіювання світла було досліджено систему (тилорон+РНК) (молярне співвідношення компонентів 1:10) у розчині, в складі якого – натрій-фосфатний буфер з додаванням 10% сироватки крові теляти. Метод мас-спектрометрії з іонізацією електророзпиленням було застосовано для дослідження міжмолекулярних взаємодій в модельних бінарних системах (тилорон+нуклеозид) (Ado або Thd, або Urd, молярне співвідношення 1:10) та трьохкомпонентній системі (тилорон + Ado + Urd) (молярне співвідношення 1:10:10), які було розчинено в полярному розчиннику – метанолі.

Результати. Дані, отримані методом динамічного розсіювання світла, свідчать, що в умовах, наближених до фізіологічних, введення тилорону у розчин РНК призводить до формування в системі молекулярних агрегатів тилорон+ssRNA, які у 10 разів перевищують за розміром частинки, присутні у вихідному розчині РНК. Результати мас-спектрометричного експерименту показують, що мас-спектри усіх досліджених бінарних систем (тилорон+нуклеозид) містять піки іонів, які характерні для індивідуальних компонентів сумішей, а в спектрі системи (тилорон + Urd) поряд з вищезазначеним реєструється досить інтенсивний сигнал стабільного іон-молекулярного кластеру Urd•Til•$2H^{2+}$. Мас-спектрометричне дослідження трьохкомпонентної модельної системи (тилорон + Ado + Urd) підтвердило дані щодо можливої вибірковості зв'язування тилорону з нуклеозидами, оскільки при наявності у спектрі сигналу нековалентного комплексу Urd•Til•$2H^{2+}$ піки кластерів Ado з тилороном в спектрі не виявлено.

Висновки. Методом динамічного розсіювання світла показано формування великорозмірних молекулярних агрегатів тилорону з РНК у розчині, який за фізико-хімічними параметрами наближений до фізіологічного. В дослідженнях методом мас-спектрометрії з іонізацією електророзпиленням виявлено утворення стабільних нековалентних комплексів Urd•Til•$2H^{2+}$ в модельних системах (тилорон + нуклеозид), утворення комплексів тилорону з Ado чи Thd не зареєстровано. Отримані дані свідчать про можливість формування стабільних нековалентних комплексів тилорону з одноланцюговими РНК та їх компонентами в біологічних системах та вказують на Urd як на один з потенційних центрів специфічного зв'язування молекул РНК з тилороном.

КЛЮЧОВІ СЛОВА: тилорон; РНК; нуклеозиди; міжмолекулярна взаємодія; динамічне розсіювання світла; мас-спектрометрія.

ИЗУЧЕНИЕ МЕЖМОЛЕКУЛЯРНОГО ВЗАИМОДЕЙСТВИЯ ПРОТИВОВИРУСНОГО АГЕНТА ТИЛОРОНА С РНК И НУКЛЕОЗИДАМИ

Пашинская В.А.[1], Жолобак Н.М.[2], Косевич М.В.[1], Гомори А.[3], Голубев П.К.[4], Маринин А.И.[4]

[1]Физико-технический институт низких температур им. Б.И. Веркина Национальной академии наук Украины,
47, пр. Науки, Харьков, 61103, Украина, pashynska@ilt.kharkov.ua;
[2]Институт микробиологии и вирусологии им. Д.К. Заболотного Национальной академии наук Украины, 154, ул. Академика Заболотного, Киев, 03680,Украина, n.zholobak2018@gmail.com;
[3] Институт органической химии Научного центра естественных наук Венгерской академии наук, Magyar tudosok korutja, 2, Budapest, H-1117, Hungary;
[4] Национальный университет пищевых технологий, 68, ул. Владимирская, Киев, 0160, Украина

Актуальность. Несмотря на использование противовирусного и интерферон-индуцирующего агента тилорона в качестве действующего вещества ряда современных фармакологических препаратов, молекулярные механизмы его антивирусного действия остаются предметом научной дискуссии. Поэтому исследования на молекулярном уровне взаимодействий тилорона с потенциальными биомолекулами-мишенями и их компонентами являются актуальными и важными для определения молекулярных механизмов его биологической активности.

Цель работы. Целью настоящей работы стало изучение межмолекулярного взаимодействия тилорона с потенциальными биомолекулами-мишенями: нуклеиновыми кислотами и их компонентами нуклеозидами, содержащими как пуриновые, так и пиримидиновые азотистые основания.

Материалы и методы. Объектами исследования были выбраны модельные системы, состоявшие из дигидрохлорида тилорона и его потенциальных молекул-мишеней одноцепочечных РНК (ssRNA), полученных из дрожжей *Saccharomyces cerevisiae*, или нуклеозидов: аденозина (Ado), тимидина (Thd), или уридина (Urd). С целью изучения возможной агрегации тилорона с биомолекулами методом динамического светорассеяния была исследована система (тилорон + РНК) (молярное соотношение компонентов 1:10) в растворе натрий-фосфатного буфера с добавлением 10% сыворотки крови телят. Метод масс-спектрометрии с ионизацией электрораспылением был использован для исследования межмолекулярных взаимодействий в модельных бинарных системах (тилорон+нуклеозид) (Ado или Thd, или Urd, молярное соотношение 1:10) и трехкомпонентной системе (тилорон + Ado + Urd) (молярное соотношение 1:10:10), растворенных в полярном растворителе метаноле.

Результаты. Данные, полученные методом динамического светорассеяния, свидетельствуют, что в условиях, приближенных к физиологическим, введение тилорона в раствор РНК вызывало формирование в модельной системе агрегатов тилорон+ssRNA, которые более чем в 10 раз превышали по размеру частицы, присутствовавшие в исходном растворе РНК. Экспериментальные результаты, полученные методом масс-спектрометрии, демонстрируют, что масс-спектры всех исследованных бинарных систем (тилорон+нуклеозид) содержат пики ионов, характерных для индивидуальных компонентов смеси, а в спектре системы (тилорон + Urd), наряду с этим, обнаружен достаточно интенсивный сигнал стабильного ион-молекулярного кластера Urd•Til•2H^{2+}. Масс-спектрометрическое исследование трехкомпонентной модельной системы (тилорон + Ado + Urd) подтвердило данные о возможной селективности связывания тилорона с нуклеозидами, поскольку при наличии в спектре системы пика нековалентного комплекса Urd•Til•2H^{2+} пики кластеров Ado с тилороном в спектре не обнаружены.

Выводы. Методом динамического светорассеяния показано формирование крупных молекулярных агрегатов тилорона с РНК в растворе, близком по физико-химическим параметрам к физиологическому. В исследованиях методом масс-спектрометрии с ионизацией электрораспылением продемонстрировано образование стабильных нековалентных комплексов Urd•Til•2H^{2+} в модельных системах (тилорон + нуклеозид). Комплексы тилорона с Ado и Thd в спектрах не зарегистрированы. Полученные данные свидетельствуют о возможности формирования стабильных нековалентных комплексов тилорона с одноцепочечными РНК и их компонентами в биологических системах и указывают на Urd как на один из потенциальных центров специфического связывания молекул РНК с тилороном.

КЛЮЧЕВЫЕ СЛОВА: тилорон; РНК; нуклеозиды; межмолекулярные взаимодействия; динамическое светорассеяние; масс-спектрометрия.

Tilorone is known as an effective antiviral and interferon-inducing agent from the seventies of the last century [1-3]. Tilorone is a reactant of the national pharmaceutical preparation Amixin IC (InterChem SLC, Odessa, Ukraine) and some other preparations which

are widely used in the treatment of a number of viral infections and some other diseases [4-8]. The interferon-inducing action of tilorone and, in particular, stimulation of synthesis of all three types of interferon in a human body is considered as the basic mechanism of the preparation activity [9].

However, in spite of active usage of tilorone in medical practice in Ukraine and some others FSU countries, the discussions about its efficiency and investigations of its pharmacological activity as well as toxicity are currently continued [10-12]. For example, there is investigation testified to miscoordination of interferon-inducing and antiviral effects of tilorone [13]. The problem of molecular mechanisms of antiviral tilorone activity is remaining open since it is still not clear whether this activity is related just to interferon-inducing activity or it is also connected with other intracellular cascade reactions and intermolecular interactions. That is why the molecular level model studies of interactions of tilorone with potential targeting biomolecules and their components are considered to be helpful in understanding the molecular mechanisms of the agent biological activity, which is necessary for development of more efficient and less toxic medicines. In particular, one of the existing hypotheses about nucleic acids and their constituents as potential molecular targets for tilorone binding requires experimental confirmation.

The current study is devoted to examining the mechanistic intermolecular interactions of tilorone with its possible molecular targets in the viral and host cells, which are believed to be RNA and nucleosides. An experimental investigation of biologically significant intermolecular interactions of tilorone with ssRNA and a number of nucleosides (adenosine (Ado), thymidine (Thd), and uridine (Urd)) has been performed by dynamic light scattering (DLS) and electrospray (ESI) ionization mass spectrometry methods.

MATERIALS AND METHODS

Materials

Tilorone – 2,7-bis[2-(diethylamino)ethoxy]-9-fluorenone dihydrochloride from the Sigma-Aldrich company (Germany) was used in all experimental investigations. The chemical structure of tilorone dihydrochloride (Til•2HCl) is presented in Scheme 1.

Single-stranded RNA (ssRNA) for DLS experiments was obtained from *Saccharomyces cerevisiae* yeast as described in [14]. The following dilution buffer composition was used as a solvent: RNA-free phosphate buffered saline solution (PBS, Sigma, USA) and 10% (volume to volume) of fetal bovine serum (FBS, Sigma, USA), pH=7.4. After preparation of solutions of tilorone ($10\ g \cdot L^{-1}$ or $2.07 \cdot 10^{-2}\ mol \cdot L^{-1}$) and ssRNA ($8\ g \cdot L^{-1}$) in the above mentioned solvent, they were *ex tempore* filtered through 0.2 μm syringe filter Minisart® NML with surfactant-free cellulose acetate (SFCA) (Sartorius AG, Germany). The samples of the model system (tilorone + ssRNA) were prepared just before DLS measurements by mixing of the two solutions to obtain the final molar ratio of tilorone to ssRNA as 1:10.

Adenosine (Ado), thymidine (Thd), and uridine (Urd) nucleosides and methanol (MeOH) for mass spectrometric experiments were purchased from the Sigma-Aldrich company (Germany). Initial solutions of tilorone and nucleosides (5 mM) were prepared in methanol (polar solvent which is commonly used in ESI mass spectrometry) and used for preparation of binary (tilorone + nucleoside) (1:10 molar ratio) and triple (tilorone + Ado + Urd) (1:10:10 molar ratio) model systems. In our study we did not investigate the model systems including guanosine, since from our previous experimental experience we know that guanine derivatives have less solubility in polar solvents in comparison with other nucleosides. It could result in distortion of mass spectrometric information about intermolecular interactions in the multicomponent model systems containing guanosine.

The mixtures were kept at the room temperature for at least 10 minutes before the ESI mass spectrometric analysis. The spraying procedure required dilution of the solutions to be studied to the final 250 μM concentration of the diluted components of the model systems in each solution.

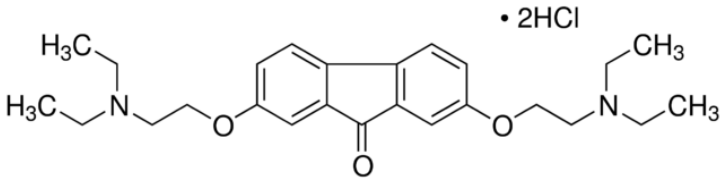

Scheme 1. Tilorone dihydrochloride (Til•2HCl) chemical structure (adapted from the web site of the Sigma-Aldrich supplier https://www.sigmaaldrich.com/catalog/product/aldrich/220957?lang=en&region=UA).

Dynamic light scattering

Dynamic light scattering (DLS) method, which is also known as photon correlation spectroscopy, is a powerful tool for studying the size distribution of molecular particles, and in particular their aggregates, basing on their diffusion behavior in solution. The diffusion coefficient, and hence the hydrodynamic radii calculated from it, depends on the size and shape of the particles present in solutions.

The particles sizes and distribution as well as polydispersity indexes (PdI) of solutions of ssRNA and (tilorone + ssRNA) mixture in the dilution buffer are measured using Malvern Zetasizer Nano-ZS instrument (Malvern Instruments Ltd., Malvern, UK) and analyzed by Zetasizer software (Malvern Instruments). For each sample a separate disposable polystyrene cuvette (Sarstedt AG & Co., Germany) is used. Water is used as a dispersant. All DSL measurements are carried out at a standard temperature of +25°C, and three measurements with at least 10 sub-runs are performed for each sample.

The Zetasizer software supplied with the instrument provides a number of analysis tools to study aggregation by the DLS. “Size Distribution by Intensity” and “Size Distribution by Volume” are the most widely used tools. The Size Distribution by Intensity method is suitable for detection of high molecular weight particles including aggregates, which scatter light disproportionately relative to smaller particles, enabling detection despite their relatively low concentration in a sample [15]. The Size Distribution by Volume method is used in our study with the aim to investigate of characteristics of the particles of ssRNA and aggregates in (tilorone + ssRNA) system in the dilution buffer.

ESI mass spectrometry

Electrospray ionization (ESI) mass spectra of the systems studied are obtained in the positive ion mode using triple quadrupole (QqQ) Micromass Quattro Micro mass spectrometer (Waters, Manchester, UK) equipped with the electrospray ion source. This source is operated in the standard ESI mode. The ESI source temperature is set to 120^{o}C and the desolvation temperature is 200^{o}C. The spraying capillary is operated at 3.5 kV. The cone voltage (CV) value of 10 V is used. The analyzed solutions (20 μL) are injected into the mass spectrometer at a constant flow rate of 0.2 mL•min^{-1} of methanol solvent. The ESI spectra are recorded in the mass range of *m/z* 100-2000. Data acquisition and processing are performed using MassLynx 4.1 software (Waters, Manchester, UK).

RESULTS AND DISCUSSION

DSL experimental study

DLS method was applied to examine the size characteristics of the particles present in solutions of ssRNA and (tilorone + ssRNA) system (1:10 molar ratio) in the dilution

buffer. The obtained (PdI) and Size Distribution by Intensity values are summarized in Table 1.

Table 1. Polydispersity Index (PdI), Size Distribution by Intensity and Z-Average data for solutions of ssRNA and (tilorone + ssRNA) in dilution buffer *

Parameter		ssRNA solution	(tilorone + ssRNA) system (1:10 molar ratio)
PdI		0.192±0.009	0.330±0.062
Size Distribution by Intensity			
Pk 1	Mean Int (d, nm)	152.6±1.99	1882±139.5
	Area Int (%)	100	75±18
Pk 2	Mean Int (d, nm)	–	5096±474.4
	Area Int (%)	–	25±18
Z-Ave	nm	126.43±1.63	not applicable

*Notes: the results are presented as Mean and St Deviation; the Size Distribution by Intensity data are represented as a certain number of peaks (Pk 1-2) corresponding to the populations of particles of certain size (Mean Int – d, nm) and their input into the total scattering intensity (Area Int – %). Z-Average size (Z-Ave) is harmonic intensity averaged particle diameter.

The summarized data on the particles Size Distribution by Volume are presented in Table 2.

Table 2. Particles Size Distribution by Volume in solutions of ssRNA and (tilorone + ssRNA)

Solutions	Particles Size Distribution (d, nm ± St Dev) by Volume
ssRNA	132.1±67.1
(tilorone + ssRNA)	1711.0±351.0

Statistic graphs of the particles size distributions in solutions of ssRNA and (tilorone + ssRNA) system by volume are presented in Fig. 1.

The experimental results demonstrate that ssRNA solution in the dilution buffer is quite monodisperse system, since it contains particles of similar sizes. Indeed, the mean diameter of these particles is between 150 and 154 nm and the size distribution is narrow, as is evidenced by the polydispersity index values (ranging from 0.18 to 0.20) (Table 1). The data obtained for PdI and Size Distribution by Intensity for the ssRNA solution most probably point to creation of similar sizes molecules aggregates of ssRNA with Bovine Serum Albumin (BSA) and/or other molecules existing in the used buffer solution (Pk1 in Table 1, peak in the statistic graph, Fig. 1). Value of Z-average (also known as the “cumulants mean”) testifies to the monodispersity of the ssRNA solution sample too.

Introduction of tilorone solution into the solution of ssRNA in the buffer resulted in almost twice reliable increase of PdI values (range of PdI value is 0.27 – 0.39) comparing with the values for the ssRNA solution itself. In the statistic graph of (tilorone + ssRNA) system (Fig. 1) there are two peaks showing the presence of two different size particles populations in the system. The first peak (which input into the total scattering intensity is 75%) is most probably related to aggregates of tilorone with the initial particles of ssRNA, and mean diameter of the aggregates is more than 10 times exceeds the mean diameter of the particles in the ssRNA solution itself. The second peak (with input into the total scattering intensity of 25%) is related to bigger aggregates of the system components (obviously, including BSA and other serum components) with the mean diameter ranging between 4.62 and 5.57 μm.

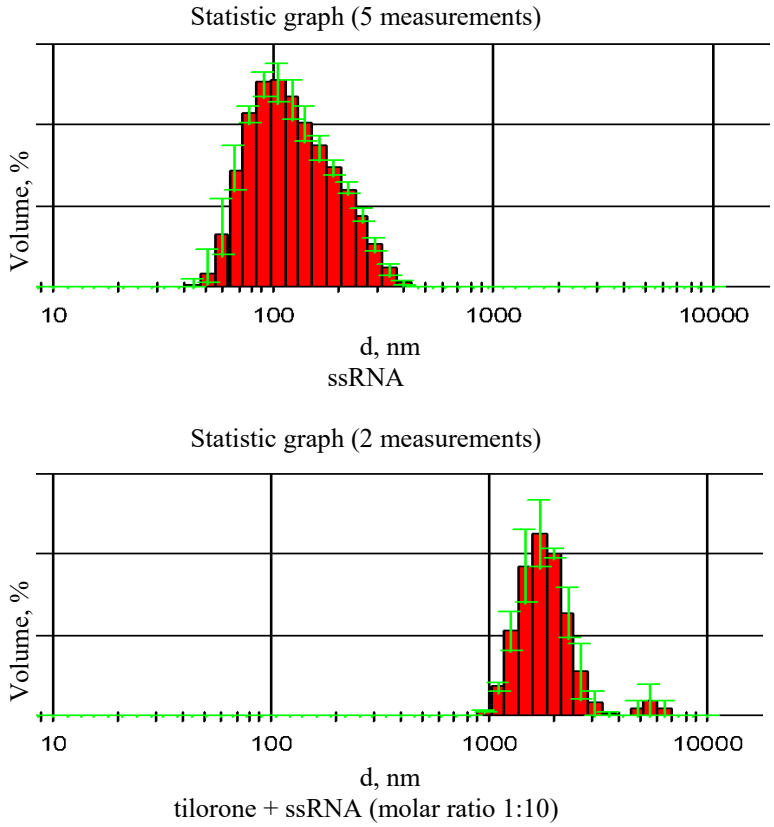

Fig. 1. Particles size distribution in solutions of ssRNA and (tilorone+ssRNA) system by volume. The results are presented as Mean with Max-Min error bar.

It should be noted that in our investigation, with the purpose of obtaining reliable results for sizes distribution and taking into account the ranges of the equipment sensitivity, we take solutions which contained more high concentrations of tilorone and ssRNA than usually are used for biological objects *in vitro* [16, 17].

Thus, the obtained DSL data demonstrate that under conditions similar to the physiological ones, the introduction of tilorone into the system of ssRNA solution in the buffer results in active aggregation of tilorone with the ssRNA particles and in enlargement of the aggregates likely contained tilorone, ssRNA and other components of the used dilution buffer. Earlier it was showed that (tilorone + ssRNA) complex with 1:10 components ratio demonstrated significant antiviral activity [16], and also induced interferon formation *in vitro* [17] as well as *in vivo* [18]. The data obtained in the current and earlier investigations are in a good agreement with the modern ideas about the effect of double-stranded allogenic RNA of different length on the formation of interferon-mediated or interferon independent antiviral resistance of the cells [19, 20].

To confirm the (tilorone + ssRNA) noncovalent complexation at the monomer level and with the purpose to find the possible RNA components which can be considered as centers of tilorone binding to the nucleic acid molecules, the following ESI mass spectrometry study of interactions of tilorone with nucleosides was performed.

ESI mass spectrometry investigations

At the first stage of the ESI mass spectrometric experimental study solution of tilorone in methanol was investigated. The characteristic mass spectrum of tilorone is presented in Fig. 2. It contains the abundant peak of the tilorone dication Til•$2H^{2+}$ (*m/z* 206.3) and set of clusters of tilorone with various number of protons and chlorine anions.

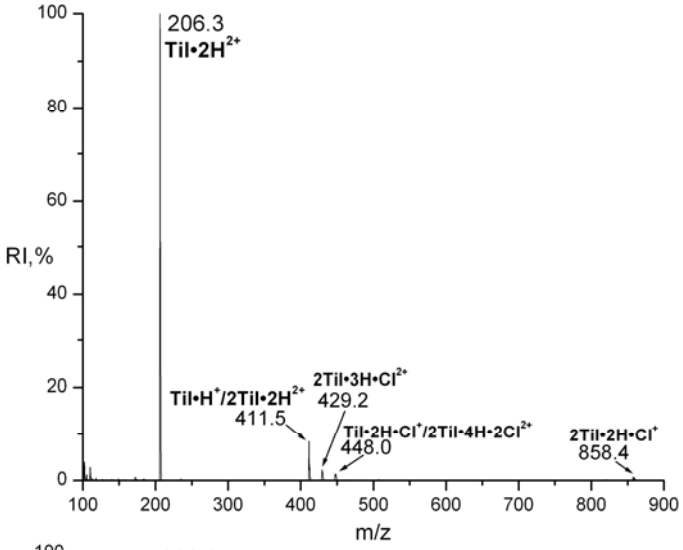

Fig. 2. Positive ion ESI mass spectrum of tilorone solution in methanol.

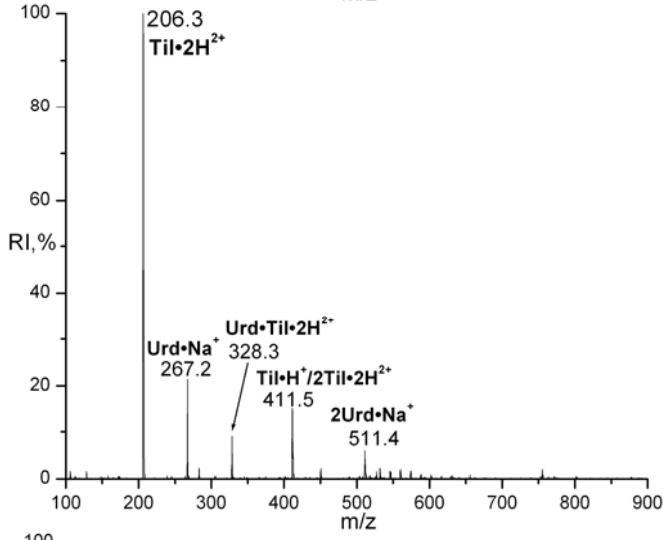

Fig. 3. ESI mass spectrum of (tilorone + Uridine) (1:10 molar ratio) model system in methanol solvent.

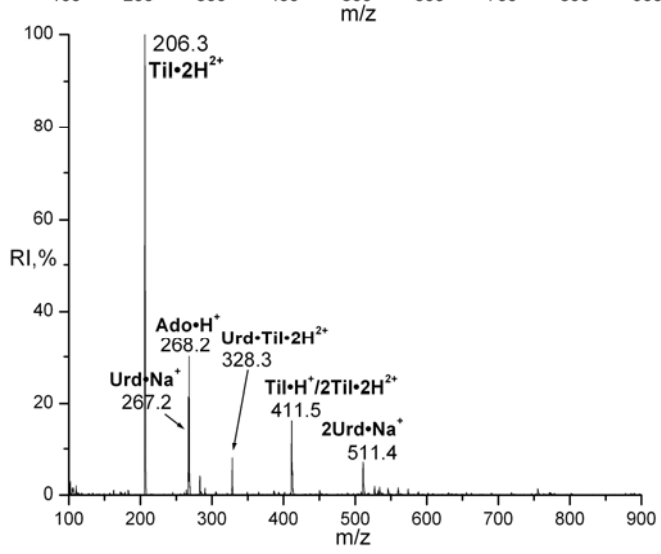

Fig. 4**.** ESI mass spectrum of (tilorone + Adenine + Uridine) (1:10:10) model system in methanol solvent.

At the next stage the intermolecular interactions of tilorone with selected nucleosides Ado, Thd, and Urd were examined by the ESI mass spectrometry probing of methanol solutions of (tilorone + nucleoside) mixtures in 1:10 molar ratio. In the current measurements, we applied the ESI approach, which we developed and effectively harnessed in our previous investigations [21-25] for the study of intermolecular interactions of biologically active compounds, including drugs, with the targeting biological molecules.

The mass spectra of all studied model systems (tilorone + nucleoside) contain ions characteristic of the individual components of the mixtures. At the same time, the most interesting result from the biophysical point of view relates to observation in the spectra of (tilorone + Urd) system (Fig. 3) the ions of stable ion-molecular clusters of uridine with tilorone dication. The presence of the peak of doubly charged ion Urd•Til•$2H^{2+}$ (*m/z* 328.3) with relative intensity about 10% in the ESI mass spectrum testifies to the formation of stable noncovalent complexes of uridine with tilorone in solution. It is notable that in the other model systems examined the formation of such complexes of tilorone with adenosine or thymidine is not detected by the ESI method.

To check the idea about selectivity of tilorone interaction with uridine we examined a three-component model system of (tilorone+Ado+Urd) (1:10:10 molar ration). The ESI mass spectrum of the triple system (Fig. 4) contains characteristic peaks of tilorone, adenosine, and uridine. The signal of the cluster of tilorone with uridine the peak of Urd•Til•$2H^{2+}$ at *m/z* 328.3 has been detected too, while the peak of the complex Ado•Til•$2H^{2+}$ with expected *m/z* 339.4 or other peaks of any noncovalent complexes of adenosine with tilorone have not been found in the spectrum.

To determine the structural and energetic parameters of the registered in the mass spectrometry experiments noncovalent complexes of tilorone with uridine we are planning to perform quantum-mechanical calculations in our following study, similarly to approach developed in [23-25]. However, right now we can suggest that registered Urd•Til•$2H^{2+}$ complexes can be stabilized by electrostatic interactions of partially negatively charged two carbonyl groups of uridine and positively charged quaternary ammonium groups of tilorone. The partially negatively charged carbonyl groups of thymidine may be less sterically accessible, because of methylation of C_5 of pyrimidine cycle in thymidine, that can cause less stability of noncovalent complexes of tilorone with thymidine (the complexes are not recorded in the mass spectrum). As for adenosine, in its structure there are no carbonyl groups with significant partial negative charge, and therefore electrostatic interactions of adenosine with positively charged protonated groups of tilorone will be weaker in comparison with the ones for uridine.

Taking into account that uridine is affiliated just with RNA (but not DNA) the obtained data testifies to the possible specificity of interactions of tilorone with the RNA (not DNA) components, which can be important for revealing the mechanisms of the tilorone biological activity.

CONCLUSIONS

The performed DLS investigations reveal the formation of large-scale molecular aggregates of tilorone with ssRNA in the buffer solution contained RNA-free phosphate buffered saline solution and 10% of fetal bovine serum, which is similar to the physiological solution in physical and chemical characteristics. The addition of tilorone into the ssRNA solution in the buffer in the molar ratio of 1:10 results in the formation of complexes of ssRNA particles with tilorone with the mean diameter of 10 times larger than the diameter of the particles in the ssRNA solution itself. We suggest that similar complexation of tilorone with ssRNA could take place in real biological systems and could provoke the tilorone antiviral effect as well as induce activation of interferon-mediated or interferon independent pathways of formation of antiviral resistance of the host cells.

The ESI mass spectrometric study of the model systems of (tilorone + nucleosides) (Ado, Urd, or Thd) demonstrates the formation of stable noncovalent complexes Urd•Til•$2H^{2+}$, while the complexes of tilorone with Ado and Thd are not detected in the experiments. It testifies to the possibility of formation of stable noncovalent complexes of tilorone with the RNA and their components in biological systems and pointed at Urd as one of the potential

centers of specific binding of tilorone to the RNA molecules. Such intermolecular interactions of tilorone with viral RNA and/or with RNA in the host cells could be considered as the molecular mechanism of antiviral activity of tilorone as well as the molecular basis of the possible drug toxicity for the host cells.

ACKNOWLEDGEMENTS

Authors acknowledge the program of cooperation between the National Academy of Sciences of Ukraine and Hungarian Academy of Sciences for the financial support of the visit to the Institute of Organic Chemistry of Research Center of Natural Sciences of the Hungarian Academy of Sciences in Budapest (Hungary), where the mass spectrometry experiments were done. Authors also thank Dr. Ivanov A. from B. Verkin Institute for Low Temperature Physics and Engineering of the National Academy of Sciences of Ukraine for the nucleosides samples providing.

CONFLICT OF INTERESTS

The authors declare that there is no conflict of interest.

Authors' ORCID ID

V.A. Pashynska https://orcid.org/0000-0001-9786-6828
N.M. Zholobak https://orcid.org/0000-0003-2792-9787
M.V. Kosevich http://orcid.org/0000-0003-0257-4588
P.K. Holubiev https://orcid.org/0000-0003-3437-4986
A.I. Marynin https://orcid.org/0000-0001-6692-7472

REFERENCES

1. Krueger R. E., Mayer G. D. Tilorone hydrochloride: an orally active antiviral agent // Science. 1970. Vol. 16(3951). P. 1213-1214. doi: 10.1126/science.169.3951.1213.
2. Mayer G. D., Krueger R. E. Tilorone hydrochloride: mode of action // Science. 1970. Vol. 169(3951). P. 1214-1215. doi: 10.1126/science.169.3951.1214
3. Stringfellow D. A., Glasgow L. A. Tilorone hydrochloride: an oral interferon-inducing agent // Antimicrobial Agents and Chemotherapy. 1972. Vol. 2(2). P. 73-78. doi: 10.1128/AAC.2.2.73
4. Ekins S., Lingerfelt M. A., Comer E. A., Freiberg A. N., Mirsalis J. C., O'Loughlin K., Harutyunyan A., McFarlane C., Green C. E., Madrid P. B. Efficacy of Tilorone Dihydrochloride against Ebola Virus Infection // Antimicrobial Agents and Chemotherapy. 2018. Vol.62(2). pii: e01711- e01717. doi:10.1128/AAC.01711-17
5. Калюжин О. В. Тилорон как средство выбора для профилактики и лечения острых респираторных вирусных инфекций // Лечащий врач. 2013. №1. С. 1-6. https://www.lvrach.ru/2013/10/15435831/.
6. Peniche A. G., Osorio Y., Renslo A. R., Frantz D. E., Melby P. C., Travi, B.L. Development of an ex vivo lymph node explant model for identification of novel molecules active against Leishmania major // Antimicrobial Agents and Chemotherapy. 2014. Vol. 58(1). P. 78-87. doi: 10.1128/AAC.00887-13.
7. Wissing M. D., Dadon T., Kim E., Piontek K. B., Shim J. S., Kaelber N. S., Liu J. O., Kachhap S. K., Nelkin B. D. Small-molecule screening of PC3 prostate cancer cells identifies tilorone dihydrochloride to selectively inhibit cell growth based on cyclin-dependent kinase 5 expression // Oncology Reports. 2014. Vol. 32. P. 419-424. doi: 10.3892/or.2014.3174.
8. Zhou D., Tuo W., Hu H., Xu J., Chen H., Rao Z., Xiao Y., Hua X., Liu P. Synthesis and activity evaluation of tilorone analogs as potential anticancer agents // European Journal of Medicinal Chemistry. 2013. Vol. 64. P. 432-441. doi: 10.1016/j.ejmech.2013.03.050.
9. Григорян С. С., Исаева Е. И., Бакалов В. В., Осипова Е. А., Бевз А. Ю., Простяков И. В., Надоров С. А. Амиксин – индукция интерферонов альфа, бета, гамма и лямбда в сыворотке крови и легочной ткани // РМЖ «Медицинское обозрение».2015. №2. С.93-99.
10. Zhuk M., Sumriy S. K. Zhuk O. V. Elimination kinetics of synthetic interferon inducer tilorone in experimental animals // Journal of Pre-Clinical and Clinical Research. 2017. Vol. 11(2). P. 127-131. doi: 10.26444/jpccr/81165.
11. Ratan R. R., Siddiq A, Aminova L., Langley B., McConoughey S., Karpisheva K.,… Gazaryan, I. Small molecule activation of adaptive gene expression: tilorone or its analogs are novel potent activators of hypoxia inducible factor-1 that provide prophylaxis against stroke and spinal cord injury // Annals of the New York Academy of Sciences. 2008. Vol. 1147 (1). P. 383-394. doi: 10.1196/annals.1427.033.

12. Feng J., Weitner M., Shi W., Zhang S., Sullivan D., Zhang Y. Identification of Additional Anti-Persister Activity against Borrelia burgdorferi from an FDA Drug Library // Antibiotics. 2015. Vol. 4(3). P. 397–410. doi: 10.3390/antibiotics4030397.
13. Giron D. J., Schmidt J. P., Pindak F. F. Tilorone hydrochloride: lack of correlation between interferon induction and viral protection // Antimicrobial Agents And Chemotherapy. 1972. Vol. 1(1). P. 78-79. doi: 10.1128/AAC.1.1.78.
14. Chatterjee S. S., Chakraborty T. Isolation of bacterial RNA from cultures // In D. Lin (Ed.) Handbook of nucleic acid purification. Boca Raton: CRC Press Taylor@Francis Group, 2009. P. 107-128.
15. Stetefeld J., McKenna S., Patel T. R. Dynamic light scattering: a practical guide and applications in biomedical sciences // Biophysical Reviews. 2016. Vol. 8 (4). P. 409-427. doi: 10.1007/s12551-016-0218-6.
16. Karpov A.V., Zholobak N. M., Spivak N. Y., Rybalko S. L., Antonenko S. V., Krivokhatskaya L. D. Virus-inhibitory effect of a yeast RNA – tilorone molecular complex in cell cultures // Acta virologica. 2001. Vol. 45(3). P. 181-184.
17. Карпов А. В., Жолобак Н. М. Изучение интерфероногенных свойств комплексов РНК-тилорон в культуре клеток // Антибиотики и химиотерапия. 1995. Т. 40, №5. С. 20-23.
18. Карпов А. В., Жолобак Н. М. Продукция интерферонов I типа в организме под действием молекулярных комплексов дрожжевая РНК-тилорон // Вопросы вирусологии. 1996. Т.41, № 1. С. 13-16.
19. Pirher N., Ivicak K., Pohar J., Bencina M., Jerala R. A second binding site for double-stranded RNA in TLR3 and consequences for interferon activation // Nature Structural & Molecular Biology. 2008. Vol. 15(7). P. 761-763. doi: 10.1038/nsmb.1453
20. DeWitte-Orr S. J., Mehta D. R., Collins S. E., Suthar M. S., Gale M., Mossman K. L. Long Double-Stranded RNA Induces an Antiviral Response Independent of IFN Regulatory Factor 3, IFN-β Promoter Stimulator 1, and IFN // The Journal of Immunology. 2009. Vol. 183(10). P. 6545-6553. doi: 10.4049/jimmunol.0900867.
21. Pashynska V. A., Kosevich M. V., Van den Heuvel H., Claeys M. Characterization of noncovalent complexes of antimalarial agents of the artemisinin type and Fe(III)-heme by electrospray ionization mass spectrometry and collisional activation tandem mass spectrometry // Journal of the American Society for Mass Spectrometry. 2004. Vol. 15. P. 1181-1190.
22. Pashynska V. A., Kosevich M. V., Gomory A., Vekey K. Investigations of the formation of noncovalent complexes between antimicrobial agent ethonium with membrane phospholipids by electrospray ionization mass spectrometry // Mass-Spectrometria. 2012. Vol. 9(2). P. 121-128.
23. Pashynska V., Kosevich M., Stepanian S., Adamowicz L. Noncovalent complexes of tetramethylammonium with chlorine anion and 2,5-dihydroxybenzoic acid as models of the interaction of quaternary ammonium biologically active compounds with their molecular targets. A theoretical study //Journal of Molecular Structure: THEOCHEM. 2007. Vol. 815. P. 55-62. doi:10.1016/j.theochem.2007.03.019.
24. Pashynska V., Stepanian S., Gomory A., Vekey K., Adamowicz L. Competing intermolecular interactions of artemisinin-type agents and aspirin with membrane phospholipids: Combined model mass spectrometry and quantum-chemical study // Chemical Physics. 2015. Vol. 455. P. 81-87. doi:10.1016/j.chemphys.2015.04.014.
25. Pashynska V., Stepanian S., Gomory A., Vekey K., Adamowicz L. New cardioprotective agent flokalin and its supramolecular complexes with target amino acids: An integrated mass-spectrometry and quantum-chemical study // Journal of Molecular Structure. 2017. Vol. 1146. P. 441-449. doi:10.1016/j.molstruc.2017.06.007.

REFERENCES

1. Krueger, R.E., Mayer, G.D. (1970) Tilorone hydrochloride: an orally active antiviral agent. *Science*, 16(3951), 1213-1214. doi: 10.1126/science.169.3951.1213.
2. Mayer, G.D., Krueger, R.E. (1970). Tilorone hydrochloride: mode of action. *Science,* 169(3951), 1214-1215. doi: 10.1126/science.169.3951.1214.
3. Stringfellow, D.A., Glasgow, L.A. (1972). Tilorone hydrochloride: an oral interferon-inducing agent. *Antimicrobial Agents and Chemotherapy,* 2(2), 73-78. doi: 10.1128/AAC.2.2.73.
4. Ekins, S., Lingerfelt, M.A., Comer, E.A., Freiberg, A.N., Mirsalis, J.C., O'Loughlin, K., Harutyunyan, A., McFarlane, C., Green, C.E., Madrid, P.B. (2018). Efficacy of Tilorone Dihydrochloride against Ebola Virus Infection. *Antimicrobial Agents and Chemotherapy,* 62(2), e01711-e01717. doi:10.1128/AAC.01711-17.
5. Kalugin, O.V. (2013). Tilorone as a chosen preparation for prevention and treatment of acute respiratory viral infections. *Lechebnoe delo*, (10), 1-6. (in Russian) https://www.lvrach.ru/2013/10/15435831/.
6. Peniche, A.G., Osorio, Y., Renslo, A.R., Frantz, D.E., Melby, P.C., Travi, B.L. (2014). Development of an ex vivo lymph node explant model for identification of novel molecules active against Leishmania major. *Antimicrobial Agents and Chemotherapy*, 58(1), 78-87. doi: 10.1128/AAC.00887-13.
7. Wissing, M.D., Dadon, T., Kim, E., Piontek, K.B., Shim, J.S., Kaelber, N.S., Liu, J.O., Kachhap, S.K., Nelkin, B.D. (2014). Small-molecule screening of PC3 prostate cancer cells identifies tilorone

dihydrochloride to selectively inhibit cell growth based on cyclin-dependent kinase 5 expression. *Oncology Reports*, 32, 419-424. doi: 10.3892/or.2014.3174.

8. Zhou, D., Tuo, W., Hu, H., Xu, J., Chen, H., Rao, Z., Xiao, Y., Hua, X., Liu, P. (2013). Synthesis and activity evaluation of tilorone analogs as potential anticancer agents. *European Journal of Medicinal Chemistry*, 64, 432-441. doi:10.1016/j.ejmech.2013.03.050.
9. Grigoryan, S.S.**,** Isaeva, E.I.**,** Bakalov, V.V., Osipova, E.A., Prostyakov, I.V., Nadorov, S.A. (2015). Amixin: induction of interferons-α, -β, -γ and -λ in serum and lung tissue. *Russkii Meditsinskii Zhurnal*, (2), 93-99. (in Russian)
10. Zhuk, M., Sumriy, S.K., Zhuk, O.V. (2017). Elimination kinetics of synthetic interferon inducer tilorone in experimental animals. *Journal of Pre-Clinical and Clinical Research*, 11(2), 127-131. doi: 10.26444/jpccr/81165.
11. Ratan, R.R., Siddiq, A, Aminova, L., Langley, B., McConoughey, S., Karpisheva, K., Gazaryan, I. (2008). Small molecule activation of adaptive gene expression: tilorone or its analogs are novel potent activators of hypoxia inducible factor-1 that provide prophylaxis against stroke and spinal cord injury. *Annals of the New York Academy of Sciences*, 1147(1), 383-394. doi: 10.1196/annals.1427.033.
12. Feng, J., Weitner, M., Shi, W., Zhang, S., Sullivan, D., Zhang, Y. (2015). Identification of Additional Anti-Persister Activity against Borrelia burgdorferi from an FDA Drug Library. *Antibiotics*, 4 (3), 397–410. doi: 10.3390/antibiotics4030397.
13. Giron, D.J., Schmidt, J.P., Pindak, F.F. (1972). Tilorone hydrochloride: lack of correlation between interferon induction and viral protection. *Antimicrobial Agents and Chemotherapy*, 1(1), 78-79. doi: 10.1128/AAC.1.1.78.
14. Chatterjee, S.S., & Chakraborty, T. (2009). Isolation of bacterial RNA from cultures. In D. Lin (Ed.) Handbook of nucleic acid purification (pp. 107-128). Boca Raton: CRC Press Taylor@Francis Group.
15. Stetefeld, J., McKenna, S., Patel, T.R. (2016). Dynamic light scattering: a practical guide and applications in biomedical sciences. *Biophysical Reviews*, 8(4), 409-427. doi: 10.1007/s12551-016-0218-6.
16. Karpov, A.V., Zholobak, N.M., Spivak, N.Y., Rybalko, S.L., Antonenko, S.V., Krivokhatskaya, L.D. (2001). Virus-inhibitory effect of a yeast RNA – tilorone molecular complex in cell cultures. *Acta virologica*, 45(3), 181-184.
17. Karpov, A.V., & Zholobak, N.M. (1995). The interferonogenic properties of yeast RNA-tilorone complexes in a cell culture. *Antibiotiki i khimioterapiia*, 40(5), 20-23. (in Russian)
18. Karpov, A.V., Zholobak, N.M. (1996). Production of type I interferons in the body exposed to yeast RNA-tiloron molecular complexes. *Voprosy virusologii*, 41(1), 13-16. (in Russian)
19. Pirher, N., Ivicak, K., Pohar, J., Bencina, M., Jerala, R. (2008). A second binding site for double-stranded RNA in TLR3 and consequences for interferon activation. *Nature Structural & Molecular Biology*, 15(7), 761-763. doi: 10.1038/nsmb.1453.
20. DeWitte-Orr, S.J., Mehta, D.R., Collins, S.E., Suthar, M.S., Gale, M., Mossman, K.L. (2009). Long Double-Stranded RNA Induces an Antiviral Response Independent of IFN Regulatory Factor 3, IFN-β Promoter Stimulator 1, and IFN. *The Journal of Immunology*, 183(10), 6545-6553. doi: 10.4049/jimmunol.0900867.
21. Pashynska, V.A., Kosevich, M.V., Van den Heuvel, H., Claeys, M. (2004). Characterization of noncovalent complexes of antimalarial agents of the artemisinin type and Fe(III)-heme by electrospray ionization mass spectrometry and collisional activation tandem mass spectrometry. *Journal of the American Society for Mass Spectrometry*, 15, 1181-1190.
22. Pashynska, V.A., Kosevich, M.V., Gomory, A., Vekey, K. (2012). Investigations of the formation of noncovalent complexes between antimicrobial agent ethonium with membrane phospholipids by electrospray ionization mass spectrometry. *Mass-Spectrometria*, 9(2), 121-128.
23. Pashynska, V., Kosevich, M., Stepanian S., Adamowicz L. (2007). Noncovalent complexes of tetramethylammonium with chlorine anion and 2,5-dihydroxybenzoic acid as models of the interaction of quaternary ammonium biologically active compounds with their molecular targets. A theoretical study. *Journal of Molecular Structure: THEOCHEM*, 815, 55-62. doi:10.1016/j.theochem.2007.03.019.
24. Pashynska, V., Stepanian, S., Gomory, A., Vekey, K., Adamowicz L. (2015). Competing intermolecular interactions of artemisinin-type agents and aspirin with membrane phospholipids: Combined model mass spectrometry and quantum-chemical study. *Chemical Physics*, 455, 81-87. doi:10.1016/j.chemphys.2015.04.014.
25. Pashynska, V., Stepanian, S., Gomory, A., Vekey, K., Adamowicz L. (2017). New cardioprotective agent flokalin and its supramolecular complexes with target amino acids: An integrated mass-spectrometry and quantum-chemical study. *Journal of Molecular Structure*, 1146, 441-449. doi:10.1016/j.molstruc.2017.06.007.

Journal of Molecular Structure 1146 (2017) 441–449

Contents lists available at ScienceDirect

Journal of Molecular Structure

journal homepage: http://www.elsevier.com/locate/molstruc

New cardioprotective agent flokalin and its supramolecular complexes with target amino acids: An integrated mass-spectrometry and quantum-chemical study

Vlada Pashynska [a, *], Stepan Stepanian [a], Ágnes Gömöry [b], Károly Vékey [b], Ludwik Adamowicz [c]

[a] B.Verkin Institute for Low Temperature Physics and Engineering of the National Academy of Sciences of Ukraine, Nauky Ave., 47, 61103 Kharkiv, Ukraine
[b] Institute of Organic Chemistry of Research Centre for Natural Sciences of the Hungarian Academy of Sciences, Magyar Tudosok Korutja, 2, Budapest H-1117, Hungary
[c] Department of Chemistry and Biochemistry, University of Arizona, Tucson, AZ 85721, USA

ARTICLE INFO

Article history:
Received 20 March 2017
Received in revised form
19 May 2017
Accepted 2 June 2017
Available online 3 June 2017

Keywords:
Flokalin
Lysine
Threonine
Supramolecular complexes
Electrospray ionization mass spectrometry
B3LYP/Aug-cc-pVDZ

ABSTRACT

This study is devoted to examining the molecular structure and molecular mechanisms of action of the recently developed cardioprotective agent flokalin (Fl), a fluorine containing analogue of pinacidil, which is known as an activator of ATP sensitive potassium membrane channels. A combined experimental and computational investigation of flokalin and its biologically relevant supramolecular complexes with selected amino acids involved in K_{ATP}-channels proteins is performed by electrospray ionization mass spectrometry (ESI MS) and by B3LYP/aug-cc-pVDZ quantum-mechanical calculations. First Fl solution is probed by ESI MS and a characteristic mass spectrum of the agent is obtained. Next the intermolecular interactions of Fl with the potentially targeted aminoacids (AA), Lys and Thr, are experimentally investigated. The spectra of the model Fl:AA systems (in 1:1 M ratio) contain information on the ions characteristic to the individual components of the mixtures; though the most interesting spectral results from the biophysical view point are related to the ions of stable molecular clusters formed by flokalin with AA. The peaks of such ions are quite prominent in the spectrum for the Fl:Lys system and less prominent for Fl:Thr. The equilibrium geometries and the corresponding interaction energies of the noncovalent supramolecular complexes registered in the mass spectra are determined in the quantum chemical calculations. The formation of the stable noncovalent complexes of Fl with Lyz and Thr revealed by the ESI MS probing and by the theoretical modelling testify to a possibility of interaction of flokalin with the K_{ATP}-channel domains enriched with the two amino acids in biological systems.

1. Introduction

The model combining experimental and theoretical studies of the molecular structures and the corresponding intermolecular interactions characteristics of biologically active compounds, including medications, with their potential molecular targets in living systems has been proven useful to elucidate the molecular action mechanisms of these compounds [1–4]. It is important for directed searching for new effective drugs.

Development of the new drugs for use as effective protective agents against hypoxia of different human organs and systems, and, in particular, as cardioprotectors is one of the most important current medical and social tasks, as the mortality from cardiovascular diseases is, according with the WHO data, one of the main global health problems [5]. One of the effective endogenous mechanisms of cardioprotection under hypoxia and ischemia of cardiac hystiocytes is related to activation and opening of ATP sensitive potassium channels (K_{ATP} channels) of sarcolemma and mitochondrial membranes [6–8]. The molecular regulation of the functioning of the K_{ATP} channels by pharmaceutical activators can be an efficacious therapeutic action in treatment of cardiological pathologies, as well as of some neurologic and nephrological diseases [6,9]. The recently developed in Ukraine cardioprotective agent flokalin, a fluorine containing analogue of pinacidil, which is

* Corresponding author.
E-mail address: vlada@vl.kharkov.ua (V. Pashynska).

http://dx.doi.org/10.1016/j.molstruc.2017.06.007
0022-2860/

a known activator of ATP sensitive potassium membrane channels, has shown high effectiveness in the treatment of myocardial infarction and ischemia in *in vitro* and *in vivo* experiments with mammals [9–11]. It also has low toxicity (3–4 times lower than some analogous produced outside Ukraine including pinacidil) [6,12–15]. It is believed that cardioprotective flokalin action is similar to pinacidil action and involves the opening of K_{ATP} channels of sarcolemma and internal mitochondrial membranes of cardiac hystiocytes and some vascular cells [6,11].

The molecular and submolecular mechanisms of the flokalin interaction with the K_{ATP} channel proteins and their components are not well studied yet, although the molecular mechanisms of the well known K_{ATP} channel-openers action and the binding sites of pinacidil in the K_{ATP} channels protein and, in particular, in the channels regulatory subunits (sulfonylurea receptors SUR1, SUR2A and SUR2B) have been recently actively investigated [16–20]. In the investigations it was revealed that a lysine (Lys) residue related to the special protein sequence motif - Walker A (W_A) - of the SUR subunits, as well as the main-chain NH atoms of the K_{ATP} channels, play a crucial role in the binding of the nucleotides to the protein [18–20]. Furthermore, mutation of a single W_A lysine in the nucleotide binding domains (NBD) of SUR1 results in abolishment of channel activation by Mg-nucleotides [21–23]. It was found that mutation of the W_A lysine in NBD1 of SUR2A abolishes the pinacidil response in the absence of added nucleotide, indicating that NBD1 structure is critical to the action of pinacidil drug even in nucleotide-free solution [23]. There is also evidence that mutation of two aminoacids in TM17 subunit of SUR1, especially replacement of methionine (Met) in position 1289 by threonine (Thr), leads to an increase of the binding affinity of the cyanoguanidines including pinacidil [24].

Thus we can conclude that the interaction of the K_{ATP} channel openers including flokalin with amino acids involved in the binding sites of K_{ATP} channel proteins is a molecular biophysics problem that needs to be addressed both experimentally by using modern physical chemistry methods and theoretically by using quantum chemical calculations.

Soft-ionization mass spectrometry is a method, which is widely used in molecular biology related research [25], as it is one of the most efficient tools to study interactions in molecular biosystems [26–28]. The electrospray ionization (ESI) massspectrometric (MS) technique based on spraying solutions of biomolecules in polar solvents has been successfully applied to investigate selective noncovalent intermolecular interactions. In particular, the technique has been applied to study the interactions between biologically active agents and medicines with targeting biomolecules [29–31]. We successfully used the ESI MS method in some mechanistic model studies of the interactions of membranothropic antimicrobial bisquaternary agents with phospholipids molecules of membranes [2,4] and the interactions of artemisinin-type antimalarial drugs with their potential molecular targets in living systems [1]. In our previous investigations we also combined the quantum chemical calculations of equilibrium geometries and interaction energies of the supermolecular complexes registered in the ESI MS experiments with their experimental characterization [1,2].

The main goal of the present work is to investigate the biologically relevant interactions of the pinacidil analogue flokalin (FI) with selected amino acids (AA) involved in K_{ATP} channel-activator binding sites using the electrospray ionization mass spectrometry (ESI MS) and quantum-chemical calculations. Lys and Thr are the amino acids selected for the investigation, as they are involved in the regulatory subunits of K_{ATP} channel proteins and are relevant in the channel activation by pinacidil according to the literature data mentioned above [21–24].

2. Experimental

2.1. Model systems

Flokalin (Fl, $C_{15}H_{20}F_2N_4O$, MW = 310,34 Da) is synthesized in the Institute of Organic Chemistry of the National Academy of Sciences of Ukraine (Fig. 1). Amino acids (AA): lysine (Lys, MW = 146,19 Da), threonine (Thr, MW = 119,12 Da), glycine (Gly, MW = 75,07 Da), and methanol (MeOH) are purchased from the Sigma-Aldrich company (Switzerland).

Initial solutions of Fl and AA (5 mM) are prepared in methanol (polar solvent) and used for preparation of binary (1:1 M ratio) model systems. The mixtures are kept at the room temperature for at least 10 min before the ESI MS analysis. The spraying procedure requires dilution of the studied solutions to the final 250 μM concentration of the diluted components of the model systems in each solution. It was shown in a number of studies [27–30] that the use of methanol as a solvent significantly improves the quality of the ESI mass spectra while the composition of the intermolecular complexes formed in methanol is similar to the ones formed in the water solution [32].

2.2. ESI mass spectrometry

The ESI mass spectra are obtained in the positive ion mode using a triple quadruple (QqQ) Micromass Quattro Micro mass spectrometer (Waters, Manchester, UK) equipped with the electrospray ion source. This source operates in the standard ESI mode. The ESI source temperature is set to 120 °C and the desolvation temperature is 200 °C. The spraying capillary is operated at 3.5 kV. The cone voltage (CV) value of 10 V is used. The analyzed solution (20 μL) is injected into the mass spectrometer at a constant flow rate of 0.2 mL/min of the methanol solvent. ESI spectra are recorded in the mass/charge range of *m/z* 100–2000. Data acquisition and processing are performed using MassLynx 4.1 software (Waters, Manchester, UK).

2.3. Quantum chemical calculations

Structures and relative stabilities of the neutral and protonated flokalin tautomers, as well as lysine and threonine conformers, are determined at the B3LYP/aug-cc-pVDZ level of theory [33–35]. The most stable geometries for the protonated supramolecular flokalin-aminoacid complexes registered in the ESI mass spectrometry experiments are also determined at the same level of theory. Since the protonation energies of flokalin and aminoacids are close, the calculations are carried out for both protonated flokalin-neutral amino acid and neutral flokalin – protonated aminoacid complexes.

Relative stabilities of the flokalin-aminoacid complexes were also calculated using the Integral Equation Formalism Polarizable Continuum Model (IEFPCM) [36–38] to account for the solvent influence. These calculations were performed for two solvents: methanol which was used in our experiments and water. Geometries of single molecules and complexes were fully optimized at the B3LYP(IEFPCM)/aug-cc-pVDZ level of theory and it was followed by

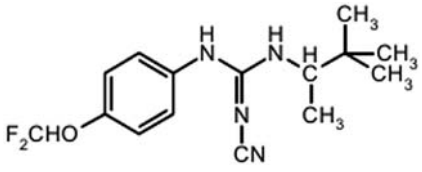

Fig. 1. Chemical formula of flokalin.

harmonic frequency calculations to account for the ZPVE correction.

All calculations are performed using the Gaussian 09 program package [39].

3. Results and discussion

3.1. ESI mass spectrometry probing of flokalin solution

In the first step of the study the solution of Fl in MeOH is investigated by ESI MS and ESI mass spectrum of the drug is obtained (Fig. 2). The spectral peaks are assigned as follows: the peak of protonated Fl, $[Fl{\cdot}H]^+$, at *m/z* 311.3 with relative intensity (RI) 100% and two peaks of Fl cationized by sodium and potassium ions - $[Fl{\cdot}Na]^+$ at *m/z* 333.3 with RI 70% and $[Fl{\cdot}K]^+$ at *m/z* 349.3 with RI 5%. It should be noted that cationization of molecules of diluted substances by the residual sodium and potassium ions in the solution is characteristic to the ion formation in the electrospray method of ionization [26–31].

The peaks of the protonated and cationized molecular clusters of Fl are also registered in the experiment: $[2Fl{\cdot}H]^+$ at *m/z* 621.7 with RI 54%; $[2Fl{\cdot}Na]^+$ at *m/z* 643.7 with RI 60%; $[2Fl{\cdot}K]^+$ at *m/z* 659.7 with RI 4%; $[3Fl{\cdot}Na]^+$ at *m/z* 954.0 with RI 30%; $[4Fl{\cdot}Na]^+$ at *m/z* 1264.4 with RI 3%. The quit intense peak of *m/z* 371.3 is also registered in the spectrum (Fig. 2). It is identified as a peak of protonated noncovalent complex of flokalin molecule with urea (carbamide, MW = 60.07Da), which is one of the most probable impurity of flokalin sample according to the literature data [12] about the way of flokalin production. The presence of quit prominent $[nFl{\cdot}H]^+$ and $[nFl{\cdot}Na]^+$ (n = 1÷4) peaks in the ESI mass spectrum of Fl provide an evidence concerning the process of formation of noncovalent homocomplexes (dimers in particular) by the drug molecules in the polar solution. The high relative intensity of the dimer's peak in the mass spectrum is probably a result of relatively strong noncovalent interactions between polar groups of two Fl molecules. The quantum chemical calculations are used to elucidate this point.

We have also probed by the ESI MS method several more diluted solutions of flokalin in methanol (with concentration of 125 μM and 62.5 μM). It is revealed that in the spectra of these more diluted flokalin solutions the similar peaks are found, but the relative intensities of $[nFl{\cdot}H]^+$ and $[nFl{\cdot}Na]^+$ peaks decrease significantly with the flokalin concentration decrease. For example, peak of $[4Fl{\cdot}Na]^+$ ions does not registered in the spectra of the diluted solutions and $[3Fl{\cdot}Na]^+$ peak is dramatically less in comparison with one in 250 μM flokalin solution spectrum (Fig. 2). Thus we selected 250 μM concentration of flokalin for formation of the model flokalin-aminoacid (1:1 M ratio) systems, because of possibility to register more diversity of hetero- and homocomplexation of flokalin molecules under ESI MS probing of the solutions of such concentration.

The peaks of the molecular and quasimolecular ions of Fl can be used as a reference to reveal the presence of the agent in any sample analyzed by ESI MS method, including biological samples and samples involving pharmacological products.

3.2. ESI mass spectrometry study of Fl:AA model systems

In the next step intermolecular interactions of Fl with Lys and Thr are examined with ESI MS. Solutions of Fl:AA with the 1:1 M ratio in MeOH are used.

The ESI MS spectra of the studied systems (Fl:AA) contain peaks corresponding to ions characteristic to the individual components of the mixtures of flokalin with lysine or flokalin with threonine, respectively. In particular, in the ESI mass spectrum of the flokalin-lysine (Fl:Lys) system (Fig. 3) the most prominent peak is the peak of protonated lysine molecule $Lys{\cdot}H^+$ at *m/z* 147.2 with RI 100%. In the spectrum of the flokalin-threonine (Fl:Thr) system (Fig. 4) there are two prominent peaks corresponding to molecular ions of Thr: $Thr{\cdot}H^+$ at *m/z* 120.1 with RI 35%, and $Thr{\cdot}Na^+$ at *m/z* 142.1 with RI 28%. The described-above characteristic peaks of Fl are also registered in the spectra of both Fl:AA systems (see Figs. 3 and 4). However, while in the spectrum of Fl:Lys solution the most prominent Fl peak, the peak of cationized ion $Fl{\cdot}Na^+$ at *m/z* 333.3 reaches just 10% on the relative intensity scale (Fig. 3), for Fl:Thr the peak of the $Fl{\cdot}H^+$ ion at *m/z* 311.3 is the dominant peak in the spectrum (RI 100%; see Fig. 4). Different ratios between the peaks of molecular ions of individual components in the ESI spectra of the Fl:Lys and FL:Thr systems (at 1:1 M ratio) can be explained by different behavior of the molecules with different structures under electrospray ionization including different abilities of the molecules to undergo protonation/cationization (this point is elucidated in the calculations described

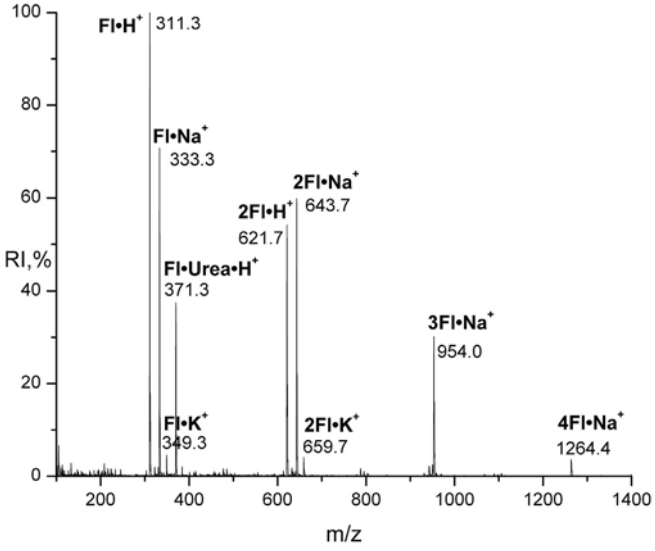

Fig. 2. ESI mass spectrum of flokalin solution in MeOH.

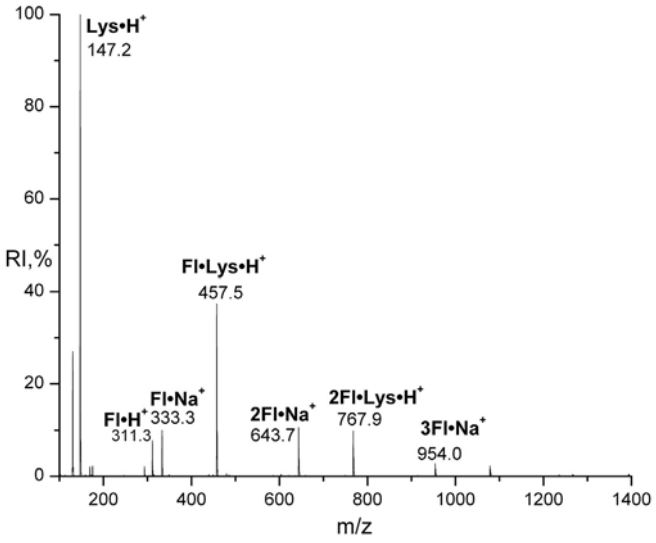

Fig. 3. ESI mass spectrum of the model system Fl:Lys (1:1).

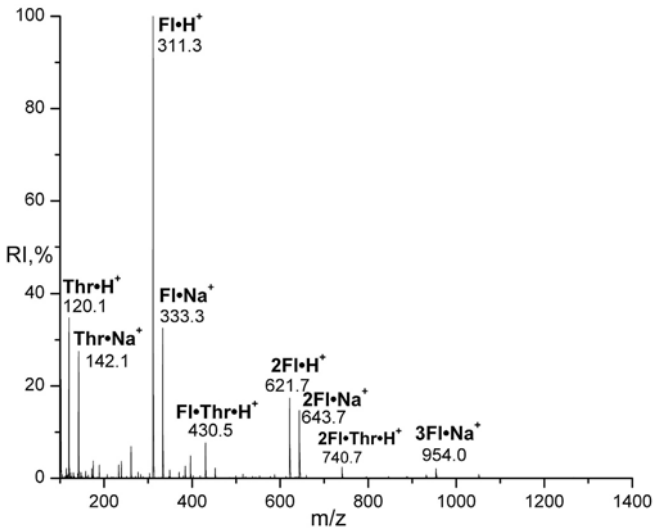

Fig. 4. ESI mass spectrum of the model system Fl:Thr (1:1).

further), by their different volatilities, and by other aspects of the multi-steps ionization process.

The most interesting result of the ESI MS experiments from the biophysical point of view is the observation in the Fl:AA spectra of peaks of stable noncovalent supramolecular complexes of flokalin with the amino acids (see Figs. 3 and 4). These peaks include an intense peak of $Fl\cdot Lys\cdot H^+$ at *m/z* 457.2 with RI 38%, and a peak of $2Fl\cdot Lys\cdot H^+$ at *m/z* 767.9 with RI 11% for the flokalin-lysine system (Fig. 3), and a peak of $Fl\cdot Thr\cdot H^+$ at *m/z* 430.5 with RA 8% for the flokalin-threonine system (Fig. 4). The peaks due to stable noncovalent complexes of Fl with Lys and Thr in the ESI MS spectra testify to substantial stability of such complexes formed in the solutions used in the ESI MS experiments. Their presence also testifies to the possibility of the selective interaction of flokalin with the K_{ATP} channel protein binding sites which contain the two amino acids in biological systems. To confirm this possibility we also investigate a model system contained flokalin and the simplest amino acid glycine, Fl:Gly (at the 1:1 M ratio), in MeOH under the same ESI MS conditions as used for Fl:Lys and Fl:Thr. In the mass spectrum of Fl:Gly (Fig. S1 in Supplementary Material) the only peaks recorded are due to the individual two components of the system: $Gly\cdot H^+$ at *m/z* 76.0, and $Gly\cdot Na^+$ at *m/z* 98.1 for Gly, and $[Fl\cdot H]^+$ at *m/z* 311.3; $[Fl\cdot Na]^+$ at *m/z* 333.3; $[Fl\cdot K]^+$ at *m/z* 349.3; $[2Fl\cdot Na]^+$ at *m/z* 643.7; $[2Fl\cdot K]^+$ at *m/z* 659.7; and $[3Fl\cdot Na]^+$ at *m/z* 954.0 for flokalin. Peaks due to noncovalent complexes $Fl\cdot Gly\cdot H^+$ (at *m/z* 386.3) and $Fl\cdot Gly\cdot Na^+$ (at *m/z* 409.3) are not recorded in the spectrum.

It is also interesting to compare the relative intensities of the peaks of the noncovalent complexes ions $nFl\cdot AA\cdot H^+$ ($n = 1\div2$) with the intensities of the peaks of protonated/cationized flokalin homoclusters $[nFl\cdot H]^+$ and $[nFl\cdot Na]^+$. In the spectrum of the Fl:Lys system (Fig. 3) the peak of $Fl\cdot Lys\cdot H^+$ at *m/z* 457.2 with RI 38% dominates over the peak of cationized flokalin dimer $2Fl\cdot Na^+$ at *m/z* 643.7 with RI 10%, and the peak of $2Fl\cdot Lys\cdot H^+$ at *m/z* 767.9 with RI 11% prevails over the peak of flokalin trimer, $3Fl\cdot Na^+$ at *m/z* 954.0 with RI 3%. This finding can be considered as an evidence of the preference of flokalin molecules to bind with lysine molecules instead of dimerizing in the model system studied. However in the spectrum of the flokalin-threonine system the peak of $Fl\cdot Thr\cdot H^+$ at *m/z* 430.5 with RI 8%, is less prominent than the peak of $2Fl\cdot H^+$ at *m/z* 621.7 with RI 17%, and the peak of $2Fl\cdot Na^+$ at *m/z* 643.7 with RI 14%. This can be an evidence of lower preference of flokalin to form noncovalent complexes with Thr in the solution than to form the homoclusters.

Formation of stable noncovalent complexes of flokalin with Lyz and Thr in the model systems revealed by the ESI MS probing gives credence to the idea of the possibility of flokalin binding with the K^+-channel domains containing these two amino acids.

3.3. Structure and protonation energy of single flokalin, lysine, and threonine: computational study

In the first step of the computational study calculations are performed to determine the most stable structures of the investigated molecules. The flokalin molecule has four nitrogen atoms and two labile protons. Thus several tautomers may appear. To locate the lowest energy flokalin structure we calculate the relative stabilities of all possible flokalin tautomers at the B3LYP/aug-cc-pVDZ level of theory. It is found that the most stable flokalin tautomer is **Fl_1** (Fig. 5). The structures of all other flokalin tautomers are shown in Fig. S2 (in Supplementary Materials) and their relative energies and Cartesian coordinates are collected in Tables S1 and S2, respectively. As it is seen in Table S1, the relative energy of the second most stable tautomer, **Fl_2,** is by 8.1 kcal/mol higher than tautomer **Fl_1**. The molecular structure of the most stable tautomer **Fl_1** (Fig. 5) exhibits symmetrical binding of two hydrogen atoms to the nitrogen atoms, which connected to −C═N−C≡N group of flokalin. We also located possible conformers of the flokalin tautomer **Fl_1**. Structure of the conformers is shown in Fig. S2 and their relative stabilities are presented in Table S1 of Supplementary Materials. In calculations of the flokalin-amino acid complexes we used the lowest energy flokalin structure (Fig. 5).

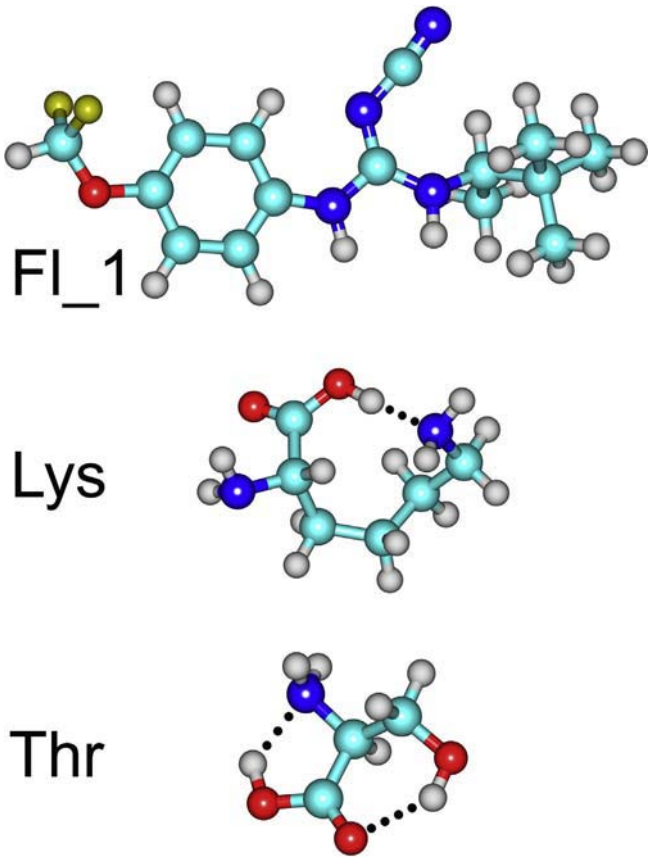

Fig. 5. Most stable structures of flokalin (**Fl_1**), lysine, and threonine molecules calculated at the B3LYP/aug-cc-pVDZ level of theory.

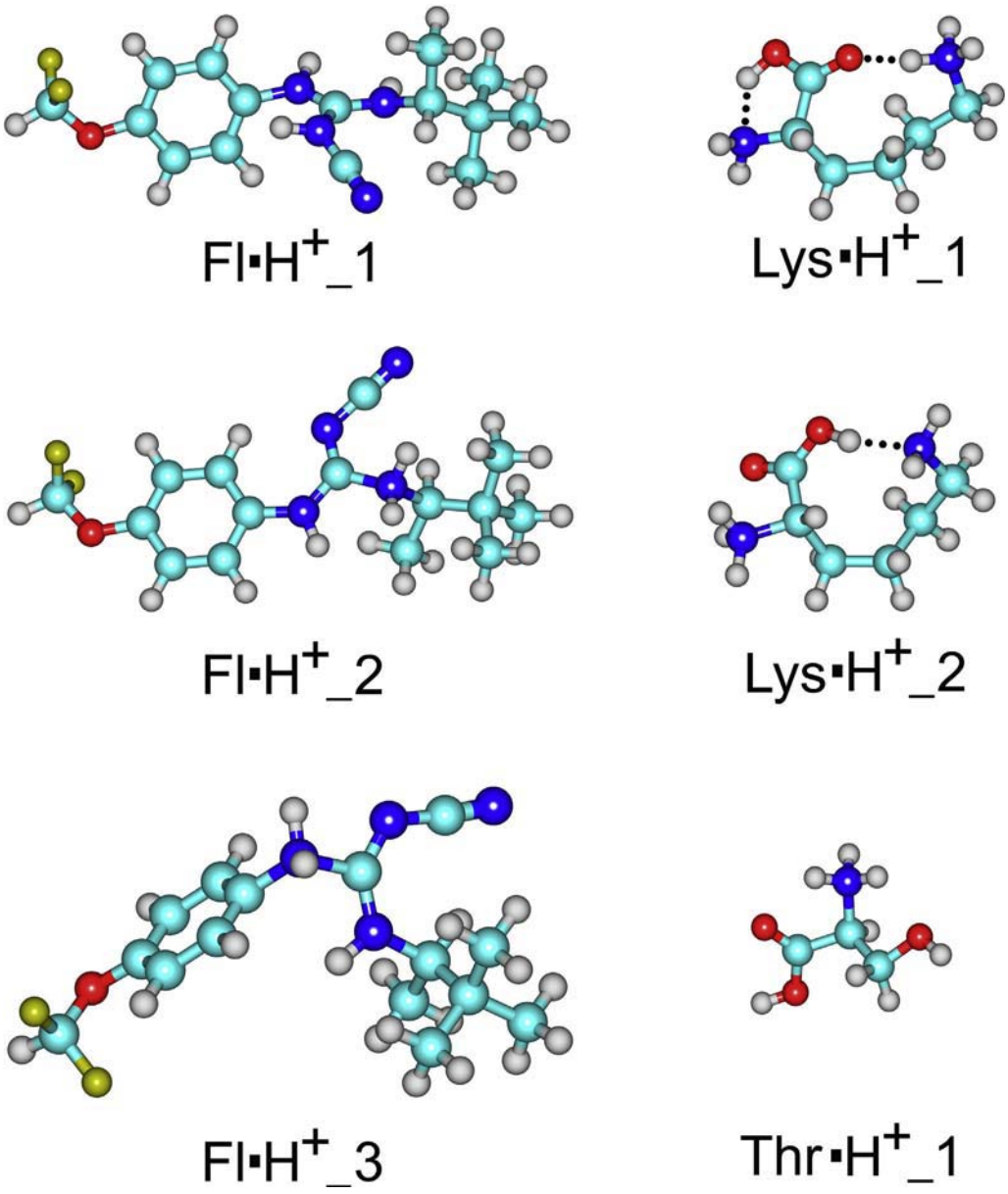

Fig. 6. Most stable structures of the protonated flokalin (**Fl·H**$^+$), lysine (**Lys·H**$^+$), and threonine (**Thr·H**$^+$) molecules calculated at the B3LYP/aug-cc-pVDZ level of theory.

As shown above, in the ESI massspectra one observes the peaks corresponding to protonated flokalin and the amino acids, and to protonated flokalin-amino acids noncovalent complexes (Figs. 2–4). In the complexes each component may be protonated and the experiment does not show where the protonation occurs. To elucidate this point the protonation energy of the lowest energy flokalin tautomer **Fl_1,** as well as of the most stable conformers of neutral lysine and threonine [40–43] (Fig. 5) need to be compared. The protonation energies of the amino acids were determined for their lowest energy conformers located in earlier works with quantum-chemistry calculations [40–43]. In our calculations, we took into account that the flokalin and lysine molecules have three and two possible protonation sites, respectively. The calculated structures of the protonated molecules under study are shown in Fig. 6 and the calculated protonation energies are collected in Table 1. One should note that amino acid molecules are highly labile and have many stable conformers with close relative energies. Additional calculations are also performed for the protonation energies of several lower-energy lysine and threonine conformers. The results of the calculations are presented in Table S3 and Fig. S3 (Supplementary Materials).

As it is seen from Table 1, the calculations predict relatively close values of the protonation energies of flokalin and the amino acids. The difference between the energies is about 6% for the lysine/flokalin pair and 3% for the threonine/flokalin pair. Such small differences do not allow for define determination which molecule in either of the two drug-amino acid complexes (flokalin or the amino acid) is protonated. Thus calculations of the protonated flokalin-amino acid complexes are carried out to elucidate this point. In Table 1 we also present the experimental gasphase protonation energy values of lysine and threonine obtained from Refs. [44,45]. As it is seen, the calculated protonation energies are in a good agreement with the experimental values. Moreover, the ratio of the relative intensities of the protonated Fl and protonated Lys and Thr peaks in our mass specta of the Fl:Lys and Fl:Thr systems (Figs. 3 and 4, respectively) is in a good qualitative correlation with the

Table 1
Protonation energies of (PE, kcal/mol) of the most stable tautomers of flokalin, lysine, and threonine calculated at the B3LYP/aug-cc-pVDZ level of theory with accounting for the thermal correction to the Gibbs Free Energy.

Neutral	Protonated[a]	PE	Experiment[b]
Fl	**Fl·H$^+$_1**	−221.4	N/A
Fl	**Fl·H$^+$_2**	−203.3	
Fl	**Fl·H$^+$_3**	−201.1	
Lys	**Lys·H$^+$_1**	−235.6	−238.1
Lys	**Lys·H$^+$_2**	−225.9	
Thr	**Thr·H$^+$_1**	−215.0	−220.5

[a] Numbers correspond to different protonation sites.
[b] Data from Refs. [44] and [45].

ratio of the protonation energy values calculated (Table 1) for these systems. These correlations testify to the good performance of the B3LYP density functional in predicting the protonation energies of molecular systems. It should be noted that, in most cases, the protonation of amino acid molecules changes their conformations as compared to the structures of the neutral forms.

3.4. Structures and interaction energies of the protonated flokalin-amino acid complexes

In the next step, structures and relative stabilities of the protonated noncovalent complexes of flokalin with lysine and threonine observed in the ESI MS experiments are determined with the calculations. The relative stabilities of the protonated complexes formed by flokalin with lysine or threonine are also determined. In the complexes observed in the experiment only one of the components of each complex is protonated (flokalin or amino acid). We use the most stable structures of the neutral and protonated components to build the initial structure of each complex. We also account for all interaction sites in flokalin and in the amino acids. The intermolecular interaction in the complex is dominated by the electrostatic interaction involving the charged component in the positively charged complex. To determine the possible interaction sites in the complexes formed by neutral flokalin and the charged protonated amino acids we first calculate the electrostatic potential energy surface (EPES) for neutral flokalin. The surface is shown in Fig. 7. As it is seen, the most negatively charged area of the potential is located at the nitrile group. Thus, the strongest interaction is likely to be observed in the complexes where the flokalin nitrile group is located closely to the positively charged protonated groups of the amino acids. Another negatively charged area is located near the flokalin oxygen atom and the two fluorine atoms (Fig. 7). The EPES is used to guess possible initial structures of the complexes to start the optimization of their geometries. The optimizations are performed at the B3LYP/aug-cc-pVDZ level of theory. They are followed with IR frequency calculations to check for any imaginary frequencies and to confirm that the obtained geometries correspond to equilibrium structures. The calculated harmonic frequencies are also used to account for the zero-point vibrational energy (ZPVE) corrections. The structures of all calculated complexes are presented in Fig. S4. The equilibrium structure and the interaction energy of the protonated flokalin dimer observed in the mass spectrometry experiments are also determined.

The calculated structures of the most stable complexes are shown in Fig. 8. In our view, these structures represent geometry of the complexes registered in the ESI MS experiments (Figss. 2–4). As mentioned, both neutral and protonated amino acids are highly structurally flexible systems. Also the interaction energies between

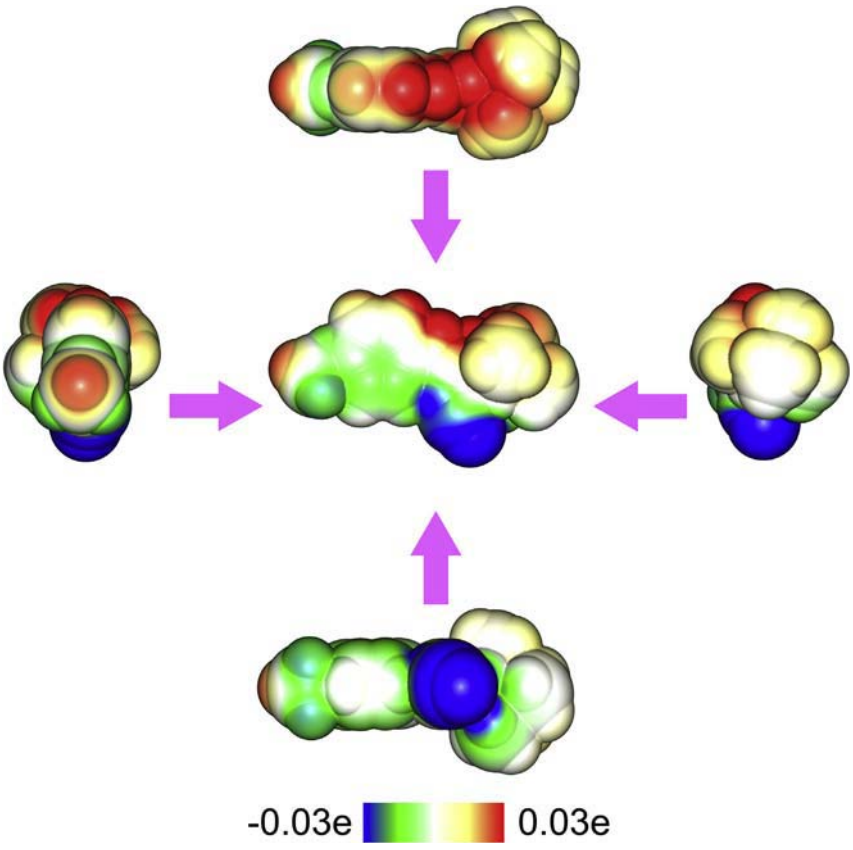

Fig. 7. The electrostatic potential surfaces of flokalin. The potential is calculated at the fixed distance of 2.5 Å from the atoms.

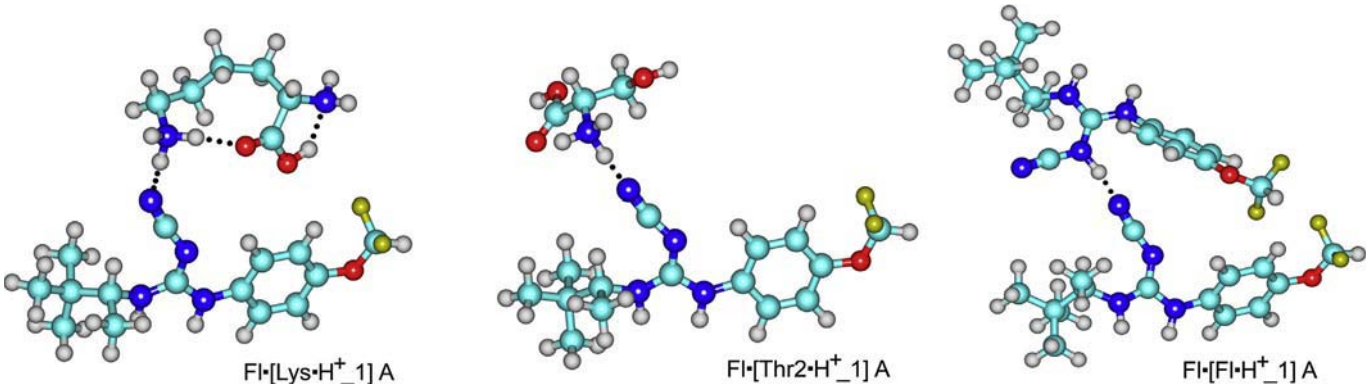

Fig. 8. The most stable structures of the protonated complexes: flokalin-lysine (**Fl·[Lys·H$^+$_1] A**), flokalin-threonine (**Fl·[Thr2·H$^+$_1] A**) and flokalin-flokalin (**Fl·[Fl·H$^+$_1] A**).

amino acids and flokalin are found to be much higher than the energy differences between the amino acid conformers. As a result the structures of the amino acid conformers are significantly altered during the optimization of the geometries of their complexes with flokalin. Thus, the notation used here to identify the amino acid conformation in a complex refers to the conformation used to initiate the geometry optimization of the complex. The interaction energies and the relative stabilities of the complexes are shown in Table 2.

An analysis of the calculated relative stabilities (see Table 2) demonstrates that the complexes formed by a neutral flokalin molecule and the protonated amino acids are the most stable among all flokalin-lysine and flokalin-threonine structures, while the interactions in the complexes formed by protonated flokalin and the neutral amino acids are much weaker. Moreover, most geometry calculations initiated with structures involving protonated flokalin and neutral amino acids geometry converge to structures involving neutral flokalin and protonated amino acids due to a barrierless intermolecular proton transfer that occurs during the optimization. Examples of the optimizations involving different protonated components of the complex at the beginning and at the end of the optimization are shown in Fig. S5. Complexes with protonated flokalin and a non-protonated amino acid are found only for structures where the proton transfer is not possible due to geometrical hindrance.

As expected, the most stable flokalin-lysine protonated complex (**Fl·[Lys·H$^+$_1] A**) is stabilized by a strong electrostatic interaction between the protonated side-chain amino group of the most stable conformer of protonated lysine and the nitrile nitrogen of neutral flokalin (Fig. 8). Two other low-energy flokalin-lysine complexes, (**Fl·[Lys2·H$^+$_1] A** and **Fl·[Lys2·H$^+$_1] B**), are also stabilized by the same interaction (Fig. S4). The interaction energies calculated for these two complexes are even higher (in absolute values) than for the **Fl·[Lys2·H$^+$_1] A** complex (Table 2), but the complexes are less stable due to lower stability of the protonated lysine conformer **Lys2·H$^+$_1** as compared to the conformer **Lys·H$^+$_1**. The flokalin-lysine complex stabilized by the interaction between the interior nitrogen atom of –C═N–C≡N group of flokalin and the protonated side-chain amino group of lysine (**Fl·[Lys2·H$^+$_1] C**) is the least stable structure formed by the lysine conformers with a protonated side chain. The interactions in the flokalin-lysine complexes formed by lysine with protonated main amino group (**Lys2·H$^+$_2**) are weaker than the interactions in the dimers formed by lysine with the protonated side chain amino group. This is particularly important as this side chain amino group of a lysine residue is present in proteins as a side group. This includes the K_{ATP}-channels proteins. The complex formed by protonated flokalin with neutral lysine (**[Fl·H$^+$_1]·Lys2 A**) is one of the least stable complexes among all complexes studied in this work.

The dependency of the relative stabilities of the flokalin-threonine complexes on their structures is generally similar to that observed for the flokalin-lysine complexes. The most stable flokalin-threonine complex, (**Fl·[Thr2·H$^+$_1] A**, Fig. 8), is also formed by neutral flokalin and the protonated aminoacid molecule. This complex is also stabilized by electrostatic interaction between the protonated amino group of threonine and the nitrile nitrogen of neutral flokalin. It should be noted that, unlike lysine, the threonine amino group participates in formation of a peptide bond when threonine affiliates itself with a protein.

All interaction energies and relative stabilities of the flokalin-amino acid complexes mentioned above were calculated in the vacuum approach. We repeated the calculations for the most stable flokalin-lysine and flokalin-threonine complexes using the Polarizable Continuum Model (PCM) approach. In the PCM calculations we used methanol and water as polar solvents. Geometry optimization of the complexes converged to the structures similar to ones obtained with the vacuum approach. Resulting interaction energies and relative stabilities of the complexes are collected in Table 3. As it is seen, the interaction energies between charged species decreased (in absolute values) in polar solvents but stability order of the flokalin-amino acid complexes in methanol and water was found to be the same as in vacuum. Although the interaction between flokalin and amino acids is found to be weaker in the both solutions, the complexes are still stable since the interaction energies are negative.

Table 2
ZPVE and BSSE corrected interaction energies (IE, kcal/mol) and relative stabilities (ΔE, kcal/mol) of the protonated flokalin-lysine, flokalin-threonine, and flokalin-flokalin complexes calculated at the B3LYP/aug-cc-pVDZ level of theory.

Complex	IE[a]	ΔE[b]	Complex	IE[a]	ΔE[b]
Flokalin-Lysine			Flokalin-Threonine		
Fl·[Lys·H$^+$_1] A	−28.7	0.0	**Fl·[Thr2·H$^+$_1] A**	−33.6	0.0
Fl·[Lys2·H$^+$_1] A	−36.9	5.9	**Fl·[Thr2·H$^+$_1] B**	−31.4	2.2
Fl·[Lys2·H$^+$_1] B	−35.7	7.1	**Fl·[Thr·H$^+$_1] A**	−28.2	5.4
Fl·[Lys2·H$^+$_1] C	−28.1	14.7	**[Fl·H$^+$_1]·Thr2 A**	−12.4	15.8
Fl·[Lys2·H$^+$_2] A	−34.5	11.0	**[Fl·H$^+$_1]·Thr2 B**	−11.5	16.9
Fl·[Lys2·H$^+$_2] B	−28.7	16.8			
Fl·[Lys2·H$^+$_2] C	−13.9	31.6	Flokalin-Flokalin		
[Fl·H$^+$_1]·Lys2 A	−16.1	25.1	**Fl·[Fl·H$^+$_1] A**	−28.7	

[a] Calculated as the difference between the total energy of the complex and the sum of the total energies of the monomers.
[b] Calculated with respect to the lowest energy of the **Fl·[Lys·H$^+$_1] A** or **Fl·[Thr2·H$^+$_1] A** complex for the flokalin-lysine and flokalin-threonine complexes, respectively.

Table 3
ZPVE and BSSE corrected interaction energies (IE, kcal/mol) and relative stabilities (ΔE, kcal/mol) of the protonated flokalin-lysine and flokalin-threonine, complexes in water and methanol calculated at the B3LYP(IEFPCM)/aug-cc-pVDZ level of theory.[a]

Complex	IE	ΔE	Complex	IE	ΔE
Flokalin-Lysine			Flokalin-Threonine		
Fl·[Lys·H$^+$_1] A	−7.8/-8.2	0.0/0.0	**Fl·[Thr2·H$^+$_1] A**	−8.4/-7.5	0.0/0.0
Fl·[Lys2·H$^+$_1] A	−9.4/-9.8	1.5/1.7	**Fl·[Thr2·H$^+$_1] B**	−7.1/-6.1	1.3/1.4
Fl·[Lys2·H$^+$_1] B	−9.3/-9.8	1.4/1.7			

[a] In water/In methanol.

4. Conclusions

A combined experimental and computational study of the molecular structure of recently developed K_{ATP}-channel activator flokalin and its biologically significant supramolecular complexes with amino acids lysine and threonine, involved in K_{ATP}-channels activators binding sites, was performed by electrospray ionization mass spectrometry (ESI MS) and by B3LYP/aug-cc-pVDZ methods for the first time. From the analysis of the data obtained in the study we can conclude the following.

Electrospray ionization mass spectrometry is found to be an effective method to study flokalin in polar solvents, as well as to study its noncovalent interactions with possible biological targets involved in the flokalin biological activity. The ESI MS experiments provide a characteristic ESI mass spectrum of flokalin. The peaks of molecular and quazimolecular ions appearing in the ESI spectrum of flokalin can be used as a reference in ESI MS studies of this compound in biological solutions and pharmacological products.

The B3LYP/aug-cc-pVDZ calculations provide the molecular structure of the most stable tautomer of flokalin in vacuum. The structure is characterized by symmetrical binding of two hydrogen atoms to the nitrogen atoms, which connected to −C═N−C≡N group of flokalin. The structure of the protonated flokalin molecule, $Fl{\cdot}H^+$, is also determined.

The ESI MS study of some model systems containing flokalin and selected amino acids (lysine or threonine) Fl:AA (in the 1:1 M ratio) in MeOH reveal the presence of prominent peaks of stable noncovalent protonated complexes of flokalin with the amino acids, $Fl{\cdot}Lys{\cdot}H^+$ and $Fl{\cdot}Thr{\cdot}H^+$ in the ESI MS spectra. In probing the flokalin-glycine (1:1 M ratio) system under the same ESI MS conditions no peaks of noncovalent complexes of flokalin with the simplest amino acid are found in the spectrum. The registration of the peaks due to stable noncovalent supramolecular complexes of flokalin with Lys and Thr in the ESI MS spectrum testifies to the high stability of these complexes in the model solutions. It also gives credence to the possibility of bonding interaction of flokalin with the K_{ATP} channel-protein sites containing these aminoacids in real biological systems. The comparison of the relative intensities of the peaks of $nFl{\cdot}AA{\cdot}H^+$ ($n = 1\div2$) with the peaks of protonated/cationized flokalin homoclusters, $[nFl{\cdot}H]^+$ or $[nFl{\cdot}Na]^+$ in the ESI mass spectra of the Fl-Lys and Fl-Thr model systems suggests preference of flokalin molecules to bind with Lys molecules instead of formation of homoclusters. This pertains to the conditions of competitive complexation in flokalin-lysine solution. It also suggests a lower preference of flokalin to form noncovalent complexes with Thr in comparison with the formation of homoclusters in the model solution.

Vacuum structural and energetic parameters of the $Fl{\cdot}AA{\cdot}H^+$ complexes registered in the ESI MS experiments are calculated at the B3LYP/aug-cc-pVDZ level of theory. It is found that the most stable flokalin-lysine protonated complex is stabilized by a strong electrostatic interaction between the protonated side-chain amino group of the most stable conformer of protonated lysine and the nitrile nitrogen of the neutral flokalin. The most stable flokalin-threonine protonated complex is also formed by neutral flokalin and a protonated aminoacid molecule. This complex is also stabilized by electrostatic interaction between the protonated amino group of threonine and the nitrile nitrogen of the neutral flokalin molecule.

The formation of the stable noncovalent complexes of flokalin with Lys and Thr revealed by the ESI MS probing and confirmed by the B3LYP/aug-cc-pVDZ calculations gives support to the idea of a strong possibility of interaction of flokalin with the K^+-channel domains enriched with Lys and Thr residues in biological systems.

Acknowledgments

Authors acknowledge the Program of cooperation between Ukrainian and Hungarian Academies of Sciences for the financial support of visit of the scientists from B. Verkin Institute for Low Temperature Physics and Engineering of the National Academy of Sciences of Ukraine to the Institute of Organic Chemistry of Research Centre for Natural Sciences of the Hungarian Academy of Sciences, where the mass spectrometry experiments have been carried out. An allocation of computer time from the Computational Center at the Institute for Low Temperature Physics and Engineering and from UA Research High Performance Computing (HPC) and High Throughput Computing (HTC) at the University of Arizona is gratefully acknowledged. Authors also thank the scientists of the Department of Cytology of Bogomoletz Institute of Physiology of the NAS of Ukraine for providing a flokalin sample for the present experimental investigation.

Appendix A. Supplementary data

Supplementary data related to this article can be found at http://dx.doi.org/10.1016/j.molstruc.2017.06.007.

References

[1] V. Pashynska, S. Stepanian, A. Gomory, K. Vekey, L. Adamowicz, Competing intermolecular interactions of artemisinin-type agents and aspirin with membrane phospholipids: combined model mass spectrometry and quantum-chemical study, Chem. Phys. 455 (2015) 81–87.
[2] V. Pashynska, O. Boryak, M.V. Kosevich, S. Stepanian, L. Adamowicz, Competition between counterions and active protein sites to bind bisquaternary ammonium groups. A combined mass spectrometry and quantum chemistry model study, Eur. Phys. J. D. 58 (2010) 287–296.
[3] V.A. Pashynska, M.V. Kosevich, H. Van den Heuvel, M. Claeys, Characterization of noncovalent complexes of antimalarial agents of the artemisinin type and Fe(III)-heme by electrospray ionization mass spectrometry and collisional activation tandem mass spectrometry, J. Am. Soc. Mass Spectrom. 15 (2004) 1181–1190.
[4] V.A. Pashinskaya, M.V. Kosevich, A. Gomory, O.V. Vashchenko, L.N. Lisetski, Mechanistic investigation of the interaction between bisquaternary antimicrobial agents and phopholipids by liquid secondary ion mass spectrometry and differential scanning calorimetry, Rapid Commun. Mass Spectrom. 16 (18) (2002) 1706–1713.
[5] http://www.who.int/mediacentre/factsheets/fs317/en/.
[6] R.B. Strutynskyi, R.A. Rovenets, O.O. Moibenko, Mechanisms of cardioprotective activity of domestic activator of K_{ATP} channels flokalin, Tavricheskiy Medico-Biological Vestnik 15 (3) (2012) 226–229 [in Ukrainian].
[7] K. Benndorf, S. Thierfelder, B. Doepher, G. Gebhardt, H. Hirche, Role of Cardiac K_{ATP}channels. Functional identity with native channels from sarcolemma of human verticular cells, Circ. Res. 83 (1998) 1132–1143.
[8] J.M. Quayle, M.T. Nelson, N.B. Standen, ATP-sensitive and inwardly rectifying potassium channels in smooth muscle, Physiol. Rev. 77 (4) (1997) 1165–1232.
[9] A. Jahandir, A. Terzic, K_{ATP} channel therapeutics at the bedside, J. Mol. Cell. Cardiol. 39 (2005) 99–112.
[10] O.O. Moibenko, R.B. Strutynskyi, L.M. Yagupolskyi, M.A. Mohort, Development and preparation to adoption of the new domestic cardioprotective preparation – fluorine containing activator of ATP-dependent potassium channels-Flokalin, Nauka innovacii 2 (4) (2006) 77–82 [in Ukrainian].
[11] R.B. Strutynskyi, The vasodilatattory effects of flocalin, a fluorine-containing K_{ATP} channel opener, Fiziol. Zh. 56 (4) (2010) 59–65 [in Ukrainian].
[12] O.O. Moibenko, R.B. Strutynskyi, L.M. Yagupolskyi, M.A. Mohort, A.S. Shalamai,

Organization of industrial production of preparation Flokalin- the new domestic myotropic spasmolyticand cardioprotector, Nauka innovacii 5 (1) (2009) 80–84 [in Ukrainian].
[13] Patent of Ukraine on useful model № 59490 A 61 K 31/00. Strutynskyi R.B., Moibenko O.O. Yagupolskyi Yu.L. Method of decrease of the size of myocardium necrotic injury under experimental ischemia- reperfusion of myocardium. №u 2011 02188; Appl. 24.02.2011; Publ. 10.05.2011. Promislova vlasnist, Bull. N9 (2011) [in Ukrainian].
[14] O.I. Voitychuk, R.B. Strutynskyi, L.M. Yagupolskii, A. Tinker, O.O. Moibenko, Y.M. Shuba, Sarcolemmal cardiac KATP channels as a target for the cardioprotective effects of the fluorine-containing pinacidil analogue flocalin, Brit J. Pharmacol. 162 (3) (2011) 701–711.
[15] R.B. Strutynskyi, R.A. Rovenets, O.P. Neshet, L.V. Tumanovska, T.M. Boychuk, B.V. Dzuran, O.O. Moibenko, Effect of the medical preparation of flokalin on myocardium ischemia- reperfusion course, Fiziol. Zh. 57 (1) (2011) 55–65 [in Ukrainian].
[16] F.M. Gribble, F. Reimann, R. Ashfield, F.M. Ashcroft, Nucleotide modulation of pinacidil stimulation of the cloned K(ATP) channel Kir6.2/SUR2A, Mol. Pharmacol. 57 (6) (2000) 1256–1261.
[17] Christophe Moreau, Hélène Jacquet, Anne-Lise Prost, Nathalie D'hahan, Michel Vivaudou, The molecular basis of the specificity of action of K_{ATP} channel openers, EMBO J. 19 (24) (2000) 6644–6651, http://dx.doi.org/10.1093/emboj/19.24.6644.
[18] P.I. Hanson, S.W. Whiteheart, AAA+ proteins: have engine, will work, Nat. Rev. Mol. Cell Biol. 6 (7) (2005) 519–529, http://dx.doi.org/10.1038/nrm1684. PMID 16072036.
[19] M.R. Carson, S.M. Travis, M.J. Welsh, The two nucleotide-binding domains of cystic fibrosis transmembrane conductance regulator (CFTR) have distinct functions in controlling channel activity, J. Biol. Chem. 270 (1995) 1711–1717.
[20] Y.H. Ko, P.L. Pedersen, The first nucleotide binding fold of the cystic fibrosis transmembrane conductance regulator can function as an active ATPase, J. Biol. Chem. 270 (1995) 22093–22096.
[21] F.M. Gribble, S.J. Tucker, F.M. Ashcroft, The essential role of the Walker A motifs of SUR1 in K-ATP channel activation by Mg-ADP and diazoxide, EMBO J. 16 (1997) 1145–1152.
[22] F.M. Gribble, S.J. Tucker, T. Haug, F.M. Ashcroft, MgATP activates the beta cell KATP channel by interaction with its SUR1 subunit, Proc. Nat. Acad. Sci. U. S. A. 95 (1998) 7185–7190.
[23] S. Shyng, T. Ferrigni, C.G. Nichols, Regulation of KATP channel activity by diazoxide and MgADP. Distinct functions of the two nucleotide binding folds of the sulfonylurea receptor, J. Gen. Physiol. 110 (1997) 643–654.
[24] A. Hambrock, T. Kayar, D. Stumpp, H. Osswald, Effect of two amino acids in TM17 of Sulfonylurea receptor SUR1 on the binding of ATP-sensitive K+ channel modulators, Diabetes 53 (Suppl. 3) (2004) S128–S134.
[25] I.A. Kaltashov, S.J. Eyles, Mass Spectrometry in Structural Biology and Biophysics: Architecture, Dynamics and Interaction of Biomolecules, second ed., John Wiley & Sons, Inc., New York, 2012, p. 316.
[26] G. Siuzdak, The Expanding Role of Mass Spectrometry in Biotechnology, second ed., MCC Press, - San Diego, 2006, p. 257.
[27] J. Laskin, C. Lifshitz (Eds.), Principles of Mass Spectrometry Applied to Biomolecules, John Wiley & Sons, Inc., Hoboken, New Jersey, 2006, p. 687.
[28] R. Cole (Ed.), Electrospray and MALDI Mass Spectrometry: Fundamentals, Instrumentation, Practicalities, and Biological Applications, second ed., John Wiley & Sons, Inc., Hoboken, New Jersey, 2010, p. 1008.
[29] J.A. Loo, Electrospray ionization mass spectrometry: a technology for studying non-covalent macromolecular complexes, Int. J. Mass Spectrom. 200 (1–3) (2000) 175–186, http://dx.doi.org/10.1016/S1387-3806(00)00298-0.
[30] Th Wyttenbach, M.T. Bowers, Intermolecular interactions in biomolecular systems examined by mass spectrometry, Annu. Rev. Phys. Chem. 58 (2007) 511–533, http://dx.doi.org/10.1146/annurev.physchem.58.032806.104515.
[31] B.J. McCullough, S.J. Gaskell, Using electrospray ionisation mass spectrometry to study non-covalent interactions, Comb. Chem. High. Throughput Screen. 12 (2) (2009) 203–211, http://dx.doi.org/10.2174/138620709787315463.
[32] R. Guevremont, K.W.M. Siu, J.C.Y. Le Blanc, S.S. Berman, Are the electrospray mass spectra of proteins related to their aqueous solution chemistry? J. Am. Soc. Mass Spectrom. 3 (1992) 216–224.
[33] A.D. Becke, Density-functional exchange-energy approximation with correct asymptotic behavior, Phys. Rev. B 38 (1988) 3098–3100, http://dx.doi.org/10.1103/PhysRevA.38.3098.
[34] C. Lee, W. Yang, R.G. Parr, Development of the Colle-Salvetti correlation-energy formula into a functional of the electron density, Phys. Rev. B 37 (1988) 785–789.
[35] S.H. Vosko, L. Wilk, M. Nusair, Accurate spin-dependent electron liquid correlation energies for local spin density calculations: a critical analysis, Can. J. Phys. 58 (1980) 1200–1211 doi: 10.1139/p80-159/.
[36] S. Miertuš, E. Scrocco, J. Tomasi, Electrostatic interaction of a solute with a continuum. a direct utilization of ab initio molecular potentials for the prevision of solvent effects, Chem. Phys. 55 (1981) 117–129, http://dx.doi.org/10.1016/0301-0104(81)85090-2.
[37] S. Miertuš, J. Tomasi, Approximate evaluations of the electrostatic free energy and internal energy changes in solution processes, Chem. Phys. 65 (1982) 239–245, http://dx.doi.org/10.1016/0301-0104(82)85072-6.
[38] J.L. Pascual-Ahuir, E. Silla, I. Tuñón, GEPOL: an improved description of molecular-surfaces. 3. A new algorithm for the computation of a solvent-excluding surface, J. Comput. Chem. 15 (1994) 1127–1138, http://dx.doi.org/10.1002/jcc.540151009.
[39] M.J. Frisch, G.W. Trucks, H.B. Schlegel, G.E. Scuseria, M.A. Robb, J.R. Cheeseman, G. Scalmani, V. Barone, B. Mennucci, G.A. Petersson, H. Nakatsuji, M. Caricato, X. Li, H.P. Hratchian, A.F. Izmaylov, J. Bloino, G. Zheng, J.L. Sonnenberg, M. Hada, M. Ehara, K. Toyota, R. Fukuda, J. Hasegawa, M. Ishida, T. Nakajima, Y. Honda, O. Kitao, H. Nakai, T. Vreven, J.J.A. Montgomery, J.E. Peralta, C. Ogliaro, M. Bearpark, J.J. Heyd, E. Brothers, K.N. Kudin, V.N. Staroverov, R. Kobayashi, J. Normand, K. Raghavachari, A. Rendell, J.C. Burant, S.S. Iyengar, J. Tomasi, M. Cossi, N. Rega, J.M. Millam, R. Klene, J.E. Knox, J.B. Cross, V. Bakken, C. Adamo, J. Jaramillo, R. Gomperts, R.E. Stratmann, O. Yazyev, A.J. Austin, R. Cammi, C. Pomelli, J.W. Ochterski, R.L. Martin, K. Morokuma, V.G. Zakrzewski, G.A. Voth, P. Salvador, J.J. Dannenberg, S. Dapprich, A.D. Daniels, O. Farkas, J.B. Foresman, J.V. Ortiz, J. Cioslowski, D.J. Fox, Gaussian 09, Revision A.02, Gaussian, Inc., Wallingford CT, 2009.
[40] Y. Leng, M. Zhang, C. Song, M. Chen, Z. Lin, A semi-empirical and ab anitio combined approach for the full conformational searches of gaseous lysine and lysine-H_2O complex, J. Mol. Str. THEOCHEM 858 (2008) 52–65, http://dx.doi.org/10.1016/j.theochem.2008.02.016.
[41] B. Boeckx, G. Maes, Experimental and theoretical observation of different intramolecular H-bonds in lysine conformations, J. Phys. Chem. B 116 (2012) 12441–12449, http://dx.doi.org/10.1021/jp306916e.
[42] M. Zhang, Z. Lin, Ab initio studies of the conformers and conformational distribution of the gaseous hydroxyamino acid threonine, J. Mol. Str. Theochem. 760 (2006) 159–166, http://dx.doi.org/10.1016/j.theochem.2005.12.008.
[43] J.L. Alonso, C. Pérez, M.E. Sanz, J.C. López, S. Blanco, Seven conformers of L-threonine in the gas phase: a LA-MB-FTMW study, Phys. Chem. Chem. Phys. 11 (2009) 617–627, http://dx.doi.org/10.1039/b810940k.
[44] E.P.L. Hunter, S.G. Lias, Evaluated gas phase basicities and proton affinities of molecules: an update, J. Phys. Chem. Ref. Data 27 (1998) 413–656, http://dx.doi.org/10.1063/1.556018.
[45] T.C. Dinadayalane, G.N. Sastry, J. Leszczynski, Comprehensive theoretical study towards the accurate proton affinity values of naturally occurring amino acids, Int. J. Quant. Chem. 106 (2006) 2920–2933, http://dx.doi.org/10.1002/qua.21117.

1.9. Підсумки до розділу 1.

З метою визначення молекулярно-фізичних механізмів біологічної дії ряду протималярійних, антисептичних та протибактеріальних, противірусних та кардіопротекторних агентів, у системах *in vitro* вивчено їхні міжмолекулярні взаємодії з потенційними біомолекулами-мішенями та їхніми компонентами з застосуванням експериментального методу мас-спектрометрії з IEP та теоретичних методів квантово-механічних розрахунків DFT та MP2. Основні підсумки проведених досліджень наведено нижче.

1. У рамках вивчення молекулярних механізмів біологічної активності протималярійних агентів уперше визначені мас-спектрометричні маркери (характеристичні мас-спектральні лінії/піки) формування в системах *in vitro* стабільних нековалентних комплексів молекул широковживаних протималярійних препаратів хінін, артемізинін, дигідроартемізинін, α-артеметер, β-артеметер та β-артеестер з їхньою потенційною молекулярною мішенню в харчових вакуолях збудника малярії - Fe(III)-гем. Таке нековалентне комплексоутворення запропоновано в якості молекулярно-фізичного механізму, пов’язаного з протималярійною активністю препаратів артемізинінового ряду, а саме з цитотоксичною дією цих агентів на еритроцитарній стадії розвитку збудника малярії в організмі хворого. Дослідження методом мас-спектрометрії з IEP складних модельних сумішей, що складалися з двох різних протималярійних засобів (що вибиралися попарно) та гему дозволили оцінити відносну інтенсивність мас-спектрометричних піків нековалентних комплексів різних протималярійних агентів із Fe(III)-гемом та встановити, що хінін (використовувався в якості агенту для порівняння) зв’язується з гемом приблизно у два рази активніше за препарати артемізинінового ряду.
2. Вперше експериментально оцінено енергетичні характеристики міжмолекулярної взаємодії в нековалентних комплексах протималярійного препарату хінін та агентів артемізинінового ряду з Fe(III)-гемом завдяки використанню потужного методу тандемної мас-спектрометрії з ДІЗ із

застосуванням низькоенергетичних молекул газу He та високоенергетичних молекул Xe для зіткнень, що індукували розпад комплексів. Показано, що нековалентний асоціат хініну з Fe(III)-гемом є стабільнішим, ніж комплекси артемізиніну та його похідних з гемом. Встановлено, що дигідроартемізинін (який вважається активним метаболітом похідних артемізиніну *in vivo)* єдиний із досліджених лікарських агентів формує комплекс із гемом, в якому протон заміщений на іон Na^+, причому енергетична стабільність такого комплексу є близькою до стабільності комплексу хінін-гем. Отримані дані свідчать, що здатність препаратів артемізинінового ряду формувати нековалентні комплекси з гемом є порівняною з такою для традиційного протималярійного препарату хінін, причому тільки для дигідроартемізиніну в утворених комплексах із гемом спостерігалися іон-молекулярні реакції за участю іону Na^+, що моделюють ймовірні молекулярні процеси за участі препаратів артемізинінового ряду в умовах фізіологічного розчину.

3. З метою встановлення фізичних молекулярних основ показаної в ряді клінічних досліджень протипухлинної активності артемізиніну та його похідних методом мас-спектрометрії з ІЕР вивчено міжмолекулярну взаємодію препаратів артемізинінового ряду з азотистими основами нуклеїнових кислот. За результатами дослідження вперше визначені мас-спектрометричні маркери, що свідчать про формування стабільних нековалентних комплексів молекул артемізиніну та дигідроартемізиніну з азотистими основами: аденіном (Ade), цитозином (Cyt) та метилтиміном (mThy). Показано, що мас-спектрометричні піки комплексів препаратів артемізинінового ряду з пуриновими азотистими основами мали більшу відносну інтенсивність, ніж піки комплексів агентів із піримідиновими основами, що свідчить про більшу відносну стабільність нековалентних комплексів протималярійних агентів із пуриновими азотистими основами. Встановлено зв’язок «структура-відносна стабільність» для досліджених нековалентних комплексів, які утворюються за рахунок міжмолекулярних сил Ван-дер-Ваальса та водневих зв’язків між полярними функціональними

групами взаємодіючих молекул. Формування нековалентних асоціатів між артемізиніновими агентами та азотистими основами нуклеїнових кислот, що можуть впливати на функціональну активність ДНК та РНК пухлинних клітин, запропоновано в якості молекулярно-фізичного механізму, що зумовлює протипухлинну дію препаратів артемізинінового ряду.

4. Методом мас-спектрометрії з ІЕР визначено мас-спектрометричні маркери пов'язаного з протиінфекційоною активністю процесу формування супрамолекулярних нековалентних комплексів дикатіонів бісчетвертинного амонієвого агенту декаметоксин (Cat^{2+}) з молекулами мембранного фосфоліпіду дипальмітоїлфосфатидилхолін (М), що моделюють взаємодію цього мембранотропного лікарського препарату з фосфоліпідними компонентами біологічних мембран. Молекулярний склад та стабільність нековалентних комплексів дикатіону декаметоксину з цим мембранним фосфоліпідом Cat•nM(n=1÷9) проаналізовано за результатами експериментів методом тандемної мас-спектрометрії з ДІЗ (з використанням Не та Хе в якості газів, індукуючих розпад комплексів).
5. З метою розвитку експериментально-методичної бази біофізичних досліджень у ході експериментів оптимізовано метод мас-спектрометрії з ІЕР для визначення міжмолекулярних взаємодій мембранотропних агентів. Зокрема, встановлено оптимальні параметри електричного потенціалу на конусному електроді (cone voltage, CV) в джерелі іонів мас-спектрометра при елекророзпиленні (оптимальний інтервал значень - між 100 та 125 В) задля можливості реєстрації в спектрах сигналів супрамолекулярних комплексів дикатіону декаметоксину з великорозмірними кластерами дипальмітоїлфосфатидилхоліну, що складаються зі значної кількості молекул фосфоліпіду та моделюють фосфоліпідні кластери біологічних мембран. Оптимізований метод мас-спектрометрії з ІЕР запропоновано у якості методики швидкого скринінгу бісчетвертинних амонієвих сполук із потенційною протиінфекційною активністю, яка зумовлена

мембранотропним ефектом цих агентів, який спричиняє дестабілізуючу дію на мембранні структури клітин бактерій.

6. У рамках вивчення міжмолекулярної взаємодії бісчетвертинних амонієвих протиінфекційних агентів із білковими компонентами біомембран уперше за результатами модельного дослідження із застосуванням теоретичних розрахункових методів та експериментального методу мас-спектрометрії з МАЛДІ визначено, що така взаємодія має відбуватися в умовах конкуренції між функціональними групами бокових радикалів амінокислот з активних центрів мембранних протеїнів та аніоном Cl^- бісчетвертинної амонієвої солі за зв'язування дикатіону протиінфекційного агенту. Зокрема, в ході розрахунків методами DFT/B3LYP/6-31^{++}G** та MP2/6-31^{++}G** доведено, що міжмолекулярна взаємодія іону тетраметіламонію (TMA^+, моделює бісчетвертинні амонієві агенти) з 2,5- дигідроксибензойною кислотою (DHB, чиї функціональні групи моделюють функціональні групи амінокислот аспартат, глутамат, триптофан, тирозин, гістидин, фенілаланін) відбувається за умов конкуренції з протиіоном хлору Cl^-. Розрахована енергія взаємодії (IE) TMA^+ з аніоном $[DHB - H]^-$ є близькою, але меншою за абсолютною величиною у порівнянні з енергію взаємодії TMA^+ з Cl^- у вакуумному наближенні. Значення енергії взаємодії іону TMA^+ з нейтральною молекулою DHB є також від'ємним, але приблизно в 10 разів меншим за модулем, ніж величина енергії взаємодії з депротонованою DHB, бо комплекс із молекулою DHB стабілізовано слабким водневим зв'язком іона TMA^+ з гідроксильною групою DHB на відміну від іонного зв'язку в комплексі TMA^+ з $[DHB - H]^-$. Завдяки застосуванню методу PCM, що дозволяє оцінити вплив сольватації на стабільність модельних комплексів, встановлено, що в полярному оточенні енергії взаємодії комплексів TMA^+ з аніонами $[DHB - H]^-$ та Cl^- мають позитивні значення, що вказує на нестабільність комплексів у цих умовах. При цьому значення IE в комплексі TMA^+ з нейтральною молекулою DHB у водному оточенні є негативною (-4.27 кДж/моль), що доводить стабільність такого комплексу, який, як показують розрахунки,

стабілізується завдяки «катіон-π» міжмолекулярній взаємодії в полярному середовищі. Отримані дані квантово-механічних розрахунків дозволили пояснити результати дослідження методом мас-спектрометрії з МАЛДІ, в якому встановлено превалювання в мас-спектрах піків комплексів дикатіону бісчетвертинного амонієвого агенту декаметоксину з DHB над піком комплексу дикатіону декаметоксину з протиіоном хлору.

7. Молекулярну конкуренцію протиіонів із функціональними групами активних центрів потенційних білкових мембранних молекул-мішеней за зв'язування з четвертинними амонієвими групами катіонів протиінфекційних агентів підтверджено в експериментальному дослідженні модельних систем, що складалися з хлориду тетраметиламонію та дигідроксибензойної кислоти методом мас-спектрометрії з БША (для бомбардування використовувався газ аргон) завдяки реєстрації в спектрах мас-спектрометричних маркерів комплексів TMA^+ з протиіоном Cl^- (з різною стехіометрією) та комплексу $2TMA^+•[DHB - H]^-$. Розрахунки структурно-енергетичних характеристик комплексів, що зареєстровані в мас-спектрометричному експерименті, методами квантово-механічних розрахунків DFT/B3LYP/6-$31^{++}G^{**}$ та MP2/6-$31^{++}G^{**}$, дозволили встановити, що комплекс $2TMA^+•Cl^-$ у вакуумі має структуру сендвіча з протиіоном хлора, розташованим між двома катіонами TMA^+, та характеризується більшим за модулем значенням енергії взаємодії (-491.68 кДж/моль за результатами розрахунків вільної енергії Гіббса) у порівнянні з енергією взаємодії в комплексі $2TMA^+•[DHB - H]^-$ (-355.15 кДж/моль). Встановлено кореляцію теоретичних та експериментальних даних щодо відносної стабільності досліджених модельних комплексів.
8. У дослідженнях інших мембранотропних протиінфекційних агентів уперше методом мас-спектрометрії з ІЕР визначено мас-спектрометричні маркери (молекулярні референтні піки), двох біогенних мембранотропних рамноліпідів, що спродуковані бактеріями штаму *Pseudomonas* sp. PS-17 та характеризуються протибактеріальною активністю. Ці мас-спектрометричні маркери запропоновано використовувати для ідентифікації методом мас-

спектрометрії означених рамноліпідів у різноманітних біологічних та технологічних зразках. У рамках вивчення методом мас-спектрометрії модельних *in vitro* систем, що складалися з рамноліпіду та фосфоліпіду дипальмітоїлфосфатидилхолін встановлено, що в результаті міжмолекулярної взаємодії компонентів систем у полярному розчиннику формуються стабільні нековалентні комплекси мембранного фосфоліпіду з рамноліпідним біосурфактантом. Формування таких комплексів, що впливає на функціональну активність фосфоліпідних компонентів бактеріальних біомембран, запропоновано в якості молекулярно-фізичного механізму, що зумовлює протибактеріальну дію досліджених рамноліпідів.

9. З метою встановлення молекулярних фізичних механізмів противірусної дії лікарської речовини тилорон (Til) вперше методом мас-спектрометрії з ІЕР вивчено міжмолекулярну взаємодію цього противірусного агенту з його потенційними молекулами-мішенями нуклеозидами (аденозин - Ado, уридин - Urd, та тимідин - Thd) у модельних бінарних системах (Til +нуклеозид) (Ado або Thd, або Urd) та трьохкомпонентній системі (Til + Ado + Urd) в полярному розчиннику. Встановлено, що тилорон формує стабільні нековалентні комплекси тільки з уридином (про що свідчить наявність у спектрах мас-спектрометричного маркеру – піку нековалентного комплексу Urd з Til та відсутність піків комплексів Til з іншими нуклеозидами). Така селективність комплексоутворення тилорону з уридином дозволяє розглядати саме РНК (в склад яких входить нуклеозид Urd) як найбільш ймовірні біомолекули-мішені противірусної дії тилорону серед нуклеїнових кислот та вказує на уридин як потенційний центр специфічного зв’язування тилорону з молекулами РНК.
10. Дослідження біологічно значущих міжмолекулярних взаємодій антивірусного препарату тилорон у складних модельних біологічних системах, що містили біогенні одноланцюгові РНК (ssRNA), які було отримано з дріжджів *Saccharomyces cerevisiae*, методом динамічного розсіювання світла (дослідження виконані колегами-співавторами з

Інституту мікробіології та вірусології НАН України [7]), показали, що в умовах, наближених до фізіологічних, введення тилорону у розчин РНК призводить до формування в системі молекулярних агрегатів Til+ssRNA, які у 10 разів перевищують за розміром частинки, присутні у вихідному розчині РНК. Формування таких міжмолекулярних комплексів тилорону з вірусною РНК або з РНК клітин організму хазяїну запропоновано в якості молекулярно-фізичного механізму, пов'язаного з противірусною дією агенту тилорон та можливими ефектами токсичності препарату по відношенню до клітин людини.

11. Вперше за результатами експериментів методом мас-спектрометрії з IEP визначено мас-спектрометричні маркери (референтні піки в мас-спектрах) нещодавно винайденого в Україні кардіопротекторного агенту флокалін (Fl), що є фторвмісним аналогом пінациділу (активатору АТФ-чутливого калієвого мембранного каналу). Ці референтні молекулярні піки агенту в мас-спектрах можуть використовуватися для ідентифікації флокаліну в різноманітних біологічних зразках та для контролю технологічних процесів синтезу препарату методом мас-спектрометрії. Квантово-механічним розрахунковим методом B3LYP/aug-cc-pVDZ встановлено структуру найбільш стабільного таутомеру Fl у вакуумному наближенні. Ця структура характеризується наявністю двох атомів водню (H), що зв'язані з атомами азоту (N), які розташовані симетрично по відношенню до -C=N-C≡N групи флокаліну. Також розраховано розподіл електростатичного потенціалу на поверхні молекули флокаліну, який є важливим для визначення характеру міжмолекулярних взаємодій Fl з біомолекулами-мішенями та їхніми компонентами.

12. Використовуючи комбінований підхід, що поєднує експериментальний метод мас-спектрометрії з IEP та теоретичний метод квантово-хімічних розрахунків B3LYP/aug-cc-pVDZ, вперше вивчено міжмолекулярні взаємодії флокаліну з потенційними молекулами-мішенями - амінокислотами лізин (Lys), треонін (Thr) та гліцин (Gly). Експериментально доведено формування

стабільних нековалентних комплексів Fl з протонованими Lys та Thr в полярному оточенні завдяки реєстрації мас-спектрометричних маркерів таких комплексів, при цьому піки кластерів Fl з Gly в мас-спектрі модельної системи не фіксувалися. Структурні та енергетичні параметри протонованих нековалентних комплексів Fl•Lys•H^+ та Fl•Thr•H^+, сигнали яких зареєстровані в мас-спектрах, розраховано квантово-хімічним методом та встановлено, що енергія взаємодії в таких комплексах має від'ємні значення як в вакуумному наближенні, так і в полярному середовищі (за даними розрахунків методом PCM), що підтверджує стабільність таких міжмолекулярних комплексів у різних середовищах. Найбільш стабільні нековалентні комплекси Fl з Lys•H^+ та Fl з Thr•H^+ стабілізовані завдяки взаємодіям електростатичної природи між протонованими аміногрупами амінокислот Lys або Thr та атомом N нітрильної групи флокаліну (що характеризується частковим негативним зарядом). Формування нековалентних комплексів між Fl та Lys або Thr запропоновано в якості молекулярного механізму взаємодії флокаліну з АТФ-чутливим калієвим мембранним каналом, що пов'язано з кардіопротекторную активністю препарату. При цьому домени регуляторних субодиниць цих мембранних каналів (рецепторів сульфонілсечовини), збагачені на залишки лізину та треоніну, розглядаються як потенційні місця зв'язування кардіопротекторного агенту флокалін із білковою молекулою-мішенню цього мембранного каналу.

РОЗДІЛ 2

Мас-спектрометричні маркери молекулярно-фізичних процесів, що здатні змінювати дію біологічно активних агентів: встановлення молекулярних механізмів модифікації активності лікарських речовин різних груп при одночасному застосуванні

У зв’язку з поширенням у сучасній медичній практиці схем лікування з сумісним застосуванням комплексу лікарських речовин, однією з актуальних проблем молекулярної біофізики вважається встановлення молекулярно-фізичних процесів, що відбуваються за участю ліків різних груп і біомолекул та можуть призводити до модифікації біологічної активності цих лікарських агентів. Верифікований у ході попередніх досліджень комплексний методичний підхід до вивчення міжмолекулярних взаємодій біологічно активних сполук, який поєднує експериментальний метод мас-спектрометрії з IEP та теоретичний метод квантово-механічних розрахунків DFT (B3LYP/aug-cc-pVDZ), було застосовано до дослідження проблеми зміни (модифікації) активності лікарських сполук різних груп при їхньому одночасному застосуванні для наступних систем: протималярійні агенти артемізинінового ряду, аспірин (ASP, ацетилсаліцилова кислота) та мембранний фосфоліпід дипальмітоїлфосфатидилхолін (DPPC); артемізинінові препарати, вітамін C (ASC, аскорбінова кислота) та DPPC; бісчетвертинні амонієві протиінфекційні агенти, аспірин та DPPC; антибіотик циклосерин, компонент пептидоглікану клітинних стінок бактерій N-ацетил-D-глюкозамін (NAG) та вітамін C.

Chemical Physics 455 (2015) 81–87

Contents lists available at ScienceDirect

Chemical Physics

journal homepage: www.elsevier.com/locate/chemphys

Competing intermolecular interactions of artemisinin-type agents and aspirin with membrane phospholipids: Combined model mass spectrometry and quantum-chemical study

Vlada Pashynska [a,*], Stepan Stepanian [a], Agnes Gömöry [b], Karoly Vekey [b], Ludwik Adamowicz [c]

[a] B.Verkin Institute for Low Temperature Physics and Engineering of the National Academy of Sciences of Ukraine, Lenin Ave., 47, 61103 Kharkov, Ukraine
[b] Institute of Organic Chemistry of Research Centre for Natural Sciences of the Hungarian Academy of Sciences, Magyar tudosok korutja, 2, Budapest H-1117, Hungary
[c] University of Arizona, Department of Chemistry and Biochemistry, Tucson, AZ 85721, USA

ARTICLE INFO

Article history:
Received 26 December 2014
In final form 22 April 2015
Available online 2 May 2015

Keywords:
Artemisinin-type agents
Aspirin
Dipalmitoylphosphatidylcholine
Competitive binding
Electrospray ionization mass spectrometry
DFT B3LYP/aug-cc-pVDZ calculations

ABSTRACT

Study of intermolecular interactions of antimalarial artemisinin type drugs and aspirin with membrane phospholipids is important in term of elucidation of the drugs activity modification under their joint usage. Combined experimental and computational study of the interaction of dihydroartemisinin, α arte mether, and artesunate with aspirin (ASP) and dipalmitoylphosphatidylcholine (DPPC) is performed by electrospray ionization (ESI) mass spectrometry and by DFT B3LYP/aug cc pVDZ methods. The results of the ESI investigation of systems containing artemisinin type agent, ASP and DPPC, reveal a competition between the antimalarial agents and ASP for binding with DPPC molecules. The complexation between the antimalarial drugs and ASP is also found. Observed phenomena suggest that membranotropic activity of artemisin type agents and aspirin is modified under their combined usage. To elucidate structure en ergy characteristics of the non covalent complexes studied the model DFT calculations are performed for dihydroartemisinin · ASP complex and complexes of the each drug with phosphatidylcholine head of DPPC in neutral and cationized forms.

1. Introduction

It is well known that the pathways of drugs to their molecular targets in the living organisms involve penetration through a mul titude of biological membrane systems; meanwhile, the majority of drugs pass into the cell directly by passive diffusion through the lipid bilayers of the cell biomembranes [1]. As far as the drugs bioavailability is essentially conditioned by the biomembranes penetration, the drugs therapeutic activity is determined as by its interaction with the proper molecular targets as by the drug inter action with the membrane molecular components.

In spite of extensive studies of the drug membrane interactions, the investigations have mainly concerned the action of individual molecules of some anesthetics, antibiotics, and anti cancer drugs on the membranes [1,2]. The situation becomes more complex when two or more drugs are administered at the same time. The combined action of several drugs involves unexpected additional effects including modulation of the drugs interaction with the membrane components. Since the problem has a principal importance for pharmacotherapy, studies of these phenomena have been traditionally carried out in the field of medicine. However, the basis of pharmacological effects of joint action of sev eral drugs lies in their physical/chemical properties and in forma tion of intermolecular complexes of the drugs molecules in particular. Thus, in the elucidation of these effects chemical phy sics methods should be applied. They can probe the underlying molecular mechanisms involved in the modification of the biolog ical activity of the drugs resulting from their joint use. Knowing these mechanisms is of a significant practical importance in thera pies involving combinations of drugs. High probability of mutual modulation of drugs used in combined (multi drug) therapeutic schemes of the present day medical practice is well documented. For example, it plays a significant role in modern multi drug approaches in the malaria treatment.

Antimalarial agent artemisinin and its derivatives, artemisinin type agents, which have been used in Chinese traditional medicine since ancient times, are currently successfully used to treat severe and/or multi drug resistant *Plasmodium falciparum* malaria [3,4]. Artemisinin type agents are increasingly being applied also in combination with other drugs, although our knowledge of molec ular mechanisms of their action and their main pharmacological

* Corresponding author. Tel.: +38 057 340 4906; fax: +38 057 340 4905.
E-mail address: vlada@vl.kharkov.ua (V. Pashynska).

http://dx.doi.org/10.1016/j.chemphys.2015.04.014
0301-0104/

properties including their intermolecular interactions with differ ent biomolecules and other drugs is still incomplete and it is actively investigated [4 8]. The understanding of these interac tions can be particularly important in, for example, the use of the Artemisinin based Combination Therapy [9] recommended by WHO for the malaria treatment. Another example involves apply ing some artemisinin type agents together with anti inflammatory and antipyretic medications. Therefore, it is clear that elucidation of the possible bioactivity and bioavailability modification of the artemisinin type and anti inflammatory medications under their joint usage is an important problem in the applied biomedical research.

In investigating the problem, along with performing tests on living organisms, model studies of the intermolecular interactions between biologically active compounds may provide an important contribution to the research. This contribution may save time and resources, which are usually involved in the experiments with the real biological objects and in medical trials, by narrowing the scope of the investigation to the most relevant problems. The modern experimental techniques allow for focusing the investigation on specific drug membrane interaction using various model mem brane systems. Modeling of the drug interaction with membrane components at the molecular level can also be carried out. The soft ionization mass spectrometry, which is a method frequently used in molecular biophysics research [10], is one of the most effi cient tools to study interactions between biomolecules [10 12]. The electrospray ionization (ESI) mass spectrometric (MS) tech nique, which is based on spraying solutions of biomolecules in polar solvents, is also successfully applied to model selective non covalent intermolecular interactions. The technique has been applied to study the interactions between biologically active agents, medicines in particular, with their specific molecular tar gets and with other biomolecules [13 16].

Our previous ESI MS study concerned the molecular mecha nisms involved in the antimalarial activity of artemisinin type agents [17]. The formation of non covalent complexes between the drugs and their potential molecular target heme *in vitro* was investigated [17]. The present model study performed with the ESI MS and quantum chemical calculations concerns the biologically significant interaction of artemisinin type drugs: dihydroartemisinin, artesunate and alfa artemether, and anti inflammatory acetylsalicylic acid (aspirin) with the membrane phospholipid molecule dipalmitoylphosphatidylcholine. The pur pose of the study is to elucidate at the molecular level the possible modification of the drugs biological activity due to multiple drug use.

2. Materials and methods

2.1. Model systems

The artemisinin derivatives, dihydroartemisinin (DHAn, MW = 284.35 Da), artesunate (ASt, MW = 384.40 Da) and alfa artemether (AMr, MW = 298.35 Da) provided by Dafra Pharma Company (Oud Tunhout, Belgium) are used in the study. Acetylsalicylic acid (aspirin, ASP, MW = 180.16 Da) is obtained from the State Scientific Centre of Medications (Kharkov, Ukraine). L α dipalmi toylphosphatidylcholine (DPPC, MW = 734.04 Da)) is purchased from "Alexis Biochemicals" (Switzerland). The structures of the investigated molecules are presented in Fig. 1.

Stock solutions of DHAn, ASP, and DPPC (5 mM) are prepared in the polar solvent methanol and used for preparation of the binary (drug:DPPC, 1:10 M ratio; artemisinin type drug:ASP, 1:1 M ratio) and ternary (artemisinin type drug:ASP:DPPC, M ration 1:1:10) model systems. The mixtures are kept at the room temperature

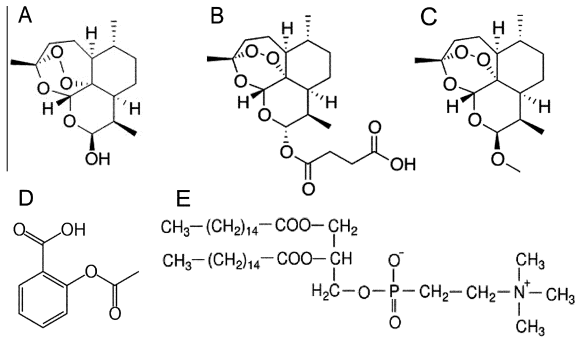

Fig. 1. Structures of the studied molecules: (A) DHAn, (B) ASt, (C) AMr, (D) ASP, (E) DPPC.

for at least 10 min before the ESI analysis. The spraying procedure required dilution of the studied solutions to the 250 μM final con centration of the most concentrated component of the model sys tems in each solution. It was shown in several studies [13 16] that utilization of methanol as a solvent significantly improves the quality of the ESI mass spectra while it does not disturb the com position of the intermolecular complexes formed in water solu tions [18].

2.2. ESI mass spectrometry

The ESI mass spectra are obtained in the positive ion mode using triple quadruple (QqQ) Micromass Quattro Micro mass spec trometer (Waters, Manchester, UK) equipped with the electrospray ion source. This source is operated in the standard ESI mode. The ESI source temperature is set to 120 °C and the desolvation tem perature is 200 °C. The spraying capillary is operated at 3.5 kV. The cone voltage (CV) value of 10 V is used. The analyzed solutions (20 μL) are injected into the mass spectrometer at a constant flow rate of 0.2 mL/min of methanol solvent. ESI spectra are recorded in the mass range of *m/z* 100 2000. Data acquisition and processing are performed using MassLynx 4.1 software (Waters, Manchester, UK).

2.3. Quantum chemical calculations

The theoretical study of non covalent complexes of one of the artemisinin derivative DHAn and ASP with the phosphatidyl choline (PCn) polar head of DPPC is performed using DFT quantum chemical calculations. We select dihydroartemisinin (DHAn) for the model study because DHAn was reported as the active metabo lite of the artemisinin type drugs in human organisms [19,20]. For modeling DPPC in the calculations we use phosphatidylcholine (PCn). This reduces the calculation time. The model provides an adequate representation of the polar head of the DPPC, which is considered to be the most accessible part of the membrane phos pholipid to interact with the drug molecules. This is because the polar head of the DPPC molecule is oriented away from the mem brane phospholipid bilayer in living cells. Moreover, the previous NMR investigation [21] showed that the interaction of aspirin with DPPC involves exactly the polar head of the phospholipid.

In the calculations, the geometries of some selected starting structures of the non covalent complexes are first fully optimized at the DFT B3LYP/aug cc pVDZ level of theory [22 24].

The PCM approach (integral equation formalism model (IEFPCM) [25]) is used in the calculations to describe the presence of the aqueous or methanol (solvent used in the ESI MS experi ments) solvent and it effect on the structure and energy of the complex.

To link up directly the results of the model calculations with the obtained experimental mass spectrometry data we also performed the DFT calculations of all mentioned above non covalent com plexes with inclusion of Na^+ ion, because the cationized complexes of the drugs with phospholipid were registered in the ESI mass spectra.

All calculations are performed using the Gaussian 09 program package [26].

3. Results and discussion

3.1. ESI mass spectrometry study of the drug DPPC model systems

In the first series of experiments ESI mass spectra of individual components of the systems studied, in particular, the artemisinin derivatives: dihydroartemisinin (DHAn), artesunate (ASt), and alfa artemether (AMr) were recorded and the experimental condi tions were optimized. In the ESI mass spectra of DHAn, as well as in the spectra of ASt and AMr, the ions of the following cationized adducts of the drugs monomer, dimer, and trimer (for DHAn) were registered: DHAn · Na^+ (*m*/*z* 307.3, RA 100%), 2DHAn · Na^+ (*m*/*z* 591.6, RA 33%), 3DHAn · Na^+ (*m*/*z* 876.2, RA 3 4%); ASt · Na^+ (*m*/*z* 407.4, RA 100%), 2ASt · Na^+ (*m*/*z* 791.8, RA 27%) and AMr · Na^+ (*m*/*z* 321.4, RA 100%), and 2AMr · Na^+ (*m*/*z* 619.8, RA 52%). Note that ionization of analytic molecules by attachment of residual sodium cations from solution is characteristic of the ESI procedure [13 16].

In the next step binary systems of all studied artemisinin type drugs with DPPC in the 1:10 M ratio were probed. The ESI mass spectra are shown in Figs. 2 4. The peaks of the ions characteristic to the studied drugs and the peaks corresponding to the ions characteristic to DPPC were registered. Also, intensive signals of the cationized non covalent complexes of drug · DPPC were registered. These ions were: DHAn · DPPC · Na^+ (*m*/*z* 1040.7, RA 24%) (Fig. 2), ASt · DPPC · Na^+ (*m*/*z* 1140.9, RA 30%) (Fig. 3), and AMr · DPPC · Na^+ (*m*/*z* 1054.8, RA 19%) (Fig. 4). The spectral data testify to the formation of stable non covalent complexes of the molecules of the antimalarial drugs with the phospholipid mole cules in the studied binary systems. This indicates a possibility of active intermolecular interactions between the antimalarial agents with the membrane phospholipids in solutions. Such interactions might play a significant role as in providing the artemisinin type drugs penetration through the membrane structures as in appear ance of the drugs effect on the membrane.

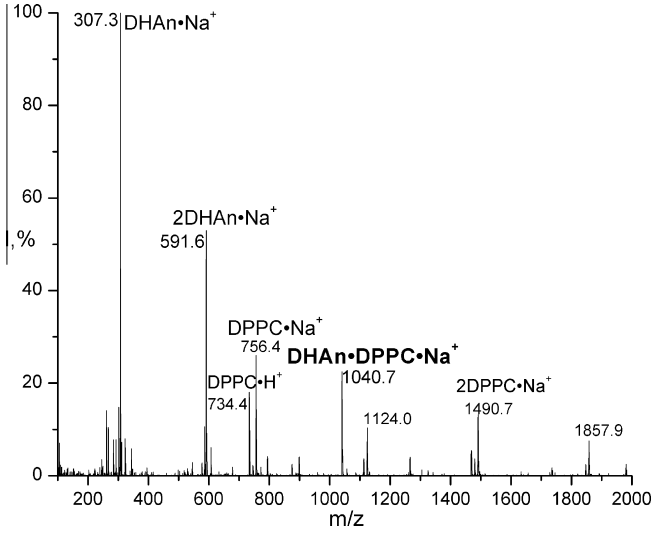

Fig. 2. ESI mass spectrum of DHAn:DPPC system.

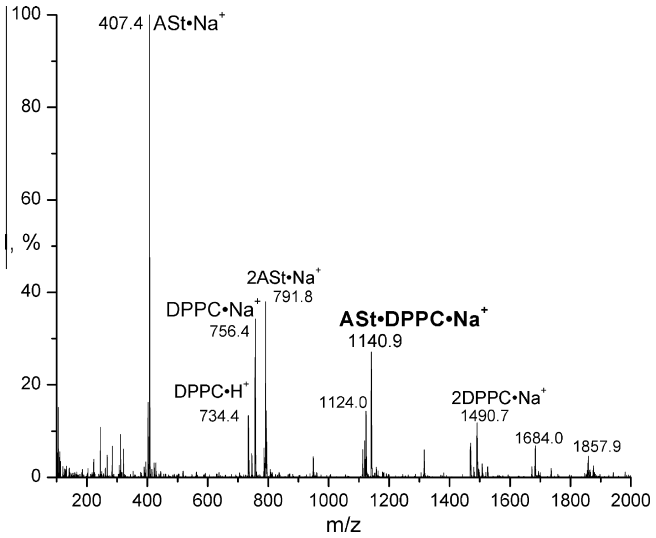

Fig. 3. ESI mass spectrum of ASt:DPPC system.

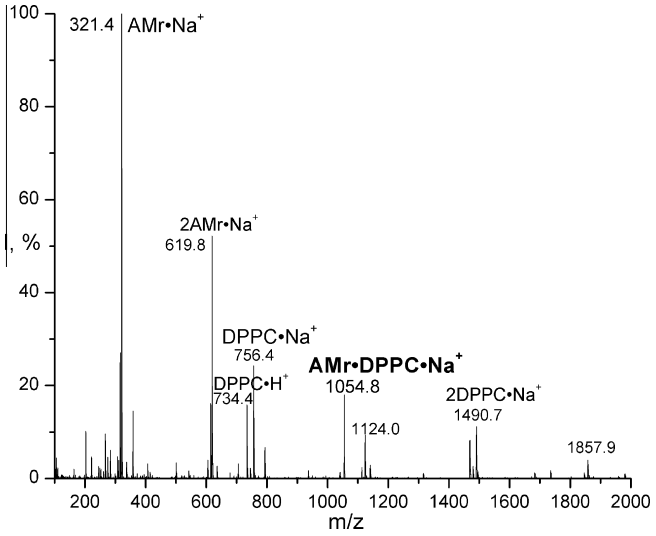

Fig. 4. ESI mass spectrum of AMr:DPPC system.

In the next step the ternary systems containing an artemisinin type agent, ASP, and DPPC in the molar ratio 1:1:10 were examined. Similarly to the earlier reported results for the systems containing a bisquaternary ammonium antimicrobial drug, ASP and DPPC [27] in the ternary systems with the studied artemisinin type drugs a competition between the antimalarial agents and ASP for binding with the DPPC molecules was revealed. The complexation between the antimalarial drugs and ASP was established based on the follow ing peaks registration in the spectra (see Figs. 5 7): DHAn · ASP · Na^+ (*m*/*z* 487.5, RA 32%), DHAn · DPPC · Na^+ (*m*/*z* 1040.7, RA 42%), DPPC · ASP · Na^+ (*m*/*z* 936.6, RA 19%), (Fig. 5); ASt · ASP · Na^+ (*m*/*z* 587.6, RA 5%), DPPC · ASP · Na^+ (*m*/*z* 936.6, RA 11%), ASt · DPPC · Na^+ (*m*/*z* 1140.9, RA 19%), (Fig. 6); AMr · ASP · Na^+ (*m*/*z* 501.5, RA 38%), DPPC · ASP · Na^+ (*m*/*z* 936.6, RA 17%), and AMr · DPPC · Na^+ (*m*/*z* 1054.7, RA 11%), (Fig. 7).

The above ESI MS results indicate the presence of the competi tion between the antimalarial agents and ASP for binding with the DPPC molecules in the model systems which were studied. It

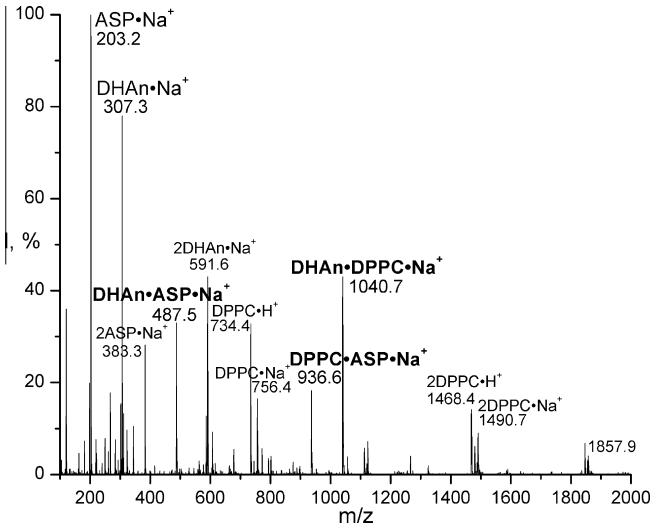

Fig. 5. ESI mass spectrum of DHAn:ASP:DPPC system.

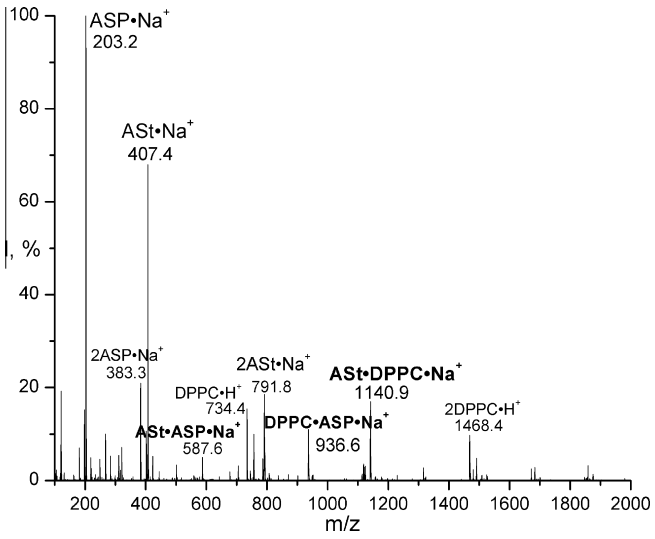

Fig. 6. ESI mass spectrum of ASt:ASP:DPPC system.

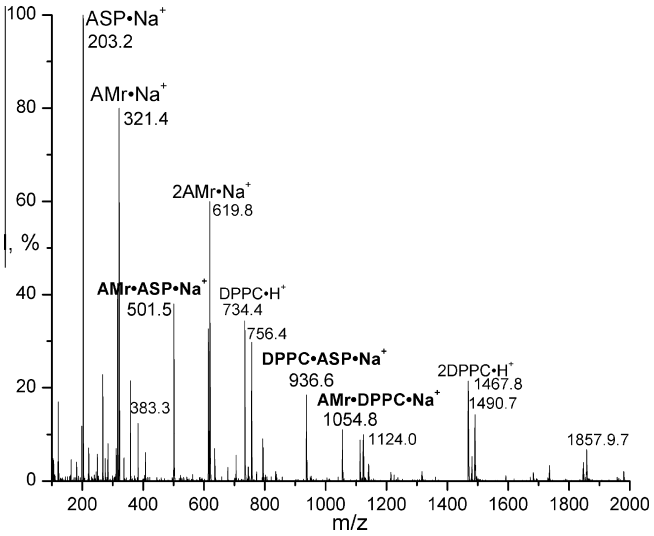

Fig. 7. ESI mass spectrum of AMr:ASP:DPPC system.

should be noted that the relative intensities of the peaks of the artemisinin type drug · DPPC and DPPC · ASP were comparable. This is particularly true for ASt and AMr. At the same time the quite intensive peaks recorded in the mass spectra of artemisinin type drug · ASP non covalent complexes revealed their quite high stability. It points to one more possible scenario of the competitive interaction between the drugs of the different classes in the ternary model mixtures and in the real biological systems.

The non covalent complexes registered in the ESI MS testify to the possibility of mutual modification of biologically significant interactions of artemisinin type agents and ASP with phospholipids that can result in modulation of the drugs activity and ability of their penetration through the cell membrane under the medications joint usage.

3.2. Quantum chemical model study of the drugs interactions with phospholipid

To elucidate the structure and energetic characteristics of the described above non covalent complexes the model DFT calculations of DHAn and ASP complexes with the polar phosphatidylcholine (PCn) head of DPPC were performed at the DFT B3LYP/aug cc pVDZ level of theory. Note that the use of PCn for modeling DPPC in the calculations has been already discussed and validated above in the Material and methods section of this work.

In spite of registration in the ESI mass spectra the non covalent complexes cationized by Na^+ in the first step of the computational study we calculated the equilibrium structures of the DHAn · PCn and ASP · PCn complexes without Na^+ inclusion, because as was mentioned in the previous experimental section the cationization is characteristic of the ESI procedure and we believe that attachment of the residual sodium ions to the dissolved molecules or complexes occurs under intensive solvent evaporation from the charged droplets during the ESI ionization process of the investigated solution. The search for the structures was initiated using three different initial geometries (A, B, and C) for each complex. These initial structures represent all possible ways the two interacting molecules can be connected through intermolecular hydrogen bonds. The final optimized geometries of the most stable drug · PCn complexes in vacuum conditions are shown in Fig. 8 (the Cartesian coordinates of the separate molecules and complexes are collected in Table S1. Atom numbering scheme is shown in Fig. S1). Structures of all calculated complexes are shown in Figs. S2 and S3 for DHAn · PCn and ASP · PCn, respectively. The calculated interaction energies for the optimized complexes are presented in Table 1.

Let us now take into account the results of the ESI MS experiments described above and let us follow the aim of this investigation which is to identify biologically relevant interactions. With that in mind and based on the analysis of the data in Table 1 we can conclude that the attractive interaction in all non covalent complexes studied in this work is confirmed. This confirmation comes from the registration of the stable peaks corresponding to these complexes in the ESI mass spectra and from the calculations which resulted in negative values of the interaction energies (IE) for all the complexes (Table 1). One can also see that the most energetically favorable geometry of the DHAn · PCn complex is the geometry C (Fig. 8, Fig. S2) with the IE = −55.6 kJ/mol. In the structure C the DHAn and PCn molecules are connected by O H(DHAn)···O P(PCn) H bond. There is also an interaction between the groups of C H(DHAn) and O C(PCn).

The most favorable geometry of the ASP · PCn non covalent complex is also structure C (Fig. 8, Fig. S3) with the IE = −107.9 kJ/mol. This structure is stabilized by the following

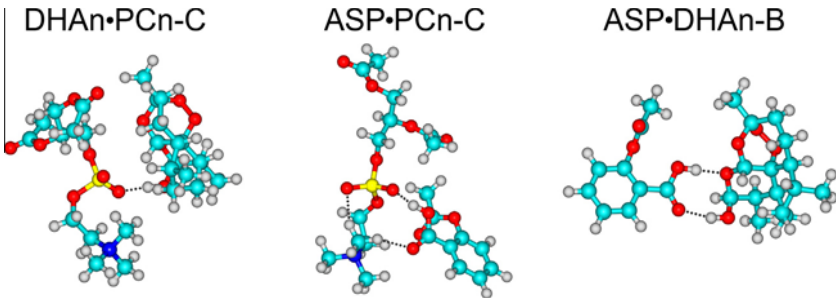

Fig. 8. Calculated at the B3LYP/aug-cc-pVDZ level of theory structures of the most stable DHAn · PCn, ASP · PCn and ASP · DHAn non-covalent complexes in vacuum.

Table 1
Interaction energies (IE, kJ/mol) in non-covalent complexes of DHAn · PCn, ASP · PCn and ASP · DHAn calculated at B3LYP/aug-cc-pVDZ level of theory in the vacuum approach and by PCM approach in methanol and water.

Complex[a]	IE, DFT B3LYP/aug-cc-pVDZ		
	Vacuum approach	PCM, methanol	PCM, water
DHAn · PC-A	−28.8	−11.6	−11.1
DHAn · PCn-B	−35.0	−7.5	−7.0
DHAn · PCn-C	−55.6	−32.2	−31.7
ASP · PCn-A	−59.9	−41.1	−40.5
ASP · PCn-B	−95.5	−55.6	−54.6
ASP · PCn-C	−107.9	−64.6	−63.5
ASP · DHAn-A	−20.5	−10.6	−10.5
ASP · DHAn-B	−56.2	−39.4	−38.8

[a] Structures of the complexes are shown in Figs. 8, S2–S4.

intermolecular bonds: O H(ASP)···O P(PCn), C O(ASP)···H C(PCn), and one more C O(ASP)···H C(PCn). Such an arrangement of the bonds in the complex facilitates a close contact of ASP with PCn that leads to the high stability of the complex in vacuum. The C geometries for the both DHAn · PCn and ASP · PCn (Fig. 8, Figs. S2 and S3) complexes in vacuum are likely the configurations of the drugs interaction with the PCn in the non covalent complexes of DHAn and ASP with DPPC registered in the present ESI MS experiments (Fig. 5).

As discussed in Introduction non covalent complexes registered in ESI mass spectra are believed to correlate with the intermolecular complexation in a solution analyzed in the ESI MS experiment [10 12]. To validate this correlation for the studied systems at the next step of our theoretical study the interaction energies calculations were performed for the DHAn · PCn and ASP · PCn complexes (in three different geometries A C) using the PCM approach. The methanol (the solvent used in our ESI MS experiments) and water environments were considered. The results of the PCM calculations are presented in Table 1. From the data shown there one can see that in the polar solvent the interaction energies of the complexes decrease in absolute values in comparison with the values obtained in the vacuum conditions. However the most energetically favorable geometries of the complexes in the polar solvents are similar to the ones in vacuum; geometry C of DHAn · PCn (Fig. 8, Fig. S2) is the most stable and has IE = −32.2 kJ/mol in methanol and IE = −31.7 kJ/mol in water; geometry C of ASP · PCn (Fig. 8, Fig. S3) is also the most stable and has IE = −64.6 kJ/mol in methanol and IE = −63.5 kJ/mol in water.

The modeling is also applied to the ASP · DHAn complex (registered in the ESI MS spectra in the cationized form (Fig. 5)) using two possible initial geometries. The most stable optimized structure of the non covalent complex obtained in the DFT B3LYP/aug cc pVDZ calculation is shown in Fig. 8 (structures of all calculated ASP · DHAn complexes are shown in Fig. S4) and the corresponding interaction energies are shown in Table 1. The most stable geometry B (Fig. 8) of the complex has IE = −56.2 kJ/mol. This value is close to IE of the DHAn · PCn complex. This combined with the evidence from the ESI MS experiments suggests the fact of strong competition between ASP and DPPC for binding to DHAn during the joint usage of the two drugs. In the B geometry the ASP · DHAn complex is stabilized by two H bonds: O H(ASP)···O C(DHAn) and C O(ASP)···H O(DHAn) (Fig. 8).

The PCM approach was also applied to study the ASP · DHAn complex. The interaction energies of the most stable configuration are the following for the two solvents: IE = −39.4 kJ/mol for methanol and IE = −38.9 kJ/mol for water. Therefore again we can conclude that the relative stability of the non covalent ASP · DHAn complex is very similar in the polar solvent as it is in vacuum.

At the final stage of the model computational study we also performed additional DFT calculation of the non covalent complexes DHAn · PCn · Na^+, ASP · PCn · Na^+ and ASP · DHAn · Na^+, because the cationized non covalent complexes of the drugs with the phospholipid were registered in the ESI mass spectra. We have used the same three different initial geometries (A, B, and C) for each complex of DHAn and ASP with PCn but with inclusion of the sodium ion. The final optimized geometries of the most stable drug · PCn · Na^+ complexes in vacuum conditions are shown in Fig. 9 (the Cartesian coordinates of the separate molecules and complexes are collected in Table S2). Structures of all calculated complexes are shown in Figs. S5 and S6 for DHAn · PCn · Na^+ and ASP · PCn · Na^+, respectively. The calculated interaction energies for the optimized complexes are presented in Table 2.

As was expected the absolute values of the interaction energies in the non covalent complexes with inclusion of the sodium ion are several times more than the ones for the complexes without Na^+ (compare the data in Tables 1 and 2), because the cationized complexes are stabilized not only by polar interactions between the molecules, but also by electrostatic interactions involving the cation. In particular the most energetically favorable geometry of the DHAn · PCn · Na^+ complex is the geometry C (Fig. 9, Fig. S5) with the IE = −403.8 kJ/mol while the IE for the DHAn · PCn C complex is equal to −55.6 kJ/mol. In the optimized C structure of the cationized complex the DHAn and PCn molecules are connected not only by O H(DHAn)···O P(PCn) H bond, but also via Na^+ ion connected with three oxygen atoms of PCn and two O atoms of DHAn.

The most favorable geometry of the ASP · PCn · Na^+ non covalent complex is also structure C (Fig. 9, Fig. S6) with the IE = −430.0 kJ/mol. This structure is stabilized also by O H(ASP)···O P(PCn) bond and by the "sodium bridge" in which the oxygen atoms of ASP and PCn are connected by Na^+ ion. From the data obtained we can see that the interaction energy values for the DHAn · PCn · Na^+ and ASP · PCn · Na^+ are close that also testifies on the model level to the reported above competition between the drugs for binding with the phospholipid target molecules which we revealed in the mass spectrometry experiment.

The calculation of ASP · DHAn · Na^+ complex using two possible initial geometries was carried out too. The most stable optimized

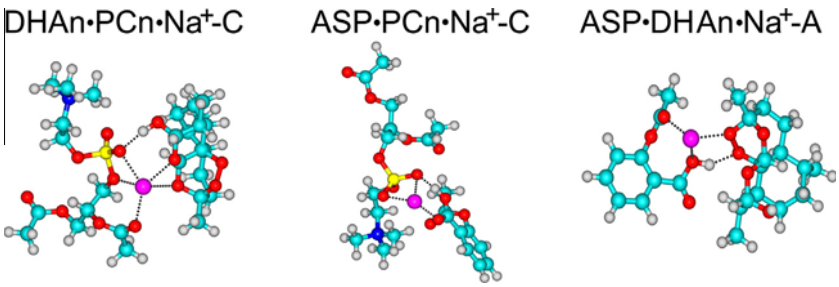

Fig. 9. Calculated at the B3LYP/aug-cc-pVDZ level of theory structures of the most stable DHAn · PCn · Na^+, ASP · PCn · Na^+ and ASP · DHAn · Na^+ non-covalent complexes in vacuum.

Table 2
Interaction energies (IE, kJ/mol) in non-covalent complexes of DHAn · PCn · Na^+, ASP · PCn · Na^+ and ASP · DHAn · Na^+ calculated at DFT B3LYP/aug-cc-pVDZ level of theory in the vacuum approach.

Complex[a]	IE B3LYP/aug-cc-pVDZ
DHAn · PC · Na^+–A	−346.6
DHAn · PCn · Na^+–B	−344.3
DHAn · PCn · Na^+–C	−403.8
ASP · PCn · Na^+–A	−327.5
ASP · PCn · Na^+–B	−408.0
ASP · PCn · Na^+–C	−430.0
ASP · DHAn · Na^+–A	−262.9
ASP · DHAn · Na^+–B	−229.9

[a] Structures of the complexes are shown in Figs. 9, S5–S7.

structure A of the non covalent complex obtained in the computational study is shown in Fig. 9 (structures of all calculated ASP · DHAn · Na^+ complexes are shown in Fig. S7) and the corresponding interaction energy is presented in Table 2. In the A geometry the ASP · DHAn · Na^+ complex is stabilized by H bond between COOH group of ASP and one of the oxygen of peroxide bridge of the DHAn and by the Na^+ ion connected with O (ASP) and the second oxigen of the peroxide bridge of the antimalarial drug. The most stable configuration A (Fig. 9) of the complex has IE = −262.9 kJ/mol. The interaction energy value in the ASP · DHAn · Na^+ complex is significantly less that the IE values for the complexes drug · PCn · Na^+ (Table 2), but very high stability of the cationized non covalent complex of ASP with DHAn also points to the one possible scenario of modification of the drugs biological activity under their joint usage.

Thus, in conclusion, the theoretical modeling study of the non covalent complexes in vacuum, as well as in polar surrounding, has allowed us to find the most stable structures of the non covalent complexes of DHAn · PCn, ASP · PCn and ASP · DHAn (Fig. 8) and DHAn · PCn · Na^+, ASP · PCn · Na^+ and ASP · DHAn · Na^+ (Fig. 9). It has also allowed us to determine the interaction energies of the complexes (Tables 1 and 2). The most energetically favorable structures of the DHAn · PCn (geometry C) and ASP · DHAn (geometry B) complexes have similar interaction energies in vacuum and in polar solvents while for the cationized non covalent complexes the close values of IE have the most energetically favorable structures of DHAn · PCn · Na^+ (geometry C) and ASP · PCn · Na^+ (geometry C).

4. Conclusions

The ESI MS experiments revealed a competition between the artemisinin type agents and aspirin for binding with the phospholipid molecules in solutions. This is concluded based on the peaks of the stable non covalent complexes of artemisinin type drugs · DPPC and ASP · DPPC, registered in the mass spectra in the cationized form. The pair complexation between the antimalarial drugs and ASP is found to be one more possible scenario of the competitive non covalent interactions between the drugs under their joint usage.

The theoretical model study by the DFT B3LYP/ aug cc pVDZ method in vacuum and by the PCM approach was performed to elucidate the equilibrium geometries of the stable non covalent complexes recorded in the ESI MS experiments for dihydroartemisinin (DHAn), the active metabolite of the artemisinin type drugs. The polar phosphatidylcholine (PCn) head of DPPC was used to model DPPC in the calculations. The most energetically favorable geometry of the DHAn · PCn complex is found to be the structure with IE = −55.6 kJ/mol where the molecules are connected with O H(DHAn)···O P(PCn) and C H(DHAn)···O C(PCn) bonds. The most favorable structure of the ASP · PCn non covalent complex has IE = −107.9 kJ/mol and it is stabilized by the following intermolecular bonds: O H(ASP)···O P(PCn) and two C O(ASP)···H C(PCn) bonds. The most stable configuration of the ASP · DHAn complex has IE = −56.2 kJ/mol and it is stabilized by two H bonds: O H(ASP)···O C(DHAn) and C O(ASP)···H O(DHAn).

Comparing the IE values of the complexes ASP · PCn, DHAn · PCn, and ASP · DHAn in vacuum shows that the complex of ASP with PCn is the most stable while the DHAn · PC and ASP · DHAn complexes have similar interaction energy values. The PCM calculations reveal that the relative stability of the complexes is similar in vacuum as it is in the polar solutions.

To link up directly the results of the model theoretical calculations and the mass spectrometry experiment data the DFT calculations of DHAn · PCn · Na^+, ASP · PCn · Na^+ and ASP · DHAn · Na^+ non covalent complexes were also performed. The results of the computation study of the drug · PCn · Na^+ complexes show that the most energetically favorable structures of the complexes DHAn · PCn · Na^+ (IE = −403.8 kJ/mol) and ASP · PCn · Na^+ (IE = −430.0 kJ/mol) are stabilized not just by O H(drug)···O P(PCn) intermolecular bonds but also by "sodium bridge" in which the oxygen atoms of the drugs and PCn molecules connected via Na^+ ion. The interaction energy values for the DHAn · PCn · Na^+ and ASP · PCn · Na^+ are close that points to the possible competition of the drugs for binding with the phospholipid target molecules. In the optimized geometry of the ASP · DHAn · Na^+ complex the COOH group of the ASP and one of the oxygens of peroxide bridge of the DHAn are connected and another O of the ASP and the second oxygen atom of the peroxide bridge of the DHAn are connected via sodium cation.

The confirmed by our experimental and theoretical model studies phenomena of competition between the artemisinin type agents and ASP for binding with the DPPC and the drugs pair complexation in the model systems point to the possibility of modification of the membranotropic and membrane penetrative activity of the artemisin type drugs and aspirin under their combined usage.

Conflict of interest

The authors declare no conflicts of interest.

Acknowledgements

Authors acknowledge the Program of cooperation between Ukrainian and Hungarian Academies of Sciences for the financial support of visit of the scientists from B. Verkin Institute for Low Temperature Physics and Engineering of the National Academy of Sciences of Ukraine to the Institute of Organic Chemistry of Research Centre for Natural Sciences of the Hungarian Academy of Sciences, where the mass spectrometry experiments were car ried out. V. Pashynska also thanks to Prof. Magda Claeys from the University of Antwerp (Belgium) for the initial joint ESI mass spec trometry study of antimalarial drugs intermolecular interactions and for provision of the samples of the artemisinin type drugs.

Appendix A. Supplementary data

Supplementary data associated with this article can be found, in the online version, at http://dx.doi.org/10.1016/j.chemphys.2015.04.014.

References

[1] M. Lucio, J.L.F.C. Lima, S. Reis, Drug-membrane interactions: significance for medicinal chemistry, Curr. Med. Chem. 17 (2010) 1795–1809.
[2] M. Lucio, Drug-membrane interactions: analysis, drug distribution, in: Joachim K. Seydel (Ed.), Michael Wiese, Wiley-VCH Verlag GmbH & Co. KGaA, 2002. p. 349.
[3] Ying Li, Qinghaosu (artemisinin): chemistry and pharmacology, Acta Pharmacol. Sin. 33 (2012) 1141–1146, http://dx.doi.org/10.1038/aps.2012.104.
[4] F. Jansen, Artesunate and Artemether. Towards the Eradication of Malaria?, Dafra Pharma Ltd, Oud-Turnhout, 2002 p. 63.
[5] Jian Li, Bing Zhou, Biological actions of artemisinin: insights from medicinal chemistry studies, Molecules 15 (2010) 1378–1397, http://dx.doi.org/10.3390/molecules15031378.
[6] F. Benoit-Vical, A. Robert, B. Meunier, In vitro and in vivo potentiation of artemisinin and synthetic endoperoxide antimalarial drugs by metalloporphyrins, Antimicrob. Agents Chemother. 44 (2000) 2836–2841.
[7] U. Eckstein-Ludwig, R. Webb, I. Van Goethem, J. East, A. Lee, M. Kimura, P. O'Neill, P. Bray, S. Ward, S. Krishna, Artemisinins target the SERCA of plasmodium falciparum, Nature 424 (2003) 957, http://dx.doi.org/10.1038/nature01813.
[8] S. Krishna, A.-C. Uhlemann, R.K. Haynes, Artemisinins: mechanisms of action and potential for resistance, Drug Resist. Updates 7 (2004) 233–244, http://dx.doi.org/10.1016/j.drup.2004.07.001.
[9] T.K. Mutabingwa, Artemisinin-based combination therapies (ACTs): best hope for malaria treatment but inaccessible to the needy!, Acta Trop 95 (3) (2005) 305–315.
[10] I.A. Kaltashov, S.J. Eyles, Mass Spectrometry in Structural Biology and Biophysics: Architecture, Dynamics and Interaction of Biomolecules, second ed., John Wiley & Sons, Inc, New York, 2012. p. 316.
[11] G. Siuzdak, The Expanding Role of Mass Spectrometry in Biotechnology, second ed., MCC Press, San Diego, 2006. p. 257.
[12] J. Laskin, Lifshitz C. Hoboken (Eds.), Principles of mass spectrometry applied to biomolecules, John Wiley & Sons, Inc., New Jersey, 2006. p. 687.
[13] , second ed.Cole R. Hoboken (Ed.), Electrospray and MALDI Mass Spectrometry: Fundamentals, Instrumentation, Practicalities, and Biological Applications, John Wiley & Sons, Inc., New Jersey, 2010. p. 1008.
[14] J.A. Loo, Electrospray ionization mass spectrometry: a technology for studying non-covalent macromolecular complexes, Int. J. Mass Spectrom. 200 (1–3) (2000) 175–186, http://dx.doi.org/10.1016/S1387-3806(00)00298-0.
[15] Th. Wyttenbach, M.T. Bowers, Intermolecular interactions in biomolecular systems examined by mass spectrometry, Annu. Rev. Phys. Chem. 58 (2007) 511–533, http://dx.doi.org/10.1146/annurev.physchem.58.032806.104515.
[16] B.J. McCullough, S.J. Gaskell, Using electrospray ionisation mass spectrometry to study non-covalent interactions, Comb. Chem. High Throughput Screening 12 (2) (2009) 203–211, http://dx.doi.org/10.2174/138620709787315463.
[17] V. Pashynska, H. Van den Heuvel, M. Claeys, M. Kosevich, Characterization of noncovalent complexes of antimalarial agents of the artemisinin type and Fe(III)-heme by electrospray ionization mass spectrometry and collisional activation tandem mass spectrometry, J. Am. Soc. Mass Spectrom. 15 (2004) 1181–1190.
[18] R. Guevremont, K.W.M. Siu, J.C.Y. Le Blanc, S.S. Berman, Are the electrospray mass spectra of proteins related to their aqueous solution chemistry?, J Am. Soc. Mass Spectrom. 3 (1992) 216–224.
[19] C.A. Morris, S. Duparc, I. Borghini-Fuhrer, D. Jung, C.S. Shin, L. Fleckenstein, Review of the clinical pharmacokinetics of artesunate and its active metabolite dihydroartemisinin following intravenous, intramuscular, oral or rectal administration, Malar J. 10 (2011) 263, http://dx.doi.org/10.1186/1475-2875-10-263.
[20] J. Grace, A. Aguilar, K. Trotman, T. Brewer, Metabolism of beta-arteether to dihydroqinghaosu by human liver microsomes and recombinant cytochrome P450, Drug Metab. Dispos. 26 (1998) 313–317.
[21] L. Panicker, V.K. Sharma, G. Datta, K. Deniz, P.S. Parvathanathan, K.V. Ramanathan, C.L. Khetrapal, Interaction of aspirin with DPPC in the lyotriopic DPPC-aspirin-H2O/D2O membrane, Mol. Cryst. Liq. Cryst. 260 (1995) 611–621.
[22] A.D. Becke, Density-functional exchange-energy approximation with correct asymptotic behavio, Phys. Rev. B 38 (1988) 3098–3100, http://dx.doi.org/10.1103/PhysRevA.38.3098.
[23] C. Lee, W. Yang, R.G. Parr, Development of the Colle–Salvetti correlation-energy formula into a functional of the electron density, Phys. Rev. B 37 (1988) 785, http://dx.doi.org/10.1103/PhysRevB.37.785.
[24] S.H. Vosko, L. Wilk, M. Nusair, Accurate spin-dependent electron liquid correlation energies for local spin density calculations: a critical analysis, Can. J. Phys. 58 (1980) 1200–1211, http://dx.doi.org/10.1139/p80-159.
[25] G. Scalmani, M.J. Frisch, Continuous surface charge polarizable continuum models of solvation. I. General formalism, J. Chem. Phys. 132 (2010) 114110.
[26] M.J. Frisch, G.W. Trucks, H.B. Schlegel, G.E. Scuseria, M.A. Robb, J.R. Cheeseman, G. Scalmani, V. Barone, B. Mennucci, G.A. Petersson, H. Nakatsuji, M. Caricato, X. Li, H.P. Hratchian, A.F. Izmaylov, J. Bloino, G. Zheng, J.L. Sonnenberg, M. Hada, M. Ehara, K. Toyota, R. Fukuda, J. Hasegawa, M. Ishida, T. Nakajima, Y. Honda, O. Kitao, H. Nakai, T. Vreven, J.J.A. Montgomery, J.E. Peralta, F. Ogliaro, M. Bearpark, J.J. Heyd, E. Brothers, K.N. Kudin, V.N. Staroverov, R. Kobayashi, J. Normand, K. Raghavachari, A. Rendell, J.C. Burant, S.S. Iyengar, J. Tomasi, M. Cossi, N. Rega, J.M. Millam, R. Klene, J.E. Knox, J.B. Cross, V. Bakken, C. Adamo, J. Jaramillo, R. Gomperts, R.E. Stratmann, O. Yazyev, A.J. Austin, R. Cammi, C. Pomelli, J.W. Ochterski, R.L. Martin, K. Morokuma, V.G. Zakrzewski, G.A. Voth, P. Salvador, J.J. Dannenberg, S. Dapprich, A.D. Daniels, O. Farkas, J.B. Foresman, J.V. Ortiz, J. Cioslowski, D.J. Fox, Gaussian 09, Revision A.02, Gaussian Inc, Wallingford CT, 2009.
[27] V.A. Pashynska, M.V. Kosevich, A. Gomory, K. Vekey, Model mass spectrometric study of competitive interactions of antimicrobial bisquaternary ammonium drugs and aspirin with membrane phospholipids, Biopolym. Cell 29 (2) (2013) 157–162, http://dx.doi.org/10.7124/bc.000814.

Journal of Molecular Structure 1232 (2021) 130039

Contents lists available at ScienceDirect

Journal of Molecular Structure

journal homepage: www.elsevier.com/locate/molstr

What are molecular effects of co-administering vitamin C with artemisinin-type antimalarials? A model mass spectrometry and quantum chemical study

Vlada Pashynska[a,b,*], Stepan Stepanian[a,c], Ágnes Gömöry[d], Ludwik Adamowicz[e,f]

[a] B Verkin Institute for Low Temperature Physics and Engineering of the National Academy of Sciences of Ukraine, 47, Nauky Ave., Kharkiv, 61103, Ukraine
[b] O. Usikov Institute for Radiophysics and Electronics of the National Academy of Sciences of Ukraine, 12, Ac. Proskura str., Kharkiv, 61085,Ukraine
[c] National Technical University «Kharkiv Polytechnic Institute», Department of Biotechnology, Biophysics and Analytical Chemistry, 2 Kyrpychova Str., Kharkiv, 61002, Ukraine
[d] Institute of Organic Chemistry of Research Centre for Natural Sciences, Magyar tudosok korutja, 2, Budapest, H-1117, Hungary
[e] University of Arizona, Department of Chemistry and Biochemistry, Tucson, Arizona 85721, USA
[f] Interdisciplinary Center for Modern Technologies, Nicolaus Copernicus University, Toruń, PL 87-100, Poland

ARTICLE INFO

Article history:
Received 6 July 2020
Revised 28 January 2021
Accepted 31 January 2021
Available online 2 February 2021

Key words:
Artemisinin-type agents
Ascorbic acid
Dipalmitoylphosphatidylcholine
Competitive binding
Electrospray ionization mass spectrometry
DFT/B3LYP/aug-cc-pVDZ calculations

ABSTRACT

In this study the electrospray ionization mass spectrometry (ESI MS) and quantum chemical modeling methods are employed to examine the interactions of molecules of artemisinin-type drugs and of ascorbic acid (ASC). These biologically significant interactions are relevant to antimalarial therapy, in particular, when artemisinin agents are co-administrated with supporting vitamin/antioxidant preparations or could be affiliated with the patient's food. The formation of stable noncovalent complexes of the artemisinin-type drugs (artemisinin, dihydroartemisinin, α-artemether, and β-arteether) with ascorbic acid molecules in a polar solvent, such as methanol, is revealed by the ESI MS probing of binary systems containing an antimalarial drug and ASC in the 1:1 molar ratio. Also, a peak corresponding to noncovalent $[ASC{\bullet}DPPC{\bullet}Na]^+$ cationized complexes is identified in the spectrum of the mixture of ASC and dipalmitoylphosphatidylcholine (DPPC, membrane phospholipid) with the 1:5 molar ratio. Next, the ternary system containing dihydroartemisinin (DHAn; the assumed active metabolite of the artemisinin-type drugs in the human organism), ASC, and DPPC in the 1:1:5 molar ratio is examined. The study reveals a competition between the antimalarial agent and ASC for binding with the DPPC molecules. The existence of the competition is supported by the observation of peaks with similar intensities corresponding to the noncovalent DHAn•DPPC and ASC•DPPC complexes in the mass spectra. An evidence for the complexation between the antimalarial drug and ASC is also found in the spectra of triple model systems studied. To elucidate the structural and energetic characteristics of the noncovalent complexes observed in the ESI MS experiments, model *ab initio* calculations of DHAn and ASC complexes and clusters of the drug molecules with the polar phosphatidylcholine head of DPPC are performed using the DFT/B3LYP/aug-cc-pVDZ approach. The results of the model study show the possibility of the noncovalent complexation and of the modulation of the biological activity of artemisin-type agents and of the ascorbic acid when they are co-administered in the therapy.

1. Introduction

Artemisinin and its derivatives are actively used worldwide in the *Artemisinin-based combination therapy (ACT)* recommended by the World Health Organization as the first- and second-line treatment to cure *Plasmodium falciparum* malaria [1-4]. The molecular mechanisms of the antimalarial agents action and their intermolecular interactions with different biomolecules and molecules of other drugs remain the subjects of a number of biomedical investigations [5-9]. Knowledge about the potential effects associated with the intermolecular interactions of molecules of different co-administered drugs are important for medical practice. This is particularly relevant in the case of ACT, which is usually concurrently administered with a supplementary anti-inflammatory or vitamin/antioxidative therapy.

* Corresponding authors.
E-mail address: pashynska@ilt.kharkov.ua (V. Pashynska).

https://doi.org/10.1016/j.molstruc.2021.130039
0022-2860/

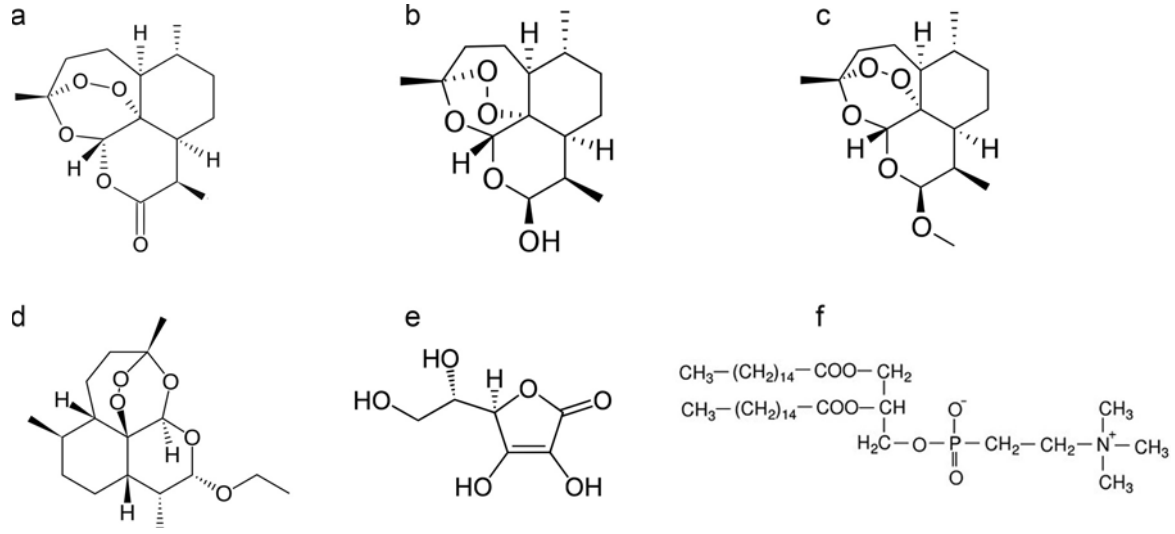

Scheme 1. Structures of the studied molecules: a) artemisinin , b) dihydroartemisinin, c) α-artemether, d) β-arteether, e) L-ascorbic acid, f) L-α-dipalmitoylphosphatidylcholine.

As reported in work [10], the vitamin C preparation (ascorbic acid, ASC) is often prescribed jointly with ACT. A number of studies showed that there are some biological activity-modulative effects present when ASC is co-administered with artemisinin-type drugs both *in vivo* and *in vitro* [11-13]. The effects are related to the well-known antioxidative activity of ASC. Therefore, elucidation of the intermolecular interactions between the molecules of artemisinin-type agents and of supporting vitamin medications, such as vitamin C, is considered as an important topic in the applied biomedical research.

One of the techniques to study the interactions of biomolecules at the molecular level is the soft ionization mass spectrometry method [14-16]. The electrospray ionization (ESI) mass spectrometry (MS) which involves spraying solutions of the studied compounds, including biologically active ones, has been successfully used to investigate selective noncovalent intermolecular interactions. For example, the technique has been applied to examine the interactions between biologically active agents, in particular, medicines, with their specific molecular targets and with other biomolecules [17-20]. In the context of these mass spectrometry studies, our long-term systematic research of intermolecular interactions of biologically active compounds, including antimicrobial and antimalarial medications, with their particular molecular targets, should be noted. The research has resulted in the development of an effective approach involving a combination of the ESI MS technique and quantum chemical calculations for examining of noncovalent interactions in systems involving drugs and various biomolecules [21-26]. For example, in one of our previous ESI MS studies concerning the molecular mechanisms involved in the antimalarial action of artemisinin-type agents, the formation of noncovalent complexes between drug molecules and their potential molecular target – heme – was investigated *in vitro* [21]. In the subsequent study, the phenomenon of the competition between the artemisinin-type agents and anti-inflammatory agent aspirin for binding with membrane phospholipids and the paired complexation between the molecules of the different drugs in the model systems was confirmed by ESI MS experiments and quantum chemical calculations [24].

In the present combined ESI MS and quantum chemical study we examine the intermolecular interactions between molecules of artemisinin-type drugs and molecules of ASC. These biologically significant interactions are involved in the above mentioned antimalarial therapy accompanied by a supporting vitamin treatment.

2. Materials and methods

2.1. Model systems

Samples of artemisinin (An, Mr=282.33), and its derivatives: dihydroartemisinin (DHAn, Mr=284.35), α-artemether (AMr, Mr=298.37), and β-arteether (AEr, Mr=312.40) provided by Dafra Pharma Company (Oud-Tunhout, Belgium) are used in the present study. L-ascorbic acid (ASC, Mr=176.12) is obtained from Sigma-Aldrich company. L-α-dipalmitoylphosphatidylcholine (DPPC, Mr=734.04) is purchased from "Alexis Biochemicals" (Switzerland). The structures of the investigated molecules are shown in Scheme 1.

Stock solutions of An and its derivatives, ASC and DPPC (5 mM), are prepared in methanol and used for the preparation of binary (artemisinin type drug:ASC with the 1:1 molar ratio and ASC:DPPC with the 1:5 molar ratio) and ternary (artemisinin type drug:ASC:DPPC with the molar ratio of 1:1:5) model systems. The mixtures are kept at the room temperature for at least 10 min before the ESI analysis. The spraying procedure require dilution of the studied solutions to the 250 μM concentration of the most dominant component of the model system in each solution. It was shown in several studies [17-20] that using methanol as a solvent significantly improves the quality of the ESI mass spectra. Also, the compositions of the intermolecular complexes formed in methanol are very similar to the complexes formed in water solutions [27].

2.2. ESI mass spectrometry

The ESI mass spectra are obtained in the positive ion mode using a triple-quadruple (QqQ) Micromass Quattro Micro mass spectrometer (Waters, Manchester, UK) equipped with an electrospray ion source. The source is operated in the standard ESI mode. The source temperature is set to 120 °C and the desolvation temperature is 200 °C. The spraying capillary is operated at 3.5 kV. The cone voltage (CV) value of 10 V is used. The analyzed solutions are injected into the mass spectrometer at a constant flow rate of 0.2 mL/min of the methanol solvent. Data acquisition and processing are performed using MassLynx 4.1 software (Waters, Manchester, UK).

2.3. Quantum chemical calculations

The structures and interaction energies of the pair complexes observed in mass spectrometry experiments are calculated using the DFT method. The following components of the complexes are used in these calculations: the artemisinin derivative – dihydroartemisinin (DHAn), L-ascorbic acid (ASC), and phosphatidylcholene head (PCn) of dipalmitoylphosphatidylcholine (DPPC). The choice of DHAn as a component used in the calculations is motivated by the fact that this compound was found to be an active metabolite of artemisinin-type drugs in human organisms [28, 29]. The PCn represents the polar head of DPPC, which is considered to be the most accessible part of the membrane phospholipid to interact with molecules of antimalarial drugs, as well as with ASC. This happens because the polar head of the DPPC molecule is oriented away from the membrane phospholipid bilayer in the living cells. The use of PCn as a model for the DPPC molecule in the present calculations allows for a significant reduction of the modeling time.

Molecules of ASC are flexible and may appear in numerous conformations. The conformational composition of ASC was a subject of several computational studies [30-35]. Based on the results of these studies, we select the following two ASC conformers to be considered in the present calculations - the most stable (in vacuum) conformer, ASC1, and conformer ASC2 observed in aqueous solutions. The structures of the conformers are shown in Fig. S1 in Supplementary Materials.

Next, the geometries of the DHAn•ASC, PCn•ASC, and DHAn•PCn noncovalent complexes are fully optimized in the current study at the DFT/B3LYP/aug-cc-pVDZ level of theory, described in [36-38]. This is followed by harmonic frequency calculations to verify if the obtained geometries correspond to minima on the potential energy surfaces (PESes) of the complexes (no imaginary frequencies are found; thus, the obtained geometries are true minima on the corresponding PESes). Next the Polarizable Continuum Model (PCM) approach is used (integral equation formalism model (IEFPCM) [39]) to determine the influence of the solvents (water and methanol - solvent used in the ESI MS experiments) on the structures and the interaction energies of the complexes. All calculations are performed using the Gaussian 16 program package [40].

3. Results and discussion

3.1. ESI mass spectrometry study of the model systems containing antimalarial drugs, ascorbic acid, and dipalmitoylphosphatidylcholine

In the first stage, the present ESI MS experiments focus on the binary model systems formed by the antimalarial drugs and ASC (*i.e.* An:ASC, DHAn:ASC, AMr:ASC, and AEr:ASC) with the 1:1 molar ratio. The ESI mass spectra obtained in the experiments are shown in Fig. 1-4. In the spectra, the peaks characteristic to the following individual components of the mixtures are recorded: for ASC - ASC•Na^+ at *m/z* 199.1 and dimer 2ASC•Na^+ at *m/z* 357.2 (see Figs. 1-4); and for cationized adducts of the appropriate antimalarial drugs monomers, dimers, and trimer - An•Na^+ (*m/z* 305.3, RA 60%), 2An•Na^+ (*m/z* 586.6, RA 100%), and 3An•Na^+ (*m/z* 869.9, RA about 8%) for An (An:ASC system; Fig. 1); DHAn•Na^+ (*m/z* 307.3, RA about 87%) and 2DHAn•Na^+ (*m/z* 591.6, RA about 76%) for DHAn (DHAn:ASC system; Fig. 2); AMr•Na^+ (*m/z* 321.4, RA about 38%) and 2AMr•Na^+ (*m/z* 619.8, RA about 26%) for AMr (Amr:ASC system; Fig. 3); and AEr•Na^+ (*m/z* 335.4, RA 100%) and 2AEr•Na^+ (*m/z* 647.8, RA about 55%) for AEr (AEr:ASC system; Fig. 4).

Importantly, that the formation of stable noncovalent complexes between the molecules of all studied artemisinin-type drugs (An, DHAn, AMr, and AEr) and ASC molecules in methanol is

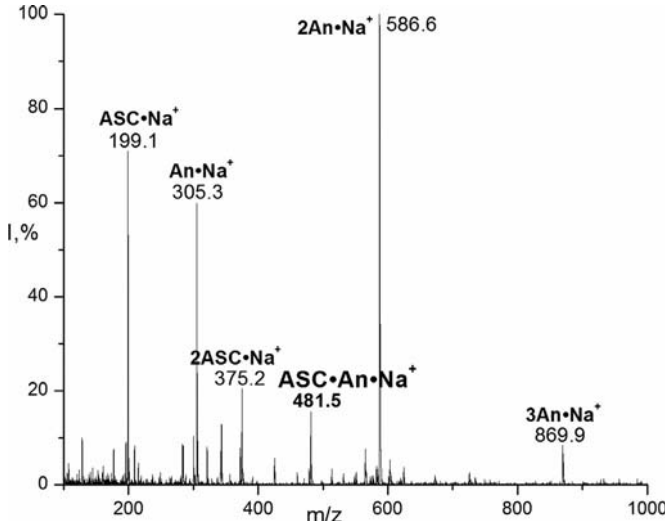

Fig. 1. ESI MS spectrum of the An:ASC system.

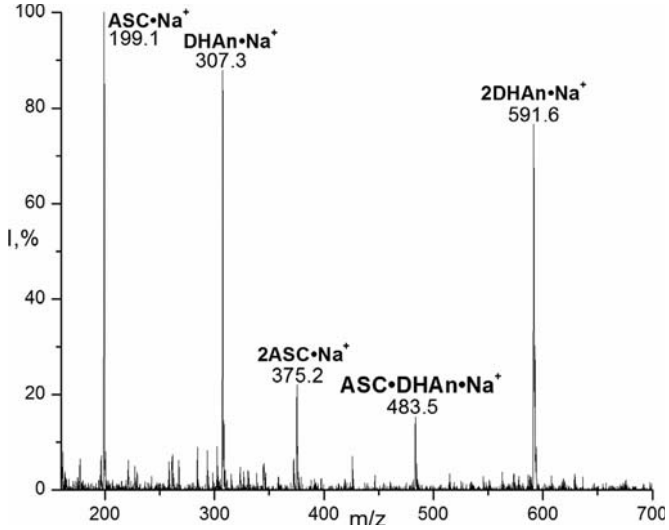

Fig. 2. ESI MS spectrum of the DAn:ASC system.

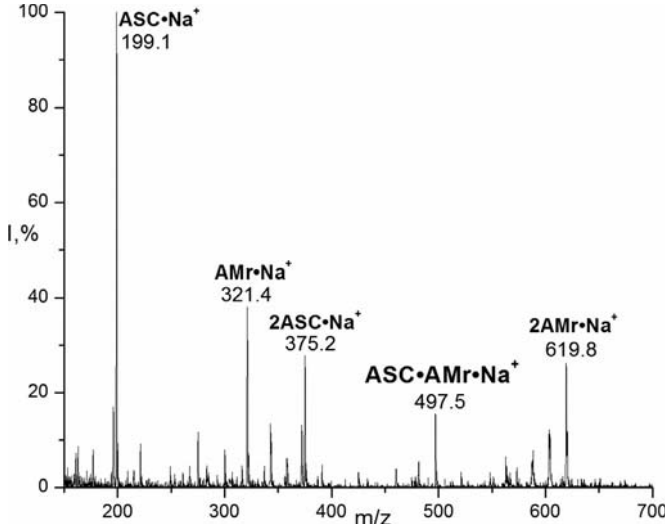

Fig. 3. ESI MS spectrum of the AMr:ASC system.

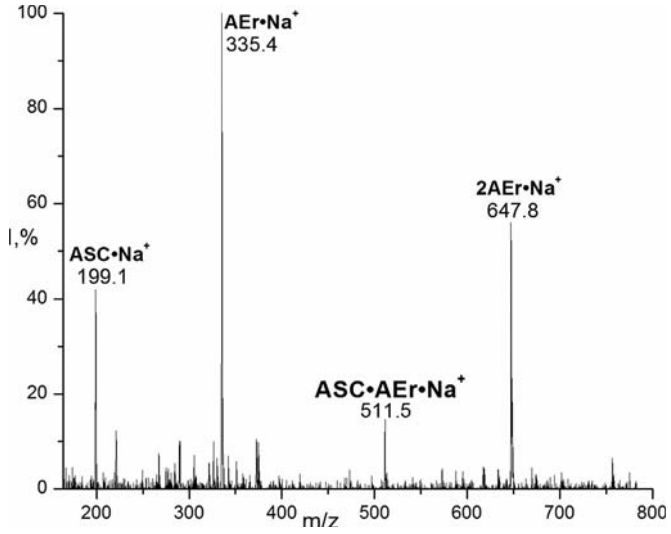

Fig. 4. ESI MS spectrum of the AEr:ASC system.

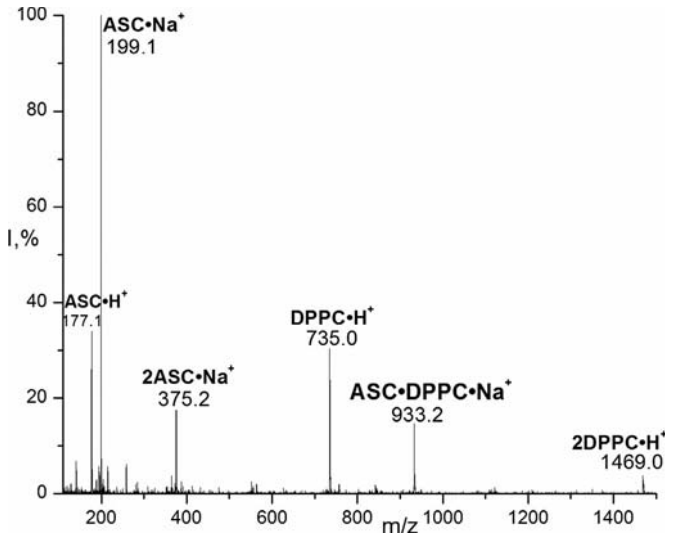

Fig. 5. ESI MS spectrum of the ASC:DPPC system.

revealed by the present ESI MS study due to the recording of the intensive peaks of cationized clusters of ASC•artemisinin-type drug•Na^+ in the spectra of each binary model system. These cationized clusters are: ASC•An•Na^+ (*m/z* 481.5, RA about 15%) for the An:ASC system (see Fig. 1); ASC•DHAn•Na^+ (*m/z* 483.5, RA about 16%) for the DHAn:ASC system (see Fig. 2); ASC•AMr•Na^+ (*m/z* 497.5, RA about 17%) for the AMr:ASC system (see Fig. 3); and ASC•AEr•Na^+ (*m/z* 511.5, RA about 14%) for the AEr:ASC system (see Fig. 4).

The noncovalent complexation between the molecules of the artemisinin-type drugs and ascorbic acid in the polar solvent indicates a possibility of modulation of the activity of the two different drugs when they are co-administered to the patient. The modulation appears at the molecular level. It should be noted that a similar noncovalent complexation between molecules of artemisinin-type drugs and acetyl salicylic acid was revealed in our previous study [24]. This phenomenon points to a common tendency of modulative effect of acidic components of supplemental medications or of specific foods on the activity of artemisinin-type drugs.

In the next step, the ESI MS experiments are performed for the model system of ASC and membrane phospholipid DPPC with the 1:5 molar ratio. The following peaks corresponding to ASC and DPPC are registered in the mass spectrum (see Fig. 5): ASC•H^+ (*m/z* 177.1, RA about 35%), ASC•Na^+ (*m/z* 199.1, RA 100%), and 2ASC•Na^+ (*m/z* 357.2, RA about 17%) for ASC; and DPPC•H^+ (*m/z* 735.0 RA about 30%) and 2DPPC•H^+ (*m/z* 1469.0 RA about 4%) for DPPC. A signal of the cationized ASC•DPPC noncovalent complex is recorded in the spectrum - ASC•DPPC•Na^+ with *m/z* 933.2 RA of about 15%. The spectral data testify to the formation of a stable noncovalent complex of ASC with the phospholipid molecules in the studied binary system. This indicates a possibility of active intermolecular interactions between the vitamin C molecules and the membrane phospholipid molecules in the solution. Such interactions can play a significant role in facilitating the ASC penetration through the membrane. They may also aid the drug effect on the membrane.

It should be noted that a similar noncovalent complexation between acetyl salicylic acid molecules and DPPC was revealed in our previous study of the system containing aspirin and DPPC [24]. It is also important that binary model systems containing artemisinin-type drugs and DPPC in methanol were studied earlier with ESI MS [24]. In that study, characteristic ion peaks corresponding to the studied drugs and DPPC were recorded in the spectra (similarly to the ASC:DPPC system, see Fig. 5). Also, intensive signals of the cationized ions of antimalarial drug•DPPC noncovalent complexes were identified. The ESI MS spectra obtained in the work [24] indicated the formation of stable binary noncovalent complexes of the molecules of the antimalarial drugs with the phospholipid molecules in polar media. Thus, one can conclude that the formation of stable noncovalent complexes of antimalarial drugs with DPPC, as well as of ASC with DPPC, is confirmed in the binary drug:DPPC model systems.

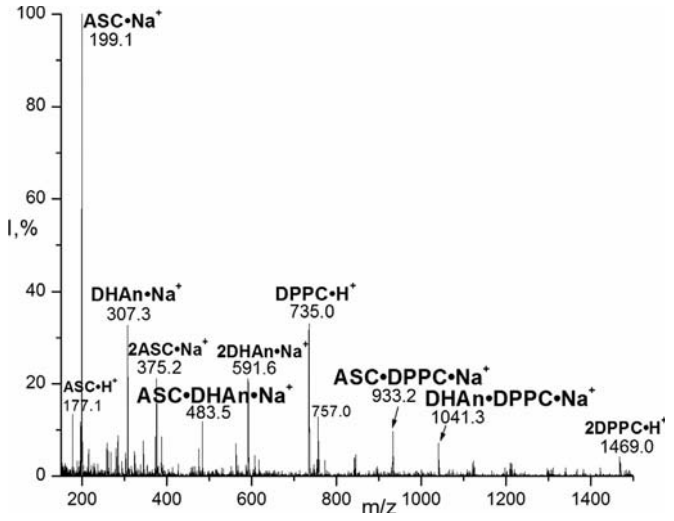

Fig. 6. ESI MS spectrum of the DHAn:ASC:DPPC system. .

In the last step of the present ESI MS study, the ternary system containing DHAn (as the active metabolite of the artemisinin-type drugs in human organisms [28, 29]), ASC, and DPPC in the molar ratio 1:1:5 are examined. The ESI MS results indicate a competition between the antimalarial agent and ASC for binding with the DPPC molecules in the model system seeing the following peaks of the noncovalent complexes artemisinin-type drug•DPPC and ASC•DPPC are observed in the mass spectrum (see Fig. 6): ASC•DPPC•Na^+ (*m/z* 933.2, RA about 9%) and DHAn•DPPC•Na^+ (*m/z* 1041.3, RA about 7%). It should be noted that the relative intensities of the peaks of the ASP•DPPC and DHAn•DPPC noncovalent complexes are comparable. An evidence of the complexation between DHAn and ASC is also found in the spectrum of the ternary model sys-

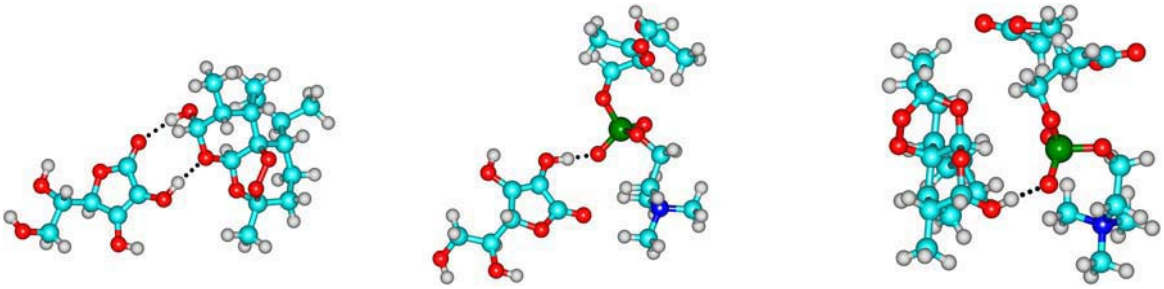

Fig. 7. Structures of the most stable complexes: a –ASC2•DHAn A; b – ASC2•PCn A and c - DHAn•PCn A calculated at the DFT/B3LYP/aug-cc-pVDZ level of theory.

tem due to recording peak - ASC•DHAn•Na^+ (*m/z* 483.5, RA about 12%; see Fig. 6) similarly to the binary DHAn:ASC model system (see Fig. 2). It points to one more possible scenario of the competing interactions between the molecules of drugs of different classes in the ternary model mixtures and in biological systems.

The noncovalent complexes observed in the ESI MS experiments testify to the possibility of mutual modification of the biologically significant interactions of the artemisinin-type agents and ASC with phospholipids and other target molecules in polar media when the medications are co-administered. The modification is due to the complexation involving the molecules of the drugs. This conclusion correlates well with the early reported results [24] of the ESI MS study of model systems containing artemisinin-type drugs, aspirin, and DPPC.

3.2. Quantum chemical study of the interaction between DHAn and ASC, and of the interaction between the drugs and phospholipid

As reported above, in the present mass spectrometric experiments, we observe a set of two-component noncovalent complexes formed by the studied compounds. The structures of the complexes involving the artemisinin derivative – dihydroartemisinin (DHAn), L-ascorbic acid (ASC), and phosphatidylcholene head of phospholipid (PCn) are determined using the DFT/B3LYP method. The molecules forming the complexes contain a significant number of functional groups that are able to participate in strong intermolecular interactions including hydrogen bonds. Additionally, the neutral PCn molecule contains a positively charged tetramethylammonium group and a negatively charged phosphate group. Six structures (three for each ASC conformer under study) designated as ASC1•DHAn A, B, C and ASC2•DHAn A, B, C are selected as starting geometries for the search for equilibrium structures of the ASC complexes with DHAn. Each structure contains two intermolecular hydrogen bonds. For complexes of PCn with ASC and DHAn, when choosing the starting structures, all possibilities of the formation of hydrogen bonds and/or contacts of the polar groups of ASC and DHAn with charged groups of PCn are considered. To aid the selection of the initial structures in the latter case, the distribution of the electrostatic potential is calculated for all studied molecules. The resulting distributions are shown in Fig. S2 (Supplementary Materials). In total, we select three starting structures for the geometry optimizations of the DHAn•PCn complex (A, B and C) and eight for the ASC•PCn heterodimer (four for each ASC conformers: ASC1• PCn A, B, C, D and ASC2• PCn A, B, C, D).

The geometries of all selected complexes are fully optimized at the DFT/B3LYP/aug-cc-pVDZ level of theory and the calculated structures of the most stable noncovalent complexes are presented in Fig. 7. All calculated noncovalent complexes are shown in Fig. S3-S5 (Supplementary Materials). The distribution of the electrostatic potential in the most stable complexes is demonstrated in Fig. S6 (Supplementary Materials). The calculated interaction energies corresponding to the optimized structures of the studied complexes are presented in Table 1.

Table 1
ZPVE and BSSE corrected interaction energies (IE, kJ/mol) of the ASC•DHAn, ASC•PCn and DHAn•PCn noncovalent complexes calculated with the B3LYP/aug-cc-pVDZ method.

Complex	IE, in vacuum	IE[a], in methanol	IE[a], in water
ASC2•DHAn A	−50.3	−32.0	−31.5
ASC2•DHAn B	−46.7	−30.1	−30.4
ASC2•DHAn C	−41.7	−24.8	−24.3
ASC1•DHAn A	−44.9	−23.2	−22.5
ASC1•DHAn B	−42.9	−29.8	−29.5
ASC1•DHAn C	−40.2	−24.1	−23.8
ASC2•PCn A	−83.0	−43.8	−42.8
ASC2•PCn B	−71.5	−53.3	−52.7
ASC2•PCn C	−69.2	−36.4	−35.6
ASC2•PCn D	−64.4	−32.7	−32.0
ASC1•PCn A	−77.1	−33.8	−32.6
ASC1•PCn B	−62.0	−48.2	−47.6
ASC1•PCn C	−49.1	−23.2	−22.3
ASC1•PCn D	−41.5	−12.6	−11.8
DHAn•PCn A	−52.6	−29.7	−29.2
DHAn•PCn B	−34.0	−6.6	−6.2
DHAn•PCn C	−27.2	−10.5	−10.0

[a] calculated with the PCM (Polarizable Continuum Model) method.

The results of the quantum chemical modeling confirm the stability of the complexes of ASC and DHAn with the polar head of the phospholipid molecule and of the binary complexes of the different drugs molecules in the vacuum approximation, since the binding energies of all calculated complexes are negative and amount to several tens of kJ/mol (Table 1). The interaction energy values for the most stable complexes of the antimalarial drug with ascorbic acid, ASC2•DHAn A (IE=−50.3 kJ/mol), and with phosphatidylcholine, DHAn•PCn A (IE=−52.6 kJ/mol), are similar. This points to possible competition between ASC and phospholipid molecules to bind antimalarial agent DHAn. The complex of ASC2•PCn A is found to be the most stable in vacuum with IE=−83.0 kJ/mol. The stability of the noncovalent complexes is mainly due to the hydrogen bonds of the -C-O-H ••• O-P- type in the ASC•PCn and DHAn•PCn complexes, and by the hydrogen bonds of the -C-O-H ••• O-C - type in the binary complexes of ascorbic acid and dihydroartemisinin (see Fig. 7).

The noncovalent complexes observed in the ESI mass spectra are believed to correspond the intermolecular complexation in the solution. Thus, in the next step, the IEs of the complexes are recalculated in methanol (the solvent used in the ESI MS experiments) and in water using the PCM approach. From the results of the PCM calculations (see Table 1) one can see that the IE values of the complexes in the polar media are all negative (*i.e.* the complexes are stable), but, as expected, their magnitudes decrease in comparison with the values in vacuum.

Thus, in the present experimental and theoretical study the phenomenon of the competition between the artemisinin-type

agents and ASC for binding with DPPC is confirmed. The study also reveals the pair complexation of the drugs of different types in the model systems. The results obtained point to the possibility of modulation of biological activities of the artemisinin-type drugs and ascorbic acid under their combined usage.

4. Conclusions

The results of the present model study performed using ESI mass spectrometry technique and quantum chemical calculations testify to the possibility of the formation of noncovalent complexes of antimalarial agents of the artemisinin type and ascorbic acid with molecules of membrane phospholipids and among themselves in polar media. In the ESI mass spectra, the formation of stable noncovalent complexes between the molecules of artemisinin-type drugs (An, DHAn, AMr, and AEr) and ascorbic acid (ASC) molecules in methanol is manifested by the presence of peaks corresponding to cationized clusters of ASC•artemisinin-type drug•Na^+. Examination of the ESI spectrum of the two-component model system containing ASC and dipalmitoylphosphatidylcholine (DPPC) show the formation of stable noncovalent complex of ASC with the phospholipid molecule in the studied system. The ESI MS investigation of a ternary model system consisting of dihydroartemisinin (DHAn), ASC, and DPPC in the 1:1:5 molar ratio points to a competition between the artemisinin-type agent and ASC for binding with the phospholipid molecules in polar solutions. This is concluded based on the peaks corresponding to the stable DHAn•DPPC and ASC•DPPC noncovalent complexes recorded in the mass spectra. The pair complexation between the antimalarial drug DHAn and ASC is also found to be one more possible scenario of a competitive noncovalent interactions between the co-administered drugs.

The theoretical model studies employing the DFT/B3LYP/aug-cc-pVDZ method performed for systems in vacuum and in solutions (using the PCM approach) are used to elucidate the equilibrium geometries of a number of the noncovalent complexes recorded in the ESI MS experiments. The studied complexes are those formed by DHAn (the active metabolite of the artemisinin-type drugs), ASC, and DPPC. The polar phosphatidylcholine (PCn) head of DPPC has been used to model DPPC in the calculations. The most energetically favorable structure of the ASC•DHAn binary complex in vacuum is the structure with IE=−50.3 kJ/mol in which the drug molecules are bonded with hydrogen bonds of the -C-O-H ••• O-C - type. The most favorable structures of the complexes formed by molecules of the different drugs with polar DPPC heads considered in this work are: the ASC•PCn noncovalent complex with IE=−83.0 KJ/mol and the DHAn•PCn complex with IE=−52.6 KJ/mol. Both complexes are stabilized by the hydrogen bonds of the -C-O-H ••• O-P- type. Comparing the IE values of the ASC•PCn, DHAn•PCn, and ASC•DHAn complexes in vacuum shows that the complex of ASC with PCn is the most stable while the DHAn•PC and ASC•DHAn complexes are less stable and have similar intermolecular interaction energies. The PCM calculations reveal that the relative stability of the complexes in vacuum is similar as in the polar methanol and water solutions.

The data obtained in this work are of practical importance because they bring up a possibility to modulate the biological action of artemisinin-type antimalarial agent and ascorbic acid at the molecular level when the two drugs are concurrently administered in a medical treatment.

Credit author statement

Vlada Pashynska: Conceptualization, Methodology, Experimental Mass Spectrometry Investigations, Participation in Quantum Chemical Calculations, Data Analysis and Presenting, Manuscript Writing, Manuscript Review and Revision.

Stepan Stepanian: Quantum Chemical Calculations, Data Analysis and Presenting, Manuscript Writing and Review.

Agnes Gomory: Participation in Mass Spectrometry Measurements, Data Analysis, Manuscript Review.

Ludwik Adamovich: Participation in Quantum Chemical Calculations, Data Analysis, Manuscript Review and Editing.

Declaration of Competing Interest

The authors declare that they have no known competing financial interests or personal relationships that could have appeared to influence the work reported in this paper.

The authors declare the following financial interests/personal relationships which may be considered as potential competing interests:

Acknowledgements

Authors acknowledge the Program of cooperation between Ukrainian and Hungarian Academies of Sciences for the financial support of visit of the scientists from B. Verkin Institute for Low Temperature Physics and Engineering of the National Academy of Sciences of Ukraine to the Institute of Organic Chemistry of Research Centre for Natural Sciences in Hungary, where the mass spectrometry experiments were carried out. This work was partially supported by the National Academy of Sciences of Ukraine (NASU) (Grant N 0120U100157). An allocation of computer time from UA Research High Performance Computing (HPC) and High Throughput Computing (HTC) at the University of Arizona is gratefully acknowledged. V. Pashynska also thanks Prof. Magda Claeys from the University of Antwerp (Belgium) for the preceding fruitful cooperation in ESI mass spectrometry study of antimalarial drugs intermolecular interactions and for provision of the samples of the artemisinin-type drugs.

Supplementary materials

Supplementary material associated with this article can be found, in the online version, at doi:10.1016/j.molstruc.2021.130039.

References

[1] World Malaria Report 2019. Available from: https://www.who.int/news-room/feature-stories/detail/world-malaria-report-2019.
[2] Antimalarial drug efficacy and drug resistance. Available from: https://www.who.int/malaria/areas/treatment/drug_efficacy/en/.
[3] Ying Li, Qinghaosu (artemisinin): Chemistry and Pharmacology // Acta Pharmacologica Sinica, 2012 V 33. P. 1141–1146. doi: 10.1038/aps.2012.104.
[4] G. Calleri, R. Balbiano, P. Caramello, Are artemisinin-based combination therapies effective against *Plasmodium malariae*? // J. Antimicrob. Chemother. V. 68 (6) (2013) 1447–1448, doi:10.1093/jac/dkt005.
[5] P.M. O'Neill, V.E. Barton, S.A. Ward, The molecular mechanisms of action of artemisinin - The debate continues // Molecules V.15 (2010) 1705–1721, doi:10.3390/molecules15031705.
[6] Jian Li and Bing Zhou, Biological Actions of Artemisinin: insights from Medicinal Chemistry Studies // Molecules.2010. V. 15. P. 1378–1397. doi:10.3390/molecules15031378.
[7] J. Golenser, J.H. Waknine, M. Krugliak, N.H. Hung, G.E. Grav, Current perspectives on the mechanism of action of artemisinins, Int. J. Parasitol. V.36. (2006) 1427–1441, doi:10.1016/j.ijpara.2006.07.011.
[8] S. Krishna, A.-C. Uhlemann, R.K Haynes, in: Artemisinins: Mechanisms of Action and Potential For Resistance //Drug Resistance Updates, V.7, 2004, pp. 233–244, doi:10.1016/j.drup.2004.07.001.
[9] J. Wang, C.J. Zhang, W.N. Chia, C.C. Loh, Z. Li, Y.M. Lee, et al., Haem-activated promiscuous targeting of artemisinin in *Plasmodium falciparum*. // Nat, Commun. V.6. (2015) 10111, doi:10.1038/ncomms10111.
[10] N. Marwaha, Ascorbic acid co-administration with artemisinin based combination therapies in falciparum malaria, Indian J. Med. Res. V.143 (2016) 539–541, doi:10.4103/0971-5916.187100.
[11] K.A. Ganiyu, M.O. Akinleye, T. Fola, A study of the effect of ascorbic acid on the antiplasmodial activity of artemether in *Plasmodium berghei* infected mice, J. Appl. Pharmaceut. Sci. V. 2. (2012) 96–100.

[12] S.D. Li, Y.D. Su, M. Li, C.G. Zou, Hemin-mediated hemolysis in erythrocytes: effects of ascorbic acid and glutathione, Acta Biochim. Biophys. Sin. (Shanghai) V.38. (2006) 63–69, doi:10.1111/j.1745-7270.2006.00127.x.
[13] M.G. McKoy, P., III Kong-Quee, D.J Pepple, *vitro* effects of co-incubation of blood with artemether/lumefantrine & vitamin C on the viscosity & elasticity of blood, Indian J. Med. Res. V. 143 (2016) 577–580, doi:10.4103/0971-5916.187105.
[14] Kaltashov I.A., Eyles S.J. Mass Spectrometry in Structural Biology and biophysics: architecture, Dynamics and Interaction of Biomolecules. 2nd edition.- New York: "John Wiley & Sons, Inc.", 2012, 316 p.
[15] Siuzdak G. The Expanding Role of Mass Spectrometry in Biotechnology. 2nd edition. - San Diego: "MCC Press", 2006. - 257 p.
[16] Principles of Mass Spectrometry Applied to Biomolecules. Edited by Laskin J. and Lifshitz C.- Hoboken, New Jersey: "John Wiley & Sons, Inc.", 2006, 687 p.
[17] Edited by Cole R.- Hoboken, in: Electrospray and MALDI Mass spectrometry: fundamentals, instrumentation, practicalities, and Biological Applications, 2nd edition, John Wiley & Sons, Inc., New Jersey, 2010, p. 1008 p. Edited by.
[18] J.A. Loo, Electrospray ionization mass spectrometry: a technology for studying non-covalent macromolecular complexes, Int. J. Mass Spectrom. 200 (1–3) (2000) 175–186 N, doi:10.1016/S1387-3806(00)00298-0.
[19] Wyttenbach Th, M.T. Bowers, Intermolecular interactions in biomolecular systems examined by mass spectrometry, Annu. Rev. Phys. Chem. 58 (2007) 511–533, doi:10.1146/annurev.physchem.58.032806.104515.
[20] B.J. McCullough, S.J. Gaskell, Using Electrospray Ionisation Mass Spectrometry to Study Non-Covalent Interactions // Comb. Chem. High Throughput Screen, 2009, pp. 203–211. **12**, doi:10.2174/138620709787315463.
[21] V. Pashynska, H. Van den Heuvel, M. Claeys, M. Kosevich, Characterization of noncovalent complexes of antimalarial agents of the artemisinin type and Fe(III)-heme by electrospray ionization mass spectrometry and collisional activation tandem mass spectrometry, J. Am. Soc. Mass Spectrom. V.15. (2004) 1181–1190.
[22] Pashynska V., Boryak O., Kosevich M.V., Stepanian S., Adamowicz L. Competition between counterions and active protein sites to bind bisquaternary ammonium groups. A combined mass spectrometry and quantum chemistry model study // Eur. Phys. J. *D*. 2010. V. 58. P. 287–296.
[23] Pashynska V.A., Kosevich M.V., Gomory A., Vekey K., Model mass spectrometric study of competitive interactions of antimicrobial bisquaternary ammonium drugs and aspirin with membrane phospholipids // Biopolymers and Cell. 2013. V. 29 (2). P. 157–162. doi: 10.7124/bc.000814.
[24] V. Pashynska, S. Stepanian, A. Gomory, K. Vekey, L. Adamowicz, Competing intermolecular interactions of artemisinin-type agents and aspirin with membrane phospholipids: combined model mass spectrometry and quantum-chemical study, Chem. Phys V.455. (2015) 81–87 http://dx.doi.org/10.1016/j.chemphys.2015.04.014.
[25] V. Pashynska, S. Stepanian, A. Gomory, K. Vekey, L. Adamowicz, New cardioprotective agent flokalin and its supramolecular complexes with target amino acids: an integrated mass-spectrometry and quantum-chemical study, J. Mol. Struct. V. 1146 (2017) 441–449 http://dx.doi.org/10.1016/j.molstruc.2017.06.007.
[26] V.A. Pashynska, N.M. Zholobak, M.V. Kosevich, A. Gomory, P.K. Holubiev, A.I. Marynin, Study of intermolecular interactions of antiviral agent tilorone with RNA and nucleosides, Biophys. Bull. V. 39 (1) (2018) 15–26 http://doi.org/10.26565/2075-3810-2018-39-02.
[27] R. Guevremont, K.W.M. Siu, J.C.Y. Le Blanc, S.S Berman, Are the electrospray mass spectra of proteins related to their aqueous solution chemistry? // J. Am. Soc. Mass Spectrom. 3 (1992) 216–224.
[28] C.A. Morris, S. Duparc, I. Borghini-Fuhrer, D. Jung, C.S. Shin, L. Fleckenstein, Review of the clinical pharmacokinetics of artesunate and its active metabolite dihydroartemisinin following intravenous, intramuscular, oral or rectal administration, Malar. J. V.10 (2011) 263, doi:10.1186/1475-2875-10-263.
[29] J. Grace, A. Aguilar, K. Trotman, T. Brewer, Metabolism of beta-arteether to dihydroqinghaosu by human liver microsomes and recombinant cytochrome P450, Drug Metab. Dispos. V. 26 (1998) 313–317.
[30] M.A. Mora, F.J. Melendez, Conformational *ab initio* study of ascorbic acid // J, Mol. Struct. (Theochem). V. 454 (1998) 175–185.
[31] R.N. Allen, M.K. Shukla, D. Reed, J. Leszczynski, Ab Initio Study of the Structural Properties of Ascorbic Acid (Vitamin C), Int. J. Quantum Chem. V. 106 (2006) 2934–2943.
[32] D.M. Bailey, W.O. George, M. Gutowski, Theoretical studies of L-ascorbic acid (vitamin C) and selected oxidised, anionic and free-radical forms, J. Mol. Struct.: THEOCHEM. V. 910 (2009) 61–68.
[33] R.A. Yadav, P. Rani, M. Kumar, R. Singh, Singh Priyanka, N.P Singh, Experimental IR and Raman spectra and quantum chemical studies of molecular structures, conformers and vibrational characteristics of L-ascorbic acid and its anion and cation, Spectrochimica Acta Part A V. 84 (2011) 6–21.
[34] S. Ebrahimi, H.A. Dabbagh, K. Eskandari, Nature of intramolecular interactions of vitamin C in view of interacting quantum atoms: the role of hydrogen bond cooperativity on geometry, Phys. Chem. Chem. Phys. V. 18 (2016) 18278–18288.
[35] G. Singh, B.P. Mohanty, G.S.S Saini, Structure, spectra and antioxidant action of ascorbic acid studied by density functional theory, Raman spectroscopic and nuclear magnetic resonance techniques, Spectrochimica Acta Part A: Mol. Biomol. Spectrosc. V. 155 (2016) 61–74.
[36] A.D. Becke, Density-functional exchange-energy approximation with correct asymptotic behavior, Phys. Rev. B V. 38 (1988) 3098–3100, doi:10.1103/PhysRevA.38.3098.
[37] C. Lee, W. Yang, R.G. Parr, Development of the Colle-Salvetti correlation-energy formula into a functional of the electron density, Phys. Rev. B. V. 37 (1988) 785 http://dx.doi.org/10.1103/PhysRevB.37.785.
[38] S.H. Vosko, L. Wilk, M. Nusair, Accurate spin-dependent electron liquid correlation energies for local spin density calculations: a critical analysis. //Can, J. Phys. V. 58 (1980) 1200–1211 doi: 0.1139/p80-159/.
[39] G. Scalmani, M.J. Frisch, Continuous surface charge polarizable continuum models of solvation. I. General formalism, J. Chem. Phys. V.132 (2010) 114110.
[40] Gaussian, Inc. (2009).

ISSN 0233–7657. Biopolymers and Cell. 2013. Vol. 29. N 2. P. 157–162 doi: 10.7124/bc.000814

UDC 577.32:615.28

Model mass spectrometric study of competitive interactions of antimicrobial bisquaternary ammonium drugs and aspirin with membrane phospholipids

V. A. Pashynska[1], M. V. Kosevich[1], A. Gomory[2], K. Vekey[2]

[1]B. I. Verkin Institute for Low Temperature Physics and Engineering, NAS of Ukraine
47, Lenin Ave., Kharkov, Ukraine, 61103

[2]Institute of Organic Chemistry of Research Centre for Natural Sciences of the Hungarian Academy of Sciences
59-67, Pusztaszeri Str., Budapest, H-1025, Hungary

vlada@vl kharkov.ua

Aim. *The aim of the study is to reveal molecular mechanisms of possible activity modulation of antimicrobial bisquaternary ammonium compounds (BQAC) and aspirin (ASP) through noncovalent competitive complexation under their combined introduction into the model systems with membrane phospholipids.* ***Methods***. *Binary and triple systems containing either decamethoxinum or ethonium, or thionium and aspirin, as well as dipalmitoylphosphatidylcholine (DPPC) have been investigated by electrospray ionization mass spectrometry.* ***Results***. *Basing on the analysis of associates recorded in the mass spectra, the types of nonocovalent complexes formed in the systems studied were determined and the supposed role of the complexation in the BQAC and ASP activity modulation was discussed. The formation of associates of BQAC dications with ASP anion is considered as one of the possible ways of deactivation of ionic forms of the medications. The formation of stable complexes of BQAC with DPPC and ASP with DPPC in binary systems as well as the complexes distribution in triple-components systems BQAC:ASP:DPPC point to the existence of competition between drugs of these two types for the binding to DPPC.* ***Conclusions***. *The results obtained point to the competitive complexation in the model molecular systems containing the BQAC, aspirin and membrane phospholipids. The observed phenomenon testifies to the possibility of modulating the activity of bisquaternary antimicrobial agents and aspirin under their combined usage, due to the competition between the drugs for binding to the target membrane phospholipid molecules and also due to the formation of stable noncovalent complexes between BQAC and ASP.*

Keywords: competitive complexation, bisquaternary ammonium compounds, aspirin, membrane phospholipids, mass spectrometry, electrospray ionization.

Introduction. Among urgent biomedical problems, the elucidation of either increase or decrease of the biological activity of several medicines at their combined use is of practical importance in connection with a high probability of mutual modulation of the medications activity in multi-drug therapeutic schemes of the modern medical practice. Along with tests on living organisms, model studies of the mechanisms of action of biologically active compounds at the molecular level permit to save time and resources prior to the experiments with real biological objects. Soft ionization mass spectrometry as an up-to-date method of molecular biophysics [1] is an efficient tool for studies of biomolecules and their intermolecular interactions [1–4]. Electrospray ionization (ESI) mass spectrometric technique based on spraying solutions of biomolecules in polar solvents is applied to modeling selective noncovalent intermolecular interactions of biologically active agents, medicines in particular, with their specific molecular targets [5–8].

In the framework of a problem of elucidation of molecular mechanisms of action of membranotropic antimicrobial agents we are developing an integrated approach to study of interactions of bisquaternary ammonium compounds (BQAC, $Cat^{2+} \cdot 2Cl^-$) with phospholi-

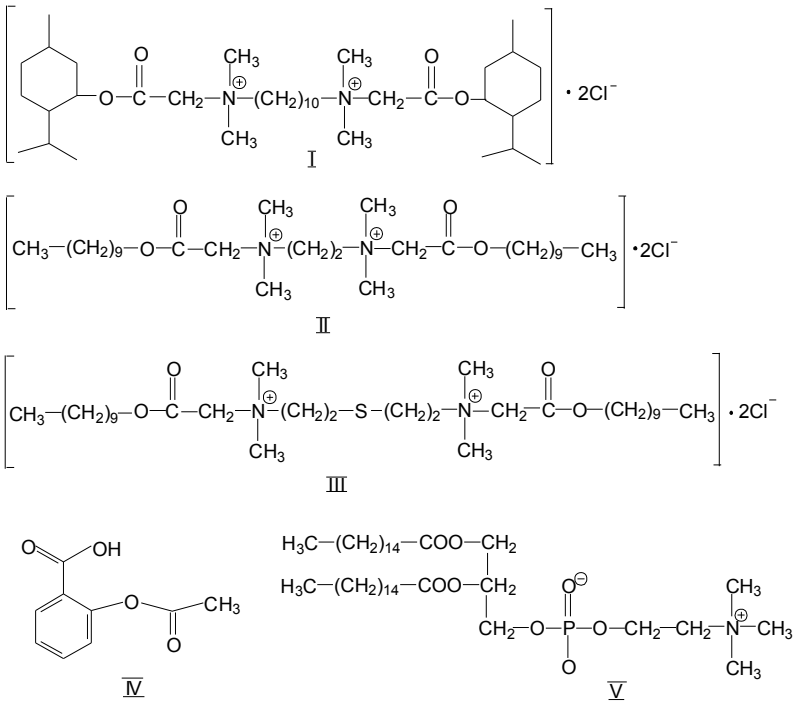

Scheme. Structures of the objects of investigation: *I* – decamethoxinum (monoisotopic molecular mass 692.5 Da); *II* – ethonium (584.4 Da); *III* – thionium (644.5 Da); *IV* – acetylsalicylic acid (180.0 Da); *V* – dipalmitoylphosphatidylcholine (733.6 Da)

pid assemblies which mimic the membranes of bacterial cells [9–13].

In our previous studies on molecular mechanisms of action of widely used antimicrobial BQACs decamethoxinum and ethonium, a combined application of ESI mass spectrometry, differential scanning calorimetry (DSC), and computer modelling [9] allowed us to reveal the formation of stable supramolecular complexes of the drugs with membrane phospholipids. The formation of such complexes is a prerequisite for the drugs incorporation into membranes, which distorts functioning of bacterial cell and thereby causes either bacteriostatic or bactericidal effect [13].

The background for addressing the above stated problem of investigation of combined action of several membranotropic and biologically active agents by means of mass spectrometry lies in an effect observed by us during characterization of BQACs by matrix-assisted laser desorption/ionization mass spectrometry [14]: substitution of inorganic Cl^- counterion of BQAC salts by anions of organic acids, 2,5-dihydrohybenzoic acid (a metabolite of aspirin) in particular, took place in a mixture. Since the formation of stable complexes of the compounds of basic and acidic types can affect and modulate the membranotropic activity of individual drugs [11], the above result stimulated us to expand the study of noncovalent interactions of BQACs with biologically significant organic acids. Among the compounds which can be administered together with BQAC antimicrobial agents for treatment of microbial infections, a popular anti-inflammatory remedy acetylsalicylic acid (aspirin, ASP), which possesses membranotropic properties as well [15], was selected.

In the current investigation different scenarios of possible activity modulation through noncovalent complexation of three antimicrobial BQACs decamethoxinum, ethonium, and thionium with aspirin under their combined mixing with a membrane phospholipid dipalmitoylphosphatidylcholine (DPPC) were examined using ESI mass spectrometry.

Materials and methods. Chemical structures of the objects of investigation are presented in the Scheme. Decamethoxinum (*I*), ethonium (*II*) and thionium (*III*) were synthesized in the Institute of Organic Chemistry of the National Academy of Sciences of Ukraine. Pure acetylsalicylic acid (aspirin) (*IV*) was obtained from the State Scientific Centre of Medications (Ukraine). Dipalmitoylphosphatidylcholine (*V*) was purchased from ALSI (Ukraine). Methanol (Super grade), being used as a solvent, was purchased from Reanal (Hungary).

Stock solutions of BQAC, ASP and DPPH (5 mM) were prepared in a polar solvent methanol and used for

binary (ASP:DPPH, ASP:BQAC) and triple (ASP: BQAC:DPPC) model systems preparation. Corresponding volumes of the stock solutions were mixed to reach the molar ratio 1:10 of drugs to phospholipid. The mixtures were kept at room temperature for at least 10 min before the ESI analysis. The spraying procedure required dilution of the solutions to be studied to provide 250 μM final concentration of the components. It was proved in numerous studies [5–8] that utilization of methanol as a solvent improves significantly the quality of ESI mass spectra and does not disturb the composition of intermolecular complexes formed in the initial solutions [16].

Mass spectral data were obtained in the positive ion mode, using triple quadruple (QqQ) Micromass Quattro Micro mass spectrometer («Waters», UK) which was equipped with the electrospray ion source. This source was operated in the standard ESI mode [5]. The potential of the spraying capillary was set at 3.5 kV. The cone voltage value of 10 V was used. ESI spectra were recorded in the mass range of 100–2000 Da. Data acquisition and processing were performed using MassLynx 4.1 software («Waters»).

Results and discussion. To reveal the formation of intermolecular complexes of membranotropic drugs and membrane phospholipid DPPH, binary and triple mixtures of the compounds under study were examined by ESI mass spectrometry.

At the initial stage of the study we have tested ASP: DPPH binary mixture with 1:10 molar ratio of the components, whose ESI mass spectrum is presented in Fig. 1. The spectrum contains peaks of the individual components: $ASP \cdot Na^+$ (*m/z* 203.1), $2ASP \cdot Na^+$ (*m/z* 383.2) for ASP and $DPPC \cdot H^+$ (*m/z* 734.6), $DPPC \cdot Na^+$ (*m/z* 756.6), $2DPPC \cdot Na^+$ (*m/z* 1491) for DPPH. Note, that cationization by sodium ion is characteristic of the ESI procedure and correlates with ion-molecule interactions under natural conditions. The presence of the peak of a cationized noncovalent complex of aspirin with phospholipid molecule, $DPPC \cdot ASP \cdot Na^+$ (*m/z* 936.5), proves the binding of aspirin to DPPH. It also testifies to the possibility of competition between aspirin and BQAC for the binding to the phospholipid molecular target.

Note that aspirin binds with a single DPPH molecule only. This contrasts with the features of binding

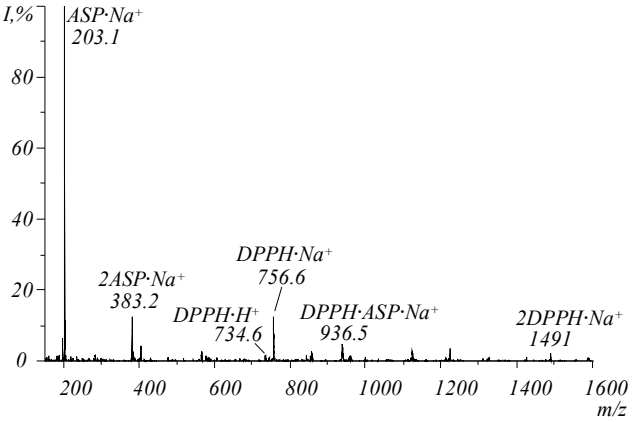

Fig. 1. ESI mass spectrum of a binary mixture of aspirin (ASP) and DPPH phospholipid in molar ratio 1:10

BQAC with DPPH in their binary mixtures, studied in our previous works [10, 12]. It was found that the diction (Cat^{2+}) of BQAC can bind up to 9 DPPH molecules. Such supramolecular complexes, nDPPH $\cdot Cat^{2+}$, can be considered as a sufficient model of complexes BQAC with phospholipid membrane assemblies. Distinctions in the types of the complexes formed by aspirin and BQACs with DPPH are in correlation with the differences in mechanisms of their intermolecular interactions with phospholipids. While the dications of surface active BQACs are incorporated as components into phospholipid assemblies, the aspirin molecule, as it was shown in [15], interacts with the glycerol moiety of a separate DPPH molecule.

At the next stage of the study, ESI mass spectra of equimolar mixtures of BQACs and aspirin were examined (Fig. 2). The abundant peak of noncovalent associate of a BQAC dication and acetylsalicylic acid anion – $Cat^{2+} \cdot (ASP\text{-}H)^-$ – was observed at *m/z* 801.6 for decamethoxinum (Fig. 2, *A*), at *m/z* 693.5 for ethonium (Fig. 2, *B*), and at *m/z* 753.6 for thionium, along with the ions characteristic of individual components (Cat^{2+} and $Cat^{2+} \cdot Cl^-$ for BQACs, $ASP \cdot Na^+$ and $2ASP \cdot Na^+$ for ASP). This result pointed to one more possible mechanism of the BQAC-based drugs action modulation by aspirin, based on the formation of stable pair complexes between the BQAC dication and the organic acid anion, which deactivated the ionic forms of the medications. Note, that no definite information can be obtained as to a possibility of the formation of triple complexes $Cat^{2+} \cdot 2(ASP\text{-}H)^-$, since they are neutral and thus undetectable by mass spectrometry.

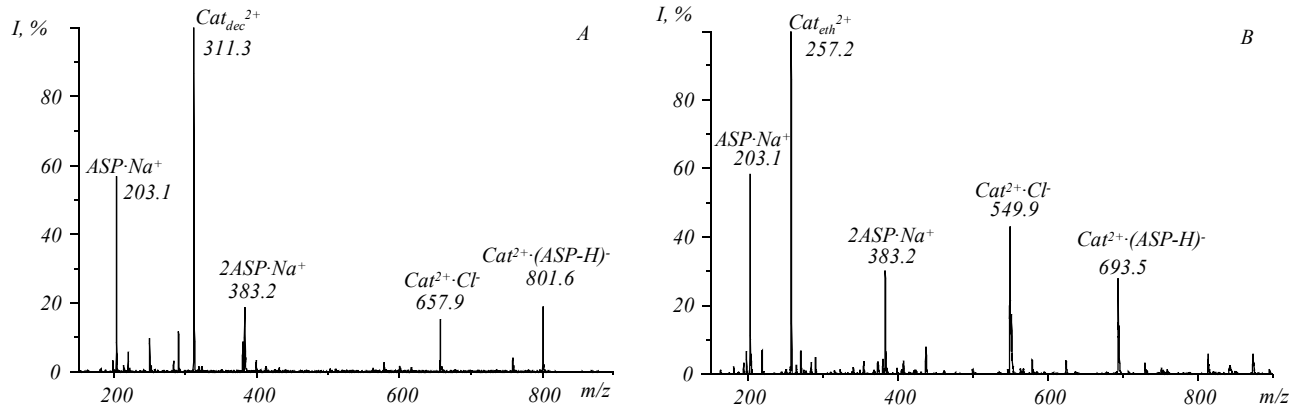

Fig. 2. ESI mass spectra of equimolar mixtures of decamethoxinum with aspirin (*A*) and ethonium with aspirin (*B*)

Finally, the triple systems BQAC:ASP:DPPC (1:1:10 molar ratio) were probed (Fig. 3).

The intermolecular complexes recorded in the mass spectra reflected the complexity of specific noncovalent interactions in the model systems. Firstly, the supramolecular complexes of the BQAC dication with up to 4 DPPC molecules were formed similarly to the drug-phospholipid associates in their binary systems [10, 12]. Secondly, aspirin bound to a single DPPH molecule similarly to its behaviour in the binary system (Fig. 1). Thirdly, the dication-anion $Cat^{2+}\cdot(ASP\text{-}H)^{-}$ complexes observed in the binary BQAC:ASP mixtures (Fig. 2) are formed in the triple system as well. The peaks distribution in the mass spectra pointed to the existence of a competition between BQACs and ASP for binding to DPPC molecules in the three systems, since abundances of the peaks of $n\text{DPPC}\cdot Cat^{2+}$ complexes, $Cat^{2+}\cdot(ASP\text{-}H)^{-}$ and $\text{DPPC}\cdot\text{ASP}\cdot Na^{+}$ associates were of comparable intensities. The competition for binding ionic forms of the drugs to DPPH molecules and the formation of dication-anion complexes, revealed on the basis of mass spectrometric data, can be considered as molecular mechanisms of the possible drugs activity modulation.

The effects observed at the molecular level were further verified at the level of model biomembranes. To prove the incorporation of the membranotropic agents into DPPC membranes and to evaluate their combined effect, DSC measurements [13] were carried out along with the mass spectrometric experiments. The results of the DSC study of the binary BQAC:DPPC, ASP:DPPC and triple BQAC:ASP:DPPC systems have shown that doping of the hydrated DPPH bilayer by individual BQAC, aspirin [13] or gentinsic acid [11, 17] decreased the temperature of phase transition in the membrane, that evidenced the disordering effect in the membrane. At the same time simultaneous addition of both BQAC and acidic agents did not cause substantial membrane disordering, which was interpreted as a confirmation of deactivation (modulation) of the drugs action.

The effect of competitive intermolecular interactions observed at the level of biomolecules and model phospholipid biomembranes permits to formulate a task for further tests of the biological activity modulation for BQAC and acidic membranotropic agents as to their combined use at the level of microbial cells.

Conclusions. The results of the ESI mass spectrometric study demonstrate the competitive complexation in the model systems containing the BQAC, aspirin and membrane DPPH phospholipids. The observed phenomenon testifies to the possibility of modulation of the activity of membranotropic BQAC-based antimicrobial agents and aspirin under their combined usage via several scenarios: due to either the competition between these two types of drugs for binding to the target phospholipid molecules, or the formation of stable pair noncovalent complexes between BQAC and aspirin ions. Owing to these competitive complexations, the activity of the both agents at their combined use can be much lower than the activity of each single agent. Thus, the mechanisms of the possible drug activity modulation are demonstrated experimentally on the model molecular level systems.

The supposed modulation effect should be further inquired at the microbial cell level.

Acknowledgements. Authors acknowledge the Program of cooperation between Ukrainian and Hungarian

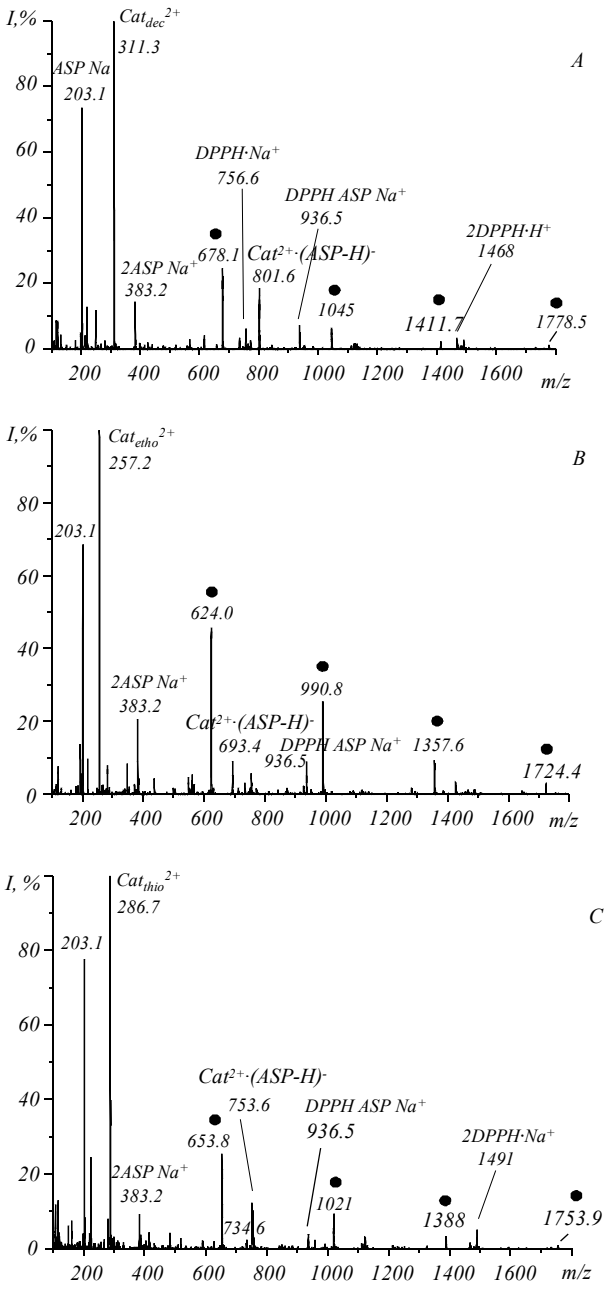

Fig. 3. ESI mass spectra of triple BQAC:ASP:DPPC systems: *A* – BQAC is decamethoxinum; *B* – BQAC is ethonium; *C* – BQAC is thionium. Sets of peaks corresponding to $[Cat \cdot nDPPC]^2$ complexes (n = = 1 ÷ 4) are marked by (•) symbol

Academies of Sciences for the financial support of the visit to the Institute of Organic Chemistry of Research Centre for Natural Sciences of the Hungarian Academy of Sciences, where the experiments were carried out. Authors are grateful to Prof. L. N. Lisetski and Dr. O. V. Vashchenko for helpful discussion of the results.

В. А. Пашинська, М. В. Косевич, А. Гоморі, К. Вєкей

Модельне мас-спектрометричне дослідження конкурентної взаємодії мембранотропних антимікробних бісчетвертинних амонієвих препаратів і аспірину з мембранними фосфоліпідами

Резюме

Мета. *Вивчення молекулярних механізмів можливої модуляції активності антимікробних бісчетвертинних амонієвих сполук (БЧАС) та аспірину (АСП) внаслідок формування нековалентних комплексів під час спільного введення препаратів двох типів у модельні системи з мембранними фосфоліпідами.* ***Методи***. *Дво- і трикомпонентні системи, які містять декаметоксин, етоній або тіоній, АСП і дипальмітоїлфосфатидилхолін (ДПФХ), досліджували методом мас-спектрометрії з іонізацією електроспреєм.* ***Результати***. *Грунтуючись на даних аналізу асоціатів, зареєстрованих у мас-спектрах, встановлено типи нековалентних комплексів, які формуються у досліджуваних системах, та обговорено їхню можливу роль у модуляції активності БЧАС і АСП. Утворення асоціатів дикатіонів БЧАС з аніоном АСП є одним з імовірних шляхів дезактивації іонних форм препаратів. Формування стабільних комплексів БЧАС з ДПФХ та АСП з ДПФХ у двокомпонентних системах, а також розподіл комплексів у трикомпонентних системах БЧАС:АСП:ДПФХ вказують на існування конкуренції між препаратами двох типів за зв'язування з ДПФХ.* ***Висновки***. *Отримані результати свідчать про конкурентне комплексоутворення у модельних молекулярних системах, що містять БЧАС, АСП і мембранні фосфоліпіди. Виявлений факт підтверджує можливість модуляції активності бісчетвертинних амонієвих протимікробних агентів і аспірину при сумісному використанні завдяки конкуренції між ліками за зв'язування з мембранними фосфоліпідами, а також внаслідок формування стабільних нековалентних комплексів між БЧАС і АСП.*

Ключові слова: конкурентне комплексоутворення, бісчетвертинні амонієві сполуки, аспірин, мембранні фосфоліпіди, мас-спектрометрія, іонізація електроспреєм.

В. А. Пашинская, М. В. Косевич, А. Гомори, К. Векей

Модельное масс-спектрометрическое исследование конкурентного взаимодействия антимикробных бисчетвертичных аммониевых препаратов и аспирина с мембранными фосфолипидами

Резюме

Цель. *Изучение молекулярных механизмов возможной модуляции активности антимикробных бисчетвертичных аммониевых соединений (БЧАС) и аспирина (АСП) посредством формирования нековалентных комплексов при совместном введении препаратов двух типов в модельные системы с мембранными фосфолипидами.* ***Методы***. *Двух- и трехкомпонентные системы, содержащие декаметоксин, этоний или тионий и АСП, а также дипальмитоилфосфатидилхолин (ДПФХ) исследовали методом масс-спектрометрии с ионизацией электроспреем.* ***Результаты***. *На основании анализа ассоциатов, зарегистрированных в масс-спектрах, установлены типы нековалентных комплексов, образующихся в исследованных системах, а также обсуждена их предполагаемая роль в модуляции активности БЧАС и АСП. Формирование ассоциатов дикатионов БЧАС с анионом АСП является одним из возможных путей дезактивации ионных форм препаратов. Образование стабильных комплексов БЧАС с ДПФХ и АСП с ДПФХ в*

двухкомпонентных системах, а также распределение комплексов в трехкомпонентных системах БЧАС:АСП:ДПФХ указывают на существование конкуренции между препаратами двух типов за связывание с ДПФХ. ***Выводы****. Полученные результаты свидетельствуют о конкурентном комплексообразовании в модельных молекулярных системах, содержащих БЧАС, АСП и мембранные фосфолипиды. Обнаруженный факт подтверждает возможность модуляции активности бисчетвертичных аммониевых противомикробных агентов и аспирина при совместном применении вследствие конкуренции между лекарствами за связывание с мембранными фосфолипидами, а также благодаря формированию нековалентных комплексов между БЧАС и АСП.*

Ключевые слова: конкурентное комплексообразование, бисчетвертичные аммониевые соединения, аспирин, мембранные фосфолипиды, масс-спектрометрия, ионизация электроспреем.

REFERENCES

1. *Kaltashov I. A., Eyles S. J.* Mass spectrometry in structural biology and biophysics: architecture, dynamics and interaction of biomolecules / 2nd edition.–New York: John Wiley & Sons, Inc., 2012.–312 p.
2. *Siuzdak G*. The expanding role of mass spectrometry in biotechnology. 2nd edition.–San Diego: MCC Press, 2006.–257 p.
3. *Lebedev A. T., Artemenko K. A., Samgina T. Yu*. Principles of mass spectrometry of proteins and peptides.–Moscow: Technosphera, 2012.–176 p. [in Russian].
4. *Principles* of mass spectrometry applied to biomolecules / Eds J. Laskin, C. Lifshitz.–New Jersey: John Wiley & Sons, Inc., 2006.–687 p.
5. *Electrospray* and MALDI mass spectrometry: fundamentals, instrumentation, practicalities, and biological applications / Ed. R. B. Cole, 2nd edition.–New Jersey: John Wiley & Sons, Inc., 2010.–863 p.
6. *Loo J. A*. Electrospray ionization mass spectrometry: a technology for studying non-covalent macromolecular complexes // Int. J. Mass Spectrom.–2000.–**200**, N 1–3.–P. 175–186.
7. *Wyttenbach Th., Bowers M. T.* Intermolecular interactions in biomolecular systems examined by mass spectrometry // Annu. Rev. Phys. Chem.–2007.–**58**.–P. 511–533.
8. *McCullough B. J., Gaskell S. J.* Using electrospray ionisation mass spectrometry to study non-covalent interactions // Comb. Chem. High Throughput Screen.–2009.–**12**, N 2.–P. 203–211.
9. *Pashinskaya V. A., Kosevich M. V., Gomory A., Vashchenko O. V., Lisetski L. N.* Mechanistic investigation of the interaction between bisquaternary antimicrobial agents and phopholipids by liquid secondary ion mass spectrometry and differential scanning calorimetry // Rapid Commun. Mass Spectrom.–2002.–**16**, N 18.–P. 1706–1713.
10. *Pashynska V. A., Kosevich M. V., Van den Heuvel H., Cuyckens F., Claeys M*. Study of non-covalent complexes formation between the bisquaternary ammonium antimicrobial agent decamethoxinum and membrane phospholipids by electrospray ionization and collision-induced dissociation mass spectrometry // Vistnyk Karazin National University. Biophys. Bull.–2004.–**637**, N 1–2 (14).–P.123–130.
11. *Vashchenko O., Pashynska V., Kosevich M., Panikarska V., Lisetski L.* Lyotropic mesophase of hydrated phospholipids as model medium for studies of antimicrobial agents activity // Mol. Cryst. Liq. Cryst.–2011.–**547**, N 1.–P. 155–163.
12. *Pashynska V. A., Kosevich M. V., Gomory A., Vekey K*. Investigation of formation of noncovalent complexes between antimicrobial agent ethonium with membrane phospholipids by electrospray ionization mass spectrometry // Mass-Spectrometria.–2012.–**9**, N 2.–P. 121–128.
13. *Vashenko O. V., Kasian N. A., Pashynska V. A., Kosevich M. V., Ermak Yu. L., Lisetskyi L. N*. Lipid membranes as a model medium for solution of the applied biomedical problems // Functional materials for scintillation technology and biomedicine.–Kharkiv: ISMA, 2012.–428 p. [in Russian].
14. *Pokrovsky V. A., Kosevich M. V., Osaulenko V. L., Chagovets V. V., Pashynska V. A., Shelkovsky V. S., Karachevtsev V. A., Naumov A. Yu*. Matrix assisted laser desorption-ionization study of bisquaternary ammonium antimicrobial agent decamethoxinum in 2,5-dixydroxybenzoic acid // Mass-Spectrometria.–2005.–**2**, N 3.–P. 183–192.
15. *Panicker L., Sharma V. K., Datta G, Deniz K. U., Parvathanathan P. S., Ramanathan K. V., Khetrapal C. L.* Interaction of aspirin with DPPC in the lyotropic, DPPC-Aspirin-H2O/D2O membrane // Mol. Cryst. Liq. Cryst.–1995.–**260**, N 1.–P. 611–621.
16. *Guevremont R., Siu K. W. M., Le Blanc J. C. Y., Berman S. S.* Are the electrospray mass spectra of proteins related to their aqueous solution chemistry? // J. Am. Soc. Mass Spectrom.– 1992.– **3**, N 3.–P. 216–224.
17. *Vashenko O. V., Pashynska V. A., Kosevich M. V., Boryak O. A., Kasian N. A., Lisetski L. N*. Investigation on combined effect of quaternary ammonium compounds and an organic acid on model phospholipid membranes // Biophys. Bull.–2010.–**25**, N 2.–P. 55–72.

Received 30.12.12

Molecular BioSystems

PAPER

Cite this: *Mol. BioSyst.*, 2014, **10**, 3155

Probing of the combined effect of bisquaternary ammonium antimicrobial agents and acetylsalicylic acid on model phospholipid membranes: differential scanning calorimetry and mass spectrometry studies

N. A. Kasian,*[a] V. A. Pashynska,[b] O. V. Vashchenko,[a] A. O. Krasnikova,[a] A. Gömöry,[c] M. V. Kosevich[b] and L. N. Lisetski[a]

Received 18th July 2014,
Accepted 10th September 2014

DOI: 10.1039/c4mb00420e

www.rsc.org/molecularbiosystems

A model molecular biosystem of hydrated dipalmitoylphosphatidylcholine (DPPC) bilayers that mimics cell biomembranes is used to probe combined membranotropic effects of drugs by instrumental techniques of molecular biophysics. Differential scanning calorimetry reveals that doping of the DPPC model membrane with individual bisquaternary ammonium compounds (BQAC) decamethoxinum, ethonium, thionium and acetylsalicylic acid (ASA) leads to lowering of the membrane melting temperature (T_m) pointing to membrane fluidization. Combined application of the basic BQAC and acidic ASA causes an opposite effect on T_m (increase), corresponding to the membrane densification. Thus, modulation of the membranotropic effects upon combined use of the drugs studied can be revealed at the level of model membranes. Formation of noncovalent supramolecular complexes of the individual BQACs and ASA with DPPC molecules, which may be involved in the mechanism of the drug membrane interaction at the molecular level, is demonstrated by electrospray ionization (ESI) mass spectrometry. In the ternary (DPPC + ASA + BQAC) model systems, the stable complexes of the BQAC dication with the ASA anion, which may be responsible for modulation of the membranotropic effects of the drugs, were recorded by ESI mass spectrometry. The proposed approach can be further developed for preliminary evaluation of the combined effects of the drugs at the level of model lipid membranes prior to tests on living organisms.

Introduction

The efficiency of combined multi-drug treatment of microbial infections can be enhanced not only by invention of new medicines, but by just avoiding possible antagonistic effects of several pharmaceuticals being applied simultaneously.[1–3] Efficient rapid evaluation of the drug activity can be achieved by means of experimental testing methods using model molecular and supramolecular systems, requiring shorter time and much smaller number of tests to be carried out on living organisms.[4] Recently, growing interest has been observed in drug–lipid membrane interactions studies using model lipid membranes [*e.g.* ref. 5–8, and references therein]. This is due to understanding of the relevance of drug–lipid interactions for pharmacokinetic properties of drugs (bioavailability, biodistribution, accumulation) and hence their pharmacological efficiency.[6–8] Another important aspect of drug–lipid interaction studies is a deeper insight into the molecular mechanism of drug activity.[5–9] Such biomimetic media as model lipid membranes can be probed by experimental techniques of molecular physics and biophysics.[5,10,11] The majority of studies in this field deal with effects of individual substances such as antibiotics, anticancer drugs, steroids, vitamins *etc.* on the physical parameters of model lipid membranes.[5–8] Evaluation of combined membranotropic effects of several substances, to the best of our knowledge, is rather uncommon. Only a few studies deal with joint membranotropic action: vitamin D_2/Ca^{2+} in dipalmitoylphosphatidylcholine (DPPC) membranes,[12,13] vitamin E/Ca^{2+} in dimyristoylphosphatidylserine membranes,[14] cholesterol/Ca^{2+} in phosphatidylserine membranes,[15] cholesterol/amphotericin B and ergosterol/amphotericin B in DPPC membranes,[16] methanol/vitamin C and ethanol/vitamin C in DPPC mono-layers.[17] In all the studies mentioned above, the simultaneous presence of two substances mutually altered their membranotropic behavior.

[a] *Institute for Scintillation Materials of the National Academy of Sciences of Ukraine, 60, Lenin ave., 61001 Kharkov, Ukraine. E mail: kasian@isma.kharkov.ua*
[b] *B. Verkin Institute for Low Temperature Physics and Engineering of the National Academy of Sciences of Ukraine, 47, Lenin ave., 61103, Kharkov, Ukraine*
[c] *Institute of Organic Chemistry of Research Centre for Natural Sciences of the Hungarian Academy of Sciences, Magyar tudósok korútja str., 2, Budapest, H 1117, Hungary*

Remarkably, no specific interactions between these substances were noted, hence these effects can be considered as membrane-mediated.

In the present work, we describe an approach to study the combined effect of drugs on model membranes based on multibilayers of hydrated DPPC. These drugs are bisquaternary ammonium compounds (BQAC), broad-spectrum antiseptics used for treatment of certain bacterial, mycotic and viral infections,[18,19] as well as a multi-functional drug - acetylsalicylic acid (ASA), with diverse therapeutic applications including symptomatic treatment of infections. The drugs are of basic and acidic nature which conditioned their potential intermolecular interaction. As known from the literature,[18–21] membranes of bacterial cells are considered as the main targets of antiseptic quaternary and bisquaternary ammonium salts, so the membranotropic effect is believed to be an important constituent of their antimicrobial activity. Investigations of bactericidal effects of the BQACs showed that these drugs caused disintegration of the bacterial membrane structures leading to an increase of their permeability and to alteration of the functioning of the membrane enzymes.[18–21] The membranotropic properties of ASA were revealed as well.[22] The idea to probe the combined effect of basic and acidic membranotropic agents emerged from our previous inter-disciplinary studies of molecular mechanisms of action of BQAC drugs decamethoxinum (DEC), ethonium (ETH) and thionium (THI) (Fig. 1). The main results of these investigations[23–31] may be summarized as follows:

(1) Probing of DPPC model membranes doped by DEC, ETH, THI by differential scanning calorimetry (DSC) revealed significant lowering of the melting temperature of membranes (T_m),[23–25,30] which is a marker of the membrane fluidization.

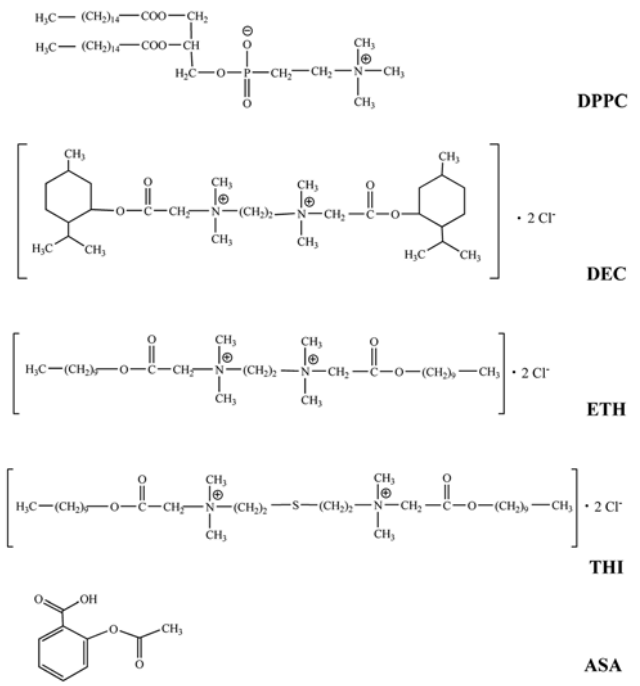

Fig. 1 Structural formulae of compounds under study: DPPC ($C_{40}H_{80}NO_8P$); DEC ($C_{38}H_{74}Cl_2N_2O_4$); ETH ($C_{30}H_{62}Cl_2N_2O_4$); THI ($C_{32}H_{66}Cl_2N_2O_4S$) and ASA ($C_9H_8O_4$).

This can be the reason for the pharmacological effect of BQACs reported above.

(2) Probing of the binary (DPPC + BQAC) systems by electrospray ionization (ESI) mass spectrometry (based on spraying of liquid solutions of biomolecules[32,33]) revealed formation of stable supramolecular complexes of the BQAC dication (Cat^{2+}) with a number (up to nine) of DPPC molecules.[29,31]

(3) From the evidence of matrix-assisted laser desorption/ionization mass spectrometry (MALDI), substitution of inorganic Cl^- counterions of BQAC salts by anions of organic 2,5-dihydroxybenzoic acid (DHB) was observed.[27,28] It should be noted that DHB used as MALDI matrix compound is a metabolite of ASA.[34]

On the basis of the above finding, it was suggested that upon simultaneous application of the basic and acidic substances, their complexes can lead to modification of their membranotropic activity. This assumption was verified by the DSC method.[25,30] For ternary (DPPC + BQAC + DHB) systems, it was demonstrated that the effect of the combined action of BQAC and DHB on T_m of DPPC membranes differed qualitatively from their individual action and consisted in an increase of T_m.[30] The data obtained stimulated us to study noncovalent interactions of BQAC with biologically significant organic acids.[29]

So the aim of the present work was to investigate the combined effect of antimicrobial drugs DEC, ETH, THI with multi-functional ASA on a DPPC model membrane using DSC and ESI mass spectrometric techniques. Such model studies of the combined action of drugs performed on molecular biosystems could be a step to their pre-biological testing.

Experimental

DEC, ETH, THI in the form of chloride salts (Fig. 1) were synthesized at the Institute of Organic Chemistry of the National Academy of Sciences of Ukraine (Kiev, Ukraine) and used without further purification. ASA was obtained from the State Scientific Centre of Medications (Kharkov, Ukraine). DPPC was purchased from ''Alexis Biochemicals'' (Switzerland).

Differential scanning calorimetry

For DSC studies, DPPC was hydrated with 70% (w/w) of bidistilled water to provide formation of the lamellar phase. Then, the samples were incubated at room temperature for 4 to 6 days with repeated heating to a temperature of approx. 50 °C (above T_m) with intense stirring. In the preparation of the DPPC membrane doped with one of the drugs studied, the same procedure was used, using the aqueous stock solutions of the drugs instead of the bidistilled water. The content of the drugs relative to dry DPPC ranged from 1 to 15% (w/w). To study the combined membranotropic action of the drugs, a series of DPPC membranes with various content of two drugs were prepared. The total amount of (BQAC + ASA) was 1% (w/w) relative to the weight of dry DPPC; molar ratios of BQAC to ASA in the system were 1 : 8, 1 : 4, 1 : 2, 1 : 1 and 2 : 1. A further procedure of model membrane preparation was applied as described for pure DPPC.

The thermodynamic properties of the model membrane systems were studied by the DSC technique using a Mettler DSC 1 calorimeter (Mettler Toledo, Switzerland). Phase transitions were detected from the low-temperature gel phase ($L_{\beta'}$) into the ripple ($P_{\beta'}$) phase (pre-transition) and then to the high-temperature liquid crystalline (L_{α}) phase (the main transition, or membrane melting).[10,35] The samples (approx. 20 mg) were placed into aluminum crucibles and sealed. The programmed scheme of the temperature scanning consisted of repeating heating–cooling cycles with a rate of 2 K min^{-1}. The parameters of the phase transitions were determined using the original Mettler DSC 1 software. The experimental error for T_m value was ±0.1 °C, for the ΔH_m value was ±1.5 kJ kg^{-1}, for FWHM ±0.2 °C, and for asymmetry ±0.04.

ESI mass spectrometry

For ESI mass spectrometry investigations, stock solutions of BQACs, ASA and DPPC (5 mM) were prepared in methanol. Corresponding volumes of the stock solutions were mixed to provide the molar ratio of the drugs to DPPC 1 : 10 in binary systems. For ternary systems (DPPC + BQAC + ASA) the molar ratio was 10 : 1 : 1. The mixtures were incubated at room temperature for at least 10 minutes before the ESI analysis. The ESI mass spectrometry spraying procedure required dilution of the solutions to provide a final concentration of 250 μM (or less) of the components.

ESI mass spectral data were obtained in the positive ion mode using a triple quadruple (QqQ) Micromass Quattro Micro mass spectrometer (Waters, Manchester, UK) which was equipped with the electrospray ion source. This source was operated in the standard ESI mode. The ESI source temperature was set to 120 °C and the desolvation temperature was 200 °C. The spraying capillary was operated at 3.5 kV. The cone voltage (CV) value of 20 V was used. The analyte solutions (20 μL) were infused into the mass spectrometer at a constant flow rate of 0.2 mL min^{-1} of the methanol solvent. ESI spectra were recorded in the mass range of m/z 100–2000. Data acquisition and processing were performed using the MassLynx 4.1 software (Waters, Manchester, UK).

Results and discussion

Membranotropic activity of individual drugs

The first step of our investigation included characterization of membranotropic effects of the individual drugs by means of DSC. DSC allows us to explore the effects of dopants on phase states of DPPC membranes, reflecting integral changes in supramolecular ordering of lipids.

The original DSC thermograms (obtained in heating mode) of binary model systems (DPPC + drug 5% w/w) are presented in Fig. 2. It is clearly seen that all the drugs cause lowering of the membrane melting temperature T_m, smearing of the melting peak and disappearance of the pre-transition peak. Decreasing of T_m indicates membrane fluidization and so increase of its permeability.

The concentration dependence of T_m shift (ΔT_m) for the (DPPC + DEC) system presented in Fig. 3 demonstrates a linear

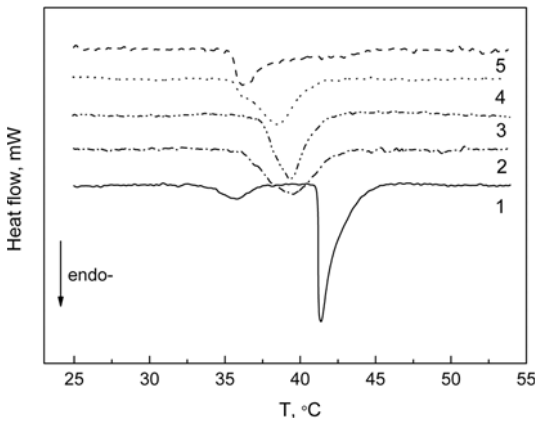

Fig. 2 DSC thermograms (heating mode) of (DPPC + drug 5% w/w): no admixture (1), THI (2), ETH (3), DEC (4), ASA (5).

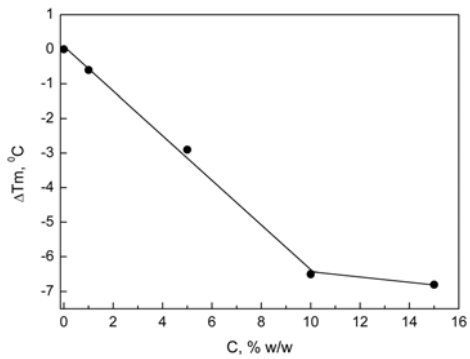

Fig. 3 Shift of the melting temperature of the (DPPC + DEC) system *vs.* DEC concentration.

character up to 10% w/w of DEC. Further increasing the DEC concentration does not result in significant changes of ΔT_m values. So, one can conclude that DEC incorporation in the DPPC membrane is limited to approximately 10% w/w.

In order to compare the membranotropic effects of different drugs, mass and molar membranotropic activity coefficients (α_{mas} and α_{mol}) were determined. These coefficients represent the shift of the membrane melting temperature ΔT_m upon addition of 1% w/w (or 1 mol%) of the admixture:

$$\alpha_{mas} = (T_m \quad T_m^o)/c_{mas}$$

$$\alpha_{mol} = (T_m \quad T_m^o)/c_{mol},$$

where T_m^o is the main phase transition temperature of the DPPC membrane without admixtures, T_m is the main phase transition temperature of the membrane with admixture, c_{mas} and c_{mol} are the admixture concentration in mass or molar percents.

The values of ΔT_m, α_{mas} and α_{mol} for the drugs studied are summarized in Table 1.

Among the drugs studied, the highest value of α_{mas} was obtained for ASA (1.0 °C), but the corresponding value accounting for the molecular mass, α_{mol}, appears close to that for ETH, THI. For DEC, both α_{mas} and α_{mol} appear to be the

Table 1 Characteristics of membranotropic effects of the drugs studied

Drug	Monoisotopic/average[a] molecular mass (Da)	ΔT_m [b] (°C)	Membranotropic activity coefficients	
			α_{mas} (°C)	α_{mol} (°C)
DEC	692.5/693.9	2.8	0.6	0.6
ETH	644.5/645.9	2.0	0.4	0.4
THI	584.4/585.7	2.0	0.4	0.3
ASA	180.0/180.2	5.1	1.0	0.3

[a] Monoisotopic mass is determined as the sum of masses of the first isotopes of all atoms of the molecule; average mass is calculated as the center of weight of the envelope of polyisotopic peaks, related to low resolution mass spectra. [b] Data for 5% (w/w) of the drugs in the DPPC membrane are presented.

highest among all BQACs. Individual membranotropic action of BQACs and ASA was similar to the effects of most dopants in liquid crystalline media,[36] *i.e.* decrease of the membrane melting temperature and smearing of the DSC phase transition peaks.

Combined membranotropic action of drugs

The next step was to study the drug effects upon their simultaneous introduction into a DPPC membrane, *i.e.* combined membranotropic action. It was demonstrated that the combined membranotropic action of (BQAC + ASA) is qualitatively different as compared to the effects of the individual substances.

Fig. 4 demonstrates that while the individual drugs (ETH and ASA) cause a decrease of T_m, their joint membranotropic action causes the opposite, *i.e.* T_m increases. The same effects were observed for (DEC + ASA) and (THI + ASA) pairs.

To specify this effect, we used the approach and methodology of so-called "quasi-binary systems" developed by Fialkov[37] and applied to model phospholipid membranes in ref. 25. According to this approach, the lipid membrane is considered as a medium where certain interactions between the admixtures could take place. In the absence of specific intermolecular interactions, the system parameters are additive with the concentration of the admixtures. In contrast, if certain specific interactions between the admixtures take place, the parameters change in a non-linear manner, and the ratio of admixtures

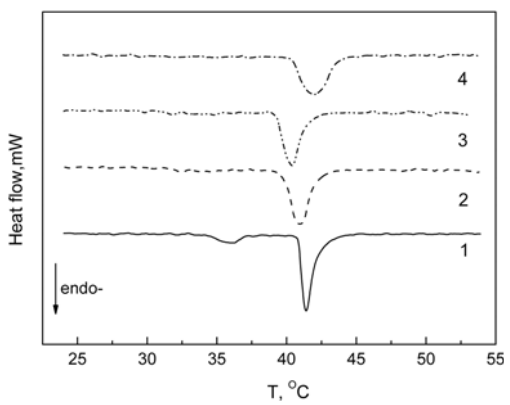

Fig. 4 DSC thermograms of the DPPC membrane (1) and the DPPC membrane containing 1% w/w of ETH (2), ASA (3) and (ETH + ASA) 1 to 2 mol mol ^{1} (4).

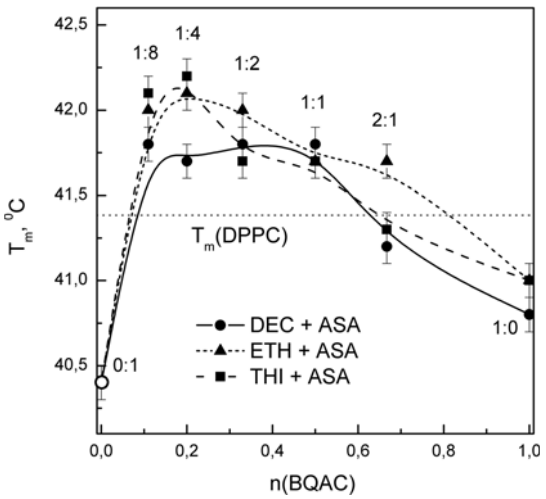

Fig. 5 Main phase transition temperature for the DPPC membrane doped with 1% w/w (BQAC + ASA) *vs.* molar fraction of BQAC in the admixture. Molar ratios BQAC to ASA are marked above the experimental points. ○ T_m for the (DPPC + ASA) system.

corresponding to the maximum deviation from additivity indicates the most probable stoichiometry of the intermolecular complex formed by the admixtures.

Based on the DSC thermograms of the DPPC membrane with individual drugs or drug pairs (BQAC + ASA) with varying molar ratios, quasi-binary phase diagrams were plotted in coordinates "T_m *vs.* n(BQAC)" (Fig. 5). Here n(BQAC) is the BQAC molar fraction in the admixture, *i.e.* $n(\text{BQAC}) = \nu_{BQAC}/(\nu_{BQAC} + \nu_{ASA})$, where ν is the number of moles in the system. The total content of the admixture(s) was 1% w/w (relative to dry DPPC) with molar ratios of BQAC to ASA 2 : 1, 1 : 1, 1 : 2, 1 : 4, and 1 : 8. The horizontal line in the plot corresponds to T_m of the non-doped DPPC membrane (41.4 °C). An imaginary straight line connecting points 0.0 and 1.0 mole fractions of BQAC corresponds to additive dependence of T_m on the molar ratio of admixtures.

As one can see from Fig. 5, the general trend of the plots for all three systems is similar. For all the pairs (DEC + ASA), (THI + ASA) and (ETH + ASA), the dependences of T_m on n(BQAC) are essentially non-linear, suggesting certain interactions between the admixtures resulting in complex formation.

For a wide range of n(BQAC) (from 0.1 to 0.7), an increase of T_m is observed. Such an effect is unusual and indicates densification of the bilayer due to increased ordering of the lipid molecules. Thus, (BQAC + ASA) complexes do interact with the DPPC membrane, but in an essentially different manner compared to the individual drugs.

Taking into account that in water medium BQACs dissociate forming dications Cat^{2+}, a noncovalent complex of Cat^{2+} with two $[ASA\text{-}H]^-$ anions is electrically neutral (each of the two charged quaternary ammonium groups of a BQAC fits to one anion of ASA). Molar ratios of BQAC to ASA 1 : 4 and 1 : 8 correspond to negatively charged complexes, whereas at the ratio 1 : 1 and 2 : 1 the complexes formed appear to be positively charged. For the (DEC + ASA) system, the plotted quasi-binary

phase diagram has no sharp maximum, but a broad plateau for 1 : 8, 1 : 4, 1 : 2, and 1 : 1 molar ratios (see Fig. 5). For the systems with ETH and THI, a maximum at 1 : 4 BQAC to ASA ratio can be noted. Though the mechanisms of interaction with the membrane depend on the charge state of the complex, the wide concentration range where increased T_m are observed suggests qualitatively similar membranotropic effects for both neutral and charged complexes.

It is interesting that less than 0.1 molar fraction of BQAC is needed to eliminate T_m decrease induced by ASA, whereas elimination of T_m decrease induced by BQAC requires ~0.35 molar fraction of ASA. Thus, ASA causes a weaker modulation effect on the membranotropic activity of BQAC as compared with the effect of the same molar fraction of BQAC on the activity of ASA.

Additional thermodynamic parameters of the systems studied are presented in Table 2. As one can see, the main phase transition enthalpy (ΔH_m) slightly decreases both in binary and in ternary systems, reflecting certain weakening in lipid–lipid interactions upon doping the DPPC membrane with drugs. No significant difference between ΔH_m values for individual and joint drugs action is noticed. In contrast to ΔH_m, the full width at half-maximum (FWHM) of the main phase transition peak exhibits a clear tendency to increase in the following sequence: undoped membrane < binary system < ternary system. So, one can conclude that under the combined action of drugs, the cooperativity of DPPC membrane phase transition (the parameter which is reciprocal to FWHM) decreases more significantly than under their individual action.

The asymmetry parameter (A) of the main phase transition peak was calculated according to ref. 25 as a ratio of the right-hand shoulder of FWHM (with respect to T_m) to the FWHM value. In the case of the admixture affinity to the $L_{\beta'}$ phase, one can observe extension of the left-hand shoulder of the melting peak; correspondingly, the right-hand shoulder extension is caused by the admixture affinity to the L_α phase. For fully symmetric peaks A = 0.5, for low-temperature phase affinity this value decreases and for high-temperature phase affinity it increases. The values obtained indicate that all BQACs possess preferential affinity to the $L_{\beta'}$ phase whereas ASA tends to stabilize the L_α phase.

Based on the results of the present work, one could make the following recommendation from the viewpoint of medical application. BQAC antiseptics should be used separately from drugs of acidic nature (such as ASA) or acidic alimentary products (such as citrus fruits).

We suppose that the approach described can be used for pre-clinical estimation of the combined efficiency of drugs in the case when the pharmacological effect of at least one of them is associated with the cell membrane.

Table 2 Parameters of main phase transition of DPPC membranes doped with the drugs in binary systems (DPPC + drug) and ternary systems (DPPC + BQAC + ASA) for BQAC to ASA 1 : 4

System	ΔH_m (kJ kg^{-1})	FWHM (°C)	A
DPPC	23.5	1.0	0.6
DPPC + DEC	19.1	2.8	0.4
DPPC + DEC + ASA	23.2	3.7	0.5
DPPC + ETH	21.1	2.3	0.5
DPPC + ETH + ASA	20.3	3.5	0.5
DPPC + THI	20.2	2.7	0.4
DPPC + THI + ASA	22.4	3.2	0.5
DPPC + ASA	23.4	1.8	0.7

Experimental errors: ΔH_m ±1.5 kJ kg^{-1}, FWHM ±0.2, °C, A ±0.04.

Mass spectrometry studies of (DPPC + drug) systems

To study the above-described combined membranotropic effect of BQAC and ASA at the molecular level, model systems containing DPPC and the drugs were examined using the ESI mass spectrometry approach, which was developed for such systems in ref. 29.

First, binary (DPPC + drug) systems were tested. In Fig. 6 the ESI mass spectrum of the (DPPC + ASA) binary mixture with a 10 : 1 molar ratio is presented. Peaks of the individual components were found in the spectrum: ASA·Na$^+$ (m/z 203.0), 2ASA·Na$^+$ (m/z 383.1) for ASA and DPPC·H$^+$ (m/z 734.6), DPPC·Na$^+$ (m/z 756.6), 2DPPC·Na$^+$ (m/z 1490.1) for DPPC. It should be noted that cationization by sodium ions is typical for the ESI mass spectrometric technique and correlates with ion–molecule interactions under natural conditions of physiological solution. Further mass spectrum analysis reveals the presence of the peak of ASA·DPPC·Na$^+$ (m/z 936.6) ion that is a cationized noncovalent complex of ASA with a phospholipid molecule formed in the system studied. The stable complexes recorded under ESI conditions prove noncovalent binding of ASA to DPPC; such a binding can be considered as a molecular mechanism of the membranotropic action of ASA confirmed by the DSC study (Table 1).

Analyzing the data more deeply we have realized that ASA binds with a single DPPC molecule only. This result differs from the features of binding of some BQAC ($Cat^{2+}\cdot 2Cl^-$) with DPPC in their binary mixtures studied in our previous studiess.[29,31] It was found that the dication Cat^{2+} of the BQAC can bind up to 9 DPPC molecules for DEC[31] and up to 4 DPPC for ETH.[29] Such supramolecular complexes, $[Cat\cdot n DPPC]^{2+}$, can be supposed to be an adequate model of complexes of BQAC

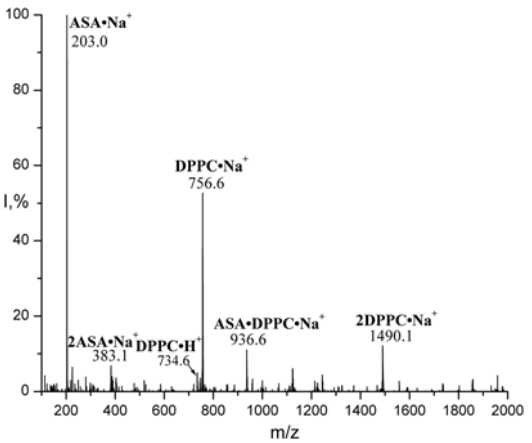

Fig. 6 ESI mass spectrum of the (DPPC + ASA) system.

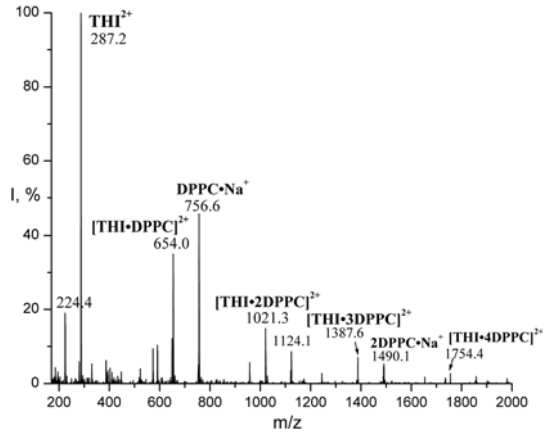

Fig. 7 ESI mass spectrum of the (DPPC + THI) system.

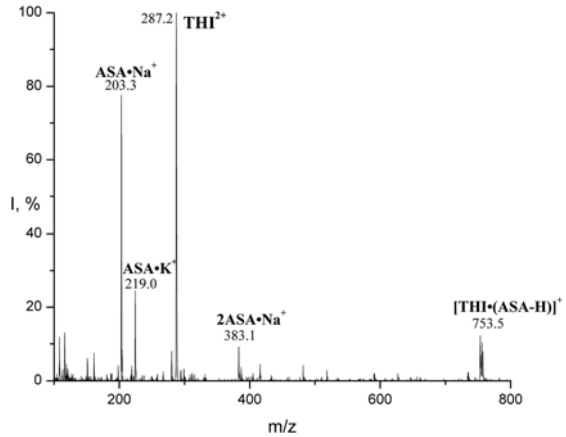

Fig. 8 ESI mass spectrum of the (ASA + THI) system.

with phospholipid membrane assemblies. In the current ESI study we have probed the (DPPC + THI) binary system in a 10 : 1 molar ratio. The spectrum of the (DPPC + THI) system is shown in Fig. 7.

Along with the characteristic ions of DPPC listed above and that of thionium (THI^{2+}, *m*/*z* 286.2) the peaks of the complexes of THI with one, two, three and four molecules of DPPC have been recorded: $[THI{\cdot}DPPC]^{2+}$, *m*/*z* 654.0; $[THI{\cdot}2DPPC]^{2+}$, *m*/*z* 1021.3; $[THI{\cdot}3DPPC]^{2+}$, *m*/*z* 1387.6; $[THI{\cdot}4DPPC]^{2+}$, *m*/*z* 1754.4. The supramolecular complexes $[THI{\cdot}nDPPC]^{2+}$ with a larger amount of phospholipid molecules could not be detected in the current experiment because of the mass range limit (2000 a.u.) of the instrument used.

Distinctions in the types of the complexes formed by ASA and BQACs with DPPC are in correlation with the differences in mechanisms of their intermolecular interactions with phospholipids. While the dications of surface active BQACs are known to be incorporated as components into the phospholipid assemblies,[7,18] the ASA molecule, as shown in ref. 22, interacts with the glycerol moiety of a separate DPPC molecule.

Thus, the results of the ESI mass spectrometric study of the binary systems (DPPC + ASA) and (DPPC + BQAC) show the formation of stable drug–phospholipids noncovalent complexes confirming at the molecular level the membranotropic activity of the drugs. They also point at one of the possible mechanisms of the modulation of the activity of drugs related to possible competition of the drugs for binding with the membrane phospholipids.

At the next stage of the mass spectrometric study, the ESI mass spectra of equimolar mixtures of the BQAC and ASA were obtained. The spectrum of the (ASA + THI) system is shown in Fig. 8 as an example. Intensive peaks of noncovalent clusters of the $Cat^{2+}{\cdot}(ASA\text{-}H)^{-}$ type were revealed for all mixtures: $[THI{\cdot}(ASA\text{-}H)]^{+}$, *m*/*z* 753.6 for (ASA + THI) mixture (Fig. 8), as well $[DEC{\cdot}(ASA\text{-}H)]^{+}$, *m*/*z* 801.6 and $[ETH{\cdot}(ASA\text{-}H)]^{+}$, *m*/*z* 693.5 for (ASA + DEC) and (ASA + ETH) systems, respectively. The ions characteristic for individual components were recorded as well: Cat^{2+} and $Cat^{2+}{\cdot}Cl^{-}$ for the BQAC, $ASA{\cdot}Na^{+}$ (*m*/*z* 203.3) and $ASA{\cdot}K^{+}$ (*m*/*z* 219.0) for ASA.

The results of the study of the (ASA + BQAC) systems point to one more possible mechanism of the BQAC-based drugs action modulation by ASA based on the formation of stable pair complexes between the BQAC dication and the organic acid anion, which deactivates the ionic forms of the drugs. It should be noted that no definite information can be obtained on the possible formation of triple complexes $Cat^{2+}{\cdot}2(ASP\text{-}H)^{-}$, since they are neutral and thus undetectable by mass spectrometry. These ESI results also directly confirm the results of the DSC experiments for the DPPC membrane doped with 1% (w/w) (BQAC + ASA) (Fig. 5) in which the increase of T_m has been registered in contrast to the decrease of T_m upon doping of DPPC membranes by individual drugs. This has been explained by formation of the drug complexes in the system with combined doping by ASA and BQAC.

Finally, the ternary systems (DPPC + ASA + BQAC) (10 : 1 : 1 molar ratio) have been probed. In Fig. 9 the spectrum of the (DPPC + ASA + THI) system is presented as an example. The spectra showed both complexation of ASA with BQAC and existence of a competition between ASA and BQAC for binding with the DPPC molecules in the systems studied, as predicted above. The two mechanisms are evidenced by comparable intensity of the peaks of the complexes of $[Cat{\cdot}nDPPC]^{2+}$ (n = 1–4), $[Cat{\cdot}(ASA\text{-}H)]^{+}$ and

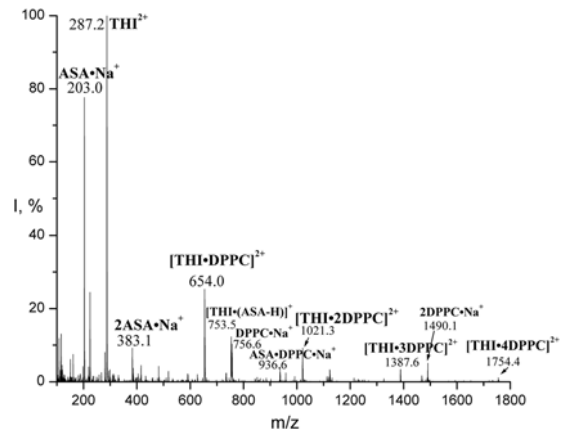

Fig. 9 ESI mass spectrum of the (DPPC + ASA + THI) system.

ASA·DPPC·Na^+ (*m*/*z* 936.6). The following peaks are recorded in the mass spectra: the characteristic peaks of ASA – ASA·Na^+ (*m*/*z* 203.0), 2ASA·Na^+ (*m*/*z* 383.1); the peak of THI intact dication THI^{2+}, *m*/*z* 287.2; the characteristic peaks of phospholipids DPPC·H^+ (*m*/*z* 734.6), DPPC·Na^+ (*m*/*z* 756.6), 2DPPC·Na^+ (*m*/*z* 1490.1) and the peaks of noncovalent complexes of ASA and THI with DPPC and pair drug complexes – ASA·DPPC·Na^+ (*m*/*z* 936.6), $[THI{\cdot}DPPC]^{2+}$, *m*/*z* 654.0; $[THI{\cdot}2DPPC]^{2+}$, *m*/*z* 1021.3; $[THI{\cdot}3DPPC]^{2+}$, *m*/*z* 1387.6; $[THI{\cdot}4DPPC]^{+}$, *m*/*z* 1754.4, $[THI{\cdot}(ASA\text{-}H)]^{+}$, *m*/*z* 753.5.

The intermolecular complexes recorded in the mass spectra reflected the complexity of specific noncovalent interactions in the model systems. Firstly, supramolecular complexes of the BQAC dication with up to 4 DPPC molecules were formed similarly to the drug–phospholipid associates in their binary systems.[23,29,31] Secondly, ASA bound to a single DPPC molecule similarly to its behaviour in the binary system (Fig. 8). Thirdly, dication–anion $Cat^{2+}{\cdot}[ASA\text{-}H]^-$ complexes observed in the binary (BQAC + ASA) mixtures are formed in the ternary system as well. The distribution of peaks in the mass spectra pointed to competition between BQACs and ASA for binding to DPPC molecules in the ternary systems, since abundances of the peaks of *n*DPPC·Cat^{2+} complexes, $Cat^{2+}{\cdot}[ASA\text{-}H]^-$ and DPPC·ASA·Na^+ associates were of comparable intensities. The competition for binding of ionic forms of the drugs to DPPC molecules and the formation of dication–anion complexes, revealed on the basis of mass spectrometric data, can be considered as molecular mechanisms of the possible modulation of the drug effects on the membrane.

Conclusions

An approach to preliminary tests of the combined effect of drugs at the level of molecular biosystems, such as DPPC model membranes, is proposed.

The membranotropic effect of the drugs is detected by changes in the membrane melting temperature determined by DSC. It is shown that doping of membranes by individual drugs DEC, ETH, THI and ASA causes T_m decrease (membrane fluidization), while the combined use of BQAC and ASA causes T_m increase (membrane densification).

Interaction of the drugs at the molecular level is probed by ESI mass spectrometry. Formation of noncovalent supramolecular complexes of the individual BQAC dications with DPPC molecules and assemblies as well as of ASA with one DPPC molecule demonstrated in the ESI mass spectrometry experiments may be involved in the molecular mechanisms of the membranotropic activity of the drugs. In the binary (BQAC + ASA) and ternary (DPPC + BQAC + ASA) systems, a new type of complex is recorded by ESI mass spectrometry, namely the complex of the BQAC dication with the deprotonated ASA anion.

The method of quasi-binary phase diagrams permits us to determine the formation of (BQAC + ASA) complexes in lipid membrane medium. Formation of such complexes may be responsible for modulation of the drug effects upon combined application.

The approach proposed can be applied for preliminary evaluation of the combined effects of various drugs at the level of molecular biosystems prior to testing on living organisms. So in the case of combined application of BQACs with ASA, we can assume that their pharmacological effect could be reduced.

Acknowledgements

Authors acknowledge the Program of cooperation between Ukrainian and Hungarian Academies of Sciences for the financial support of visit of the scientists from B. Verkin Institute for Low Temperature Physics and Engineering of the National Academy of Sciences of Ukraine to the Institute of Organic Chemistry of Research Centre for Natural Sciences of the Hungarian Academy of Sciences, where the mass spectrometry experiments were carried out.

Notes and references

1 T. C. Chou, *Cancer Res.*, 2010, **70**(N2), 440.
2 J. R. Pritchard, P. M. Bruno, L. A. Gilbert, K. L. Capron, D. A. Lauffenburger and M. T. Hemann, *Proc. Natl. Acad. Sci. U. S. A.*, 2013, **110**, 170.
3 A. K. Srivastava and Y. K. Gupta, *Indian J. Physiol. Pharmacol.*, 2001, **45**, 475.
4 T. C. Chou, *Leuk. Lymphoma*, 2008, **49**, 2059.
5 T. Pignatello, L. Musumeci, C. Basile, C. Carbone and G. Puglisi, *J. Pharm. BioAllied Sci.*, 2011, **3**, 4.
6 C. Peetla, A. Stine and V. Labhasetwar, *Mol. Pharmaceutics*, 2009, **6**, 1264.
7 J. K. Seydel and M. Wiese, *Drug-Membrane Interactions: Analysis, Drug Distribution, Modeling*, Wiley-VCH Verlag GmbH, Weinheim, 2002, p. 349.
8 M. Lucio, J. L. F. C. Lima and S. Reis, *Curr. Med. Chem.*, 2010, **17**, 1795.
9 I. Fournier, J. Barwicz, M. Auger and P. Tancrède, *Chem. Phys. Lipids*, 2008, **151**, 41.
10 S. Tristram-Nagle and J. F. Nagle, *Chem. Phys. Lipids*, 2004, **127**, 3.
11 M. H. Chiu and E. J. Prenner, *J. Pharm. BioAllied Sci.*, 2011, **3**, 39.
12 N. Toyran and F. Severcan, *Spectroscopy*, 2002, **16**, 399.
13 N. Toyran and F. Severcan, *Chem. Phys. Lipids*, 2003, **123**, 165.
14 M. P. Sfinchez-Migallon, F. J. Aranda and J. C. Gomez-Fernamdez, *Biochim. Biophys. Acta*, 1996, **1281**, 23.
15 S. Choi, W. Ware, S. R. Lauterbach and W. M. Phillips, *Biochemistry*, 1991, **30**, 8563.
16 I. Fournier, J. Barwicz, M. Auger and P. Tancr'ede, *Chem. Phys. Lipids*, 2008, **151**, 41.
17 M. Weis and M. Kopani, *Eur. Biophys. J.*, 2008, **37**, 893.
18 A. N. Vievskij, *Tenside, Surfactants, Deterg.*, 1997, **34**, 18.
19 A. Vievskiy, *Mechanisms of biological activity of cationic surface active compounds Kiev*, 1991, p. 250 (in Russian).
20 P. Gilbert and L. E. Moor, *J. Appl. Microbiol.*, 2005, **99**, 703.

21 N. N. D. Daoud, N. A. Dickinson and P. Gilbert, *Microbios*, 1983, **37**, 75.
22 L. Panicker, V. K. Sharma, G. Datta, K. Deniz, P. S. Parvathanathan, K. V. Ramanathan and C. L. Khetrapal, *Mol. Cryst. Liq. Cryst.*, 1995, **260**, 611.
23 V. A. Pashinskaya, M. V. Kosevich, A. Gomory, O. V. Vashchenko and L. N. Lisetski, *Rapid Commun. Mass Spectrom.*, 2002, **16**, 1706.
24 L. N. Lisetski, O. V. Vashchenko, A. V. Tolmachev and K. B. Vodolazhskiy, *Eur. Biophys. J.*, 2002, **31**, 554.
25 O. Vashchenko, V. Pashynska, M. Kosevich, V. Panikarska and L. Lisetski, *Mol. Cryst. Liq. Cryst.*, 2011, **507**, 155.
26 V. A. Pashynska, M. V. Kosevich, A. Gomory and K. Vekey, *Mass Spectrom.*, 2012, **9**, 121.
27 V. A. Pokrovsky, M. V. Kosevich, V. L. Osaulenko, V. V. Chagovets, V. A. Pashynska, V. S. Shelkovsky, V. A. Karachevtsev and A. Yu. Naumov, *Mass Spectrom.*, 2005, **2**, 183.
28 V. Pashynska, M. Kosevich, S. Stepanian and L. Adamowicz, *THEOCHEM*, 2007, **815**, 55.
29 V. A. Pashynska, M. V. Kosevich, A. Gomory and K. Vekey, *Biopolym. Cell*, 2013, **29**, 157.
30 O. V. Vashchenko, V. A. Pashynska, M. V. Kosevich, V. D. Panikarska and L. N. Lisetski, *Biopolym. Cell*, 2010, **26**, 472.
31 V. A. Pashynska, M. V. Kosevich, H. Van den Heuvel, F. Cuyckens and M. Claeys, *Biophys. Bull.*, 2004, **1–2**, 123 (in Russian).
32 *Electrospray and MALDI Mass Spectrometry: Fundamentals, Instrumentation, Practicalities, and Biological Applications*, ed. C. R. Hoboken, John Wiley & Sons, Inc., New Jersey, p. 1008.
33 Th. Wyttenbach and M. T. Bowers, *Annu. Rev. Phys. Chem.*, 2007, **58**, 511.
34 K. Ashidate, M. Kawamura, D. Mimura, H. Tohda, S. Miyazaki, T. Teramoto, Y. Yamamoto and Y. Hirata, *Eur. J. Pharmacol.*, 2005, **513**, 173.
35 R. Koynova and M. Caffrey, *Biochim. Biophys. Acta*, 1998, **1376**, 91.
36 P. K. Mukherjee, *Liq. Cryst.*, 1997, **22**, 239.
37 Yu. Ia. Fialkov, A. N. Zhitomirskij and Yu. A. Tarasenko, *Physical Chemistry of Non-Aqueous Solutions*, Khimija, Leningrad, 1973, p. 376 (in Russian).

MOLECULAR BIOPHYSICS

Original article
https://doi.org/10.26565/2075-3810-2020-43-11

UDC 577.32:615.28:544.173

MASS SPECTROMETRY STUDY OF NONCOVALENT COMPLEXES FORMATION OF ANTIBIOTIC CYCLOSERINE WITH N-ACETYL-D-GLUCOSAMINE AND ASCORBIC ACID

V.A. Pashynska[1], M.V. Kosevich[1], A. Gomory[2]
[1]*B. Verkin Institute for Low Temperature Physics and Engineering of the National Academy of Sciences of Ukraine, 47 Nauky Ave., Kharkiv, 61103, Ukraine*
e-mail: pashynska@ilt.kharkov.ua
[2]*Institute of Organic Chemistry of Research Centre for Natural Sciences, 2 Magyar tudosok korutja, Budapest, H-1117, Hungary*
Submitted December 18, 2019
Accepted January 28, 2020

Background: While antibiotic cycloserine (CYS) is widely applied in the treatment of tuberculosis, our knowledge of the drug intermolecular interactions with targeting biomolecules and other drugs remains incomplete. It is believed that the CYS antibacterial activity is related to inhibiting the bacterial cell wall biosynthesis. On the other hand, intermolecular interactions of CYS with ascorbic acid (ASC) molecules is worth of studying taking into account that ASC can be used as supporting vitamin preparation or can be affiliated with the patients nutrition.
Objectives: The purpose of the current model study are to examine biologically significant intermolecular interactions of CYS with N-acetyl-D-glucosamine (NAG) as one of the main component of peptidoglycan of bacterial cell wall and to verify the possibility of noncovalent complexes formation between CYS and ASC molecules using electrospray ionization mass spectrometry (ESI MS) technique.
Materials and methods: The objects of the study are model systems composed of CYS and NAG or CYS and ASC prepared in a polar methanol solvent for the ESI MS probing. ESI mass spectra are obtained using the approach earlier developed by us for investigation of the noncovalent complexation of drugs with targeting biomolecules.
Results: The experiments reveal that the ESI mass spectrum of (CYS–NAG) model system contains peaks of protonated molecular clusters of CYS with NAG: $[CYS{\bullet}NAG{\bullet}H]^+$ and $[CYS{\bullet}2NAG{\bullet}H]^+$. Existing of such peaks in the spectrum testifies to formation of stable noncovalent complexes between CYS and NAG in the studied solution. ESI MS examining of (CYS–ASC) system reveals the noncovalent pair complexation of CYS and ASC molecules confirmed by the recording of intensive peak of $[CYS{\bullet}ASC{\bullet}H]^+$ cluster in the spectrum.
Conclusions: The ESI MS findings point to the possibility of noncovalent complexation of CYS with NAG in the polar media including biological systems. Such complexation between the antibiotic and NAG as component of peptidoglycan of bacterial cell wall is considered to be biologically significant for the process of the cell wall biosynthesis inhibiting by CYS. Stable noncovalent complexes formation between the CYS and ASC molecules is suggested as a potential molecular mechanism of the drugs activity modulation under their joint usage.
KEY WORDS: cycloserine; N-acetyl-D-glucosamine; ascorbic acid; noncovalent complexes; electrospray ionization mass spectrometry.

МАС-СПЕКТРОМЕТРИЧНЕ ДОСЛІДЖЕННЯ ФОРМУВАННЯ НЕКОВАЛЕНТНИХ КОМПЛЕКСІВ АНТИБІОТИКА ЦИКЛОСЕРИНА З N-АЦЕТИЛ-D-ГЛЮКОЗАМІНОМ ТА АСКОРБІНОВОЮ КИСЛОТОЮ

В.А. Пашинська[1], М.В. Косевич[1], А. Гоморі[2]
[1]*Фізико-технічний інститут низьких температур ім. Б.І. Вєркіна Національної академії наук України, просп. Науки, 47, Харків, 61103, Україна*
[2]*Інститут органічної хімії Наукового центру природничих наук, Бульвар Мадьяр тудосок, 2, Будапешт, H-1117, Угорщина*

Актуальність. Антибіотик циклосерин (CYS) активно застосовується при лікуванні туберкульозу, проте наші знання щодо міжмолекулярної взаємодії молекул цього препарату з біомолекулами-

мішенями та з молекулами інших ліків наразі є обмеженими. Вважається, що антибактеріальна дія CYS пов'язана з пригніченням процесу біосинтезу клітинної стінки бактерій. Поряд з цим певний інтерес становить вивчення міжмолекулярних взаємодій CYS з молекулами аскорбінової кислоти (ASC), оскільки вона може використовуватися як допоміжний вітамінний препарат при лікуванні туберкульозу або знаходитися у їжі пацієнтів.

Мета роботи. Задачами даного модельного дослідження стали вивчення біологічно важливих міжмолекулярних взаємодій циклосерину з N-ацетил-D-глюкозаміном (NAG), що є одним з головних компонентів полімерного пептидоглікану клітинної стінки бактерій, та перевірка можливості формування нековалентних комплексів між молекулами CYS та ASC за допомогою методу мас-спектрометрії з іонізацією електророзпиленням (MCIEP).

Матеріали й методи. Об'єктами дослідження обрано модельні системи, складовими яких є CYS та NAG або CYS та ASC, розчинені у полярному розчиннику метанолі для MCIEP експериментів. Мас-спектри було отримано з використанням розробленого нами раніше підходу до дослідження нековалентного комплексоутворення між молекулами лікарських агентів та біологічними молекулами-мішенями.

Результати. Показано, що мас-спектр IEP модельної системи (CYS–NAG) містить піки протонованих молекулярних кластерів CYS та NAG: $[CYS•NAG•H]^+$, $[CYS•2NAG•H]^+$. Наявність цих піків у спектрі свідчить про формування стабільних нековалентних комплексів між CYS та NAG у дослідженому розчині. MCIEP дослідження системи (CYS–ASC) виявило утворення нековалентних парних комплексів молекул CYS та ASC, що підтверджується наявністю у спектрі інтенсивних піків кластерів $[CYS•ASC•H]^+$.

Висновки. Результати MCIEP експериментів вказують на можливість нековалентного комплексоутворення між молекулами CYS та NAG у полярному середовищі, включаючи біологічні системи. Ми вважаємо, що таке зв'язування молекул протитуберкульозного антибіотика CYS з NAG-компонентами пептидоглікану клітинної стінки бактерій може бути біологічно важливим для процесу пригнічення біосинтезу клітинної стінки. Виявлене формування стабільних нековалентних комплексів молекул CYS та ASC в розчині пропонується як потенційний молекулярний механізм модуляції активності цих лікарських засобів при їх одночасному застосуванні.

КЛЮЧОВІ СЛОВА: циклосерин; N-ацетил-D-глюкозамін; аскорбінова кислота; нековалентні комплекси; мас-спектрометрія з іонізацією електророзпиленням.

МАСС-СПЕКТРОМЕТРИЧЕСКОЕ ИССЛЕДОВАНИЕ ФОРМИРОВАНИЯ НЕКОВАЛЕНТНЫХ КОМПЛЕКСОВ АНТИБИОТИКА ЦИКЛОСЕРИНА С N-АЦЕТИЛ- D-ГЛЮКОЗАМИНОМ И АСКОРБИНОВОЙ КИСЛОТОЙ

В.А. Пашинська[1], М.В. Косевич[1], А. Гомори[2]

[1]Физико-технический институт низких температур им. Б.И. Веркина НАН Украины, просп. Науки, 47, Харьков, 61103, Украина

[2]Институт органической химии Научного центра естественных наук, Бульвар Мадьяр тудосок, 2, Будапешт, H-1117, Венгрия

Актуальность. Антибиотик циклосерин (CYS) широко используется при лечении туберкулеза, однако наши знания о межмолекулярных взаимодействиях этого лекарственного препарата с биомолекулами-мишенями и молекулами других лекарств остаются неполными. Предполагается, что антибактериальное действие CYS связано с ингибированием биосинтеза клеточной стенки бактерий. Наряду с этим определенный интерес представляет изучение межмолекулярных взаимодействий CYS с молекулами аскорбиновой кислоты (ASC), поскольку она может применяться как вспомогательный витаминный препарат при лечении туберкулеза или находиться в пище пациента.

Цель работы. Задачами настоящего модельного исследования стали изучение биологически значимых межмолекулярных взаимодействий CYS с N-ацетил-D-глюкозамином (NAG), который является основным составным компонентом пептидогликана клеточной стенки бактерий, а также оценка возможности формирования нековалентных комплексов между молекулами CYS и ASC методом масс-спектрометрии с ионизацией электрораспылением (МСИЭР).

Материалы и методы. Объектами исследования были выбраны модельные двухкомпонентные системы, состоящие из CYS и NAG или CYS и ASC, приготовленные на основе полярного растворителя метанола для МСИЭР анализа. Масс-спектры получали, используя разработанный нами ранее подход для исследований нековалентного комплексообразования между молекулами лекарственных агентов и биомолекулами-мишенями.

Результаты. Показано, что масс-спектр ИЭР модельной системы (CYS–NAG) содержит пики протонированных молекулярных кластеров CYS и NAG: $[CYS•NAG•H]^+$, $[CYS•2NAG•H]^+$. Наличие этих пиков в спектре свидетельствует о формировании стабильных нековалентных комплексов CYS и NAG. МСИЭР исследование системы (CYS–ASC) выявило формирование парных нековалентных комплексов молекул CYS и ASC, что подтверждается присутствием в спектре интенсивных пиков кластеров $[CYS•ASC•H]^+$.

Выводы. Результаты МСИЭР экспериментов указывают на возможность нековалентного комплексообразования между молекулами CYS и NAG в полярном окружении, включая биосистемы. Считаем, что такое связывание молекул противотуберкулезного антибиотика CYS с NAG-компонентами пептидогликана клеточной стенки бактерий может быть биологически значимым для процесса ингибирования биосинтеза клеточной стенки. Обнаруженное формирование стабильных нековалентных комплексов молекул CYS и ASC в растворе предлагается как потенциальный молекулярный механизм модуляции активности этих лекарственных агентов при их совместном применении.

КЛЮЧЕВЫЕ СЛОВА: циклосерин; N-ацетил-D-глюкозамин; аскорбиновая кислота; нековалентные комплексы; масс-спектрометрия с ионизацией электрораспылением.

Antibiotic cycloserine (CYS) is widely used in medical practice to treat a number of infection diseases, foremost tuberculosis and its drug resistant forms [1, 2]. At the same time our knowledge on molecular mechanisms of CYS antimicrobial and, in particular anti-tuberculosis activity remains incomplete and requires further advancement anticipating the demand in overcoming of drug resistance of the pathogens [3–6].

It is believed that CYS reveals its antibacterial effect by inhibiting the biosynthesis of bacteria cell wall peptidoglycan and this inhibition may result from multi-targeting action of D-cycloserine in the bacteria cell [3–6], e.g. reaction with enzyme alanine racemase [6] or binding to another enzyme involved in peptidoglycan biosynthesis — D-alanine:D-alanine ligase [3,4]. Moreover recently it was shown that the inhibition of D-alanine:D-alanine ligase by D-cycloserine can be proceeded via a distinct phosphorylated form of the drug [4]. Taking into account the continued studies of the mentioned enzymatic mechanisms of CYS antimicrobial activity and sharing the idea that the antibacterial agents can target multiple activities in the bacterial cells metabolism [7, 8], we think that from biophysical point of view it would be interesting to investigate the intermolecular interactions of CYS not just with the enzymes of the peptidoglycan biosynthesis, but also with the reagents participated in this crucial for bacteria biosynthetical process.

A purpose of the current model study is to examine the biologically significant intermolecular interactions of CYS with one of the main sugar component of peptidoglycan of bacterial cell wall — N-acetyl-D-glucosamine (NAG) applying electrospray ionization mass spectrometry (ESI MS) technique.

Furthermore, the multi-drugs schemes of therapy of infection diseases are commonly applied presently. A number of supporting preparations, such as anti-inflammatory agents, vitamin preparations, etc, may be used by patients jointly with antibiotic preparations; in this connection the effects of the drugs activity modulation on the molecular level is considered as an important subject to be investigated. In this light another task of the current work is to investigate possible complexation of the CYS molecules with ascorbic acid (ASC), known as vitamin C, which can be used in anti-tuberculosis therapy as supporting vitamin medication or could be affiliated with the patient's food.

To examine the problems stated above and to investigate the intermolecular interactions of CYS with its possible targeting molecule of NAG and with ascorbic acid we used ESI MS approach which was developed and successfully applied by us in our previous investigations of the drugs molecules interactions with biomolecules and other biologically active agents [9-12].

MATERIALS AND METHODS

Materials

In our experiments we used cycloserine produced by company "Enamine" (Ukraine); N-acetyl-D-glucosamine and L-ascorbic acid (99% of purity) were provided by "Sigma-Aldrich" international company. Structures of the compounds under study are presented in Scheme 1.

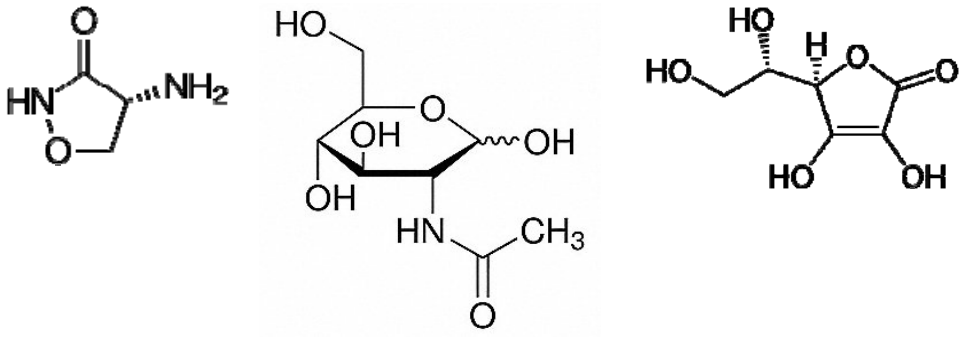

a b c

Scheme 1. Structures of compounds under study: a) cycloserine (CYS); b) N-acetyl-D-glucosamine (NAG); c) L-ascorbic acid (ASC).

The 5 mM stock solutions of CYS, NAG and ASC were prepared in polar solvent methanol and model systems containing CYS and NAG (1:5 molar ratio) or CYS and ASC (1:1 molar ratio) were obtained by mixing on the appropriate volume parts of the stock solutions.

The mixtures were kept at the room temperature for at least 10 minutes before the ESI mass spectrometric analysis. For spraying procedure in the ESI MS experiments the primary CYS solution to be examined and the model systems (CYS–NAG) and (CYS–ASC) were diluted by methanol to the final 250 μM concentration of CYS in each solution.

Note that methanol as the most appropriate solvent is recommended for standard ESI probing of biomolecules and their intermolecular interactions basing on a number of authoritative studies [13–17]. As to noncovalent intermolecular complexes of bioactive molecules, it was shown that their composition in water and methanol-based solutions is similar [17].

Electrospray ionization mass spectrometry

ESI mass spectra of the model systems under study were obtained in the positive ion mode using triple quadrupole (QqQ) Micromass Quattro Micro mass spectrometer (Waters, Manchester, UK) equipped with the electrospray ion source. This source was operated in the standard ESI mode. The ESI source temperature was set to 120°C and the desolvation temperature was 200°C. The spraying capillary was operated at 3.5 kV. The cone voltage value of 10 V was applied. The analyzed solutions (20 μL) were injected into the mass spectrometer at a constant flow rate of 0.2 mL·min^{-1} of methanol solvent. The ESI spectra were recorded in the mass range of 100-2000 Da. Data acquisition and processing were performed using MassLynx 4.1 software (Waters, Manchester, UK).

RESULTS AND DISCUSSION

Electrospray mass spectrometry probing of neat cycloserine solution

At the first stage of the experimental study the solution of the antibiotic CYS in methanol was investigated by ESI MS. It was established that characteristic ESI mass

spectrum of the preparation (Fig. 1) contained intensive peaks of the protonated molecule of CYS $[Cys•H]^+$ at m/z 103.2, cationized molecule $[Cys•Na]^+$ at m/z 125.2 and less intense peak of the protonated CYS dimer $[2Cys•H]^+$ at m/z 205.4.

High quality of the obtained mass spectrum of the drug, characterized by a high signal to noise ratio, confirms the applicability of the ESI MS method for investigation of CYS containing model systems, including the systems generated for study of intermolecular interactions of CYS with biologically active molecules, as well as the effectiveness of the ESI MS for CYS identification in different biological and pharmacological samples in any clinical or technological investigations.

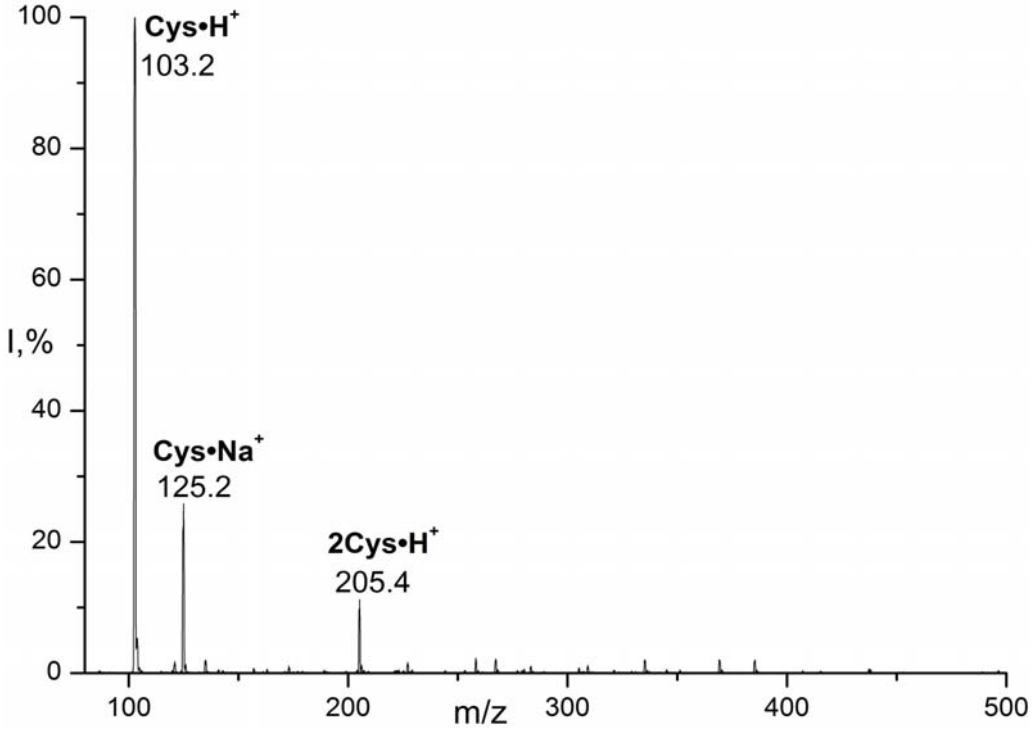

Fig. 1. ESI mass spectrum of CYS solution in methanol.

Electrospray mass spectrometric study of cycloserine-N-acetyl-D-glucosamine model system

At the next stage, the model system of CYS with NAG (1:5 molar ratio) in methanol was probed with the purpose to examine the possibility of noncovalent complexes formation between the molecules of the system components. In the obtained ESI mass spectrum (Fig. 2) the ions characteristic of the individual components of the mixture such as:$[Cys•H]^+$ at m/z 103.2, $[Cys•Na]^+$ at m/z 125.2, $[2Cys•H]^+$ at m/z 205.4 for CYS and $[NAG•H]^+$ at m/z 222.2, $[NAG•Na]^+$ at m/z 244.2, $[2NAG•H]^+$ at m/z 443.4, $[2NAG•Na]^+$ at m/z 465.4 for NAG; were accompanied by the peaks of protonated molecular clusters of CYS with NAG: $[Cys•NAG•H]^+$ at m/z 324.4 and $[Cys•2NAG•H]^+$ at m/z 545.6.

Such molecular clusters recorded in the ESI mass spectrum testifies to the formation of stable noncovalent complexes between CYS and NAG in the studied model system and these complexes stability is sufficient to provide the clusters surveillance under the electrospray ionization processes. The ESI MS findings point to the possibility of noncovalent complexation of CYS with NAG in the polar media, including solutions in polar solvents like methanol or water, that model the media in biological systems. Such intermolecular interaction between the molecules of antibiotic CYS and the NAG components of bacteria

cell wall peptidoglycan is considered to be biologically significant for the process of the bacterial wall biosynthesis inhibition induced by CYS as well as can affect the drug penetration into the bacterial cell.

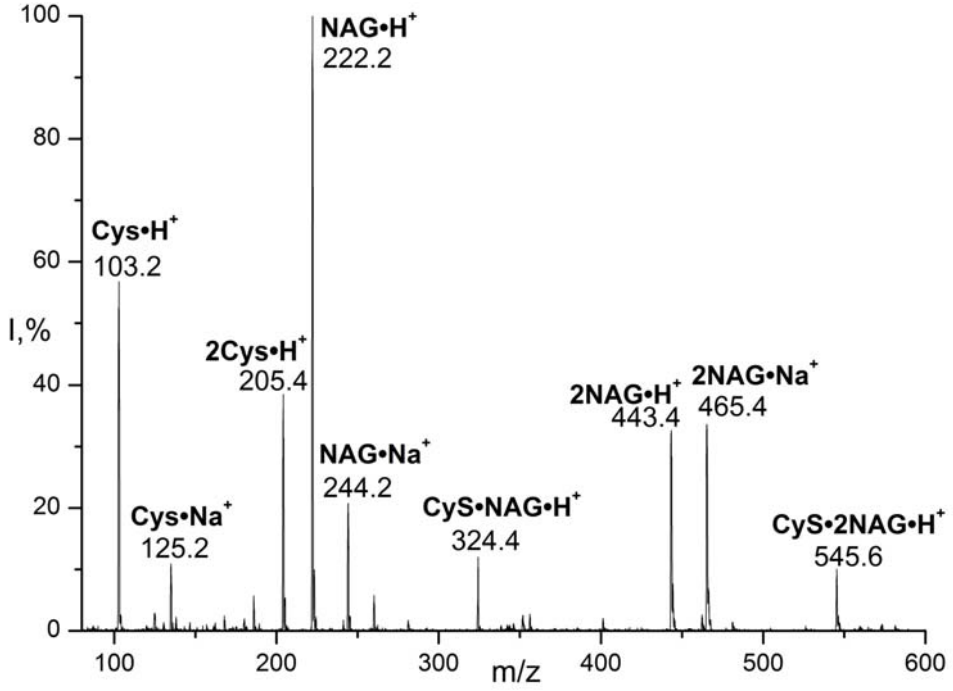

Fig. 2. ESI mass spectrum of (CYS–NAG) model system.

Electrospray mass spectrometry study of cycloserine-ascorbic acid model system

As the second task of this study we investigated the model system containing CYS and ASC. The obtained ESI mass spectrum of the studied system can be seen in Fig. 3.

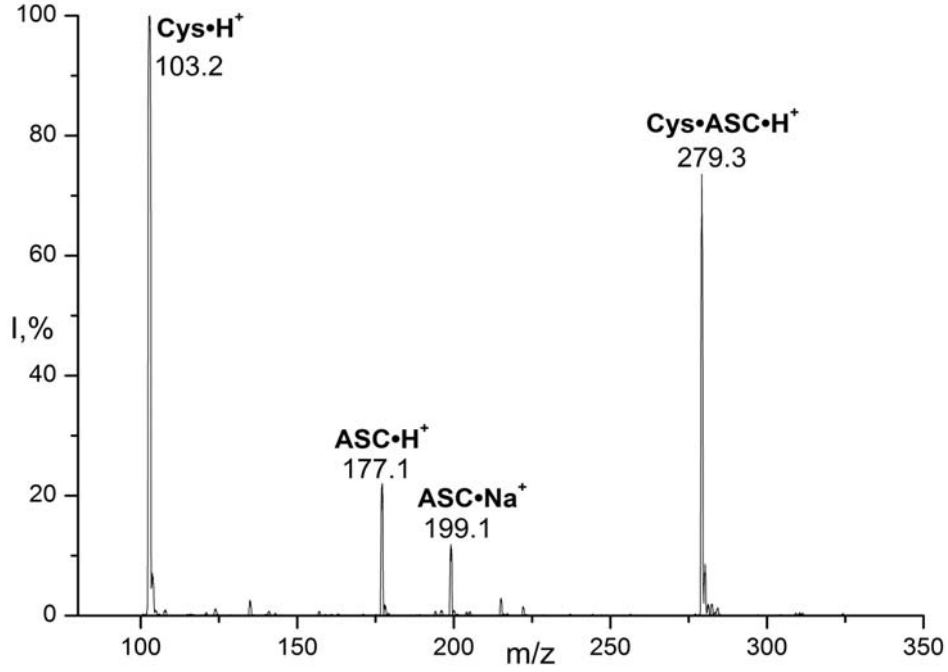

Fig. 3. ESI mass spectrum of (CYS–ASC) model system.

Similarly to the described above model system of (CYS–NAG), in the spectrum of (CYS–ASC) mixture the characteristic peaks of the system components are present: $[Cys•H]^+$ at m/z 103.2 for CYS and $[ASC•H]^+$ at m/z 177.1 and $[ASC•Na]^+$ at m/z 199.1 for ASC. At the same time, neither cationized CYS — $[Cys•Na]^+$ nor CYS dimer — $[2Cys•H]^+$ peaks can be found in the spectrum of (CYS–ASC) system (Fig. 3), in contrast to the spectra of the neat CYS (Fig. 1) and (CYS–NAG) mixture (Fig. 2). Absence of the $[Cys•Na]^+$ ion in the presence of $[ASC•Na]^+$ ion points to the competition for the metal cation binding in favour of more acidic ascorbic acid, while the absence of CYS dimer peak in the spectrum can be connected with the change of the conditions for CYS dimerization reaction caused in the presence of ascorbic acid in the model system.

The most interesting from the biophysical point of view result is recording in the spectrum of high intensive peak of a cluster of CYS with ASC — $[Cys•ASC•H]^+$, m/z 279.3, I=75% (Fig. 3). This peak points to the intensive process of formation of stable noncovalent complexes of CYS with ASC molecules in the polar solvent methanol.

Noncovalent complexation revealed between the molecules of cycloserine and ascorbic acid in solvents can modulate the drugs activity under their joint usage.

CONCLUSIONS

Realization of biologically significant noncovalent complexation of antibiotic cycloserine molecules with the components of bacterial cell wall and with ascorbic acid in polar solvent is proved as the main result of the present model study by means of ESI MS.

The possibility of noncovalent clusters formation between the molecules of CYS and the main sugar component of peptidoglycan of the bacterial cell wall, N-acetyl-D-glucosamine, in polar medium is demonstrated. The intermolecular complexes formation between CYS and peptidoglycan components can play an important role in molecular mechanisms of the bacteria cell wall biosynthesis inhibiting induced by the CYS antimicrobial action.

ESI MS examining of the model system containing CYS and ASC points to the intensive process of formation of the pair noncovalent clusters of the different drugs molecules in the polar solution. Such complexation between the molecules of CYS and ASC under joint usage of the drugs by patients can modulate the individual drugs activity and should be taken into account in medical practice.

The performed mass spectrometry study also confirms the effectiveness of the ESI MS method for investigation of intermolecular interactions in cycloserine containing systems and for the drug identification in the biological and technological solutions in clinical and industrial applications.

ACKNOWLEDGEMENTS

Authors acknowledge the Program of cooperation between Ukrainian and Hungarian Academies of Sciences for the financial support of the visits of the scientists from B. Verkin Institute for Low Temperature Physics and Engineering of the National Academy of Sciences of Ukraine to the Research Centre for Natural Sciences and the Hungarian Academy of Sciences, where the mass spectrometry experiments were carried out. We also thank Vashchenko O.V. and other colleagues from the Institute for Scintillation Materials of STC ”Institute for Single Crystals” of the NAS of Ukraine for providing the cycloserine samples.

CONFLICT OF INTERESTS

The authors declare that there is no conflict of interest.

Authors' ORCID ID

V.A. Pashynska https://orcid.org/0000-0001-9786-6828
M.V. Kosevich http://orcid.org/0000-0003-0257-4588
A. Gomory http://orcid.org/0000-0001-5216-0135

REFERENCES

1. Cycloserine. [No authors listed] Tuberculosis (Edinb). 2008 Mar:88(2):100–1. https://doi.org/10.1016/S1472-9792(08)70007-6
2. Perri GD, Bonora S. Which agents should we use for the treatment of multidrug-resistant *Mycobacterium tuberculosis*? J Antimicrob Chemother. 2004 Sep:54(3):593–602. https://doi.org/10.1093/jac/dkh377
3. Prosser GA, de Carvalho LPS. Reinterpreting the Mechanism of Inhibition of *Mycobacterium tuberculosis* d-Alanine:d-Alanine Ligase by d-Cycloserine. Biochemistry. 2013:52(40):7145–49. https://doi.org/10.1021/bi400839f
4. Batson S, de Chiara C, Majce V, Lloyd AJ, Gobec S, Dean Rea, et. al. Inhibition of D-Ala:D-Ala ligase through a phosphorylated form of the antibiotic D-cycloserine. Nature Communications. 2017:8:1939. https://doi.org/10.1038/s41467-017-02118-7
5. Neuhaus FC, Lynch JL. The enzymatic synthesis of D-alanyl-D-alanine. 3. On the inhibition of D-alanyl-D-alanine synthetase by the antibiotic D-cycloserine. Biochemistry. 1964:3(4):471–80. https://doi.org/10.1021/bi00892a001
6. Lambert MP, Neuhaus FC. Mechanism of D-cycloserine action: alanine racemase from *Escherichia coli* W. J Bacteriol. 1972 Jun:110(3):978–87.
7. East SP, Silver LL. Multitarget ligands in antibacterial research: progress and opportunities. Expert Opin Drug Discov. 2013 Feb:8(2):143–56. https://doi.org/10.1517/17460441.2013.743991
8. Walsh CT, Wencewicz TA. Prospects for new antibiotics: a molecule-centered perspective. J Antibiot. 2014 Jan:67(1):7–22. https://doi.org/10.1038/ja.2013.49
9. Pashynska VA, Kosevich MV, Gomory A, Vekey K. Model mass spectrometric study of competitive interactions of antimicrobial bisquaternary ammonium drugs and aspirin with membrane phospholipids. Biopolym Cell. 2013:29(2):157–62. https://doi.org/10.7124/bc.000814
10. Pashynska V, Stepanian S, Gomory A, Vekey K, Adamowicz L. Competing intermolecular interactions of artemisinin-type agents and aspirin with membrane phospholipids: Combined model mass spectrometry and quantum-chemical study. Chem Phys. 2015:455:81–7. https://doi.org/10.1016/j.chemphys.2015.04.014
11. Pashynska V, Stepanian S, Gomory A, Vekey K, Adamowicz L. New cardioprotective agent flokalin and its supramolecular complexes with target amino acids: An integrated mass-spectrometry and quantum-chemical study. J Mol Struct. 2017:1146:441–9. https://doi.org/10.1016/j.molstruc.2017.06.007
12. Pashynska VA, Zholobak NM, Kosevich MV, Gomory A, Holubiev PK, Marynin AI. Study of intermolecular interactions of antiviral agent tilorone with RNA and nucleosides. Biophys Bull. 2018:39(1):15–26. https://doi.org/10.26565/2075-3810-2018-39-02
13. Cole R, editor. Electrospray and MALDI mass spectrometry: fundamentals, instrumentation, practicalities, and biological applications. 2nd edition. Hoboken, New Jersey: John Wiley & Sons, Inc.; 2010. 896 p. ISBN: 978-0-471-74107-7
14. Loo JA. Electrospray ionization mass spectrometry: a technology for studying non-covalent macromolecular complexes. Int J Mass Spectrom. 2000:200(1–3):175–86. https://doi.org/10.1016/S1387-3806(00)00298-0
15. Wyttenbach Th, Bowers MT. Intermolecular interactions in biomolecular systems examined by mass spectrometry. Annu Rev Phys Chem. 2007:58:511–33. https://doi.org/10.1146/annurev.physchem.58.032806.104515
16. McCullough BJ, Gaskell SJ. Using electrospray ionisation mass spectrometry to study non-covalent interactions. Comb Chem High Throughput Screen. 2009:12(2):203–11. https://doi.org/10.2174/138620709787315463
17. Guevremont R, Siu KWM, Le Blanc JCY, Berman SS. Are the electrospray mass spectra of proteins related to their aqueous solution chemistry? J Am Soc Mass Spectrom. 1992 Mar:3(3):216–24. https://doi.org/10.1016/1044-0305(92)87005-J

2.6. Підсумки розділу 2.

У рамках вирішення проблеми встановлення молекулярно-фізичних механізмів модифікації активності лікарських агентів різних груп при їхньому одночасному застосуванні за результатами поєднання експериментального методу мас-спектрометрії IEP та теоретичного методу квантово-механічних розрахунків B3LYP/aug-cc-pVDZ визначено мас-спектрометричні маркери молекулярно-фізичних процесів конкуренції молекул ряду протималярійних та протиінфукційних амонієвих ліків із молекулами протизапальних та вітамінних агентів (аспірин та вітамін С), за зв'язування з мембранними фосфоліпідами (на прикладі DPPC). Також встановлено маркери парного комплексоутворення між молекулами досліджених лікарських речовин різних груп у полярному розчині. Ці міжмолекулярні конкурентні процеси комплексоутворення запропоновано розглядати в якості молекулярно-фізичних механізмів явища модифікації біологічної дії зазначених лікарських сполук при їхньому одночасному введенні в медичній практиці вже на стадії проникнення лікарських сполук через мембранні структури клітин.

1. У рамках проведених досліджень вперше визначено мас-спектрометричні маркери молекулярно-фізичного процесу конкуренції, що відбувається між молекулами протималярійних агентів артемізинінового ряду (дигідроартемізинін, α-артеметер, артезунат) та аспірину (ASP), за нековалентну асоціацію з мембранним фосфоліпідом дипальмітоїлфосфатидилхоліном (DPPC) в полярному середовищі. Ця конкуренція підтверджується присутністю в IEP мас-спектрах дво- та трикомпонентних модельних систем (що складалися з лікарських агентів різних груп, молекул DPPC та розчинника метанолу) піків стабільних нековалентних комплексів артемізинінових агентів з DPPC та ASP з DPPC. Важливо, що в мас-спектрах також ідентифіковано піки нековалентних комплексів похідних артемізиніну з ASP, які є мас-спектрометричними маркерами ще одного можливого сценарію міжмолекулярних взаємодій,

модифікуючих біоактивність лікарських агентів різних груп при одночасному введенні.

2. Результати модельних розрахунків методом B3LYP/aug-cc-pVDZ структурно-енергетичних характеристик комплексів дигідроартемізиніну (DHAn) з аспірином та/або з фосфатидилхоліном (PCn, моделює полярну головку DPPC) підтвердили стабільність комплексів та міжмолекулярну конкуренцію між фосфоліпідом та ASP за зв'язування з протималярійним агентом: у визначеній найбільш стабільній структурі нековалентного комплексу DHAn•PCn у вакуумному наближенні енергія взаємодії дорівнює IE =-55.6 кДж/моль та є близькою до значення енергії взаємодії в комплексі ASP•DHAn (IE =-56.2 кДж/моль). За даними розрахунків найбільш енергетично стабільним виявився кластер аспірину з фосфатидилхоліном ASP•PCn (IE = -107.9 кДж/моль), який стабілізується трьома парами водневих зв'язків на відміну від двох пар водневих зв'язків в попередньо зазначених комплексах.
3. Встановлене явище міжмолекулярної конкуренції між протималярійними агентами артемізинінового ряду та аспірином за нековалентне зв'язування з мембранними фосфоліпідами, а також формування стабільних парних міжмолекулярних асоціатів між молекулами препаратів різних груп уперше запропоновано в якості молекулярно-фізичних механізмів модифікації біологічної активності цих лікарських агентів при їхньому одночасному застосуванні в медичній практиці вже на стадії проникнення ліків через мембранні структури клітин.
4. Вперше методом мас-спектрометрії з IEP експериментально доведено можливість конкурентного формування стабільних міжмолекулярних нековалентних комплексів молекул протималярійних агентів артемізинінового ряду (артемізинін, дигідроартемізинін, α-артеметер, β-артеестер) та аскорбінової кислоти (вітамін С, ASC) з молекулою DPPC та між собою в системах *in vitro*. Конкуренція на молекулярному рівні між протималярійними препаратами та вітаміном С за нековалентне зв'язування з

мембранним фосфоліпідом та формування стабільних парних асоціатів молекул артемізинінових агентів із молекулами вітаміну С запропоновані в якості молекулярно-фізичних механізмів модуляції біологічної дії протималярійних ліків при одночасному застосуванні в лікувальній практиці.

5. Квантово-механічні *ab initio* розрахунки методом B3LYP/aug-cc-pVDZ структурно-енергетичних параметрів кластерів протималярійного агенту DHAn з ASC та з PCn підтвердили високу стабільність цих нековалентних комплексів. Найбільш стабільний нековалентний кластер ASC•DHAn у вакуумному наближенні характеризується енергією зв'язку IE=−50.3 кДж/моль, яка є близькою за значенням до енергії зв'язку в комплексі DHAn•PCn (IE=−52.6 кДж/моль), що підтверджує міжмолекулярну конкуренцію між вітаміном С та мембранним фосфоліпідом за комплексоутворення з протималярійним агентом (подібно до ситуації з аспірином). Нековалентний кластер ASC•PCn за даними квантово-механічних розрахунків у вакуумному наближенні має найбільшу за абсолютною величиною енергію зв'язку (IE=−83.0 кДж/моль) серед визначених міжмолекулярних комплексів. Розрахунки методом PCM показали, що відносна стабільність цих нековалентних асоціатів у вакуумному наближенні є подібною до їх відносної стабільності в полярних розчинниках – у воді та в метанолі.
6. У рамках вивчення молекулярних механізмів модифікації активності протиінфекційних бісчетвертинних амонієвих агентів уперше визначені мас-спектрометричні маркери формування стабільних нековалентних комплексів дикатіонів декаметоксину, етонію та тіонію з молекулами аспірину та процесу конкуренції молекул лікарських сполук різних груп за зв'язування з молекулой мембранного фосфоліпіду DPPC в полярному середовищі. Ці міжмолекулярні конкурентні процеси комплексоутворення за участю протиінфекційних бісчетвертинних агентів та аспірину запропоновано розглядати як молекулярно-фізичні механізми модифікації та зниження активності цих ліків при одночасному застосуванні.

7. Запропонований на основі мас-спектрометричних досліджень з ІЕР молекулярно-фізичний механізм взаємної модифікації біологічної дії (через нековалентне конкурентне комплексоутворення) протиінфекційних бісчетвертинних амонієвих агентів та аспірину при одночасному введенні підтверджено в дослідженнях, що проводилися колегами-співавторами з Інституту сцинтиляційних матеріалів НАН України, на модельних молекулярних біосистемах більш високого рівня організації (в модельних біслойних фосфоліпідних мембранах, що складалися з гідратованого DPPC) [12, 33]. Результати досліджень наших співавторів методом диференціальної скануючої калориметрії показали наступне: якщо введення індивідуально декаметоксину, або етонію, або тіонію, або аспірину в модельні фосфоліпідні мембрани призводить до зниження температури плавлення модельних мембран Tm, то сукупне введення будь-якого з цих мембранотропних бісчетвертинних амонієвих агентів та аспірину в модельні системи має за результат протилежний ефект - збільшення температури Tm, що вказує на певне ущільнення мембран [12, 33]. Отримані колегами-співавторами дані свідчать про модифікацію мембранотропної біологічної дії досліджених препаратів різних груп на мембранні структури при їхньому одночасному введенні, що добре корелює з отриманими здобувачем мас-спектрометричними результатами сумісних досліджень [12, 33].
8. При вивченні молекулярно-фізичних механізмів активності представника групи протитуберкульозних лікарських агентів уперше методом мас-спектрометрії з ІЕР ідентифіковано мас-спектрометричні маркери формування стабільних міжмолекулярних кластерів молекул антибіотика циклосерин з потенційною біомолекулою-мішенню в клітинній стінці бактерій - N-ацетил-D-глюкозаміном (NAG), що утворюються в умовах полярного розчину. Таке нековалентне комплексоутворення між молекулами протитуберкульозного агенту та NAG-компонентами пептидоглікану клітинної стінки бактерій розглядається як молекулярно-фізична складова процесу пригнічення біосинтезу клітинної стінки, пов’язаного з

протиінфекційною дією циклосерину. У подальших мас-спектрометричних експериментах виявлено формування стабільних нековалентних комплексів молекул циклосерину та аспірину в системі *in vitro*, що запропоновано як потенційний молекулярно-фізичний механізм модифікації активності цих лікарських речовин різних груп при їхньому одночасному застосуванні в лікувальній практиці.

РОЗДІЛ 3

Біологічно активні агенти в умовах гідратного або іншого сольватного оточення: молекулярно-структурна стабільність лікарських сполук та взаємодія з молекулами та іонами сольватного оточення за даними м’якоіонізаційної мас-спектрометрії та модельних розрахунків

Стабільність молекулярної структури біологічно активних речовин (включаючи ліки та компоненти довкілля) та їхня міжмолекулярна взаємодія з гідратним або іншим сольватним оточенням є визначальними для молекулярних механізмів реалізації біологічної дії цих речовин, яка відбувається в фізіологічних умовах або в навколишньому середовищі. У рамках комплексного вивчення молекулярної стабільності протиінфекційних лікарських агентів та особливості їхньої взаємодії з компонентами сольватного оточення проведено дослідження методами м’якоіонізаційної мас-спектрометрії (ІЕР та МАЛДІ), а також методом напівемпіричних квантово-механічних розрахунків модельних систем, що містили бісчетвертинні амонієві протиінфекційні сполуки (декаметоксин, етоній) та молекули сольватного оточення, зокрема води, або спиртів (етанол чи метанол), або дигідроксибензойної кислоти (DHB).

Вісн. Харк. ун-ту, № 497 БІОФІЗИЧНИЙ ВІСНИК. Вип. 2(7) 2000

УДК 577.7

МОЛЕКУЛЯРНА БІОФІЗИКА

КВАНТОВОМЕХАНИЧЕСКОЕ ИССЛЕДОВАНИЕ СТРУКТУРЫ ГИДРАТИРОВАННОГО БИСЧЕТВЕРТИЧНОГО АММОНИЕВОГО СОЕДИНЕНИЯ ДЕКАМЕТОКСИНА

В.А. Пашинская, М.В. Косевич, С.Г. Степаньян

Физико-технический институт низких температур им. Б.И. Веркина НАН Украины, пр. Ленина, 47, 61164, Харьков

Поступила в редакцию 16 ноября 2000 года

Проведено полуэмпирическое квантовомеханическое исследование структуры комплекса дикатиона антимикробного бисчетвертичного аммониевого препарата декаметоксина с 36 молекулами воды, моделирующими первую гидратную оболочку дикатиона. Показано, что структура гидратированного дикатиона декаметоксина близка к наиболее энергетически выгодной конформации дикатиона в вакууме, соответствующей вытянутой конфигурации центральной углеводородной цепочки между четвертичными группами азота. Рассчитанная полная энергия межмолекулярных взаимодействий в гидратном комплексе декаметоксина составляет -1361,4 кДж/моль, в том числе -553,1 кДж/моль составляет энергия взаимодействия декаметоксин-вода. Расчет гидратного комплекса дикатиона декаметоксина в конформации с изогнутой центральной углеводородной цепочкой показал, что изменение геометрии органического дикатиона, связанное с изгибом углеводородной цепочки, вызывает увеличение полной энергии системы. Результаты исследования позволяют предположить, что важнейшим фактором, стабилизирующим вытянутую структуру дикатиона декаметоксина как в отсутствии растворителя, так и в гидратном окружении, является электростатическое отталкивание между положительно заряженными четвертичными группами дикатиона.

КЛЮЧЕВЫЕ СЛОВА: декаметоксин, гидратация, квантовомеханические расчеты

Одной из актуальных задач молекулярной биофизики является выявление молекулярных механизмов действия биологически активных соединений, применяемых в качестве фармакологических препаратов. Среди них значительный интерес вызывают бисчетвертичные аммониевые соли, некоторые из которых успешно используют в медицине в качестве химиотерапевтических средств [1]. В ходе систематического изучения структуры и физико-химических свойств широко применяемого в Украине антимикробного бисчетвертичного аммониевого препарата декаметоксина [2] была рассчитана геометрия наиболее стабильной структуры дикатиона декаметоксина в вакуумном приближении, определен характер его масс-спектрометрической фрагментации, коррелирующий с наиболее вероятными путями распада препарата в различных средах [3,4]. В работах [5,6] предложен молекулярный механизм антимикробного действия этого препарата, состоящий в образовании невалентных комплексов дикатиона декаметоксина с фосфолипидами мембран клеток бактерий и влиянии таких взаимодействий на параметры фазовых переходов мембранного фосфолипидного матрикса. На основании экспериментальных исследований методами масс-спектрометрии и дифференциальной сканирующей калориметрии, а также квантовомеханических расчетов показано [5,6], что дикатион декаметоксина взаимодействует преимущественно с полярными головками фосфолипидов и предложена модель такого взаимодействия, в которой дикатион декаметоксина в вытянутой конформации углеводородной цепочки (наиболее энергетически выгодной в вакуумном приближении) координируется с полярными головками двух молекул одного из наиболее распространенных фосфолипидных компонентов мембран грамположительных бактерий - дипальмитоилфосфатидилхолина. В связи с предложенной моделью закономерен вопрос, будет ли изменяться конформация дикатиона декаметоксина в присутствии молекул воды (что более адекватно физиологической ситуации) и правомерна ли предложенная с использованием вакуумной конформации модель взаимодействия декаметоксина с головками дипальмитоилфосфатидилхолина для случая гидратированного дикатиона декаметоксина. Поиск ответа на этот вопрос и составил предмет настоящего квантовомеханического исследования, а цель работы можно сформулировать как определение структуры дикатиона бисчетвертичного аммониевого соединения декаметоксина в водном окружении, моделирующем первую гидратную оболочку.

ОБЪЕКТЫ И МЕТОД ИССЛЕДОВАНИЯ

Объектом исследования являлся представитель класса бисчетвертичных аммониевых соединений - декаметоксин, структурная формула молекулы которого имеет вид

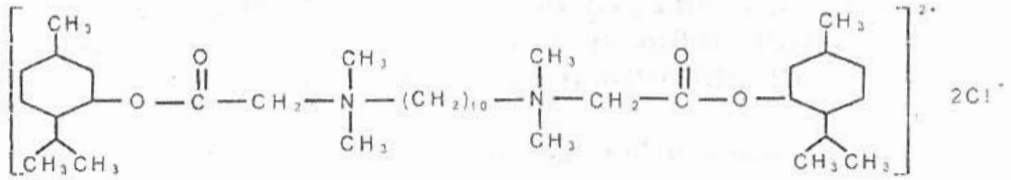

Как видно из структурной формулы дикатион декаметоксина имеет в своем составе два четвертичных азота, разделенных углеводородной цепочкой из 10 метиленовых групп, и терминальные ментильные кольца. Общее число атомов в дикатионе декаметоксина - 118. Для установления влияния воды на структуру декаметоксина проведен расчет комплекса дикатиона с 36 молекулами воды, моделирующими его первую гидратную оболочку. Количество молекул воды, вводимое в начальную геометрию комплекса для расчета, определялось необходимостью гидратации всех атомных групп дикатиона, несущих наиболее существенный избыточный положительный заряд, обусловленный зарядом дикатиона в целом, а также протоноакцепторных групп -CO-O- . Число атомов в комплексе дикатион декаметоксина + 36 H_2O составляет 226.

Поскольку количество атомов в системе дикатион декаметоксина и 36 молекул воды исключает возможность использования неэмпирических методов расчета для определения структурных параметров системы, оптимизация геометрии гидратированного комплекса дикатиона проводилась полуэмпирическим квантовохимическим методом AM1 (Austin Model). Полуэмпирические методы успешно применялись для расчета гидратных комплексов протонированных молекул фармакологических препаратов грамицидина, брадикинина, иона тетраметиламмония [7].

Выбор в качестве метода исследования AM1, основанного на приближении MNDO (Modified Neglect of Diatomic Overlap), обусловлен тем, что энтальпии образования и геометрии молекул, рассчитанные этим методом, находятся в лучшем согласии с экспериментом по сравнению с другими полуэмпирическими методами расчета [8], причем метод AM1 основан на приближении нулевого двухцентрового дифференциального перекрывания, которое приводит к значительному сокращению числа двухэлектронных интегралов и более простой вычислительной процедуре. Отмечается также эффективность метода AM1 при расчетах органических катионов с гетероатомами [8], что особенно важно при выборе расчетного метода для дикатионов бисчетвертичных аммониевых соединений. Следует также подчеркнуть, что метод AM1 дает результаты, не уступающие по точности данным неэмпирических расчетов методом HF/ 4-31G, причем затраты времени ЭВМ в 1000 раз меньше [8].

Расчеты методом AM1 проводились на PC Pentium II 400 с использованием пакета программ GAMESS [9].

РЕЗУЛЬТАТЫ И ОБСУЖДЕНИЕ

Геометрия дикатиона декаметоксина в водном окружении

В результате расчета с полной оптимизацией геометрии получена структура комплекса дикатиона декаметоксина с 36 молекулами воды, представленная на рис.1. Гидратированный органический дикатион имеет геометрию, соответствующую вытянутой конформации углеводородного радикала между четвертичными азотами и сходную с наиболее энергетически выгодной геометрией изолированного дикатиона в вакуумном приближении, описанной в [3]. В таблице 1 приведены некоторые структурные параметры рассчитанных геометрий дикатиона декаметоксина в изолированном состоянии и в комплексе с водой. Сравнение этих данных показывает, что эти параметры при гидратации дикатиона практически не изменяются. Расстояние между четвертичными азотами в дикатионе при гидратации 36 молекулами воды уменьшается на величину 0,36 Å. Уменьшение средней длины -C-C- связи при гидратации дикатиона не превышает 0,01 Å, а угла между связями в углеродной цепочке - 0,1°. Приведенные данные свидетельствуют о сохранении в гидратированном дикатионе декаметоксина вытянутой конформации полиметиленовой цепочки $-(CH_2)_{10}-$.

Метильные заместители при четвертичных азотах, как для изолированного декаметоксина, так и для гидратированного ориентированы в противоположных направлениях относительно оси полиметиленовой цепочки, также как и ментильные кольца находятся в *транс*-положении относительно оси.

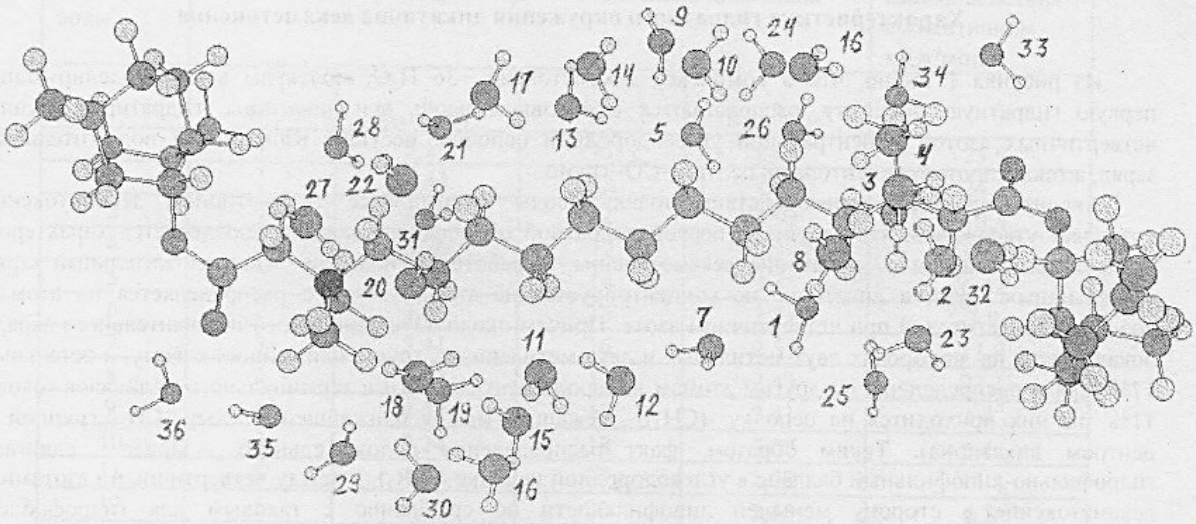

Рис.1. Структура комплекса дикатиона декаметоксина с 36 молекулами H_2O. Номера молекул воды соответствуют таковым в табл. 2.

Таблица 1. Структурные параметры дикатиона декаметоксина в изолированном состоянии и в комплексе с 36 молекулами воды.

Параметр	Дикатион декаметоксина в вакуумном приближении	Гидратированный дикатион декаметоксина
Расстояние между четвертичными азотами $r_{N\text{-}N}$, Å	13,87	13,51
Средняя длина связи -C-C- в углеводородной цепочке, Å	1,518	1,515
Средний угол между атомами углерода в цепочке, град	110,47	110,37

Факт сохранения вытянутой конформации декаметоксина при его взаимодействии с водой позволяет сделать вывод, что решающий вклад в конформацию органического дикатиона вносит электростатическое отталкивание между положительно заряженными четвертичными группами, которое слабо экранируется в присутствии 36 молекул воды.

Энергия межмолекулярных взаимодействий в комплексе декаметоксин +36 молекул воды составляет -1361,4 кДж/моль, причем -553,1 кДж/моль приходится на взаимодействие декаметоксин-вода и -808,3 кДж/моль на взаимодействие вода-вода.

Для выявления возможности реализации других конформаций дикатиона декаметоксина в гидратном окружении проведен расчет комплекса 36 молекул воды с дикатионом декаметоксина с изогнутой конформацией центрального углеводородного радикала (при задании начальной геометрии перегиб в центре цепочки дикатиона декаметоксина составлял 120^0 по сравнению с вытянутой конформацией дикатиона). Полная энергия гидратного комплекса дикатиона декаметоксина в вытянутой и изогнутой конформации углеводородного радикала составляет -739,820704 а.е. и -739,791291 а.е. соответственно. Эти данные показывают, что изгиб углеводородной цепочки в органическом дикатионе, уменьшающий расстояние между четвертичными азотами ($r_{N\text{-}N}$ в вытянутой конформации составляет 13,87 Å в сравнении с 13,23 Å в изогнутой конформации гидратированного дикатиона), приводит к значительному увеличению энергии системы на величину 77,1 кДж/моль.

Проведенные расчеты свидетельствуют о том, что более выгодной в гидратном окружении является структура дикатиона декаметоксина, близкая к наиболее вытянутой конформации углеводородной цепочки дикатиона.

Характеристика гидратного окружения дикатиона декаметоксина

Из рисунка 1 видно, что в комплексе декаметоксин +36 H_2O, молекулы воды, моделирующие первую гидратную оболочку, располагаются в основном вдоль оси дикатиона, гидратируя группы четвертичных азотов и центральной углеводородной цепочки, несущие избыточный положительный заряд, а также протоноакцепторные центры -CO- групп.

Анализ характера взаимодействия молекул воды в комплексе с дикатионом декаметоксина позволяет утверждать, что структура первой гидратной оболочки полностью определяется характером распределения заряда в дикатионе декаметоксина. В работе [2] показано, что положительный заряд четвертичных групп в дикатионе не концентрируется на атомах азота, а распределяется по атомам водорода заместителей при четвертичном азоте. Причем около 83% единичного положительного заряда локализуется на водородах двух метильных и двух метиленовых групп, ближайших к азоту, а остальные 17% заряда распределены по другим атомам водорода центрального и терминального радикалов (около 11% из них приходится на цепочку $-(CH_2)_4-$, лежащую между ближайшей к азоту $-CH_2-$ группой и центром дикатиона). Таким образом, факт распределения положительного заряда сдвигает гидрофильно-липофильный балланс в углеводородной цепочке $-(CH_2)_{10}-$ между четвертичными азотами в декаметоксине в сторону меньшей липофильности по сравнению с таковым для гидрофобной полиметиленовой цепочки $CH_3-(CH_2)_{10}-CH_3$. Даже минимальный из всех зарядов на водородах в цепочке декаметоксина - заряд на атомах водорода при центральных атомех С цепочки - углеродах С5и С6- составляет +0,088, а в полиметиленовой цепочке заряд на всех атомах водорода одинаков и составляет +0, 079. Проведенные методом AM1 дополнительные расчеты комплексов дикатиона декаметоксина с одной молекулой воды и полиметиленовой цепочки с одной молекулой воды, локализованной вблизи одного из центральных атомов - углероде С5 цепочки $-(CH_2)_{10}-$, показали, что меньшая гидрофобность цепочки у декаметоксина приводит к значительному возрастанию по абсолютной величине энергии взаимодействия декаметоксина с молекулой воды по сравнению с таковой для $CH_3-(CH_2)_{10}-CH_3$. Так, энергия межмолекулярного взаимодействия полиметиленовой цепочки с одной молекулой воды составляет -5,5 кДж/моль, а энергия взаимодействия дикатиона декаметоксина с молекулой воды практически в три раза больше по абсолютной величине: -15, 4 кДж/моль.

Для энергетического описания характера взаимодействия молекул воды в комплексе с дикатионом проведены расчеты энергии взаимодействия каждой молекулы воды из гидратного окружения с дикатионом. Данные расчетов, приведенные в табл. 2, показывают, что наибольшая энергия взаимодействия у молекул воды, локализованных вблизи кислородов карбоксильных групп дикатиона (атомы кислорода O57 и O88 дикатиона) и углеводородных групп, ближайших к четвертичным азотам (атомы C1, C2, C9, C10, C32, C33, C34, C45, C46, C47 дикатиона). Ряд молекул воды имеют очень малую энергию взаимодействия с дикатионом, сравнимую с величиной энергии взаимодействия молекулы воды с полиметиленовой цепочкой $CH_3-(CH_2)_{10}-CH_3$.

Приведенные выше данные о характере делокализации заряда в дикатионе декаметоксина хорошо объясняют факт наибольшей гидратации в рассчитанной геометрии атомов первой координационной сферы четвертичных азотов в дикатионе и присутствия молекул воды вдоль углеводородной цепочки между четвертичными азотами.

На рис.2 представлена гистограмма распределения молекул воды гидратного комплекса дикатиона декаметоксина по энергиям их взаимодействия с дикатионом. Из гистограммы видно, что семь молекул воды имеют энергию взаимодействия с дикатионом меньше по абсолютной величине, чем -5 кДж/моль (энергия взаимодействия молекулы воды с гидрофобной полиметиленовой цепочкой). Эти молекулы слабо взаимодействуют с дикатионом и могут не рассматриваться при моделировании первой гидратной оболочки дикатиона декаметоксина.

Наибольшее количество молекул воды (18) из гидратного окружения декаметоксина имеет энергию взаимодействия с дикатионом, лежащую в интервале от -5 кДж/моль до -20 кДж/моль. Одиннадцать молекул воды имеют энергию взаимодействия по абсолютному значению превышающую величину -20 кДж/моль (средняя энергия взаимодействия молекул воды в димере), что позволяет отнести их к числу сильно связанных молекул гидратного окружения. Из них энергия пяти молекул воды лежит в интервале от -20 кДж/моль до -30 кДж/моль, а шесть молекул воды, гидратирующих наиболее гидрофильные группы дикатиона, имеет энергию взаимодействия от -30 кДж/моль до -40 кДж/моль.

Таблица 2 Структурные и энергетические параметры гидратного окружения дикатиона декаметоксина

Номер молекулы воды	Положение молекулы воды относительно дикатиона				Энергия взаимодействия с дикатионом, кДж/моль
	N^A	$R_{O\text{-}C}{}^B$, A^0	N^C	$R_{H\text{-}H}{}^D$, A^0	
1	1	3,19	11	2,61	-25,9
2	1	3,41	12	2,31	-24,3
3	1	4,99	12	3,97	-10,4
4	2	3,76	12	2,34	-33,1
5	2	3,62	14	2,35	-6,42
6	2	3,35	13	2,41	-3,9
7	3	3,41	16	2,35	-11,9
8	3	3,57	15	2,42	-23,1
9	4	4,32	17	2,41	1,4
10	4	3,24	18	2,07	0,4
11	5	4,24	23	2,93	-14,4
12	5	3,29	20	2,45	-5,8
13	6	3,39	21	2,46	-10,8
14	6	3,54	17	2,56	-1,8
15	7	3,84	27	2,57	-4,2
16	7	5,43	23	4,48	-1,9
17	8	3,17	21	2,24	-11,3
18	9	3,37	27	2,39	-17,9
19	9	2,96	28	2,23	-31,7
20	10	3,67	29	2,32	-7,9
21	10	3,62	17	2,17	-8,4
22	32	3,14	43	2,42	-38,1
23	33	3,20	40	2,29	-18,3
24	34	4,11	43	2,51	-8,5
25	34	2,65	40	2,10	-15,9
26	45	3,23	50	2,71	-36,1
27	45	3,20	29	2,37	-35,9
28	46	3,69	30	2,28	-4,0
29	46	4,12	53	2,33	-16,4
30	47	3,06	56	2,69	-17,2
31	46	2,84	53	2,29	-25,8
32	47	3,15	51	2,47	-8,4
33	62	3,80	79	2,17	-7,6
	N^E	$R_{H\text{-}O}{}^F$, A^0	N^C	$R_{H\text{-}H}{}^D$, A^0	
34	57	3,05	38	2,5	-25,1
35	88	2,21	54	2,54	-31,7
36	88	2,21	54	3,1	-11,5

N^A - номер атома С дикатиона декаметоксина;
$R_{O\text{-}C}{}^B$ - расстояние атома О молекулы воды до ближайшего атома С дикатиона;
N^C - номер атома Н дикатиона;
$R_{H\text{-}H}{}^D$ - расстояние атома Н молекулы воды до ближайшего атома Н дикатиона;
N^E - номер атома О дикатиона;
$R_{H\text{-}O}{}^F$ - расстояние атома Н молекулы воды до ближайшего атома О дикатиона.

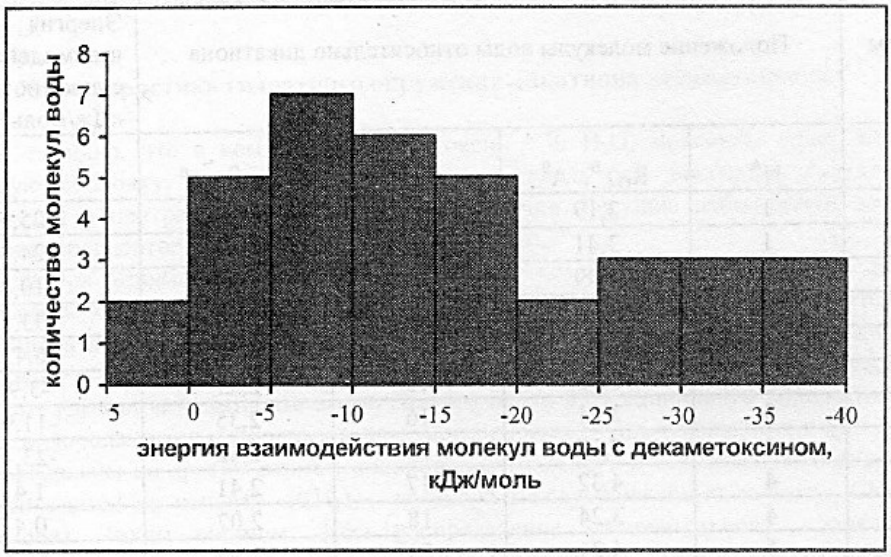

Рис.2. Распределение молекул воды гидратного окружения дикатиона декаметоксина по энергиям взаимодействия с дикатионом.

ВЫВОДЫ

Проведенное в данной работе квантовомеханическое исследование комплекса дикатиона декаметоксина с 36 молекулами воды, моделирующими его первую гидратную оболочку, позволило сделать следующие выводы:

1) Структура дикатиона декаметоксина в присутствии 36 молекул воды близка к наиболее энергетически выгодной конформации изолированного дикатиона в вакуумном приближении и соответствует вытянутой геометрии углеводородной цепочки между четвертичными группами азота.
2) Характер взаимодействия молекул воды гидратного окружения дикатиона декаметоксина определяется характером делокализации зарядов в дикатионе. Наиболее гидратированными оказываются атомные группы, имеющие наибольшую плотность заряда.

СПИСОК ЛИТЕРАТУРЫ

1. Виевский А.Н. Механизмы биологического влияния катионных поверхностно-активных веществ.- М.:Б.И, 1991.- 250 с.
2. Машковский М.Д. Лекарственные средства. Часть 2.- М.: Медицина, 1978. - 560 с.
3. Косевич М.В., Пашинская В.А., Шилаги З., Векей К., Шелковский В.С., Благой Ю.П. // Вісник Харк. ун-ту № 422. Біофізичний вісн. - 1998.- Вип.2.- С.15-23.
4. Kosevich M.V., Pashinskaya V.A., Stepanian S.G., Shelkovsky V.S., Orlov V.V., Blagoy Yu.P. // Вісник Харк. ун-ту № 434. Biophys. Bulletin.- 1999.-Вип. 1.- P .31-38.
5. Пашинская В.А., Косевич М.В., Гомори А., Векей К., Корзовская О.В., Лисецкий Л.Н., Благой Ю.П. // Вісник Харк. ун-ту № 450. Biophys. Bulletin. - 1999. - Вип. 2. - С. 59-62.
6. Korzovskaya O.V., Pashinskaya V.A., Kosevich M.V., Lisetski L.N. // Вісник Харк. ун-ту № 450. Biophys. Bulletin. - 1999. - Вип. 2. - P. 35-39.
7. Sang-Won Lee, Freivogel P.,Schindler T.. Beauchamp J.L. // J. Am. Chem. Soc. - 1998. - V.120. - P. 11758-11765.
8. Dewar M.J.S., Zoebish E.G., Healy E.F., Stewart J.J.P. // J. Am.Chem.Soc. - 1985. - V.107.- P. 3902-3909.
9. Schmidt M.W., Baldridge K.K., Boatz J.// J. Comput. Chem. - 1993. - V.14. - P. 1347.

RAPID COMMUNICATIONS IN MASS SPECTROMETRY
Rapid Commun. Mass Spectrom. 2006; **20**: 755–763
Published online in Wiley InterScience (www.interscience.wiley.com). DOI: 10.1002/rcm.2371

RCM

The effect of cone voltage on electrospray mass spectra of the bisquaternary ammonium salt decamethoxinum

V. A. Pashynska[1,2]*, M. V. Kosevich[1], H. Van den Heuvel[2] and M. Claeys[2]

[1]B. Verkin Institute for Low Temperature Physics and Engineering of the National Academy of Sciences of Ukraine, 47, Lenin ave., Kharkov 61103, Ukraine
[2]University of Antwerp (Campus Drie Eiken), Department of Pharmaceutical Sciences, Universiteitsplein 1, BE-2610 Antwerp, Belgium

Received 24 November 2005; Revised 30 December 2005; Accepted 3 January 2006

The effect of cone voltage (CV) variation on the mass spectral pattern of the bisquaternary ammonium salt decamethoxinum in the electrospray ionization (ESI) mode was studied. The advantage of decamethoxinum as a test compound in ESI mass spectrometry lies in the production of two types of ions, i.e. the doubly charged organic dication Cat^{2+} and its singly charged cluster with a Cl^- counterion, $Cat \cdot Cl^+$. This makes it possible to monitor the fragmentation patterns of these ions under identical experimental conditions. Pronounced qualitative and quantitative changes in the ESI mass spectra were observed upon a gradual increase of the CV. The model compound decamethoxinum allowed us to reveal the extreme situation, in which the mass spectra at a CV below and over approximately 100 V look quite different, in that they contain different product ions of Cat^{2+} and $Cat \cdot Cl^+$. While this effect may be much less pronounced for other classes of organic compounds, it should be properly taken into account for the adequate description of fragmentation pathways of bisquaternary ammonium compounds with ESI. Comparison of ESI, FAB-SIMS and MALDI mass spectra of decamethoxinum shows that taking into account CV effects also permits us to gain information on energy deposition into ions generated with the different ionization techniques.

Quaternary ammonium salts are popular test compounds that have been studied by various soft mass spectrometric techniques,[1–10] since the presence of fixed 'preformed' charges in their organic cations facilitates investigations on the fundamentals of ion generation and on fragmentation pathways. In our previous studies[11–17] we selected the bisquaternary ammonium compound decamethoxinum as a structure and energy probe for soft ionization methods, because it demonstrated a strong dependence of the types of ions recorded in the mass spectra on the mass spectrometric technique and experimental conditions applied. Data on the fragmentation of decamethoxinum obtained with liquid secondary ion mass spectrometry (SIMS)[11] and matrix-assisted laser desorption/ionization (MALDI)[12] techniques were reported. In the present study we focus on the behavior of decamethoxinum in the electrospray ionization (ESI) mode with a view to obtaining further insights into the mechanisms of ion formation.

In addition to the advantages of the technique as a whole,[18] ESI offers the possibility of controlling the degree of ion excitation by changing the potential between the capillary or nozzle and the skimmer in the ESI source.[9,10,17–42] In different publications this potential is referred to as the declustering potential,[30] orifice potential,[10] capillary-skimmer,[31] needle-skimmer,[9] nozzle-skimmer[19,34] potential, or sampling cone voltage (CV).[10,37–42] It is believed that the CV effect is due to an in-source collision-induced dissociation (CID) (up-front CID) process. The initially sprayed charged species can undergo collisions with the residual or bath gas on their path between the nozzle and the skimmer, and the change of the ion velocity caused by CV variation affects their kinetic energy and, consequently, their collision energy.[18]

The possibility of controlling the charge state of the ions, the desolvation process and the degree of fragmentation of the ions by CV variation offers the prospect of many useful applications of this technique, mainly in studies of supramolecular noncovalent complexes.[25–36] For example, a method was suggested for evaluating the stability of chemotherapeutic non-intercalating drugs binding to DNA on the basis of monitoring DNA-drug complex decomposition upon CV increase, which correlates with the thermal decomposition of the complex.[25,26] CV adjustment is also of critical importance in probing the structures of surfactant micelles generated under ESI conditions.[30,31] In-source CID is used along with collision-cell tandem mass spectrometric (MS/MS) CID in studies of protein structures.[19–21,32–36] Comparison of in-cell CID and in-source CID[32] permits us to obtain more comprehensive information on the molecular structures of analytes. A method, denoted as energy-dependent ESI mass spectrometry (EDESI-MS), employing CV variation, has been reported for fragmentation studies of metalloorganic compounds.[37–41]

**Correspondence to*: V. A. Pashynska, B. Verkin Institute for Low Temperature Physics and Engineering of the National Academy of Sciences of Ukraine, 47, Lenin ave., Kharkov 61103, Ukraine.
E-mail: pashynska@ilt.kharkov.ua
Contract/grant sponsor: Research Council of the University of Antwerp.

Although the dependence of the degree of fragmentation of precursor ions on CV is mentioned in some publications,[9,10,19,23] systematic investigations of gradual CV variation on fragmentation pathways of selected compounds are rather limited.[35,39,42] In the present work we have undertaken a detailed study of the effect of CV variation on the ESI mass spectral pattern of decamethoxinum to clarify some peculiarities of the ESI processes of bisquaternary compounds. An important feature of decamethoxinum is its ability to form several types of intact ions, i.e. the intact dication Cat^{2+}, the dication complex with the chlorine counterion $Cat \cdot Cl^{+}$, and the singly charged deprotonated cation $[Cat–H]^{+}$. This ability permits the simultaneous monitoring of the behaviors of the latter types of structurally related singly and doubly charged precursor ions under identical experimental conditions. Our study reveals that the CV determines the course of the fragmentation of ions and their energy deposition under ESI conditions.

EXPERIMENTAL

The mass spectral data were obtained in the positive ion mode using an Autospec-oa-TOF mass spectrometer (Micromass, Manchester, UK), which was equipped with an ESI source. The instrument is comprised of a double-focusing stage of *EBE* configuration, coupled to an orthogonal acceleration time-0f-flight (oaTOF) analyzer for MS/MS experiments. The ESI source was operated at 4 kV. Nitrogen was used both as bath gas (100°C; 250 L/h) and nebulizing gas (15 L/h). ESI spectra were recorded in the mass range *m/z* 100–1400. The analyte solutions were introduced into the mass spectrometer by a syringe pump (Harvard Apparatus, South Natick, MA, USA), employing a 500 μL syringe at a constant flow rate of 5 μL/min.

The CV effect on the fragmentation of decamethoxinum was examined by varying the CV from 0 to 250 V in steps of 10 V. Low- and high-energy CID spectra were obtained at a laboratory frame collision energy (E_{lab}) of 400 eV using He and Xe, respectively, as collision gas. Data acquisition and processing were performed using OPUS V3.1X software. All scans were acquired in the continuum mode. Stock solutions of decamethoxinum were prepared (5 mM) either in ethanol or methanol with addition of a drop of CH_2Cl_2 for a better solubilization of the salt. For the actual analysis a methanolic or ethanolic salt solution was used at a final concentration of 0.5 mM and 5 μM.

Decamethoxinum was synthesized at the Institute of Organic Chemistry of the National Academy of Sciences of Ukraine (Kiev, Ukraine). Ethanol and methanol (analytical grade) were purchased from Lab-Scan (Dublin, Ireland).

RESULTS AND DISCUSSION

SIMS and ESI CID data on the fragmentation of decamethoxinum

The structure of the bisquaternary ammonium salt decamethoxinum ($C_{38}H_{74}N_2O_4Cl_2$) is as follows:

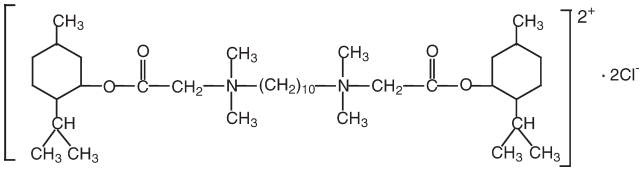

(1)

The following generalized formula will be used in the fragmentation schemes:

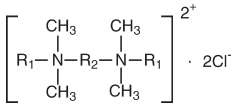

(2)

In the organic dication of the salt, designated as Cat^{2+}, two quaternary nitrogen atoms are connected by a rather long polymethylene $(CH_2)_{10}$ chain, R_2, and each of the nitrogen atoms has two CH_3 and one R_1 substituents. The side groups R_1 contain menthyl rings R_m attached by an ester bond. *Ab initio* quantum chemical calculations on decamethoxinum[11] show that the distance between the quaternary nitrogen atoms for the extended conformation of the R_2 chain is approximately 14 Å. A significant feature of the electronic structure of the organic dication[11] is the delocalization of the positive charge over a number of hydrogen atoms of the quaternary groups.

The main features of the behavior of decamethoxinum under mass spectrometric conditions were established in our previous study[11] on the basis of MS/MS data on metastable decay and CID of SIMS-generated ions. Control experiments with collision-cell CID of the same types of decamethoxinum ions generated by ESI gave qualitatively similar CID spectral patterns. Two main primary types of ions, Cat^{2+} (*m/z* 311) and $Cat \cdot Cl^{+}$ (*m/z* 657), are produced under both liquid SIMS and ESI conditions. To avoid the term 'molecular ion', which is inappropriate for both the organic dication Cat^{2+} and its cluster with a Cl^{-} counterion, we shall adopt the term 'precursor ions'. Fragmentation of these precursor ions may proceed through at least two successive steps with formation of first- and second-order product ions.

The main pathways of Cat^{2+} fragmentation, observed under both metastable decay and CID conditions, involve the loss of one and two menthyl rings, R_m, accompanied by proton transfer:

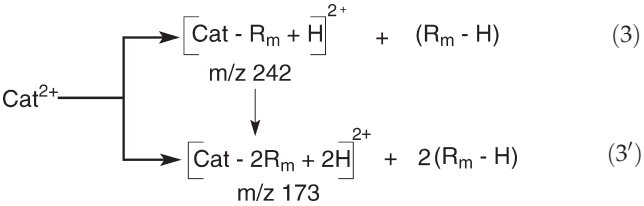

(3)

(3′)

The abundance of the product ion $[Cat–2R_m+2H]^{2+}$ (3′) increases noticeably under CID compared with its abundance under metastable decay. An intriguing feature of this pathway is the preservation of the doubly charged state in the product ions of the primary dication. It was suggested that such unusual stability of the decamethoxinum dication[11] resulted from the structural peculiarities of decamethoxinum, with its long distance of 14 Å between the quaternary

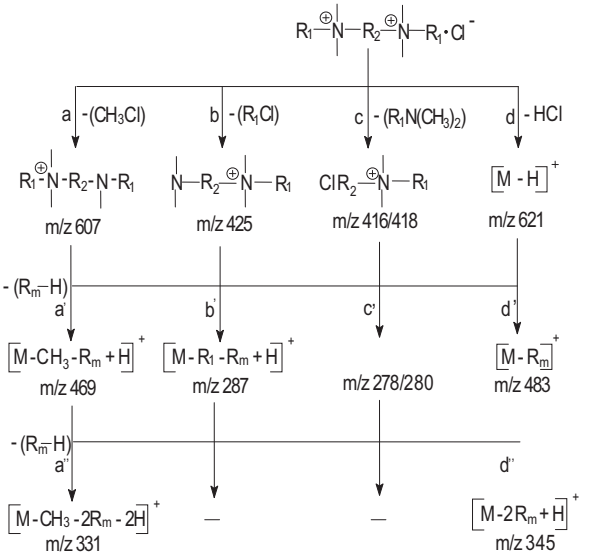

Scheme 1. Fragmentation pathways of the decamethoxinum $Cat \cdot Cl^+$ precursor ion.

nitrogen atoms, the charge smearing over the nearest substituents of the quaternary nitrogens and intramolecular solvation.

The main fragmentation pathways of the $Cat \cdot Cl^+$ precursor are summarized in Scheme 1. The fragmentation is dominated by dequaternization reactions (reactions *a–c*) which proceed via halogenalkyl (RCl) elimination. All four substituents at the quaternary nitrogens, that is CH_3, R_1, R_2 (the latter with the adjacent segment of the dication), as well as H (reaction *d*), can be eliminated in combination with chlorine. These pathways coincide with thermal degradation processes of quaternary salts. The products formed in reactions *a–d* can undergo further fragmentation via a specific pathway that involves the side groups R_1 of decamethoxinum, namely via the loss of a menthyl ring moiety (R_m–H) with the mass of 138 Da (*a′–d′*). The second menthyl ring can be eliminated from two secondary product ions, which have retained one R_1 group (*a″*, *d″*). Note that Cat^{2+} is never formed by dissociation of $Cat \cdot Cl^+$.

The pathway of charge separation driven by Coulomb repulsion between two positively charged groups is observed for many bisquaternary compounds.[1] In the case of decamethoxinum, products of such a process for the dication Cat^{2+} (*g*, *h*, Scheme 2) are more than an order of magnitude less abundant than those of fragmentation routes (3, 3′). Again this was explained by a relatively high stability

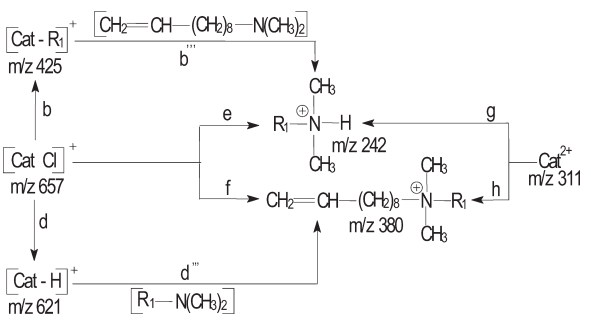

Scheme 2. Fragmentation via cleavage of a C–N bond in a number of precursor ions.

of the doubly charged state of the organic cation of decamethoxinum.[11] At the same time a cleavage of the C–N bond (accompanied by proton transfer) in the singly charged $Cat \cdot Cl^+$ is possible, as shown in Scheme 2 (reactions *e* and *f*). Secondary products of first-order singly charged product ions $[M–R_1]^+$ and $[M–H]^+$ can also contribute to the abundances of the ions at *m/z* 242 (*b‴*) and *m/z* 380 (*d‴*) (Scheme 2).

The destruction of the central polymethylene chain is observed under high-energy CID only. It should be noted that under SIMS all product ions of different precursor ions superimpose in the total mass spectrum of decamethoxinum. A complete list of some other minor fragmentation pathways can be found in our previous report.[11]

Dependence of ESI spectral pattern on cone voltage

Let us consider now the changes in the ESI spectral pattern of decamethoxinum with CV variation. Figure 1 presents spectra obtained by infusing a 0.5 mM ethanolic solution of decamethoxinum with a stepwise CV increase. It is known that lower CV values favor preservation both of higher charge states and of noncovalent clusters.[9] In agreement with this theory, an abundant dication Cat^{2+} (*m/z* 311) and an abundant singly charged $Cat \cdot Cl^+$ (*m/z* 657) ion were recorded at a low CV of between 25 and 50 V (Figs. 1(a) and 1(b)). The level of fragmentation was negligibly low. The absolute abundance of the two precursor ions increased about three-fold on a CV rise from 25 to 50 V, which may be connected with a more efficient desolvation process. On further CV increase up to 75 V (Fig. 1(c)) the Cat^{2+} started to fragment in accordance with pathways (3, 3′) by successive loss of the two menthyl rings R_m. The corresponding product ions, $[Cat–R_m+H]^{2+}$ (*m/z* 242) and $[Cat–2R_m+2H]^{2+}$ (*m/z* 173), are also doubly charged. As already mentioned, preservation of the doubly charged state on fragmentation of a relatively small dication is a rarity. In the case of decamethoxinum, stabilization of the doubly charged species is explained by the structural peculiarities of its organic dication.[11] Pathways (3, 3′) are the major ones for Cat^{2+} independently of the source of excitation: they were observed earlier for metastable decay and CID of ions sputtered under SIMS,[11] and in the present study upon in-source CID of electrosprayed dications. At a relatively low CV of 75 V, the loss of only one menthyl ring is dominant and the product ion $[Cat–R_m+H]^{2+}$ (*m/z* 242) is more abundant than that resulting in $[Cat–2R_m+2H]^{2+}$ (*m/z* 173) corresponding to the loss of the two menthyl rings. As expected, a further increase in CV up to 90 V led to more extensive fragmentation via loss of the second menthyl ring. Characteristic product ions of the $Cat \cdot Cl^+$ precursor were not observed at these voltages. A possible stabilizing role of the Cl^- anion binding to the dication cannot explain this phenomenon. A more likely explanation is that the singly charged ions acquire a twice lower kinetic energy than the doubly charged ones and, consequently, their collisions with residual gas will not be efficient at the given voltage. It is worth noting that in a previous study on bisquaternary compounds[9] the influence of CV increase consisted of a redistribution of Cat^{2+} and $Cat \cdot Cl^+$ abundances in favor of

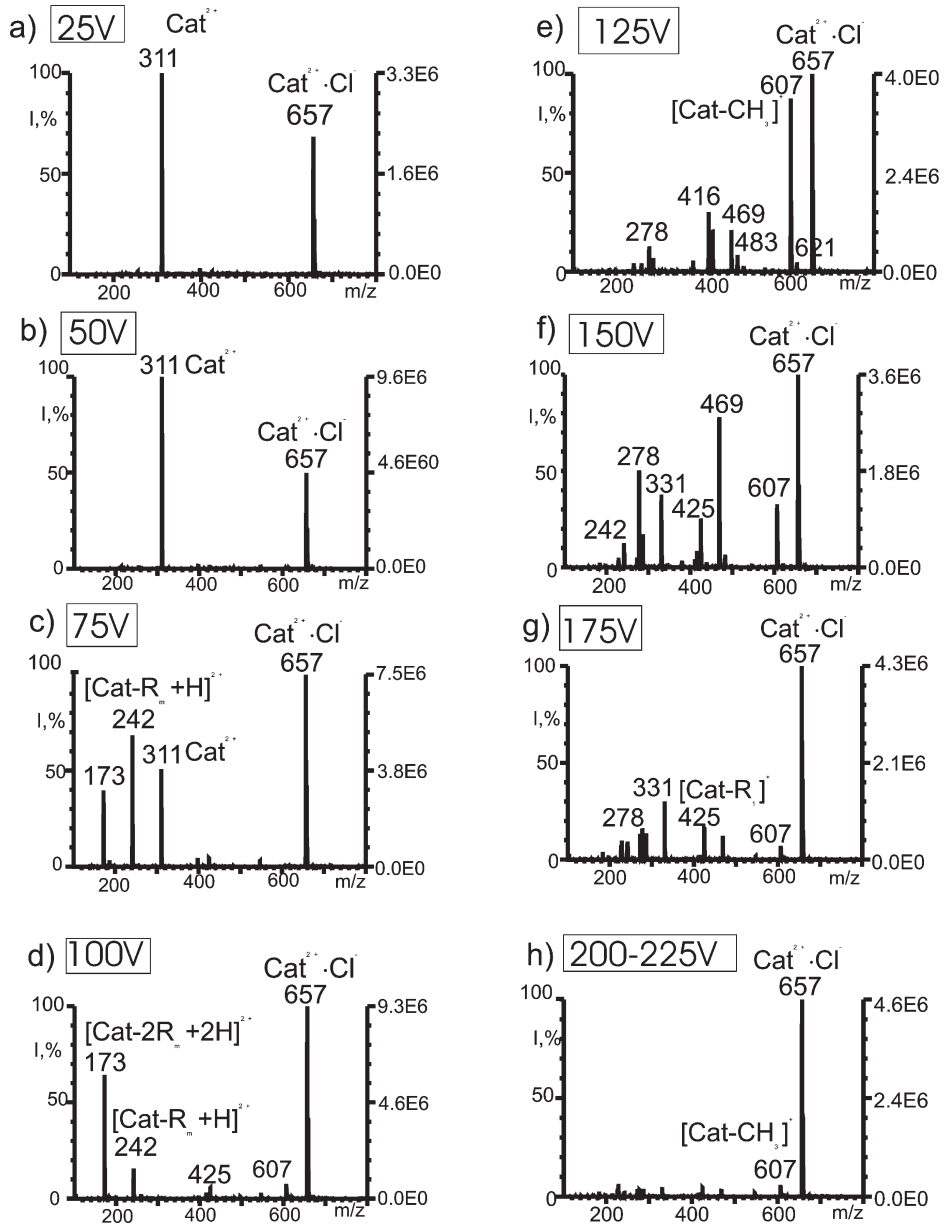

Figure 1. Cone voltage dependence on the appearance of ESI mass spectra obtained for a 0.5 mM decamethoxinum solution in ethanol.

an increase in the $Cat \cdot Cl^+$ abundance, and that fragmentation of these ions was practically absent. Using decamethoxinum as a test compound we can demonstrate that the decrease of the dication yield with CV increase occurs due to enhancement of Cat^{2+} fragmentation under in-source CID.

At a CV of 90 V the Cat^{2+} ion at *m/z* 311 practically vanishes and the abundances of its product ions at *m/z* 173 and 242 start to decrease, which means that the majority of the dications no longer survive under these conditions. Obviously, the first-order product ions have sufficiently high excitation energy to undergo further decay to lower mass product ions. At a CV of 100 V (Fig. 1(d)), fragmentation of $Cat \cdot Cl^+$ starts and progresses with further CV increase. At a CV of 125 V (Fig. 1(e)), the spectrum is comprised only of product ions of $Cat \cdot Cl^+$, while those of Cat^{2+} have disappeared completely. Note that the spectra at CVs of 75 V (Fig. 1(c)) and 125 V (Fig. 1(e)) look quite different and, in fact, contain sets of product ions originating from different precursors. This behavior points to the need to select the CV properly for a precise description of the fragmentation of complicated compounds such as bisquaternary ammonium salts.

The initial step of $Cat \cdot Cl^+$ fragmentation, which became observable at a CV of 100 V, coincides with the most abundant pathway elucidated earlier under metastable decay and CID of SIMS-generated ions, namely dequaternization (see first steps *a*, *b*, and *c* in Scheme 1). At a CV of 125 V, the abundance of ions at *m/z* 607, 425, 416/418 increases noticeably.

In contrast to Cat^{2+} fragmentation (3, 3′), the loss of (R_m–H) does not occur for $Cat \cdot Cl^+$. It starts only as the second-step fragmentation of the first-order product ions (see second-order steps *a*′, *b*′, and *c*′ in Scheme 1) at a CV of 125 V. At a CV of 150 V (Fig. 1(f)), the abundances of ions at *m/z* 607, 425 and 416/418 corresponding to the first-order product ions (*a*–*c*)

decrease, while those of the second-order product ions at *m/z* 278/280, 287 and 469 (*a*′–*c*′) grow significantly. More extensive third-order fragmentation (*a*″) is shown by the $[Cat–CH_3]^+$ (*m/z* 607) product ion: similar to a stepwise loss of the first and the second menthyl rings observed for Cat^{2+} (3, 3′), the $[Cat–CH_3]^+$ product ion successively loses one and two R_m rings. At a CV of 125 V, only a $[Cat–CH_3–R_m+H]^+$ (*m/z* 469) ion is present; at a CV of 150 V, both *m/z* 469 (*a*′) and 331 $[Cat–CH_3–2R_m+2H]^+$ (*a*″) ions are present; and, at a CV of 175 V (Fig. 1(g)), the ion at *m/z* 331 becomes more abundant.

The yield of pathways *d*–*d*′–*d*″ under ESI is negligible for a relatively concentrated solution; a weak $[M–H]^+$ ion (*m/z* 621) is recorded at a CV of between 125 and 150 V only, and the observation of a *m/z* 483 product ion (*d*′) correlates with the presence of the $[M–H]^+$ precursor in the spectra. Yields of pathways corresponding to charge separation and a cleavage of the C–N bond are negligibly small for both the Cat^{2+} and $Cat \cdot Cl^+$ precursor ions under ESI. An ion at *m/z* 242, which corresponds to the doubly charged (confirmed by a proper peak width) product ion of Cat^{2+} at a CV up to about 100 V, is noted and then disappears. The ion at *m/z* 242 was registered again at a CV in the range of 150–175 V, but now it corresponds to a singly charged ion which may originate from $Cat \cdot Cl^+$ according to reactions *e* and *b*–*b*‴ (see Scheme 2). The product ion at *m/z* 380 is mainly associated with the (*d*–*d*‴) pathway (Scheme 2) since it appears together with $[Cat–H]^+$ (*m/z* 621) and *m/z* 438 ions at a CV in the range of 125–150 V.

At a CV ≥200 V (Fig. 1(h)), the abundances of characteristic product ions in relation to $Cat \cdot Cl^+$ decrease noticeably while the absolute abundance of $Cat \cdot Cl^+$ remains relatively high. This behavior contrasts with that observed for Cat^{2+} where the decrease of the abundance of characteristic product ions followed that of the precursor Cat^{2+}. At least three explanations can be suggested for this puzzling experimental result. The first could be a purely instrumental factor in that the focusing of high-energy product ions formed at high CV values is less efficient;[18] however, in this case, we would expect that the absolute abundance of the $Cat \cdot Cl^+$ precursor would also decrease. The second possible explanation is that such a high kinetic energy of precursor ions causes a decrease in the number of their effective collisions with residual gas in the nozzle-skimmer region, decreasing the cross-section of fragmentation processes. However, these two explanations are contestable because product ions are observed at high CV values for dilute solutions, as will be discussed further. Finally, it is possible that the $Cat \cdot Cl^+$ ion present in the spectra recorded at high CV is actually due to fragmentation of larger clusters. It is logical to consider that $Cat \cdot Cl^+$ 'monomeric' precursors initially formed in the spraying process can be fragmented into smaller ions at a CV > 200 V similarly to the fragmentation of Cat^{2+} (which is completed at lower CV values), but that the $Cat \cdot Cl^+$ ions released in collisions from larger clusters may be relatively 'cool' and may be recorded under these conditions. A singly charged cluster of two cations and three anions $2Cat \cdot 3Cl^+$ at *m/z* 1349 was recorded in the ESI spectra, but it was rather hard to make unambiguous conclusions as to its behavior on CV variation. MS/MS CID of $2Cat \cdot 3Cl^+$ with He as collision gas showed $Cat \cdot Cl^+$ as the only CID product ion while use of the heavier Xe gas caused more extensive fragmentation, with the formation of product ions characteristic of $Cat \cdot Cl^+$ decomposition (results not shown). Decomposition of large low molecular weight salt clusters into smaller ones as a source of ions in the ESI mass spectra has been reported for some other bisquaternary compounds.[10]

It may be concluded that in-source CID of decamethoxinum produces the same types of product ions as in collision-cell CID under MS/MS. However, the abundance and distribution of the product ions show a dramatic dependence on the CV, and product ions originating from different precursors replace one another as the CV increases. Nevertheless, the appearance of certain types of product ions at different cone voltages can provide valuable information on the energy requirements of fragmentation pathways.

Spectral dependence on analyte concentration and type of solvent

To evaluate the dependence of the extent of the CV effect on the analyte concentration, a set of spectra similar to that shown in Fig. 1 was obtained for a 5 μM ethanolic solution of decamethoxinum (Fig. 2). Comparison of these two sets of spectra revealed some differences. At a low CV in the range of 25–50 V, the spectra contain two intact precursor ions, Cat^{2+} (*m/z* 311) and $Cat \cdot Cl^+$ (*m/z* 657). The relative abundance of Cat^{2+}, however, is noticeably higher for the dilute sample (cf. Figs. 1a, 1b, 2a and 2b)). The extent of fragmentation of the Cat^{2+} dication via pathways (3, 3′), which starts at approximately the same CV of about 75 V for both concentrated and dilute solutions, seems to be smaller for the dilute one (see Figs. 1c and 2c)). Fragmentation of the $Cat \cdot Cl^+$ ion starts at the same CV of around 100 V, regardless of the analyte concentration. The fragmentation pathways of the $Cat \cdot Cl^+$ precursor in both solutions are practically the same. The general trend of more extensive fragmentation, that is the appearance of the second- and third-order product ions with CV increase, is preserved for the dilute solution. The relative abundances of the product ions are somewhat different for the concentrated and the dilute samples at the same CV values (Figs. 1(d)–1(g), 2(d)–2(g)), but a quantitative comparison is beyond the scope of the present work.

The qualitative distinction of ESI spectra of the dilute solution consists of the presence of a relatively abundant $[Cat–H]^+$ (*m/z* 621) ion in the CV range of 100–225 V (Figs. 2(d)–2(h)). The product ions formed from this precursor, namely the ions at *m/z* 483 (*d*′), *m/z* 345 (*d*″) and *m/z* 380 (*d*‴), are also present under these conditions and are most pronounced for a CV of 150 V (cf. Figs. 1f and 2f)). It can be seen that at CV ≥ 200 V the product ions arising from fragmentation of $Cat \cdot Cl^+$, although of low abundance, are present in the mass spectrum of the dilute sample (Fig. 2(h)). This spectrum is in contrast to that of the concentrated sample, which lacks product ions at these high CV values (Fig. 1(h)). Thus, three distinctive features of the ESI mass spectra of the dilute decamethoxinum solution are revealed as opposed to those observed for the concentrated one: an increased abundance of the Cat^{2+} dication, a comparably high abundance of the $[Cat–H]^+$ ion and its product ions, and the presence of $Cat \cdot Cl^+$ product ions at a CV ≥ 200 V. The following reasons for these differences may be proposed.

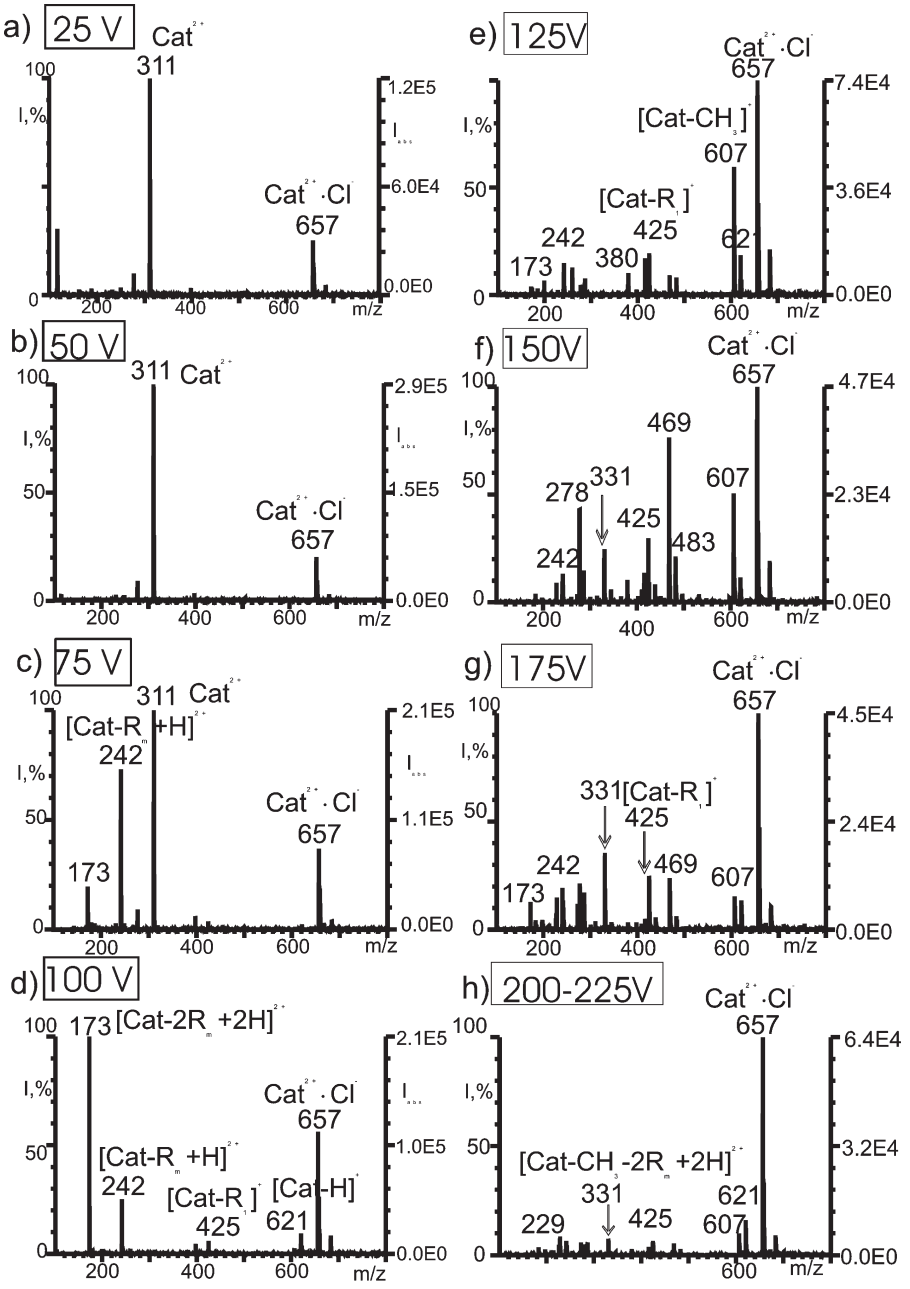

Figure 2. Cone voltage dependence on the appearance of ESI mass spectra obtained for a 5 μM decamethoxinum solution in ethanol.

A concentration effect consisting of an increase of multiply charged ions upon dilution is well known and has been reported earlier for other bisquaternary salts.[9,18] It is reasonable to assume that a higher degree of dissociation of a salt solute in low-concentrated solutions enhances the probability of the occurrence of single cations of the organic salt Cat^{2+} in the final droplet without clustering with the counterion.[43] It should be noted that our[11] and literature[10,22] data show that the Cat^{2+} ion is never formed by fragmentation of the $Cat^{2+} \cdot Cl^-$ cluster. Literature data confirm that the Cat^{2+} ion of bisquaternary compounds is released on desolvation of the dication-solvent molecule clusters.[10] The noticeable increase in the $[Cat–H]^+$ ion abundance for dilute solutions can also be explained as arising from the dication-solvent clusters by a process involving proton transfer to a solvent molecule (or the solvent anion[22]). This suggestion is supported by the following facts. Firstly, the $[Cat–H]^+$ ion is not formed from the bare Cat^{2+} precursor ion, as was confirmed by CID.[11] Secondly, the yield of pathway (d) of $[Cat–H]^+$ formation from $Cat \cdot Cl^+$ is rather low under ESI, as is shown for the concentrated solution where the abundance of the $Cat \cdot Cl^+$ precursor is high. Thirdly, the growth of the $[Cat–H]^+$ ion abundance with CV increase, observed in our experiments (Figs. 2(d)–2(h)) and other studies,[10] is consistent with a $[Cat–H]^+$ release due to decomposition of larger clusters. This permits consideration of the dication-solvent clusters as the most probable precursors of the $[Cat–H]^+$ ion.

The probability of formation of relatively large $[Cat_n \cdot Cl_{2n-1}]^+$ clusters must also be lower on spraying of dilute solutions. This phenomenon may help to explain the observation of rather abundant product ions at a CV $\geq$ 200 V.

If the above assumption on the noticeable yield of the $Cat \cdot Cl^+$ product ion due to decomposition of large clusters in concentrated solutions at high CV holds, this source of stable $Cat \cdot Cl^+$ ions should diminish for dilute samples. Consequently, the absolute abundance of $Cat \cdot Cl^+$ becomes lower for dilute solutions than for the concentrated ones at a $CV \geq 200$ V and the relative product ion yield of $Cat \cdot Cl^+$ ions originating from the same source as at the lower CV remains noticeable.

The effect of the solvent on the appearance of ESI mass spectra of bisquaternary compounds has been reported.[9] It was shown that solvents of higher polarity favor the formation of gas-phase ions of higher charge states; e.g. the abundance of Cat^{2+} decreases monotonously in relation to that of $Cat \cdot Cl^+$ when alcoholic solvents with a polarity decreasing in the order methanol > ethanol > propanol > butanol are employed.[9]

To check the fulfillment of this rule for decamethoxinum, ESI mass spectra of a methanolic decamethoxonium solution were obtained. Figure 3 illustrates mass spectra of a 0.5 mM methanolic decamethoxonium solution at two CV values of 25 and 100 V.

It can be seen that the abundance of the Cat^{2+} ion in the case of methanol (Fig. 3(a)) is noticeably higher than with ethanol (Fig. 1(a)), which is in agreement with the above hypotheses.[9] The relative yield of two characteristic Cat^{2+} product ions at *m*/*z* 173 and 242 in the case of methanol (Fig. 3(b)) is higher than with ethanol (Fig. 1(d)) for the same CV of 100 V, which is consistent with a higher generation of the Cat^{2+} precursor ion in the former case. Fragmentation of the $Cat \cdot Cl^+$ ion on CV increase is qualitatively similar for both ethanol and methanol solvents. At a $CV \geq 200$ V the relative contribution of product ions decreases for the methanolic sample in a similar way to the ethanolic one. A decrease in the analyte concentration of the methanolic solution (5 μM) (results not shown) induces a further increase in the relative abundance of the doubly charged Cat^{2+} ion at low CV values. At a CV of 50 V the abundance of the $Cat \cdot Cl^+$ ion in relation to that of Cat^{2+} is only about 2%. After the disappearance of the Cat^{2+} ion at a CV > 100 V the $Cat \cdot Cl^+$ ion becomes the most abundant ion in the spectra, while its absolute signal intensity remains practically the same as at lower CV values. The CV ranges for which changes of fragmentation patterns are observed are practically the same for the concentrated and dilute methanolic solutions. The $[Cat–H]^+$ ion is prominent in dilute methanol at a CV > 125 V, which is similar to the case of dilute ethanolic samples. At a CV > 200 V the product ions of $[Cat–H]^+$ are noticeable and the abundance of the $[Cat–H]^+$ ion reaches about 40% of that of the $Cat \cdot Cl^+$ ion. Such a significant change in $[Cat–H]^+$ abundance may be because of the additional yields of Cat^{2+} due to both the higher polarity of the solvent and the dilution of the solution.

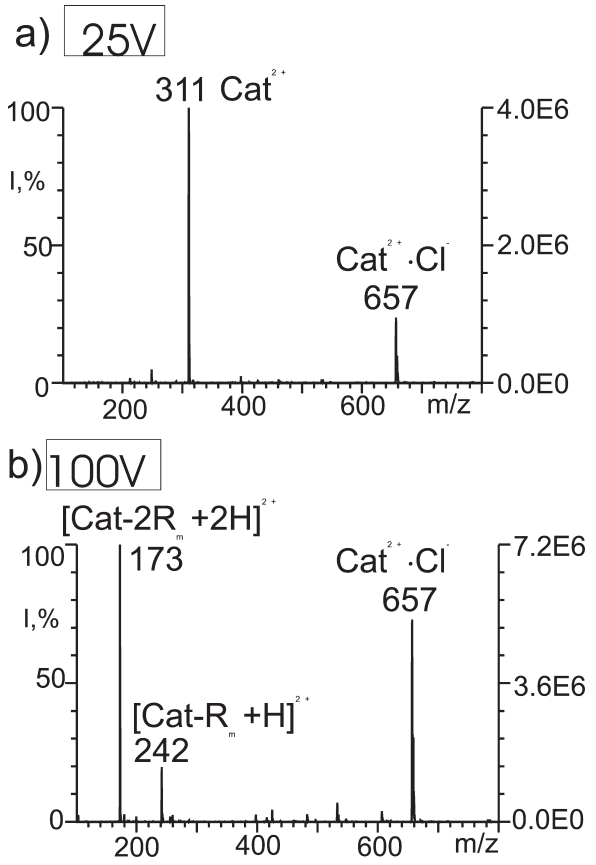

Figure 3. ESI mass spectra of a 0.5 mM solution of decamethoxinum in methanol at CV values of 25 V and 100 V.

Comparison of ESI, FD, MALDI and SIMS/FAB mass spectra

When comparing ion generation and energy deposition with different soft ionization techniques, it is of interest to compare mass spectra of decamethoxinum obtained by ESI at different CV values with those obtained in earlier studies with other desorption techniques.[11–16] Such a comparison shows that the mass spectra obtained at different CV values under ESI never coincide completely with those obtained with FD, FAB and liquid SIMS.

The FD spectrum of decamethoxinum[16] contains abundant Cat^{2+} and $Cat \cdot Cl^+$ ions, which makes it similar to ESI spectra obtained at the lowest CV. However, in contrast to ESI, the level of Cat^{2+} fragmentation is negligible under FD, while products of the dequaternization of $Cat \cdot Cl^+$ via RCl loss are present. On the one hand, it is obvious that the absence of desolvational cooling under FD may lead to 'hotter' $Cat \cdot Cl^+$ ions; on the other hand, a significant increase of the $[Cat–CH_3]^+$ and $[Cat–R_1]^+$ ion yield on increase of the FD emitter temperature points to the possibility of the desorption of these species as products formed by direct thermal decomposition on the FD emitter surface.

Under liquid SIMS/FAB conditions the relative abundance of Cat^{2+} is relatively low due to its efficient pairing with the anion,[11] and the level of $Cat \cdot Cl^+$ fragmentation is relatively high. It could be predicted that the SIMS spectrum would be similar to some of the ESI spectra recorded in a CV range of 150–200 V. As already mentioned, however, complete coincidence is never achieved. The most abundant fragments in the SIMS spectrum are the first-order products of dequaternization reactions (see the first row in Scheme 1) while the abundance of their second-step fragments formed via (R_m–H) loss (the second row in Scheme 1) is low. Under ESI the abundance of dequaternization products increases with CV at first (see Fig. 1(e)), but then decreases because of

more extensive fragmentation via loss of menthyl rings, reflected in a significant growth of the abundance of the second-order product ions (Fig. 1(f)). One additional distinct feature of SIMS spectra is the presence of relatively abundant products of reactions (*e*, *f*, Scheme 2) at *m*/*z* 242 and 380.

With MALDI using 2,5-dihydroxybenzoic acid (DHB) matrix,[12] Cat^{2+} is not recorded, while two other diagnostic ions, $Cat \cdot Cl^+$ and $[Cat–H]^+$, are present. The abundance of $[Cat–H]^+$ is comparable with or higher than that of $Cat \cdot Cl^+$. The pathways of fragmentation under MALDI are similar to those observed with SIMS and ESI, but the total yield of fragment ions is much higher. The distribution of fragment ions differs for the linear and reflectron modes of measurements, which is connected with the post-source decay effect. The main distinctive feature of the MALDI mass spectra of decamethoxinum is the presence of an abundant cluster of the dication with a DHB matrix molecule, $[Cat+DHB–H]^+$. No decamethoxinum clusters with solvent molecules were ever recorded with SIMS/FAB and ESI. A high abundance of the $[Cat–H]^+$ ion and its fragments with MALDI is observed along with abundant clusters of the dication with organic matrix molecules. This supports the idea formulated above that $[Cat–H]^+$ formation is due to decay of these clusters.

Thus, while the main directions of fragmentation of decamethoxinum precursor ions are the same with all the above techniques, the mass spectra are not reproducible with different ionization techniques and, moreover, depend on the conditions applied in each technique.

CONCLUSIONS

It is shown in the present study that the bisquaternary ammonium antimicrobial agent decamethoxinum exhibits pronounced qualitative and quantitative changes in its ESI spectra on variation of the cone voltage. At the lowest CV values up to 50 V, only two intact precursors, Cat^{2+} and $Cat \cdot Cl^+$, are present in the spectra. On further CV increase, fragmentation of Cat^{2+} via its characteristic pathways starts while $Cat \cdot Cl^+$ remains intact. This is explained by the higher kinetic energy and the correspondingly higher collision energy of the doubly charged ion than of the singly charged one. The abundances of the Cat^{2+} product ions grow while the abundance of Cat^{2+} decreases with CV increase up to 90 V when Cat^{2+} vanishes from the spectra. At a CV of about 100 V fragmentation of $Cat \cdot Cl^+$ starts and progresses as the CV increases. A consequence of the above spectral changes is that the mass spectra recorded in the CV ranges below and above approximately 100 V look quite different in that they contain product ions originating from the different precursor ions, Cat^{2+} and $Cat \cdot Cl^+$.

The dependence of ESI mass spectra on the concentration of decamethoxinum solution was investigated and different solvents (ethanol and methanol) were evaluated. The results show that a more concentrated solution and the use of ethanol as a solvent allow us to observe a more abundant $Cat \cdot Cl^+$ ion, while dilution of the analyte and use of methanol as solvent facilitate Cat^{2+} formation at similar CV values.

Control of the kinetic energy of ions by variation of the CV in the ESI source results in qualitatively different fragmentation pathways that resemble those obtained with other techniques. At a low CV, the softest conditions, similar to those in FD, are achieved while at higher CV high-energy fragmentation such as in SIMS/FAB is observed. However, comparison of ESI and liquid SIMS spectra of decamethoxinum shows that the spectra are never completely similar. The main differences in the MALDI spectra in comparison with the ESI spectra are the dominance of the $[Cat–H]^+$ ion, the absence of Cat^{2+}, the high total level of fragmentation, and the presence of the dication-matrix clusters which are absent with other techniques.

Acknowledgements

This study was supported by the Research Council of the University of Antwerp through a visiting postdoctoral fellowship (12 months) to V. Pashynska.

REFERENCES

1. Veith HJ. *Mass Spectrom. Rev*. 1983; **2**: 419.
2. Ryan TM, Day RJ, Cooks RG. *Anal. Chem*. 1980; **52**: 2054.
3. Hercules DM, Day RJ, Balasanmugan K, Dang TA, Li CP. *Anal. Chem*. 1982; **54**: 280A.
4. Dang TA, Day RG, Hercules DM. *Anal. Chem*. 1984; **56**: 868.
5. Heller DN, Yergey J, Cotter RJ. *Anal. Chem*. 1983; **55**: 1310.
6. Schmelzeisen-Redeker G, Rollgen FW, Wirtz H, Vogtle F. *Org. Mass Spectrom*. 1985; **20**: 752.
7. Prokai L, Hsu BH, Farag H, Bodor N. *Anal. Chem*. 1989; **61**: 1723.
8. Claereboudt J, Claeys M, Geise H, Gijbels R, Vertes A. *J. Am. Soc. Mass Spectrom*. 1993; **4**: 798.
9. Wang G, Cole RG. *J. Am. Soc. Mass Spectrom*. 1996; **7**: 1050.
10. Milman BL. *Rapid Commun. Mass Spectrom*. 2003; **17**: 1344.
11. Pashynska VA, Kosevich MV, Gomory A, Szilagyi Z, Vekey K, Stepanian SG. *Rapid Commun. Mass Spectrom*. 2005; **19**: 785.
12. Pokrovsky VA, Kosevich MV, Osaulenko VL, Chagovets VV, Pashynska VA, Shelkovsky VS, Karachevtsev VA, Naumov AYu. *Mass Spectrom. (Russ)*. 2005; **2**: 183.
13. Pashynska VA, Kosevich MV, Van den Heuvel H, Cuyckens F, Claeys M. *Visnyk of V.N. Karazin Kharkov National University, Biophysical Bulletin* 2004; **637**: 123.
14. Kosevich MV, Pashynska VA, Van den Heuvel H, Claeys M. *21st Informal Meeting on Mass Spectrometry*, 11–15 May 2003, Antwerp, Belgium, 2003; 107–108.
15. Pashynskaya VA, Kosevich MV, Gomory A, Vashchenko OV, Lisetski LN. *Rapid Commun. Mass Spectrom*. 2002; **16**: 1706.
16. Sukhodub LF, Kosevich MV, Shelkovsky VS, Volyanski YuL. *Antibiotics Chemother. (Russ.)* 1989; **34**: 823.
17. Kosevich MV, Derrick PJ. *Proc. 16th Informal Meeting on Mass Spectrometry*, 4–6 May 1998, Budapest, Hungary, 1998; 82.
18. Cole RB. *Electrospray Ionization Mass Spectrometry. Fundamentals, Instrumentation and Applications*. John Wiley: Chichester, 1997.
19. Kaltashov IA, Eyles SJ. *Mass Spectrometry in Biophysics: Conformation and Dynamics of Biomolecules*. John Wiley: New York, 2005.
20. Aleksandrov ML, Gall LN, Krasnov NV, Nikolaev VI, Pavlenko VA, Shkurov VA. *Dokl. Acad. Nauk SSSR*. 1984; **277**: 397.
21. Aleksandrov ML, Baram GI, Gall LN, Grachev MA, Knorre VD, Krasnov NV, Kusner YS, Mirgorodskaya OA, Nikolaev VI, Shkurov VA. *Bioorg. Khim. (Russ.)* 1985; **11**: 705.
22. Evans CS, Startin JR, Goodall DM, Keely BJ. *Rapid Commun. Mass Spectrom*. 2001; **15**: 1341.
23. Alfassi ZB, Huie RE, Milman BL, Neta P. *Anal. Bioanal. Chem*. 2003; **377**: 159.
24. Hao C, March RE, Croley TR, Smith JC, Rafferty SP. *J. Mass Spectrom*. 2001; **36**: 79.
25. Gabelica V, Rosu F, De Pauw E. *J. Mass Spectrom*. 1999; **34**: 1328.
26. Gabelica V, Rosu F, Houssier C, De Pauw E. *Rapid Commun. Mass Spectrom*. 2000; **14**: 464.

27. Gabelica V, De Pauw E. *J. Mass Spectrom*. 2001; **36**: 397.
28. Akashi S, Osawa R, Nishimura Y. *J. Am. Soc. Mass Spectrom*. 2005; **16**: 116.
29. Guo X, Bruis MF, Davis DL, Bentzle CM. *Nucleic Acids Res*. 2005; **33**: 3659.
30. Siuzdak G, Bothner B. *Angew. Chem. Int. Ed. Engl*. 1995; **34**: 2053.
31. Nohara D, Bitoh M. *J. Mass Spectrom*. 2000; **35**: 1434.
32. Van Dongen WD, Van Wijk JIT, Green BN, Heerma W, Haverkamp J. *Rapid Commun. Mass Spectrom*. 1999; **13**: 1712.
33. Eyles SJ, Speir P, Kruppa G, Giearsch LM, Kaltashov IA. *J. Am. Chem. Soc*. 2000; **122**: 495.
34. Bure C, Lange C. *Curr. Org. Chem*. 2003; **7**: 1613.
35. Harrison AG, Siu MKW, El Aribi H. *Rapid Commun. Mass Spectrom*. 2003; **17**: 869.
36. Kubwabo C, Vais N, Benoit FM. *Rapid Commun. Mass Spectrom*. 2005; **19**: 597.
37. Dyson PJ, Johnson BFG, McIndoe JS, Langridge-Smith PRR. *Rapid Commun. Mass Spectrom*. 2000; **14**: 311.
38. Dyson PJ, Hearley AK, Johnson BFG, McIndoe JS, Langridge-Smith PRR, Whyte C. *Rapid Commun. Mass Spectrom*. 2001; **15**: 895.
39. Butcher CPG, Dyson PJ, Johnson BFG, Langridge-Smith PRR, McIndoe JS, Whyte C. *Rapid Commun. Mass Spectrom*. 2002; **16**: 1595.
40. Butcher CPG, Johnson BFG, McIndoe JS, Yang X, Wang X-B, Wang L-S. *J. Chem. Phys*. 2002; **116**: 6560.
41. Dyson PJ, McIndoe JS, Zhao D. *Chem. Commun*. 2003; 508.
42. Harrison AG. *J. Mass Spectrom*. 1999; **34**: 1253.
43. Kebarle P. *J. Mass Spectrom*. 2000; **35**: 804.

Mass Spectrometry & Purification Techniques

Pashynska et al., Mass Spectrom Purif Tech 2015, 1:1
DOI: 10.4172/2469-9861.1000103

Research Article Open Access

Variable Electrospray Ionization and Matrix-Assisted Laser Desorption/Ionization Mass Spectra of the Bisquaternary Ammonium Salt Ethonium

VA Pashynska[1], MV Kosevich[1*], A Gömöry[2], K Vékey[2], M Claeys[3], VV Chagovets[1] and VA Pokrovskiy[4]

[1]*B. Verkin Institute for Low Temperature Physics and Engineering of the National Academy of Sciences of Ukraine, Lenin Avenue 47, Kharkov, Ukraine*
[2]*Institute of Organic Chemistry of Research Center for Natural Sciences of the Hungarian Academy of Sciences, Magyar tudósok körútja 2, Budapest, Hungary*
[3]*University of Antwerp, Department of Pharmaceutical Sciences, Universiteitsplein 1, Antwerp, Belgium*
[4]*A.A. Chujko Institute of Surface Chemistry of the National Academy of Sciences of Ukraine, General Naumov Str. 17, Kiev, Ukraine*

Abstract

Determination of a single "fingerprint" mass spectrum of a biologically active compound, required for compound identification in mixtures and biological materials in such applied tasks as ecological monitoring and biological imaging, may become a nontrivial problem for labile compounds whose mass spectra depend strongly on the applied experimental conditions. In the present communication, qualitatively different mass spectral patterns obtained for the bisquaternary ammonium salt ethonium Cat^{2+}•$2Cl^-$ under varied conditions of electrospray ionization and matrix-assisted laser desorption/ionization (MALDI) are described and systematized. It is shown that qualitative changes in the electrospray mass spectra of ethonium occur upon a cone voltage increase from 10 V to 100 V, which are caused by the subsequent appearance and destruction of several primary ions: the intact dication Cat^{2+}, the dication-counterion cluster Cat^{2+}•Cl^- and$[Cat - H]^+$ and $[Cat - CH_3]^+$ ions. Novel experimental evidence of survival of the gas-phase dication Cat^{2+} with the shortest possible distance of *ca* 4 Å between the quaternary nitrogen atoms provided by two CH_2 groups and Cat^{2+} fragmentation with preservation of the doubly charged state of the fragments are revealed under soft electrospray conditions. The interpretation of the MALDI mass spectrum is made taking into account the formation of a salt of the bisquaternary ammonium base and 2,5-dihydroxybenzoic acid, which results in the absence of any chlorine-containing ions in the mass spectra and a fragment ion distribution that is different from that observed under electrospray ionization conditions. The main mass spectral features revealed for ethonium may aid in the identification of other types of bisquaternary ammonium compounds.

Keywords: Bisquaternary ammonium compounds; Ethonium; Electrospray; Matrix-assisted laser desorption/ionization; Organic dication

Introduction

Widening of the scope of mass spectrometry from straightforward identification of compounds to studies of interactions in supramolecular assemblies of fragile biomolecules and to biological imaging brings to life new requirements to the mass spectra obtained by soft ionization techniques. The trivial task of determining the "fingerprint" mass spectrum characteristic of an individual compound can be significantly complicated by the chemical reactivity, lability, and degradability of some types of compounds, which are reflected in their mass spectra. High sensitivity of such compounds to variation of external conditions leads to noticeable qualitative differences in their mass spectral patterns obtained not only by different ionization/desorption methods, but on variation of experimental parameters in the framework of a single ionization technique as well. In the present work, we report a case of a representative bisquaternary ammonium compound (BQAC), ethonium (Scheme 1), which produces qualitatively different mass spectral patterns under different mass spectrometric conditions (Scheme 1)

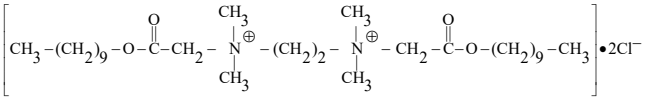

Scheme 1: Structure of the bisquaternary ammonium salt ethonium.

Bisquaternary ammonium salts, including gemini surfactants and bolaforms, find many useful applications as disinfectants, herbicides, industrial detergents and emulsifiers, chemotherapeutic agents, components of various pharmacological and cosmetic formulations, building blocks of nanosized materials, and others [1-7]. Surfactants based on BQACs used as chemotherapeutic antimicrobial agents [6-9] possess such advantages as low toxicity towards humans, practical absence of mutagenic effects, and slow microbial resistance development. Ethonium is used as an antimicrobial agent for wound healing in surgical and stomatological practice [10,11]. In our previous molecular biophysical studies [12-14] it was shown that the molecular mechanisms of action of ethonium and similar membranotropic agents involve non-covalent intermolecular interactions with phospholipids of microbial cell membranes. To continue investigations on the interactions of ethonium with its molecular targets by means of soft ionization mass spectrometry [14] knowledge of its mass spectrometric characteristics is required. In this context, the aim of the present work was to systematize the experimental conditions-dependent features of electrospray (ESI) and matrix-assisted laser desorption/ionization (MALDI) mass spectra of ethonium. A brief summary of basic information on the peculiarities of mass spectra of BQACs, obtained earlier by various techniques [15-31] and relevant to the subject of the present investigation, is as follows. The main types of primary ions expected in the soft ionization mass spectra of BQACs are the salt dication Cat^{2+} and its cluster with the salt anion Cat^{2+}•$Anion^-$. Doubly-charged ions are a rarity in liquid secondary ion mass spectrometry (SIMS), fast atom bombardment (FAB), laser desorption/ionization (LDI), and MALDI, but are detected under field desorption (FD) and

***Corresponding author:** M.V. Kosevich, B. Verkin Institute for Low Temperature Physics and Engineering of the National Academy of Sciences of Ukraine, Lenin Avenue 47, 61103 Kharkov, Ukraine, Tel: +(380)-57-340-22-23; E-mail: mvkosevich@ilt.kharkov.ua

Received August 25, 2015; **Accepted** September 05, 2015; **Published** September 08, 2015

Citation: Pashynska VA, Kosevich MV, Gomory A, Vekey K, Claeys M, et al. (2015) Variable Electrospray Ionization and Matrix-Assisted Laser Desorption/Ionization Mass Spectra of the Bisquaternary Ammonium Salt Ethonium. Mass Spectrom Purif Tech 1: 103. doi:10.4172/2469-9861.1000103

ESI conditions. The stability of the dication Cat^{2+}, and, consequently, its abundance in the mass spectra, is determined by structural parameters of Cat^{2+} such as the distance between the two quaternary nitrogen atoms. It is believed that the distance-dependent Coulombic repulsion between two positive charges is the main driving force for dication fragmentation via charge separation or charge elimination. The extent of so-called dequaternization leading to the transformation of quaternary groups to tertiary amines, which is similar to the main thermal degradation pathway of quaternary compounds, can be considered as a measure of the thermal excitation acquired by the BQAC under given conditions. Under ESI conditions the mass spectral pattern of a BQAC depends strongly on such a parameter of the electrospray ion source as the cone voltage (CV) (called also nozzle-skimmer potential or orifice potential) [28,31]. Usually, at low CV values the salt dication Cat^{2+} dominates, while at higher CV it is destroyed and replaced by the dication-counterion cluster Cat^{2+}•$Anion^-$ [26-28,31]. Since the pathways of fragmentation of Cat^{2+} and Cat^{2+}•$Anion^-$ are different, the spectra obtained at low and high CV values may appear as spectra of two different compounds [31].

In our more recent quantum chemical modeling of alkylammonium BQACs [29,32,33] some new features of the electronic structure of quaternary compounds have been revealed. It was shown that there is no single positive charge located at the quaternary nitrogen atom but that the charge is smeared over the hydrogen atoms of the CH_3 and CH_2 groups adjacent to the quaternary nitrogen. Due to this phenomenon the density of the delocalized charge becomes lower (as compared to the single unit charge), which, in turn, decreases the magnitude of the electrostatic repulsion between the alkylammonium groups and provides a higher stability to the BQAC dication. The stabilization of the BQAC dication in the gas phase was further supported in SIMS [30] and ESI [31] studies of the BQAC decamethoxinum whose main structural distinctions from ethonium are in a much longer spacer of ten CH_2 groups and menthyl rings in the side chains. Namely, along with the expected observation of the Cat^{2+} stability due to the relatively large distance (*ca* 14 Å [29]) between the quaternary nitrogen atoms, an unexpected feature of preferential Cat^{2+} fragmentation with preservation of the doubly-charged state of the fragments has been revealed. Further, stable gas-phase noncovalent clusters of two tetramethyl ammonium (TMA^+) cations which model two quaternary sites of BQAC with the Cl^- counterion were produced by soft ionization techniques [33]. This demonstrates that the repulsion between two closely located $N^+(CH_3)_4$ cations is not sufficient for their separation even in a noncovalent complex.

As for the MALDI technique, the necessity to account for the effect of possible chemical reactions of the 2,5-dihydroxybenzoic acid (DHB) matrix compound with basic analytes on the mass spectra has been demonstrated [34]. In particular, for quaternary ammonium salts it was proved that the competitive substitution of an inorganic anion of the salts by organic $(DHB - H)^-$ anion in the course of sample preparation leads to formation of a new salt Cat^+•$(DHB - H)^-$ or $(Cat^{2+}$•$2(DHB - H)^-$ ion) [34]. Due to this effect the MALDI mass spectra contain the latter new salt ion species and are characterized by ions related to the cation of the initial salt in the positive ion mode and $[DHB - H]^-$ anions in the negative ion mode [34,35].

In the present study of ethonium by ESI and MALDI techniques some additional novel features are revealed. The intact dication Cat^{2+} is detected under ESI conditions for the BQAC with the minimal possible distance provided by two methylene groups between the two quaternary nitrogen atoms. Moreover, the fragmentation of this dication is observed with preservation of the doubly-charged state of its fragments. Qualitative changes in the ethonium ESI mass spectral pattern with CV increase are revealed and explained by the consecutive appearance and destruction of at least three types of primary ions. For MALDI the effect of formation of the salt consisting of bisquaternary ammonium base and DHB acid on the MALDI mass spectral pattern is confirmed.

Materials and Methods

ESI mass spectra were obtained with a triple quadruple (QqQ) Micromass Quattro micro mass spectrometer (Waters, Manchester, UK). The electrospray ion source temperature was 120°C (393 K), while the desolvation temperature was 200°C. The capillary potential was 3.5 kV. For obtaining the dependences of the ESI mass spectral pattern on cone voltage (CV) the latter was varied from 10 V to 100 V with a step of 10 V. Data acquisition and processing were performed using MassLynx 4.1 software (Waters, Manchester, UK).

Collision-induced dissociation (CID) measurements were performed using an Autospecoa- TOF mass spectrometer (Micromass, Manchester, UK) which was equipped with an ESI ion source. The instrument was comprised of a double-focusing stage of *EBE* configuration coupled to an orthogonal acceleration time-of flight (oaTOF) analyzer for MS/MS experiments. Nitrogen was used both as bath gas (100°C; 250 L/h) and as nebulizing gas (15 L/h). The ESI source was operated at 4 kV. CID spectra were obtained at a laboratory frame energy (E_{lab}) of 400 eV using Xe as collision gas and by reducing the precursor ion beam to 70% of its original value Data acquisition and processing were performed using OPUS V3.1X software. The 10^{-4} M analyte solutions in methanol were infused into the mass spectrometer by a syringe pump (Harvard Apparatus, South Natick, MA, USA), employing a 500 μL syringe, at a constant flow rate of 5 μL/min.

MALDI experiments were performed using an Autoflex II time-of-flight mass spectrometer (Bruker Daltonik GmbH, Germany) equipped with a nitrogen laser (wavelength 337 nm). Positive and negative ion spectra were recorded in the linear mode with ion acceleration up to 20 keV with the delayed extraction time set to 20 ns. The energy of the laser beam was attenuated down to 40% of the full laser power. The digitizer acquisition rate was 2 GS·s^{-1}. Spectra were recorded by summing 100 laser shots. Data were processed using the acquisition software FlexControl 2.2 (Bruker Daltonik GmbH, Germany). For sample preparation equal volumes of 10^{-2} M ethonium and saturated DHB solutions in deionized water were mixed in an Eppendorf vial. A 1 μL droplet of the mixture was deposited on the standard metal sample holder and dried at ambient conditions.

Ethonium ($C_{30}H_{62}N_2O_4Cl_2$, monoisotopic molecular mass 584.4 Da) was synthesized at the Institute of Organic Chemistry of the National cademy of Sciences of Ukraine (Kiev, Ukraine). Methanol was acquired from Reanal (Budapest, Hungary). 2,5- dihydroxybenzoic acid (DHB) was purchased from Sigma-Aldrich (St. Louis, MI, USA).

Results and Discussion

Electrospray mass spectra

The structure of ethonium (Scheme 1) can be schematically represented as $Cat^{2+} \bullet 2Cl^-$ or $[R_1-(CH_3)_2N-R_2-N(CH_3)_2-R_1]^{2+} \bullet 2Cl^-$ where R_2 is a short polymethylene chain $(CH_2)_2$ spacer (linker) between two quaternary nitrogen atoms and the two side substituents R_1 are composed of rather long polymethylene chains CH_3-$(CH_2)_9$-(marked further as "terminal" R_t radicals) attached by ester linkages.

The pattern of electrospray mass spectra of ethonium dissolved

in methanol shows a strong dependence on CV variation (Figure 1a-1h). It is remarkable that the mass spectral pattern not only reflects the expected quantitative changes consisting in an increase of fragmentation (in-source decay) on increase of energy of primary ions collisions with the residual gas, but also undergoes qualitative transformations. It can be seen that the ESI mass spectral patterns of ethonium look qualitatively different at a CV of 10 V (Figure 1a), 30 V (Figure 1c), and CV ≥ 50 V (Figure 1e-1h). In general, the qualitative changes observed on CV increase can be attributed to the consecutive appearance and destruction of several primary (precursor) ions: the intact dication Cat^{2+} (*m/z* 257) (occurring in the CV range from 10 V to 40 V), the dication-counterion cluster $Cat^{2+}\bullet Cl^-$ (*m/z* 549/551) (CV from 10 V to 70 V), and two ions $[Cat - H]^+$ (*m/z* 513) and $[Cat - CH3]^+$ (*m/z* 499) (CV from 30 V to 100 V).

The first type of the mass spectral patterns is determined by the ethonium dication Cat^{2+} and its fragmentation. At low CV values below 10 V (Figure 1a) the peak of the intact dication Cat^{2+} (*m/z* 257) is the most abundant one in the mass spectrum. This behavior is consistent with the known preference of preservation of multiply charged species at low CV [28], but it is unexpected taking into account the small distance (of about 4 Å [12,29]) between the quaternary nitrogen atoms, which is believed to be the cause of a dramatic destabilization of dications. The fragmentation of Cat^{2+} is absent at a CV of 10 V. On gradual increase of CV two interconnected processes are observed: the decrease of Cat^{2+} abundance down to its practical disappearance at a CV of 40 V (Figure 1d) and consecutive appearance, growth and decline of its fragments in the CV range from 20 V to 50 V (Figure 1b-1e). The main pathways of the Cat^{2+} fragmentation, confirmed by CID data (see "Experimental"), consist in the loss of one or two terminal radicals R_t (141 Da) accompanied by hydrogen transfer: (Equation 1)

$$Cat^{2+} \rightarrow [Cat - R_t + H]^{2+} + (R_t - H) \quad \text{m/z 187} \qquad (1)$$

$$Cat^{2+} \rightarrow [Cat - 2R_t + 2H]^{2+} + 2(R_t - H) \quad \text{m/z 117} \qquad (1')$$

The pathway (1) of elimination of one R_t radical dominates at a CV of 20 V (Figure 1b) and is gradually replaced by the loss of two R_t radicals (1') on further CV increase up to 30 V (Figure 1c). The fragment $[Cat - 2R_t + 2H]^{2+}$ becomes the most abundant one in the spectrum at a CV of 40 V (Figure 1d) and almost disappears at a CV of 50 V (Figure 1e). Thus, it can be concluded that the ethonium bare dication and its fragments are completely destroyed at a CV of 50 V. The low CV peak observed at *m/z* 257, which corresponds to the doubly charged ion and contains proper isotopic satellites at half mass values (Figure 2a), is replaced by a peak at *m/z* 256 corresponding to a singly charged ion (to be interpreted below) starting from a CV of 40 V (Figure 2b). It is remarkable that the products of fragmentation of the dication Cat^{2+} ((1) and (1')) preserve the doubly charged state. A peculiar fragment observed at *m/z* 373 at the lowest CV only (Figure 2b) corresponds the loss of R_t^+; to be singly charged it must have a zwitterionic structure. It should be noted also that several rather exotic clusters (not shown in the mass range of Figure 1), which demonstrate a trend of self-assembling of the ethonium surfactant, are present at a low CV and disappear on its increase, as, for example, the singly charged aggregate $2Cat^{2+}\bullet 3Cl^-$ (monoisotopic mass 1131.8 Da, the most abundant peak in the group at *m/z* 1133.8) and a doubly charged one $3Cat^{2+}\bullet 4Cl^-$ (monoisotopic mass 1683.3 Da, the most abundant peak in the doubly charged ion group at *m/z* 842.6). The second group of changes in the mass spectral pattern is connected with the transformations of the $Cat^{2+}\bullet Cl^-$ (*m/z* 549/551) ion. This ion appears in the mass spectra at the lowest CV value and starts to decrease from a CV of 20 V on (Figure 1b) because of the decomposition of the $Cat^{2+}\bullet Cl^-$ ion and is practically complete at a CV approaching 70 V (Figure 1g). In the CV range from 20 V to 40 V the mass spectra are a superposition of the fragments of both Cat^{2+} and $Cat^{2+}\bullet Cl^-$ precursors. The main pathway of fragmentation known for dication-anion clusters of BQACs is the so called dequaternization process, which is similar to the pathway of thermal degradation of $Cat^+\bullet Cl^-$ and $Cat^{2+}\bullet 2Cl^-$ salts [15,16,24,29,30]. The dequaternization via dealkylation of alkylammonium ion consists in the elimination of any substituent at a quaternary nitrogen $^-CH_3$ (2), R_1 (2'), and R_1-$N(CH_3)_2$-R_2 (2") in the present case – in combination with the Cl^- anion with formation of a neutral tertiary nitrogen: (Equation 2)

$$Cat^{2+}\bullet Cl^- \rightarrow [Cat - CH_3]^+ + CH_3Cl \quad \text{m/z 499} \qquad (2)$$

$$Cat^{2+}\bullet Cl^- \rightarrow [R_1\text{-}N(CH_3)_2\text{-}R_2\text{-}N(CH_3)_2]^+ + R_1Cl \quad \text{m/z 315} \qquad (2')$$

$$Cat^{2+}\bullet Cl^- \rightarrow [R_1\text{-}N(CH_3)_2\text{-}R_2\text{-}Cl]^+ + (CH_3)_2\text{-}N\text{-}R_1 \quad \text{m/z 306/308} \qquad (2")$$

The chlorine attack at the N-C bond with the R_2 spacer leads to a pair consisting of a neutral $(CH_3)_2$-N-R_1 product and a chlorinated charged fragment $[R_1\text{-}N(CH_3)_2\text{-}CH_2\text{-}CH_2\text{-}Cl]^+$ (*m/z* 306/308) (2"). Elimination of one charge can also be achieved *via* elimination of a HCl neutral leading to formation of a [Cat – H]+ (*m/z* 513) ion: (Equation 3).

$$Cat^{2+}\bullet Cl^- \rightarrow [Cat - H]^+ + HCl \qquad (3)$$

Analysis of CID data aimed at supporting the fragmentation pathways observed for the $Cat^{2+}\bullet Cl^-$ precursor (Figure 3). Interestingly, the CID experiments reveal an unexpected feature in that the product of the loss of the smallest substituent (pathway (2)), known as the preferential route for alkylammonium compounds [15], is absent, as well as that of the reaction (3). There is a relatively small contribution of the products of pathways (2') and (2"), and a more noticeable contribution of fragments with *m/z* 270 and 242. The latter ions appear to be the main CID products of the $[Cat - H]^+$ precursor as well. In this connection, it can be suggested that the $[Cat - H]^+$ product ion of the reaction (3) occurring under CID appears to be highly excited and further undergoes a more deep fragmentation resulting in the fragments with *m/z* 270 and 242. Since the most probable location of the Cl^- anion in the $Cat^{2+}\bullet Cl^-$ cluster is in the vicinity of the positively charged alkylammonium groups, the loss of HCl must destabilize the bonds adjacent to nitrogen atoms resulting in cleavage of N-C bonds [24] and release of either $[R_1\text{-}N(CH_3)_2\text{-}CH{=}CH_2]^+$ (*m/z* 270) or $[CH_2{=}N(CH_3)\text{-}R_1]^+$ (*m/z* 242) singly charged fragments and their neutral counterparts. The abundance of the fragment ions at *m/z* 270 and 242 increased significantly in relation to that of the $Cat^{2+}\bullet Cl^-$ precursor in the CV range from 20 V to 70 V (Figure 1b-1g).

The above described discrepancies between the CID and the expected in-source decay of $Cat^{2+}\bullet Cl^-$ can be explained by a difference in the precursor species generated in the two methods: under CID the bare isolated precursor is subjected to collisions with the collision gas, while precursor-solvent clusters can be present in the skimmer-nozzle space and produce specific dissociation products on collisions with the residual gas. The $[Cat - H]^+$ fragment ion produced from the $Cat^{2+}\bullet Cl^-$ precursor via pathway (3) under CID may be instable and undergo secondary fragmentation as described above. The $[Cat - H]^+$ species produced as primary ions on the desolvation of the analyte-solvent clusters under in-source decay may be more stable in comparison with the identical fragments of CID origin due to "desolvational cooling". Possible origins of the $[Cat - H]^+$ ion involving analyte-solvent clusters has been discussed earlier [25,31,36]. The absence of a $[Cat - CH_3]^+$ product ion in the CID mass spectra of the $Cat^{2+}\bullet Cl^-$ precursor is not clear; it can be tentatively suggested that a rather short R_2 spacer

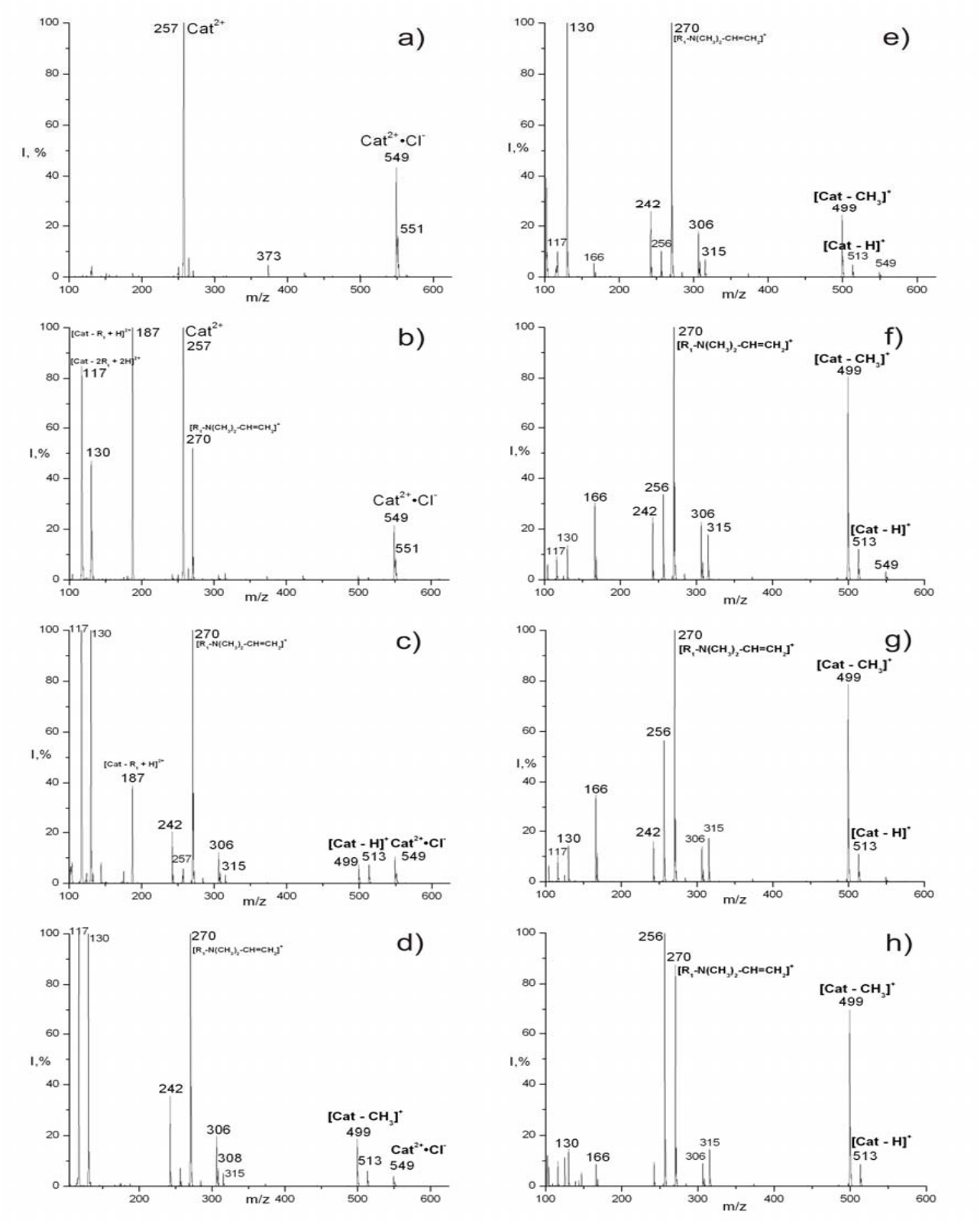

Figure 1: Electrospray ionization mass spectra of ethonium obtained on cone voltage variation: a) 10 V; b) 20 V; c) 30 V; d) 40 V; e) 50 V; f) 60 V; g) 70 V; h) 100 V.

is in some way responsible for the suppression of pathway (2). The appearance and growth of the $[Cat - CH_3]^+$ ion in the ESI mass spectra at a CV higher than 30 V leads us to suggest that it is formed upon decomposition of the analyte-solvent clusters as well, where the solvent molecules may assist the separation of CH_3Cl from the $Cat^{2+}\bullet Cl^-$ precursor. The growth of abundances of $[Cat - H]^+$ and $[Cat - CH_3]^+$ ions with increase of CV, which facilitates desolvation, supports a desolvation origin of these ions. Thus, the third group of changes of the mass spectral pattern at higher CV values is related to $[Cat - H]^+$ and $[Cat - CH_3]^+$ precursor ions originating directly from the analyte-solvent clusters. Both ions appear at a CV of 30 V (Figure 1c) and survive up to a CV of 100 V (Figure 1h). Products of $[Cat - H]^+$ fragmentation with *m/z* 270, 242 continue to contribute to the abundance of the corresponding peaks at a CV higher than 80 V, where the $Cat^{2+}\bullet Cl^-$ precursor is already practically destroyed. In accord with CID data the most abundant fragment of $[Cat - CH_3]^+$ precursor is at *m/z* 256; it can be formed via cleavage of a N-R_2 bond. This fragment accompanies its precursor from a CV of 40 V on (Figure 1d), but grows significantly starting from a CV of 60 V (Figure 1f) indicating an increase of the precursor decomposition. Note, that the absence of a primary fragment $[Cat - CH_3]^+$ (2) in the CID mass spectrum of the $Cat^{2+}\bullet Cl^-$ precursor (Figure 3) agrees with the practical absence of its secondary fragment at *m/z* 256. More deep fragmentation of practically all fragment ions consists in the loss of a (R_1 - H) moiety similar to the primary reaction (1). The loss of 140 Da from the precursors at *m/z* 270, 256 and 242 results in the fragments at *m/z* 130, 116 and 102, respectively. The chlorine containing precursor ion at *m/z* 306/308 (2") produces the chlorine-containing fragment at *m/z* 166/168. It should be noted that in ESI experiments with ethanol as a solvent the ratio of abundances of Cat^{2+} and $Cat^{2+}\bullet Cl^-$ ions of ethonium are much smaller than in the case of methanol solvent at the same low CV values. A similar effect was observed earlier for decamethoxinum [14] and other BQAC [27,28], and is explained by a difference in ion pair stability in solvents with different polarity [27]. The existence of several different types of primary ions and their characteristic fragments, cation-anion clustering, and strong dependence on the CV applied are factors that may hamper detection of ethonium in a sample by means of ESI. Therefore, in further ESI studies of ethonium interactions with biomolecules, low CV values necessary for survival of the ethonium dication that enable the observation of noncovalent complexes involving the dication need to be applied.

MALDI mass spectrum

The MALDI mass spectrum of ethonium obtained by the common method of drying a drop of an aqueous solution of ethonium and the DHB matrix mixture is presented in Figure 4. It can be seen that the MALDI mass spectral pattern does not match with any of the ESI patterns obtained under varying CV values.

The most abundant precursor ion in the upper mass region of the MALDI mass spectra is $[Cat - H]^+$ (*m/z* 513). Two other intense peaks at *m/z* 242 and 270 correspond to its characteristic fragments, as evidenced by the CID data for the gas-phase $[Cat - H]^+$ ion obtained under ESI conditions. There is also a low abundant precursor $[Cat - CH^3]^+$ (*m/z* 499) ion with its characteristic fragment at *m/z* 256. The most intense peak in the mass spectrum at *m/z* 315 corresponds to the fragment $[Cat - R_1]^+$. Chlorine-containing ions are not detected, nor is Cat^{2+} observed. The absence of the intact dication Cat^{2+} was expected in connection with the rarity that multiply charged species survive under ordinary MALDI conditions [37,38].

The observed MALDI pattern of ethonium is consistent with the features of MALDI mass spectra of quaternary ammonium compounds obtained with DHB matrix, which were reported in our previous paper [34]. In accord with these findings, a chemical substitution reaction of the Cl^- anion of the quaternary ammonium salt ethonium for the $(DHB - H)^-$ anion of organic acid DHB must take place in water solution at the stage of sample preparation. As a result, a new salt $Cat^{2+}\bullet 2(DHB - H)^-$ (instead of the initial $Cat^{2+}\bullet 2Cl^-$) is precipitated upon sample drying and the mass spectrum obtained corresponds to this new compound. The MALDI mass spectra of ethonium satisfy completely this rule: formation of the new salt composed of Cat^{2+} and $(DHB - H)^-$ leaves no space for $Cat^{2+}\bullet Cl^-$ and its chlorine-containing fragments; protonated and cationized DHB molecules have a rather low abundance in the positive ion mode (Figure 4), but there is an abundant $[DHB - H]^-$ (*m/z* 153) anion in the negative ion mode.

The absence of the $Cat^{2+}\bullet(DHB - H)^-$ ion in the MALDI mass spectrum (Figure 4) points to a low stability of the ethonium dication cluster with the relatively large organic anion in the gas phase. At the same time the presence of the $[Cat - H]^+$ ion confirms our suggestion made above on the basis of CID of electrospray-generated ions concerning the origin of $[Cat - H]^+$ ion from the analyte-solvent (or DHB in the present case) clusters. Indeed, under MALDI conditions the release of the ethonium dication to the gas phase from the laser-sputtered material necessitates its "desolvatation" from both DHB anions and residual neutral DHB matrix molecules. The latter are the only, in the sample available, candidates for a proton subtraction from the dication in the course of $[Cat - H]^+$ formation.

The $[Cat - CH_3]^+$ ion and abundant $[Cat - R_1]^+$ ions can be formed following decomposition of precursors containing Cat^{2+} and the $(DHB - H)^-$ organic anion in dealkylation reactions similar to (2) and (2') proposed for dequaternization of the Cat^{2+} clusters with the inorganic Cl^- anion. In this context, MALDI data obtained on decamethoxinum [34] revealed a similar noticeable increase of the relative abundance of the $[Cat - R_1]^+$ fragment of decamethoxinum under MALDI with DHB matrix in comparison with other techniques. Furthermore, an increased abundance of the $[Cat - R_1]^+$ ion was observed in the liquid SIMS mass spectra of an ethonium-sodium dodecylsulfate (SDS) mixture, in which the precursor consisting of the ethonium dication and the SDS anion was present [39]. This set of data allows us to assume that the pathway of elimination of R_1 is strongly enhanced by the preceding clustering of the dication with organic anions as compared with the pathway (2') of R_1Cl elimination for the ethonium-chlorine cluster.

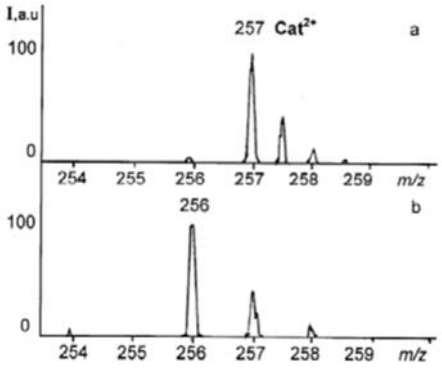

Figure 2: Change of types of positive ions of ethonium, recorded in the electrospray mass spectra in the region of 256-257 Da at different cone voltage values: a) CV=30 V, Cat^{2+} doubly charged ion; b) CV=40 V, *m/z* 256 singly charged fragment.

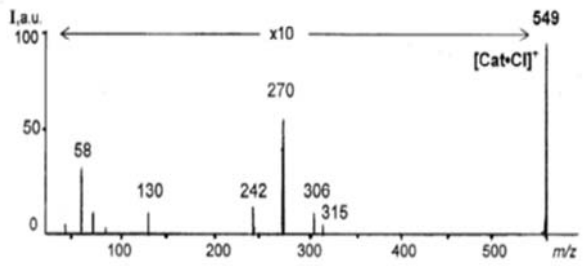

Figure 3: Collision induced dissociation mass spectrum of Cat^{2+}•Cl^- precursor ion of ethonium. Collision gas is Xe.

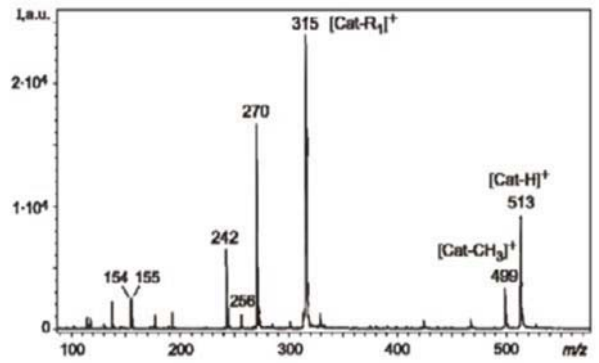

Figure 4: MALDI mass spectrum of ethonium-DHB system.

It may be concluded that the absence of the Cat^{2+} and chlorine-containing ions in the MALDI mass spectra of ethonium, as well as its interactions with the DHB matrix, complicates *de novo* identification of a given compound on the basis of its conventional MALDI mass spectrum only. Interaction of ethonium with organic acids in the complex mixtures may influence its MALDI mass spectral pattern as well. At the same time the $[Cat - H]^+$ ion and a set of abundant peaks of fragments at *m/z* 242, 270, 315 and 499 in the MALDI mass spectrum can support the presence of the ethonium dication in the sample.

Comparison of data for ethonium and decamethoxinum

It is of interest to compare the ESI mass spectra of ethonium with those obtained earlier for the BQAC decamethoxinum [12,29,31,35,39], which differs from ethonium by a longer R_2 spacer composed of ten CH_2 groups and by R_t radicals comprised by menthyl rings. The idea of comparison is connected with the search of distinctions in the mass spectra caused by differences in the so-called inter-charge distance [16-19], that is the distance between the two quaternary groups of the BQAC, which was estimated as 14 Å and 4 Å for decamethoxinum and ethonium, correspondingly [12,29].

The dependence of the ESI mass spectra of decamethoxinum on CV [31] is qualitatively similar to that revealed for ethonium in the present work. However, the specific quantitative changes in the spectra occur in different CV ranges for the two compounds. The dication Cat^{2+} of decamethoxinum, appearing at the lowest CV, begins to fragment at a higher, as compared with ethonium, CV value of about 75 V (*vs* 20 V for ethonium). The Cat^{2+} of decamethoxinum and its fragments disappear from the spectra at a CV above 100 V *vs* 50 V for ethonium. The Cat^{2+}•Cl^- cluster of decamethoxinum survives up to the highest applied CV of 225 V, while it vanishes at a CV of 70 V for ethonium. The higher CV-dependent energy required for destruction of the dication of decamethoxinum points to its higher stability in comparison with that of ethonium. This behavior is expected on the basis of literature data describing the decrease of stability of the dications of BQACs with decrease of the intercharge distance in the dications [16-19].

An unexpected feature of the ESI mass spectra of ethonium is the survival of its dication with the shortest possible distance between two quaternary nitrogen atoms provided by two CH_2 groups only. Another uncommon feature is the preservation of the doubly charged state of the fragments in pathways (1) and (1') of the Cat^{2+} decay, characteristic of both ethonium and decamethoxinum. In the early literature on BQACs the main driving force leading to destabilization of the gas-phase dications was believed to be the Coulomb repulsion between two positive charges, according to which the main pathway of Cat^{2+} fragmentation should be "charge separation" or "charge minimization", leading to a complete destruction of dications with a small inter-charge distance [16-19]. In this connection, the occurrence of the decay pathways (1) and (1') for the decamethoxinum dication was rather surprising [29,31], and for the ethonium dication it was even more surprising. Among possible reasons of the BQAC dication stabilization in the gas phase is the effect of delocalization (smearing) of the unit positive charge over the hydrogen atoms of the alkylammonium quaternary groups [29], mentioned in the introduction, which can reduce the electrostatic repulsion as compared to that between two localized point charges.

It is worth noting that the fission of the labile ether linkages (1) and (1') observed for the gas-phase dications of ethonium and decamethoxinum follows the direction of their biodegradation in that it appears to be more favored than that involving "charge separation". As to biodegradation, the drug design of antimicrobial agents of this type includes the incorporation of the ester linkage into the structure of their dications to allow for their proper metabolization in the living organism [40,41], an approach that is similar to that utilized currently in the design of some biodegradable polyesters [42].

Internal energy dependence on cone voltage

To obtain insights into the survival of the intact ethonium dication under ESI conditions and to evaluate the contribution of the Coulomb repulsion to the destabilization of the dication, the internal energy acquired by Cat^{2+} at different CV values has been estimated. It is known that the extent of in-source fragmentation under ESI is governed by the internal energy acquired by an ion on its collisions with the residual gas in the orifice-skimmer region. An approach to the quantitative evaluation of the dependence of the internal energy of ions on CV was developed in a number of works [43,44] for small organic molecules and peptides. Evaluation of large sets of ESI data obtained with instruments of the same design as that used in the present work (Quattro Micromass) resulted in an empirical equation for the mean internal energy $<E_{int}>$ [44]:

$$<E_{int}> = [405 \times 10^{-6} - 480 \times 10^{-9}(DOF)](CV)T + E_{therm}(T) \qquad (4)$$

where (CV) is the cone voltage value, T (in Kelvin scale) is the source temperature, DOF is the number of degrees of freedom (determined as 3N-6, where N is the number of atoms in the ion), and $E_{therm}(T)$ is the mean internal energy corresponding to the source temperature at zero CV value. The authors of the equation (4) [44] stressed that the values of the numerical parameters (405×10^{-6} and 480×10^{-9}) may depend on pressure variation in the ion source. Since in the framework of the present investigation we were interested in comparing the relative internal energies of certain ions rather than in measuring their exact

values, we have used equation (4) as it is, assuming slight variations of standard pressure values in the instrument settings.

We have applied the equation (4) to estimate the dependence of internal energy of singly and doubly charged ions of ethonium and decamethoxinum on CV value. The value of $E_{therm}(T)$ at the source temperatures of 300 K and 393 K were derived from the values tabulated in the paper [45] on the base of calculations made by *MassKinetics* software [46]. The results for the ethonium dication Cat^{2+} (98 atoms, DOF=288) and $[Cat - H]^+$ cation (97 atoms, DOF=285), as well as for the decamethoxinum dication Cat^{2+} (118 atoms, DOF=348) and $[Cat - H]^+$ cation (117 atoms, DOF=345) are presented in Figure 5a and 5b, respectively. The trend of the plot for the singly charged cluster $Cat•Cl^+$ (not shown) is similar to that of the $[Cat - H]^+$ ion.

The numerical values of the mean internal energy obtained by the dications of ethonium and decamethoxinum at several CV values, which are connected with the qualitative changes in the ESI mass spectra patterns of the two compounds, are presented in Table 1.

It should be reminded that, although the mass values of the dication Cat^{2+} and the singly charged ion $[Cat - H]^+$ differ in one atomic mass unit only, the kinetic energy gained by the dication during its movement in the electric field, being proportional to the charge of the ion, is twice as high than that of the singly charged ions. This results in different slopes of the dependences for Cat^{2+} and $[Cat - H]^+$ (or $Cat•Cl^+$) in the plots in Figure 5 and explains mechanistically, why the dication is destroyed at lower CV values than the mono-cations. For example, while the Cat^{2+} of ethonium obtains an internal energy of 12.5 eV (at 393 K) at a CV value of 50 V, sufficient for its complete decomposition, the $[Cat - H]^+$ and $Cat•Cl^+$ acquire the same energy at a CV of about 100 V.

It should be noted that equation (4) considers the number of the atoms (DOF) in the ion only and does not take into account any of its structural features. Nevertheless, the data of the plots in Figure 5 provides interesting information related to the above stated problem of the dication stability in dependence of the inter-charge distance. It can be seen that the internal energies gained by the dications of the two compounds with different inter-charge distance are comparable at the same CV values. However, the decomposition of Cat^{2+} of ethonium takes place at a CV value of 50 V, which is much lower than a CV of 100 V, required for complete decomposition of the decamethoxinum dication [31]. It can be assumed that the destruction of the ethonium dication at a CV value in 50 V lower than that required for the decamethoxinum dication is facilitated by the contribution of the energy of electrostatic repulsion between the two closely located quaternary groups of ethonium. Very rough estimates show that addition of Coulomb repulsion energy, evaluated for the ethonium dication as about 4 eV, to the internal energy of 9 eV, acquired by the dication at a CV of 50 V at 300 K (Table 1), gives a product comparable to the internal energy of 15.4 eV acquired by the decamethoxinum dication at the same conditions.

On the other hand this means that the Coulomb repulsion between the quaternary groups *per se* is not sufficient for fragmentation even in the dications with the smallest possible distance between the quaternary groups. The intact ethonium dication can be transferred to the gas phase under very gentle conditions, such as under electrospray at the minimal CV value, and it survives in the gas phase in the absence of additional excitation. The gain in internal energy of 3-4 eV acquired by the ethonium dication at the lowest CV value of 10 V is not sufficient to initiate fragmentation neither. It can be speculated on this basis, that the failure to detect the dications with small inter charge distance in other ionization/desorption techniques is caused by the acquisition of an internal energy higher than 10-15 eV by the sputtered/desorbed ions. In particular, the patterns of the ethonium mass spectra obtained under fast atom bombardment (FAB) [29] and liquid SIMS [29,39] conditions resemble the pattern obtained under electrospray at a CV of 40-50 V (Figure 1d and 1e) with the exception of fragments resulting from Cat^{2+} (which are never generated for ethonium under FAB/SIMS). Such a similarity supports the assumption that in both cases the

CV, V	Mean internal energy $<E_{int}>$,eV			
	Ethonium		decamethoxinum	
	300 K	393 K	300 K	393 K
10	2.7	4.1	2.8	4.3
20	4.3	6.2	4.2	6.1
50	9.0	12.5	8.4	11.7
100	16.8	23.0	15.4	21.1

Table 1: Mean internal energy $< E^{int} >$ of Cat^{2+} of ethonium and decamethoxinum at different cone voltage (CV) values and electrospray ion source temperatures T.

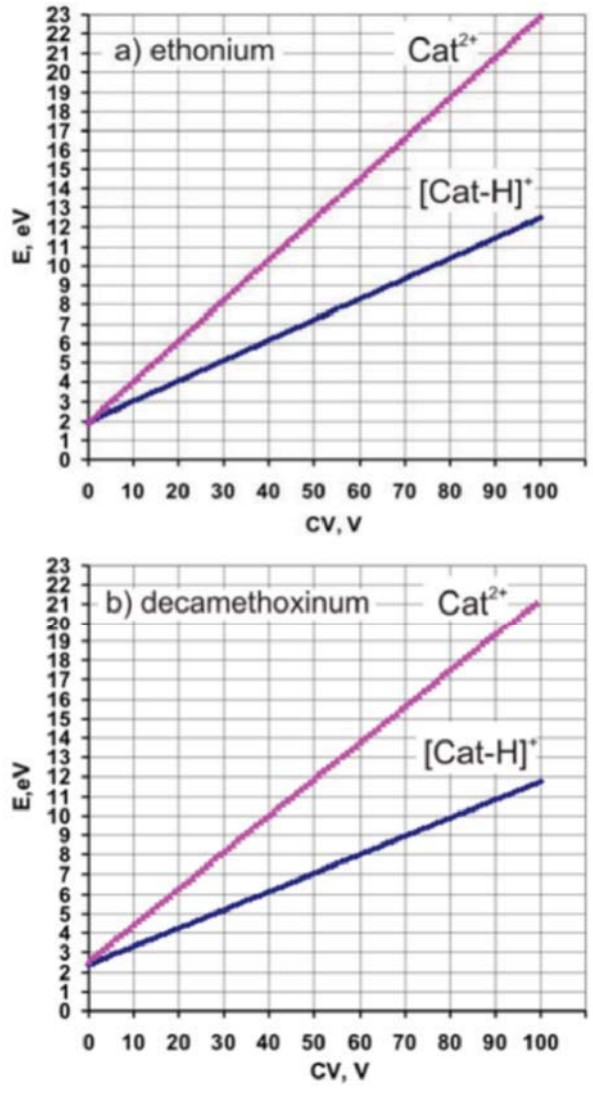

Figure 5: Dependence of mean internal energy $<E_{int}>$ on cone voltage (CV) value for doubly charged Cat^{2+} and singly charged $[Cat – H]^+$ ions of ethonium (a) and decamethoxinum (b). Ion source temperature is 393 K (+120°C).

mass spectral pattern is determined by the $Cat^{2+}•Cl^-$ primary ion and its characteristic fragments, while the Cat^{2+} does not survive. It can be tentatively suggested that the energy necessary for fragmentation of the $Cat^{2+}•Cl^-$ cluster obtained upon collisions with the residual gas under ESI at a CV of 40-50 V and upon collisions with the matrix molecules in the excited zone during the sputtering event under FAB/SIMS is of the same order of magnitude. The distinction between the electrospray mass spectral patterns generated upon significant CV increase (Figure 1f) and those observed for FAB/SIMS is consistent with the appearance of the new precursor ions and their fragments at more energetic conditions which are not achieved under FAB/SIMS.

As to the mono-cations of comparable mass, $Cat•Cl^+$ and $[Cat - H]^+$, which must gain comparable energies upon in-source decay, the destruction of $Cat•Cl^+$ at a CV value of 70 V and survival of $[Cat - H]^+$ at much higher CV values add support to the hypothesis of different sources of these two types of ions. Namely, we have proposed that the $[Cat - H]^+$ ion may originate from larger, presumably solvated species, which acquire the internal energy necessary for their decay with $[Cat - H]^+$ formation at relatively high CV values.

Conclusions

A representative of bisquaternary ammonium salts, ethonium, produces qualitatively different mass spectra in dependence of the experimental conditions applied. It is shown that the distinctions of electrospray mass spectral patterns in different cone voltage ranges are caused by subsequent appearance and destruction of several primary ions: the intact dication Cat^{2+} (occurring in the CV range from 10 V to 40-50 V), the dication-counterion cluster $Cat^{2+}•Cl^-$ (survival range 20 V-80 V), and two ions $[Cat - H]^+$ and $[Cat - CH_3]^+$ (30 V-100 V). In the overlapping CV ranges the spectra are a superposition of the spectra originating from several precursor ions. From the practical point of view, namely, for ethonium identification in mixtures and extracts using electrospray ionization, the established types of ions are to be looked for and monitored when applying different CV values.

From a basic point of view, the survival of the dication of noncyclic BQACs with the shortest possible distance between the quaternary nitrogen atoms is a nontrivial feature, as well as the dominant pathways of fragmentation of Cat^{2+} resulting in formation of the doubly charged fragments instead of more common singly charged "charge separation" products. We provide an explanation for this behavior on the basis of analysis of the mean internal energy acquired by the ethonium ions in the electrospray ion source at different CV values and structural features of the organic dication of ethonium. The higher internal energy acquired by a dication as compared to singly charged species allows to explain its destruction at comparably low CV values. At the same time the survival of Cat^{2+} means that the energy of Coulomb repulsion between the charged groups of the dication (*ca* 4 eV), which is believed to be the main driving force of its fragmentation, appears to be insufficient for the decomposition of the Cat^{2+} of ethonium at the lowest CV values. The failure of the dication to fragment in spite of the electrostatic repulsion is explained by the delocalization of the unit positive charges over the hydrogen atoms of alkylammonium quaternary groups. An additional gain in internal energy of about 10-12 eV is required for the fragmentation of the ethonium dication. It could be speculated on this basis that the absence of intact dications of BQACs with short inter-charge distance in other desorption/ionization techniques is caused by the acquisition of internal energy exceeding the threshold determined in the present work. A low internal energy enables the survival of the dication's doubly charged fragments $[Cat - R_t + 2H]^{2+}$ and $[Cat - 2R_t + 2H]^{2+}$ as well. The weakest bonds involved in the formation of the above fragments appear to be the ester bonds.

The mass spectral pattern of ethonium observed under MALDI with DHB matrix is in agreement with the revealed earlier formation of salts between an ammonium base and acidic matrix compound at the stage of sample preparation. Formation of such a salt hampers the observation of both diagnostic chlorine-containing precursor and fragment ions of the initial salt. Energetic conditions of the laser-generated plume do not permit the dication survival. Thus, the MALDI mass spectral pattern of ethonium does not match any of its electrospray patterns obtained in the whole range of CV values. The diagnostic ions which are to be looked for in the case of ethonium identification by MALDI are $[Cat - H]^+$ and $[Cat - CH_3]^+$ precursors and abundant fragments at *m/z* 242, 270, and 315.

The main mass spectral features revealed for ethonium may be applied to the identification of other types of BQACs compounds that are similar in structure.

Acknowledgements

The authors are grateful to the Inter-academy Cooperation Program between Ukrainian and Hungarian Academies of Sciences, to the Center for collective use of MALDI Autoflex II mass spectrometer of the National Academy of Sciences of Ukraine and to the University of Antwerp for the possibility of collecting ethonium mass spectra using different instruments, and to Dr. Laszlo Drahos for helpful discussion.

References

1. Menger FM, Keiper JS (2000) Gemini surfactants. Angew Chemie Int Ed 39: 1906-1920.
2. Shukla D, Tyagi VK (2006) Cationic gemini surfactants: a review. J Oleo Sci 55: 381-390.
3. Zana R (1996) Gemini (dimeric) surfactants. Current Opinion in Colloid Interface Science 1: 566-571.
4. Fuhrhop JH, Wang T (2004) Bolaamphiphiles. Chem Rev 104: 2901-2938.
5. Voronin MA, Gabdrakhmanov DR, Semenov VE, Valeeva FG, Mikhailov A S, et al. (2011) Novel bolaamphiphilic pyrimidinophane as building block for design of nanosized supramolecular systems with concentration-dependent structural behavior. ACS Appl Mater Interfaces 3: 402-409.
6. Vievsky AN (1990) Mechanisms of biological action of cationic surface-active compounds (Russ.). Moscow University, Moscow.
7. Vievsky A (1997) Cationic surfactants: new perspectives in medicine and biology. Tenside, Surfactants, Deterg 34: 18-21.
8. Kourai H, Yabuhara T, Shirai A, Maeda T, Nagamune H (2006) Syntheses and antimicrobial activities of a series of new bis-quaternary ammonium compounds. Eur J Med Chem 41: 437-444.
9. Sun XZ, Wang N, Cao D, Hu ZY, Mao P, et al. (2011) The antimicrobial activities of a series of bis-quaternary ammonium compounds. Chinese Chem Lett 22: 887-890.
10. Rogovaia EP, Garazha N N (2001) Clinical and microbiological efficiency of silard gelimmobilized ethonium in the treatment of periodontal inflammations [Article in Russian]. Stomatologiia 80: 18-21.
11. Babak OI, Kushnir IE (1996) Ethonium in the treatment of patients with gastric and duodenal peptic ulcers [Article in Russian]. Lik Sprava 3-4: 123-125.
12. Pashynskaya VA, Kosevich MV, Gomory A, Vashchenko OV, LisetskiLN (2002) Mechanistic investigation of the interaction between bisquaternary antimicrobial agents and phospholipids by liquid secondary ion mass spectrometry and differential scanning calorimetry. Rapid Commun Mass Spectrom 16: 1706-1713.
13. Vashchenko O, Pashynska V, Kosevich M, Panikarska V, Lisetski L (2011) Lyotropic mesophase of hydrated phospholipids as model medium for studies of antimicrobial agents activity. Mol Cryst Liq Cryst 547: 1845-1853.
14. Pashynska VA, Kosevich MV, Gomory A, Vekey K (2012) Investigation of formation of noncovalent complexes between antimicrobial agent ethonium with membrane phospholipids by electrospray ionization mass spectrometry. Mass-Spektrometria 9: 121-128.
15. Veith HJ (1983) Mass spectrometry of ammonium and iminium salts. Mass

Spectrom Rev 2: 419-446.

16. Ryan TM, Day RJ, Cooks RG (1980) Secondary ion mass spectra of diquaternary ammonium salts. Anal Chem 52: 2054-2057.
17. Hercules DM, Day RJ, Balasanmugan K, Dang TA, Li CP (1982) Laser microprobe mass spectrometry. Applications in structural analysis. Anal Chem 54: 280A-305A.
18. Dang TA, Day RG, Hercules DM (1984) Laser mass spectrometry of diquaternary ammonium salts. Anal Chem 56: 866-871.
19. Heller DN, Yergey J, Cotter RJ (1983) Doubly charged ions in desorption mass spectrometry. Anal Chem 55: 1310-1313.
20. Schmelzeisen-Redeker G, Rollgen FW, Wirtz H, Vogtle F (1985) Thermospray mass spectrometry of diazonium, di-, tri- and tetra-quaternary onium salts. Org Mass Spectrom 20: 752-756.
21. Aubagnac J-L, Gilles I, Calas M, Cordina G, Piquet G, et al. (1995) Fast atom bombardment, frit fast atom bombardment and electrospray ionization mass spectrometric study of organic salts $C^{2+}2X^{-}$: Matrix and anion effects. J Mass Spectrom 30: 985-992.
22. Evans CS, Startin JR, Goodall DM, Keely BJ (2001) Formation of gas-phase clusters monitored during electrospray mass spectrometry: a study of quaternary ammonium pesticides. Rapid Commun Mass Spectrom 15: 1341-1345.
23. Giuliani A, Debois D, Laprévote O (2006) Study of a bisquaternary ammonium salt by atmospheric pressure photoionization mass spectrometry. Eur J Mass Spectrom 12: 189-197.
24. Aimé C, Plet B, Manet S, Schmitter JM, Huc I, et al. (2008) Competing gas-phase substitution and elimination reactions of gemini surfactants with anionic counterions by mass spectrometry. Density functional theory correlations with their bolaform halide salt models. J Phys Chem B 112: 14435-14445.
25. Milman BL (2003) Cluster ions of diquat and paraquat in electrospray ionization mass spectra and their collision-induced dissociation spectra. Rapid Commun Mass Spectrom 17: 1344-1349.
26. Wang G, Cole RB (1995) Mechanistic interpretation of the dependence of charge state distributions on analyte concentrations in electrospray ionization mass spectrometry. Anal Chem 67: 2892-2900.
27. Wang G, Colecor RB (1996) Effects of solvent and counterion on ion pairing and observed charge states ofdiquaternary ammonium salts in electrospray ionization mass spectrometry. J Am Soc Mass Spectrom 7: 1050-1058.
28. Cole RB (1997) Electrospray ionization mass spectrometry: Fundamentals, instrumentation and applications. Wiley-Interscience, New York.
29. Pashynska VA, Kosevich MV, Gomory A, Szilagyu Z, Vekey K, et al. (2005) On the stability of the organic dication of the bisquaternary ammonium salt decamethoxinum under liquid secondary ion mass spectrometry. Rapid Commun Mass Spectrom 19: 785-797.
30. Sukhodub LF, Kosevich MV, Shelkovskii VS, Boriak VA, Volyianskii YuL, et al. (1990) Identification of bis-quaternary ammonium compounds using mild ionization mass spectrometry [Article in Russian] Antibiot Khimioter 35: 10-12.
31. Pashynska VA, Kosevich MV, Van den Heuvel H, Claeys M (2006) The effect of cone voltage on electrospray mass spectra of the bisquaternary ammonium salt decamethoxinum. Rapid Commun Mass Spectrom 20: 755-763.
32. Pahynska V, Kosevich M, Stepanian S, Adamowicz L (2007) Noncovalent complexes of tetramethylammonium with chlorine anion and 2,5-dihydroxybenzoic acid as models of the interaction of quaternary ammonium biologically active compounds with their molecular targets. A theoretical study. J Mol Struct: THEOCHEM 815: 55 62.
33. Pashynska V, Boryak O, Kosevich MV, Stepanian S, Adamovicz L (2010) Competition between counterions and active protein sites to bind bisquaternary ammonium groups. A combined mass spectrometry and quantum chemistry model study. Eur Phys J D 58: 287-296.
34. Kosevich MV, Boryak OA, Chagovets VV, Pashynska VA, Orlov VV, et al. (2007) “Wet chemistry” and crystallochemistry reasons for acidic matrix suppression by quaternary ammonium salts under MALDI conditions. Rapid Commun Mass Spectrom 21: 1813-1819.
35. Pokrovsky VA, Kosevich MV, Osaulenko VL, Chagovets VV, Pashynska VA, et al. (2005) Matrix-assisted laser desorption/ionization study of bisquaternary ammonium antimicrobial agent decamethoxinum in 2,5-dihydroxybenzoic acid. Mass-spektrometria 2: 183-192.
36. Wickens JR, Sleeman R, Keely BJ (2007) Adduction of solvent molecules by ions isolated within an ion trap mass spectrometer under atmospheric pressure ionization conditions. Rapid Commun Mass Spectrom 21: 2491-2496.
37. Karas M, Gluckman M, Schafe J (2000) Ionization in matrix-assisted laser desorption/ionization: singly charged molecular ions are the lucky survivors. J Mass Spectrom 35: 1-12.
38. Jaskolla TW, Karas M (2011) Compelling evidence for lucky survivor and gas phase protonation: the unified MALDI analyte protonation mechanism. J Am Soc Mass Spectrom 22: 976-988.
39. Kosevich MV, Chagovets VV, Shelkovsky VS, Boryak OA, Orlov VV, et al. (2007) Is there a “matrix suppression effect” under fast atom bombardment liquid secondary ion mass spectrometry of ionic surfactants in glycerol? Rapid Commun Mass Spectrom 21: 466-478.
40. Bodor N, Kaminski JJ, S. Selk S (1980) Soft drugs. 1. Labile quaternary ammonium salts as soft antimicrobials. J Med Chem 23: 469-474.
41. Tehrani-Bagha AR, Oskarsson H, van Ginkel CG, Holmberg K (2007) Cationic estercontaining gemini surfactants: chemical hydrolysis and biodegradation. J Colloid Interface Sci 312: 444-452.
42. Ratner BD, Hoffman AS, Schoen FJ, Lemons JE, Editors (2004) Biomaterials science: An Introduction to materials in medicine. Elsevier Academic Press: Boston.
43. Naban-Maillet J, Lesage D, Bossée A, Gimbert Y, Sztáray J, Vékey K, Tabet JC (2005) Internal energy distribution in electrospray ionization. J Mass Spectrom. 40: 1-8.
44. Pak A, Lesage D, Gimbert Y, Vékey K, Tabet JC (2008) Internal energy distribution of peptides in electrospray ionization : ESI and collision-induced dissociation spectra calculation. J Mass Spectrom 43: 447-455.
45. Drahos L, Vekey K (1999) Determination of the thermal energy and its distribution in peptides. J Am Soc Mass Spectrom 10: 323-328.
46. Drahos L, Vekey K (2001) MassKinetics: a theoretical model of mass spectra incorporating physical processes, reaction kinetics and mathematical descriptions. J Mass Spectrom 36: 237-263.

RAPID COMMUNICATIONS IN MASS SPECTROMETRY
Rapid Commun. Mass Spectrom. 2007; **21**: 1813–1819
Published online in Wiley InterScience (www.interscience.wiley.com) DOI: 10.1002/rcm.3020

RCM

Letter to the Editor

To the Editor-in-Chief
Sir,

'Wet chemistry' and crystallochemistry reasons for acidic matrix suppression by quaternary ammonium salts under matrix-assisted laser desorption/ionization conditions

In discussions of a matrix suppression effect (MSE) observed under matrix-assisted laser desorption/ionization (MALDI) conditions[1–8] models accounting for interactions of ionic and neutral species in the gas phase of a plume generated by a laser shot are usually applied,[2,9] while the role played by 'wet chemistry' reactions which can occur at the stage of sample preparation in liquid solutions is often underestimated. The function of various matrix additives in enhancing the performance of MALDI is considered mainly from the point of view of affecting the balance of gas-phase reactions.[3,9] It is taken for granted that organic acids used as 'host' matrices are chemically inert in relation to the majority of analytes and additives in solutions.

In the present communication we propose a model which demonstrates how possible chemical reactions between quaternary ammonium compounds, alkylammonium halide salts in particular, and organic acids of matrix compounds in aqueous solutions, resulting in formation of new salts, can lead to an apparent MSE in MALDI positive ion mass spectra and its absence in negative ion spectra. The postulation of these reactions for a particular class of quaternary ammonium compounds does not undermine the possibility of other processes being responsible for the suppression effect for other analytes, since qualitatively different pathways may lead to similar mass spectra.

The MSE in the presence of (alkyl) ammonium salts in the sample consists of the significant decrease or complete disappearance (at some analyte-to-matrix ratios) of all ions related to the MADLI matrix compound (**M**) in the positive ion mode, while the deprotonated matrix molecule $[\mathbf{M}–H]^-$ produces the main signal in the negative ion mode.[3,10] At the same time the alkylammonium cation Cat^+ (and its fragments, if any) is detected in the positive ion mode. If one has such a pair of positive and negative ion mass spectra for *de novo* identification of an unknown compound without any presumption of the sample composition, the probable conclusion is that the spectra correspond to a pure salt of $Cat^+ \cdot (\mathbf{M}–H)^-$ composition.

A very simple experiment can be carried out to demonstrate a chemical reaction resulting in the formation of the ammonium salt of 2,5-dihydroxybenzoic acid (2,5-DHB). On mixing a colourless aqueous solution of 2,5-DHB with a colourless aqueous ammonia solution (ammonium hydroxide) the liquid gradually acquires a reddish colour. The crystals precipitating on drying such a solution are magenta-red. A new salt $NH_4^+ \cdot (DHB–H)^-$ is synthesized in this way. No additional efforts to those used in the common method of MALDI sample preparation are involved. The crystallographic structure for a salt crystalline hydrate $NH_4^+ \cdot C_7H_5O_4^- \cdot H_2O$ of another DHB structural isomer, 2,6-DHB, was reported recently.[11] The crystals formed by the two isomers are of same red colour, indicating that 2,6-DHB and 2,5-DHB form similar ammonium salts. X-ray and crystal chemistry literature data on alkylammonium and heterocyclic ammonium dihydroxybenzoates usually spontaneously formed by the simple mixing of solutions of reagents will be discussed later in this letter.

First we shall describe a model postulating the effect of the formation of new salts on MALDI mass spectra and then analyze some existing data from the point of view of this model.

Quaternary ammonium (including alkylammonium and heterocyclic) salts are compounds with two charged parts: a cation (NR_4^+ or Cat^+) and anion (An^-) which can be presented by halogens Cl^-, Br^-, I^- or acetate, citrate, phosphate, etc. anions. The ionic (charged) state is the inherent property of these compounds: the cations and anions are present in the ionic crystalline lattice in the solid state and are released into liquid solution due to electrolytic dissociation. We reiterate these concepts here to stress the crucial distinction of these ionic species from other types of transient 'preformed' ions considered in mass spectrometric models,[12–15] which are formed by protonation/deprotonation or cationization/anionization in the condensed state. Many classical MALDI matrices (**M**) are organic acids which, by definition, dissociate in aqueous solution via detachment of a proton. Reactions between salts and acids in aqueous solutions are quite common. In the present context, on the preparation of a sample composed of a quaternary ammonium salt and an acidic matrix for MALDI measurements, we have the following set of ions in aqueous solution:

$$(Cat^+An^-) + \mathbf{M} \rightarrow \text{dissociation} \rightarrow Cat^+ + An^- + (\mathbf{M}-H)^- + H^+ \quad (1)$$

Exchange of anions is an allowed reaction in such a system. It is known, for example, that alkylammonium groups are active components of ion-exchange resins which trap various types of anions efficiently.[16] If the competitive binding is resolved in favour of the organic (matrix) anion, a new salt and a new acid may precipitate on drying of the solution:

$$Cat^+ + An^- + (\mathbf{M}-H)^- + H^+ \rightarrow \text{drying} \rightarrow Cat^+ \cdot (\mathbf{M}-H)^- + AnH \quad (2)$$

(We use parentheses to distinguish $(\mathbf{M}–H)^-$ anion in solution vs. square brackets for the $[\mathbf{M}–H]^-$ type of ion recorded in mass spectra.)

In the ideal case of complete anion exchange (reaction (2)) one obtains ionic crystals consisting of a new compound, the (alkyl)ammonium salt containing the organic $(\mathbf{M}–H)^-$ anion. There is no initial matrix compound left in such a sample.

RCM

The predictable mass spectrum of the new salt fits well the spectra observed in the MALDI mass spectra of alkylammonium salts in acidic matrices. The main components of the plume include neutrals $Cat^+ \cdot (\mathbf{M}–H)^-$ (not detected by MALDI, but detected by some other techniques[17]), cations Cat^+ (detected in the positive ion mode) and anions $(\mathbf{M}–H)^-$ (detected in the negative ion mode). In the particular case of bisquaternary ammonium compounds a $Cat^{2+} \cdot (\mathbf{M}–H)^-$ associate, which discloses directly the type of the anion, is detected.[10] There is no source for the formation of $[\mathbf{M}+H]^+$ ions (and their fragments). Nor is there a source for $\mathbf{M}^{+\cdot}$ ions (which are abundant, in particular, in the spectra of neat DHB). Thus, $[\mathbf{M}+H]^+$ and $\mathbf{M}^{+\cdot}$ species seem to be 'suppressed' in the spectra, while the actual reason for their absence (*viz*. MSE) is the absence of '**M**' molecules in the sample (or, at least, at the ablated spot).

Primary reactions[9] occurring on a laser shot are sufficient for Cat^+ and $(\mathbf{M}–H)^-$ ions to be released from the salt. Larger charged clusters built of various combinations of Cat^+ and $(\mathbf{M}–H)^-$ (being the only constituents of the sample) can be formed either directly on desorption/ablation of the sample,[13–15,18] or in secondary reactions in the plume.[9] The stability of relatively small cations and anions in the gas phase hampers their fragmentation and provides clean noiseless spectra in the low mass range.[3] A lower plume density and, consequently, smaller number of collisions involved in the formation of Cat^+ and $[\mathbf{M}–H]^-$ ions and a lower metastable decay rate may be reasons for better resolution (reported, e.g., for the MALDI spectra obtained on cetyltrimethylammonium bromide (CTAB) addition to α-cyano-4-hydroxycinnamic acid (CHCA)[3]). Thus, an individual compound, a salt with a UV-light-absorbing anion, produces clean and simple mass spectra.

Further, if halogen anions are present in the initial (alkyl)ammonium salts, volatile acids such as HCl and HBr can be released in reaction (2). These acids may promote protonation of an analyte, since some amino acids commercially available in the form of hydrochloride salts produce abundant protonated molecules in desorption mass spectrometric techniques.

On new salt formation the only species left from the matrix acid are $(\mathbf{M}–H)^-$ anions. This means that only $[\mathbf{M}–H]^-$ anions are available for in-plume chemistry following the laser desorption of the salt sample. It is of interest that the idea 'that matrix anions, $[\mathbf{M}–H]^-$, mediate most of the reactions' was expressed by Frankevich *et al*.[19] In this[19] and related works[20] the $[\mathbf{M}–H]^-$ anions, however, were formed due to interaction of electrons with matrix and analyte in the plume. This is an excellent example of how the same effect can be caused by different processes (mechanisms).

It is remarkable also that the recently reported ionization energy for the $(DHB–H)^-$ anion, 3.09 eV (HF/6-31+G** calculations) or 4.53 eV (Koopmans' theorem), is much lower than that of the neutral DHB molecule (8.05 eV from experiment or 8.11 eV calculated).[17] This opens new pathways for photoreactions of the 'preformed' $(DHB–H)^-$ anion directly ablated/desorbed from the salt crystals.

The suggested model of a new salt formation as a reason for MSE is supported by a number of facts: (1) MALDI data on quaternary ammonium salts, including our results on bisquaternary ammonium salt decamethoxinum in 2,5-DHB matrix[16] and literature data on matrix suppression by the addition of some cationic surfactants, such as CTAB;[3] (2) quantum-chemical estimations of the interaction energies of the tetramethylammonium cation (TMA^+) with Cl^- and $(DHB–H)^-$ anions;[21] (3) observation of the colloidal properties of solutions of decamethoxinum with 2,5-DHB; (4) fast atom bombardment (FAB) studies of glycerol solutions of DHB with decamethoxinum; and (5) crystallographic data for salts composed of the DHB anion and various quaternary ammonium cations.

The first fact that drew our attention to the possibility of $(\mathbf{M}–H)^-$ acting as an anion in alkylammonium salts was the observation of an abundant $Cat^{2+} \cdot (DHB–H)^-$ cluster along with a relatively low abundance 'native' associate $Cat^{2+} \cdot Cl^-$ in the MALDI mass spectrum of the bisquaternary ammonium salt decamethoxinum ($(R–O–CO–CH_2–N^+(CH_3)_2–(CH_2)_{10}–N^+(CH_3)_2–CH_2–CO–O–R) \cdot 2Cl^-$, where R is a menthyl moiety) in 2,5-DHB matrix.[10] Here an advantage of bisquaternary compounds was demonstrated: the possibility to reveal the type of the anion of the salt in the positive ion mass spectra, while neutral $Cat^+ \cdot An^-$ complexes of monoquaternary salts are 'invisible' in the spectra and the yield of $Cat^+_{(n+1)} \cdot An^-_n$ clusters may be negligibly small. $[DHB+H]^+$ and $DHB^{+\cdot}$ ions were substantially suppressed in the positive ion mode, while the absolute signal intensities of $[DHB–H]^-$ and $[2DHB–H]^-$ were high in the negative ion mode.[10] The question arises as to whether the spectrum was that of a new $Cat^{2+} \cdot 2(DHB–H)^-$ salt or, alternatively, Cl^- to $(DHB–H)^-$ anion exchange took place in the in-plume reaction.

Secondly, to provide quantitative estimates to support an assumption concerning competition between Cl^- and $(DHB–H)^-$ for NR_4^+ cation binding, we have performed quantum-chemical calculations of Cl^- and $(2,5\text{-}DHB–H)^-$ interactions with the tetramethylammonium (TMA) cation (taken as a model of the main active part of alkylammonium cations). The description of the calculations performed by the *ab initio* MP2/6-31++G** (ZPVE and BSSE corrected) method will be published elsewhere,[21] but here we present the main results relevant to the current discussion. As expected, the energy of interaction in the isolated (gas-phase, optimized geometry) $TMA^+ \cdot Cl^-$ complex ($-378.86\ kJ \cdot mol^{-1}$) appeared to be higher than that in the $TMA^+ \cdot (DHB–H)^-$ complex ($-351.66\ kJ \cdot mol^{-1}$). The higher charge density around the monoatomic anion than around the COO^- group of $(DHB–H)^-$ is the main reason for the stronger binding of Cl^-. This means that in the gas-phase reactions binding with Cl^- will be preferred, contradicting the observed preferential formation of decamethoxinum $Cat^{2+} \cdot (DHB–H)^-$ clusters,[10] if interpreted in the framework of in-plume interaction MALDI models. At the same time a method of calculating aqueous media using a polarizable continuum model (PCM)[21] results in higher destabilization of the $TMA^+ \cdot$

DOI: 10.1002/rcm

Cl^- complex ($+11.55\ kJ \cdot mol^{-1}$) than of $TMA^+ \cdot (DHB–H)^-$ ($+4.34\ kJ \cdot mol^{-1}$). The data agree with the behaviour of these salts and acids in aqueous solutions; namely they reflect a trend of dissociation of the $TMA \cdot Cl$ electrolyte and, obviously, a higher probability of anion exchange resulting in the formation of the $TMA^+ \cdot (DHB–H)^-$ associate. Thus, the data are evidence for the association of TMA^+ with $(DHB–H)^-$ in solution, rather than in the gas phase. Other alkylammonium ions may plausibly follow the same trend.

Thirdly, the appearance of the decamethoxinum and 2,5-DHB mixed solution in water has engaged our attention. While the solutions of both individual compounds were transparent, turbidity appeared on their mixing. The characteristic opalescence of the solution and the observation of a Tindal cone were indicators of formation of a colloidal micelle solution. Since individual compounds in the starting solution do not produce such an effect, it can be suggested that mixed micelles are formed from either some components of the two compounds or a new compound that has emerged due to anion exchange. Less soluble complexes of the decamethoxinum dication Cat^{2+} and $(DHB–H)^-$ can form the core of such micelles. If DHB is in excess (which is the case in common MALDI samples), then $(DHB–H)^-$ anions will form the next layer of the micelle shell. The example of the micelles shows that more complex nanostructures, not just simple 'ion pairs', can be formed in solution to be solidified as samples for MALDI. Micelle formation, however, is only one spectacular manifestation of interactions in solution and is not a necessary precondition for anion exchange. The micelles are destroyed on drying of the solution, but close contacts of Cat^{2+} with $(DHB–H)^-$ species provided by micelles may facilitate nucleation of the crystals of a new salt $Cat^{2+} \cdot 2(DHB–H)^-$. It should be also stressed that there are no isolated 'ion pairs', but a continuous ordered alteration of cations and anions in the salt crystalline lattice.

Fourthly, we have checked the interaction of DHB with decamethoxinum in glycerol solution by the independent FAB technique. In the FAB mass spectra of surface-active decamethoxinum and 2,5-DHB solution in glycerol two characteristic groups of ions (with appropriate isotopic distribution) with comparable abundance corresponding to $Cat^{2+} \cdot Cl^-$ (reported earlier in FAB/SIMS studies on decamethoxinum[22,23]) and $Cat^{2+} \cdot (DHB–H)^-$ were recorded, pointing to the occurrence of partial anion exchange. It is important here that we probe not some separate 'ion pair' associates in the liquid, but a continuous two-dimensional surface layer formed by the cations and anions of the surface-active organic salt.[23] Detection of the $Cat^{2+} \cdot (DHB–H)^-$ ion is a firm confirmation of the binding of $(DHB–H)^-$ to Cat^{2+} or, more precisely, of the incorporation of $(DHB–H)^-$ anions into the surface monolayer formed by the decamethoxinum surfactant (with a composition correlating roughly with the composition of micelles formed in solution).[23] Since FAB/SIMS sputtering affects mainly the surface layers of a sample, a 'competition for the surface' dependent on surface activity of the analytes causes the suppression effect in FAB/SIMS.[24] Analyte compounds which are not incorporated into such a surface layer are 'invisible' in FAB spectra. Since DHB is not a surfactant, it can be extracted into the surface layer occupied by the ionic surfactant only as a counterion in the surface electric double layer formed by the decamethoxinum organic dication and the original Cl^- anions.[23]

It is interesting that MSE shows up in relation to glycerol liquid matrix in the presence of surfactants under FAB/SIMS conditions,[23,24] although its nature and mechanisms[23] are completely different from those of MSE in MALDI. Complete glycerol (G) matrix suppression is observed in the positive ion mass spectra of decamethoxinum, while abundant production of $[nG–H]^-$ ($n = 1, 2$) ions is seen in the negative ion mode.[23] In spite of the apparent similarity with the suppression of the matrix signals in only one charge state under MALDI conditions, the cluster of the decamethoxinum dication with glycerol matrix anion $Cat^{2+} \cdot (G–H)^-$ is not detected in the FAB/SIMS spectra. At the same time the $Cat^{2+} \cdot (DHB–H)^-$ cluster appears on the addition of DHB to the solution. This points to the selectivity of the interactions of alkylammonium cations with organic anions.

Fifthly, X-ray crystallography structural data on the salts of acids which are used as matrices in MALDI can provide direct information on the solid sample structure. To the best of our knowledge crystallographic and crystallochemistry data on crystals of new compounds formed by matrix acids and organic molecules have not been systematically considered in the context of laser desorption/ionization. There are X-ray data on the structures of some pure matrix compounds[25,26] and descriptions of the biomolecule-doped matrix crystals.[26,27] Various empirical approaches to the evaluation of the MALDI sample structure[1,28–31] and morphology[32–36] have been applied and qualitative descriptions and models of the solid sample structure have been reported.[13–15,28,31] Electron microscopy and spectroscopy methods, however, do not provide direct information on the charge state of the analyte and possible analyte-matrix adducts in the crystals. A method of inclusion of dyes into matrix crystals[28] made it possible to prove the preservation of the solution charged state of the dyes in the solid samples, but the type and exact position of the counterions remained uncertain.

Forestalling a survey of the X-ray data it is necessary to make some remarks concerning the terminology. The term cocrystallization, often used in the description of MALDI sample preparation, should not be misinterpreted. Its strict meaning in crystallography refers to the formation of a regular crystalline lattice in which two or more nonidentical atoms or molecules are arranged in a repetitive order in the crystallographic cells. An alternative is a 'solid solution', a homogeneous crystalline structure (a single phase) in which some 'solute' atoms or molecules substitute for the original atoms or molecules; this is the most probable arrangement of large biomolecules in MALDI samples.[30] There is also a possibility of the random inclusion of minor components or admixtures into the cavities or defects of the crystalline lattice, or their adsorption on the surface of the

DOI: 10.1002/rcm

RCM

crystal. Further, for new compounds formed in solutions or in peritectic reactions on solidification (the case of crystalline hydrates) from several initial components, the term 'cocrystallization' is not relevant, since formation of single crystals of the new individual compound takes place.

While crystallographic data on the objects formed on solidification of solutions of the common matrix compounds with large biomolecules are few in number,[26,27] information on the cocrystallization of benzoic acid derivatives with organic molecules of comparable size is readily available. The majority of structural data that we have found were related to the DHB structural isomers;[11,17,37–55] more extended screening is necessary for other compounds used as MALDI matrices. The great attention paid to DHB isomers results from their potential for use in crystal engineering, the construction of supramolecular two- and three-dimensional aggregates with hydrogen-bond networks and $\pi-\pi$ interactions.[37,38]

The structures found can be divided into two groups. First, there are true cocrystals formed by neutral acid molecules and intact molecules of the second compound, e.g. phenazine-2,6-DHB ($C_{12}H_8N_2 \cdot C_7H_6O_4$)[39] or 4,4′-bipyridine-2,4-DHB ($C_{10}H_8N_2 \cdot C_7H_6O_4$),[40] glycine-3,5-DHB hydrate[41] cocrystals. Secondly, salts can be formed on dissolution of organic acids with other compounds to be cocrystallized. In the particular case which is the object of our current discussion, the crystal contains the (**M**–H)$^-$ anion and a cation. Actually, this is not a cocrystal, but a crystal of a new compound. The described procedures of synthesis of these compounds are usually very simple and consist of merely stirring of the reagents in solution. The simplest case mentioned at the beginning of the letter is that of ammonium 2,4-dihydroxybenzoate monohydrate ($NH_4^+ \cdot C_7H_5O_4^- \cdot H_2O$).[11] For 2,5-DHB the structure of its salt with a heterocyclic cation containing quaternary nitrogen, 3-hydroxypyridinium 2,5-dihydrobenzoate ($C_5H_6NO^+ \cdot C_7H_5O_4^-$), has been reported.[42] A number of structures of the salts of DHB isomers with organic cations have been established: imidazolium 2,4-dihydroxybenzoate ($C_3H_5N_2^+ \cdot C_7H_5O_4^-$);[43] 2,6-dimethylpyridinium 2,4-dihydroxybenzoate 2,6-dimethylpyridine solvate ($C_7H_{10}N^+ \cdot C_7H_5O_4^- \cdot C_7H_9N$);[44] benzimidazolium 3,5-dihydroxybenzoate ($C_7H_7N_2^+ \cdot C_7H_5O_4^-$);[45] and benzimidazolium 3,5-dihydroxybenzoate benzimidazole ($C_7H_7N_2^+ \cdot C_7H_5O_4^- \cdot C_7H_6N_2$).[46]

More complex metal-organic compounds form salts with DHB, e.g. bis(benzimidazole-κ*N*)bis(3,5-dihydroxybenzoato-κ*O*)copper(II) trihydrate ($[Cu(C_7H_5O_4)_2(C_7H_6N_2)_2] \cdot 3H_2O$);[47] aqua(2,4-dihydroxybenzoato-κO^1)bis(1,10-phenanthroline-κ$^2N,N'$)nickel(II) 2,4-dihydroxybenzoate monohydrate ($[Ni(C_7H_5O_4)(C_{12}H_8N_2)_2(H_2O)](C_7H_5O_4) \cdot H_2O$).[48]

The formation of such salts on the 'wet chemistry' stage of MALDI sample preparation and their further crystallization on sample drying can facilitate the desorption/ablation of 'preformed' cations and anions characteristic of the salts.

In some cases crystalline hydrates[11,17,47–53,55] or solvates (containing, e.g., methanol[38] or acetonitrile[49]) are formed in DHB-containing crystals. The possibility of the formation of such species on MALDI sample preparation provides a crystallochemical explanation for the earlier reported solvent retention in MALDI samples.[28,30] Solvent molecules detected in the matrix crystals by independent techniques (e.g. NMR of redissolved crystals[28]) can be preserved in crystalline hydrates/solvates. Rather slow dehydration (desolvation) on heating or on the vacuum storage of such samples agrees with the known behaviour of crystalline hydrates. Microscopic quantities of non-bound solvent entrapped in the crystalline defects, 'pockets', 'liquid inclusions',[15,30] are proved to be present in the DHB samples (by field emission scanning electron microscopy[30]), but their role in the incorporation of the analyte molecules has been questioned.[30]

DHB isomers also form hydrate and solvate salts with metal ions: $[Cu_2(3,5\text{-DHB–H})_4 \cdot (acetonitrile)_2] \cdot 8H_2O$, $Cu_2(3,5\text{-DHB–H})_4 \cdot H_2O_2] \cdot 11H_2O$,[49] $Me(2,6\text{-DHB–H})_2 \cdot 8H_2O$ (Me=Mn, Fe, Co, Ni, Zn; $Cu(2,6\text{-DHB–H})_2(H_2O)_2$,[50] $Me(2,5\text{-DHB–H})_2 \cdot 4H_2O$ (Me=Mn, Co, Ni, Zn, Cu, Cd),[51] $[Ni(C_7H_5O_4)_2(H_2O)_4] \cdot 3H_2O$,[52] and many others.[53] These data show that the presence of metal ions provides retention of a noticeable number of solvent molecules in the crystals of crystalline hydrates/solvates.

Some cocrystals contain both the charged and the neutral form of one of the components, where it is said that the neutrals solvate ionic components in the crystal.[44,46,54] This particular type of crystalline structure is formed by alkylammonium salt – 'tetrabutylammonium 2,6-dihydrobenzoate 2,6-dihydrobenzoic acid solvate', $C_{16}H_{36}N^+ \cdot C_7H_5O_4^- \cdot C_7H_6O_4$ (red crystals).[54] To preserve 1:1 positive to negative charge electrical balance and, at the same time, to accommodate the relatively large tetrabutylammonium cation one neutral DHB molecule is included into the crystalline lattice along with one (DHB–H)$^-$ anion per one cation. Thus, deptrotonated anionic and intact neutral forms of the DHB molecule can be found in the same crystal.

The latter example of incorporation of a relatively large cation can shed light on the inclusion of medium-size biomolecules into the matrix crystals. In particular, a mechanism of preservation of the 'pre-charged' protonated state of some analytes in the solid matrix, described in the framework of the 'lucky survivors',[13] and related[14,15] models can be clarified. The counterions formed from (M–H)$^-$ acidic matrix anions can balance positively charged (basic) sites of the analyte molecule, while the rest of the matrix remains neutral in the crystal. Thus, there is no need for any other anions and some remains in the liquid solvent (other than that included in the crystalline hydrate/solvate structure[56]) to maintain the charge on the analyte. In amino acids and peptides some basic sites are at amino groups which can form ion pairs with matrix anions. X-ray data show that 3,5-DHB forms hydrated salts with organic diamines: piperazine-3,5-DHB-water (1/2/4) $[H_2N(CH_2CH_2)_2NH_2]^{2+} \cdot 2(C_7H_5O_4)^- \cdot 4H_2O$,1,2-diaminoethane-3,5-DHB-water (1/2/2) $[H_3NCH_2CH_2NH_3]^{2+} \cdot 2(C_7H_5O_4)^- \cdot 2H_2O$, 1,4-diazabicyclo [2.2.2] octane-3,5-DHB-water (1/1/1), $[HN(CH_2CH_2)_3N]^+ \cdot (C_7H_5O_4)^- \cdot 2H_2O$ [55] and bis(2-aminoethyl)amine-3,5-DHB salt (1/2) $[HN(CH_2CH_2NH_3)_2]^{2+} \cdot [(C_7H_5O_4)^-]_2$.[38]

DOI: 10.1002/rcm

Recently, cocrystals of amino acids with DHB have been reported.[17,41] In the crystals of the molecular complex of glycine · 3,5-DHB hydrate[41] glycine is shown to be in a zwitterionic form, while DHB is not deprotonated. The case of arginine[17] as one of the most basic amino acids is of particular interest. In arginine · 2,5-DHB hydrate crystals arginine exists in a zwitterionic protonated form, while DHB is deprotonated. The water molecule bridges one DHB with two arginine units. There is 'a double hydrogen bond (salt bridge) between the guanidinium group of arginine and the (deprotonated) carboxylate group of DHB',[17] which means that a salt is formed. Thus, the exact location of the counterions (originating from the 'matrix' compound) next to the positively charged site of the amino acid is determined.

The concept of the formation of DHB salts with analytes containing quaternary nitrogen groups, which is supported by the above-cited demonstration of the existence of the arginine-2,5-DHB hydrate salt[17] and salts of DHB with amines,[55] provides a direct '*ab initio*' basis for hypothetical models of incorporation of peptides into acidic matrices for MALDI.[13–15] Basic sites of peptides are preserved in the positively charged protonated state as salts with the anions coming from the matrix acid (DHB at least), while the remaining matrix molecules 'solvating' the peptide remain neutral.

The significance of the preservation of the multiply protonated state of peptides and proteins in the form of salt-type adducts with the matrix anions in the solid state for further facilitation of 'ionization' on laser desorption remains, however, ambiguous. In the framework of cluster precursor models,[13–15,17] primarily desorbed/ablated analyte-matrix clusters undergo desolvation. It was shown recently[14,15] that anions of stronger and less basic acids, such as perchloric and hexafluorophosphoric acids, and bis (trifluoromethylsulfonyl)imide, which can survive desolvation under certain conditions, remain attached to the ablated proteins. It is thus possible that DHB matrix anions balancing the charged quaternary nitrogen sites of the analyte can be included, along with neutral matrix molecules, into the primary ablated analyte-containing cluster (this is confirmed, e.g., by observation of the above-mentioned $Cat^{2+} \cdot (DHB–H)^-$ associate for decamethoxinum). The mechanism of further desolvation of such species is intriguing. It is known that the most favourable pathway of thermally induced decomposition of ammonium salts is so-called dequaternization, i.e. formation of tertiary amines via loss of neutral or alkyl-anion molecules.[10,22,57] It is observed on thermal evaporation of (alkyl)ammonium salts for analysis in the gas phase (e.g. by electron ionization), or as an abundant pathway of in-source, metastable and collision-induced decay in desorption techniques. Under MALDI the thermal excitation in the primary cluster seems to be sufficient for the initiation of 'dequaternization' of the protonated basic sites (BH^+) with loss of the neutral matrix acid (**M**) molecule:

$$[BH^+ \cdot (\mathbf{M} - H)^-] \rightarrow B + \mathbf{M} \quad (3)$$

This mechanism comprises an easy alternative to neutralization of the multiply protonated sites by multiple collisions with anions in the in-plume reactions. The possibility of process (3) means, in fact, that the acidic matrix preserves the charged state of the analyte in the solid state, but efficiently 'deprotonates' its protonated basic amino (imino, guanidino) sites at the desorption/desolvation stage. In this connection a single positive charge usually left on peptides and proteins under MALDI must be really a 'lucky survivor' or be acquired in subsequent reactions of the desolvated neutral analyte.[18]

X-ray data on the exact structures and intermolecular interactions in the crystals (either cocrystals or crystals of new compounds) of small molecules with DHB can serve as a starting point for establishing quantitative correlations between the known structure of the solid and MALDI mechanisms, at least for small analytes. The first step in this direction is an explanation of MSE, suggested in the present letter.

Returning to possible reactions occurring on MALDI sample preparation it can be noted that few chemical reactions have 100% product yield. In more general cases, reaction (2) is written as:

$$\begin{aligned} x[Cat^+ + An^- + (\mathbf{M} - H)^- + H^+] \\ \rightarrow \text{drying} \\ \rightarrow y[(Cat^+ \cdot An^-) + \mathbf{M}] \\ + z[Cat^+ \cdot (\mathbf{M} - H)^- + AnH] \end{aligned} \quad (4)$$

where the relative yields of the products (y, z) depend on the chemical equilibrium established in the system. Observation of the suppression effect is possible not only at a 1:1 salt to acid molar ratio, since the distribution of the new product in the solid sample depends also on phase separation during drying, resulting in complex morphology of the sample. The main features of the sample morphology effect on MALDI mass spectra are well established.[33–36]

Without going into detail it can be said that an average multicomponent sample may contain crystals or areas of different chemical composition. Even if relatively large crystals of the matrix are precipitated (e.g. on the rims of the DHB spot), they can be covered by smaller crystals or a layer formed on solidification of the last portions of the solution (more probably of the eutectic composition). Due to this the MSE, as well as abundant production of the analyte ions, can be recorded for some so-called 'hot' or 'sweet spots' of the sample. There are no obvious means to overcome the rules of physical chemistry, and it is hard to predict *a priori* a variety of phenomena accompanying solidification of complex multicomponent systems. This hampers the routine automated analysis of heterogeneous samples. The optimal solution to the problem seems to be in harnessing the practically unlimited capabilities of computerized data handling by advancement of selective data accumulation.[2c]

Studies on matrix suppression effects are of interest not only for the fundamentals of ion formation under MALDI, but for increasing the analytical capabilities of MALDI by searching for more efficient matrices, in particular for the study of low molecular weight compounds and for biopolymer sequencing applications. The above discussion shows a new direction for design of 'noiseless' salt

DOI: 10.1002/rcm

RCM

MALDI matrices in which the UV-absorbing part will serve as the anion of the salt. Selection of an organic cation which provides only one ion in the positive ion mode, a decreased degree of clustering, sufficient volatility and at the same time stability of the salt on storage will require further chemical searching for more efficient salt matrix compounds. It should be noted that two-component matrices with onium[58] and ammonium salts[59,60] treated as additives have been suggested. The present discussion supported by crystallographic data[11,54] shows that a one-component ammonium-(matrix anion) salt was probably involuntarily synthesized in these studies. In some discussions most attention was paid to the surfactant properties of the additives, while the present work shows that the presence of the alkylammonium group and its reactions play the main role in MSE. Another promising type of liquid matrices composed of a mixture of a room-temperature ionic liquid and some common MALDI matrix (DHB, sinapinic acid, CHCA) has been suggested recently.[61,62] The charge of the cationic (tributylammonium, pyridinium, 1-methylimidazolium) part of these ionic liquids is due to quaternary nitrogen atoms. A large variety of 'tailor-made' salts can be produced by varying the combinations of ionic liquids and common matrix organic acids. Many of these new salts are viscous liquids, with the exception of some of those that contain pyridinium cations.[62] The absence of ions related to the anionic counterparts of these salts in the positive ion mode makes the ionic liquid matrices suitable for the analysis of low molecular weight compounds.

Acknowledgements

The authors are grateful to Drs V. A. Pokrovsky, V. L. Osaulenko and A. Yu. Naumov for their help in obtaining MALDI mass spectra of decamethoxinum.

Marina V. Kosevich, Oleg A. Boryak, Vitalij V. Chagovets, Vlada A. Pashynska, Vadim V. Orlov, Stepan G. Stepanian and Vadim S. Shelkovsky*

B. Verkin Institute for Low Temperature Physics and Engineering of the National Academy of Sciences of Ukraine, 47 Lenin Avenue, Kharkov 61103, Ukraine

**Correspondence to: M. V. Kosevich, B. Verkin Institute for Low Temperature Physics and Engineering of the National Academy of Sciences of Ukraine, 47 Lenin Avenue, Kharkov 61103, Ukraine.*
E-mail: mvkosevich@ilt.kharkov.ua

REFERENCES

1. (a) Chan T-WD, Colburn AW, Derrick PJ. *Org. Mass Spectrom.* 1991; **26**: 342. DOI: 10.1002/oms.1210260428; (b) Chan T-WD, Colburn AW, Derrick PJ, Gardiner DJ, Bowden M. *Org. Mass Spectrom.* 1992; **27**: 188. DOI: 10.1002/oms.1210270307.
2. (a) Knochenmuss R, Dubois F, Dale MJ, Zenobi R. *Rapid Commun. Mass Spectrom.* 1996; **10**: 871. DOI: 10.1002/(SICI)1097-0231(19960610)10:8<871::AID-RCM559>3.0.CO;2-R; (b) Knochenmuss R, Karbach V, Wiesli U, Breuker K, Zenobi R. *Rapid Commun. Mass Spectrom.* 1998; **12**: 529. DOI: 10.1002/(SICI)1097-0231(19980515)12:9<529::AID.-RCM188>3.0.CO;2-E; (c) McCombie G, Knochenmuss R. *Anal. Chem.* 2004; **76**: 4990. DOI: 10.1021/ac049581r.
3. Guo Z, Zhang Q, Zou H, Guo B, Ni J. *Anal. Chem.* 2002; **74**: 1637. DOI: 10.1021/ac010979m.
4. Cohen LH, Gusev AI. *Anal. Bioanal. Chem.* 2002; **373**: 571. DOI: 10.1007/s00216-002-1321-z.
5. Donegan M, Tomlinson AJ, Nair H, Juhasz P. *Rapid Commun. Mass Spectrom.* 2004; **18**: 1885. DOI: 10.1002/rcm.1568.
6. Zhu X, Papayannnopoulos IA. *J. Biomol. Technol.* 2003; **14**: 298.
7. Smirnov IP, Zhu X, Taylor T, Huang Y, Ross P, Papayanopoulos IA, Martin SA, Pappin DJ. *Anal. Chem.* 2004; **76**: 2958. DOI: 10.1021/ac035331jS0003-2700(03)05331-9.
8. Pan Ch, Xu S, Zhou H, Fu Y, Ye M, Zou Y. *Bioanal. Chem.* 2007; **387**: 193. DOI: 10.1007/s00216-006-0905-4.
9. (a) Zenobi R, Knochenmuss R. *Mass Spectrom. Rev.* 1998; **17**: 337. DOI: 10.1002/(SICI)1098-2787(1998)17:5<337::AID-MAS2>3.0.CO;2-S; (b) Knochenmuss R, Stortelder A, Breuker K, Zenobi R. *J. Mass Spectrom.* 2000; **35**: 1237. DOI: 10.1002/1096-9888(200011)35:11<1237::AID-JMS74>3.0.CO;2-O; (c) Knochenmuss R, Zenobi R. *Chem. Rev.* 2003; **103**: 441. DOI: 10.1021/cr0103773; (d) Breuker K, Knochenmuss R, Zhang J, Stortelder A, Zenobi R. *Int. J. Mass Spectrom.* 2003; **226**: 211. DOI: 10.1016/S1387-3806(02)00965-X.
10. Pokrovsky VA, Kosevich MV, Osaulenko VL, Chagovets VV, Pashynska VA, Shelkovsky VS, Karachevtsev VA, Naumov AYu. *Mass Spectrometria* 2005; **2**: 183. (A journal of Russian MS Society, ISSN 1817-969X).
11. Wei L-H. *Acta Cryst* 2006; **E62**: 5542. DOI: 10.1107/S1600536806044357.
12. Lehman E, Knochenmuss R, Zenobi R. *Rapid Commun. Mass Spectrom.* 1997; **11**: 1483. DOI: 10.1002/(SICI)1097-0231(199709)11:14<1483::AID.-RCM982>3.0.CO;2-F.
13. Karas M, Glückmann M, Schäfer J. *J. Mass Spectrom.* 2000; **35**: 1. DOI: 10.1002/(SICI)1096-9888(200001)35:1<1::AID-JMS904>3.0.CO;2-0.
14. Krüger R, Karas M. *J. Am. Soc. Mass Spectrom.* 2002; **13**: 1218. DOI: 10.1016/S1044-0305(02)00450-6.
15. Karas M, Krüger R. *Chem. Rev.* 2003; **103**: 427. DOI: 10.1021/cr010376a.
16. Meloan CE. *Chemical Separations: Principles, Techniques and Experiments*, John Wiley: New York, 1999.
17. Kinsel GR, Zhao Q, Narayanasamy J, Yassin FH, Dias HVR, Niesner B, Prater K, St. Marie C, Ly L, Marynick DS. *J. Phys. Chem. A* 2004; **108**: 3153. DOI: 10.1021/jp031207s S1089-5639(03)01207-6.
18. (a) Fournier I, Brunot A, Tabet JC, Bolbach G. *Int. J. Mass Spectrom.* 2002; **213**: 203. DOI: 10.1016/S1387-3806(01)00540-1; (b) Fournier I, Brunot A, Tabet JC, Bolbach G. *J. Mass Spectrom.* 2005; **40**: 50. DOI: 10.1002/jms.772.
19. Frankevich VE, Zhang J, Friess SD, Dashtiev M, Zenobi R. *Anal. Chem.* 2003; **75**: 6063. DOI: 10.1021/ac034436j.
20. (a) Gorshkov MV, Frankevich VE, Zenobi R. *Eur. J. Mass Spectrom.* 2002; **8**: 67. DOI: 10.1255/ejms.474; (b) Frankevich V, Zenobi R. *Int. J. Mass Spectrom.* 2002; **220**: 11. DOI: 10.1016/S1387-3806(02)00766-2.
21. Pashynska VA, Kosevich MV, Stepanian SG, Adamowicz L. *J Mol. Struct. THEOCHEM.* 2007; in press. DOI:10.1016/j.theochem.2007.03.019.
22. Pashynska VA, Kosevich MV, Gomory A, Szilagyu Z, Vekey K, Stepanian SG. *Rapid Commun. Mass Spectrom.* 2005; **19**: 785. DOI: 10.1002/rcm.1846.
23. Kosevich MV, Chagovets VV, Shelkovsky VS, Boryak OA, Orlov VV, Gomory A, Vegh P. *Rapid Commun. Mass Spectrom.* 2007; **21**: 466. DOI: 10.1002/rcm.2859.
24. Ligon WV, Dorn SB. *Int. J. Mass Spectrom. Ion Processes* 1987; **78**: 99. DOI: 10.1016/0168-1176(87)87044-1.
25. (a) Haisa M, Kashino S, Hanada S-I, Tanaka K, Okazaki S, Shibagaki M. *Acta Crystallogr.* 1982; **B38**: 1480. DOI: 10.1107/S0567740882006189; (b) Gdaniec M, Gilski M, Denisov GS. *Acta Crystallogr.* 1994; **C50**: 1622. DOI: 10.1107/S0108270194000557; (c) Okabe N, Kyoyama H. *Acta Crystallogr.* 2001; **E57**: 1224. DOI: 10.1107/S1600536801018682.
26. Beavis RC, Bridson JN. *J. Phys. D: Appl. Phys.* 1993; **26**: 442. DOI: 10.1088/0022-3727/26/3/015.
27. Strupat K, Kampmeier J, Horneffer V. *Int. J. Mass Spectrom.* 1997; **169**: 43. DOI: 10.1016/S0168-1176(97)00225-5.
28. Krüger R, Pfenninger A, Fournier I, Glückmann M, Karas M. *Anal. Chem.* 2001; **73**: 5812. DOI: 10.1021/ac010827r.
29. (a) Horneffer V, Dreisewerd K, Lüdemann H-C, Hillenkamp F, Läge M, Strupat K. *Int. J. Mass Spectrom.* 1999; **185–187**: 859. DOI: 10.1016/S1387-3806(98)14218-5; (b) Glückmann M, Pfenninger A, Krüger R, Hierolf M, Karas M, Horneffer V, Hillenkamp F, Strupat K. *Int. J. Mass. Spectrom.* 2001; **210**: 121. DOI:

10.1016/S1387-3806(01)00450-X; (c) Horneffer V, Forsmann A, Strupat K, Hillenkamp F, Kubitscheck U. *Anal. Chem.* 2001; **73**: 1016. DOI: 10.1021/ac000499f.
30. Horneffer V, Reichelt R, Strupat K. *Int. J. Mass Spectrom.* 2003; **226**: 117. DOI: 10.1016/S1387-3806(02)00979-X.
31. Dreisewerd K. *Chem. Rev.* 2003; **103**: 395. DOI: 10.1021/cr010375i.
32. Luxembourg SL, McDonnell LA, Duursma MC, Guo X, Heeren RMA. *Anal. Chem.* 2003; **75**: 2333. DOI: 10.1021/ac026434p.
33. Spengler B, Hubert M. *J. Am. Soc. Mass Spectrom.* 2002; **13**: 735. DOI: 10.1016/S1044-0305(02)00376-8.
34. Garden RW, Sweedler JV. *Anal. Chem.* 2000; **72**: 30. DOI: 10.1021/ac9908997.
35. Hanton SD, Cornelio CPA, Owens KG. *J. Am. Soc. Mass Spectrom.* 1999; **10**: 104. DOI: 10.1016/S1044-0305(98)00135-4.
36. Dai Y, Whittal RM, Li L. *Anal. Chem.* 1996; **68**: 2494. DOI: 10.1021/ac960238z S0003-2700(96)00238-7.
37. Davey RJ, Blagden N, Righini S, Alison H, Quayle MJ, Fuller S. *Crystal Growth and Design* 2001; **1**: 59. DOI: 10.1021/cg000009c.
38. (a) Gregson RM, Glidewell C, Ferguson G, Lough AJ. *Acta Crystallogr.* 2000; **B56**: 39. DOI: 10.1107/S0108768199006072; (b) Glidewell C, Ferguson G, Gregson RM, Campana CF. *Acta Crystallogr.* 2000; **B56**: 68. DOI: 10.1107/S0108768199009714.
39. Gdaniec M, Polonski T. *Acta Crystallogr.* 2007; **E63**: o707. DOI: 10.1107/S1600536807001195.
40. Wang Z-L, Wei L-H, Li M-X. *Acta Crystallogr.* 2006; **E62**: o3031. DOI: 10.1107/S160053680602201X.
41. Chen H, Xue L, Che Y-X, Zheng J-M. *Chin. J. Struct. Chem.* 2006; **25**: 229.
42. Fukunaga T, Kashino S, Ishida H. *Acta Crystallogr.* 2003; **E59**: 420. DOI: 10.1107/S1600536803004525.
43. Lin D-D, Liu J-G, Xu D-J. *Acta Crystallogr.* 2006; **E62**: o451. DOI: 10.1107/S1600536805043035.
44. Wei L-H. *Acta Crystallogr.* 2007; **E63**: o368: DOI: 10.1107/S160053680605375X.
45. Huang X, Liu J-G, Xu D-J. *Acta Crystallogr.* 2006; **E62**: o276. DOI: 10.1107/S160053680504170X.
46. Huang X, Liu J-G, Xu D-J. *Acta Crystallogr.* 2006; **E62**: o1833. DOI: 10.1107/S1600536806011639.
47. Huang X, Xiao L-P, Xu D-J. *Acta Crystallogr.* 2006; **E62**: m2246. DOI: 10.1107/S1600536806032417.
48. Yang Q, Zhang L, Xu D-J. *Acta Crystallogr.* 2006; **E62**: m2678. DOI: 10.1107/S160053680603772X.
49. Papaefstathiou GS, Darrow BG, MacGillivray LR. *J. Chem. Crystallogr.* 2002; **32**: 191. DOI: 10.1023/A:1020291903742.
50. Cariati F, Erre L, Micera G, Panzanelli A, Ciani G, Sironi A. *Inorg. Chim. Acta* 1983; **80**: 57. DOI: 10.1016/S0020-1693(00)91262-3.
51. Micera G, Strinna EL, Piu P, Cariati F, Ciani G, Sironi A. *Inorg. Chim. Acta* 1985; **107**: 223. DOI: 10.1016/S0020-1693(00)80707-0.
52. Wang H-Y, Gao S, Ng SW. *Acta Crystallogr.* 2005; **E61**: m2639. DOI: 10.1107/S1600536805036792.
53. Griffith WP, Nogueira HIS, Parkin BC, Sheppard RN, White AJP, Williams DJ. *J. Chem. Soc., Dalton Trans.* 1995; 1775. DOI: 10.1039/DT9950001775.
54. Almeida Paz FA, Soares-Santos PCR, Nogueira HIS, Trindade T, Klinowski J. *Acta Crystallogr.* 2003; **E59**: o506. DOI: 10.1107/S1600536803004987.
55. Burchell CJ, Ferguson G, Lough AJ, Gregson RM, Glidewell C. *Acta Crystallogr.* 2001; **B57**: 329. DOI: 10.1107/S0108768100019832.
56. Görbitz CH, Hersleth H-P. *Acta Crystallogr.* 2000; **B56**: 526. DOI: 10.1107/S0108768100000501.
57. Veith HJ. *Mass Spectrom. Rev.* 1983; **2**: 419. DOI: 10.1002/rcm.2480.
58. Ueki M, Yamaguchi M. *Rapid Commun. Mass Spectrom.* 2006; **20**: 1615. DOI: 10.1002/rcm.2480.
59. Cheng S-W, Dominic Chan T-W. *Rapid. Commun. Mass Spectrom.* 1996; **10**: 907. DOI: 10.1002/(SICI)1097-0231(19960610)10:8<907::AID-RCM576>3.3.CO;2-B
60. Zhu YF, Taranenko NI, Allman SL, Martin SA, Haff L, Chen CH. *Rapid Commun. Mass Spectrom.* 1996; **10**: 1591. DOI: 10.1002/(SICI)1097-0231(199610)10:13<1591::AID-RCM715>3.0.*CO*;2 − *W*
61. Armstrong DW, Li-Kang Zhang L-K, He L, Gross ML. *Anal. Chem.* 2001; **73**: 3679. DOI: 10.1021/ac010259f.
62. Tholey A, Heinzle E. *Anal. Bioanal. Chem.* 2006; **386**: 24. DOI: 10.1007/s00216-006-0600-5.

Received 7 March 2007
Revised 6 April 2007
Accepted 10 April 2007

ISSN 1993-6842. Biopolymers and cell. 2010. vol. 26. N 6.P. 472-477. Translated from Ukrainian

Modulation of bisquaternary ammonium agents effect on model biomembranes by complex formation with an organic anion

O. V. Vashchenko, V. A. Pashynska[1], M. V. Kosevich[1], V. D. Panikarskaya, L. N. Lisetski

Institute for Scintillation Materials NAS of Ukraine
60, Prospekt Lenina, Kharkiv, Ukraine, 61085

[1]Institute for Low Temperature Physics and Engineering NAS of Ukraine
47, Prospekt Lenina, Kharkiv, Ukraine, 61103

olga_v@isma.kharkov.ua

Aim. *To study membranotropic activity modulation of bisquaternary ammonium compounds (BQAC) decamethoxinum and aethonium determined by their interaction with dihydroxybenzoic acid (DHB) organic anion.* ***Methods***. *Differential scanning calorimetry, mass spectrometry.* ***Results***. *Doping phospholipid membranes with individual BQAC or DHB leads to a considerable decrease in the membrane melting temperature. At the same time, when BQAC and DHB are introduced together, a certain increase in the membrane melting temperature is observed, implying non-additivity of their action and incorporation of their complexes into the membranes.* ***Conclusions***. *DHB decreases the efficiency of BQAC destabilizing action on the membranes, i. e. DHB is a modulator of their membranotropic activity. A possible molecular mechanism of the modulation consists in the compensation of charges of the BQAC dications by organic DHB anions on the complex formation; parameters of the complex interaction with the membrane structures differ from those of individual ionic compounds.*

Key words: membranotropic agents, phospholipid membranes, bisquaternary ammonium compounds, dihydroxybenzoic acid, activity modulation, differential scanning calorimetry.

Introduction. It is known that the efficiency of pharmacological preparations is determined by their main active compound and the modulation of activity by other substances present in the pharmaceutical form. The present investigation was aimed at modulating influence of antimicrobial preparations based on bisquarternary ammonium compounds (BQAC) by their binding to organic anions. One of the main mechanisms of activity of membranotropic BQAC, which are the cation surface active compounds (surfactants), is believed to be their binding to the cytoplasmic membranes of microorganisms, resulting in their malfunction [1]. In the series of our previous publications [2–4], dedicated to systematic study on the molecular mechanisms of activity of the BQAC-based antimicrobial preparations, decamethoxinum and aethonium (Fig.1, *a*, *b*), we showed that these preparations interacted with model phospholipid membranes and formed stable non-covalent complexes with phospholipids. The

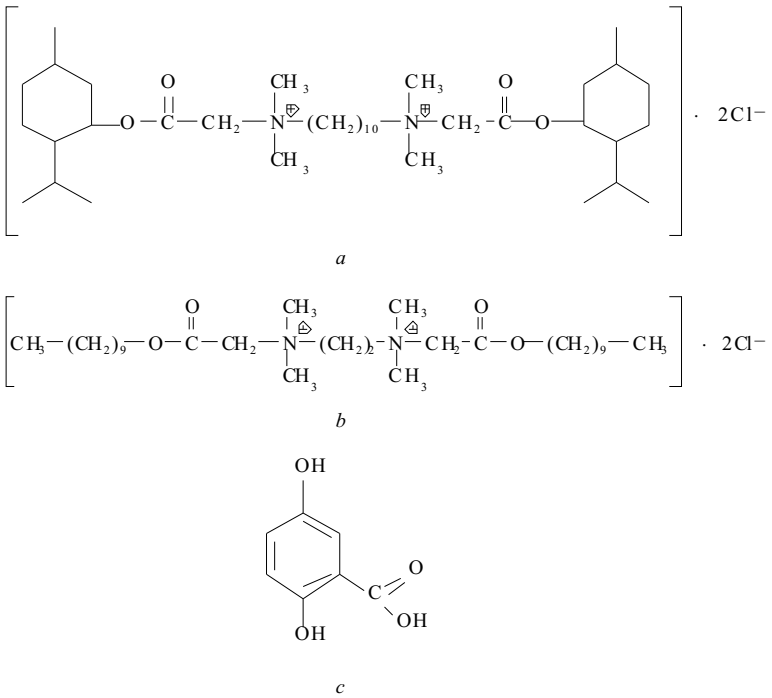

Fig. 1. Structural formulas of dichlorides of BQAC of decamethoxinum (*a*), aethonium (*b*), and 2.5-dihydroxybenzoic acid (*c*)

further mass-spectrometry experiments revealed that an anion of organic 2, 5-dihydroxybenzoic acid (DHB) is able to replace a counter-ion of chloride, thus forming a stable complex with decamethoxinum dication. This fact allowed us to suppose a possibility of formation of such complexes as a result of joint action of these two substances on phospholipid membranes, as well as to assume an effect of binding BQAC dications to DHB organic anions on their membranotropic activity. To check this assumption, a model system was selected as water dispersions of dipalmitoylphosphatidylcholine (DPPC) ? multilayer lamellar structures consisting of phospholipid bilayers separated by water layers, which imitate phospholipid membranes. BQAC decamethoxinum and aethonium were introduced separately or in combination with DHB. It should be noted that DHB was chosen as a compound modelling the acid and aromatic groups present in a number of amino acids [5]. The main method of investigation was differential scanning calorimetry (DSC) allowing determining changes in the calorimetric parameters of phase transitions in the model membranes when they are affected by membranotropic agents (MTA).

Materials and Methods. The DSC studies were carried out using the Mettler TA 3000 thermoanalytic system (Switzerland). Samples of 15–25 mg were placed into aluminium crucibles with half-closed lids. Programmed scheme of temperature scanning consisted of consecutive cycles of heating and cooling with the rate of 2 K/min.

Crystalline DPPC and BQAC were mixed and water dispersions of this composition with mass ratio DPPC: water of 50:50 [were prepared] using the standard method, described in [6]. While introducing BQAC and DHB simultaneously, we chose the concentrations to ensure the ratio between quaternary groups and DHB as 2:1, 1:1, and 1:2, corresponding to the molar ratios of 1:1, 1:2, and 1:4. The investigation of all the systems was performed at pH 7, the total amount of MTA, introduced into phospholipid matrix, was 5% (mass).

The investigation by matrix-assisted laser desorption/ionization (MALDI) mass-spectrometry was performed using a time-of-flight mass spectrometer MALDI-TOF AutoFlex (*Bruker Daltonics*, Germany). In these experiments, one of the components of investigated systems, namely, DHB, functioned also as a UV-absorbing matrix for MALDI.

Preparations of DPPC (5.45% humidity) of *Alexis Biochemicals* (Switzerland) and 2, 5-dihydroxybenzoic acid of *Sigma* (Germany) were

Parameters of phase transitions for systems of hydrated DPPC + MTA

Composition of membranotropic agents	Heating		Cooling		Hysteresis
	T_m, °C	ΔH, J/g	T_m, °C	ΔH_m, J/g	ΔT, °C
no MTA	41,5	23,4	41,4	40,3	0,1
DHB	37,1	20,3	36,1	23,9	1,0
Decamethoxinum	35,7	15,8	35,2	24,5	0,5
Decamethoxinum:DHB 1:1	37,9	15,3	35,0	26,0	2,9
Decamethoxinum:DHB 1:2	41,8	15,8	40,5	17,7	1,3
Decamethoxinum:DHB 1:4	41,7	24,5	41,5	5,0	0,2
Aethonium	39,8	17,8	39,7	18,5	0,1
Aethonium:DHB 1:1	40,0	13,7	39,5	16,6	0,5
Aethonium:DHB 1:2	41,6	17,8	40,2	21,7	1,4
Aethonium:DHB 1:4	41,6	18,8	40,9	30,8	0,7

used in the work. Decamethoxinum and aethonium were synthesized in the Institute of Organic Chemistry, NAS of Ukraine.

Results and Discussion. The formation of stable non-covalent complex of BQAC decamethoxinum dication with DHB anion was registered in the conditions of MALDI mass-spectrometry experiment using solid samples obtained from dried water solution of decamethoxinum and DHB (Fig.2). Along with the dication associate with one chloride anion Cat^{+2}•Cl^-, *m*/*z* 657, characteristic ion in mass-spectra of pure decamethoxinum [2], the dication associate with DHB anion Cat^{2+}•$(DHB–H)^-$, *m*/*z* 775 is formed. At equimolar ratio of components in initial solution, the intensity of associate Cat^{2+}•(DHB–H) in MALDI mass-spectra is considerably higher than that of associate Cat^{2+}•Cl^-, which indicates the competition between anions and predominate binding of organic anion to dication $(DHB–H)^-$.

DSC method was used to determine the calorimetric parameters of phase transitions in model membranes in the range of physiological temperatures, namely, transition from gel phase into liquid crystalline

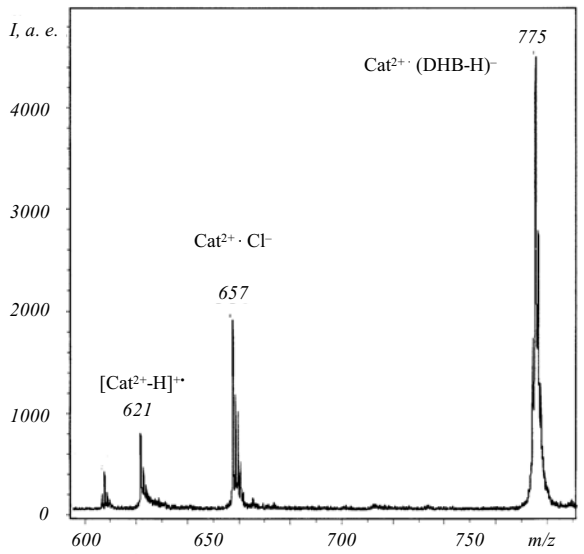

Fig. 2. Part of MALDI mass-spectrum of decamethoxinum sample in DHB matrix containing dication associates of decamethoxinum with chloride anion Cat^{+2}•Cl^- and anion of deprotonated DHB Cat^{2+}•$(DHB–H)^-$

state. The study was performed on water dispersions of DPPC alone, DPPC with addition of BQAC of decamethoxinum, aethonium, and DHB, and mixtures of BQAC: and DHB .Table 1 presents the data of DSC: temperature (T_m) and enthalpy (ΔH_m) of the main phase transition, determined in the regimes of heating and cooling, as well as hysteresis (ΔT).

To solve the question about stoichiometry of possible complexes, we analyzed the initial data using the method of quasibinary systems [7, 8]. In this method, the phospholipid medium is considered as a matrix, in which two dissolved components interact. In the absence of interaction, any thermodynamic feature of the system, expressed in corresponding units, is additive with respect to the relative concentrations of components and vice versa, specific interaction results in a deviation from the additivity.

Fig.3 presents quasibinary phase diagrams for the systems containing hydrated DPPC with additions of BQAC of decamethoxinum and aethonium, as well as DHB acids. The straight line connecting two extreme points corresponding to T_m of BQAC and DHB relates to the diagram in case of T_m additivity. The length of the perpendicular dropped from the maximum of the experimental curve on this line characterizes the deviation from additivity; the location of the curve

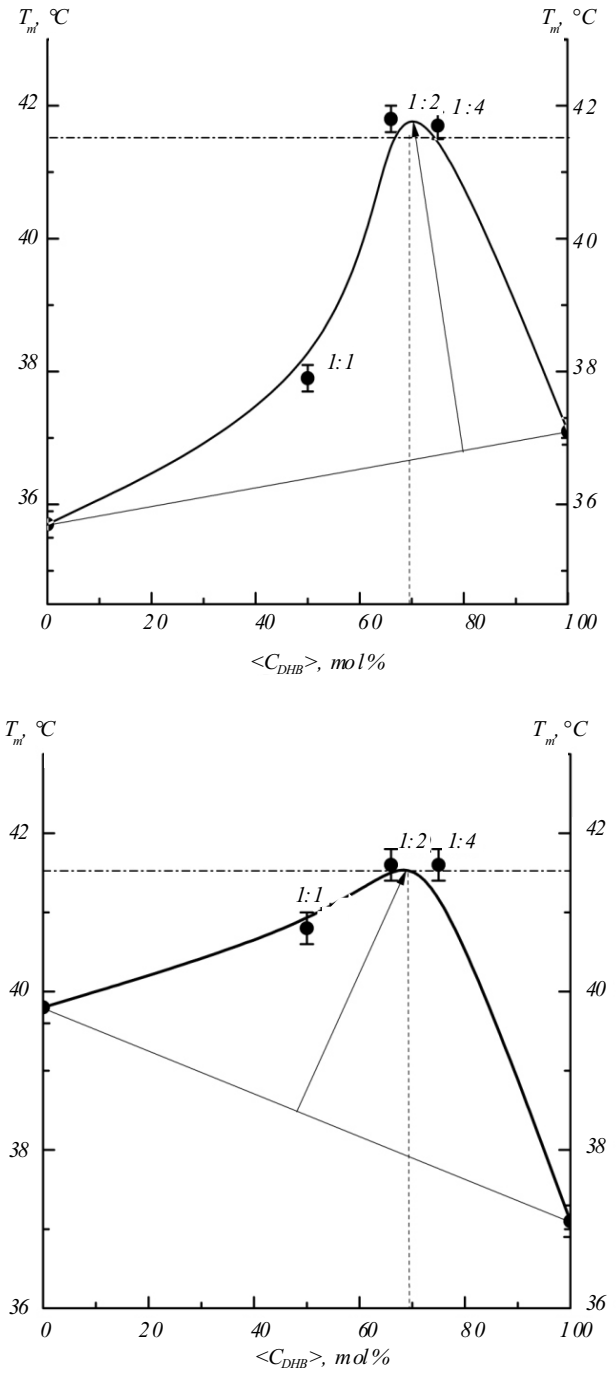

Fig. 3. Phase diagrams of quasibinary systems: decamethoxinum–DHB (*a*), aethonium–DHB (*b*) in the medium of hydrated DPPC (total MTA concentration in all the systems is 5 mass. %). Corresponding molar ratios of MTA are indicated in markings of experimental points

maximum points to the most advantageous stoichiometry of the complexes incorporated into the membrane.

The analysis of the data obtained gives grounds for the following conclusions. The change in thermodynamic parameters of model membranes at introducing individual MTA into the water dispersion of DPPC proves the interaction of all investigated MTA with phospholipid bilayers. The introduction of MTA considerably decreases the temperature of the main phase transition, i.e. it results in disorder of phospholipid bilayers. As quaternary ammonium compounds and DHB acid dissociate in water solution, it is possible to suppose that these MTA are built into the membrane in the form of ions: dications of decamethoxinum and aethonium Cat^{2+} and anion $(DHB–H)^-$.

Simultaneous introduction of BQAC and DHB into DPPC dispersion also changes its thermodynamic parameters, but there is no observed additivity of BQAC and DHB effects related to the concentration of introduced components. A considerable deviation from additivity in systems (DPPC + BQAC + DHB) is an evidence of specific interaction between the additives introduced into phospholipid matrix. The complexes of BQAC and DHB are likely to be formed similarly to the complexes of Cat^{2+}• $(DHB–H)^-$ registered in the mass-spectrometry experiment ([see] Fig.2) due to Coulomb interaction between corresponding cations and anions.

Plotting of quasibinary diagrams allowed determining the stoichiometry of complexes BQAC: DHB 1:2, which is notable for the maximal deviation from additivity ([see] Fig.3). In these complexes one DHB anion corresponds to each ammonium group in the composition of BQAC.

The degree of effect of simultaneously introduced BQAC and DHB on the system calorimetric parameters significantly depends on the ratio between components. If molar ratio BQAC to DHB is 1:1, T_m values for the three-component system (DPPC + BQAC + DHB) do not differ much from those for the binary system (DPPC + BQAC). If BQAC ratio to DHB is 1:2 and 1:4, there are qualitative changes: a shift of the main transition temperature changes the sign with respect to T_m of non-doped DPPC; however, an increase in T_m absolute value is insignificant. This effect may be considered as elimination of disordering influence of BQAC on membranes in the presence of

definite DHB concentrations. Therefore, it is possible to regard DHB as a modulator of BQAC activity. On the other hand, complex formation with BQAC decreases the DHB activity.

Neutralization of the charge of BQAC dication while forming its complex with DHB seems to be the most probable molecular mechanism of the abovementioned effect of modulation of the BQAC activity. This assumption is based on the fact that the transition from decrease to increase in melting temperature T_m in the system (DPPC + BQAC + DHB) occurs at the DHB content that either equals or exceeds the amount of positively charged ammonium groups (two groups per one BQAC molecule), which is sufficient for their neutralization at the complex formation. If molecular ratio BQAC to DHB is 1:1, one of the dication positive centres on average is not "compensated" by DHB anion and the calorimetric parameters still change in accordance with the effect of ion MTA on the membrane.

It should be noted that previously we described the dependence of membranotropic activity of the BQAC-based surfactants on their structure, i.e. the nature of hydrophobic "tail" and a distance between positively charged atoms of quaternary nitrogen, on the example of decamethoxinum and aethonium [2, 3]. The structure of aethonium dication, including a polar "head" of two closely located ammonium groups and two hydrophobic carbohydrate chains, is generally similar to the structure of DPPC molecules, which provides the building of aethonium dication into the membrane due to the substitution of DPPC molecule. A more complicated structure of hydrophobic "tails" of decamethoxinum, containing methyl residues, as well as rather large distance between positively charged ammonium groups result in greater destabilizing effect of decamethoxinum on the membranes in comparison to aethonium.

As for enthalpy values of the main phase transition in model membranes determined in the regime of sample heating, they demonstrate a general tendency to decreasing when MTA is introduced into the system. At first sight, this fact shows that disordering of membranes requires much less energy in the presence of destabilizing agents in their composition. The processes occurring during cooling of the system are related to the peculiarities of MTA inclusion into the liquid crystal structure of membranes, which is a subject of further studies beyond the framework of this review.

Conclusions. The possibility of modulation of the activity of MTA, based on BQAC salts, was considered for the case of their simultaneous with organic acid DHB introduction into the model phospholipid membranes.

The data of DSC research demonstrated the absence of additivity of calorimetric parameters, which is a characteristic of the model membranes containing individual MTA, in the case of simultaneous introduction of the mixture of DHB with BQAC decamethoxinum and aethonium into the water dispersion of hydrated DPPC. This experimental fact evidences the insertion of MTA complexes instead of individual MTA into the membranes.

The data of mass-spectrometry showed the possibility of formation of stable complexes of cations of quaternary ammonium compounds with DHB anion.

The analysis of calorimetric parameters of the systems investigated revealed that the insertion of dissociated in solution individual components in ionic state into the membranes, results in a decrease in the temperature of main transition and corresponding disordering of the membrane structure. The similar effect of decrease in the membrane melting temperature is observed if components of the MTA mixtures added are in the ratio sustaining a charged state of their complexes. In case of the formation of neutral complexes of BQAC dications with DHB anion, an increase in the temperature of main transition is revealed along with ordering the membrane structure. This effect may be considered as BQAC deactivation, i.e. modulation of the BQAC activity by organic acid. Neutralization of ionic MTA due to the formation of cation-anion complexes was suggested as a molecular mechanism of such modulation.

The possibility of weakening membranotropic activity of the BQAC-based antimicrobial agents, revealed at their introduction together with organic acid, should be taken into account while developing polycomponent drugs of antimicrobial activity. The approach proposed in this work may be used on a broader scale for testing the combined activity of MTA of various nature.

О. В. Ващенко, В. А. Пашинская[1], М. В. Косевич[1], В. Д. Паникарская, Л. Н. Лисецкий

Модуляция воздействия четвертичных аммониевых соединений на модельные биомембраны посредством комплексообразования с органическим анионом

Институт сцинтилляционных материалов НТК «Институт монокристаллов» НАН Украины
Проспект Ленина, 60, Харьков, Украина, 61001

[1]Физико-технический институт низких температур им. Б. И. Веркина НАН Украины
Проспект Ленина, 47, Харьков, Украина, 61103

Резюме

Цель. *Изучить модуляцию мембранотропной активности бисчетвертичных аммониевых соединений (БЧАС) декаметоксина и этония, обусловленную их взаимодействием с органическим анионом дигидроксибензойной кислоты (DHB).* ***Методы****. Дифференциальная сканирующая калориметрия, масс-спектрометрия.* ***Результаты****. Обнаружено, что добавление индивидуальных БЧАС или DHB к фосфолипидным мембранам значительно снижает температуру перехода «гель–жидкий кристалл». При совместном введении БЧАС и DHB температура фазового перехода мембраны несколько повышается, что свидетельствует об отсутствии аддитивности действия этих веществ и встраивании в мембраны их комплексов.* ***Выводы****. DHB уменьшаает эффективность дестабилизирующего эффекта БЧАС на мембраны, то есть является модулятором их активности. Возможный молекулярный механизм модуляции заключается в компенсации зарядов дикатиона БЧАС и органических анионов DHB при образовании их комплекса, взаимодействие которого с мембранными структурами отличается от такового ионных форм индивидуальных соединений.*

Ключевые слова: мембранотропные агенты, фосфолипидные мембраны, бисчетвертичные аммониевые соединения, дигидроксибензойная кислота, модуляция активности, дифференциальная сканирующая калориметрия.

О. В. Ващенко, В. А. Пашинська, М. В. Косевич, В. Д. Панікарська, Л. М. Лисецький

Модуляція впливу бісчетвертинних амонієвих сполук на модельні біомембрани внаслідок комплексоутворення з органічним аніоном

Резюме

Мета*. Вивчити модуляцію мембранотропної активності бісчетвертинних амонієвих сполук (БЧАС) декаметоксину та етонію, зумовлену їхньою взаємодією з органічнім аніоном дигідроксибензойної кислоти (DHB).* ***Методи****. Диференційна скануюча калориметрія, мас-спектрометрія.* ***Результати****. Виявлено, що додавання індивідуальних БЧАС або DHB до фосфоліпідних мембран значно знижує температуру фазового переходу «гель–рідкий кристал». При одночасному введенні БЧАС і DHB температура фазового переходу мембрани дещо підвищується, що свідчить про відсутність адитивності дії цих речовин та інкорпорацію у мембрани утворених ними комплексів.* ***Висновки****. DHB зменшує ефективність дестабілізувальної дії БЧАС на мембрани, тобто слугує модулятором їхньої активності. Ймовірний молекулярний механізм модуляції полягає у компенсації зарядів дикатіона БЧАС та органічних аніонів DHB при утворенні їхнього комплексу, взаємодія якого з мемб- ранними структурами є відмінною від такої іонних форм інди- відуальних сполук.*

Ключові слова: мембранотропні агенти, фосфоліпідні мембрани, бісчетвертинні амонієві сполуки, дигідроксибензойна кислота, модуляція активності, диференційна скануюча калориметрія.

REFERENCES

1. *Vievskij A. N.* Cationic surfactants: New perspectives in medicine and biology // Tenside, Surfactants, Detergents.–1997.–**34**, N 1.–P. 18–21.
2. *Pashynskaya V. A., Kosevich M. V., Gomory A., Vashchenko O. V., Lisetski L. N.* Mechanistic investigation of the interaction between bisquaternary antimicrobial agents and phospholipids by liquid secondary ion mass spectrometry and differential scanning calorimetry // Rapid Commun. Mass Spectrom.–2002.–**16**, N 18.–P. 1706–1713.
3. *Korzovskaya O. V., Pashinskaya V. A., Kosevich M. V., Lisetski L. N.* Interaction of antimicrobial agents decamethoxinum and aethonium with model membranes // Proc. Kharkiv State Univ., Biophys. Bull.–1999.–**450**, N 2.–P. 35–39.
4. *Pashynska V. A., Kosevich M. V., Van den Heuvel H., Cuyckens F., Claeys M.* Study of non-covalent complexes formation between the bisquaternary ammonium antimicrobial agent decamethoxinum and membrane phospholipids by electrospray ionization and collision-induced dissociation mass spectrometry // Proc. Kharkiv State Univ., Biophys. Bull.–2004.–**637**, N 1–2 (14).– P. 123–130.
5. *Pahynska V., Kosevich M., Stepanian S., Adamowicz L.* Noncovalent complexes of tetramethylammonium with chlorine anion and 2,5-dihydroxybenzoic acid as models of the interaction of quaternary ammonium biologically active compounds with their molecular targets. A theoretical study // J. Mol. Struct.: THEOCHEM.– 2007.–**815**, N 1–3.–P. 55–62.
6. *Korzovskaya O. V., Lisetski L. N., Panikarskaya V. D.* UV-spectroscopy and structura features of model membranes and liquid-crystalline biomimetic systems // Proc. Kharkiv State Univ., Biophys. Bull.–1998.–**422**, N 2.–P. 85–89.
7. *Fialkov Yu. Ya., Zhitomirskij A. N., Tarasenko Yu. A.* Physical chemistry of non-aqueous solution.–Leningrad: Khimiya, 1973.–376 p.
8. *Solutions* of non-electrolytes in liquids.–Moskva: Nauka, 1989.–264 p.

UDC 577.352:615.2
Received 29.03.10

3.6. Підсумки розділу 3.

Застосування м’якоіонізаційних мас-спектрометричних методик з ІЕР та МАЛДІ, а також напівемпіричного методу квантово-механічних розрахунків AM1 для дослідження модельних систем, що містили біологічно активні бісчетвертинні амонієві сполуки в оточенні або води, або спиртів (етанол чи метанол), або 2,5-дигідроксибензойної кислоти, дозволили визначити особливості гідратації та мас-спектрометричні маркери структурної стабільності досліджених лікарських агентів та їхніх сольватних комплексів в умовах мас-спектрометричного експерименту під впливом ряду фізичних факторів, серед яких - електричне поле, зіткнення з високоенергетичними частинками тощо. У рамках проблеми пошуку характеристичних мас-спектрометричних маркерів (сукупності піків спектру - мас-спектрометричних «відбитків пальців», “fingerprint”) структурної стабільності бісчетвертинних амонієвих агентів для їхньої ефективної ідентифікації в різних середовищах та біомедичних зразках проведено порівняльне дослідження розчинів бісчетвертинних амонієвих протиінфекційних агентів декаметоксин та етоній за допомогою методик мас-спектрометрії з ІЕР та МАЛДІ. Основні підсумки розділу наведено нижче.

1. Уперше визначено структурно-енергетичні характеристики гідратного комплексу дикатіону бісчетвертинного амонієвого протиінфекційного агенту декаметоксин із 36 молекулами води, що моделюють першу гідратну оболонку дикатіону, за результатами розрахунків напівемпіричним методом AM1. Доведено, що структура дикатіону декаметоксіну в гідратному оточенні близька до найбільш енергетично вигідної структури дикатіону у вакуумному наближенні та відповідає витягнутій конформації центрального вуглеводневого ланцюга між четвертинними азотами (відстань між четвертинними азотами гідратованого дикатіону дорівнює 13.51 Å у порівнянні з 13.87 Å для дикатіону в умовах вакуумного наближення). Така структура дикатіону декаметоксину зумовлена силами електростатичного

відштовхування, що діють як у відсутності розчинника, так і в гідратному оточенні між делокалізованими позитивними зарядами четвертинних азотних груп. Розрахована методом AM1 повна енергія міжмолекулярної взаємодії в гідратному комплексі декаметоксину з 36 молекулами води становить -1361.4 кДж/моль, включаючи енергію взаємодії між дикатіоном та молекулами води, що дорівнює -553.1 кДж/моль. За результатами розрахунків встановлено, що взаємодія молекул води гідратного оточення з дикатіоном декаметоксину визначається делокалізацією позитивного заряду в дикатіоні: найбільш гідратованими є вуглеводневі групи дикатіону, які найближчі до четвертинних азотів та характеризуються найбільшою щільністю делокалізованого позитивного заряду.

2. У рамках експериментальних досліджень молекулярно-фізичних характеристик бісчетвертинних амонієвих протиінфекційних агентів уперше описано динамічну поведінку мас-спектрометричних маркерів молекулярно-структурної стабільності декаметоксину в умовах сольватного оточення в залежності від електричного потенціалу на конусному електроді (CV) в джерелі іонів для IEP. Визначено, що в діапазоні значення CV від 0 до 50 В у мас-спектрах присутні обидва мас-спектрометричні маркери структурної стабільності цього бісчетвертинного агенту: піки інтактного дикатиону Cat^{2+} та комплексу дикатіону з протиіоном хлору $Cat^{2+}\cdot Cl^{-}$. З ростом CV в IEP мас-спектрах декаметоксину, розчиненого в етанолі, з'являються піки фрагментів розпаду дикатіону, при цьому відносна інтенсивність самого піку Cat^{2+} знижується, поки сигнал від Cat^{2+} зовсім не зникає в спектрі при значенні CV=90 В. Важливо, що мас-спектрометричні маркери фрагментації іону $Cat^{2+}\cdot Cl^{-}$ в діапазоні CV до 90 В не спостерігаються. Така поведінка мас-спектрометричних маркерів структурної стабільності декаметоксину підтверджує, що комплекс дикатіону декаметоксину з протиіоном є стабільнішим за інтактний дикатіон в умовах мас-спектрометричного експерименту, що пояснюється набуттям більшої кінетичної енергії іоном Cat^{2+} у порівнянні з іоном комплексу $Cat^{2+}\cdot Cl^{-}$ та пов'язаною з цим більшою

енергією зіткнення дикатіону з молекулами висушуючого газу в мас-спектрометрі. Результати дослідження показують, що найбільш м'які умови іонізації, за яких у спектрах ідентифікується найбільше мас-спектрометричних маркерів збереження структурної стабільності дикатіонів бісчетвертинних амонієвих сполук та найменше маркерів їхньої фрагментації, спостерігаються в мас-спектрометричних експериментах з IEP при низьких значеннях потенціалу на конусному електроді.

3. Завдяки дослідженню розчинів бісчетвертинного амонієвого агенту етоній методом мас-спектрометрії з IEP встановлено, що спектральна картина (особливості розподілу мас-спектрометричних піків - маркерів структурної стабільності та процесів фрагментації дикатіона етонію), як це спостерігалося й для декаметоксину, переважно визначається значеннями потенціалу на конусному електроді джерела іонів мас-спектрометра. З ростом значення CV мас-спектри етонію змінюються та свідчать про інтенсифікацію процесу фрагментації дикатіону препарату. Так мас-спектрометричний маркер стабільності інтактного дикатіону етонію Cat^{2+} присутній в IEP спектрах в діапазоні CV від 10 до 50 В, пік кластеру дикатіону з протиіоном хлору $Cat^{2+}\cdot Cl^{-}$ наявний у спектрах в інтервалі CV від 20 до 80 В. Поведінка мас-спектрометричних маркерів молекулярно-структурної стабільності етонію в IEP спектрах свідчить про цікаве явище збереження двозарядового стану фрагментів дикатіону етонію (з найменшою серед досліджених бісчетвертинних амонієвих сполук відстанню в 4Å між четвертинними азотами, що розділені двома метильними групами) при розпаді дикатіону в умовах IEP. Проведені розрахунки значень середньої внутрішньої енергії, що набувають іони-прекурсори етонію при різних значеннях CV та температури в джерелі іонів мас-спектрометру, дозволили встановити наступне. Явище збереження двозарядових фрагментів етонію пояснюється недостатністю енергії електростатичного відштовхування для фрагментації дикатіону з розділенням заряду в умовах мас-спектрометрії з IEP при низьких значеннях CV через делокалізацію позитивного заряду дикатіону.

4. Мас-спектрометричні маркери структурної стабільності етонію, що отримані в дослідженнях методом МАЛДІ із застосуванням матриці 2,5-дигідроксибензойної кислоти (DHB) значно відрізняються від таких, які було визначено методом мас-спектрометрії з ІЕР, що зумовлено відмінністю умов іонізації та міжмолекулярною взаємодією дикатіону етонію з аніоном DHB. В МАЛДІ спектрі етонію відсутні піки інтактного дикатіону Cat^{2+} та піку комплексу $Cat^{2+}\cdot Cl^{-}$, при цьому визначальними характеристичними піками в спектрі є піки квазімолекулярних іонів $[Cat - H]^{+}$ and $[Cat - CH3]^{+}$ та іонів фрагментів з *m/z* 242, 270, та 315. Визначені особливості мас-спектрометрів етонію є корисними для ідентифікації в різних зразках інших бісчетвертинних амонієвих сполук методом мас-спектрометрії з МАЛДІ.
5. Уперше пояснено ефект пригнічення сигналів матриці (відсутність мас-спектрометричних піків матриці) в мас-спектрах четвертинних амонієвих агентів, що отримані методом МАЛДІ із застосуванням матриці, що належить до органічних кислот. При дослідженнях модельної системи, що складалася з гідроксиду амонію в DHB, та систем, що містили протиінфекційні препарати декаметоксин та етоній, розчинені в матриці DHB, встановлено факт конкуренції аніонів (OH^{-} або Cl^{-}) четвертинних сполук та кислотного аніону $[DHB - H]^{-}$ за зв'язування з четвертинним амонієвим катіоном. Аналіз отриманих мас-спектрометрів показує, що утворення стабільних комплексів четвертинних амонієвих катіонів з органічним кислотним аніоном превалює в умовах мас-спектрометричного експерименту, що зумовлює ефект пригнічення сигналів самої матриці в МАЛДІ мас-спектрах цих сполук, отриманих в режимі позитивних іонів.
6. Формування стабільних комплексів дикатіону декаметоксину з органічним аніоном $[DHB - H]^{-}$ як складової сольватного оточення, показане в МАЛДІ експерименті, дозволяє пояснити модифікаційний ефект органічних кислот на мембранотропну активність цього бісчетвертинного амонієвого агенту. В експериментах, що проведені колегами-співавторами спільних публікацій [18, 43] з Інституту сцинтиляційних матеріалів НАН України методом

диференціальної скануючої калориметрії показано, що одночасне введення бісчетвертинних амонієвих сполук (декаметоксину або етонію) з DHB в модельні фосфоліпідні мембрани призводить до підвищення температури фазового переходу мембрани, яке вказує на відсутність адитивності дії цих сполук [18, 43], що пояснюється інкорпорацією в модельні мембрани зареєстрованих в мас-спектрометричних експериментах комплексів дикатіонів четвертинних агентів з аніоном DHB.

7. Результати досліджень, викладені в цьому розділі дисертації, вказують на важливість урахування умов збереження структурної стабільності біологічно активних агентів і ліків, та їхньої взаємодії з компонентами сольватного оточення для прогнозування функціональної активності цих агентів та встановлення молекулярних механізмів їхньої біологічної дії.

РОЗДІЛ 4

Мас-спектрометричні маркери органічних компонентів частинок атмосферних аерозолів та молекулярних процесів за їхньою участю

Взаємодія біологічно активних речовин із біомолекулами та сольватним оточенням відіграє важливу роль не тільки в процесах, що відбуваються в клітинах живих організмів, а й у молекулярно-фізичних процесах у довкіллі, зокрема в атмосфері. Летючі органічні сполуки біогенного та антропогенного походження, потрапляючи до атмосфери, можуть вступати як в хімічні, так і в молекулярно-фізичні процеси, зокрема нековалентні взаємодії з іншими компонентами довкілля, і як самотужки, так і вже в складі сформованих асоціатів чинити вплив на живі організми. Водорозчинні органічні полярні сполуки в атмосфері завдяки особливостям своєї молекулярної структури та фізичним властивостям активно взаємодіють з молекулами води, іншими компонентами сольватного оточення та молекулами інших атмосферних складових, що забезпечує їх активну участь у біологічно та кліматично важливих молекулярно-фізичних процесах, зокрема в формуванні вторинних органічних аерозолів, гідратації та хмароутворенні тощо. Умови мас-спектрометричного експерименту якнайкраще підходять для моделювання молекулярно-фізичних процесів за участю біологічно активних речовин, що відбуваються в атмосфері, а також для вивчення молекулярного складу та міжмолекулярної взаємодії в частинках атмосферних аерозолів. Однак, у той час як методи вивчення міжмолекулярних взаємодій лікарських речовин із біомолекулами активно розвивалися останнім часом завдяки бурхливому розвитку фармакології та медичних досліджень, мас-спектрометричні методи визначення маркерів атмосферних молекулярно-фізичних процесів за участю біологічно активних речовин ще потребують подальшого удосконалення. Тому у рамках даної роботи виконувалися дослідження в напрямку розвитку методики на базі фізичного методу, який поєднує газову хроматографію і мас-

спектрометрію (ГХ/МС), задля вивчення особливостей молекулярного складу та міжмолекулярних взаємодій у нековалетних частинках атмосферних аерозолів, зокрема й біологічно-активних вторинних органічних аерозолів, які при попаданні в організм людини або тварини при диханні реалізують свій біологічний (часто негативний) вплив.

JOURNAL OF MASS SPECTROMETRY
J. Mass Spectrom. 2002; **37**: 1249–1257
Published online in Wiley InterScience (www.interscience.wiley.com). DOI: 10.1002/jms.391

JMS

Development of a gas chromatographic/ion trap mass spectrometric method for the determination of levoglucosan and saccharidic compounds in atmospheric aerosols. Application to urban aerosols†

Vlada Pashynska,[1‡] Reinhilde Vermeylen,[1] Gyorgy Vas,[1] Willy Maenhaut[2] and Magda Claeys[1]*

[1] University of Antwerp (UIA), Department of Pharmaceutical Sciences, Universiteitsplein 1, B-2610 Antwerp, Belgium
[2] Ghent University, Institute for Nuclear Sciences, Proeftuinstraat 86, B-9000 Ghent, Belgium

Received 21 May 2002; Accepted 17 September 2002

We developed and validated a gas chromatographic/ion trap mass spectrometric method for the determination of levoglucosan and the related monosaccharide anhydrides, mannosan, galactosan and 1,6-anhydro-β-D-glucofuranose in urban atmospheric aerosols collected on quartz fiber filters. The method is based on extraction with dichloromethane–methanol (80 : 20, v/v), trimethylsilylation, multiple reaction monitoring in the tandem mass spectrometric mode using the ion at *m/z* 217, and the use of an internal standard calibration procedure with the structurally related compound methyl β-L-arabinopyranoside. In addition, the method allows the quantification of other saccharidic compounds, arabitol, mannitol, glucose, fructose, inositol and sucrose, which were found to be important in summer aerosols. The recovery of levoglucosan was estimated by spiking blank filters and was better than 90%. The precision evaluated by analyzing parts of the same filters was about 2% for the monosaccharide anhydrides and 7% for the other saccharidic compounds in the case of a winter aerosol sample, and the corresponding values for a summer aerosol sample were 5% and 8%. The method was applied to urban PM_{10} (particulate matter of <10 μm aerodynamic diameter) aerosols collected at Ghent, Belgium, during a 2000–2001 winter and a 2001 summer episode and revealed interesting seasonal variations. While monosaccharide anhydrides were relatively more important during the winter season owing to wood burning, the other saccharidic compounds were more prevalent during the summer season, with some of them, if not all, originating from the vegetation.

KEYWORDS: atmospheric aerosols; biomass burning; gas chromatography/mass spectrometry; ion trap; levoglucosan; organic carbon; saccharides

INTRODUCTION

Water-soluble organic carbon (WSOC) constitutes a major fraction of atmospheric aerosols in both polluted and remote areas. Our knowledge of the composition is, in general, insufficient to judge the possible effects on climate and human health. In recent years, the investigation of aerosol WSOC compounds which contribute to the ability of particles to act as cloud condensation nuclei and also participate in the complex organic liquid-phase chemistry of clouds has received considerable attention.[1,2] It has been stressed by Fuzzi *et al.*[2] that reliable determinations of the molecular forms of WSOC in atmospheric aerosols are still lacking and are needed in order to arrive at model compounds which can be used to simulate the chemical and physical properties of the entire organic carbon mass of aerosols. The WSOC fraction of atmospheric aerosols has been demonstrated to contain three main classes of compounds: (1) neutral/basic compounds, (2) mono- and dicarboxylic acids and (3) polyacidic compounds. Characterization by ^{1}H NMR spectroscopy showed that the neutral/basic fraction was mainly composed of polyols,[1] and levoglucosan has been proposed as a model compound for this fraction.[2]

Levoglucosan arises from the pyrolysis of cellulose, the main building material of wood, at temperatures higher than 300 °C and is accompanied by minor quantities of

*Correspondence to: Magda Claeys, University of Antwerp (UIA), Department of Pharmaceutical Sciences, Universiteitsplein 1, B-2610 Antwerp, Belgium. E-mail: claeys@uia.ua.ac.be
†Paper presented at the 20th Informal Meeting on Mass Spectrometry, Fiera di Primiero, Italy, 12–16 May 2002.
‡On leave from the Institute for Low Temperature Physics and Engineering, National Academy of Sciences of the Ukraine, 47 Lenin Avenue, 61164 Kharkov, Ukraine.
Contract/grant sponsor: Belgian Federal Office of Scientific, Technical and Cultural Affairs (OSTC); Contract/grant numbers: PODO II, EV/06/11B; PODO II, EV/06/11A.
Contract/grant sponsor: Research Council of the University of Antwerp (UA-BOF-ASPEO).
Contract/grant sponsor: Fonds voor Wetenschappelijk Onderzoek—Vlaanderen.

isomers, namely 1,6-anhydro-β-D-glucofuranose, mannosan (1,6-anhydro-β-D-mannopyranose) and galactosan (1,6-anhydro-β-D-galactopyranose).[3] Whereas 1,6-anhydro-β-D-glucofuranose is also formed by pyrolysis of cellulose, mannosan and galactosan result from the pyrolysis of hemicelluloses.[3] In contrast to other molecular markers of biomass burning (i.e. diterpenoids, triterpenones, triterpadienes and methoxylated phenolics), levoglucosan is emitted in large amounts, is sufficiently stable, is specific to cellulose-containing substances and meets all important criteria to serve as an ideal molecular marker of biomass burning.[4–8]

In a previous paper, we reported a method for the quantitative determination of levoglucosan and related monosaccharide anhydrides, mannosan and galactosan, in atmospheric aerosols, based on capillary gas chromatography with flame ionization detection, extraction with dichloromethane, trimethylsilylation and the use of an external recovery standard.[9] It was shown that the atmospheric concentration of the monosaccharide anhydrides, levoglucosan, mannosan and galactosan, in the PM_{10} (particulate matter of <10 μm aerodynamic diameter) aerosol at Ghent, Belgium, was 0.56 μg m^{-3} for the winter season, which was about a factor of 20 higher than for the summer season, and that the carbon in the monosaccharide anhydrides accounted for about 2% of the organic carbon in Ghent winter aerosols. The primary objective of the present study was to elaborate the above method[9] by using gas chromatography (GC)/ion trap mass spectrometry (MS), taking advantage of ion trap MS/MS technology, and by resorting to an internal calibration procedure with a compound structurally similar to the monosaccharide anhydrides (i.e. methyl β-L-arabinopyranoside). The advantages of ion trap MS/MS technology for selective and sensitive detection have been well documented in the analysis of polychlorodibenzo-*p*-dioxins.[10–12] Other advantages of ion trap instruments, in addition to economic considerations, i.e. high MS/MS efficiencies and versatility in the control of the ion dissociation process, have been described by Plomley and co-workers.[10,11]

The developed method was applied to urban PM_{10} aerosols collected on quartz fiber filters in Ghent, Belgium, during a 2000–2001 winter and a 2001 summer period. To our surprise, we detected saccharidic compounds other than monosaccharide anhydrides (i.e. arabitol, mannitol, glucose, fructose, inositol and sucrose) in summer aerosols, with some compounds at apparently higher concentrations than those of levoglucosan in winter aerosols. In view of the possible significance of these saccharidic compounds as model compounds for aerosol WSOC, we also quantified them by using a response factor relative to methyl β-L-arabinopyranoside. To our knowledge, the present study constitutes the first work on the occurrence of saccharidic compounds other than monosaccharide anhydrides in urban atmospheric aerosols, their possible sources and their seasonal variations.

EXPERIMENTAL

Chemicals

Standards of levoglucosan (1,6-anhydro-β-D-glucopyranose), mannosan (1,6-anhydro-β-D-mannopyranose), galactosan (1,6-anhydro-β-D-galactopyranose), D-(+)-arabitol, D-(+)-mannitol, methyl β-L-arabinopyranoside and methyl β-L-xylanopyranoside were obtained from Sigma (St. Louis, MO, USA). D-(+)-Glucose, D(-)-fructose, *myo*-inositol and sucrose were purchased from Merck (Darmstadt, Germany). *N*-Methyl-*N*-trimethylsilyltrifluoroacetamide (MSTFA) containing 1% trimethylchlorosilane (TMCS) and anhydrous pyridine used for trimethylsilylation were obtained from Pierce (Rockford, IL, USA). Dichloromethane (SupraSolv grade) was supplied by Merck and methanol (Super grade) by Lab-Scan (Dublin, Ireland). Chemical structures of the saccharidic compounds determined in this study are given in Fig. 1.

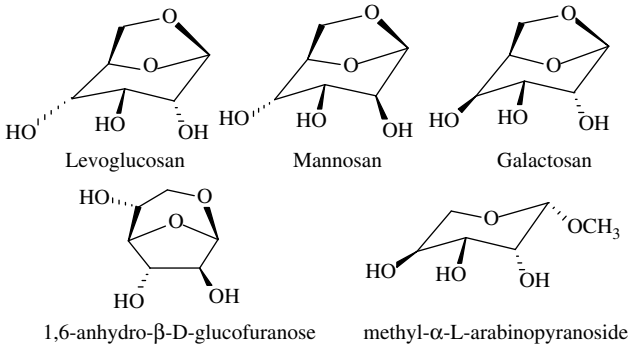

Figure 1. Structures of the compounds studied.

Aerosol collections

Urban aerosols were collected during a winter (9 November 2000 to 8 March 2001) and a summer (28 May–9 September 2001) period at the Institute for Nuclear Sciences (coordinates: 51°01′N, 3°44′E), which is located within the city of Ghent about 3 km to the south of the city center. The major sources of air pollution in the close vicinity are expected to be residential heating, automotive emissions from a major highway and highway intersection, a municipal incinerator and some chemical (plastics) industries. The sampler was an open-faced 'total' filter sampler, equipped with a cylindrical intake tube facing downward, and essentially collected the PM_{10} aerosol;[13,14] it used a Whatman QM-A quartz fiber filter (o.d. 47 mm) and was operated at a flow-rate of 150 l min^{-1}. The collection time per sample was typically 24 or 48 h. In addition to the actual samples, a number of field blanks were also taken using a sampling time of only 10 s.

Sample preparation

The part of the filter sample used for extraction was one-eighth of the whole filter area. Before extraction, the recovery standard methyl β-L-arabinopyranoside was added (6 μg for winter and 1 μg for summer aerosol samples). The spiked filter part was extracted three times, each time for 30 min with 20 ml of dichloromethane–methanol (80 : 20, v/v) under ultrasonic agitation in 25 ml Pyrex glass flasks with Teflon-lined stoppers, following a protocol that was established in previous studies.[15,16] The combined extracts were reduced with a rotary evaporator (213 hPa, 35 °C) to about 1 ml. Subsequently, the concentrated extract was filtered through a Teflon syringe filter (0.45 μm) and completely dried under a stream of nitrogen. Finally, the dried sample was dissolved in

200 μl of dichloromethane–methanol (50 : 50, v/v). Standard solutions of the saccharidic compounds were prepared in methanol. For derivatization, part of the final sample extract (one-fifth) was transferred to a 1 ml silylation vial and dried under a stream of nitrogen. Then, 40 μl of the trimethylsilylation mixture containing the reagent MSTFA + 1% TMCS and pyridine (2 : 1, v/v) were added and the reaction was carried out for 60 min at 70 °C. After trimethylsilylation, 1 μl was immediately analyzed by GC/MS. For derivatization of standard solutions of monosaccharide anhydrides and other saccharidic compounds, the same procedure was applied.

Instrumentation

Qualitative and quantitative analyses were performed on a GC/MS system consisting of a TRACE GC2000 gas chromatograph and a Polaris Q ion trap mass spectrometer fitted with an external electron ionization source (ThermoFinnigan, San Jose, CA, USA). Major advantages of this recent technology are that the ion trap is less prone to contamination and can be easily cleaned and the ion source can be replaced without venting the instrument. For data acquisition and processing, Xcalibur version 1.2 software was used. The gas chromatograph was equipped with a deactivated silica precolumn (2 m × 0.25 mm i.d.) and a CP Sil 8CB low-bleed capillary column (95% dimethyl-, 5% phenylpolysiloxane, 0.25 μm film thickness, 30 m × 0.25 mm i.d.) (Chrompack, Middelburg, The Netherlands).

For analysis, a sample volume of 1 μl was injected into a split/splitless injector, operated in the splitless mode (splitless time: 0.5 min) at 250 °C. The carrier gas was helium at a flow-rate of 1.2 ml min^{-1}. The temperature of the transfer line was 280 °C. The temperature program was initial temperature at 120 °C held for 2 min, a gradient of 5 °C min^{-1} up to 200 °C, held for 2 min, then 20 °C min^{-1} to 300 °C, held for 2 min. The total analysis time was 27 min. The mass spectrometer was operated in the electron ionization (EI) mode at an electron energy of 70 eV and an ion source temperature of 220 °C. For qualitative analysis the full-scan mode was applied in the mass range m/z 45–500. For quantitative analysis the instrument was operated in the selected ion monitoring (SIM) or the multiple reaction monitoring (MRM) mode. In both modes the fragment ion at m/z 217 was selected because this ion is characteristic of all saccharidic compounds considered in the present study. For operation in the SIM mode the scan time was 0.24 s, whereas for operation in the MRM mode the scan time was 0.38 s, the product ion mass range was m/z 110–217, the collision-induced dissociation (CID) amplitude of the supplementary potential was 1.2 V_{p-p} (peak-to-peak) and the duration of the excitation was 15 ms. The signal-to noise (S/N) ratios were calculated using the program 'Signal to Noise Calculator' (version 1.1, ThermoQuest, 1999), which is based on the root mean square (r.m.s) of noise calculations and is part of the Xcalibur version 1.2 software.

The quantification of the monosaccharide anhydrides, levoglucosan, mannosan and galactosan, was based on an internal standard calibration procedure employing methyl β-L-arabinopyranoside as internal standard, whereas that of the other saccharidic compounds, arabitol, mannitol, glucose, fructose, inositol and sucrose, was based on the use of a response factor relative to methyl β-L-arabinopyranoside. For assessing the amount of 1,6-anhydro-β-D-glucofuranose, for which no reference compound was available, the response factor of levoglucosan was used.

RESULTS AND DISCUSSION

Optimization of the analytical procedure

As the primary objective of our study was to develop a reliable and robust method for the determination of the monosaccharide anhydrides, levoglucosan, mannosan and galactosan, in atmospheric aerosol samples, and since it is well established that levoglucosan is the major contributor to this class of compounds and an ideal marker for biomass combustion,[4–9,17] the optimization of the method was mainly directed towards levoglucosan.

In a first series of experiments, attention was given to the selection of a suitable solvent mixture for the extraction of the monosaccharide anhydrides, levoglucosan, mannosan and galactosan, from aerosols collected on quartz fiber filters. In previous work, it was demonstrated that the monosaccharide anhydride, levoglucosan, could be extracted from such filter samples using the non-polar solvent dichloromethane with an extraction efficiency of about 60%[9] although it is water-soluble. Taking into account the polar character of levoglucosan, in the present work we evaluated dichloromethane–methanol (80 : 20, v/v) and compared it with pure dichloromethane and pure methanol for the extraction of levoglucosan, its stereoisomers, mannosan and galactosan, and glucose from a Ghent winter aerosol sample. On the basis of this comparison (Fig. 2), which revealed that dichloromethane–methanol (80 : 20, v/v) was as efficient as methanol for the extraction of the monosaccharide anhydrides and even for the more polar glucose, it was selected for further determinations. The extraction recovery employing dichloromethane–methanol (80 : 20, v/v) was assessed by spiking blank filter parts (one-eighth) with known amounts of levoglucosan and was estimated to be 90.0 ± 2.4% (n = 3) and 97.0 ± 4.0% (n = 3) at the 2 μg and 740 ng levels, respectively.

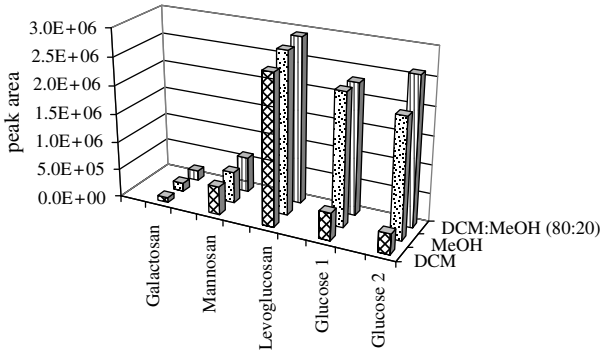

Figure 2. Peak areas of levoglucosan, galactosan, mannosan and glucose obtained for the analyses of a winter aerosol sample extracted with dichloromethane, methanol and dichloromethane–methanol (80 : 20, v/v). The GC/MS analyses were performed in the total scan mode. Abbreviations: DCM, dichloromethane; MeOH, methanol.

With regard to derivatization, the procedure developed in our previous study using MSTFA + 1% TMCS,[9] which was shown to yield a single TMS derivative for each of the monosaccharide anhydrides, levoglucosan, mannosan and galactosan, was followed. While one derivative was observed for the latter compounds, and for methyl β-L-arabinopyranoside, methyl β-L-xylanopyranoside, arabitol, mannitol, inositol and sucrose, multiple peaks were observed for glucose (two) and fructose (three), in agreement with literature data.[18,19]

For the selective detection of the monosaccharide anhydrides, levoglucosan, mannosan, galactosan and 1,6-anhydro-β-D-glucofuranose, the saccharidic compounds, arabitol, mannitol, glucose, fructose, inositol and sucrose, and the internal standard, methyl β-L-arabinopyranoside, in the SIM and MRM modes, the ion at *m/z* 217 was selected because it is characteristic of the TMS derivative(s) of all these compounds and is also abundant (Fig. 3 and Table 1).

Using the SIM mode, qualitative information is given by the retention time. In contrast, in the MRM mode employing MS/MS technology, after selection of the fragment ion (*m/z* 217) and subsequent CID, the whole fragment ion spectrum is acquired, providing specific spectral information (i.e. MS/MS) in addition to the retention time. The conditions for the dissociation of the selected fragment ion at *m/z* 217 were optimized for levoglucosan by varying the amplitude of the supplementary potential between 0.7 and 1.5 V_{p-p}. Fragment ion mass spectra were acquired for the *m/z* 217 ion of levoglucosan-TMS with different CID amplitudes (Fig. 4). A CID amplitude of 1.2 V_{p-p} was selected because under these conditions the abundance ratio between the product ions (*m/z* 143 and 147) and the ion at *m/z* 217 were high and the ion at *m/z* 217 was still fairly abundant (relative abundance (RA) = 35%). Evaluation of the S/N ratios for the analysis of a summer aerosol sample containing small amounts of the monosaccharide anhydrides, in the MRM mode (*m/z* 217), revealed that for all the peaks corresponding to the minor contributors to this class of compounds, galactosan, mannosan and 1,6-anhydro-β-D-glucofuranose, the S/N ratios were all >10. The product ion *m/z* 217 spectra for the other saccharidic compounds determined in this study (not shown) were very similar to that of levoglucosan (Fig. 4(b)) except for arabitol (Fig. 4(d)) and mannitol (not shown), for which the ion at *m/z* 129 was the base peak. These results suggest that in the case of arabitol and mannitol the ion at *m/z* 217 has a different structure or a different internal energy.

We also compared the MRM mode with the SIM mode, both using the ion at *m/z* 217, by analyzing a winter aerosol sample and evaluating the S/N ratios for all the detected saccharidic compounds, and found that the S/N ratios were about a factor of two better in the SIM mode. Because the sensitivity was not a critical issue and spectral information (i.e. MS/MS) was also considered important, further quantitative determinations were carried out in the MRM mode.

As internal standards, two compounds structurally related to the monosaccharide anhydrides, levoglucosan, galactosan and mannosan, namely, methyl β-L-arabinopyranoside and methyl β-L-xylanopyranoside, were evaluated. Both compounds contain three hydroxy groups and a ketal function as the monosaccharide anhydrides (Fig. 1). Methyl β-L-arabinopyranoside was selected because its TMS derivative eluted in an interference-free region of the total ion chromatogram when analyzing real aerosol samples. In contrast, the TMS derivative of methyl β-L-xylanopyranoside eluted close to that of mannosan (the retention times were 13.36 and 13.56 min for the TMS derivative of methyl β-L-xylanopyranoside and mannosan, respectively) and co-eluted with a minor compound present in aerosol samples.

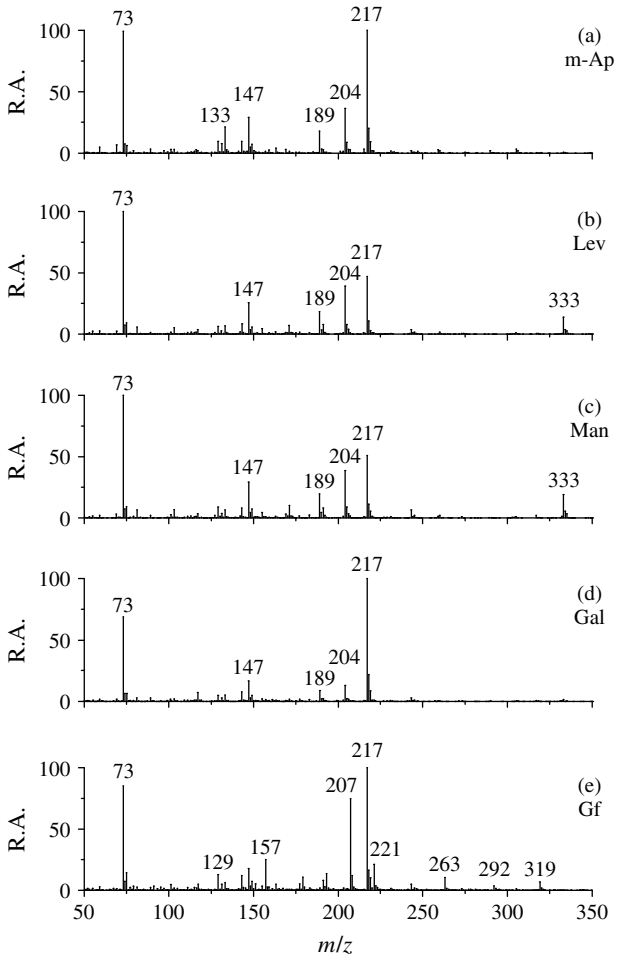

Figure 3. EI mass spectra obtained for the TMS derivatives of (a) methyl β-L-arabinopyranoside, used as internal standard; (b) levoglucosan (1,6-anhydro-β-D-glucopyranose); (c) mannosan (1,6-anhydro-β-D-mannopyranose); (d) galactosan (1,6-anhydro-β-D-galactopyranose); and (e) 1,6-anhydro-β-D-glucofuranose. All mass spectra were obtained on reference compounds, except in (e), for which no reference compound was available, obtained in the analysis of a winter aerosol sample. The last compound was characterized on the basis of its chromatographic retention time.[3] The peaks at *m/z* 157, 207, 221, 263 and 292 are due to interferences. Abbreviations: m-Ap, methyl β-L-arabinopyranose; Lev, levoglucosan; Man, mannosan; Gal, galactosan; Gf, 1,6-anhydro-β-D-glucofuranose.

Table 1. Summary of mass spectral data obtained by GC/ion trap MS for saccharidic compounds

Compound	Formula	M_r	t_r(min)	Fragment ions, m/z (RA, %)
Arabitol-TMS_5	$C_{20}H_{52}O_5Si_5$	512	14.24	395 (2), 322 (9), 319 (17), 307 (15), 277 (7), 243 (6), 217 (100), 205 (10), 191 (8), 147 (79), 129 (33), 117 (12), 103 (11), 79 (8), 73 (76), 50 (4)
D-Fructose-TMS_5	$C_{21}H_{52}O_6Si_5$	540	15.98/16.14/16.20	437 (45/41/58), 347 (21/17/27), 319 (9/10/25), 295 (16/8/5), 281 (4/6/5), 257 (40/39/35), 235 (3/15/3), 221 (9/7/8), 217 (56/65/27), 207 (34/40/39), 204 (5/4/56), 191 (20/17/20), 179 (8/13/4), 157 (11/8/14), 149 (23/14/17), 147 (56/52/59), 129 (15/14/19), 95 (9/10/11), 79 (38/29/29),73 (100/100/100), 69 (13/7/16), 52 (13/13/14)
D-Glucose-TMS_5	$C_{21}H_{52}O_6Si_5$	540	17.75/19.76	435 (4/4), 345 (4/6), 317 (3/3), 305 (6/4), 291 (4/4), 243 (6/6), 217 (22/27), 204 (100/100), 191 (42/55), 189 (19/25), 169 (6/5), 147 (43/40), 129 (15/12), 73 (73/84)
D-Mannitol-TMS_6	$C_{24}H_{62}O_6Si_6$	512	18.44	419 (4), 345 (8), 331 (9), 319 (71), 307 (6), 255 (5), 229 (8), 217 (57), 205 (19), 191 (13), 157 (48), 147 (92), 129 (64), 117 (16), 73 (100)
myo-Inositol-TMS_6	$C_{24}H_{60}O_6Si_6$	612	21.52	432 (20), 393 (5), 343 (7), 318 (63), 305 (100), 291 (6), 265 (22), 217 (72), 204 (13), 191 (32), 177 (9), 147 (61), 129 (22), 103 (15), 73 (85)
Sucrose-TMS_8	$C_{36}H_{86}O_{11}Si_8$	918	25.18	437 (19), 361 (100), 331 (5), 319 (6), 271 (18), 243 (13), 217 (21), 204 (8), 191 (6), 169 (35), 147 (19), 129 (11), 73 (48)

Calibration curves for each monosaccharide anhydride, levoglucosan, mannosan and galactosan, were obtained using MRM from the injection of 1 µl of different solutions in two different concentration ranges. For quantitative determination in winter aerosol samples, the ranges of the calibration curves were 0–70 ng μl^{-1} for levoglucosan and 0–14 ng μl^{-1} for mannosan and galactosan, whereas for that in summer aerosol samples, the ranges were 0–12.5 ng μl^{-1} for levoglucosan and 0–2.5 ng μl^{-1} for mannosan and galactosan. For each monosaccharide anhydride and each concentration range, high correlation coefficients ($R^2 > 0.99$, $n = 6$–11) were obtained. Calibration curves used for quantitative determination in summer aerosol samples are illustrated in Fig. 5.

In the course of our work, we found that special attention needs to be paid not to overload the GC/ion trap MS system. In the case of aerosol samples containing high amounts of levoglucosan, the peak observed for it was severely distorted owing to overloading of the capillary column giving rise to an unusual peak shape (i.e. heading) and because the number of ions admitted to the ion trap is controlled. This overloading phenomenon could easily be monitored because it results in abnormal peak ratios between levoglucosan and its stereoisomers, mannosan and galactosan, present at much lower concentrations in aerosol samples and in calibration solutions. If the overloading phenomenon occurred, the samples used for injection into the GC/MS system were simply diluted.

The day-to-day precision of the method was evaluated by analyzing parts of the same filter samples on three different days. For a winter aerosol sample, the RSD was about 2% for the monosaccharide anhydrides and 7% for the other saccharidic compounds, whereas the corresponding values for a summer aerosol sample were 5% and 8%.

Application of the method to urban aerosol samples

The method was applied to nine quartz fiber filter samples from the 2000–2001 winter collection at Ghent and to 10 filter samples from the 2001 summer period. Figure 6 illustrates typical chromatograms, obtained in the MRM mode (m/z 217), for a winter and two summer aerosol samples. For all samples from each period, we had measured the particulate mass (PM) by weighing[16] and the contents of organic carbon (OC) and elemental carbon (EC) by a thermal–optical transmission (TOT) technique.[9,20] The atmospheric concentrations of the monosaccharide anhydrides, levoglucosan, mannosan, galactosan and 1,6-anhydro-β-D-glucofuranose, and of the other saccharidic compounds, arabitol, mannitol, glucose, fructose, inositol and sucrose, in the nine winter and 10 summer samples are summarized in Table 2. The concentrations of the PM, OC and EC in these same samples are also included in Table 2. The percentages of OC attributed to each of the saccharidic compounds and to their sum are given in Table 3. The atmospheric concentrations of the monosaccharide anhydrides and their percentage contributions to the OC are higher in winter than in summer, in good agreement with those obtained in a previous study on aerosol samples collected in 1998 at the same urban site.[9] In a recent study by Poore[21] on $PM_{2.5}$ aerosols collected at the Fresno air monitoring site in California, USA, during 2000, it was found that the atmospheric concentration of levoglucosan was higher in winter than in summer and that it contributed more to the particulate mass in winter. The results imply that wood burning is much more pronounced

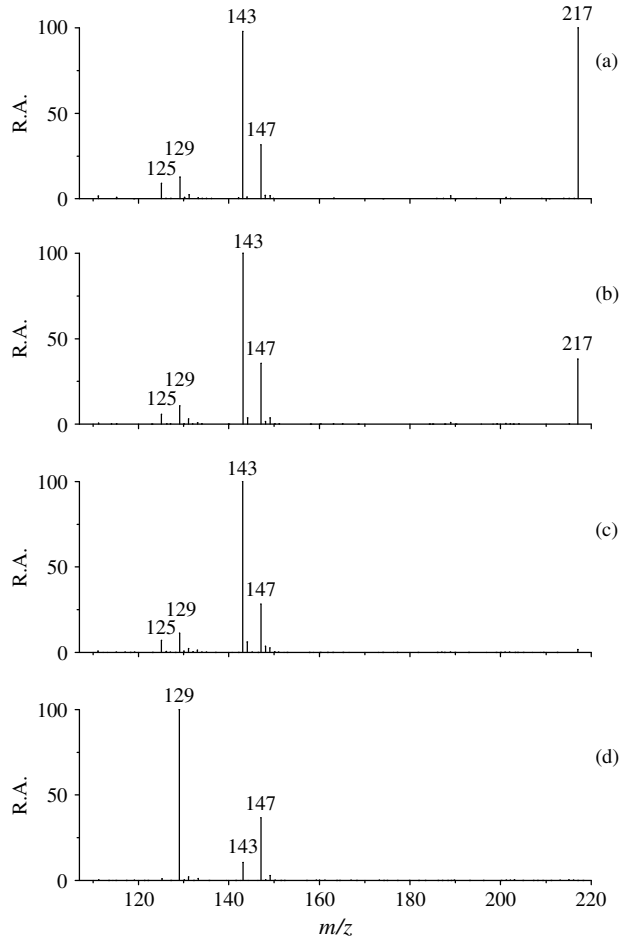

Figure 4. Fragment ion mass spectra obtained for the ion at *m/z* 217 of the TMS derivative of levoglucosan (a–c) employing different CID amplitudes of (a) 0.9, (b) 1.2 and (c) 1.5 V_{p-p}, and of arabitol (d) employing a CID amplitude of 1.2 V_{p-p}. The duration of excitation was 15 ms.

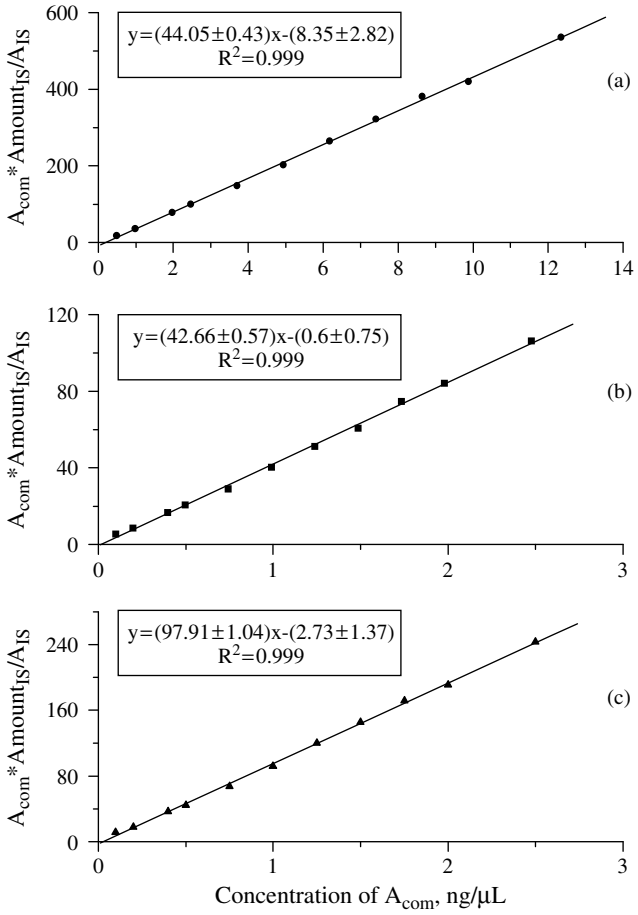

Figure 5. Calibration curves used for the quantitative determination of (a) levoglucosan, (b) mannosan and (c) galactosan for summer aerosol samples. Abbreviations: com, compound; IS, internal standard (= methyl *β*-L-arabinopyranoside).

Table 2. Average atmospheric concentrations and concentration ranges for PM, OC, EC and the saccharidic compounds in the 2000–2001 winter and 2001 summer PM_{10} aerosol sample sets from Ghent, Belgium

	Winter ($n = 9$)		Summer ($n = 10$)	
	Mean	(Range)	Mean	(Range)
PM (µg m^{-3})	48	(13–168)	33	(19–53)
OC (µg m^{-3})	10.7	(2.4–45)	5.9	(3.5–9.2)
EC (µg m^{-3})	1.13	(0.38–3.5)	1.24	(0.81–1.73)
Sum of saccharides (µg m^{-3})	0.71	(0.19–2.8)	0.73	(0.39–1.32)
Levoglucosan (ng m^{-3})	420	(96–1900)	19.1	(9.1–27)
Mannosan (ng m^{-3})	61	(10–290)	3.0	(2.0–3.9)
Galactosan (ng m^{-3})	25	(4.9–115)	1.02	(0.67–1.17)
Glucofuranose (ng m^{-3})	32	(7.5–140)	1.57	(0.90–2.5)
Arabitol (ng m^{-3})	26	(6.3–59)	105	(45–260)
Mannitol (ng m^{-3})	26	(7.8–70)	97	(31–220)
Glucose (ng m^{-3})	73	(30–153)	270	(110–610)
Fructose (ng m^{-3})	37	(10–126)	193	(39–440)
Inositol (ng m^{-3})	4.7	(1.3–17.2)	40	(3.0–97)
Sucrose (ng m^{-3})	48	(7.2–98)	100	(7.7–200)

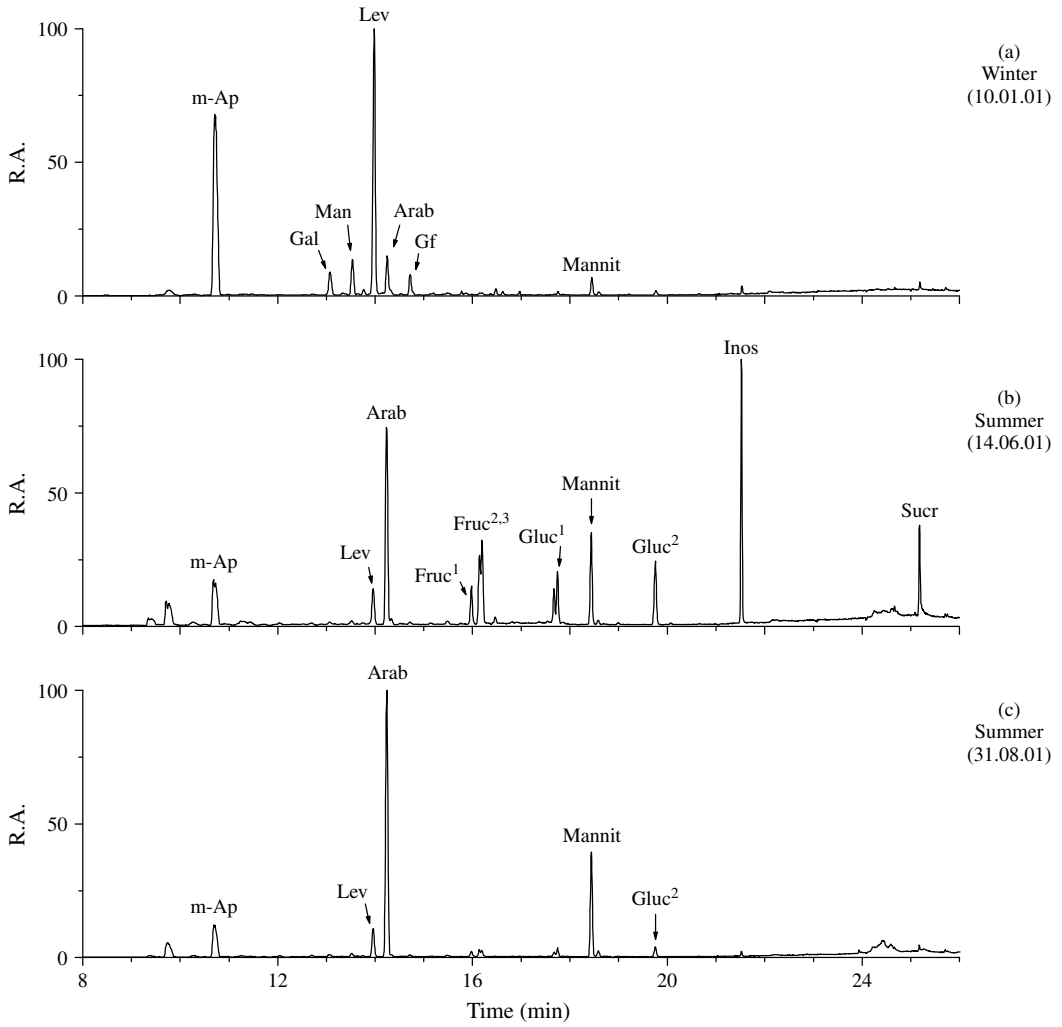

Figure 6. Total ion chromatograms in the MRM mode (*m/z* 217; CID amplitude, 1.2 V_{p-p}; duration of excitation, 15 ms) obtained on (a) a winter aerosol sample and (b, c) summer aerosol samples. Abbreviations: for m-Ap, Lev, Man, Gal and Gf, see Fig. 3; Arab, arabitol; Mannit, mannitol; Gluc, glucose; Fruc, fructose; Inos, inositol; Sucr, sucrose. Retention times: m-Ap, 10.70; Gal, 13.07; Man, 13.54; Lev, 13.99; Arab, 14.24; Gf, 14.72; Fruc (three peaks), 15.94, 16.15 and 16.20; Gluc (two peaks), 17.74 and 19.72; Mannit, 18.44; Inos, 21.53; Sucr, 25.18 min.

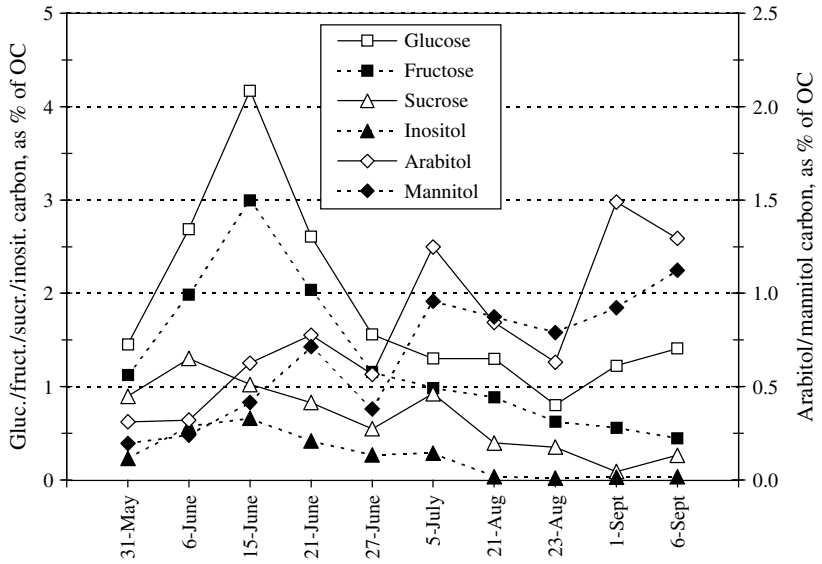

Figure 7. Percentage contribution of carbon from glucose, fructose, inositol, sucrose, arabitol and mannitol to the organic carbon (OC) in the individual samples of the 2001 summer PM_{10} aerosol sample set from Ghent, Belgium. The dates in the abscissa indicate the collection dates.

Table 3. Average percentage contribution (mean ± stanadard deviation) of carbon from the saccharidic compounds to the organic carbon in the 2000–2001 winter and 2001 summer PM_{10} aerosol sample sets from Ghent, Belgium

	Winter ($n = 9$)	Summer ($n = 10$)
Sum of saccharidic compounds	3.56 ± 1.58	5.73 ± 2.03
Levoglucosan	1.71 ± 0.49	0.16 ± 0.08
Mannosan	0.22 ± 0.06	0.025 ± 0.009
Galactosan	0.096 ± 0.021	0.008 ± 0.003
Glucofuranose	0.135 ± 0.043	0.013 ± 0.005
Arabitol	0.21 ± 0.22	0.81 ± 0.41
Mannitol	0.20 ± 0.24	0.66 ± 0.33
Glucose	0.50 ± 0.45	1.85 ± 1.01
Fructose	0.18 ± 0.09	1.28 ± 0.81
Inositol	0.022 ± 0.008	0.26 ± 0.24
Sucrose	0.29 ± 0.23	0.66 ± 0.39

in winter than in summer. For the other saccharidic compounds, arabitol, mannitol, glucose, fructose, inositol and sucrose, their atmospheric concentrations and percentage contributions to the OC are higher in summer than in winter. The atmospheric levels of glucose, fructose, inositol and sucrose and their contributions to the OC were highest at the beginning of summer (in June; see contributions to the OC in Fig. 7), whereas for the sugar alcohols, arabitol and mannitol, highest levels and contributions to the OC were noted later in summer (July–September; see Fig. 7). The sugar alcohols, arabitol and mannitol, are primary photosynthesis products in mature leaves, and are attributed to the vegetation,[22] although other sources, such as fungi[23] and algae[24] cannot be excluded. The source of the other saccharidic compounds, glucose, fructose, inositol and sucrose, is still unclear but a possible source could be developing leaves.

The carbon in the saccharidic compounds contributes on average 3.6% of the OC during winter and 5.7% of the OC during summer (Table 3). Expressed as percentages of organic aerosol mass (organic matter, OM), thereby using a multiplying factor of 1.4 to convert the measured OC value into OM,[16,25] the average contributions of the saccharidic compounds to the OM amount to 5.4% during winter and 8.9% during summer. In a previous study at the same Ghent sampling site,[16] it was found that the identified extractable and elutable organic matter represented 3.1% of the OM during both a 1998 winter and a 1988 summer episode. About 100 compounds were quantified in that study, which belonged to seven classes, i.e. (1) n-alkanes, (2) fatty acids, (3) dicarboxylic and oxocarboxylic acids, (4) diterpenoic acids, (5) lignin pyrolysis products, (6) polyaromatic hydrocarbons and (7) other compounds. Phthalates were the major contributers to the class of other compounds, and the class of the fatty acids was the most prominent of the seven classes, particularly during winter. The present study indicates that the saccharidic compounds contribute more to the OM than the sum of the above seven classes at the Ghent sampling site. During summer, the contribution of the saccharidic compounds is almost three times larger than that of the above seven classes combined.

CONCLUSIONS

We have developed and validated a gas chromatographic/ion trap mass spectrometric method for the determination of levoglucosan and the related monosaccharide anhydrides, mannosan, galactosan and 1,6-anhydro-β-D-glucofuranose, in urban atmospheric aerosols collected on quartz fiber filters. The method is based on extraction with dichloromethane–methanol (80:20, v/v), trimethylsilylation, multiple reaction monitoring in the MS/MS mode using the ion at m/z 217, and the use of an internal standard calibration procedure with the structurally related compound methyl β-L-arabinopyranoside. In addition, the method allows the quantification of other saccharidic compounds, arabitol, mannitol, glucose, fructose, inositol and sucrose, which were found to be important in summer aerosols. The recovery of levoglucosan was estimated by spiking blank filters and was better than 90%. The precision, evaluated by analyzing parts of the same filters, was about 2% for the monosaccharide anhydrides and 7% for the other saccharidic compounds in the case of a winter aerosol sample, whereas the corresponding values for a summer aerosol sample were 5% and 8%. Special precautions were taken not to overload the GC/ion trap MS system.

The method was applied to urban PM_{10} aerosols collected at Ghent, Belgium, during a 2000–2001 winter and a 2001 summer episode and revealed interesting seasonal variations. Whereas monosaccharide anhydrides were relatively more important during the winter season due to wood burning, the other saccharidic compounds were more prevalent during the summer season, with some of them, if not all, originating from the vegetation. Furthermore, the saccharidic compounds appeared to be more important contributors to the organic aerosol mass than the seven compound classes measured in a previous study.[16] In future work, we will examine in more detail how the concentrations of the saccharidic compounds correlate with those of other markers of atmospheric processes (alkanes, pollen, etc.). Furthermore, it would be relevant to determine their concentrations in different size fractions. As the monosaccharide anhydrides and the saccharidic compounds considered in the present study are fairly polar and water-soluble, they may be relevant for the hygroscopic properties of atmospheric aerosol particles. To our knowledge, this study constitutes the first work on the occurrence of saccharidic compounds other than monosaccharide anhydrides in urban atmospheric aerosols, their possible sources and their seasonal variations.

Acknowledgements

The authors are indebted to the Belgian Federal Office of Scientific, Technical and Cultural Affairs (OSTC) (PODO II, Contract Nos EV/06/11B and EV/06/11A), the Research Council of the University of Antwerp (UA-BOF-ASPEO) and the 'Fonds voor Wetenschappelijk Onderzoek—Vlaanderen' for research support. V. Pashynska acknowledges the OSTC for a postdoctoral fellowship within the programme to promote more intensive collaboration between researchers of Central and Eastern Europe and of Belgium.

Jan Cafmeyer is thanked for performing the aerosol collections and Xuguang Chi is acknowledged for assisting in the measurements for organic and elemental carbon.

REFERENCES

1. Decesari S, Facchini MC, Fuzzi S, Tagliavini E. *J. Geophys. Res.* 2000; **105**: 1481.
2. Fuzzi S, Decesari S, Facchini MC, Matta E, Mircea M, Tagliavini E. *Geophys. Res. Lett.* 2001; **20**: 4079.
3. Shafizadek F. In *The Chemistry of Pyrolysis and Combustion*, Rowell R (ed.). Advances in Chemistry Series 207. American Chemical Society: Washington DC, 1984; 489.
4. Simoneit BRT, Schauer JJ, Nolte CG, Oros DR, Elias VO, Frazer MP, Rogge WF, Cass GR. *Atmos. Environ.* 1999; **33**: 173.
5. Nolte CG, Schauer JJ, Cass GR, Simoneit BRT. *Environ. Sci. Technol.* 2001; **35**: 1912.
6. Simoneit BRT, Elias VO. *Mar. Chem.* 2000; **69**: 301.
7. Frazer MP, Lakshmanan K. *Environ. Sci. Technol.* 2000; **34**: 4560.
8. Elias VO, Simoneit BRT, Cordeiro RC, Turcq B. *Geochim. Cosmochim. Acta* 2001; **65**: 267.
9. Zdráhal Z, Oliveira J, Vermeylen R, Claeys M, Maenhaut W. *Environ. Sci. Technol.* 2002; **36**: 747.
10. Plomley JB, Mercer RS, March RE. *Organohalogen Compd.* 1995; **23**: 7.
11. Plomley JB, Lausevic M, March RE. *Mass Spectrom. Rev.* 2000; **19**: 305.
12. Helen C, Lemasle M, Laplanche A, Genin E. *J. Mass Spectrom.* 2001; **36**: 546.
13. Claeys M, Vermeylen R, Kubatova A, Cafmeyer J, Maenhaut W. In *Proceedings of EUROTRAC Symposium '98, Transport and Chemical Transformation in the Troposphere*, Borrell PM, Borrell P (eds). WIT Press: Southampton, 1999; 501.
14. Kubátová A, Vermeylen R, Claeys M, Cafmeyer J, Maenhaut W. *J. Aerosol Sci.* 1999; **30**: S905.
15. Kubátová A, Vermeylen R, Claeys M, Cafmeyer J, Maenhaut W, Roberts G, Artaxo P. *Atmos. Environ.* 2000; **34**: 5037.
16. Kubátová A, Vermeylen R, Claeys M, Cafmeyer J, Maenhaut W. *J. Geophys. Res.* 2002; **107**: 8047.
17. Graham B, Mayol-Bracero OL, Guyon P, Roberts GC, Decesari S, Facchini MC, Artaxo P, Maenhaut W, Köll P, Andreae MO. *J. Geophys. Res.* 2002; **107**: 8343.
18. Bartolozzi F, Bertazza G, Bassi D, Cristoferi G. *J. Chromatogr. A* 1997; **758**: 99.
19. Poole CF. In *Handbook of Derivatives for Chromatography*, Blau K, King G (eds). Heyden: London, 1977; 152.
20. Birch ME, Cary RA. *Aerosol Sci. Technol.* 1996; **25**: 221.
21. Poore MW. *J. Air Waste Manage. Assoc.* 2002; **52**: 3.
22. Loewus FA, Dickinson MW. In *Encyclopedia of Plant Physiology, New Series*, vol. 13, Loewus FA, Tanner W (eds). Springer: Berlin, 1982; 194.
23. Davis JM, Fellman JK, Loescher WH. *Plant Physiol.* 1988; **86**: 129.
24. Reed RH, Davidson IR, Chudek JA, Foster R. *Phycology* 1985; **24**: 35.
25. Turpin BJ, Saxena P, Andrews E. *Atmos. Environ.* 2000; **34**: 2983.

total surface. Second, near the tops of the barriers to isomerization, where isomerization is slow, the potential for vibrationally mode-specific effects exists if the SEP process deposits energy in modes that are closely associated with the reaction coordinate(s). Third, if isomerization involves H atom tunneling, it may be possible to use these methods to explore the conformational mixture of the tunneling levels as a function of vibrational level and energy relative to the classical barrier height. Finally, there may be circumstances where the spectra will provide evidence for competing pathways turning off certain open channels for isomerization as other more efficient pathways open up.

References and Notes

1. D. A. Evans, D. J. Wales, *J. Chem. Phys.* **118**, 3891 (2003).
2. D. J. Wales, *Energy Landscapes* (Cambridge Univ. Press, Cambridge, 2003).
3. T. Ebata, K. Kouyama, N. Mikami, *J. Chem. Phys.* **119**, 2947 (2003).
4. B. C. Dian, A. Longarte, P. R. Winter, T. S. Zwier, *J. Chem. Phys.* **120**, 133 (2004).
5. D. Evans, D. Wales, B. C. Dian, T. S. Zwier, *J. Chem. Phys.* **120**, 148 (2004).
6. B. C. Dian, G. M. Florio, A. Longarte, T. S. Zwier, *J. Chem. Phys.*, in press.
7. M. Silva, R. Jongsma, R. W. Field, A. M. Wodtke, *Annu. Rev. Phys. Chem.* **52**, 811 (2001).
8. T. Burgi, T. Droz, S. Leutwyler, *Chem. Phys. Lett.* **246**, 291 (1995).
9. Y. D. Park, T. R. Rizzo, L. A. Peteanu, D. H. Levy, *J. Chem. Phys.* **84**, 6539 (1986).
10. L. A. Philips, D. H. Levy, *J. Chem. Phys.* **89**, 85 (1988).
11. Y. R. Wu, D. H. Levy, *J. Chem. Phys.* **91**, 5278 (1989).
12. L. L. Connell, T. C. Corcoran, P. W. Joireman, P. M. Felker, *J. Phys. Chem.* **94**, 1229 (1990).
13. J. R. Carney, T. S. Zwier, *J. Phys. Chem. A* **104**, 8677 (2000).
14. J. R. Carney, T. S. Zwier, *Chem. Phys. Lett.* **341**, 77 (2001).
15. B. C. Dian, J. R. Clarkson, T. S. Zwier, data not shown.
16. Studies of this type can be used to test statistical theories of isomerization rates which assume that intramolecular vibrational redistribution is fast compared to the rate of isomerization. See D. M. Leitner, B. Levine, J. Quenneville, T. J. Martinez, P. G. Wolynes, *J. Phys. Chem. A* **107**, 10706 (2003).
17. J. C. Keske, B. H. Pate, *Annu. Rev. Phys. Chem.* **51**, 323 (2000).
18. T. M. Korter, N. V. Tri, J. T. Yi, D. W. Pratt, personal communication (2003).
19. In Fig. 4, it is assumed that C(2) is the conformer responsible for the 747 cm^{-1} upper bound in the C→B spectrum on the basis of the relative energies of other barriers shown.
20. Density functional theory calculations at the Becke3LYP/6-31+G(d) level of theory predict barriers for the A-B and A-F isomerizations that are several hundred wavenumbers higher than experiment. However, the computed barriers for A→C(1), A→D, and A→E are close to those measured. This suggests that the pathway for A-B and A-F isomerizations may proceed by some pathway other than the direct one computed.
21. Supported by the National Science Foundation (CHE-0242818). We thank D. W. Pratt and his group for providing the results of their high-resolution spectra on TRA before publication.

Supporting Online Material

www.sciencemag.org/cgi/content/full/303/5661/1169/DC1

Figs. S1 and S2

17 November 2003; accepted 13 January 2004

Formation of Secondary Organic Aerosols Through Photooxidation of Isoprene

Magda Claeys,[1]* Bim Graham,[2,3] Gyorgy Vas,[1] Wu Wang,[1] Reinhilde Vermeylen,[1] Vlada Pashynska,[1] Jan Cafmeyer,[4] Pascal Guyon,[2] Meinrat O. Andreae,[2] Paulo Artaxo,[5] Willy Maenhaut[4]

Detailed organic analysis of natural aerosols from the Amazonian rain forest showed considerable quantities of previously unobserved polar organic compounds, which were identified as a mixture of two diastereoisomeric 2-methyltetrols: 2-methylthreitol and 2-methylerythritol. These polyols, which have the isoprene skeleton, can be explained by OH radical–initiated photooxidation of isoprene. They have low vapor pressure, allowing them to condense onto preexisting particles. It is estimated that photooxidation of isoprene results in an annual global production of about 2 teragrams of the polyols, a substantial fraction of the Intergovernmental Panel on Climate Change estimate of between 8 and 40 teragrams per year of secondary organic aerosol from biogenic sources.

Aerosols are of climatic interest because they act as cloud condensation nuclei (*1*) and scatter and absorb solar radiation (*2*). It has been well established that photooxidation products of monoterpenes (e.g., α- and β-pinene) (*3*, *4*), which are biogenic volatile organic compounds (VOCs) emitted mainly by terrestrial vegetation, contribute to the aerosol budget (*5*, *6*). However, it has been assumed that the much larger emissions of isoprene (*7*) do not result in secondary organic aerosol (SOA) formation in the atmosphere (*8*). Knowledge of the degradation mechanisms of isoprene, which represents almost 50% of all biogenic non-methane hydrocarbons on the global scale (*7*), is of considerable interest for air quality modeling (*9*). It has recently been proposed that the heterogeneous reaction of isoprene on acidic particles could be an important source of humic-like substances, which contribute 20 to 50% of the water-soluble organic aerosol at urban and rural sites in Europe (*10*). Here, we report evidence that photooxidation of isoprene is a substantial source of SOA, contrary to previous assumptions.

[1]Department of Pharmaceutical Sciences, University of Antwerp, Universiteitsplein 1, B-2610 Antwerp, Belgium. [2]Biogeochemistry Department, Max Planck Institute for Chemistry, Post Office Box 3060, D-55020 Mainz, Germany. [3]Atmospheric Research, Commonwealth Scientific and Industrial Research Organisation, PMB 1, Aspendale, Victoria 3195, Australia. [4]Department of Analytical Chemistry, Institute for Nuclear Sciences, Ghent University, Proeftuinstraat 86, B-9000 Gent, Belgium. [5]Institute of Physics, University of São Paulo, Rua do Matão, Travessa R, 187, CEP 05508–900 São Paulo, Brazil.

*To whom correspondence should be addressed. E-mail: magda.claeys@ua.ac.be

As part of the Cooperative Large-Scale Biosphere-Atmosphere Experiment in Amazonia Airborne Regional Experiment (LBA-CLAIRE) 1998 and 2001 experiments, atmospheric aerosols were collected at Balbina (1°55′S, 59°24′W), 125 km north of Manaus, Brazil, during the wet season (*11*). Backward air mass trajectories indicated that this site was not affected by anthropogenic sources, given that surface air masses originated from the northeast to east and had traveled 1000 km over the most remote regions of the Amazonian rain forest for almost a week before being sampled. The organic compounds present in the aerosol samples are, therefore, believed to be characteristic of local and regional atmospheric chemical phenomena rather than of long-range transport. The Amazon basin contains the world's largest humid forest ecosystem, which is known to emit large quantities of VOCs (*7*, *12*). Because solar radiation and the production of OH radicals are at a maximum in the tropics, the formation of photooxidation products from natural VOCs is expected to be important.

Selected aerosol samples were subjected to analysis by gas chromatography–mass spectrometry (GC-MS) for detailed characterization of organic compounds (*11*). Figure 1 presents a GC-MS total ion current chromatogram of the trimethylsilylated (TMS) extract of the fine size fraction [particulate matter with diameter <2.5 μm (PM2.5)] of a typical aerosol sample collected during the CLAIRE 2001 campaign with a high-volume (Hi-Vol) air sampler. Compounds **1** and **2** correspond to the newly found compounds, which were identified as diastereoisomeric forms (threo and erythro) of a polyol, specifically 2-methylthreitol and 2-methylerythritol. The structures of these compounds were elucidated with a combination of electron ionization (EI) and methane chemical ionization GC-MS, and then confirmed by a comparison of the GC-MS data with data from synthesized reference compounds (*11*).

Mass spectra of the TMS derivatives of compounds **1** and **2** are shown in figs. S1 and S2, and those of the synthesized reference compounds are given in fig. S3.

Taking into account that 2-methylthreitol and 2-methylerythritol have the C_5 isoprene skeleton, it is logical to propose that isoprene is the precursor for their formation in the atmosphere. To date, the photooxidation of isoprene in the atmosphere has been believed to result only in volatile products—particularly formaldehyde, methacrolein, and methyl vinyl ketone—and not in condensable products that can be found in the aerosol phase. A primary plant origin of the 2-methyltetrols could be ruled out because they are not known to be present in plant leaves (*13*), they were not found in a composite sample of leaves from Amazonian tree species (*11*), and they occur as a mixture of diastereoisomers, consistent with a non-enzymatic formation process. Because the 2-methyltetrols are not of primary biogenic origin, they have to be considered as SOA components. The 2-methyltetrols have, to our knowledge, not been reported before, either in chamber experiments with isoprene or from ambient aerosols. A possible reason that they have not been detected in earlier aerosol composition studies is that the methods generally used are targeted to the determination of dicarboxylic acids. These methods are based on methylation of carboxylic groups and GC-MS, or on direct liquid chromatography–MS with electrospray ionization in the negative ion mode, and are not well suited to the analysis of neutral polyols.

Chamber experiments with isoprene under simulated atmospheric conditions have generally been performed in the presence of relatively high levels of ozone and NO_x (*8*), conditions that are different from natural tropical atmospheric conditions, which, except in the burning season, are characterized by low NO_x concentrations [(NO) $<$ 100 parts per thousand (ppt)] (*14*). It is known that the photooxidation of isoprene is dominated by its reaction with OH radicals, because its reaction with ozone is relatively slow (*15*). When the OH radical–initiated photooxidation of isoprene has been investigated in the absence of NO_x, aerosol formation has been noted (*8*), and furthermore, the formation of 1,2-diol derivatives (i.e., 2- and 3-methyl-3-butene-1,2-diol) has been demonstrated (*16*). For the formation of the 1,2-diols, a reaction mechanism involving a reaction with $HO^{\cdot}/O_2$ followed by self- and cross-reactions of peroxyradicals ($RO_2^{\cdot}$) has been proposed (*16*). The formation of the 2-methyltetrols from isoprene in the present study under tropical atmospheric conditions can be explained by two cycles of these reactions (Fig. 2) [further discussion of potential formation mechanisms is available in the supporting online material (SOM) text]. The yield of the 2-methyltetrols from isoprene oxidation of 0.2% (0.4% in mass terms) is consistent with the low aerosol carbon yields in chamber experiments (*8*). The vapor pressures of the 2-methyltetrols are expected to be very low ($<1.6 \times 10^{-5}$ Torr, the value calculated for 2,3,4-pentanetriol at 27°C), so that these products are expected to be predominantly in the condensed phase (*17*). A gas-to-particle transfer mechanism, most likely condensation onto preexisting particles, operates in aerosol formation from 2-methyltetrols.

The 2-methyltetrols, 2-methylthreitol and 2-methylerythritol, are expected to be hygroscopic and to have a water solubility comparable to those reported for racemic D,L-threitol (i.e., 8.8 g ml^{-1} water) and meso-erythritol (i.e., 0.64 g ml^{-1} water), respectively (*18*). The hygroscopic growth of submicrometer aerosol particles has been studied with tandem differential mobility analysis at the same remote rain forest site in central Amazonia during the LBA-CLAIRE 1998 campaign (*19*). In that study, hygroscopic particles could be identified that were typical of the pristine rain forest atmosphere and were believed to contain oxidation products of biogenic compounds. In addition, it has been demonstrated that most aerosol particles contain enough water-soluble material to be able to act efficiently as cloud condensation nuclei (*20*).

In addition to the 2-methyltetrols, the extract of the fine size fraction of the wet season aerosols contained other oxygenated organic compounds, i.e., mono- and dihydroxydicarboxylic acids and polysaccharidic compounds (Fig. 1). The mono- and dihydroxydicarboxylic acids and saccharidic compounds were identified by comparing their EI mass spectra and GC behaviors with those of authentic standards. The mono- and dihydroxydicarboxylic acids included malic acid, α-hydroxyglutaric acid, tartaric acid, and previously unobserved minor compounds, which occurred as a mixture of diastereoisomers (threo and erythro) and were tentatively identified as 2,3-dihydroxyglutaric acids (Fig. 1, compounds **4** and **6**) (*11*). The major identified saccharidic compounds were levoglucosan, arabitol, mannitol, and glucose. Of the mono- and dihydroxydicarboxylic acids, malic, tartaric, and α-hydroxyglutaric acid have been previously reported in Amazonian aerosols at appreciable atmospheric concentrations ($>$10 ng m^{-3}) (*21*). As for the atmospheric origin of these compounds, malic acid has been proposed to be a late product in the photochemistry of unsaturated fatty acids (*22*), but other biogenic sources, such as *n*-alkanes emitted by the forest vegetation, could also be considered. The other mono- and dihydroxydicarboxylic acids, tartaric acid, α-hydroxyglutaric acid, and the 2,3-dihydroxyglutaric acids likely have the same atmospheric origin as malic acid. Levoglucosan (1,6-anhydro-β-D-glucopyranose) is a molecular marker for biomass burning (*23*), which has proven useful for monitoring biomass burning in Amazonian aerosols (*21*, *24*). The sugar alcohols, arabitol and mannitol, are attributed to natural background and are believed to originate from fungal spores, whereas the monosaccharide, glucose (a common plant sugar), is likely due to pollen (*25*).

To determine whether compounds were asso-

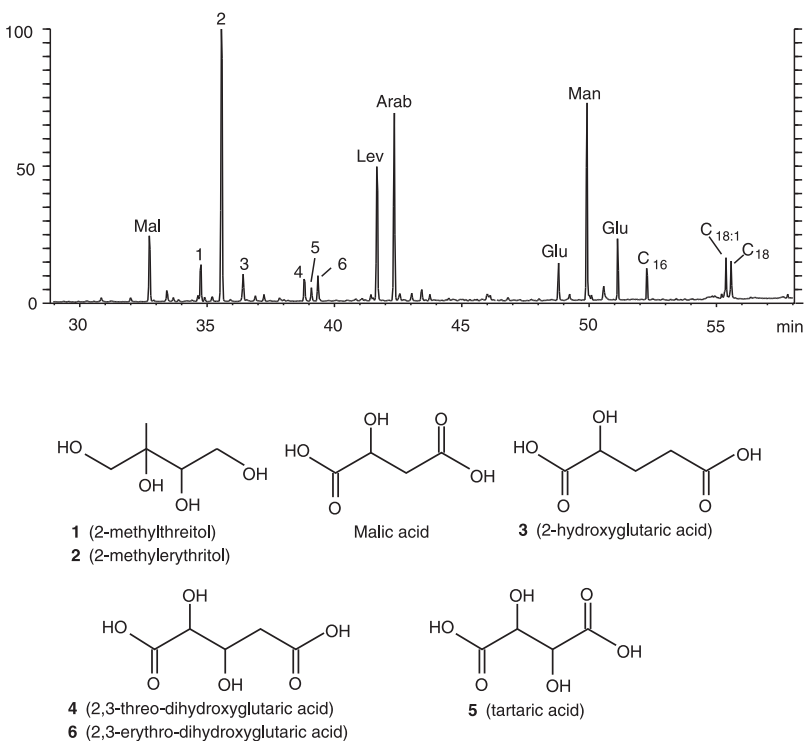

Fig. 1. GC-MS total ion current chromatogram obtained for a trimethylsilylated extract of the fine size fraction of a Hi-Vol sample collected during the LBA-CLAIRE 2001 campaign (25 to 27 July, day sampling only). Mal, malic acid; Lev, levoglucosan; Arab, arabitol; Glu, glucose (2 peaks); Man, mannitol; C_{16}, palmitic acid; $C_{18:1}$, oleic acid; C_{18}, stearic acid. Compounds **1** and **2** correspond to the previously unobserved 2-methyltetrols, i.e., 2-methylthreitol and 2-methylerythritol, respectively, arising from the photooxidation of isoprene.

ciated with fine- or coarse-mode particles, we analyzed a set of fine and coarse filter samples from daytime and nighttime collections during LBA-CLAIRE 2001. Quantitative determinations of the 2-methyltetrols, mono- and dihydroxydicarboxylic acids, and saccharidic compounds were performed by GC–flame ionization detection (Table 1) (*11*). The results obtained for the 2-methyltetrols show that they are enriched in the fine size fraction, suggesting that they are SOA components (i.e., formed by gas-to-particle conversion processes). The observation that 2-methyltetrols, formed by the daytime photooxidation of isoprene, are present at a considerable concentration in the nighttime sampling can be explained by the high chemical stability of the 2-methyltetrols and the lower nighttime temperatures, which favor condensation onto particles. Table 1 also shows that the 2-methyltetrols explain about 2% of the organic carbon (OC) in PM2.5 aerosols. Similarly, the mono- and dihydroxydicarboxylic acids—malic acid, α-hydroxyglutaric acid, the 2,3-dihydroxyglutaric acids, and tartaric acid—are enriched in the fine size fraction, as expected for SOA components. Levoglucosan, a primary organic aerosol component and a molecular marker for wood combustion (*23*), is associated with the fine size fraction, consistent with formation by a high-temperature combustion process. In contrast, the sugar alcohols, arabitol and mannitol, and the sugar, glucose, are enriched in the coarse size fraction, as could be expected for compounds typical of fungal spores and plant pollen (*25*). It is seen from Table 1 that the atmospheric concentration of the 2-methyltetrols is larger than that of malic acid, which was found to be the major hydroxydicarboxylic acid. The concentration of the 2-methyltetrols was comparable to that of oxalic acid, a dicarboxylic acid which is typically the major water-soluble organic species identified in atmospheric aerosols (*26*). The concentration of oxalic acid during the LBA-CLAIRE 2001 campaign was on average 57 ng m^{-3} for the fine size fraction and 63 ng m^{-3} for the coarse fraction (*25*).

The atmospheric concentrations of the 2-methyltetrols, malic acid, levoglucosan, arabitol, mannitol, and glucose in 10 selected total filter samples from the LBA-CLAIRE 1998 wet season campaign are provided in table S1. During the 1998 campaign, the atmospheric concentration of levoglucosan was quite low (average, 0.46 ng m^{-3}; range, 0 to 3.0 ng m^{-3}), indicating clean air conditions that were not affected by biomass smoke. The combined atmospheric concentration of the two 2-methyltetrols and their percentage relative to the OC mass were 31 ng m^{-3} and 0.61 ± 0.39%, respectively, and, similar to the 2001 campaign, the concentration and percentage were higher than those of malic acid (7.2 ng m^{-3} and 0.10 ± 0.06%, respectively).

In a study on VOCs performed at the same remote site in the Amazonian rain forest during the 1998 campaign (*12*), isoprene and its photooxidation products were measured, and it was concluded that isoprene chemistry can be regarded as a dominant process within this area. The isoprene mixing ratios were between 4 and 10 parts per billion (ppb), whereas those of the major photooxidation products of isoprene (methacrolein and methyl vinyl ketone) were always substantially below 1 ppb, pointing to a low oxidation capacity of the pristine atmosphere over the Amazonian rain forest; this is in agreement with ozone concentrations, which were always below 20 ppb. The median combined atmospheric concentration of the 2-methyltetrols found in the present work was 31 ng m^{-3}, or 10 ppt, corresponding to about 0.2% of the isoprene mixing ratio (calculated for a mixing ratio of 5 ppb). It can thus be concluded that aerosol formation from isoprene has a low yield, but considering the large amounts of isoprene that are emitted by the rain forest vegetation, this source may be very important for SOA formation. The apparent yield of 0.2% (0.4% in mass terms) of the 2-methyltetrols can be used to estimate the global contribution of isoprene oxidation to SOA formation (SOM text). An annual global emission of isoprene of about 500 Tg (*7*) suggests a SOA source strength of about 2 Tg, which can be compared with the Intergovernmental Panel on Climate Change (*27*) estimate of between 8 and 40 Tg per year of SOA from biogenic sources.

Our results indicate that natural aerosols collected in Amazonia, Brazil, contain considerable amounts of the 2-methyltetrols, 2-methylthreitol and 2-methylerythritol, which can be explained by OH radical–initiated photooxidation of isoprene, as well

Table 1. Concentrations (ng m^{-3}) of OC, elemental carbon (EC), polyhydroxylated compounds, and mono- and dihydroxydicarboxylic acids in fine and coarse filter samples from day and night collections with a Hi-Vol dichotomous sampler during the LBA-CLAIRE 2001 wet season campaign in Balbina, Brazil. The percentage carbon contributions to the OC are given in parentheses.

	Collection time 25 to 27 July 2001 day		Collection time 25 to 28 July 2001 night	
	Fine	Coarse	Fine	Coarse
OC	1550	2440	830	1610
EC	66	28	56	27
2-Methyltetrols (threo + erythro)	64.7 (1.84)	40.9 (0.74)	49.2 (2.62)	–*
Malic acid	32 (0.74)	10.9 (0.16)	11.6 (0.50)	–
α-Hydroxy glutaric acid	16.9 (0.44)	–	7.1 (0.35)	–
2,3-Dihydroxy glutaric acids (threo + erythro)	30 (0.71)	–	12.0 (0.53)	–
Tartaric acid	7.5 (0.15)	–	3.6 (0.14)	–
Levoglucosan	38 (1.10)	–	12.2 (0.66)	–
Arabitol	5.9 (0.17)	19.1 (0.34)	9.7 (0.51)	48 (1.31)
Mannitol	9.4 (0.24)	32 (0.52)	8.4 (0.40)	68 (1.68)
Glucose	15.6 (0.40)	134 (2.20)	0.6 (0.03)	2.7 (0.07)

*The dash denotes that the concentration was less than 10% of that in the fine size fraction; it is not given because of the large associated uncertainty. (The amount on the coarse filter has been corrected for the contribution from fine particles.)

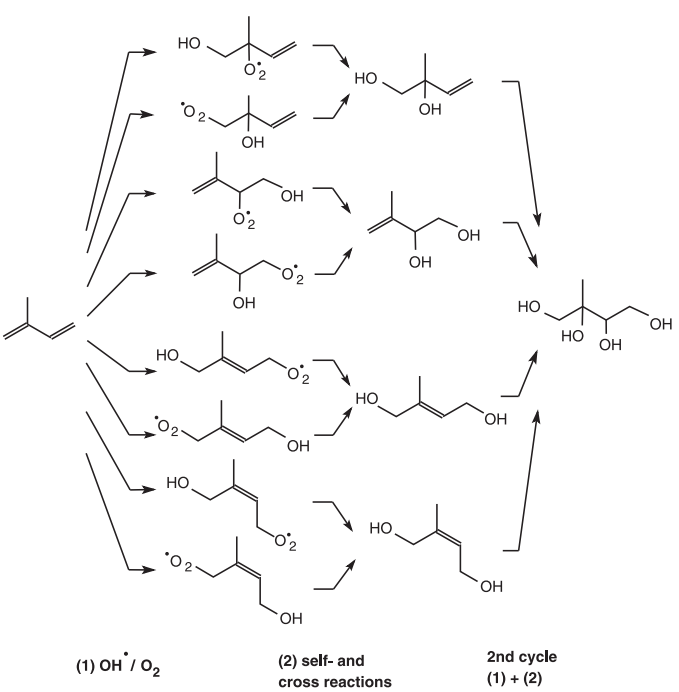

Fig. 2. Proposed formation of the 2-methyltetrols from isoprene by reaction with $OH^{\bullet}O_2$ followed by self- and cross-reactions of peroxyradicals. The intermediate 1,2-diols have been reported in chamber experiments with isoprene under low NO_x conditions (*16*).

as smaller amounts of mono- and dihydroxydicarboxylic acids. The 2-methyltetrols were identified as major oxygenated organic compounds in the fine size fraction, and it is estimated that they represent a SOA source strength of about 2 Tg per year. These compounds have low vapor pressure and are hygroscopic; they can therefore contribute to particle growth (*28*), enhance the ability of aerosols to act as cloud condensation nuclei, and result in the formation of haze (*29*) above forests. The 2-methyltetrols can be regarded as specific molecular markers for the photooxidation of isoprene in the ambient atmosphere and are, as such, of potential interest for source apportionment and air quality modeling studies. Contrary to widespread assumption, we suggest that photooxidation of isoprene emitted by forest vegetation results in substantial SOA formation.

References and Notes

1. T. Novakov, J. E. Penner, *Nature* **365**, 823 (1993).
2. M. O. Andreae, P. J. Crutzen, *Science* **276**, 1052 (1997).
3. T. Hoffmann *et al*., *J. Atmos. Chem.* **26**, 189 (1997).
4. T. Hoffmann, R. Bandur, U. Marggraf, M. Linscheid, *J. Geophys. Res.* **103**, 25569 (1998).
5. I. G. Kavouras, N. Mihalopoulos, E. G. Stephanou, *Nature* **395**, 683 (1998).
6. I. G. Kavouras, E. G. Stephanou, *Environ. Sci. Technol.* **36**, 5083 (2002).
7. A. Guenther *et al*., *J. Geophys. Res.* **100**, 8873 (1995).
8. S. N. Pandis, S. E. Paulson, J. H. Seinfeld, R. C. Flagan, *Atmos. Environ.* **25A**, 997 (1991).
9. H. Geiger, I. Barnes, I. Bejan, T. Benter, M. Spittler, *Atmos. Environ.* **37**, 1503 (2003).
10. A. Limbeck, M. Kulmala, H. Puxbaum, *Geophys. Res. Lett.* **30**, 1996 10.1029/2003GL0177738 (2003).
11. Materials and methods are available as supporting material on *Science* Online.
12. J. Kesselmeier *et al*., *Atmos. Environ.* **34**, 4063 (2000).
13. D. H. Lewis, D. C. Smith, *New Phytol.* **66**, 143 (1967).
14. A. L. Torres, H. Buchan, *J. Geophys. Res.* **93**, 1396 (1988).
15. R. Atkinson, W. P. L. Carter, *Chem. Rev.* **84**, 437 (1984).
16. L. Ruppert, K. H. Becker, *Atmos. Environ.* **34**, 1529 (2000).
17. J. H. Seinfeld, S. N. Pandis, *Atmospheric Chemistry and Physics: From Air Pollution to Climate Change* (Wiley, New York, 1998), pp. 724–743.
18. S. Cohen, Y. Marcus, Y. Migron, S. Dikstein, A. Shafran, *J. Chem. Soc. Faraday Trans.* **89**, 3271 (1993).
19. J. Zhou, E. Swietlicki, H. C. Hansson, P. Artaxo, *J. Geophys. Res.* **107**, 8055 10.1029/2000JD00203 (2002).
20. G. C. Roberts, M. O. Andreae, J. Zhou, P. Artaxo, *Geophys. Res. Lett.* **28**, 2807 (2001).
21. B. Graham *et al.*, *J. Geophys. Res.* **107**, 8047 10.1029/2001JD000336 (2002).
22. K. Kawamura, R. Sempéré, Y. Imai, M. Hayashi, *J. Geophys. Res.* **101**, 18721 (1996).
23. B. R. T. Simoneit *et al*., *Atmos. Environ.* **33**, 173 (1999).
24. Z. Zdráhal, J. Oliveira, R. Vermeylen, M. Claeys, W. Maenhaut, *Environ. Sci. Technol.* **36**, 747 (2002).
25. B. Graham *et al.*, *J. Geophys. Res.* **108**, 4766 10.1029/2003JD003990 (2003).
26. P. Saxena, L. M. Hildemann, *J. Atmos. Chem.* **24**, 57 (1996).
27. J. T. Houghton *et al*., Eds. *Climate Change 2001: The Scientific Basis* (Cambridge Univ. Press, Cambridge, 2001).
28. W. R. Leaitch *et al*., *J. Geophys. Res.* **104**, 8095 (1999).
29. F. W. Went, *Nature* **187**, 641 (1960).

30. This work is a contribution to the Large Scale Biosphere-Atmosphere Experiment in Amazonia (LBA). We thank the Belgian Federal Science Policy Office, the University of Antwerp, the "Fonds voor Wetenschappelijk Onderzoek–Vlaanderen," the European Commission, the Max Planck Gesellschaft, Germany, and the Fundacão de Apoio a Pesquisa do Estado de São Paulo and Conselho Nacional de Desemvolvimento Cientifico e Tecnologico, Brazil, for research support; the National Botanic Garden of Belgium for tree leaf specimens; and J. Kesselmeier and anonymous reviewers for constructive comments.

Supporting Online Material

www.sciencemag.org/cgi/content/full/303/5661/1173/DC1
Materials and Methods
SOM Text
Figs. S1 to S4
Schemes S1 and S2
Table S1
References

21 October 2003; accepted 21 January 2004

Repeating Seismic Events in China

David P. Schaff[1]* and Paul G. Richards[1,2]

About 10% of seismic events in and near China from 1985 to 2000 were repeating events not more than about 1 kilometer from each other. We cross-correlated seismograms from ~14,000 earthquakes and explosions and measured relative arrival times to ~0.01 second, enabling lateral location precision of about 100 to 300 meters. Such precision is important for seismic hazard studies, earthquake physics, and nuclear test ban verification. Recognition and measurement of repeating signals in archived data and the resulting improvement in location specificity quantifies the inaccuracy of current procedures for picking onset times and locating events.

Each day, hundreds of seismic events are located by the traditional method of picking onset times of seismic waves recorded by seismometer networks and then interpreting these data with a travel time model to infer the epicenter (latitude/longitude), depth, and origin time of each event. Pick errors (i.e., errors in picking onset times) and errors in the models lead to uncertainties in event location amounting to a few percent of the station spacing. These errors frustrate efforts to understand the interactions between neighboring events and to obtain more precise models of Earth structure. Model error may be reduced by locating many earthquakes simultaneously, and pick error may be reduced by measuring relative arrival times by cross-correlation when possible (instead of onset times). Reduction in both types of error can lead to improvement in location precision of up to three orders of magnitude in specialized studies of small regions, typically using short windows (lengths of a few seconds) based on the *P*- and *S*-wave onsets (*1*–*8*). Here, we report improvements in epicentral locations over a broad area of diffuse seismicity, namely China and surrounding regions, using waveform cross-correlation on a large scale.

Repeating earthquakes or doublets arise when two events display nearly identical seismograms at a common station, implying that the events have similar focal mechanisms and similar locations. Doublets have primarily been observed in the creeping zones of major faults (*9*–*12*) and more recently in subduction zones (*13*–*15*). Clusters of repeating events are often called multiplets.

[1]Lamont-Doherty Earth Observatory, [2]Department of Earth and Environmental Sciences, Columbia University, Palisades, NY 10964, USA.

*To whom correspondence should be addressed. E-mail: dschaff@ldeo.columbia.edu

The cross-correlation coefficient *CC* quantifies waveform similarity, with values from 0 (no similarity) to 1 (a perfect match). We processed 12 GB of waveform data for about 14,000 events in and surrounding China as listed in the Annual Bulletin of Chinese Earthquakes (ABCE) from January 1985 to April 2000 (*16*, *17*). The waveforms were acquired from several networks of stations that are archived by the IRIS Consortium (*18*).

We define a doublet to be an event pair having $CC \geq 0.8$ for time windows from 5 s before the *P*-wave to 40 s after the *Lg*-wave recorded at least at one station. An example of a pair of events in China (magnitude ~ 4.5) with similar waveforms, recorded at a station ~1100 km away, yields $CC = 0.8$ for a 220-s window bandpass-filtered from 0.5 to 5 Hz (Fig. 1). *Lg* is the largest amplitude phase and shows a high degree of correlation, even though it is a complex, scattered wave. The waveforms are similar even for unknown phases and coda as well as for the *P*- and *S*-waves.

An automated search isolated 1301 events that have $CC \geq 0.8$ with at least one other event (Fig. 2). These comprise 950 doublets, which can be grouped as 494 multiplets of various sizes (table S1). They are well distributed throughout seismic zones in and near China and represent more than 9% of the ABCE events from 1985 to 2000. Most events satisfy $CC \geq 0.8$ at only one station because of the sparse station coverage. As a general rule, high similarity of complex multiply scattered waves for an event pair requires the events to be no farther apart than about one-quarter of the dominant wavelength, which in our case is ~0.8 km (*19*, *20*). If the signal-to-noise ratio is good enough to see different phases overlay, it further supports the hypothesis that the

Atmos. Chem. Phys., 6, 375–402, 2006
www.atmos-chem-phys.org/acp/6/375/
SRef-ID: 1680-7324/acp/2006-6-375
European Geosciences Union

Atmospheric Chemistry and Physics

Characterization of the organic composition of aerosols from Rondônia, Brazil, during the LBA-SMOCC 2002 experiment and its representation through model compounds

S. Decesari[1], S. Fuzzi[1], M. C. Facchini[1], M. Mircea[1], L. Emblico[1], F. Cavalli[1], W. Maenhaut[2], X. Chi[2], G. Schkolnik[3], A. Falkovich[3], Y. Rudich[3], M. Claeys[4], V. Pashynska[4], G. Vas[4], I. Kourtchev[4], R. Vermeylen[4], A. Hoffer[5], M. O. Andreae[5], E. Tagliavini[6,7], F. Moretti[6], and P. Artaxo[8]

[1]Istituto Scienze dell'Atmosfera e del Clima – C.N.R., Bologna, Italy
[2]Department of Analytical Chemistry, Institute for Nuclear Sciences, Ghent University, Gent, Belgium
[3]Department of Environmental Sciences, Weizmann Institute, Rehovot, Israel
[4]Department of Pharmaceutical Sciences, University of Antwerp, Antwerp, Belgium
[5]Biogeochemistry Department, Max Planck Institute for Chemistry, Mainz, Germany
[6]Dipartimento di Chimica "G. Ciamician", Università di Bologna, Bologna, Italy
[7]Centro di Ricerche per le Scienze Ambientali, Università di Bologna, Ravenna, Italy
[8]Instituto de Fisica, Universidade de Sao Paulo, Sao Paulo, SP, Brazil

Received: 2 May 2005 – Published in Atmos. Chem. Phys. Discuss.: 9 August 2005
Revised: 28 November 2005 – Accepted: 27 December 2005 – Published: 7 February 2006

Abstract. The chemical composition of carbonaceous aerosols collected during the LBA-SMOCC field experiment, conducted in Rondônia, Brazil, in 2002 during the transition from the dry to the wet season, was investigated by a suite of state-of-the-art analytical techniques. The period of most intense biomass burning was characterized by high concentrations of submicron particles rich in carbonaceous material and water-soluble organic compounds (WSOC). At the onset of the rainy period, submicron total carbon (TC) concentrations decreased by about 20 times. In contrast, the concentration of supermicron TC was fairly constant throughout the experiment, pointing to a constant emission of coarse particles from the natural background. About 6–8% of TC (9–11% of WSOC) was speciated at the molecular level by GC-MS and liquid chromatography. Polyhydroxylated compounds, aliphatic and aromatic acids were the main classes of compounds accounted for by individual compound analysis. Functional group analysis by proton NMR and chromatographic separation on ion-exchange columns allowed characterization of ca. 50–90% of WSOC into broad chemical classes (neutral species/light acids/humic-like substances). In spite of the significant change in the chemical composition of tracer compounds from the dry to the wet period, the functional groups and the general chemical classes of WSOC changed only to a small extent. Model compounds representing size-resolved WSOC chemical composition for the different periods of the campaign are then proposed in this paper, based on the chemical characterization by both individual compound analysis and functional group analysis deployed during the LBA-SMOCC experiment. Model compounds reproduce quantitatively the average chemical structure of WSOC and can be used as best-guess surrogates in microphysical models involving organic aerosol particles over tropical areas affected by biomass burning.

Correspondence to: S. Decesari
(s.decesari@isac.cnr.it)

1 Introduction

The Large Scale Biosphere-Atmosphere Experiment in Amazonia – Smoke, Aerosols, Clouds, Rainfall and Climate (LBA-SMOCC) experiment was conducted in the Amazon Basin in the period September – mid-November 2002, with the principal purpose of investigating how and to what extent aerosol particles produced by biomass burning alter cloud formation. Previous studies have highlighted that smoke particles emitted by biomass burning are enriched in organic carbon (OC) and also contain a variable amount of elemental carbon (EC), operationally defined as the fraction of carbon that is refractory at high temperature in an inert atmosphere (Chow et al., 2001; Mayol-Bracero et al., 2002a, b). Elemental carbon is often used as a synonym for "soot carbon" defined by IPCC(2001) as "Particles formed during the quenching of gases at the outer edge of flames of organic vapors, consisting predominantly of carbon, with lesser

amounts of oxygen and hydrogen present as carboxyl and phenolic groups and exhibiting an imperfect graphitic structure".

Although carbonaceous aerosols are less hygroscopic than particles consisting of sulfate or sodium chloride, the polar organic compounds known to occur in biomass burning aerosol may absorb water from the gas phase, thus enhancing the ability to nucleate cloud droplets ("CCN ability") of the particles (Svenningsson et al., 2005). The organic compounds that have an affinity to water are generally isolated by extracting aerosol samples with water and measuring their total carbon concentration by liquid total organic carbon (TOC) analysis. These water-soluble organic compounds (WSOC) constitute a variable fraction of the aerosol TC. They can be internally or externally mixed with other aerosol constituents (e.g., inorganic soluble and insoluble components) and, most importantly, they contain a wide range of chemical species that are expected to show very different water solubilities (Mochida and Kawamura, 2004). All these factors are of primary importance in determining the CCN ability of biomass burning particles.

In order to evaluate the net effect of carbonaceous particles from biomass burning on the formation of clouds, it is indicated to compare their characteristics with those formed during unpolluted episodes in the same region. The SMOCC aircraft campaign revealed that forested areas distant from the biomass burning sources show a background of CCN with low concentrations and a rather constant vertical profile in the troposphere (Andreae et al., 2004). Previous studies highlighted the occurrence of natural sources of aerosol particles from the biota in the same area (Graham et al., 2003). The processes responsible for particle formation in the Amazon basin – biomass burning and biogenic emission – are geographically distinct and follow very different temporal trends. In particular, the dramatic increase in the aerosol load observed during the dry period in the rural areas of Rondônia and Mato Grosso can be mainly attributed to biomass burning. In the same period, biomass burning products strongly impact the TC concentrations and composition in the neighboring forested areas. Biogenic organic aerosols have mainly been characterized at forest sites located at a large distance from the main pollution sources (Kubátová et al., 2000; Graham et al., 2003; Claeys et al., 2004a). However, primary biological particles (e.g., pollen and fungal spores) were found to increase also in rural areas at the end of the dry period, when the increase in precipitation impedes extensive burning activities (Graham et al., 2002).

The chemical composition of carbonaceous particles produced by biomass burning in Rondônia was characterized during the 1999 LBA-EUSTACH-2 campaign (Mayol-Bracero et al., 2002a). It was found that WSOC account for 45–75% of TC and that a substantial fraction of the thermally refractory carbon determined by evolved gas analysis (EGA) analysis is also water-soluble. This soluble refractory carbonaceous material was linked to complex polycarboxylic acids, which are denoted by the generic term "HULIS" (humic-like substances) and were determined by analysis of water extracts. Another important fraction of WSOC was identified as neutral compounds mainly consisting of sugar-like compounds such as levoglucosan, which is the most abundant product of the pyrolysis of cellulose at temperatures higher than 300°C (Shafizadeh, 1984).

Except for levoglucosan, linking the organic composition of the aerosol to the chemical reactions occurring during the complex and varying combustion processes remains an issue. The relatively low concentrations of sugars in biomass burning smoke, compared to the abundance of their degradation products, likely results from the fact that biomolecules undergo pronounced chemical transformations, even at relatively low temperatures (<200°C), owing to heterogeneous reactions with oxygen and reactions between amines and sugars (Moens et al., 2004). Combustion studies on Graminaceae (Knicker et al., 1996) have shown that at 350°C cellulose and hemicelluloses are completely degraded to volatile products (with levoglucosan as a major compound) in a time span of 1 min. The remaining char products contain mainly complex aliphatic compounds and newly formed aromatic compounds, and have a very low content of oxygenated substances. The composition of these char residues is completely different from that of biomass burning aerosol which instead shows a large fraction of oxygenated compounds (Graham et al., 2002). The oxygenated compounds may form during the low-temperature stages of combustion. In addition, a substantial fraction of compounds volatilized at the high temperatures of the combustion process may condense onto particles, when the smoke plume cools down. Finally, photochemical production of newly formed condensable compounds within the plume and in the regional haze will increase the fraction of oxygenated species relative to soot (Gao et al., 2003; Reid et al., 2005). Therefore, there are a number of processes that are responsible for the high content of oxygenated water-soluble organic compounds in biomass burning particles, ranging from combustion itself, through the early aging stages to actual in-situ secondary processes. Chemical transformation within the aerosol particles, e.g., polymerization of low-molecular weight compounds, is not a likely mechanism for altering significantly the oxygen to carbon ratio of the organic matter. However, it may alter its solubility through the modification of functional groups of specific classes of compounds, for example, benzoic acids may be converted to high-molecular weight aromatic acids (Hoffer et al., 2005) and unsaturated acids may be further oxidized to dihydroxy acid derivatives (Claeys et al., 2004b).

The biogenic sources of organic aerosols are still only partly understood and cover a wide range of different sources and source processes. The identification of biomolecules (mainly sugars and lipids) in the coarse fraction of aerosols collected at forest sites has highlighted the importance of the direct emission of primary biological particles, like spores, pollen, plant debris, soil detritus and insect body parts, to

the atmosphere (Graham et al., 2003; Simoneit et al., 2004). Recently, another source process has been characterized for the formation of secondary organic aerosols, i.e., photo-oxidation of isoprene which is emitted in large amounts by the tropical forest vegetation (Claeys et al., 2004a; Wang et al., 2005).

Biomass burning and biogenic sources show a very different seasonal dependence. In a simplified scheme (since the Amazon forest ecosystem is productive throughout the year, while biomass burning mainly occurs in the dry period), the latter gives rise to episodes of very high aerosol loads, which are superimposed on a relatively constant natural background of primary biological particles and photo-oxidation products of biogenic volatile organic compounds (secondary organic aerosol). Consequently, the atmospheric concentrations of biomass burning aerosols, along with their composition, will vary according to the strength and type of the combustion sources, as well as the ambient conditions, with strong diel and day-to-day variations (Falkovich et al., 2005; Schkolnik et al., 2005; Fuzzi et al., 2006[1]). The aim of this study is to trace the changes in the organic aerosol composition during the transition from the biomass burning period to the rainy period, with particular focus on WSOC. A combination of state-of-the-art techniques for speciation of polar organic compounds has been exploited for the chemical characterization, together with functional group analysis by ^{1}HNMR. The results and implications of some specific analytical methods have been published in separate papers (Falkovich et al., 2005; Schkolnik et al., 2005). Here, they are included to provide comprehensive compositions for the main periods of the LBA-SMOCC field campaign. In past studies on tropical areas affected by biomass burning, only limited analyses (e.g., ion chromatography or GC-MS) on selected samples have been performed, providing sets of measurements that are difficult to intercompare (Reid et al., 2005). Here, we provide what is probably the most complete set of analyses of biomass burning aerosols, for a full assessment of the organic chemical composition. Finally, we propose a model representation of the water-soluble fraction of OC, derived from both individual compounds and functional group composition for the different periods of the campaign. These model compositions should be useful in microphysical models of aerosol hygroscopic growth, as well as in laboratory studies for the determination of the hygroscopic behavior of mixed organic/inorganic systems (Svenningsson et al., 2005).

[1] Fuzzi, S., Decesari, S., Facchini, M. C., Cavalli, F., Emblico, L., Mircea, M., Andreae, M. O., Trebs, I., Hoffer, A., Guyon, P., Artaxo, P., Rizzo, L.V., Lara, L. L., Pauliquevis, T., Maenhaut, W., Raes, N., Chi, X., Mayol-Bracero, O. L., Soto, L., Claeys, M., Kourtchev, I., Rissler, J., Swietlicki, E., Tagliavini, E., Schkolnik, G., Falkovich, A. H., Rudich, Y., Fisch G., and Gatti, L. V.: Overview of the inorganic and organic composition of size-segregated aerosol in Rondônia, Brazil, from the biomass burning period to the onset of the wet season, J. Geophys. Res., in review, 2006.

2 Experimental

2.1 Sampling

The SMOCC field campaign was conducted at a ground-based station on the Fazenda Nossa Senhora Aparecida (FNS) (10°45′44″ S, 62°21′27″ W, 315 m a.s.l.), which is located approximately 8 km southwest of the town Ouro Preto do Oeste in the state of Rondônia, Brazil. The place was deforested by fire about 20 years ago and the area is now a pasture site with *Brachiaria brizantha* as a dominant grass species. Sampling of aerosol particles was conducted from 9 September to 14 November 2002, by deploying a series of impactors and filter-based techniques. A full description of the sampling platform is provided by Fuzzi et al. (2006[1]). According to meteorological conditions, the sampling period was subdivided into dry (intense burning; 11 September to 7 October), transition (8 October to 29 October) and wet (30 October to 14 November) periods. With respect to the determination of total carbon (TC) and organic and elemental carbon (OC and EC), and of the organic chemical composition, sampling was conducted with: a) a stacked filter unit (SFU) sampler that separates coarse ($10>d>2.0\,\mu$m, where d is the aerodynamic diameter) and fine particles ($d<2.0\,\mu$m) by sequential filtration on 8.0 and 0.4 μm pore-size Nuclepore® polycarbonate filters, with a flow rate of 10–15 l/min, operated by the Institute of Physics of the University of Sao Paulo (IFUSP); b) two SFU samplers equipped with quartz fiber filters (front and back-up) with a flow rate of 17 l/min and PM_{10} and $PM_{2.5}$ inlets, respectively, both operated by Ghent University (UGent); c) three high-volume dichotomous impactors (HVDS) with front and back quartz fiber filters, segregating fine (PM2.5) and coarse ($>2.5\,\mu$m) particles, operating at a flow rate of ca. 300 l/min, and deployed by UGent ($HVDS1_{UGent}$ and $HVDS2_{UGent}$) and by the Max Planck Institute for Chemistry (MPIC) ($HVDS_{MPIC}$); d) two microorifice uniform deposit impactors ($MOUDI_{IFUSP}$, from the University of Sao Paulo) with Nuclepore® polycarbonate filters as impaction foils, the other ($MOUDI_{UGent}$, from Ghent University) with aluminum foils on the impaction stages; e) a 5-stage Berner impactor with aluminum and Tedlar foils on the impaction stages, deployed by ISAC (Istituto Scienze dell'Atmosfera e del Clima). Sampling time varied from 12 h in the dry period (when the highest aerosol concentrations were encountered) to 24 and 48 h at the end of the campaign. Positive artifacts during sampling were either avoided by using inert substrates (polycarbonate, Tedlar, Aluminum) or corrected by the analysis of back-filters (in the case of quartz filters). In contrast, presumably semi-volatile organic compounds (Eatough et al., 2003) could not be efficiently collected by our sampling apparatus.

The comparison of aerosol measurements performed with analogous sampling systems (e.g., HVDS and SFU) indicates that the uncertainties in the flow measurement and potential other minor sampling biases, such as differences in the size cutoff between samples, led to differences of up to 25% in the concentration data reported from the various samplers and groups. Where such biases could be quantified and corrections applied, this is indicated in the text and tables. Otherwise, values are reported as obtained from the species mass measured on the particular samples and the sample volumes determined with the flow meters attached to the individual samplers.

2.2 TC/OC/EC analysis

Ghent University (UGent) analyzed the PM_{10} and $PM_{2.5}$ quartz fiber filters (both front and back-up) of the SFU samples and the fine and coarse filter samples (both front and back) of two HiVol samplers ($HVDS1_{UGent}$ and $HVDS2_{UGent}$) for OC, EC and TC (TC=OC+EC) with a thermal-optical transmission (TOT) technique (Birch and Cary, 1996; Schmid et al., 2001), using a thermal-optical carbon analyzer from Sunset Laboratory Inc. (Tigard, OR, USA). The analysis was done in a two-stage procedure; one or two 1.5-cm^2 rectangular punches of each quartz filter were heated stepwise (up to 900°C) in a non-oxidizing helium (He) atmosphere, and then (again up to 900°C) in an oxidizing atmosphere of 2% oxygen and 98% He. The carbon that evolves at each temperature is oxidized to carbon dioxide (CO_2), and then reduced to methane (CH_4) for quantification with a flame ionization detector (FID). The transmittance of light from a He-Ne laser through the filter punches is continuously monitored and used for setting the OC/EC "split" point, thereby correcting for pyrolysis/charring during the first stage of the analysis.

Max Planck Institute for Chemistry (MPIC) measured total carbon (TC) and the elemental carbon after water extraction (EC_w) on HiVol samples ($HVDS_{MPIC}$) by evolved gas analysis (EGA) (Mayol-Bracero et al., 2002; Hoffer et al., 2005). The combustion was performed in an oxygen atmosphere, the temperature was increased linearly from 50°C to 780°C at a rate of 20°C/min, and the conversion was completed over a MnO_2 catalyst at 800°C. The EC concentration was determined integrating the last peaks of the thermograms obtained after water extraction (Mayol-Bracero et al., 2002).

2.3 TOC analysis

UGent analyzed the fine ($<2.5\,\mu$m) filter samples (both front and back filters) from $HVDS1_{UGent}$ for total organic carbon (TOC). Filter punches of 1 or 1.5 cm^2 were placed in a 15 mL tube, 5 or 10 mL Millipore Simplicity water was added, and the tube was hand-shaken during 5 min, after which it was allowed to stand for 30 min. The sample extract was then filtered through a PVDF syringe filter (pore size 0.2 μm) and analyzed for TOC, thereby correcting for the inorganic carbon, with a Shimadzu TOC-V CPH analyzer. The TOC data were used as water-soluble OC.

ISAC subjected a sub-set of coarse HiVol ($HVDS2_{UGent}$) filter samples, having collected supermicron particles ($>2.5\,\mu$m), to TOC analysis. Upon extraction of $\frac{1}{4}$ of filter with 30 ml of deionized water, samples were filtered to remove the filter debris and analyzed by a Shimadzu TOC5000A analyzer. Blank levels were 1 ppm C and 0.25 ppm C, when filtering with hydrophilic cellulose filters and PTFE hydrophobic filters, respectively. Only coarse ($>2.5\,\mu$m) filters from the transition and the wet periods could be analyzed, because of the relatively low interference from fine particles (Graham et al., 2002).

Pre-cleaned Tedlar substrates mounted on a 5-stage Berner impactor were extracted by ISAC in 6 ml of deionized water in an ultrasonic bath, and analyzed by means of a Shimadzu TOC5000A analyzer. Blank levels were around 0.2 ppm C and a total of 37, 12, 5 size-segregated samples were analyzed for the dry, transition and wet periods, respectively.

2.4 GC-MS_{MPIC}

MPIC analyzed the fine fraction of the aerosols collected by the $HVDS_{MPIC}$ sampler for individual polar compounds by gas chromatography-mass spectrometry (GC-MS) (Hewlett Packard 6890 GC-MSD) after derivatization. The method was adapted from Graham et al. (2002). The samples (3.5–5.3 cm^2 of the filter) were extracted in 4–6 ml of acetonitrile for 1 h, agitated once every 15 min. The extract was then filtered through a 0.45 μm pore size PTFE syringe filter (Pall). An internal standard (3,3-dimethylglutaric acid) was added to 3 ml of filtered sample solution, which was then brought to dryness under a gentle stream of N_2. After this process, 50 μl pyridine and 50 μl bis(trimethylsilyl)trifluoroacetamide (BSTFA), containing 1% trimethylchlorosilane (TMCS) as a catalyst (Supelco), were added to the samples, which were then put into an oven at 70°C for 30 min. The sample was injected onto a HP5-MS column (30 m×250 μm; 0.25 μm film thickness) equipped with a Supelco guard column (deactivated methylsiloxane, 1 m×0.32 mm) in the splitless mode at 280°C. The temperature of the oven was held at 65°C for 10 min and ramped at 10°C/min to 310°C and held for 10 min. The mass spectrometer was operated both in the selected ion monitoring and full scan mode, and it was calibrated with aliquots of a stock solution of authentic standards. Repeated analysis of the samples showed that the precision of the method was about 20%.

2.5 GC-MS_{UA}

The University of Antwerp (UA) determined a series of polar organic compounds in aerosol samples, i.e., in the front fine filters of all $HVDS1_{UGent}$ samples and the aluminum

foils from selected $MOUDI_{UGent}$ collections, by using gas chromatography-mass spectrometry (GC-MS) following derivatization into trimethylsilyl derivatives. Two methods were employed: the first method was targeted to the quantitation of sugar-like compounds (i.e., anhydrosugars, the 2-methyltetrols, C_5 alkene triol derivatives of isoprene, the monosaccharides, and the sugar-alcohols), while the second method was targeted to the quantitation of acidic compounds (i.e., hydroxy monocarboxylic acids, dicarboxylic acids, hydroxy dicarboxylic acids and aromatic acids).

Method 1: The first method was adapted from one previously described for the determination of levoglucosan in urban aerosols (Pashynska et al., 2002). Before extraction, the recovery standard, methyl β-L-xylanopyranoside was added. The aluminum foils were also spiked with a second internal recovery standard, deuterated (d_3) – malic acid (2,2,3-d_3-malic acid; Cambridge Isotope Laboratories, Andover, MA, USA), for measurement of malic acid. Sample workup consisted of extraction with 3 times 20 ml dichloromethane:methanol (4:1, v/v) and trimethylsilylation of the extract residue with 50 μl of a 3:5 (v/v) mixture of pyridine and N-methyl-N-trimethylsilyltrifluoroacetamide containing 1% trimethylchlorosilane (MSTFA+1% TMCS). GC-MS analysis was performed with a TRACE GC2000 gas chromatograph and a Polaris Q ion trap mass spectrometer equipped with an external electron ionization source (ThermoFinnigan, San Jose, CA, USA) using an electron energy of 70 eV. The gas chromatograph was equipped with a deactivated silica precolumn (2 m $\times$ 0.25 mm i.d.) and a CP Sil 8CB low-bleed capillary column (95% dimethyl-, 5% phenylpolysiloxane, 0.25 μm film thickness, 30 m $\times$ 0.25 mm i.d.; Chrompack, Middelburg, The Netherlands). The following temperature program was applied: the initial temperature was 50°C and kept for 5 min, the temperature was then increased to 200°C at the rate of 3°C/min and kept at that temperature for a further 2 min and then raised to 310°C at the rate of 30°C/min. The total analysis time was 62 min. For derivatization of standard solutions of all saccharidic compounds, the same procedure was applied. The quantification was based on an internal standard calibration procedure employing methyl β-L-xylanopyranoside (and d_3-malic acid in case of the Al foils) as internal recovery standard and pure reference compounds, if available.

Method 2: The second method employs the same analytical principles as method 1 and is also based on the use of internal recovery standards. All glassware used for sample workup was deactivated with 5% dimethyldichlorosilane in toluene in order to minimize adsorption and loss of polar acidic compounds. Before extraction, three recovery standards (3.75 μg of each) were added to the filter sample: (a) deuterated glutaric acid (2,2,4,4-d_4-pentanedioic acid; Cambridge Isotope Laboratories), (b) deuterated malic acid (2,2,3-d_3-malic acid; Cambridge Isotope Laboratories) and (c) tropic acid (3-hydroxy-2-phenylpropionic acid; Fluka, Buchs, Switzerland). Deuterated glutaric acid served as internal recovery standard for the dicarboxylic acids, i.e., glutaric acid, succinic acid and fumaric acid. Deuterated malic acid served as internal recovery standard for the hydroxy mono- and dicarboxylic acids, i.e., malic acid, glyceric acid, α- and β-hydroxy glutaric acid, threonic acid, an isomer of threonic acid, and tartaric acid. Tropic acid served as internal recovery standard for the aromatic acids, i.e., 2-, 3- and 4-hydroxybenzoic acid, vanillic acid and isovanillic acid. Extraction was performed in 25 mL Pyrex flasks with methanol (3 times with 20 mL) under ultrasonic agitation for 15 min. The subsequent steps were the same as for method 1. For assessing the amounts of the analytes, the response factor of pure reference compounds was used.

For both methods, duplicate analyses show that the precision of the determinations was about 10%. All reported concentrations are corrected for procedural blanks.

2.6 IC

The Weizmann Institute (WI) performed analyses of filter and impactor samples by ion chromatography (IC). For $HVDS2_{UGent}$ samples, a $\frac{1}{4}$ fraction of the fine filter was extracted twice into 5 ml of water, by short vortex agitation followed by 15 min of gentle shaking. The combined extract was centrifuged for 5 min and filtered through a GHP Acrodisk® syringe filter (25 mm, 0.45 μm pore size; Gelman, Pall Corporation, NY, USA), which had been previously washed with 10 ml water. Selected $MOUDI_{IFUSP}$ samples and half of each SFU sample were extracted in the same manner into 4 ml of water. These were filtered using a GHP Acrodisk® syringe filter (13 mm, 0.45 μm pore size). It has been validated that further extraction was not needed.

IC analysis was carried out using a Varian ProStar HPLC system equipped with a Dionex ED50 electrochemical detector. Anions were determined using a Dionex AS11 analytical column and ASRS-Ultra suppressor in autosuppression mode. For simultaneous separation of inorganic and short-chain (C_1-C_9) organic anions, gradient elution by 0.4–25 mM NaOH (2 mL/min) was employed (duration of the analysis: 20 min). Cations were determined using a Dionex CS12 column and CSRS-Ultra suppressor in autosuppression mode with 20 mM methanesulfonic acid (MSA) as an eluent (1 ml min^{-1}). A thorough validation of extraction and analytical method can be found in Falkovich et al. (2004).

2.7 IEC

Sample extracts of the $HVDS2_{UGent}$ samples obtained as described for IC analysis were further analyzed by ion exclusion chromatography (IEC) by WI. The extracts were purified using Accell™ QMA solid-phase extraction cartridges (Waters, MA, USA) in order to eliminate HULIS, which interfered with detection. The samples were separated using ion exclusion liquid chromatography using a Dionex ICE-AS1 column and a Varian ProStar 230I HPLC pump, and

polyhydroxy compounds were detected by photodiode array (Varian ProStar 330) at 194 nm (for a detailed description of the method, see Schkolnik et al., 2005). The method uncertainty is 15% for concentrations $>0.2\,\mu g/m^3$, and 23% for concentrations $<0.2\,\mu g/m^3$.

2.8 IC-UV

ISAC employed ion-exchange chromatography with UV detection (IC-UV) to fractionate WSOC according to their ionic nature at pH 8. The whole set of 5-stage Berner impactor samples collected during the SMOCC field campaign was analyzed by the IC-UV technique, implemented on a Hitachi L-7100 HPLC system equipped with a Gilson autosampler, a Toso-Haas DEAE-TSK gel column (7.5 mm i.d. × 7.5 cm l.), and an UV detector (260 nm). The aliquots of samples for HPLC analysis were dried under vacuum and re-dissolved with 300 μl of mobile phase A, necessary to fill the 100 μl loop of the HPLC system. The injection of samples dissolved in the first mobile phase instead of water allowed the suppression of the injection peak in the chromatogram, in order to perform a more accurate integration of the peak arising from non-retained analytes.

The mobile phase was an aqueous solution of 20% acetonitrile and $NaClO_4$ at the following concentrations: A) 0 M; B) 0.02 M; C) 0.4 M. The pH of the mobile phases B and C was held constant at 8.0 with a 0.01 M TRIS:HCl buffer. A first isocratic elution was followed by a gradient (from 12 to 15 min) changing the solvent composition from A to B; after 6 min of isocratic conditions, a second gradient from 21 to 26 min allowed the system to reach the 100% C composition. A last five minute gradient changed the composition of the mobile phase to 100% A. Flow rate was 0.7 ml min^{-1}. The compounds eluted A) with the first eluent (from 3 to 17 min), B) after the increase of the $NaClO_4$ concentration to 0.02 M (from 17 to 26 min), or C) after the second increase of the ionic strength (from 26 to 32 min) were classified as neutral compounds (NC), mono-/diacids (MDA) and polyacids (PA), respectively. Compared to the original analytical procedure proposed by Decesari et al. (2000), the elution method used in the present study improves the separation between NC and the acidic fractions, allowing to overcome the elution problems with the phenolic compounds (Chang et al., 2005). The attribution of the separated fractions to chemical classes has been verified by injection of standard compounds (their retention time in minutes is indicated in parentheses in the following listing) selected to represent all the classes of polar organic compounds known to occur in biomass burning aerosol (Graham et al., 2002). NC: D-galactal (4.5), D-glucal (4.5), furfuryl alcohol (5.0), benzyl alcohol (5.6), vanillin (9.8), phenol (10.2), m-cresol (11.9); MDA: glyoxylic acid (19.2), sodium formate (19.7), sodium oxalate (23.4), malic acid (23.9), potassium hydrogen-phthalate (25.1); PA: 1,3,5-benzene-tricarboxylic acid (28.3), citric acid (28.5), Suwannee River fulvic acid (ca. 29). Clearly, the retention times of all the standards match with those expected according to the classification into the three main chromatographic fractions (Decesari et al., 2005).

Calibration factors to convert the peak areas of NC, MDA and PA into their specific carbon concentrations were provided by chromatographic fractions isolated on preparative glass columns of DEAE-cellulose gel. Buffer solutions of ammonium bicarbonate were used for selective elution of NC, MDA and PA. In order to improve the resolution while keeping low the volume of mobile phase necessary to elute the strongly retained compounds, two columns, A and B (lengths: 1 cm+4 cm), were initially used in series to separate NC from the acidic compounds retained on the column. MDA were subsequently eluted with the 0.02 M buffer, while in a second step PA were eluted with 1 M buffer directly from column A by-passing B. This procedure allows the elution of each fraction with an amount of ammonium bicarbonate low enough to be easily removed by rotary evaporation. The isolated fractions were then analyzed for TOC and by HPLC, providing an external calibration for the HPLC technique. The precision of the procedure for providing calibration factors is 8% for NC and PA and 20% for MDA, while the variability between samples belonging to homogeneous sets (e.g., the samples of the dry, transition or wet periods) introduces an uncertainty of 10–20% up to 30% in the case of NC in the coarse aerosol samples.

2.9 ^{1}HNMR spectroscopy

The water extracts of Tedlar foils from two Berner impactor samples collected in the dry period (on 23 September during daytime, and during the night of 25–26 September) were dried and redissolved in 0.7 mL of D_2O containing an internal standard (0.24 mM sodium 3-trimethylsilyl-2,2,3,3-d_4-propanoate (TSP)) for ^{1}HNMR analysis at 400 MHz. From the sample collected on 23 September, only the three impactor stages corresponding to the size fractions 0.05–0.14, 0.14–0.42 and 0.42–1.2 μm provided sufficient amounts of sample for the ^{1}HNMR analysis. Water extracts of $HVDS2_{UGent}$ samples representative of the three periods of the campaign were also dried and redissolved with 0.24 mM TSP in D_2O for ^{1}HNMR analysis at 400 MHz or 600 MHz. Finally, the same procedure was applied to the chromatographic fractions isolated on preparative glass columns of DEAE-cellulose gel (see previous section) from the water extract of the $PM_{2.5}$ $HVDS2_{UGent}$ sample (front filter) collected during the night of 25–26 September, under very polluted conditions in the dry period. Details of the ^{1}HNMR experimental conditions are reported by Tagliavini et al. (2005). The concentration of carboxylic groups (COOH) was directly determined in selected samples, through a derivatization procedure into methyl esters, as also discussed by Tagliavini et al. (2005). Samples undergoing derivatization-^{1}HNMR analysis included $HVDS2_{UGent}$ fine and coarse filters representative of the three campaign periods, and the

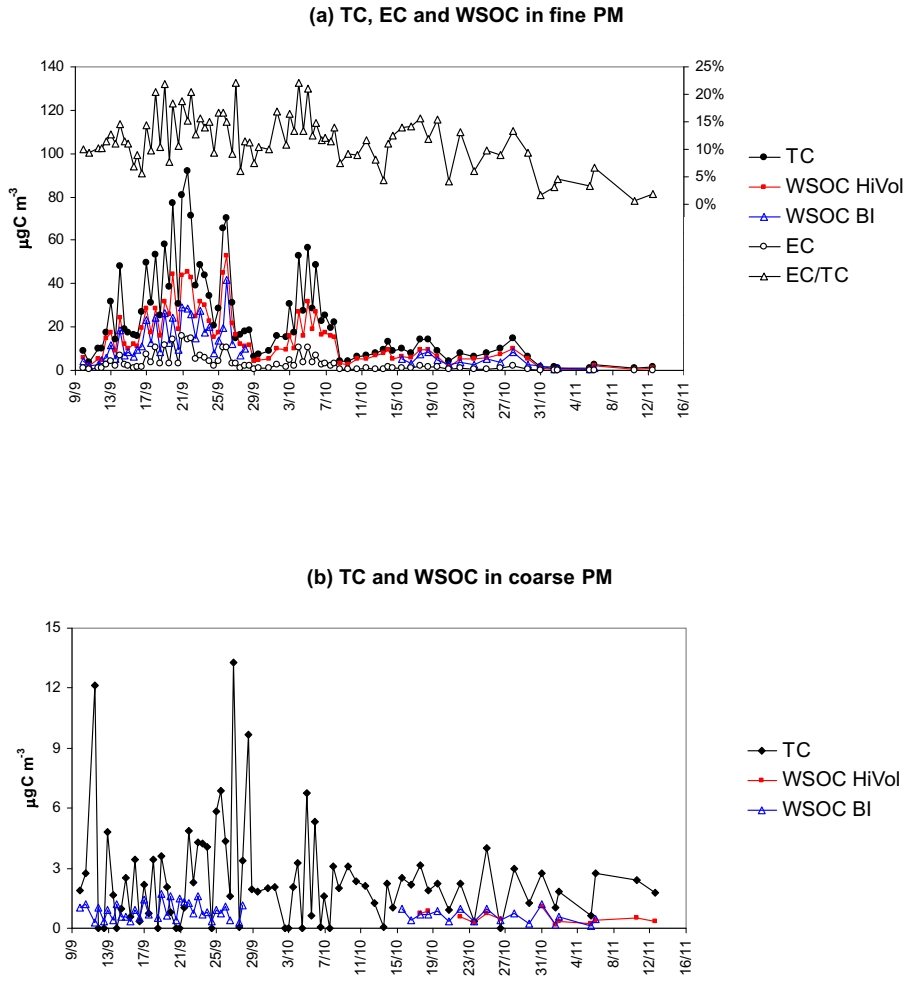

Fig. 1. Trends of TC, EC and WSOC concentrations (μg C m^{-3}) in the fine **(a)** and coarse **(b)** fractions of the aerosol during the LBA-SMOCC experiment. The profile of the EC/TC (%) ratio is also reported for the fine fraction. TC concentrations were determined on PM_{10} and $PM_{2.5}$ SFU samples equipped with quartz fiber filters, and deployed by UGent. The concentration of EC was obtained by EGA analysis of $PM_{2.5}$ $HVDS_{MPIC}$ filter samples. The WSOC concentrations were determined in the fine and coarse fractions of the aerosol on $HVDS1_{UGent}$ and $HVDS2_{UGent}$ filter samples, respectively. All concentrations determined on HVDS samples have been corrected for sampling biases relative to the UGent SFU samplers. WSOC concentrations determined on the Berner impactor (BI) samples are also reported for the fine fraction (0.05–1.2 μm) and for the coarse one (1.2–10 μm).

three chromatographic fractions obtained from the sample $HVDS2_{UGent}$ collected on 25–26 September. The overall ^{1}HNMR experiment was conducted by the University of Bologna (UniBO).

3 Results

3.1 Concentrations and trends of TC, EC and total WSOC

Figure 1 shows the temporal trends of TC from the TOT analysis of the SFU samples in the fine and coarse size fractions throughout the experiment. EC data provided by EGA analysis of water-extracted $HVDS_{MPIC}$ filters (fine fraction) are also reported after correction for sampling biases between the HiVol and the SFU systems. Data are already corrected for the back-up filter contribution. EC accounts for 5 to 20% of TC in the fine fraction of the aerosol (Table 1). These data are in agreement with results reported in the literature on biomass burning in tropical forests (Reid et al., 2005). It should be noted that the EC values provided by EGA analysis of water-extracted filters are about six-fold higher than those measured by TOT analysis (not shown in the figure), while they are in reasonable agreement with those determined by means of a Ruprecht and Patashnik (R&P) 5400 carbon analyzer (Fuzzi et al., 2006[1]). The partitioning between OC and EC in TOT analysis depends strongly on the temperature program used (Schmid et al., 2001), especially for biomass smoke aerosols, and suffers from artifacts when filters are heavily loaded (Kubátová et al., 1999).

Table 1. (a) EC/TC for the fine fraction of the aerosol and **(b)** WSOC/TC ratios for the fine and coarse fractions in the different periods of the LBA-SMOCC campaign. EC/TC data were obtained by EGA analysis of $HVDS_{MPIC}$ samples, whereas WSOC/TC ratios were obtained on $HVDS1_{UGent}$ and $HVDS2_{UGent}$ filter samples. Average values and standard deviations (in parentheses) are reported for all the samples in each period (N/D), and specifically for the samples collected at night (N) and day-time (D).

(a) EC/TC

period	fine		
	N/D	N	D
dry	0.13 (0.04)	0.15 (0.04)	0.10 (0.03)
trans.	0.10 (0.03)	0.12 (0.02)	0.08 (0.03)
wet	0.03 (0.02)	0.04 (0.02)	0.03 (0.00)
all samples	0.11 (0.05)		

(b) WSOC/TC

period	fine			coarse		
	N/D	N	D	N/D	N	D
dry	0.64 (0.08)	0.61 (0.06)	0.67 (0.08)	0.37 (0.13)	0.35 (0.13)	0.37 (0.13)
trans.	0.69 (0.09)	0.66 (0.03)	0.68 (0.12)	0.31 (0.07)	0.31 (0.02)	0.28 (0.05)
wet	0.53 (0.11)	0.54 (0.16)	0.46 (0.06)	0.28 (0.12)	0.33 (0.14)	0.21 (0.04)
all samples	0.64 (0.09)			0.34 (0.12)		

The figure also shows the concentrations of total WSOC determined on $HVDS1_{UGent}$ and $HVDS2_{UGent}$ filters after correction for the sampling biases with relative to the SFU filters, plus the total WSOC determined on the Berner impactor samples obtained by lumping the impactor stages corresponding to an aerosol diameter $<1.2\,\mu$m (fine fraction), and those sampling between 1.2 and 10 μm (coarse fraction). Generally, the Berner impactor was less efficient than the filter-based techniques in sampling WSOC in the fine fraction, providing concentrations 30% lower on average during the first part of the campaign, when the aerosol concentrations were highest and the discrepancy between the samplers largest. The air concentrations of WSOC are always well correlated with those of TC and PM (the latter are not shown in the figure), with temporal trends that reflect the main factors controlling the aerosol loads in the boundary layer as discussed in a parallel paper (Fuzzi et al., 2006[1]). Clearly, the high aerosol concentrations of submicrometer carbonaceous particles observed in September and the beginning of October (i.e., the dry period) must be attributed to the intense biomass burning activities in Rondônia and Mato Grosso, and other upwind Brazilian states at that time. Under high pressure meteorological conditions, the height of the tropical continental boundary layer undergoes a diurnal cycle, which causes fluctuations in the aerosol loads with clear maxima during the night. After the intense precipitation event on 8 October, the concentrations of biomass burning particles started to increase again but without reaching the peaks observed in the dry period. This period was denoted as the "transition period". Finally, "wet" conditions with frequent rain episodes became established after 1 November, leading to a substantial decrease in the concentrations of the fine particles, down to approx. 4% relative to the average concentrations observed in the dry period.

Conversely, the TC in the coarse fraction underwent a much less pronounced decrease from the dry to the wet period (Fig. 1b), suggesting that its concentrations were only partly affected by the biomass burning emissions and were controlled mainly by other sources that also hold for periods of intense precipitation. In contrast to the strong dominance of submicrometer WSOC mass during dry conditions, the concentrations of the WSOC in the fine and coarse fractions were of the same order of magnitude (0.90 and 0.45 μg C/m^3 on average, respectively) during the wet period. The trends in WSOC concentrations in the fine and coarse fractions closely follow those of TC. However, the average WSOC/TC ratios are different, indicating that coarse carbonaceous particles have a lower WSOC content (Table 1b). The analysis of the chemical tracers indicates that biological particles contributed to the coarse fraction of the aerosol (see the following discussion). Large biological particles emitted by vegetation typically contain substances that are essentially water-unextractable, such as cell membranes and walls, epi-cuticular materials, as well as water-soluble compounds trapped inside intact cells (Graham et al., 2003). Therefore, the occurrence of large biological particles is a plausible explanation for the less soluble character of coarse carbonaceous particles collected at FNS. Conversely, WSOC dominate the composition of TC in fine particles from biomass burning sources. During the dry period, a limited but significant increase in the WSOC percentage was observed during day-time compared to the night. This difference can be

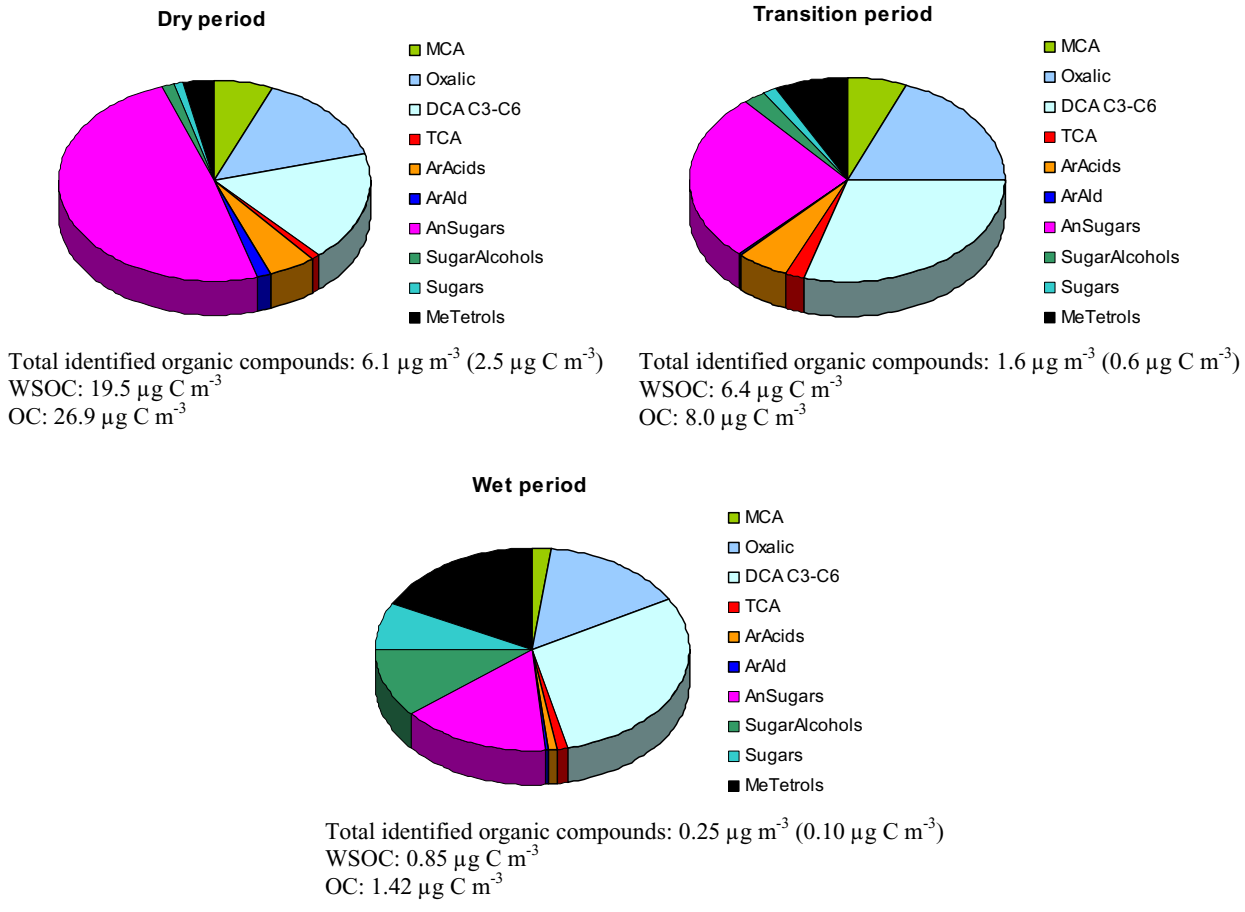

Fig. 2. Mean composition of the WSOC fraction speciated at the molecular level by GC-MS, IC and IEC methods in fine filter samples collected in the different periods of the campaign. Average concentrations of monocarboxylic acids (MCA) and oxalic acid were obtained by the results of IEC and IC analysis of the $HVDS2_{UGent}$ and IFUSP SFUs samples (Table 2). Mean concentrations for C_3-C_6 dicarboxylic acids (DCA C3-C6), aromatic aldehydes (ArAld), sugar-alcohols, sugars and 2-methyltetrols (MeTetrols) were provided by GC-MS analysis of the $HVDS1_{UGent}$ and $HVDS_{MPIC}$ filters. The concentrations of the other classes of compounds (tricarboxylic acids (TCA), aromatic acids (ArAcids) and anhydrosugars (AnSugars)) are averages of the mean values for the different sets of HVDS and SFU samples analyzed by GC-MS, IC and IEC. For each period of the campaign, the reconstructed total concentration of the organic compounds identified by GC-MS, IC and IEC is reported together with the average OC and WSOC concentrations determined on HVDS samples by TOT (for TC), EGA (for EC_w) and TOC (for WSOC) analysis. All concentrations determined for the HVDS samples are corrected for the sampling biases between each HiVol system and the SFU samplers with quartz fiber filters operated by UGent, as for Table 2.

attributed either to the different combustion stages occurring during the day compared to night (i.e., more frequent flaming than smoldering fires), or to the photochemical production of secondary organic compounds during day (Hoffer et al., 2005). Therefore, different sources of biomass burning aerosols and secondary processes are likely to affect the soluble/insoluble character of the fine particles in the dry period.

3.2 OC speciation in the fine and coarse aerosol

Using the diverse analytical techniques for individual compound analysis, as described in the experimental section, we identified and quantified a series of polar organic compounds with 1 to 12 carbon atoms per molecule, comprising different chemical classes: monocarboxylic, dicarboxylic and tricarboxylic acids, aromatic acids and aldehydes, sugars, sugar-alcohols and anhydrosugars. A summary of the results of WSOC speciation from the analysis of filter samples is given in Table 2, while a pie chart (Fig. 2) shows the relative concentrations of the main categories of compounds identified in fine PM for the various periods of the campaign. The four sets of data available for the composition of submicron particles exhibit discrepancies in the concentrations of specific classes of compounds. However, since the statistics for each series are not based on the same number of samples, a general conclusion on the recovery of the different sampling systems and analytical methods cannot be provided here.

Table 2a. Concentrations of the identified organic compounds (in ng m^{-3}) in fine and coarse filter samples, following GC-MS, IC and IEC analysis. Average values and range of variation are reported for the dry (Table 2a), transition (Table 2b) and wet (Table 2c) periods. Total identified organic compounds, WSOC, OC and TC data are reported as $\mu g\,m^{-3}$. MCA: aliphatic mono-carboxylic acids; DCA: aliphatic dicarboxylic acids; TCA aliphatic tricarboxylic acids. TC determinations on $HVDS_{MPIC}$ samples were performed by evolved gas analysis (Hoffer et al., 2005), while TC/OC analyses for the two HVDS systems operated by UGent were performed by TOT. Finally, total WSOC concentrations were determined by TOC analysis. Concentrations determined for the HVDS samples are corrected for the sampling biases between each HiVol system and the SFU samplers with quartz fiber filters operated by UGent. Sampling biases were estimated by comparing the TC values obtained on the different sets of samples, and therefore could not be assessed for the SFU_{IFUSP} samples, which were equipped with Nuclepore® substrates unsuitable for TC analysis.

Dry period	Fine				Coarse
	$HVDS1_{UGent}$ GC-MS_{UA} (N=51)	$HVDS_{MPIC}$ GC-MS_{MPIC} (N=17)	$HVDS2_{UGent}$ IC+IEC (N=16)	SFU_{IFUSP} IC (N=19)	SFU_{IFUSP} IC (N=19)
MCA			594 (119–1472)	139 (22.9–413)	80.3 (6.1–264)
glyceric acid	71.4 (22.1–169)	58.0 (22.9–98.0)			
formic acid			137 (56.2–294)	88.5 (12.1–370)	17.2 (2.5–43.8)
MSA			12.7 (4.9–18.4)	25.2 (0.0–213)	32.0 (0.0–465)
glyoxylic acid			79.8 (19.4–181)	40.5 (0.0–115)	0.80 (0.0–15.1)
Oxalic acid			1233 (409–2463)	516 (92.2–932)	162 (19.2–305)
DCA C_3-C_9			874 (169–1497)	566 (139–1026)	19.7 (0.0–106)
malonic acid		153 (23.3–350)	127 (55.5–287)	53.7 (0.0–210)	
methylmalonic acid		5.8 (3.0–9.3)			
succinic acid	659 (125–2213)	149 (61.8–261)			
methylsuccinic acid		18.3 (7.2–34.8)			
maleic acid		21.5 (7.0–75.0)	25.7 (10.3–52.6)	9.8 (0.0–29.3)	
fumaric acid	71.1 (22.5–276)	10.7 (4.9–17.5)	8.9 (2.2–21.7)	5.2 (0.0–20.3)	
malic acid	397 (152–858)	169 (96–228)			
glutaric acid	57.5 (9.0–187)	24.1 (11.0–40.3)			
α−hydroxyglutaric acid	186 (61.7–449)				
β−hydroxyglutaric acid	46.8 (16.2–111)				
2-ketoglutaric acid		31.7 (0.0–50.9)			
threonic acid (+isomer)	83.5 (24.3–206)				
tartaric acid	50.9 (18.6–104)				
adipic acid		7.9 (3.8–16.8)			
pimelic acid		4.9 (2.8–9.4)			
azelaic acid			10.1 (0.0–30.9)		
TCA					
citric acid			54.1 (20.3–95.2)	48.4 (0.0–114)	
tricarballylic acid		23.0 (15.0–36.5)	57.0 (6.4–14.4)	42.8 (0.0–89.3)	
Aromatic acids					
phtalic acid		30.5 (16.2–57.2)	22.0 (0.0–55.3)		
isophtalic acid		3.7 (1.3–7.4)			
2-hydroxybenzoic acid	5.6 (0.5–20.3)				
3-hydroxybenzoic acid	3.0 (0.2–14.5)	10.6 (2.8–22.6)	83.2 (26.4–183)	78.2 (0.0–183)	
4-hydroxybenzoic acid	33.3 (2.3–117)	48.9 (15.0–124)			
3,4-dihydroxybenzoic acid		51.2 (23.2–109)			
vanillic acids	81.1 (4.9–255)	54.1 (12.4–136)	93.7 (26.0–174)	16.8 (0.0–67.3)	
syringic acid		74.6 (6.8–194)	109 (31.2–342)	86.4 (0.0–225)	
Aromatic aldehydes					
4-hydroxybenzaldehyde		4.6 (0.6–16.0)			
vanillin		10.2 (1.3–27.6)			
syringaldehyde		66.8 (6.2–216)			
Other aromatics					
4-methylbenzcatechin		5.2 (1.1–16.6)			
Anhydrosugars					
galactosan	58.7 (7.7–261)	80.3 (16.4–193)			
mannosan	152 (23.7–543)	151 (34.0–345)			
levoglucosan	2222 (284–7485)	3698 (763–7903)	1307 (92–6514)		
anhydroglucofuranose	97.8 (16.3–435)				
Sugar-alcohols					
glycerol		14.3 (6.6–35.8)			
erythritol		51.7 (18.5–155)			
threitol		11.9 (1.4–24.0)			
arabitol	16.7 (0.0–41.4)	30.9 (9.0–57.4)			
mannitol	21.9 (3.8–52.3)	25.0 (7.5–44.6)			
sorbitol		1.0 (0.4–1.9)			
inositol		1.0 (0.0–2.1)			
Sugars					
fructose		20.7 (11.2–44.3)			
sucrose		4.9 (1.3–11.0)			
Methyl-tetrols					
2-methyl-threitol	53.7 (8.7–98.3)				
2-methyl-erythritol	148 (26.7–318)				
Total identified	4.5 (1.1–13.3)	6.2 (1.7–12.7)	3.4 (1.0–6.4)	1.68 (0.36–3.69)	0.26 (0.08–0.55)
WSOC	20.5 (4.4–52.6)	33.3 (19.0–55.2)	23.3 (9.4–49.7)		
OC	31.6 (6.1–76.3)		35.2 (14.4–69.8)		
TC	32.7 (6.4–78.2)	51.7 (24.9–90.9)	36.4 (14.9–72.0)		

Table 2b.

Transition	Fine				Coarse
	$HVDS1_{UGent}$ $GC\text{-}MS_{UA}$ (N=20)	$HVDS_{MPIC}$ $GC\text{-}MS_{MPIC}$ (N=13)	$HVDS2_{UGent}$ IC+IEC (N=5)	SFU_{IFUSP} IC (N=8)	SFU_{IFUSP} IC (N=8)
MCA			164 (112–215)	27.8 (8.4–46.0)	10.6 (0.3–25.7)
glyceric acid	32.4 (16.3–47.6)	13.7 (6.9–19.3)			
formic acid			32.5 (19.0–45.8)	17.0 (3.7–31.5)	2.0 (0.1–4.3)
MSA			6.9 (3.3–11.7)	3.4 (0.0–11.1)	
glyoxylic acid			25.1 (19.6–31.7)	10.9 (0.0–24.4)	
Oxalic acid			434 (347–490)	177 (65.9–265)	55.5 (8.4–123)
DCA C_3-C_9			345 (257–463)	295 (63.6–514)	
malonic acid		31.5 (3.0–58.1)	48.2 (30.1–59.6)	14.4 (0.0–43.8)	
methylmalonic acid		1.1 (0.4–1.9)			
succinic acid	276 (99.9–609)	22.3 (8.4–47.3)			
methylsuccinic acid		3.1 (1.2–5.3)			
maleic acid		4.7 (1.0–19.2)	18.3 (9.3–28.5)	7.3 (0.0–15.8)	
fumaric acid	36.5 (13.3–63.1)	2.7 (1.2–5.0)	5.3 (3.7–8.5)	3.5 (0.0–7.7)	
malic acid	268 (163–413)	69.7 (39.3–104)			
glutaric acid	21.7 (8.3–43.4)	3.5 (1.3–7.3)			
α−hydroxyglutaric acid	77.7 (37.5–133)				
β−hydroxyglutaric acid	26.7 (13.1–45.7)				
2-ketoglutaric acid		8.4 (2.9–23.4)			
threonic acid (+ isomer)	41.9 (23.1–60.6)				
tartaric acid	47.9 (25.5–78.3)				
adipic acid		1.3 (0.5–2.9)			
pimelic acid		0.7 (0.4–1.3)			
azelaic acid					
TCA					
citric acid			21.1 (14.8–33.8)	22.9 (7.3–44.9)	
tricarballylic acid		11.3 (5.9–18.7)	16.7 (14.4–20.9)	16.0 (4.9–31.7)	
Aromatic acids					
phtalic acid			4.0 (0.0–6.7)		
isophtalic acid		0.9 (0.4–1.5)			
2-hydroxybenzoic acid	0.7 (0.1–2.3)				
3-hydroxybenzoic acid	0.4 (0.0–1.5)	0.8 (0.2–2.3)	55.4 (40.8–86.4)	38.2 (6.1–79.5)	
4-hydroxybenzoic acid	4.9 (0.7–14.4)	4.6 (0.8–13.5)			
3,4-dihydroxybenzoic acid		8.0 (1.5–17.8)			
vanillic acids	12.8 (1.9–39.1)	3.2 (0.5–9.5)	9.9 (0.0–26.1)	12.6 (0.0–24.0)	
syringic acid		6.3 (0.4–16.6)	30.8 (25.3–42.9)	39.0 (0.0–77.1)	
Aromatic aldehydes					
4-hydroxybenzaldehyde		0.4 (0.1–1.6)			
vanillin		1.0 (0.2–2.9)			
syringaldehyde		3.7 (0.7–12.0)			
Other aromatics					
4-methylbenzcatechin		0.4 (0.1–0.8)			
Anhydrosugars					
galactosan	11.4 (2.7–32.2)	9.0 (1.4–22.7)			
mannosan	30.6 (7.3–69.6)	16.8 (3.3–39.1)			
levoglucosan	399 (106–858)	425 (89.9–893)	256 (32.6–609)		
anhydroglucofuranose	22.5 (6.8–41.9)				
Sugar-alcohols					
glycerol		3.3 (1.3–5.6)			
erythritol		7.5 (3.1–15.3)			
threitol		1.4 (0.3–2.7)			
arabitol	9.9 (4.5–22.1)	12.0 (5.2–24.4)			
mannitol	20.2 (9.5–46.8)	18.1 (3.8–46.3)			
sorbitol		0.8 (0.2–2.1)			
inositol		0.4 (0.0–0.7)			
Sugars					
fructose		5.8 (1.9–9.1)			
sucrose		1.6 (0.8–4.6)			
Methyl-tetrols					
2-methyl-threitol	26.1 (7.6–89.1)				
2-methyl-erythritol	93.9 (22.4–312)				
Total identified	1.4 (0.7–2.3)	0.9 (0.3–1.6)	1.1 (0.9–1.3)	0.63 (0.1–1.25)	0.1 (0.0–0.2)
WSOC	6.2 (1.5–10.1)	7.2 (5.1–10.2)	7.3 (5.5–9.2)		
OC	8.6 (2.9–15.2)		10.5 (7.5–13.6)		
TC	9.0 (3.1–15.8)	9.4 (5.4–14.9)	10.9 (8.0–14.0)		

Table 2c.

Wet period	Fine				Coarse
	$HVDS1_{UGent}$ $GC\text{-}MS_{UA}$ (N=7)	$HVDS_{MPIC}$ $GC\text{-}MS_{MPIC}$ (N=7)	$HVDS2_{UGent}$ IC+IEC (N=0)	SFU_{IFUSP} IC (N=7)	SFU_{IFUSP} IC (N=7)
MCA				5.2 (2.5–6.7)	11.2 (4.6–20.8)
glyceric acid	4.0 (1.3–6.3)	1.5 (0.5–2.5)			
formic acid				9.4 (6.6–18.0)	0.4 (0.0–1.3)
MSA					
glyoxylic acid					
Oxalic acid				36.7 (23–51.6)	16.0 (7.7–28.3)
DCA C_3-C_9				33.9 (14.7–61.0)	4.0 (0.0–11.4)
malonic acid		5.0 (1.8–7.1)		5.2 (0.0–8.1)	
methylmalonic acid		0.2 (0.1–0.4)			
succinic acid	28.6 (8.4–48.8)	2.5 (1.2–3.8)			
methylsuccinic acid		0.3 (0.1–0.5)			
maleic acid		0.9 (0.3–2.7)			
fumaric acid	7.1 (3.9–12.3)	0.5 (0.3–0.9)			
malic acid	76.7 (39.5–113)	15.5 (8.3–24.6)			
glutaric acid	4.4 (0.0–11.7)	0.4 (0.2–0.8)			
α−hydroxyglutaric acid	8.7 (3.8–18.0)				
β−hydroxyglutaric acid	4.6 (2.0–7.1)				
2-ketoglutaric acid		0.8 (0.0–1.3)			
threonic acid (+ isomer)	6.7 (3.6–10.7)				
tartaric acid	14.6 (5.9–24.2)				
adipic acid		0.4 (0.2–0.5)			
pimelic acid		0.2 (0.1–0.4)			
azelaic acid					
TCA					
citric acid					
tricarballylic acid		2.7 (1.3–5.3)			
Aromatic acids					
phtalic acid		1.5 (0.4–2.3)			
isophtalic acid		0.1 (0.0–0.4)			
2-hydroxybenzoic acid	0.1 (0.0–0.1)				
3-hydroxybenzoic acid	0.0 (0.0–0.1)	0.1 (0.0–0.3)			
4-hydroxybenzoic acid	0.3 (0.1–0.6)	0.0 (0.0–0.1)			
3,4-dihydroxybenzoic acid		0.4 (0.1–1.0)			
vanillic acid	1.1 (0.2–3.5)	0.3 (0.1–0.8)			
isovanillic acid					
syringic acid		0.4 (0.0–1.1)			
Aromatic aldehydes					
4-hydroxybenzaldehyde		0.0 (0.0–0.1)			
vanillin		0.2 (0.0–0.8)			
syringaldehyde		0.1 (0.0–0.4)			
Other aromatics					
4-methylbenzcatechin		0.1 (0.0–0.2)			
Anhydrosugars					
galactosan	1.1 (0.0–2.4)	0.6 (0.2–1.1)			
mannosan	4.2 (1.9–7.9)	1.3 (0.4–2.5)			
levoglucosan	59.7 (15.7–160)	35.8 (9.6–74.3)	44.5 (0.0–89.1)		
anhydroglucofuranose	2.4 (1.1–4.9)				
Sugar-alcohols					
glycerol		1.3 (0.8–2.4)			
erythritol		2.2 (0.5–3.3)			
threitol		0.2 (0.1–0.4)			
arabitol	8.9 (5.4–11.9)	10.4 (5.8–13.6)			
mannitol	18.0 (11.2–21.2)	23.5 (12.1–31.5)			
sorbitol		1.1 (0.7–1.4)			
inositol		0.1 (0.1–0.2)			
Sugars					
fructose		4.0 (2.5–5.9)			
sucrose		0.9 (0.4–2.4)			
Methyl-tetrols					
2-methyl-threitol	9.3 (3.1–20.3)				
2-methyl-erythritol	34.7 (13.2–65.6)				
Total identified	0.3 (0.2–0.5)	0.1 (0.1–0.2)		0.09 (0.05–0.13)	0.03 (0.01–0.04)
WSOC	0.9 (0.7–2.0)	1.4 (0.9–1.8)			
OC	1.4 (0.9–2.5)				
TC	1.5 (0.9–2.7)	1.7 (0.9–2.2)			

In general, the IC analysis provided higher concentrations of monocarboxylic, tricarboxylic and aromatic acids compared to the GC-MS methods. The GC-MS analysis following the UA methods (denoted by GC-MS_{UA}) provided higher values for the dicarboxylic acids and lower for the sugar-derivatives compared to the analysis performed with the MPIC method (denoted by GC-MS_{MPIC}). The recovery of low-molecular weight compounds, such as C_3–C_6 dicarboxylic acids (DCA) by GC-MS can be affected by the different extraction techniques employed. The levoglucosan concentrations obtained with the GC-MS_{UA} method are in agreement with the results of the IEC-UV method which does not require a derivatization step (Schkolnik et al., 2005). Therefore, the deviation between the two methods shown in the table is merely due to the different sets of samples analyzed. Further, it is noted that the levoglucosan concentrations obtained with the GC-MS_{UA} method are in good agreement with those for the LBA-EUSTACH-2 campaign, which had been conducted at the same pasture site (Graham et al., 2002). A possible reason for the large discrepancies obtained for measurement of polar carboxylic acids between the two GC-MS methods is the different polarity of the extraction solvents used: the GC-MS_{UA} method uses methanol as an extraction solvent, and internal recovery standards that allow to correct for losses during sample workup, while the GC-MS_{MPIC} method uses acetonitrile (less polar than methanol) as extraction solvent and assumes a 100% recovery.

The pie charts in Fig. 2 were obtained by averaging the mean concentrations for the different sets of HVDS and SFU samples analyzed by GC-MS, IC or IEC. However, given the systematic differences between the analytical methods with respect of the recovery for specific categories of compounds, the average concentrations for MCA and oxalic acid were based only on the $HVDS2_{UGent}$ and SFU samples analyzed by IC, while we retrieved average concentrations for DCA C_3-C_9, aromatic aldehydes, sugar-alcohols, sugars and 2-methyl-tetrols only from the sets of HVDS samples analyzed by GC-MS.

The data in Tables 2a and b can be directly compared with the GC-MS results from the 1999 LBA-EUSTACH-2 campaign (Graham et al., 2002). The coarse filters collected during the SMOCC campaign were subjected to a less comprehensive set of analyses than used in LBA-EUSTACH, and sugar-derivatives were not measured. In the case of the submicron particles, on the other hand, the combination of speciation methods in the present study, comprising both GC and LC techniques provided a more detailed picture of the organic composition. In particular, in addition to the di- and tricarboxylic acids, benzoic and vanillic acids, and sugar-derivatives already identified and measured by Graham et al. (2002), the analysis of the LBA-SMOCC samples indicated higher concentrations of monocarboxylic acids and significant concentrations of dicarboxylic acids, hydroxy mono- and dicarboxylic acids, and 2-methyltetrols. The identified chemical compounds are classified as follows:

- *C_1-C_3 monocarboxylic acids:* acetic, formic, methanesulfonic, lactic, glyoxylic and glyceric acids. They represent 4 to 7% of total aliphatic acids. Monocarboxylic acids have multiple sources, including both biomass burning and biogenic emissions (Souza et al., 1999);

- *C_2-C_9 aliphatic dicarboxylic acids:* oxalic acid was found to be by far the most abundant carboxylic acid identified, followed by malonic, succinic and malic acid, and with a clear increase in the relative contribution of the latter species towards the end of the campaign. Oxalic acid can originate from multiple sources, both primary and secondary. It was recently found as the most abundant carboxylic acid in biomass burning smoke in South Africa (Gao et al., 2003). Conversely, malic acid shows a more pronounced biogenic origin and was found to accompany photooxidation products of isoprene (i.e., 2-methyltetrols) in the Amazon basin (Claeys et al., 2004a);

- *Aliphatic tricarboxylic acids:* they include citric and tricarballylic acids, and account for only 1 to 2% of the mass of total speciated organic compounds. They have been previously reported (Graham et al., 2002);

- *One-ring aromatic acids and aldehydes:* the aromatic compounds include methoxylated species (vanillin, syringaldehyde and the corresponding acids) and hydroxy-benzoic acids. The methoxylated compounds are more abundant compared to the hydroxy-benzoic acids in the dry season, whereas the contrary holds starting from the transition period. The concentration of the aromatic compounds clearly decreases relatively to aliphatic acids from 1:5 in the dry period to 1:25 in the wet period. One-ring aromatic acids and aldehydes are primary compounds known to be produced by the combustion of lignins (Simoneit, 2002) and are, therefore, enriched in fresh biomass burning smoke;

- *Sugars and sugar-derivatives:* they comprise both pyrogenic (anhydrosugars; Graham et al., 2002; Zdráhal et al., 2002) and biogenic (sugars and sugar-alcohols; Simoneit et al., 2004) compounds. Levoglucosan is the most abundant single compound identified in submicron aerosols during the whole campaign, including the wet period. However, the concentration of levoglucosan and the other anhydrosugars clearly decreases relative to the biogenic compounds (sugars and sugar-alcohols), from 10:1 in the dry to 9:10 in the wet period;

- *2-Methyltetrols:* they were identified as major biogenic compounds in the Amazon basin, and were attributed to photo-oxidation of isoprene (Claeys et al., 2004a). Principal component analysis confirmed that the concentrations of 2-methyltetrols in the SMOCC filter samples do not correlate with those of pyrogenic compounds,

such as levoglucosan and potassium sulfate (Maenhaut et al., 2005, in preparation). Figure 2 also shows that 2-methyltetrols account for a very small fraction of the identified WSOC mass during the dry period, whereas they add up to 10% of the speciated mass in the wet period, following the decrease of the concentrations of the pyrogenic organic compounds.

The tracer analysis clearly indicates a more pronounced signature of the biogenic sources in the wet period compared to the previous periods of the campaign. After averaging the concentrations from the various filter substrates and analytical techniques (Fig. 2), the classes of identified organic compounds of clearly pyrogenic origin (i.e., aromatic acids and aldehydes and anhydrosugars) account for 55, 33 and 16% of the total speciated compounds in the dry, transition and wet periods, respectively, while the corresponding fractions for the biogenic species (i.e., sugars, sugar-alcohols and 2-methyl-tetrols) are 6, 11 and 36%. The relatively high concentrations of levoglucosan and other pyrogenic compounds in the samples from November suggest that the biomass burning activity was not totally suppressed at the beginning of the wet season. In that period, persistent fire activity could be detected in Rondônia and Mato Grosso in areas temporarily free from precipitations (http://www.master.iag.usp.br/queimadas/). Finally, the increase in the concentrations of aliphatic carboxylic acids compared to anhydrosugars and aromatic compounds towards the end of the campaign may reflect more pronounced secondary sources due to oxidation of either pyrogenic and biogenic VOCs. The enrichment of the aliphatic carboxylic acids compared to anhydrosugars is known to occur during the transport of biomass burning products (Gao et al., 2003). After the onset of wet conditions, a longer transport from distant sparse fires, as well as more pronounced in-cloud processing, would favor the production of secondary organic compounds, rendering a more chemically aged character to the aerosol OC. The same conclusion can be derived from the change in the size-segregated inorganic chemical composition from the dry to the wet period (Fuzzi et al., 2006[1]).

Table 2 also reports the sum of concentrations of identified organic compounds and the aerosol TC, OC and WSOC for the same periods. The recovery of the speciation methods is higher in the case of the GC-MS_{UA} analysis on the $HVDS1_{UGent}$ samples, where the identified compounds account for 6 to 8% of TC, and 9 to 11% of WSOC on a carbon basis. When comparing the reconstructed total concentration of the compounds identified by GC-MS_{UA}, GC-MS_{MPIC}, IC and IEC techniques with the average OC and WSOC concentrations for the three main periods of the campaign (Fig. 2), we obtain a recovery of 7–9% for OC and of 10–13% for WSOC (Fig. 2). These values must be treated with caution, since the sets of samples analyzed by GC-MS_{MPIC}, IC and IEC are a subset of the filters used for TC and WSOC determination. In any case, it is clear that a large part of the organic matter was not amenable to GC-MS, IC and IEC analysis because it could not be eluted or derivatized into stable products, and eventually eluded identification at the molecular level.

3.3 OC speciation in the size-segregated samples

Selected samples of the 12-stage $MOUDI_{UGent}$ were subjected to OC speciation by GC-MS_{UA}, while samples of the 10-stage $MOUDI_{IFUSP}$ were analyzed by IC and IEC-UV techniques, providing the size-distributions of the most important identified organic compounds in the three periods of the campaign (Falkovich et al., 2004; Claeys et al., 2006, 2006[2]; Schkolnik et al., 2005). The resulting size-segregated organic composition in terms of identified chemical classes is plotted for samples representative from the dry, transition and wet periods in Figs. 3a and b. The concentrations of the speciated OC classes are expressed as percentages of the aerosol mass in each size bin. Figure 3a reports the size-segregated composition of the carboxylic acids determined by IC analysis. Monocarboxylic acids, oxalic acid and C_3-C_9 dicarboxylic acids are the main contributors to the acidic organic fraction in all the size intervals, although aromatic compounds are also important in the dry and transition periods, but only for particles with a diameter lower than 1 μm. Conversely, aromatic acids were not detected in the sample from the wet period in all size intervals. In all periods, the carboxylic acids are less abundant in the finest size range, as well as in the coarse fraction. Their contribution to aerosol mass is also higher in the dry compared to the other two periods. The contribution of the 2-methyltetrols determined by GC-MS_{UA} to PM (Fig. 3b) also shows a decrease toward the wet period, but only in the submicron fraction, whereas the opposite holds for the coarse fraction. Anhydrosugars are the most abundant compounds in all seasons, with levoglucosan as the main species in the submicron and supermicron fractions, respectively. Sugar-alcohols (arabitol and mannitol) contribute up to almost two thirds of the speciated polyhydroxylated compounds in the size intervals 1.8–10 μm in the dry period, but this fraction increases to 60–90% in the transition phase and to 80–100% in the wet period. Finally, the contribution of the 2-methyltetrols to OC increases significantly in the wet period, but only in the submicron size intervals.

The data reported in Figs. 3a and b show that the contribution of the identified classes of organic compounds to aerosol PM changes with the aerosol diameter, and is generally highest in the 0.4–4 μm range. Since TC was not determined

[2]Claeys, M., Kourtchev, I., Pashynska, V., Vas, G., Vermeylen, R., Cafmeyer, J., Chi, X., Artaxo, P., and Maenhaut, W.: Polar organic marker compounds in boundary layer aerosols during the LBA-SMOCC 2002 biomass burning experiment in Rondônia, Brazil: time trends, diurnal variations and size distributions, in preparation, 2006.

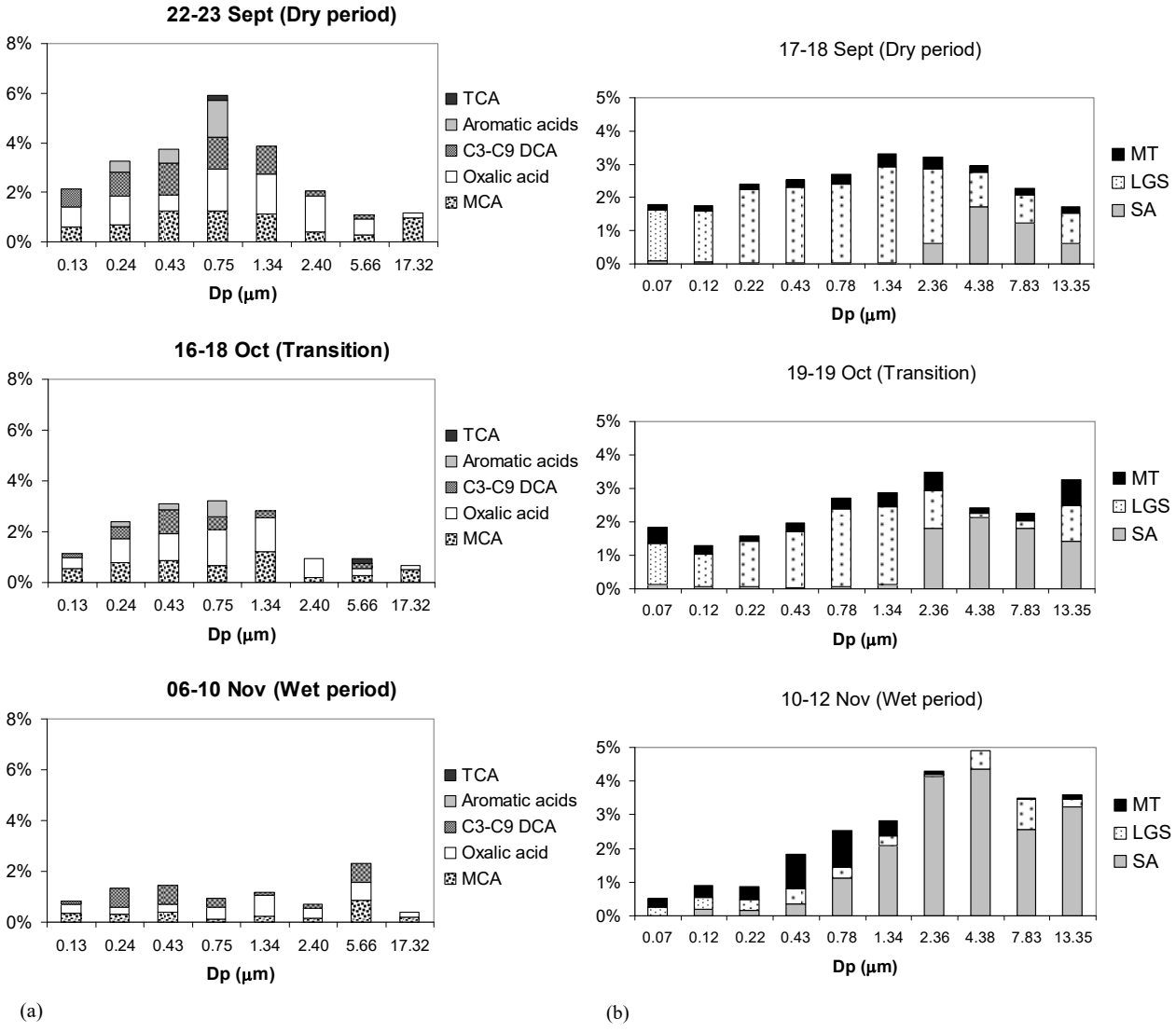

Fig. 3. Fraction of PM accounted for by the organic compounds speciated in size-segregated aerosol samples. **(a)** Carboxylic acids from IC analysis of IFUSP MOUDI samples: aliphatic monocarboxylic acids (MCA), oxalic acid, C_3-C_9 dicarboxylic acids (DCA), C_7-C_8 aromatic acids and aliphatic tricarboxylic acids (TCA). **(b)** Polyhydroxylated compounds from GC-MS analysis of UGent MOUDI samples: 2-methyltetrols (MT), levoglucosan (LGS) and sugar-alcohols (SA) (arabitol and mannitol). Both figures report the results for three different samples representative of the three main periods of the campaign. The horizontal axis gives the geometric mean of the lower and upper cut-off diameters of the MOUDI stages.

systematically on MOUDI samples, a size-segregated carbon balance was not attempted in this study.

3.4 Apportionment of WSOC into main chemical classes

Compared to the methods for WSOC speciation discussed so far, the IC-UV technique presented in the experimental section is a chromatographic method for the separation of broad chemical classes of WSOC, which is not targeted to speciation at the molecular level. The neutral compounds (NC), mono-/diacids (MDA) and the polyacids (PA) separated by IC-UV were identified mainly on the basis of their chromatographic behavior (i.e., the retention time). The quantitative analysis is based on the determination of the TOC on isolated fractions used to calibrate the UV detector. Therefore, the concentrations of NC, MDA and PA could be derived only as μg of carbon per cubic meter, as for total WSOC. Other than some improvements in the chromatographic conditions, the method is essentially the same as the one used for the analysis of $PM_{2.5}$ samples during the LBA-EUSTACH campaign (Mayol-Bracero et al., 2002a).

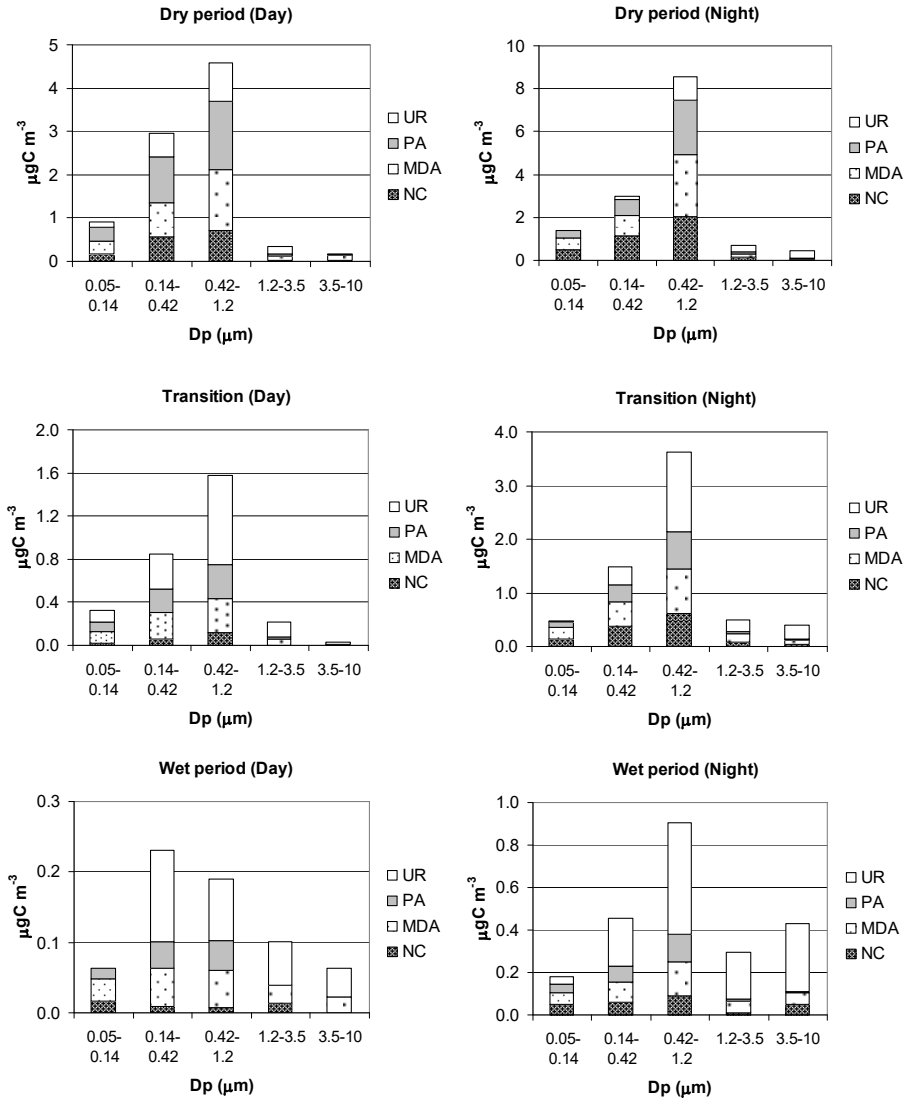

Fig. 4. Average concentrations of the WSOC chemical classes determined by the IC-UV method on the Berner impactor samples. NC: neutral compounds; MDA: mono-/diacids; PA: polyacids; UR: unresolved, i.e., WSOC fraction not accounted for by IC-UV analysis. Mean concentrations are reported for the three main periods of the campaign and separately for the samples collected during night-time and those collected during day-time.

The NC, MDA and PA were detected by UV absorption at 260 nm in all samples analyzed, provided that the injected WSOC amount exceeded 500 ng C. Using calibration following the procedure described in the experimental section, the HPLC peak areas of the three main regions of the chromatogram provided the concentrations of NC, MDA and PA in the size range 0.05–3.5 μm (stages I to IV of the Berner impactor) for 37 samples from the dry period, 12 samples from the transition period and 5 samples from the wet period, whereas the concentrations in larger particles (3.5–10 μm) were often below the detection limit. Table 3 reports the statistics for the concentrations of NC, MDA and PA in size-segregated samples from the three periods and also separately for nocturnal and diurnal samples. The mean relative contributions of the three IC-UV classes to the total water-soluble carbon are also included. Average size-segregated distributions for the three chemical classes and for the WSOC fraction unresolved by the IC-UV method are shown in Fig. 4 for the three main periods of the campaign.

A constant feature for all samples is the substantially lower relative concentration of PA in the coarse size range compared to the submicron size fraction. PA show a particularly low abundance in coarse particles from the wet period. MDA exhibit rather constant contributions to WSOC in the submicron particles, whereas their contribution to WSOC in the coarse particles is quite variable. Finally, the NC fraction of

Table 3. Concentrations of WSOC, neutral compounds (NC), mono-/diacids (MDA) and polyacids (PA) determined by the IC-UV method for the Berner impactor. Mean values and standard deviations (in parentheses) are reported for the whole set of samples for each period (N/D), and specifically for the samples collected at night (N) and during day-time (D).

			Concentrations (μg C m^{-3})				% WSOC		
		Dp (μm)	WSOC	NC	MDA	PA	NC	MDA	PA
Dry period	N/D (n=37)	0.05–0.14 1.35 (0.93)	0.40 (0.38)	0.46 (0.31)	0.38 (0.24)	28%	35%	31%	
		0.14–0.42	3.59 (2.17)	0.99 (0.89)	1.08 (0.75)	1.08 (0.76)	26%	30%	30%
		0.42–1.2	8.96 (6.94)	2.18 (2.20)	2.97 (2.56)	2.72 (2.66)	21%	32%	31%
		1.2–3.5	0.64 (0.63)	0.12 (0.18)	0.18 (0.17)	0.10 (0.13)	15%	28%	14%
		3.5–10	0.29 (0.18)	0.04 (0.02)	0.09 (0.04)	0.02 (0.01)	9%	18%	5%
	N (n=18)	0.05–0.14	1.75 (1.10)	0.65 (0.41)	0.60 (0.33)	0.43 (0.24)	43%	37%	25%
		0.14–0.42	3.73 (2.24)	1.32 (1.01)	1.18 (0.75)	0.97 (0.76)	28%	31%	25%
		0.42–1.2	12.76 (7.70)	3.43 (2.42)	4.17 (2.91)	3.65 (3.38)	24%	34%	26%
		1.2–3.5	0.91 (0.81)	0.20 (0.23)	0.24 (0.21)	0.15 (0.17)	18%	25%	12%
		3.5–10	0.40 (0.17)	0.04 (0.02)	0.06 (0.04)	0.02 (0.01	8%	17%	4%
	D (n=18)	0.05–0.14	1.12 (0.56)	0.20 (0.14)	0.35 (0.22)	0.39 (0.21)	17%	34%	35%
		0.14–0.42	3.61 (2.09)	0.70 (0.63)	1.04 (0.76)	1.23 (0.76)	17%	27%	31%
		0.42–1.2	5.58 (3.44)	1.05 (1.07)	1.91 (1.52)	1.93 (1.28)	16%	31%	32%
		1.2–3.5	0.38 (0.19)	0.05 (0.06)	0.11 (0.07)	0.07 (0.05)	9%	31%	13%
		3.5–10	0.16 (0.07)	0.03 (0.02)	0.03 (0.06)	0.01 (0.01)	11%	32%	11%
Transition	N/D (n=12)	0.05–0.14	0.47 (0.19)	0.13 (0.07)	0.18 (0.08)	0.12 (0.05)	24%	37%	26%
		0.14–0.42	1.33 (0.56)	0.32 (0.17)	0.37 (0.15)	0.32 (0.14)	21%	28%	24%
		0.42–1.2	2.87 (1.44)	0.46 (0.37)	0.74 (0.44)	0.61 (0.34)	14%	25%	21%
		1.2–3.5	0.37 (0.14)	0.11 (0.04)	0.13 (0.06)	0.04 (0.02)	28%	37%	12%
		3.5–10	0.25 (0.15)	0.07 (0.02)	0.07 (0.01)	0.01 (0.00)	24%	29%	4%
	N (n=4)	0.05–0.14	0.47 (0.24)	0.15 (0.10)	0.20 (0.12)	0.11 (0.05)	29%	42%	25%
		0.14–0.42	1.48 (0.47)	0.38 (0.18)	0.45 (0.16)	0.32 (0.12)	25%	30%	21%
		0.42–1.2	3.62 (1.55)	0.62 (0.45)	0.84 (0.29)	0.69 (0.26)	16%	24%	19%
		1.2–3.5	0.49 (0.03)	0.08 (0.02)	0.16 (0.03)	0.04 (0.01)	16%	33%	9%
		3.5–10	0.40 (0.15)	0.05 (0.05)	0.08 (0.01)	0.01 (0.00)	14%	21%	3%
	D (n=3)	0.05–0.14	0.32 (0.12)	0.02 (0.02)	0.11 (0.05)	0.09 (0.04)	12%	34%	27%
		0.14–0.42	0.84 (0.18)	0.06 (0.07)	0.24 (0.06)	0.22 (0.06)	14%	29%	26%
		0.42–1.2	1.58 (0.34)	0.12 (0.04)	0.32 (0.08)	0.31 (0.08)	7%	20%	19%
		1.2–3.5	0.22 (0.04)	0.00 (0.00)	0.06 (0.02)	0.02 (0.01)		26%	8%
		3.5–10	0.09 (0.02)	0.00 (0.00)	0.01 (0.03)	0.00 (0.00)		51%	
Wet period	N/D (n=5)	0.05–0.14	0.12 (0.09)	0.04 (0.01)	0.05 (0.02)	0.03 (0.02)	38%	47%	24%
		0.14–0.42	0.37 (0.13)	0.05 (0.03)	0.08 (0.03)	0.06 (0.02)	10%	23%	16%
		0.42–1.2	0.62 (0.48)	0.07 (0.04)	0.12 (0.07)	0.10 (0.05)	8%	22%	18%
		1.2–3.5	0.21 (0.14)	0.03 (0.01)	0.04 (0.02)	0.01 (0.00)	25%	25%	4%
		3.5–10	0.28 (0.28)	0.05 (0.04)	0.04 (0.02)	0.00 (0.00)	12%	26%	2%
	N (n=3)	0.05–0.14	0.18 (0.10)	0.05 (0.01)	0.06 (0.02)	0.04 (0.02)	29%	35%	21%
		0.14–0.42	0.46 (0.07)	0.06 (0.02)	0.10 (0.01)	0.07 (0.02)	13%	21%	16%
		0.42–1.2	0.91 (0.40)	0.09 (0.03)	0.16 (0.04)	0.13 (0.02)	10%	19%	16%
		1.2–3.5	0.29 (0.11)	0.01 (0.02)	0.05 (0.01)	0.01 (0.00)	13%	19%	4%
		3.5–10	0.43 (0.28)	0.05 (0.04)	0.06 (0.02)	0.00 (0.00)	11%	15%	2%
	D (n=2)	0.05–0.14	0.05 (0.00)	0.02 (0.02)	0.03 (0.02)	0.01 (0.00)	56%	59%	26%
		0.14–0.42	0.23 (0.04)	0.01 (0.01)	0.05 (0.02)	0.04 (0.02)	7%	23%	16%
		0.42–1.2	0.19 (0.00)	0.01 (0.01)	0.05 (0.02)	0.04 (0.02)	8%	28%	22%
		1.2–3.5	0.09 (0.02)	0.01 (0.02)	0.03 (0.00)	0.00 (0.00)	37%	31%	
		3.5–10	0.06 (0.01)	0.00 (0.00)	0.02 (0.00)	0.00 (0.00)		37%	

WSOC decreased steadily from the finest size range (0.05–0.14 μm) to the coarsest, although a mode in the range 1.2–3.5 μm was also observed in some samples from the transition and wet periods. Table 3 also highlights some systematic differences in the composition of the aerosol samples collected at night-time compared to day-time. In particular, the

NC fraction is significantly higher during the night (often by a factor of two compared to the day) in all periods. Conversely, PA are relatively more abundant during day in the dry period, but differences in the other two seasons are less evident. MDA also show limited diel variations, tending towards enrichment during night (similar to NC), especially in the finest size fraction during the transition period. The high content of neutral compounds of nocturnal samples is clearly correlated with the higher nocturnal concentrations observed for levoglucosan (Schkolnik et al., 2004). Therefore, the diel variations in the IC-UV composition can be interpreted in terms of different combustion conditions (e.g., smoldering vs. flaming processes) active at different times of the day. The production of PA during the day can also be explained by heterogeneous chemical processes promoted by sunlight (Hoffer et al., 2005. Although the chemical classes separated by the IC-UV method are not unambiguous tracers of the WSOC sources, the variations in their relative concentrations can be interpreted on the basis of the correlation with other chemical constituents of the aerosol (e.g., K), which can be more readily associated with a particular source or source processes. A full treatment of this subject is given in a parallel paper (Fuzzi et al., 2006[1]).

The fraction of WSOC not accounted for by the sum of NC, MDA and PA is size-dependent, being around 0–15% for the smallest particles, and increasing to 70% in the coarsest size range. The proportion is lower in the dry period, compared to the transition and especially the wet period, during which 50% of WSOC could not be accounted for even in the accumulation mode size range. The organic materials that can contribute to WSOC, especially in the wet period, and not accounted for by the IC-UV analysis could be either semi-volatile compounds that were lost during the calibration procedure, or hydrophilic colloids (very high molecular weight humic-like particles, fragments of biological membranes and other cell constituents) that are extracted from the impactor foils but escape analysis by HPLC.

3.5 ^{1}HNMR functional group composition

^{1}HNMR analysis provides the functional group composition of the mixture, but little information on the speciation into individual compounds. Furthermore, it does not provide information on the distribution of the functional groups into chemical classes. This explains why a pre-separation by preparative chromatography on DEAE columns was necessary to obtain the functional group compositions of NC, MDA and PA. ^{1}HNMR analysis in D_2O solution provided direct measurements of the functional groups carrying hydrogen atoms bound to carbon atoms: a) alkylic groups (CH); b) aliphatic groups bound to an unsaturated carbon atom (HC-C=); c) alkoxyl groups (HC-O); d) acetal groups (O-CH-O) and e) aromatic groups (HC=). For the samples subjected to the derivatization procedure presented in Sect. 2.6, the concentration of COOH groups was also obtained. The complete results are discussed in the companion paper by Tagliavini et al. (2005). As a brief overview, we outline the following points: 1) significant differences were observed between the three periods as regards the composition of the fine particles, with the samples from the wet period exhibiting a lower content of aromatic groups and more unsaturated and hydroxylated aliphatic moieties; 2) the coarse fraction of the aerosol from the transition and wet periods, on the other hand, is dominated by oxygenated carbon atoms, indicating the occurrence of polyhydroxy-compounds; 3) carboxylic groups (COOH) represent 13.3%, 19.7% and 18.4% of the water-soluble carbon accounted for by NMR analysis in fine aerosol samples collected during the dry, transition and wet periods, respectively; 4) when applied to size-segregated samples, the functional group approach provides significantly different compositions in the 0.05–0.14 μm size range compared to the 0.42–1.2 μm range, the former containing much more alkyl and less oxygenated moieties; 5) the picture derived from IC separated fractions is consistent with what has been previously observed, i.e., that the neutral fraction is dominated by polyols (e.g., levoglucosan, mannitol), but still contains polyhydroxy and polyalkoxy benzenes; the mono-/diacids fraction can be seen as a mixture of hydroxylated alkyl and benzoic monocarboxylic and dicarboxylic acids, and the polyacidic fraction exhibits a humic-like character.

4 Discussion

4.1 Speciated WSOC and chemical classes

The analytical techniques described in the experimental section can be grouped into methods for individual compound analysis (GC-MS, IC and IEC-UV), and methods targeted to the separation of main chemical classes (IC-UV). The former allow the identification and measurement of six categories of polar organic compounds, but leave uncharacterized a substantial fraction of OC. Conversely, the IC-UV technique provides a high recovery in the measurement of the water-soluble fraction of OC by fractionation into three main categories, whose specific chemical compositions, however, rests poorly defined. Therefore, in general, the IC-UV chromatographic classes do not correspond directly to any of the categories of polyols and carboxylic acids accounted for by individual compound analyses, but are more likely to include them.

To better understand the chemical nature of the "neutral compounds", "mono-/diacids" and "polyacids", the WSOC speciated by GC-MS, IC and IEC in size-segregated samples can be classified according to their number of carboxylic groups per molecule; the estimation of their contribution to each of the three IC-UV classes is then straightforward. However, the concentrations of the identified WSOC were obtained on MOUDI samples, while those of total WSOC

Table 4. Contribution of levoglucosan and carboxylic acids identified by IEC and IC, respectively, to total WSOC and neutral compounds (NC), mono-/diacids (MDA) and polyacids (PA) measured by the IC-UV method. The speciated carboxylic acids include C_1-C_3 aliphatic monocarboxylic acids (MCA), oxalic acid, C_3-C_9 aliphatic dicarboxylic acids (DCA), C_7-C_8 aromatic acids and C_6 aliphatic tricarboxylic acids (TCA). Average mass balances were calculated on a carbon basis for the dry and transition periods, on the basis of a limited number of samples for which the $MOUDI_{IFUSP}$ and the five-stage Berner impactor were operated approximately in parallel. The concentrations of the polar organic compounds determined on the MOUDI samples by IEC and IC were converted into five-stage size-distributions for comparison with the total WSOC and NC, MDA and PA data, according to the procedure described in the text.

		%WSOC						%NC	%MDA				%PA
	Size intervals	Levoglu-	Aliphatic carboxylic acids				Aromatic	Levoglu-	Aliphatic carboxylic acids			Aromatic	Aliphatic
	(μm)	cosan	MCA	Oxalic	C_3-C_9 DCA	TCA	acids	cosan	MCA	Oxalic	C_3-C_9 DCA	acids	TCA
Dry period	0.05–0.14	0.3%	0.3%	0.5%	0.5%		0.1%	1.0%	0.8%	1.4%	1.2%	0.3%	
	0.14–0.42	1.3%	0.6%	0.8%	1.1%	0.1%	1.9%	7.5%	1.9%	2.6%	3.6%	6.3%	0.2%
	0.42–1.2	2.7%	1.1%	1.3%	1.6%	0.1%	1.6%	12%	3.1%	3.5%	4.4%	4.3%	0.3%
	1.2–3.5	4.7%	1.2%	1.9%	1.4%	0.1%	1.2%	28%	3.7%	5.7%	4.1%	4.1%	0.3%
	3.5–10	0.0%	1.0%	1.8%	0.9%	0.1%	2.6%	0.1%	0.6%	1.0%	0.7%	2.1%	1.6%
Transition	0.05–0.14	0.2%	0.4%	0.2%	0.4%	0.1%	0.2%	0.6%	1.0%	0.9%	1.0%	0.6%	0.3%
period	0.14–0.42	0.1%	0.2%	0.2%	0.2%	0.1%	0.5%	0.3%	0.6%	1.4%	0.9%	2.1%	0.2%
	0.42–1.2	2.2%	0.9%	0.7%	1.4%	0.2%	1.1%	13%	3.0%	4.5%	4.6%	3.7%	0.7%
	1.2–3.5	4.5%	3.1%	1.0%	0.9%	0.1%	0.7%	11%	7.0%	4.7%	1.8%	1.9%	0.4%
	3.5–10		0.6%	0.3%	0.7%	0.5%	1.7%		2.1%	2.5%	2.8%	7.1%	10%

and of NC, MDA and PA were available only for the Berner impactor, making the comparison difficult owing to the different size resolutions and sampling efficiencies of the two impactors. To make the two sets of data comparable, we first defined a sub-set of four pairs of $MOUDI_{IFUSP}$ and Berner impactor (BI) samples that were collected approximately in parallel:

- $MOUDI_{IFUSP}$ 22 September 23:42 UT to 23 September 23:12 UT vs. BI 22 September 22:30 UT to 23 September 22:00 UT;
- $MOUDI_{IFUSP}$ 25 September 00:20 UT to 25 September 22:08 UT vs. BI 24 September 23:00 UT to 25 September 21:45 UT;
- $MOUDI_{IFUSP}$ 16 October 22:40 UT to 18 October 12:46 UT vs. BI 16 October 13:00 UT to 18 October 11:00 UT;
- $MOUDI_{IFUSP}$ 18 October 13:55 UT to 20 October 10:40 UT vs. BI 18 October 12:00 UT to 20 October 10:40 UT.

Then, the MOUDI size-distributions for the identified WSOC and inorganic compounds were converted to continuous size-distributions according to an inversion algorithm, using the MICRON inversion program (Wolfenbarger and Seinfeld, 1990), which takes into account the collection efficiency and species concentration in each MOUDI stage. A more detailed description of the use of the program is given by Havránek et al. (1996). The concentrations of the chemical species measured in MOUDI samples could then be retrieved for the size intervals of the Berner impactor by integrating the continuous size distributions between the Berner cut-offs. To take into account the different sampling efficiencies of the two impactors, the concentrations of organic species were normalized to those of sulfate, which had been measured on both sets of impactor samples. The identified WSOC from $MOUDI_{IFUSP}$ were then expressed as μgC m^{-3} and compared to the concentrations of total WSOC and of the IC-UV classes from the Berner impactor.

Table 4 shows the resulting average carbon budget for the dry period (n=2) and for the transition phase (n=2). Levoglucosan accounts for 1 to 12% of NC in the fine fraction, and for an even higher percentage in the size range 1.2–3.5 μm. Similarly, the identified mono- and di-carboxylic acids account for 6 to 16% of total MDA in the fine fraction, and 9–18% in coarse particles. In contrast, the contribution of the identified tricarboxylic acids (citric and tricarballylic) to total PA is very low, usually less than 1%. In conclusion, the speciated WSOC represent around 1.5% of the total water-soluble carbon in the 0.05–0.14 μm size interval, and up to 10% in the 0.42–3.5 μm size range. The identified WSOC are mostly NC and MDA, while PA remains essentially uncharacterized at the molecular level. This finding supports the hypothesis that PA consist mostly of medium-to-high molecular weight compounds (HULIS). These results for the identified fractions of the three IC-UV classes analyzed in the impactor samples are in agreement with analogous data obtained on comparable $PM_{2.5}$ samples collected during the 1999 LBA-EUSTACH-2 experiment (Mayol-Bracero et al., 2002a).

4.2 A synthetic representation of the WSOC composition by model compounds

In the previous section, the chemical characterization of the IC-UV chromatographic classes was attempted in terms of organic compounds identified at the molecular level, showing

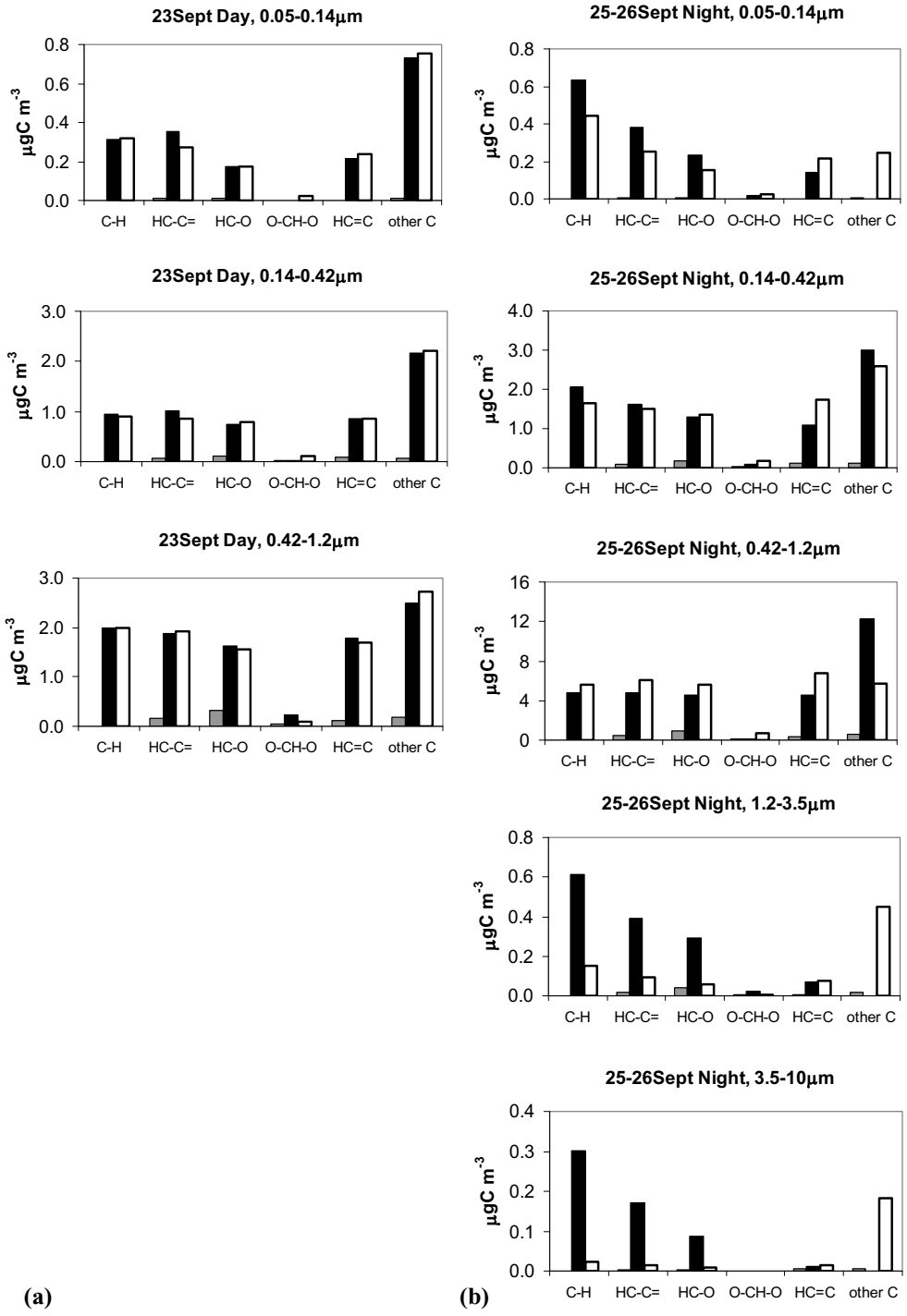

Fig. 5. Comparison between the functional group composition (black bars) determined by ^{1}HNMR analysis of size-segregated samples and HVDS2U$_{Gent}$ filters and that reconstructed on the basis of the individual compounds identified by GC-MS, IC and IEC techniques (gray bars). WSOC functionalities of the mixtures of model compounds are also reported (white bars). The comparison is shown for the selected samples: **(a, b)** Two size-segregated samples from the dry period; **(c)** three $PM_{2.5}$ HVDS samples from the dry, transition and wet periods, respectively; **(d)** chromatographic fractions of the $PM_{2.5}$ HVDS sample collected on 25–26 September: NC (neutral compounds); MDA (mono-/diacids); PA (polyacids); **(e)** a coarse (PM>2.5) HVDS sample from the transition period.

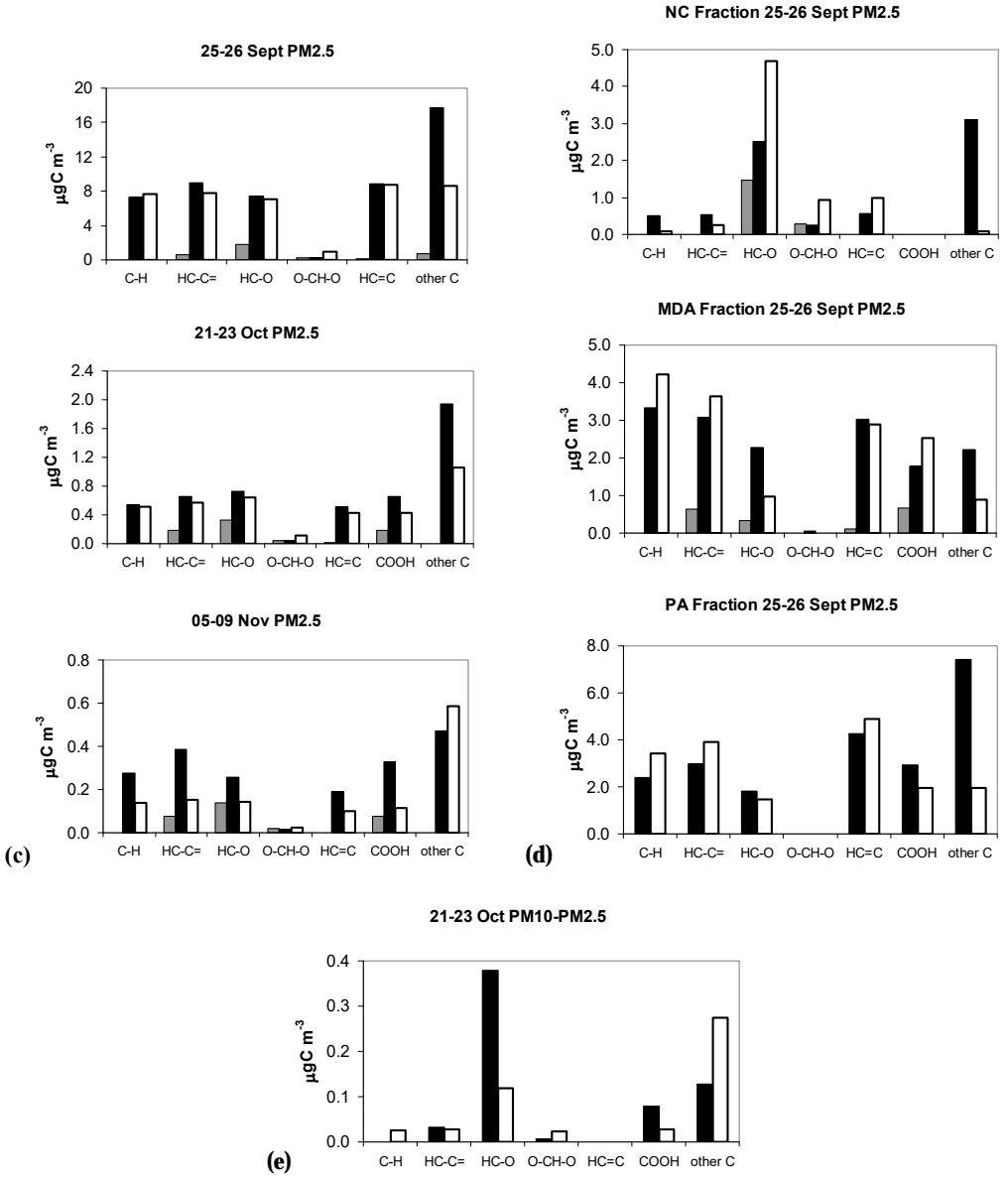

Fig. 5. Continued.

that large fractions of NC, MDA and especially PA could not be speciated using this approach. For the large fraction of the WSOC which eluded any speciation at the molecular level, only data on the neutral/acidic character and the average ^{1}HNMR functional group composition could be obtained. Following the approach of Fuzzi et al. (2002), ^{1}HNMR data and IC-UV fractionation can be exploited to provide at least a representation of the unidentified WSOC by a set of "model compounds". Model compounds are hypothetical that allow to reproduce the observed carbon content, functional group composition and other chemical properties of a mixture (or a fraction) of WSOC. The molecular formulae of the model compounds do not follow unequivocally from the functional group composition, but they are constrained by it. Using this approach the chemical composition of a mixture or a fraction of WSOC is represented in terms of a limited number of compounds, in cases where the speciation of organic compounds is not feasible, but a substantial pool of structural data and other information on the chemical properties of the mixture is however available. The main advantage of the representation through model compounds is that they can be directly used in microphysical models describing the physico-chemical properties of organic aerosols.

In a first step aimed at evaluation of model compounds, the functional group distributions characteristic of the unidentified WSOC were obtained from the available ^{1}HNMR

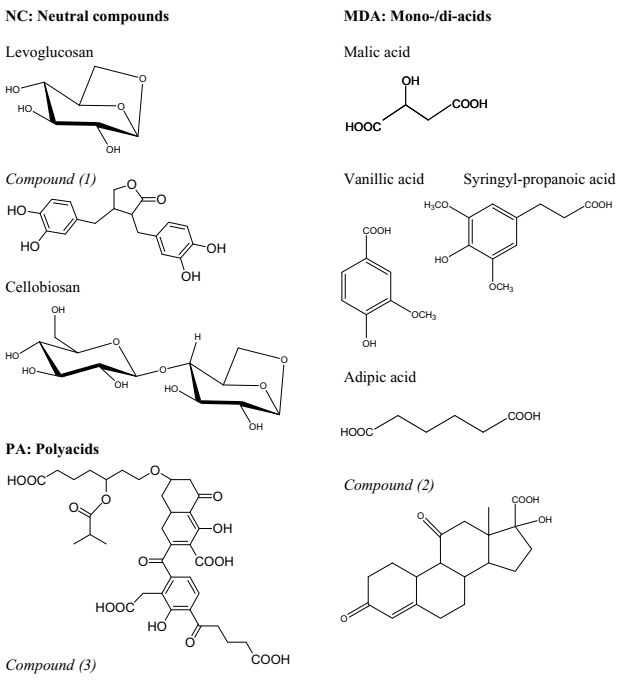

Fig. 6. Model compounds proposed to represent the chemical composition of WSOC on the basis of both speciation methods and functional group analysis. The three compounds labeled with numbers are hypothetical and not available commercially. On the basis of the chemical structure, they can be approximated to: the organic compound with CAS number 580-72-3 (Compound 1); the organic compound with CAS 53-06-5 (Compound 2); the Suwannee River fulvic acid (reference standard from IHSS).

compositions by the subtraction of the contribution of the individual compounds identified by GC-MS, IC and IEC. The contribution of the speciated compounds to the ^{1}HNMR composition was computed on the basis of their concentrations and molecular structure (e.g., anhydrosugars contain five H-C-O groups and one O-CH-O group per molecule, while malic acid contains one HC-(C=), one H-C-O and two COOH groups). The calculation was performed for samples representative of the three periods of the campaign and for which ^{1}HNMR data are available (Fig. 5): a, b) two Berner impactor samples from the dry period, one diurnal and one nocturnal; c) three $PM_{2.5}$ $HVDS2_{UGent}$ samples from the dry, transition and wet periods, respectively; and d) IC-UV fractions isolated from one $PM_{2.5}$ $HVDS2_{UGent}$ sample collected in the dry period. ^{1}HNMR data collected for these $HVDS2_{UGent}$ samples are compared in the figure to the functional groups accounted for by $GC\text{-}MS_{UA}$ analysis of the $HVDS1_{UGent}$ samples collected exactly in parallel. By contrast, for the two impactor samples, the proportion of functional groups attributable to identified compounds was extrapolated from the average amount of WSOC accounted for by levoglucosan, MCA, DCA and aromatic acids in the dry period (Table 4). In general, COOH and H-C-O groups are the functional groups for which the individual compound analysis provides the best recoveries. Conversely, there is a large amount of water-soluble carbon occurring as aliphatic and aromatic C-H groups that cannot be covered by the available set of speciated organic compounds, and for which only a representation through model compounds is possible.

A minimum of six model compounds aimed to represent the unspeciated WSOC was necessary to explain the observed variability in the functional group composition of the samples. The molecular structure of the model compounds and their relative concentrations were chosen in order to match as closely as possible the chemical composition of the samples in Fig. 5 with respect to the functional groups (from ^{1}HNMR characterization) and main chemical classes (NC, MDA and PA from IC-UV analysis), as shown in Table 5 for the example of the 23 September impactor sample. This sample was used to provide the model WSOC chemical composition for the dry period (daytime). The WSOC fraction accounted for by molecular speciation was expressed by the three model compounds, "levoglucosan", "malic acid" and "vanillic acid", introduced respectively as proxies of: a) the speciated polyhydroxylated compounds (anhydrosugars, sugar-alcohols, saccharides, 2-methyltetrols), b) the identified C_1-C_9 aliphatic mono- and dicarboxylic acids, and c) the identified aromatic acids[3,4]. Their concentrations relative to that of total WSOC were set fixed to the values reported in Table 4. Provided that the total concentrations of neutral compounds, mono-/di-acids and polyacids in the chemical model correspond to those determined by IC-UV analysis, the chemical structure and relative concentrations of the model compounds representing the WSOC fraction eluding molecular speciation were varied in an iterative process, until the functional group composition of the mixture reached good agreement with that measured by ^{1}HNMR analysis. In the case of the chemical model evaluated for the dry period (night-time), the functional group composition of model neutral species (levoglucosan+compound 2+cellobiosan), mono-/diacids (malic acid+vanillic acid+compound 3+syringyl propanoic acid+adipic acid) and polyacids (compound 3) was also validated against the ^{1}HNMR functional group compositions obtained for the three chromatographic fractions of the nocturnal sample collected on 25–26 September

[3]No specific class for the identified tricarboxylic acids was introduced because of their very low contribution to PA.

[4]As regards the wet period samples, size-segregated data for the contribution of model compounds "levoglucosan" and "malic acid" to WSOC were extrapolated from the average data for the transition period (Table 4), while the contribution of "vanillic acid" was set to zero. This is qualitatively in agreement with Fig. 3, showing that low-molecular weight aromatic compounds were not detected in the wet period, and that, despite the decrease of anhydrosugars, the content of polyhydroxylated compounds in the fine fraction of PM decreased only slightly from the transition to the wet period, due to the simultaneous increase of the 2-methyltetrol concentrations.

(Fig. 5d). The functional groups of the model compounds constrained by the ^{1}HNMR measurements were the alkyl (C-H), unsaturated aliphatic (HC-C=), alkoxyl (HC-O), acetal (O-CH-O) and aromatic (HC=) groups, plus, in the case of HVDS samples, carboxyl groups (COOH).

The resulting WSOC model compounds are shown in Fig. 6. Beside the three proxies of the compounds identified at the molecular level, two surrogates were introduced for the unidentified neutral species, three for the unidentified mono-/diacids and one for the polyacids:

- Cellobiosan accounts for the unidentified polyhydroxylated compounds. The occurrence of oligomers of anhydrosugars in biomass smoke was suggested by Gao et al. (2003).
- "Compound (1)", a compound close to matairesinol, a plant phenolic compound that has also been found in biomass smoke (Simoneit et al., 2003), reproduces the aromatic and H-C-C= groups of the NC.
- Adipic acid, a C_6 aliphatic dicarboxylic acid, accounts for the excess COOH groups determined by the derivatization-NMR technique.
- Syringyl-propionic acid (Nolte et al., 2001), a methoxylated C_{11} aromatic acid representing the unidentified aromatic species.
- "Compound (2)", a hypothetical C_{19} aliphatic monocarboxylic acid, which reproduces the abundance of saturated aliphatic moieties determined by ^{1}HNMR, especially in the 0.05–0.14 and 3.5–10 μm size intervals of the nocturnal sample from the dry season. Acyclic compounds like compound (2) have previously been reported for biomass smoke particles (Simoneit et al., 2003[5]).
- The polyacidic fraction is represented in all samples by the same single species, "Compound (3)", a fulvic-like substance. This is a hypothetical compound, whose structure is based on the functional group composition of the polyacidic fraction of sample HVDS2$_{UGent}$ collected on 25–26 September (Fig. 5d). It resembles that of the Suwannee River fulvic acid (Averett et al., 1989), but is less aromatic while showing more saturated aliphatic moieties. Therefore, the choice of the Suwannee River fulvic reference material to reproduce the chemical properties of the PA fraction in laboratory experiments cannot be considered as optimal, although it is still preferable to the other commercial standards of humic substances or of other high-molecular weight water-soluble substances.

It is noted that the resulting model NC composition lacks the saturated aliphatic moieties observed in the samples, for which a suitable candidate molecule could not be found. Therefore, the closure of the observed functional group composition of NC could be only partially achieved (Fig. 5d).

The composition of the mixture of model compounds simulating the functional group composition of the 23 September BI sample is reported in Table 5, while the comparison with the NMR data is graphically shown in Fig. 5a. The simulated functional group compositions for the other samples from the various periods of the campaign is also shown in Figs. 5b, c, e. The composition of the mixtures of model compounds used in each case is reported in Table 6, expressed using mass fractions of each compound in the mixtures. Figure 5 shows that good agreement is reached for fine aerosol samples from the dry and the transition period (Fig. 5c), for the size-segregated composition of the 23 September BI sample (Fig. 5a) and for the 25–26 September BI sample in the submicron size range (accounting for most of the PM). By increasing the proportion of the aliphatic carboxylic acid "Compound 2" in the coarse size range of the BI sample collected on 25–26 September, we could reproduce the observed increase of aliphatic groups only to a limited extent (Fig. 5b). In the case of the $PM_{2.5}$ sample from the wet period (Fig. 5c), the WSOC fraction recovered by the IC-UV method and represented through model compounds could not account for the total functional groups estimated by ^{1}HNMR. Therefore, only a relative functional group composition could be reproduced. Finally, the ^{1}HNMR composition of the HVDS coarse filter (Fig. 5e) shows a very high content of hydroxyl groups, which could not be fully accounted for by the model polyhydroxylated neutral compounds.

The above paragraphs describe how to evaluate model WSOC compositions constrained by ^{1}HNMR data and the IC-UV grouping method. As a final remark, it should be emphasized that the molecular weight of the model compounds representing the (large) fraction of WSOC not speciated at the molecular level cannot be constrained by the present approach. It can be assumed that the derivatization-GC-MS and ion chromatography methods were rather efficient in the determination of the low-molecular weight fraction of WSOC. Consequently, the model compounds introduced to represent the uncharacterized fraction must include medium-high molecular weight species. In the model presented here, the compounds with molecular weight higher than 300 account for 60–70% of WSOC in the fine fraction, consistent with the results of EGA analysis, which indicates a fraction of 60–80% on the basis of the thermal evolution behavior. The maximum molecular weight attributable to the model compounds reproducing the more refractory fraction of WSOC

[5] In this study, the acyclic compounds were found prevalently in the water-insoluble fraction. Compound (2) must exhibit a limited solubility in water, probably higher than that of cortisone, a compound with similar structure but with no carboxylic groups and a water solubility of 0.28 g/kg H_2O. This solubility can be sufficient for the extraction of compound (2)-like WSOC, for which a minimum amount of water of 15 g per 0.1 mg C of sample was always used.

Table 5. Example of model composition of WSOC constrained by chromatographic and spectroscopic analysis of a size-segregated aerosol sample. The composition of the three size intervals corresponding to the Berner impactor stages collecting the fine fraction of the aerosol is shown. The TOC and IC-UV analyses as well as the ^{1}HNMR data refer to the dry period sample collected on 23 September in daytime. The IC-UV classes are: NC (neutral compounds), MDA (mono-/diacids) and PA (polyacids), while UR is the unrecovered WSOC fraction. The classes of compounds speciated at the molecular level are here represented by three proxies: levoglucosan (LGS), malic acid (MA) and vanillic acid (VA). Their concentration relative to total WSOC was derived from Table 4. All data obtained by the chemical analyses are reported in italics in the table. The model compounds introduced to represent the WSOC recovered by the IC-UV techniques but not speciated at the molecular level are: Compound 1 (C1), cellobiosan (CBS), syringyl-propanoic acid (SPA), Compound 2 (C2), adipic acid (AD), Compound 3 (C3) (Fig. 6). Table 5a shows that the proportions of the model neutral species, mono-/diacids and polyacids, are set fixed to those determined by IC-UV analysis. The concentrations of the model compounds (bottom of Table 5a) and their specific functional groups (upper part of Table 5b) are then used to simulate the WSOC functional group composition (column labeled "total" in Table 5b) to be validated against the measured ^{1}HNMR composition (right column of Table 5b). †Simulated total "other C" (i.e., the functional groups that cannot be detected by ^{1}HNMR analysis) includes the "other C" of the model compounds plus the carbon not recovered (UR) by the IC-UV analysis.

(a)

Composition of the mixture of model compounds (% WSOC)									
size range (μm)	LGS	C1	CBS	MA	VA	C2	SPA	AD	C3
0.05–0.14	*0.3%*	2.0%	7.1%	*1.3%*	*0.1%*	15.4%	2.9%	11.6%	32%
0.14–0.42	*1.3%*	3.1%	10.4%	*2.5%*	*1.9%*	11.8%	2.6%	10.2%	32%
0.42–1.2	*2.7%*	3.6%	10.7%	*4.0%*	*1.6%*	15.9%	3.1%	12.4%	39%

Concentration of the organic fractions (μg C m^{-3}) from TOC and IC-UV analysis					
size range (μm)	WSOC	NC	MDA	PA	UR
0.05–0.14	*1.78*	*0.17*	*0.56*	*0.57*	*0.49*
0.14–0.42	*5.76*	*0.86*	*1.67*	*1.86*	*1.37*
0.42–1.2	*9.97*	*1.69*	*3.69*	*3.93*	*0.66*

Concentrations of the model compounds (μg C m^{-3})									
size range (μm)	LGS	C1	CBS	MA	VA	C2	SPA	AD	C3
0.05–0.14	0.005	0.035	0.127	0.023	0.002	0.275	0.052	0.207	0.569
0.14–0.42	0.076	0.180	0.600	0.144	0.109	0.679	0.147	0.588	1.859
0.42–1.2	0.266	0.356	1.072	0.399	0.160	1.586	0.308	1.234	3.930

(b)

Functional groups breakdown of model compounds										
		LGS	C1	CBS	MA	VA	C2	SPA	AD	C3
	C-H		1/18				10/20		2/6	7/36
	HC-C=		3/18		2/5		4/20	2/11	2/6	8/36
	HC-O	5/6	1/18	10/12	1/5	1/8		2/11		3/36
	O-CH-O	1/6		2/12						
	HC=C		12/18			6/8	2/20	6/11		10/36
	other C		1/18		2/5	1/8	4/20	1/11	2/6	8/36

Functional groups concentrations (μg C m^{-3}) of model compounds												NMR functional groups
size range (μm)		LGS	C1	CBS	MA	VA	C2	SPA	AD	C3	total	(μg C m^{-3})
0.05–0.14	C-H		0.002				0.137		0.069	0.111	0.319	*0.310*
	HC-C=		0.006		0.009		0.055	0.009	0.069	0.126	0.275	*0.356*
	HC-O	0.004	0.002	0.106	0.005	0.000		0.009		0.047	0.174	*0.175*
	O-CH-O	0.001		0.021							0.022	
	HC=C		0.023			0.001	0.027	0.028		0.158	0.238	*0.212*
	other C		0.002		0.009	0.000	0.055	0.005	0.069	0.126	0.757†	*0.730*
0.14–0.42	C-H		0.010				0.340		0.196	0.362	0.907	*0.941*
	HC-C=		0.030		0.058		0.136	0.027	0.196	0.413	0.859	*1.022*
	HC-O	0.063	0.010	0.500	0.029	0.014		0.027		0.155	0.798	*0.749*
	O-CH-O	0.013		0.100							0.113	*0.031*
	HC=C		0.120			0.082	0.068	0.080		0.516	0.866	*0.853*
	other C		0.010		0.058	0.014	0.136	0.013	0.196	0.413	2.213†	*2.159*
0.42–1.2	C-H		0.020				0.793		0.411	0.764	1.988	*1.989*
	HC-C=		0.059		0.160		0.317	0.056	0.411	0.873	1.877	*1.928*
	HC-O	0.222	0.020	0.893	0.080	0.020		0.056		0.327	1.618	*1.547*
	O-CH-O	0.044		0.179							0.223	*0.100*
	HC=C		0.237			0.120	0.159	0.168		1.092	1.775	*1.685*
	other C		0.020		0.160	0.020	0.317	0.028	0.411	0.873	2.491†	*2.722*

Table 6. Model composition of water-soluble carbon in size-segregated samples from the different periods of the SMOCC campaign. Model compounds with underscored names were evaluated on the basis of WSOC speciation, while the others were based only on functional group analysis and the apportionment of WSOC into the three main chemical classes from the IC-UV method: neutral compounds (NC), mono-/diacids (MDA) and polyacids (PA). Model compounds corresponding to organic species never detected in aerosol samples are hypothetical compounds labeled with numbers 1 to 3 in the table. Their structure is shown in Fig. 6, and recommendations for suitable surrogates among the commercial standards are given in the footnotes.

			Dry (day)			Dry (night)			Dry (day/night)		Transition			Wet			Transition/ Wet
Size range (μm)			0.05–0.14	0.14–0.42	0.42–1.2	0.05–0.14	0.14–0.42	0.42–1.2	1.2–3.5	3.5–10	0.05–0.14	0.14–0.42	0.42–1.2	0.05–0.14	0.14–0.42	0.42–1.2	1.2–10
	levoglucosan	$C_6H_{10}O_5$	0.5%	2.1%	3.4%	0.4%	1.9%	3.2%	10.7%	0.2%	0.2%	0.1%	3.9%	0.3%	0.1%	4.4%	18.5%
NC	compound 1 [a]	$C_{18}H_{22}O_6$	2.3%	3.4%	3.2%	2.5%	3.0%	3.1%	5.7%	4.1%	6.0%	6.8%	4.8%	5.1%	5.4%	4.5%	0.0%
	cellobiosan	$C_{12}H_{20}O_{10}$	12.0%	16.4%	13.8%	13.1%	14.5%	13.8%	2.9%	9.7%	27.3%	30.9%	18.2%	23.1%	24.6%	16.4%	46.5%
	malic acid	$C_4H_6O_5$	2.7%	4.9%	6.3%	2.2%	4.4%	5.9%	12.8%	18.1%	1.5%	1.0%	6.4%	2.2%	1.6%	7.3%	4.2%
	vanillic acid	$C_8H_8O_4$	0.1%	2.3%	1.6%	0.1%	2.1%	1.5%	2.1%	8.0%	0.2%	0.5%	1.5%	0.0%	0.0%	0.0%	0.0%
MDA	adipic acid	$C_6H_{10}O_4$	17.7%	14.4%	14.3%	2.4%	10.2%	10.7%	0.0%	0.0%	33.6%	32.7%	30.3%	35.3%	34.3%	32.5%	30.8%
	syringyl-propionic acid	$C_{11}H_{14}O_5$	3.7%	3.0%	3.0%	1.7%	10.1%	7.2%	0.0%	0.0%	2.4%	2.2%	2.1%	0.0%	0.0%	0.0%	0.0%
	compound 2 [b]	$C_{19}H_{24}O_5$	16.7%	11.9%	13.0%	45.7%	16.6%	8.9%	46.4%	43.0%	3.5%	3.2%	3.0%	2.8%	2.4%	2.4%	0.0%
PA	compound 3 [c]	$C_{36}H_{42}O_{16}$	44.3%	41.6%	41.4%	32.0%	37.2%	45.8%	19.2%	16.9%	25.2%	22.7%	29.8%	31.2%	31.6%	32.5%	0.0%

[a] Can be approximated to compound with CAS 580-72-3;
[b] Can be approximated to compound with CAS 53-06-5
[c] Can be approximated to the Suwannee River fulvic acid (reference standard from IHSS).

cannot be determined accurately. However, it cannot be very high for the less polar compounds, like compounds (1) and (2), whose homologs with 30 carbon atoms would probably be insoluble even in the large excess of water used for extraction of the samples. Conversely, the polyhydroxylated species with more than six carbon atoms, represented in the model by cellobiosan, can be perfectly soluble even when occurring in very large polymeric forms. Although polyhydroxylated compounds larger than cellobiosan have not yet been found in samples of ambient aerosol, such polymers may form in wood smoke (Kawamoto et al., 2003), and therefore the molecular weight of the WSOC fraction represented by the model compound "cellobiosan" remains largely uncertain.

The list of model compounds representative of the WSOC composition in the aerosol samples collected during the SMOCC campaign is more complex than that presented in the previous work by Fuzzi et al. (2001), based on samples from the Po Valley. In contrast to the former study, a more detailed picture of the low-molecular weight WSOC emerged from the GC-MS and IC analyses performed during the LBA-SMOCC experiment. The identified species are represented by distinct model compounds (levoglucosan, malic acid and vanillic acid). They constitute a subset of model compounds known with a higher confidence, whereas the remaining unidentified compounds are more susceptible to modifications following different approaches in defining the chemical classes, and improvements in the characterization of un-speciated WSOC. For this reason, it is thought that the current representation is more flexible and provides a better integration of the information from the individual compound analysis with the results from the functional group characterization.

5 Conclusions

During the LBA-SMOCC field campaign, biomass burning emissions frequently caused episodes of very high concentrations of submicron carbonaceous aerosol (submicron TC concentrations $>50\,\mu gC\,m^{-3}$) in the period 9 September–8 October 2002, while at the beginning of November, after the end of the intense burning period, the measured submicron TC concentrations were 20 times lower. At the same time, biogenic sources produced a constant background of aerosol throughout the campaign, which was found predominantly in the coarse mass fraction. Fine and coarse aerosol TC differ also with respect to their water-soluble fraction, which is 64% on average in the first case and only 34% in the latter. The EC accounted for 12% on average of TC in the fine fraction of the aerosol. A unique combination of analytical techniques for individual compound analysis was employed to speciate the aerosol organic compounds, resulting in the apportionment of up to 8% of the submicron TC (ca. 11% of WSOC). Carboxylic acids and polyhydroxylated compounds, comprising both pyrogenic and biogenic species, were the main classes of compounds speciated. Pyrogenic compounds include anhydrosugars, aromatic acids and aldehydes, while biogenic species include sugars, sugar-alcohols, 2-methyltetrols and malic acid. The ratio between total identified pyrogenic and biogenic compounds changed from 10:1 in the dry period to 1:3 in the wet period, showing that biomass burning was still active at the end of the field campaign.

Three main chemical classes of WSOC isolated by the IC-UV method (i.e., neutral compounds, mono-/diacids and polyacids) were detected in size-segregated aerosol samples throughout the campaign, although the concentrations

of polyacids were low in the coarse fraction, especially at the onset of the wet period. The speciated polyhydroxylated compounds and low-molecular weight carboxylic acids contributed 1–20% to both, neutral compounds and mono-/diacids. Conversely, the polyacidic fraction remained almost entirely uncharacterized at the molecular level. An insight into the unresolved fraction of WSOC was provided by ^{1}HNMR functional group analysis, showing that most of the less polar compounds, characterized by extended saturated aliphatic and aromatic moieties, escaped molecular speciation.

The size-segregated composition of WSOC was summarized by a set of model compounds, which reproduce both the composition of the identified organic compounds and the functional groups of the whole WSOC mixture. The model compounds retain the average structural information on WSOC derived by the chemical characterization. The main advantage of the representation of the complex mixture of WSOC through model compounds is that they can be directly used in microphysical models for prediction of the aerosol hygroscopic properties and CCN ability starting from the chemical composition. In this respect, an application of the mixtures of model organic compounds evaluated in the present study is discussed in a companion paper (Mircea et al., 2005).

It is remarkable that despite the significant change in the relative strength of pyrogenic and biogenic sources from the dry to the wet period, the main chemical classes and functional groups of WSOC (and consequently the sets of model compounds) change only to a limited extent. This must be attributed to the fact that the decrease in the hydroxylated compounds and carboxylic acids of pyrogenic origin toward the end of the campaign was compensated by the increased contribution of analogous classes of compounds of biogenic nature. In this way, the pyrogenic and biogenic emissions provided a rather constant pool of very polar organic compounds in the submicron fraction of the aerosol throughout the dry-to-wet season transition. One consequence of this fact is the surprisingly similar cloud droplet nucleating ability (CCN ability) of the pyrogenic and biogenic aerosols over Amazonia (Andreae et al., 2004).

Acknowledgements. This work was carried out within the frame work of the Smoke, Aerosols, Clouds, Rainfall, and Climate (SMOCC) project, a European contribution to the Large-Scale Biosphere-Atmosphere Experiment in Amazonia (LBA). It was financially supported by the Environmental and Climate Program of the European Commission (contract No. EVK2-CT-2001-00110 SMOCC), the Max Planck Society (MPG), the Fundação de Amparo à Pesquisa do Estado de São Paulo, and the Conselho Nacional de Desenvolvimento Científico (Instituto do Milênio LBA). Research at ISAC was also supported by the Italian Ministry of Environment (Italy-USA Cooperation on Science and Technology of Climate Change) and by the Project FISR Modellistica Molecolare. Research at Ghent University and the University of Antwerp was also supported by the Belgian Federal Science Policy Office through the project "Characterization and sources of carbonaceous atmospheric aerosols" (contracts EV/02/11A and EV/06/11B). We thank all members of the LBA-SMOCC and LBA-RACCI Science Teams for their support during the field campaign, especially A. C. Ribeiro, M. A. L. Moura, J. von Jouanne, L. Tarozzi, and J. Cafmeyer.

Edited by: T. Hoffmann

References

Andreae, M. O., Rosenfeld, D., Artaxo, P., Costa, A. A., Frank, G. P., Longo, K. M., and Silva-Dias, M. A. F.: Smoking rain clouds over the Amazon, Science, 303, 1337–1342, 2004.

Averett, R. C., Leenheer, J. A., McKnight, D. M., and Thorn, K. A. (Eds.): Humic substances in the Suwannee River, Georgia: Interaction, properties, and proposed structures, USGS Report 87-557, U.S. Geological Survey, Denver, CO, 1989.

Birch, M. E. and Cary, R. A.: Elemental carbon-based method for monitoring occupational exposures to particulate diesel exhaust, Aerosol Sci. Technol., 25, 221–241, 1996.

Chang, H., Herckes, P., and Collett Jr., J. L.: On the use of anion exchange chromatography for the characterization of water soluble organic carbon, Geophys. Res. Lett., 32, L01810, doi:10.1029/2004GL021322, 2005.

Chow, J. C., Watson, J. G., Crow, D., Lowenthal, D. H., and Merrifield, T.: Comparison of IMPROVE and NIOSH Carbon measurements, Aerosol. Sci. Technol., 34, 23–34, 2001.

Claeys, M., Graham, B., Vas, G., Wang, W., Vermeylen, R., Pashynska, V., Cafmeyer, J., Guyon, P., Andreae, M. O., Artaxo, P., and Maenhaut, W.: Formation of secondary organic aerosols through photooxidation of isoprene, Science, 303, 1173–1176, 2004a.

Claeys, M., Wang, W., Ion, A. C., Kourtchev, I., Gelencsér, A., and Maenhaut, W.: Formation of secondary organic aerosols from isoprene and its gas-phase oxidation products through reaction with hydrogen peroxide, Atmos. Environ., 38, 4093–4098, 2004b.

Decesari, S., Facchini, M. C., Fuzzi, S., and Tagliavini, E.: Characterization of water soluble organic compounds in atmospheric aerosol: A new approach, J. Geophys. Res., 105, 1481–1489, 2000.

Decesari, S., Moretti, F., Fuzzi, S., Facchini, M. C., and Tagliavini, E.: Comment on "On the use of anion exchange chromatography for the characterization of water soluble organic carbon" by Chang et al., Geophys. Res. Lett., 32, L24814, doi:10.1029/2005GL023826, 2005.

Eatough, D. J., Eatough, N. L., Pang, Y., Sizemore, S., Kirchstetter, T. W., Novakov, T., and Hobbs, P. V.: Semivolatile particulate organic material in southern Africa during SAFARI 2000, J. Geophys. Res., 108, 8479, doi:10.1029/2002JD002296, 2003.

Falkovich, A. H., Schkolnik, G., Ganor, E., and Rudich, Y.: Adsorption of organic compounds pertinent to urban environments onto mineral dust particles, J. Geophys. Res., 109, D02208, doi:10.1029/2003JD003919, 2004.

Falkovich, A. H., Graber, E. R., Schkolnik, G., Rudich, Y., Maenhaut, W., and Artaxo, P.: Low molecular weight organic acids in aerosol particles from Rondonia, Brazil, during the biomass-burning, transition and wet periods, Atmos. Chem. Phys., 5, 781–

797, 2005,
SRef-ID: 1680-7324/acp/2005-5-781.

Fuzzi, S., Decesari, S., Facchini, M. C., Matta, E., Mircea, M., and Tagliavini, E.: A simplified model of the water soluble organic component of atmospheric aerosols, Geophys. Res. Lett., 20, 4079–4082, 2001.

Gao, S., Hegg, D. A., Hobbs, P. V., Kirchstetter, T. W., Magi, B. I., and Sadilek, M.: Water-soluble organic components in aerosols associated with savanna fires in southern Africa: Identification, evolution, and distribution, J. Geophys. Res., 108, 8491, doi:10.1029/2002JD002324, 2003.

Graham, B., Mayol-Bracero, O. L., Guyon, P., Roberts, G., Decesari, S., Facchini, M. C., Artaxo, P., Maenhaut, W., Koll, P., and Andreae, M. O.: Water-soluble organic compounds in biomass burning aerosols over Amazonia. 1. Characterization by NMR and GC-MS, J. Geophys. Res., 107, 8047, doi:10,1029/2001JD000336, 2002.

Graham, B., Guyon, P., Taylor, P. E., Artaxo, P., Maenhaut, W., Glovsky, M. M., Flagan, R. C., and Andreae, M. O.: Organic compounds present in the natural Amazonian aerosol: Characterization by gas chromatography-mass spectrometry, J. Geophys. Res., 108(D24), 4766, doi:10.1029/2003JD003990, 2003.

Havránek, V., Maenhaut, W., Ducastel, G., and Hanssen, J. E.: Mass size distribution for atmospheric trace elements at the Zeppelin background station in Ny Alesund, Spitsbergen, Nucl. Instr. Meth. B, 109/110, 465–470, 1996.

Hoffer, A., Gelencsér, A., Blazsó, M., Guyon, P., Artaxo, P., and Andreae, M. O.: Chemical transformation in organic aerosol from biomass burning, Atmos. Chem. Phys. Discuss., 5, 8027–8054, 2005,
SRef-ID: 1680-7375/acpd/2005-5-8027.

Kawamoto, H., Murayama, M., and Saka, S.: Pyrolysis behavior of levoglucosan as an intermediate in cellulose pyrolysis: polymerization into polysaccharide as a key reaction to carbonized product formation, J. Wood. Sci., 49, 469–473, 2003.

Knicker, H., Almendros, G., Gonzales-Vila, F. J., Martin, F., and Ludemann, H. D.: ^{13}C and ^{15}N-NMR spectroscopic examination of the transformation of organic nitrogen in plant biomass during thermal treatment, Soil Biol. Biochem., 28, 1053–1060, 1996.

Kubátová, A., Vermeylen, R., Claeys, M., Cafmeyer, J., and Maenhaut, W.: Carbonaceous aerosols and particulate organic compounds in Gent, Belgium, during winter and summer of 1998, J. Aerosol Sci., 30, suppl. 1, S905–S906, 1999.

Kubátová, A., Vermeylen, R., Claeys, M., Cafmeyer, J., Maenhaut, W., Roberts, G., and Artaxo, P.: Carbonaceous aerosol characterization in the Amazon basin, Brasil: novel dicarboxylic acids and related compounds, Atmos. Environ., 34, 5037–5051, 2000.

Mayol-Bracero, O. L., Guyon, P., Graham, B., Roberts, G. C., Andreae, M. O., Decesari, S., Facchini, M. C., Fuzzi, S., and Artaxo, P.: Water-soluble organic compounds in biomass burning aerosols over Amazonia: 2. Apportionment of the chemical composition and importance of the polyacidic fraction, J. Geophys. Res., 107, 8091, doi:10.1029/2001JD000522, 2002a.

Mayol-Bracero, O. L., Gabriel, R., Andreae, M. O., Kirchstetter, T. W., Novakov, T., Ogren, J., Sheridan, P., and Streets, D. G.: Carbonaceous aerosols over the Indian Ocean during the Indian Ocean Experiment (INDOEX): Chemical characterization, optical properties and probable sources, J. Geophys. Res., 107, 8030, doi:10.1029/2000JD000039, 2002b.

Mircea, M., Facchini, M. C., Decesari, S., Cavalli, F., Emblico, L., Fuzzi, S., Vestin, A., Rissler, J., Swietlicki, E., Frank, G., Andreae, M. O., Maenhaut, W., Rudich, Y., and Artaxo, P.: Importance of the organic aerosol fraction for modeling aerosol hygroscopic growth and activation: a case study in the Amazon Basin, Atmos. Chem. Phys., 5, 3111–3126, 2005,
SRef-ID: 1680-7324/acp/2005-5-3111.

Mochida, M. and Kawamura, K.: Hygroscopic properties of levoglucosan and related organic compounds characteristic to biomass burning aerosol particles, J. Geophys. Res., 109, D21202, doi:10.1029/2004JD004962, 2004.

Moens, L., Evans, R. J., Looker, M. J., and Nimlos, M. R.: A comparison of the Maillard reactivity of proline to other amino acids using pyrolysis-molecular beam mass spectrometry, Fuel, 83, 1433–1443, 2004.

Nolte, C., Schauer, J. J., Cass, G. R., and Simoneit, B. T.: Highly polar organic compounds present in wood smoke and in the ambient atmosphere, Environ. Sci. Technol., 35, 1912–1919, 2001.

Pashynska, V., Vermeylen, R., Vas, G., Maenhaut, W., and Claeys, M.: Development of a gas chromatography/ion trap mass spectrometry method for determination of levoglucosan and saccharidic compounds in atmospheric aerosols: Application to urban aerosols, J. Mass Spectrom., 37, 1249–1527, 2002.

Reid, J. S., Koppmann, R., Eck, T. F., and Eleuterio, D. P.: A review of biomass burning emissions, part II: Intensive physical properties of biomass burning particles, Atmos. Chem. Phys., 5, 799–825, 2005,
SRef-ID: 1680-7324/acp/2005-5-799.

Schkolnik, G., Falkovich, A. H., Rudich, Y., Maenhaut, W., and Artaxo, P.: A new analytical method for the determination of levoglucosan, polyhydroxy compounds and 2-methylerythrol and its application to smoke and rainwater samples, Environ. Sci. Technol., 39, 2744–2742 2005.

Schmid, H., Laskus, L., Abraham, H. J., Baltensperger, U., Lavanchy, V., Bizjak, M., Burba, P., Cachier, H., Crow, D., Chow, J., Gnauk, T., Even, A., ten Brink, H. M., Giesen, K.-P., Hitzenberger, R., Hueglin, C., Maenhaut, W., Pio, C., Carvalho, A., Putaud, J.-P., Toom-Sauntry, D., and Puxbaum, H.: Results of the carbon conference international aerosol carbon round robin test stage I, Atmos. Environ., 35, 2111–2121, 2001.

Shafidazeh, F.: The chemistry of pyrolysis and combustion, in: Chemistry of Solid Wood, edited by: Rowell, R., Advances in Chemistry Series 207, American Chemical Society, Washington D.C., 489–529, 1984.

Simoneit, B. R. T.: Biomass burning – a review of organic tracers for smoke from incomplete combustion, Appl. Geochem., 17, 129–162, 2002.

Simoneit, B. R. T., Elias, V. O., Kobayashi, M., Kawamura, K., Rushdi, A. I., Medeiros, P. M., Rogge, W. F., and Didyk, B. M.: Sugars-Dominant water-soluble organic components in soils and characterization as tracers in atmospheric particulate matter, Environ. Sci. Technol., 38, 5939–5949, 2004.

Souza, S. R., Vasconcellos, P. C., and Carvalho, L. R. F.: Low molecular weight carboxylic acids in an urban atmosphere: Winter measurements in Sao Paulo City, Brazil, Atmos. Environ. 33, 2563–2574, 1999.

Svenningsson, B., Rissler, J., Swietlicki, E., Mircea, M., Bilde, M., Facchini, M. C., Decesari, S., Fuzzi, S., Zhou, J., Monster, J.,

and Rosenorn, T.: Hygroscopic growth and critical supersaturations for mixed aerosol particles of inorganic and organic compounds of atmospheric relevance, Atmos. Chem. Phys. Discuss., 5, 2833–2877, 2005,
SRef-ID: 1680-7375/acpd/2005-5-2833.

Tagliavini, E., Moretti, F., Decesari, S., Facchini, M. C., Fuzzi, S., and Maenhaut, W.: Functional group analysis by H NMR/chemical derivatization for the characterization of organic aerosol from the SMOCC field campaign, Atmos. Chem. Phys. Discuss., 5, 9447–9491, 2005,
SRef-ID: 1680-7375/acpd/2005-5-9447.

Wang, W., Kourtchev, I., Graham, B., Cafmeyer, J., Maenhaut, W., and Claeys, M.: Characterization of oxygenated derivatives of isoprene related to 2-methyltetrols in Amazonian aerosols using trimethylsilylation and gas chromatography/ion trap mass spectrometry, Rapid Commun. Mass Spectrom., 19, 1343–1351, 2005.

Wolfenbarger, J. K. and Seinfeld, J. H.: Inversion of aerosol size distribution data, J. Aerosol Sci., 21, 227–247, 1990.

Wurzler, S., Herrmann, H., Neusüß, C., Wiedensohler, A., Stratmann, F., Wilck, M., Trautmann, T., Andreae, M. O., Helas, G., Trentmann, J., Langmann, B., Graf, H., and Textor, C.: Impact of vegetation fires on the composition and circulation of the atmosphere: Introduction of the research project EFEU, J. Aerosol Sci., 32 (Suppl), 199–200, 2001.

Zdráhal, Z., Oliveira, J., Vermeylen, R., Claeys, M., and Maenhaut, W.: Improved method for quantifying levoglucosan and related monosaccharide anhydrides in atmospheric aerosols and application to samples from urban and tropical locations, Environ. Sci. Technol., 36, 747–753, 2002.

Atmos. Chem. Phys., 10, 9319–9331, 2010
www.atmos-chem-phys.net/10/9319/2010/
doi:10.5194/acp-10-9319-2010

Atmospheric Chemistry and Physics

Polar organic marker compounds in atmospheric aerosols during the LBA-SMOCC 2002 biomass burning experiment in Rondônia, Brazil: sources and source processes, time series, diel variations and size distributions

M. Claeys[1], I. Kourtchev[1,*], V. Pashynska[1,], G. Vas[1,***], R. Vermeylen[1], W. Wang[1], J. Cafmeyer[2], X. Chi[2], P. Artaxo[3], M. O. Andreae[4], and W. Maenhaut[2]**

[1]Department of Pharmaceutical Sciences, University of Antwerp (Campus Drie Eiken), Antwerp, Belgium
[2]Department of Analytical Chemistry, Institute for Nuclear Sciences, Ghent University, Gent, Belgium
[3]Institute of Physics, University of São Paulo, São Paulo, Brazil
[4]Biogeochemistry Department, Max Planck Institute for Chemistry, Mainz, Germany
[*]present address: Institute for Reference Materials and Measurements (IRMM), European Commission, Joint Research Centre, Geel, Belgium
[**]present address: B. Verkin Institute for Low Temperature Physics and Engineering, National Academy of Sciences of Ukraine, Kharkov, Ukraine
[***]present address: Cordis Corporation, Analytical Technology, Spring House, PA, USA

Received: 7 April 2010 – Published in Atmos. Chem. Phys. Discuss.: 23 April 2010
Revised: 11 September 2010 – Accepted: 21 September 2010 – Published: 5 October 2010

Abstract. Measurements of polar organic marker compounds were performed on aerosols that were collected at a pasture site in the Amazon basin (Rondônia, Brazil) using a high-volume dichotomous sampler (HVDS) and a Micro-Orifice Uniform Deposit Impactor (MOUDI) within the framework of the 2002 LBA-SMOCC (Large-Scale Biosphere Atmosphere Experiment in Amazônia – Smoke Aerosols, Clouds, Rainfall, and Climate: Aerosols From Biomass Burning Perturb Global and Regional Climate) campaign. The campaign spanned the late dry season (biomass burning), a transition period, and the onset of the wet season (clean conditions). In the present study a more detailed discussion is presented compared to previous reports on the behavior of selected polar marker compounds, including levoglucosan, malic acid, isoprene secondary organic aerosol (SOA) tracers and tracers for fungal spores. The tracer data are discussed taking into account new insights that recently became available into their stability and/or aerosol formation processes. During all three periods, levoglucosan was the most dominant identified organic species in the $PM_{2.5}$ size fraction of the HVDS samples. In the dry period levoglucosan reached concentrations of up to 7.5 µg m^{-3} and exhibited diel variations with a nighttime prevalence. It was closely associated with the PM mass in the size-segregated samples and was mainly present in the fine mode, except during the wet period where it peaked in the coarse mode. Isoprene SOA tracers showed an average concentration of 250 ng m^{-3} during the dry period versus 157 ng m^{-3} during the transition period and 52 ng m^{-3} during the wet period. Malic acid and the 2-methyltetrols exhibited a different size distribution pattern, which is consistent with different aerosol formation processes (i.e., gas-to-particle partitioning in the case of malic acid and heterogeneous formation from gas-phase precursors in the case of the 2-methyltetrols). The 2-methyltetrols were mainly associated with the fine mode during all periods, while malic acid was prevalent in the fine mode only during the dry and transition periods, and dominant in the coarse mode during the wet period. The sum of the fungal spore tracers arabitol, mannitol, and erythritol in the $PM_{2.5}$ fraction of the HVDS samples during the dry, transition, and wet periods was, on average, 54 ng m^{-3}, 34 ng m^{-3}, and 27 ng m^{-3}, respectively, and revealed minor day/night variation. The mass size distributions of arabitol and mannitol during all periods showed similar patterns and

Correspondence to: M. Claeys
(magda.claeys@ua.ac.be)

an association with the coarse mode, consistent with their primary origin. The results show that even under the heavy smoke conditions of the dry period a natural background with contributions from bioaerosols and isoprene SOA can be revealed. The enhancement in isoprene SOA in the dry season is mainly attributed to an increased acidity of the aerosols, increased NO_x concentrations and a decreased wet deposition.

1 Introduction

The Amazon basin is a region where widespread biomass burning takes place during the dry season which significantly alters the chemical properties of the tropical pristine background atmosphere. The carbonaceous aerosol over the Amazon basin has been intensively studied during recent years since it contains a large fraction of water-soluble organic carbon (WSOC). The latter fraction is of climatic relevance since it enhances the ability of the aerosol to act as cloud condensation nuclei (e.g., Novakov and Penner, 1993; Novakov and Corrigan, 1996; Mochida and Kawamura, 2004) and may as such affect cloud processes (e.g., Shulman et al., 1996; Facchini et al., 1999; Roberts et al., 2002; Mircea et al., 2005). As to chemical composition studies of the Amazonian carbonaceous aerosol, emphasis has been formerly placed on the measurement and/or characterization of individual compounds that are hygroscopic and/or can serve as tracers for aerosol sources and/or processes, i.e., anhydrosugars, sugars, 2-methyltetrols, polyols, hydroxyacids, dicarboxylic acids, and phenolic acids (Kubátová et al., 2000; Zdráhal et al., 2002; Graham et al., 2002, 2003; Claeys et al., 2004; Falkovich et al., 2005; Schkolnik et al., 2005), as well as of humic-like substances (HULIS) that represent a large fraction of the WSOC (Mayol-Bracero et al., 2002).

The major anhydrosugar detected in the aerosol samples is levoglucosan (1,6-anhydro-β-D-glucopyranose), which is formed through pyrolysis of cellulose, the main building material of wood, at temperatures higher than 300 °C (Shafizadeh, 1982). It is accompanied by minor stereoisomers, including 1,6-anhydro-β-D-glucofuranose, mannosan (1,6-anhydro-β-D-mannopyranose), and galactosan (1,6-anhydro-β-D-galactopyranose), all resulting from the pyrolysis of hemicelluloses present in wood. Levoglucosan is a well-established tracer for pyrolysis of cellulose in biomass smoke (Simoneit et al., 1999; Nolte et al., 2001; Simoneit, 2002) and has been extensively used to monitor biomass smoke in the Amazon basin (Zdráhal et al., 2002; Graham et al., 2002, 2003; Schkolnik et al., 2005) and in other tropical and subtropical areas where biomass burning takes place such as, for example, southern Africa (Gao et al., 2003). Levoglucosan has for a long time thought to be fairly inert; however, recent laboratory studies show that it decays upon a time scale relevant to particle lifetimes by heterogeneous OH radical-initiated oxidation (Hoffmann et al., 2010; Hennigan et al., 2010). Sugars present in atmospheric aerosol comprise the monosaccharides, glucose and fructose, and the disaccharides, sucrose and trehalose. Glucose, fructose, and sucrose originate from plant material such as pollen, fruits, and their fragments (Bartolozzi et al., 1997; Baker et al., 1998; Pacini, 2000; Yttri et al., 2007), but in addition glucose may also result from cellulose pyrolysis (Shafizadeh, 1982), while trehalose is due to fungal spores (Lewis and Smith, 1967; Bieleski, 1982). The sugar alcohols, arabitol, mannitol, and erythritol, which are denoted by polyols, are marker compounds for fungal spores (Lewis and Smith, 1967; Bieleski, 1982).

The 2-methyltetrols (2-methylthreitol and 2-methylerythritol) and the C_5-alkene triols [2-methyl-1,3,4-trihydroxy-1-butene (*cis* and *trans*) and 3-methyl-2,3,4-trihydroxy-1-butene] have first been identified in Amazonian aerosols (Claeys et al., 2004; Wang et al., 2005) and were, based on their C_5-isoprene skeleton, proposed to be photooxidation products of isoprene. In subsequent laboratory (smog chamber) experiments it was confirmed that the 2-methyltetrols are formed through photooxidation of isoprene under varying NO_x regimes (Edney et al., 2005; Böge et al., 2006; Surratt et al., 2006, 2010; Sato, 2008), while the C_5-alkene triols could only be detected in the absence of NO_x (Surratt et al., 2006, 2010; Kleindienst et al., 2009). Dicarboxylic acids and hydroxycarboxylic acids comprise a very large group of compounds; a major hydroxycarboxylic acid is malic acid, which can be regarded as intermediate in the oxidation of C_n ($n \leq 6$) semivolatile carboxylic acids (which are also oxidation products of unsaturated fatty acids) and is believed to be formed through further photooxidation of succinic acid (Kawamura and Gagosian, 1990; Kawamura and Ikushima, 1993). Dicarboxylic acids are known to have many sources, both anthropogenic and biogenic ones (Rogge et al., 1993; Limbeck and Puxbaum, 1999). A recent study examined the molecular profiles of dicarboxylic acids (C_2-C_{11}) and related compounds (ketocarboxylic acids and dicarbonyls) in $PM_{2.5}$ samples from the intensive biomass burning period of the LBA-SMOCC 2002 campaign and found higher ratios of the latter compounds to biomass burning tracers (i.e., levoglucosan, K^+) during daytime, suggesting the importance of photochemical production (Kundu et al., 2010).

In the present study, we focus on major polar organic marker compounds and discuss their time series, diel variations, mass size distributions, and aerosol formation processes. The major polar organic marker compounds include: (a) levoglucosan, (b) malic acid, (c) photooxidation products of isoprene, i.e., 2-methyltetrols and C_5-alkene triols, and (d) polyols (arabitol, mannitol, and erythritol). The latter compounds were selected for two reasons: (a) they correspond to major single compounds that can be detected in the fine ($PM_{2.5}$) size fraction of high-volume dichotomous samples

by gas chromatography/mass spectrometry (GC/MS) with prior trimethylsilylation in the full scan mode, and (b) they provide important information on aerosol sources and source processes. Part of the presented data have been reported by Decesari et al. (2006) on the overall composition of the carbonaceous aerosol in Rondônia during the LBA-SMOCC campaign and its representation through model compounds, and by Fuzzi et al. (2007) on the inorganic and organic composition of the corresponding size-segregated aerosol; these earlier presented data are included here to allow a more detailed and coherent discussion on time series, diel variations, and size distributions of major polar organic marker compounds.

2 Experimental

2.1 Site description

Ground-based measurements were performed as part of the LBA-SMOCC campaign from 9 September till 14 November 2002 (66 days) at a pasture site (Fazenda Nossa Senhora Aparecida, 10°04′44″ S, 62°21′27″ W, 315 m a.s.l.). This site is located within Rondônia, Brazil, a region where extensive deforestation took place in recent years. The campaign covered a dry period (9 September–8 October), corresponding to the end of the dry season (biomass burning season), a transition period (8–30 October), and a wet period (30 October–14 November), corresponding to the beginning of the wet season. For a more detailed description of the sampling site, see Andreae et al. (2002). For an overview of the meteorological conditions, including temperature, during the campaign, see Fuzzi et al. (2007). The temperature showed little variability during the period considered, with monthly mean values around 25.0 °C, although there was a variation in the daily maximum temperature span: 10.7 °C in September, 9.4 °C in October and 8.0 °C in November. During the dry season, and, to a lesser extent, the transition period, widespread fire activity was observed in Rondônia and Mato Grosso, as well as in other states along the southern and south eastern margin of the Amazon forest. Conversely, biomass burning was substantially reduced at the beginning of November after the onset of persistent wet conditions (Andreae et al., 2004).

2.2 Aerosol sampling

A high-volume dichotomous virtual sampler (HVDS), located 2 m above ground level, was used to collect samples in two size fractions, a fine [<2.5 µm aerodynamic diameter (AD)] and a coarse (>2.5 µm AD) fraction (Solomon et al., 1983). Double Pallflex quartz fiber filters (of 102 mm diameter), which had been pre-fired at 550 °C to remove organic contaminants, were used to collect each of the two size fractions. For collection of size-fractionated aerosol samples, a ten-stage Micro-Orifice Uniform Deposit Impactor (MOUDI), with 50% aerodynamic cutoff diameters for the pre-impaction stage (stage 0) and 10 regular stages of 18, 9.9, 6.2, 3.1, 1.8, 1.0, 0.603, 0.301, 0.164, 0.094, and 0.053 µm, was employed. Aluminum foils of 37 mm diameter (pre-fired at 550 °C) were used as collection substrates in the MOUDI. Separate day- and nighttime samples were collected during most days of the dry period and part of the transition period. During the rest of the transition period, the collection time was 24 h, whereas during the wet period, day- and nighttime samples were collected for 48 h. A total of 80 HVDS samples and 80 MOUDI sample sets were collected.

PM_2 mass data were derived from the fine (<2 µm AD) size fraction of a Gent PM_{10} stacked filter unit (SFU) sampler that was operated in parallel. A Pall Teflo filter was used as fine filter in the SFU sampler.

2.3 Aerosol analysis

PM mass data were obtained by weighing the SFU filters and the MOUDI aluminum foils before and after sampling with a microbalance of 1 µg sensitivity. The weighings were done at 20 °C and 50% relative humidity (RH) and the filters were equilibrated at these conditions for 24 h prior to weighing. All filters of the HVDS samples were analyzed for organic carbon (OC) and elemental carbon (EC) by a thermal-optical (TOT) technique (Birch and Cary, 1996) and the fine size fraction filters also for WSOC as described by Viana et al. (2006).

Selected polar organic marker compounds in the front fine filters of all HVDS quartz fiber filter samples and in the aluminum foils of selected MOUDI samples were quantified using GC/MS techniques that incorporated a derivatization step in order to convert carboxylic and hydroxyl groups to trimethylsilylated ester and ether derivatives, respectively. The method was targeted to the quantitation of sugar-like compounds, including anhydrosugars (levoglucosan, mannosan, galactosan, and 1,6-anhydro-β-D-glucofuranose), 2-methyltetrols (2-methylthreitol and 2-methylerythritol), monosaccharides (fructose and glucose), and polyols (erythritol, arabitol, and mannitol). The analytical procedure was adapted from a method previously described and validated for the determination of levoglucosan in urban aerosols (Pashynska et al., 2002). In addition to the above mentioned sugar-like compounds, malic acid was also measured with the same method; however, more accurate data for malic acid were obtained with a method targeted to the analysis of polar hydroxycarboxylic acids, as has been reported in a previous study (Decesari et al., 2006). The malic acid data used in the present study for the fine HVDS samples were, therefore, obtained with the latter method (method 2 of the cited study). In addition, succinic acid data obtained with the latter method were also used for the detailed interpretation of the malic acid data.

A part of the front quartz filter sample (1/16 or 1/32) or of the aluminum foil (1/2 or 1/4) was used for extraction. Before extraction, the recovery standards,

methyl-β-L-xylanopyranoside and deuterated (D_3) malic acid (2,2,3-D_3-malic acid; Cambridge Isotope Laboratories, Andover, MA, USA) were added. Briefly, the sample work-up procedure consisted of extraction with 3 times 20 mL dichloromethane:methanol (4:1, v/v) and derivatization of the residues into trimethylsilylether derivatives with 50 µL of a 3:5 (v/v) mixture of pyridine and N-methyl-N-trimethylsilyltrifluoroacetamide (MSTFA) containing 1% trimethylchlorosilane (TMCS) (Pierce, Rockford, IL, USA). GC/MS analysis was performed with a TRACE GC2000 gas chromatograph and a Polaris Q ion trap mass spectrometer equipped with a CP Sil 8CB low-bleed capillary column (95% dimethyl-, 5% phenylpolysiloxane, 0.25 µm film thickness, 30 m × 0.25 mm i.d.; Chrompack, Middelburg, The Netherlands), which was preceded by a deactivated silica precolumn (2 m × 0.25 mm i.d.). The following temperature program was applied: the initial temperature was 50 °C and kept for 5 min, the temperature was then increased to 200 °C at the rate of 3 °C min^{-1} and kept at that temperature for a further 2 min and then raised to 310 °C at the rate of 30 °C min^{-1}; the total analysis time was 62 min. For the analysis of the HVDS samples, the GC/MS instrument was operated in the electron ionization and the full scan modes (mass range *m/z* 45–500), and quantification was based on mass chromatographic data (i.e., extracted ion chromatograms), while for the analysis of the MOUDI samples, the instrument was operated in the selected ion monitoring mode (instead of the full scan mode) with an ion dwell time of 25 ms. The selected ions were at *m/z* 204 and 217 for the internal recovery standard (IS), methyl-β-D-xylanopyranoside, and for levoglucosan, *m/z* 219 and 277 for the 2-methyltetrols (2-methylthreitol and 2-methylerythritol), *m/z* 233 and 307 for malic acid, *m/z* 236 and 310 for deuterated (D_3) malic acid, *m/z* 217 and 319 for arabitol and mannitol, and *m/z* 231 for the alkene triol derivatives of isoprene (2-methyl-1,3,4-trihydroxy-1-butene (*cis* and *trans*) and 3-methyl-2,3,4-trihydroxy-1-butene). For derivatization of standard solutions of all saccharidic compounds, the same procedure as that used for the aerosol extracts was applied. The quantification of the monosaccharide anhydrides (levoglucosan, mannosan, and galactosan), the polyols (arabitol, mannitol, and erythritol), the monosaccharides (fructose and glucose), and the 2-methyltetrols was based on an internal standard calibration procedure employing methyl-β-L-xylanopyranoside as internal recovery standard and pure reference compounds, if available. For assessing the amounts of the 2-methyltetrols and C_5-alkene triols, for which no pure reference compounds were available, the response factor of erythritol was used, while for assessing the amount of malic acid, the response factor of deuterated (D_3) malic acid was used. Duplicate analyses showed that the precision of the determinations was about 10%. All reported concentrations were corrected for procedural blanks.

3 Results and discussion

3.1 GC/MS chromatograms

Figure 1 presents a typical total ion chromatogram (TIC) obtained for a trimethylsilylated extract of a fine daytime HVDS filter sample collected during the transition period (26–27 October). The chromatogram is dominated by levoglucosan and smaller peaks are clearly observed for malic acid, the 2-methyltetrols, the C_5-alkene triols, and anhydrosugars that are isomeric to levoglucosan (mannosan and 1,6-anhydro-β-D-glucofuranose). It is worth noting that the latter compounds can be detected in the TIC so that more selective detection, i.e., mass chromatographic or selected ion monitoring detection, was not necessary. However, in the present study, mass chromatography using specific ions was utilized to obtain more clear chromatographic peaks for less abundant compounds, i.e., polyols (arabitol, mannitol, and erythritol), and, in most cases, C_5-alkene triols (2-methyl-1,3,4-trihydroxy-1-butene (*cis* and *trans*) and 3-methyl-2,3,4-trihydroxy-1-butene), while selected ion monitoring was performed for the analysis of aluminum foils collected with the MOUDI, where the amounts found on the different stages are much lower than on the HVDS filter samples.

3.2 Time series, diurnal variations and size distributions

3.2.1 PM, OC, EC, and levoglucosan

Table 1 summarizes median and mean concentrations and concentration ranges for OC, EC, WSOC, and the selected organic species in the fine size fraction of the HVDS filter samples for the dry, transition, and wet periods of the LBA-SMOCC 2002 campaign. In addition, Table 1 presents mean percentages of the fine OC that is attributable to the carbon in the organic compounds. Figure 2 shows the time series for fine PM (PM_2), and OC, EC, and levoglucosan for the fine size fraction of the HVDS samples. It can be seen that all four parameters show substantial variation throughout the campaign and are fairly well correlated with each other. The correlations between the PM (PM_2) and OC, EC, and levoglucosan for the dry period were 0.83, 0.84, and 0.75, respectively. During the dry period, which is characterized by intense deforestation fires, high $PM_{2.5}$ levels of levoglucosan are measured (mean value 2.1 µg m^{-3}), while during the transition and wet periods, the mean levels decrease to 0.40 µg m^{-3} and 0.06 µg m^{-3}, respectively. It can also be seen in Fig. 2 that diel differences are observed for the fine PM (PM_2), OC, EC, and levoglucosan during the dry period when separate day- and nighttime sampling was carried out and that the highest concentrations are found at night. The higher nighttime concentrations can be partly explained by trapping of the pyrogenic aerosol under the shallow nocturnal

Table 1. Median and mean concentrations and concentration ranges for OC, EC, WSOC, and selected organic species (and mean percentages of the OC attributable to the carbon in the organic compounds) in the front filters of the fine size fraction of the HVDS filter samples for the dry, transition, and wet periods of the LBA-SMOCC 2002 campaign.

Species	Dry period ($N = 53$) Conc., ng m^{-3} (* µg m^{-3})			Mean	Transition period ($N = 20$) Conc., ng m^{-3} (* µg m^{-3})			Mean	Wet period ($N = 7$) Conc., ng m^{-3} (* µg m^{-3})			Mean
	Median	Mean	Range	% OC	Median	Mean	Range	% OC	Median	Mean	Range	% OC
OC*	27	32	4.1–79	n/a	8.4	9.1	3.9–15.7	n/a	1.80	1.60	0.93–2.3	n/a
EC*	0.98	1.11	0.30–2.4	n/a	0.42	0.42	0.18–0.66	n/a	0.07	0.09	0.04–0.18	n/a
WSOC*	17.5	21	2.6–53	66	6.0	6.6	2.5–10.5	73	0.98	1.04	0.65–1.92	64
levoglucosan	1380	2100	126–7500	2.63	350	400	106–1860	1.91	26	58	15.7–150	1.46
mannosan	88	148	10.1–540	0.18	27	31	7.3–70	0.15	2.8	4.1	1.9–7.4	0.11
galactosan	26	57	4.3–260	0.07	10.1	11.4	2.8–32	0.05	0.9	1.1	<0.5–2.4	0.03
arabitol	14.7	16.8	<2.0–41	0.03	9.8	9.8	4.5–22	0.05	8.2	8.7	5.3–11.8	0.27
mannitol	19.4	23	3.9–52	0.05	8.3	20	9.5–47	0.10	19.2	17.7	11.1–20	0.50
erythritol	12.8	14.4	2.3–37	0.02	4.1	4.4	1.6–8.0	0.02	1.1	1.0	0.7–1.3	0.03
glucose	47	52	15.1–130	0.09	34	34	16.6–53	0.17	27	27	16.3–37	0.74
fructose	13.9	15.2	<2.0–44	0.03	8.5	8.0	2.5–13.2	0.04	4.8	5.1	1.2–12.5	0.14
2-methylthreitol	51	52	4.8–98	0.09	19.0	26	7.6–89	0.13	8.2	9.1	3.0–20	0.26
2-methylerythritol	145	143	13.7–320	0.25	68	94	22–310	0.48	29	34	13.3–66	1.00
C_5-alkene triols	42	54	5.3–164	0.11	29	37	9.9–93	0.22	6.3	8.7	4.3–16.0	0.29
malic acid	390	400	138–860	0.57	260	270	163–410	1.15	74	76	37–110	1.69
succinic acid	500	640	53–2200	0.83	270	280	100–610	1.23	26	28	8.5–48	0.69

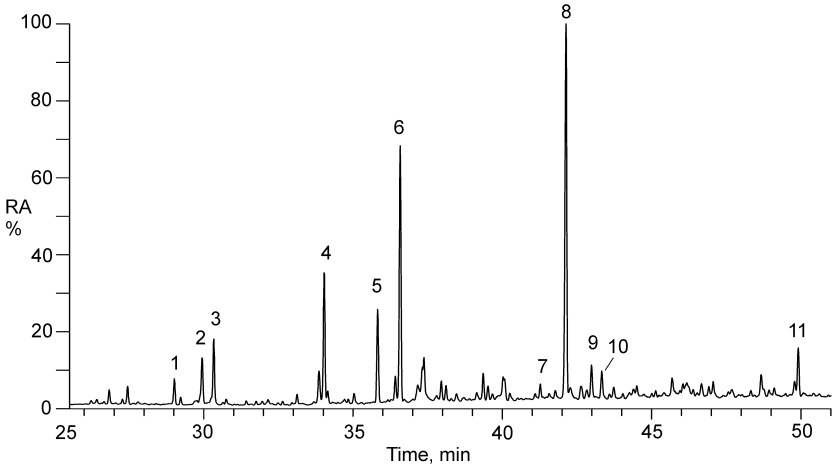

Fig. 1. GC/MS total ion chromatogram (TIC) obtained for a fine daytime HVDS filter sample collected during the transition period (26–27 October). (1) *cis*-2-methyl-1,3,4-trihydroxy-1-butene; (2) 3-methyl-2,3,4-trihydroxy-1-butene; (3) *trans*-2-methyl-1,3,4-trihydroxy-1-butene; (4) malic acid; (5) 2-methylerythritol; (6) 2-methylthreitol; (7) mannosan; (8) levoglucosan; (9) 1,6-anhydro-β-D-glucofuranose; (10) arabitol; and (11) mannitol.

boundary layer. This concentration effect is due to evolution of the boundary layer, which is much thinner at night, as a result of decreased vertical mixing and dilution (Fish et al., 2004; Rissler et al., 2006). An additional explanation for the higher nighttime concentrations of levoglucosan is photochemical degradation during daytime. In this respect, it has recently been shown that levoglucosan decays upon a time-scale relevant to particle lifetimes by heterogeneous OH radical-initiated oxidation (Hoffmann et al., 2010; Hennigan et al., 2010).

Figure 3 shows levoglucosan carbon as a percentage of the OC. It is clear that levoglucosan contributes more to the OC during the night, on average $3.1 \pm 0.9\%$ at night versus $1.8 \pm 0.7\%$ during the daytime. This diel variation can be explained by a different combustion stage with flaming combustion taking place during daytime when fires are started and smoldering combustion resulting in a less complete oxidation of biomass dominating at night, as has been discussed in more detail by Schkolnik et al. (2005). Our results can also be compared with those of Gao et al. (2003)

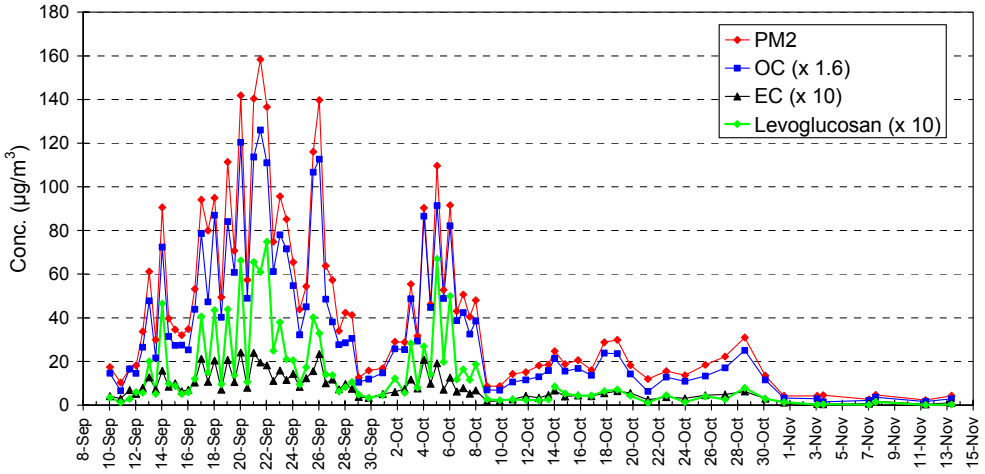

Fig. 2. Time series for fine PM (PM_2), and for OC, EC, and levoglucosan in the fine filters of the HVDS samples.

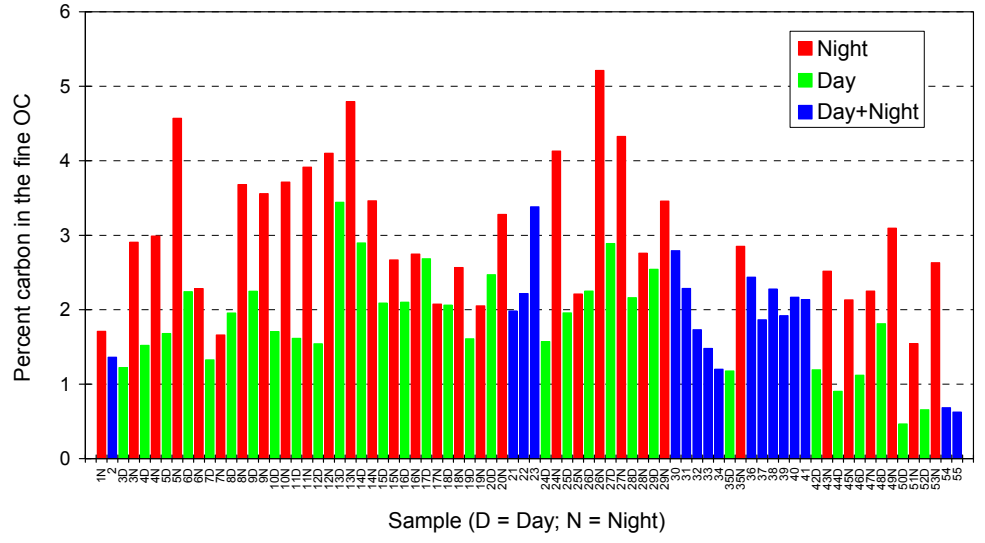

Fig. 3. Time series for the levoglucosan carbon as percent of the fine OC in the HVDS samples. Samples 1N through 29N are from the dry period, 30 through 48D from the transition period, and 49N through 55 from the wet period.

for smoke aerosol from the SAFARI 2000 experiment in southern Africa, which showed that certain organic species including levoglucosan are more enriched in smoke aerosol from the smoldering than the flaming phase. In addition, the diel variation of levoglucosan can to some extent also be explained by photochemical degradation of levoglucosan during daytime (Hoffmann et al., 2010; Hennigan et al., 2010). However, the data obtained within this field study do not allow to determine which of the two processes, i.e., the combustion stage or the photochemical degradation of levoglucosan during daytime, govern the atmospheric concentrations of levoglucosan, since flaming combustion which is prevalent during daytime is in itself a highly oxidative process. We also examined the diel variation of levoglucosan by expressing its carbon as a percentage of the water-insoluble OC (WIOC = OC − WSOC), which can be considered as a rough proxy for non-SOA OC. Following this procedure, we see that levoglucosan carbon (be it that it is itself water-soluble) represents only a slightly larger percentage of the WIOC fraction during night than during the day, i.e., on average $8.6 \pm 2.1\%$ at night versus $6.4 \pm 2.6\%$ during the daytime. This night/day difference is (in relative terms; the ratio between the two percentages is 1.34) substantially smaller than that found for the difference in the percentage of levoglucosan carbon to the OC between night and day (the ratio between the two percentages is here 1.72). It may well be that only the difference in levoglucosan carbon to the WIOC between day and night is attributable to further oxidation of levoglucosan during the daytime.

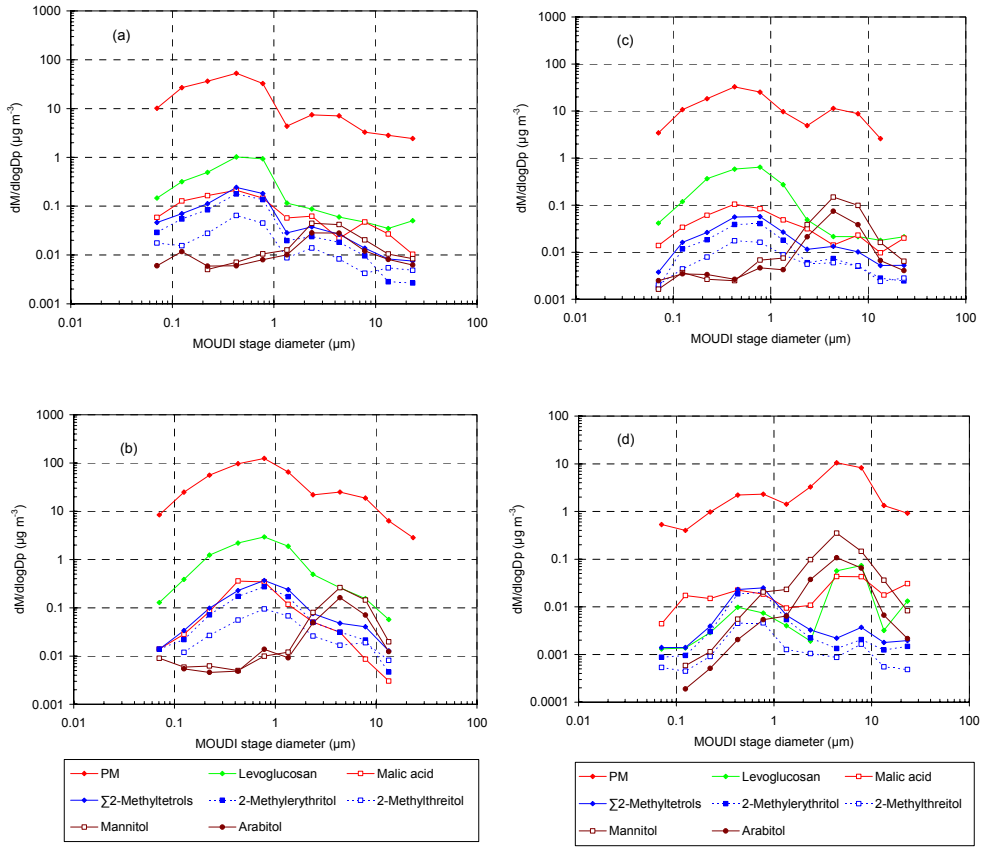

Fig. 4. Mass-size distributions of selected polar organic marker compounds and the PM during the 17 September 2002 day **(a)** and night **(b)** of the dry period, a 24-h sampling on 17 October 2002 of the transition period **(c)**, and a 48-h sampling, 10–12 November 2002, of the wet period **(d)**.

Figure 4a–d present typical size distributions of the PM and levoglucosan, as well as of malic acid, the 2-methyltetrols, mannitol and arabitol, for the dry, transition, and wet periods of the LBA-SMOCC 2002 campaign. Other indicator compounds such as glucose, fructose, erythritol, galactosan, and mannosan were also detected. However, a detailed examination of those compounds was not performed since they correspond to minor compounds; some of them (galactosan and mannosan) are known to accompany the emission of levoglucosan (Shafizadeh, 1984). It can be seen that the mass size distribution of the PM depends strongly on the period: during the dry period most of the PM is in the fine mode (Fig. 4a and b), while in the transition period a substantial fraction of it is in the coarse mode (Fig. 4c), and in the wet period the coarse mode has become more abundant than the fine one (Fig. 4d). Furthermore, it can be noted that there is a clear difference in the day- and nighttime mass-size distributions for the dry period with a more pronounced coarse mode at night than during daytime. Levoglucosan follows quite closely the PM and is mainly associated with the fine size mode, except in the wet period where it peaks in the coarse mode. The latter phenomenon can be explained by a lack of pre-existing fine aerosol surface that is required for condensation of biomass smoke and by the hydrophilic properties of levoglucosan that facilitates its adsorption on the wet surface of coarse biological particles. A similar size distribution as ours for levoglucosan during the dry period was reported by Blazsó et al. (2003) for the LBA-EUSTACH 1999 dry season experiment at the same site.

3.2.2 Malic acid, 2-methyltetrols and C_5-alkene triols

Figure 5 shows the time series of malic acid, the 2-methyltetrols and the C_5-alkene triol derivatives of isoprene [sum of 2-methyl-1,3,4-trihydroxy-1-butene (*cis* and *trans*) and 3-methyl-2,3,4-trihydroxy-1-butene]. The time series of malic acid and the 2-methyltetrols are quite different from those of levoglucosan (Fig. 3), consistent with different aerosol sources or source processes. It can be seen that the concentrations of both malic acid and the 2-methyltetrols are higher in the dry and transition periods than in the wet period. The mass-size distributions of malic acid (Fig. 4a–d) show that it follows quite closely that of levoglucosan; it is mainly associated with the fine size mode, except in the wet

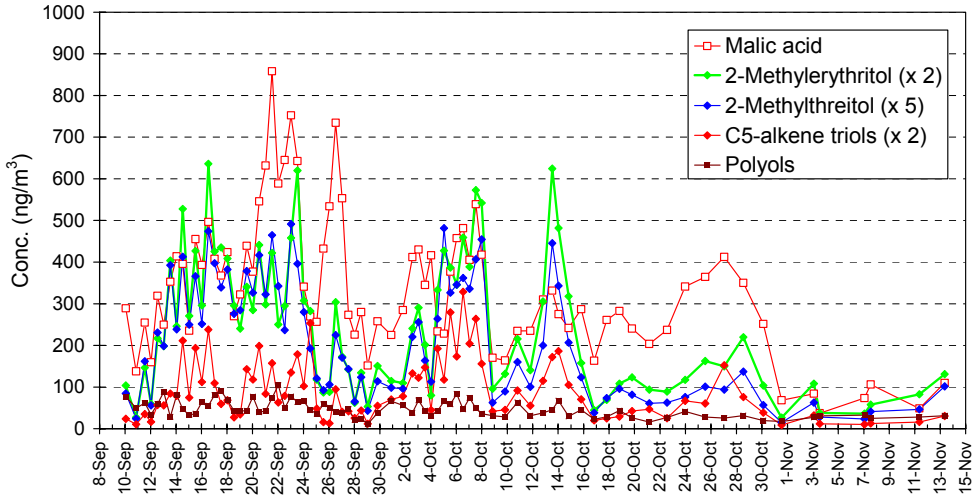

Fig. 5. Time series for malic acid, 2-methyltetrols (2-methylthreitol and 2-methylerythritol), C_5-alkene triol derivatives of isoprene (sum of 2-methyl-1,3,4-trihydroxy-1-butene (*cis* and *trans*) and 3-methyl-2,3,4-trihydroxy-1-butene) and polyols (sum of arabitol, mannitol, and erythritol) in the fine filters of the HVDS samples.

period where it is also more abundant in the coarse mode. The similar behaviors of levoglucosan and malic acid suggest the same aerosol formation process, namely, condensation of low-volatile organic vapors that are either emitted during deforestation fires by a high temperature process (in the case of levoglucosan) or formed by photooxidation of biogenic emissions and vapors released during the fires (in the case of malic acid). The different size distributions of malic acid and levoglucosan during the wet season, where both compounds are mainly associated with the coarse size mode, can be explained by a lack of fine aerosol surface onto which low-volatile organic vapors can condense. As to the origin of malic acid, it has been proposed that it is formed from C_n ($n \leq 6$) semivolatile carboxylic acids, i.e., further photooxidation of succinic acid (Kawamura and Gagosian, 1990; Kawamura and Ikushima, 1993), which in the present case can be explained by daytime photooxidation of semivolatile carboxylic acids that are emitted during biomass burning (Kundu et al., 2010). A fairly good correlation was found between the concentrations of malic and succinic acid during the dry and transitions periods ($r = 0.76$), supporting that both tracers have the same aerosol source and are formed through photooxidation of C_n ($n \leq 6$) semivolatile carboxylic acids. It is noted that an even better correlation ($r = 0.92$) between the concentrations of malic and succinic acid has been reported for $PM_{2.5}$ aerosols collected from K-puszta, Hungary, during a 2003 summer period (Kourtchev et al., 2009). As can be seen in Fig. 5, malic acid does not reveal a diel variation; this behavior of malic acid has been noted in previous field studies such as, for example, during a 2003 summer campaign in K-puszta, Hungary (Ion et al., 2005), and has been explained by its formation from both anthropogenic and biogenic sources over a relatively long time scale.

It can be seen in Fig. 5 that the 2-methyltetrols, 2-methylthreitol and 2-methylerythritol, closely follow each other. The ratio between the *threo* and *erythro* isomers was on average 0.30 and a statistically significant correlation was found between them ($r = 0.94$), consistent with their formation through the same aerosol formation process, namely, photooxidation of isoprene. The ratio *threo*/*erythro* of 0.30 compares well with the ratio of between 0.33 and 0.58 found for aerosol ($PM_{2.5}$, PM_1, or total aerosol) collected at other forested sites (e.g., 0.37, Ion et al., 2005; 0.40, Cahill et al., 2006; 0.48, Kourtchev et al., 2008a; 0.33, Clements and Seinfeld, 2007; 0.58, Xia and Hopke, 2006; 0.41, Kourtchev et al., 2008b). The higher concentrations of the 2-methyltetrols during the dry and transition periods compared to the wet period can in part be explained by a difference in the acidity of the aerosol. Smog chamber studies with isoprene (Edney et al., 2005; Surratt et al., 2007a, b) as well as field studies (Kourtchev et al., 2008a; Lewandowski et al., 2007) have demonstrated that the formation of 2-methyltetrols is strongly affected by the acidity of the aerosol. It is noted that during the LBA-SMOCC 2002 experiment the mixing ratios of the acidic trace gases HNO_3 and SO_2 were considerably higher during the dry and transition periods than the wet period, and that the same trends were found for aerosol NO_3^- and SO_4^{2-} anions showing maxima of 1.25 ppb and 0.6 ppb, respectively (Trebs et al., 2004). In addition, the higher concentrations of the 2-methyltetrols during the dry and transition periods compared to the wet period may in part be explained by differences in the emission rate of isoprene, the NO_x concentration and the removal by wet deposition. As to seasonal variations in the emission rate of isoprene in the Amazon basin, only slightly higher emissions in the dry than in the wet season were measured

(i.e., at National Forest of the Tapajos mean isoprene mixing ratios were 2.8 ± 0.9 ppb, 1.4 ± 0.5 ppb and 1.9 ± 1.2 ppb in the dry, transition, and wet periods, respectively, Trostdorf et al., 2004), so that other factors such as the aerosol acidity, the NO_x concentration and wet deposition mainly determine the concentrations of the 2-methyltetrols. As to seasonal variations in the NO_x concentration, substantial differences were reported by Trebs et al. (2006), who measured median NO_x mixing ratios in the dry, transition, and wet periods of 4.6 ppb, 3.0 ppb, and 0.9 ppb, respectively. It is very likely that the 2-methyltetrol concentrations were also affected by the NO_x concentration, since NO_x is known to play a role in their formation (Sato, 2008; Szmigielski et al., 2010). During the dry period, the 2-methyltetrol concentrations show a clear diel variation with highest concentrations during daytime. This is in accordance to observations made for aerosol (PM_1 or $PM_{2.5}$) from other forested sites (Ion et al., 2005; Plewka et al., 2006; Kourtchev et al., 2008a), where a diel pattern was found for the 2-methyltetrol concentrations with maxima during daytime, which is consistent with their fast photochemical formation from locally emitted isoprene. The 2-methyltetrols were poorly correlated with malic acid ($r = 0.55$), as could be expected since they have a different aerosol source. No conclusions could be made regarding diel variations in the 2-methyltetrol concentrations during the transition and wet periods, since there were not sufficient day/night samples taken during these periods. In addition to the 2-methyltetrols, the C_5-alkene triols were detected at significant concentrations during the dry and transition periods, and also exhibited higher concentrations during daytime. The latter photooxidation products of isoprene have been reported at high concentrations in PM_1 aerosol from a boreal forest site, Hyytiälä, southern Finland, during 2004 and 2005 summer periods (Kourtchev et al., 2005, 2008a), especially during an episode that was characterized by a higher acidity. The percentage concentration ratios C_5-alkene triols/2-methyltetrols were 28%, 31%, and 20% for the dry, transition, and wet periods of the LBA-SMOCC campaign, respectively, and are thus higher than the percentage ratios of less than 10% measured in laboratory isoprene photooxidation experiments performed in the absence of NO_x (Kleindienst et al., 2009). Possible reasons for this discrepancy are that the NO_x regimes are different under the ambient conditions and that the RH in the moist tropical atmosphere is much higher (it was, on average, 78% during the SMOCC campaign) than that employed in the latter laboratory study (i.e., <3%). It is worth noting that during all periods of the LBA-SMOCC 2002 campaign the NO_x regime cannot be regarded as a low-NO_x one (<10 ppt) since the median NO_x mixing ratios in the dry, transition and wet periods were 4.6 ppb, 3.0 ppb and 0.9 ppb, respectively (Trebs et al., 2006). With respect to the effect of the RH, it has been reported in a recent laboratory study in the absence of NO_x (considered as low-NO_x) by Surratt et al. (2010) that the concentration ratio C_5-alkene triols/2-methyltetrols is strongly affected by the RH. The mass size distributions of the 2-methyltetrols (Fig. 4a–d) show that they have the same pattern as those of levoglucosan and malic acid, and are mainly associated with the fine size mode during the dry and transition periods. However, it is noted that the mass size distributions of the 2-methyltetrols are distinctly different from those of levoglucosan and malic acid during the wet period, where the 2-methyltetrols remain associated with the fine size mode. The latter behavior of the 2-methyltetrols is consistent with an aerosol formation process that is different from that for levoglucosan and malic acid; in the case of the 2-methyltetrols a heterogeneous process is suggested, while that for levoglucosan and malic acid involves condensation of low-volatile organic vapors onto pre-existing aerosol particles. The C_5-alkene triols in the MOUDI sample sets from the dry and transition periods were below the detection limit, but could be measured in the fine size fractions of the wet period MOUDI sample set, where their concentrations were about 20% of those of the 2-methyltetrols (results not shown).

Both the 2-methyltetrols and C_5-alkene triols are isoprene SOA tracers under low-NO_x conditions (Surratt et al., 2006; Kleindienst et al., 2009); the formation of 2-methyltetrols can be explained by acid-catalyzed degradation of C_5-trihydroxyhydroperoxides (Kleindienst et al., 2009) and/or C_5-epoxydiols (Paulot et al., 2009; Surratt et al., 2010), while that of the C_5-alkene triols can be explained by acid-catalyzed degradation of C_5-epoxydiols (Wang et al., 2005; Surratt et al., 2010). It is noted that during the dry and transition periods of the LBA-SMOCC campaign the NO_x mixing ratios were in the 1–5 ppb range (Trebs et al., 2006), which can be considered as an intermediate NO_x regime, suggesting that the C_5-alkene triols may not be as unique to low-NO_x conditions as originally thought (Surratt et al., 2006). It can be seen that the size distribution observed during the wet season for the 2-methyltetrols (Fig. 4d) differs from that of other polar compounds that partition from the gas to the particle phase such as levoglucosan and malic acid. A possible explanation is that only the freshly generated fine particles are sufficiently acidic to generate the 2-methyltetrols from their gas-phase precursors through acid-catalyzed reactions. In this context, it is worth noting that both the 2-methyltetrols (Fig. 4a–d) and inorganic sulfate (Fig. 4 in Fuzzi et al., 2007) are mainly associated with the fine size mode.

3.2.3 Arabitol, mannitol, and erythritol

Arabitol, mannitol, and erythritol are marker compounds for airborne fungal spores (Lewis and Smith, 1967; Bieleski, 1982) that are expected to be mainly associated with the coarse aerosol (Matthias-Maser and Jaenicke, 1995; Bauer et al., 2002a, b). However, together with fungal spores also fragments may be released from moldy surfaces (Górny et al., 2002), explaining why these polyols are also present in

the $PM_{2.5}$ HVDS samples, as has been reported in previous studies (Graham et al., 2003; Yttri et al., 2007). The time series for the polyols (arabitol, mannitol, and erythritol) (Fig. 5) reveals little variation throughout the dry, transition, and wet periods of the LBA-SMOCC 2002 campaign, as could be expected for these compounds since the humid tropical rain forest remains active throughout the whole year in producing fungal material. In addition, no clear day/night variations could be noted for their $PM_{2.5}$ concentrations (Fig. 5).

The mass size distributions of arabitol and mannitol (Fig. 4a–d) show that they have similar patterns and are mainly associated with the coarse mode. The day- and nighttime data for samplings in the dry period (Fig. 4a and b) show that the concentrations of arabitol and mannitol are about two times higher at night than during daytime, consistent with observations made by Graham et al. (2003) during the LBA-CLAIRE 2001 wet season campaign on the coarse size fractions of HVDS samples. These day/night differences have been explained by a nocturnal increase in wet spore discharging fungi such as *Ascomycota* and *Basidiomycota* (Elbert et al., 2007); an alternative explanation for this phenomenon, however, is trapping of the released fungal material under the shallow nocturnal boundary layer. The mass size distributions of arabitol and mannitol for the 48-h sampling during the wet period (Fig. 4d) clearly show a tail into the fine size mode, suggesting an enhanced release of fungal fragments from the biota during this period compared to the transition and dry periods. Size-fractionated aerosol data revealing similar patterns for arabitol and/or mannitol were reported for samples from a rural meadow site in Melpitz, Germany (Carvalho et al., 2003) and from urban sites in Norway (Yttri et al., 2007), where arabitol and/or mannitol clearly peaked in the coarse mode between 1.3 and 4.2 µm, which is the size range for spores of typical airborne fungal strains (Bauer et al., 2002b).

4 Conclusions

Sources, source processes, time series, diel variations, and size distributions of organic marker compounds were investigated for carbonaceous aerosols that were collected during the LBA-SMOCC field experiment, conducted in Rondônia, Brazil, in 2002 during dry, intermediate, and wet periods. During all three periods levoglucosan was found to be the most dominant organic species in $PM_{2.5}$ samples and reached up to 7.5 µg m^{-3} during the dry period, which was characterized by intense deforestation fires. During the dry period, levoglucosan exhibited diel variations with a nighttime prevalence. In the size-segregated samples, levoglucosan was found to be closely associated with the PM and mainly found in the fine mode, except during the wet period, where it peaked in the coarse mode. Isoprene oxidation products were found to be important species in $PM_{2.5}$ at this pasture site (on average 250 ng m^{-3} during the dry period versus 157 ng m^{-3} during the transition period and 52 ng m^{-3} during the wet period) and the seasonal differences were mainly attributed to differences in the acidity of the aerosols, the NO_x concentration and wet deposition. In addition, during the dry period clear diel variations were observed for the isoprene oxidation products with a daytime prevalence, which is consistent with their fast formation from locally emitted isoprene. In size-segregated samples, malic acid and the 2-methyltetrols exhibited a different distribution pattern. While the 2-methyltetrols were found to be mainly associated with the fine mode during all periods, malic acid was found to be prevalent in the fine mode only during the dry and transition periods and in the coarse mode during the wet period, indicating that the aerosol formation processes for those species are distinctly different. The unique behavior of the 2-methyltetrols is explained by heterogeneous chemistry, likely involving acid-catalyzed degradation of their gas-phase precursors onto an acidic particle surface. Marker compounds for airborne fungi included arabitol, mannitol, and erythritol. The sum of these polyols in $PM_{2.5}$ during the dry, transition, and wet periods was, on average, 54 ng m^{-3}, 34 ng m^{-3}, and 27 ng m^{-3}, respectively and revealed minor day/night variation. The mass size distributions of arabitol and mannitol during all periods showed similar patterns and an association with the coarse mode, which is consistent with their primary source origin.

Acknowledgements. This work was carried out within the framework of the Smoke, Aerosols, Clouds, Rainfall, and Climate (SMOCC) project, a European contribution to the Large-Scale Biosphere-Atmosphere Experiment in Amazonia (LBA). It was financially supported by the Environmental and Climate Program of the European Commission (contract No. EVK2-CT-2001-00110 SMOCC), the Max Planck Society (MPG), the Belgian Federal Science Policy Office through the project "Characterization and sources of carbonaceous atmospheric aerosols" (contracts EV/06/11B and EV/02/11A), a postdoctoral visiting fellowship to V. Pashynska within the programme to promote collaboration between researchers of Central and Eastern Europe and of Belgium, the Fund for Scientific Research – Flanders, the Fundação de Amparo à Pesquisa do Estado de São Paulo, and the Conselho Nacional de Desenvolvimento Científico (Instituto do Milênio LBA). We thank all members of the LBA-SMOCC and LBA-RACCI Science Teams for their support during the field campaign, especially A. C. Ribeiro, M. A. L. Moura and J. von Jouanne.

Edited by: A. Chen

References

Andreae, M. O., Artaxo, P., Brandão, C., Carswell, F. E., Ciccioli, P., da Costa, A. L., Culf, A. D., Esteves, J. L., Gash, J. H. C., Grace, J., Kabat, P., Lelieveld, J., Malhi, Y., Manzi, A. O., Meixner, F. X., Nobre, A. D., Ruivo, M. d. L. P., Silva-Dias, M. A., Stefani, P., Valentini, R., von Jouanne, J., and Waterloo, M. J.: Biogeochemical cycling of carbon, water, energy, trace gases,

and aerosols in Amazonia: The LBA-EUSTACH experiments, J. Geophys. Res., 107, 8066, doi:10.1029/2001JD000524, 2002.

Andreae, M. O., Rosenfeld, D., Artaxo, P., Costa, A. A., Frank, G. P., Longo, K. M., and Silva-Dias, M. A. F.: Smoking rain clouds over the Amazon, Science, 303, 1337–1342, 2004.

Baker, H. G., Baker, I., and Hodges, S. A.: Sugar composition of nectars and fruits consumed by birds and bats in the tropics and subtropics, Biotropica, 30, 559–586, 1998.

Bartolozzi, F., Bertazza, G., Bassi, D., and Cristofori, G.: Simultaneous determination of soluble sugars and organic acids as their trimethylsilyl derivatives in apricot fruits by gas-liquid chromatography, J. Chromatogr. A, 758, 99–107, 1997.

Bauer, H., Kasper-Giebl, A., Löflund, M., Giebl, H., Hitzenberger, R., Zibuschka, F., and Puxbaum, H.: The contribution of bacteria and fungal spores to the organic carbon content of cloud water, precipitation and aerosols, Atmos. Res., 64, 109–119, 2002a.

Bauer, H., Kasper-Giebl, A., Zibuschka, F., Hitzenberger, R., Kraus, G. F., and Puxbaum, H.: Determination of the carbon content of airborne fungal spores, Anal. Chem., 74, 91–95, 2002b.

Bieleski, R. L.: Sugar alcohols, in: Encyclopedia of Plant Physiology, volume 13A, Plant Carbohydrates, volume I, Intracellular Carbohydrates, edited by: Loewis, A. and Tanner, W., Springer-Verlag, Berlin, 158–170, 1982.

Birch, M. E. and Cary, R. A.: Elemental carbon-based method for monitoring occupational exposures to particulate diesel exhaust, Aerosol Sci. Technol., 25, 221–241, 1996.

Blazsó, M., Janitsek, S., Gelencsér, A., Artaxo, P., Graham, B., and Andreae, M. O.: Study of tropical organic aerosol by thermally assisted alkylation-gas chromatography mass spectrometry, J. Anal. Appl. Pyrol., 68/69, 351–369, 2003.

Böge, O., Miao, Y., Plewka, A., and Herrmann, H.: Formation of secondary organic particle phase compounds from isoprene gas-phase oxidation products: an aerosol chamber and field study, Atmos. Environ., 40, 2501–2509, 2006.

Cahill, T. M., Seaman, V. Y., Charles, M. J., Holzinger, R., and Goldstein, A. H.: Secondary organic aerosols formed from oxidation of biogenic volatile organic compounds in the Sierra Nevada Mountains of California, J. Geophys. Res., 111, D16312, doi:10.1029/2006JD007178, 2006.

Carvalho, A., Pio, C., and Santos, C.: Water-soluble hydroxylated organic compounds in German and Finnish aerosols, Atmos. Environ., 37, 1775–1783, 2003.

Claeys, M., Graham, B., Vas, G., Wang, W., Vermeylen, R., Pashynska, V., Cafmeyer, J., Guyon, P., Andreae, M. O., Artaxo, P., and Maenhaut, W.: Formation of secondary organic aerosols through photooxidation of isoprene, Science, 303, 1173–1176, 2004.

Clements, A. and Seinfeld, J. H.: Detection and quantification of 2-methyltetrols in ambient aerosol in the southeastern United States, Atmos. Environ., 41, 1825–1830, 2007.

Decesari, S., Fuzzi, S., Facchini, M. C., Mircea, M., Emblico, L., Cavalli, F., Maenhaut, W., Chi, X., Schkolnik, G., Falkovich, A., Rudich, Y., Claeys, M., Pashynska, V., Vas, G., Kourtchev, I., Vermeylen, R., Hoffer, A., Andreae, M. O., Tagliavini, E., Moretti, F., and Artaxo, P.: Characterization of the organic composition of aerosols from Rondônia, Brazil, during the LBA-SMOCC 2002 experiment and its representation through model compounds, Atmos. Chem. Phys., 6, 375–402, doi:10.5194/acp-6-375-2006, 2006.

Edney, E. O., Kleindienst, T. E., Jaoui, M., Lewandowski, M., Offenberg, J. H., Wang, W., and Claeys, M.: Formation of 2-methyl tetrols and 2-methylglyceric acid in secondary organic aerosol from laboratory irradiated isoprene/NO_x/SO_2/air mixtures and their detection in ambient $PM_{2.5}$samples collected in the eastern United States, Atmos. Environ., 39, 5281–5289, 2005.

Elbert, W., Taylor, P. E., Andreae, M. O., and Pöschl, U.: Contribution of fungi to primary biogenic aerosols in the atmosphere: wet and dry discharged spores, carbohydrates, and inorganic ions, Atmos. Chem. Phys., 7, 4569–4588, doi:10.5194/acp-7-4569-2007, 2007.

Facchini, M. C., Mircea, M., Fuzzi, S., and Charlson, R. J.: Cloud albedo enhancement by surface-active organic solutes in growing droplets, Nature, 401, 257–259, 1999.

Falkovich, A. H., Graber, E. R., Schkolnik, G., Rudich, Y., Maenhaut, W., and Artaxo, P.: Low molecular weight organic acids in aerosol particles from Rondônia, Brazil, during the biomass-burning, transition and wet periods, Atmos. Chem. Phys., 5, 781–797, doi:10.5194/acp-5-781-2005, 2005.

Fisch, G., Tota, J., Machado, L. A. T., Dias, M., Lyra, R. F. D., Nobre, C. A., Dolman, A. J., and Gash, J. H. C.: The convective boundary layer over pasture and forest in Amazonia, Theor. Appl. Climatol., 78, 47–59, 2004.

Fuzzi, S., Decesari, S., Facchini, M. C., Cavalli, F., Emblico, L., Mircea, M., Andreae, M. O., Trebs, I., Hoffer, A., Guyon, P., Artaxo, P., Rizzo, L. V., Lara, L. L., Pauliquevis, T., Maenhaut, W., Raes, N., Chi, X., Mayol-Bracero, O. L., Soto-García, L., Claeys, M., Kourtchev, I., Rissler, J., Swietlicki, E., Tagliavini, E., Schkolnik, G., Falkovich, A. H., Rudich, Y., Fisch G., and Gatti, L. V.: Overview of the inorganic and organic composition of size-segregated aerosol in Rondônia, Brazil, from the biomass burning period to the onset of the wet season, J. Geophys. Res., 112, D01201, doi:10.1029/2005JD006741, 2007.

Gao, S., Hegg, D. A., Hobbs, P. V., Kirchstetter, T. W., Magi, B. I., and Sadilek, M.: Water-soluble organic components in aerosols associated with savanna fires in southern Africa: identification, evolution, and distribution, J. Geophys. Res., 108, 8491, doi:10.1029/2002JD002324, 2003.

Górny, R. L., Reponen, T., Willeke, K., Robine, E., Boissier, M., and Grinshpun, S. A.: Fungal fragments as indoor biocontaminants, Appl. Environ. Microbiol., 68, 3522–3531, 2002.

Graham, B., Mayol-Bracero, O. L., Guyon, P., Roberts, G. C., Decesari, S., Facchini, M. C., Artaxo, P., Maenhaut, W., Köll, P., and Andreae, M. O.: Water-soluble organic compounds in biomass burning aerosols over Amazonia: 1. Characterization by NMR and GC-MS, J. Geophys. Res., 107, 8047, doi:10.1029/2001JD000336, 2002.

Graham, B., Guyon, P., Taylor, P. E., Artaxo, P., Maenhaut, W., Glovsky, M. M., Flagan, R. C., and Andreae, M. O.: Organic compounds present in the natural Amazonian aerosol: characterization by gas chromatography-mass spectrometry, J. Geophys. Res., 108, 4766, doi:10.1029/2003JD003990, 2003.

Hennigan, C. J., Sullivan, A. P., Collett, J. L., and Robinson, A. L.: Levoglucosan stability in biomass burning particles exposed to hydroxyl radicals, Geophys. Res. Lett., 37, L09806, doi:10.1029/2010GL043088, 2010.

Hoffmann, D., Tilgner, A., Iinuma, Y., and Herrmann, H.: Atmospheric stability of levoglucosan: A detailed laboratory and modeling study, Environ. Sci. Technol., 44, 694–699, 2010.

Ion, A. C., Vermeylen, R., Kourtchev, I., Cafmeyer, J., Chi, X., Ge-

lencsér, A., Maenhaut, W., and Claeys, M.: Polar organic compounds in rural $PM_{2.5}$ aerosols from K-puszta, Hungary, during a 2003 summer field campaign: Sources and diel variations, Atmos. Chem. Phys., 5, 1805–1814, doi:10.5194/acp-5-1805-2005, 2005.

Kawamura, K. and Gagosian, R. B.: Mid-chain ketocarboxylic acids in the remote marine atmosphere: Distribution patterns and possible formation mechanisms, J. Atmos. Chem., 11, 107–122, 1993.

Kawamura, K. and Ikushima, K.: Seasonal changes in the distribution of dicarboxylic acids in the urban atmosphere, Environ. Sci. Technol., 27, 2227–2235, 1993.

Kleindienst, T. E., Lewandowski, M., Offenberg, J. H., Jaoui, M., and Edney, E. O.: The formation of secondary organic aerosol from the isoprene + OH reaction in the absence of NO_x, Atmos. Chem. Phys., 9, 6541–6558, doi:10.5194/acp-9-6541-2009, 2009.

Kourtchev, I., Ruuskanen, T., Maenhaut, W., Kulmala, M., and Claeys, M.: Observation of 2-methyltetrols and related photo-oxidation products of isoprene in boreal forest aerosols from Hyytiälä, Finland, Atmos. Chem. Phys., 5, 2761–2770, doi:10.5194/acp-5-2761-2005, 2005.

Kourtchev, I., Ruuskanen, T. M., Keronen, P., Sogacheva, L., Dal Maso, M., Reissell, A., Chi, X., Vermeylen, R., Kulmala, M., Maenhaut, W., and Claeys, M.: Determination of isoprene and α-/β-pinene oxidation products in boreal forest aerosols from Hyytiälä, Finland: diel variations and possible link with particle formation events, Plant Biology, 10, 138–149, 2008a.

Kourtchev, I., Warnke, J., Maenhaut, W., Hoffmann, T., and Claeys, M.: Polar organic marker compounds in PM2.5 aerosol from a mixed forest site in western Germany, Chemosphere, 73, 1309–1314, 2008b.

Kourtchev, I., Copolovici, L., Claeys, M., and Maenhaut, W.: Characterization of aerosols at a forested site in central Europe, Environ. Sci. Technol., 43, 4665–4671, 2009.

Kubátová, A., Vermeylen, R., Claeys, M., Cafmeyer, J., Maenhaut, W., Roberts, G., and Artaxo, P.: Carbonaceous aerosol characterization in the Amazon basin, Brasil: novel dicarboxylic acids and related compounds, Atmos. Environ., 34, 5037–5051, 2000.

Kundu, S., Kawamura, K., Andreae, T. W., Hoffer, A., and Andreae, M. O.: Molecular distributions of dicarboxylic acids, ketocarboxylic acids and α-dicarbonyls in biomass burning aerosols: implications for photochemical production and degradation in smoke layers, Atmos. Chem. Phys., 10, 2209–2225, doi:10.5194/acp-10-2209-2010, 2010.

Lewandowski, M., Jaoui, M., Kleindienst, T. E., Offenberg, J. H., and Edney, E. O.: Composition of $PM_{2.5}$ during the summer of 2003 in Research Triangle Park, North Carolina, Atmos. Environ., 41, 4073–4083, 2007.

Lewis, D. H. and Smith, D. C.: Sugar alcohols (polyols) in fungi and green plants: 1. Distribution, physiology and metabolism, New Phytol., 66, 143–184, 1967.

Limbeck, A. and Puxbaum, H.: Organic acids in continental background aerosols, Atmos. Environ., 33, 1847–1852, 1999.

Matthias-Maser, S. and Jaenicke, R.: Size distribution of primary biological aerosol particles with radii $\geq$ 0.2 µm, Atmos. Res., 39, 279–286, 1995.

Mayol-Bracero, O. L., Guyon, P., Graham, B., Roberts, G. C., Andreae, M. O., Decesari, S., Facchini, M. C., Fuzzi, S., and Artaxo, P.: Water-soluble organic compounds in biomass burning aerosols over Amazonia: 2. Apportionment of the chemical composition and importance of the polyacidic fraction, J. Geophys. Res., 107, 8091, doi:10.1029/2001JD000522, 2002.

Mircea, M., Facchini, M. C., Decesari, S., Cavalli, F., Emblico, L., Fuzzi, S., Vestin, A., Rissler, J., Swietlicki, E., Frank, G., Andreae, M. O., Maenhaut, W., Rudich, Y., and Artaxo, P.: Importance of the organic aerosol fraction for modeling aerosol hygroscopic growth and activation: a case study in the Amazon Basin, Environ. Sci. Technol., 5, 3111–3126, 2005.

Mochida, M. and Kawamura, K.: Hygroscopic properties of levoglucosan and related organic compounds characteristic to biomass burning aerosol particles, J. Geophys. Res., 109, D21202, doi:10.1029/2004JD004962, 2004.

Nolte, C., Schauer, J. J., Cass, G. R., and Simoneit, B. R. T.: Highly polar organic compounds present in wood smoke and in the ambient atmosphere, Environ. Sci. Technol., 35, 1912–1919, 2001.

Novakov, T. and Penner, J. E.: Large contribution of organic aerosols to cloud-condensation-nuclei, Nature, 365, 823–826, 1993.

Novakov, T. and Corrigan, C. E.: Cloud condensation nucleus activity of the organic component of biomass smoke particles, Geophys. Res. Lett., 23, 2141–2144, 1996.

Pacini, E.: From anther and pollen ripening to pollen presentation, Plant Sys. Evol., 222, 19–43, 2000.

Pashynska, V., Vermeylen, R., Vas, G., Maenhaut, W., and Claeys, M.: Development of a gas chromatography/ion trap mass spectrometry method for determination of levoglucosan and saccharidic compounds in atmospheric aerosols: Application to urban aerosols, J. Mass Spectrom., 37, 1249–1527, 2002.

Paulot, F., Crounse, J. D., Kjaergaard, H. G., Kürten, A., St. Clair, J. M., Seinfeld, J. H., and Wennberg, P. O.: Unexpected epoxide formation in the gas-phase photooxidation of isoprene, Science, 325, 730–733, 2009.

Plewka, A., Gnauk, T., Brüggeman, E., and Herrmann, H.: Biogenic contribution to the chemical composition of airborne particles in a coniferous forest in Germany, Atmos. Environ., 40, S103–S115, 2006.

Rissler, J., Vestin, A., Swietlicki, E., Fisch, G., Zhou, J., Artaxo, P., and Andreae, M. O.: Size distribution and hygroscopic properties of aerosol particles from dry-season biomass burning in Amazonia, Atmos. Chem. Phys., 6, 471–491, doi:10.5194/acp-6-471-2006, 2006.

Roberts, G. C., Artaxo, P., Zhou, J., Swietlicki, E., and Andreae, M. O.: Activity of CCN spectra on chemical and physical properties of aerosol: a case study from the Amazon basin, J. Geophys. Res., 107, 8070, doi:10.1029/2001JD000583, 2002.

Rogge, W. F., Hildemann, L. M., Mazurek, M. A., Cass, G. R., and Simoneit, B. R. T.: Quantification of urban organic aerosols at a molecular level: identification, abundance and seasonal variation, Atmos. Environ., 27, 1309–1330, 1993.

Sato, K.: Detection of nitrooxypolyols in secondary organic aerosol formed from the photooxidation of conjugated dienes under high-NO_x conditions, Atmos. Environ., 42, 6851–6861, 2008.

Shafizadeh, F.: The chemistry of pyrolysis and combustion, in: Chemistry of Solid Wood, Rowell, R. (Ed), Advances in Chemistry Series 207, American Chemical Society, Washington DC, 489–529, 1984.

Solomon, P. A., Moyers, J. L., and Fletcher, R. A.: High-volume

dichotomous virtual impactor for the fractionation and collection of particles according to aerodynamic size, Aerosol Sci. Technol., 2, 455–464, 1983.

Schkolnik, G., Falkovich, A. H., Rudich, Y., Maenhaut, W., and Artaxo, P.: New analytical method for the determination of levoglucosan, polyhydroxy compounds, and 2-methylerythritol and its application to smoke and rainwater samples, Environ. Sci. Technol., 39, 2744–2752, 2005.

Shulman, M. L., Jacobson, M. C., Charlson, R. J., Synovec, R. E., and Young, T. E.: Dissolution behavior and surface tension effects of organic compounds in nucleating cloud droplets, Geophys. Res. Lett., 23, 277–280, 1996.

Simoneit, B. R. T., Schauer, J. J., Nolte, C. G., Oros, D. R., Elias, V. O., Fraser, M. P., Rogge, W. F., and Cass, G. R.: Levoglucosan, a tracer for cellulose in biomass burning and atmospheric particles, Atmos. Environ., 33, 173–182, 1999.

Simoneit, B. R. T.: Biomass burning – a review of organic tracers for smoke from incomplete combustion, Appl. Geochem., 17, 129–162, 2002.

Surratt, J. D., Murphy, S. M., Kroll, J. H., Ng, N. L., Hildebrandt, L., Sorooshian, A., Szmigielski, R., Vermeylen, R., Maenhaut, W., Claeys, M., Flagan, R. C., and Seinfeld, J. H.: Chemical composition of secondary organic aerosol formed from the photooxidation of isoprene, J. Phys. Chem. A, 110, 9665–9690, 2006.

Surratt, J. D., Kroll, J. H., Kleindienst, T. E., Edney, E. O., Claeys, M., Sorooshian, A., Ng, N. L., Offenberg, J. H., Lewandowski, M., Jaoui, M., Flagan, R. C., and Seinfeld, J. H.: Evidence for organosulfates in secondary organic aerosol, Environ. Sci. Technol., 41, 517–527, 2007a.

Surratt, J. D., Lewandowski, M., Offenberg, J. H., Jaoui, M., Kleindienst, T. E., Edney, E. O., and Seinfeld, J. H.: Effect of acidity on secondary organic aerosol formation from isoprene, Environ. Sci. Technol., 41, 5363–5369, 2007b.

Surratt, J. D., Chan, A. W. H., Eddingsaas, N. C., Chan M. N., Loza, C. L., Kwan, A. J., Hersey, S. P., Flagan, R. C., Wennberg, P. O., and Seinfeld, J. H., Reactive intermediates revealed in secondary organic aerosol formation from isoprene, Proc. Natl. Acad. Sci. USA, 107, 6640–6645, 2010.

Szmigielski, R., Dommen, J., Metzger, A., Maenhaut, W., Baltensperger, U., and Claeys, M.: The acid effect in the formation of 2-methyltetrols from the photooxidation of isoprene in the presence of NO_x, Atmos. Res., doi:10.1016/j.atmosres.2010.02.012, in press, 2010.

Trebs, I., Meixner, F. X., Slanina, J., Otjes, R., Jongejan, P., and Andreae, M. O.: Real-time measurements of ammonia, acidic trace gases and water-soluble inorganic aerosol species at a rural site in the Amazon Basin, Atmos. Chem. Phys., 4, 967–987, doi:10.5194/acp-4-967-2004, 2004.

Trebs, I., Lara, L. L., Zeri, L. M. M., Gatti, L. V., Artaxo, P., Dlugi, R., Slanina, J., Andreae, M. O., and Meixner, F. X.: Dry and wet deposition of inorganic nitrogen compounds to a tropical pasture site (Rondônia, Brazil), Atmos. Chem. Phys., 6, 447–469, doi:10.5194/acp-6-447-2006, 2006.

Trostdorf, C. R., Gatti, L. V., Yamazaki, A., Potosnak, M. J., Guenther, A., Martins, W. C., and Munger, J. W.: Seasonal cycles of isoprene concentrations in the Amazonian rainforest, Atmos. Chem. Phys. Discuss., 4, 1291–1310, doi:10.5194/acpd-4-1291-2004, 2004.

Viana, M., Chi, X., Maenhaut, W., Querol, X., Alastuey, A., Mikuška, P., and Večeřa, Z.: Organic and elemental carbon concentrations in carbonaceous aerosols during summer and winter sampling campaigns in Barcelona, Spain, Atmos. Environ., 40, 2180–2193, 2006.

Wang, W., Kourtchev, I., Graham, B., Cafmeyer, J., Maenhaut, W., and Claeys, M.: Characterization of oxygenated derivatives of isoprene related to 2-methyltetrols in Amazonian aerosols using trimethylsilylation and gas chromatography/ion trap mass spectrometry, Rapid Commun. Mass Spectrom., 19, 1343–1351, 2005.

Xia, X. and Hopke, P. K.: Seasonal variation of 2-methyltetrols in ambient air samples, Environ. Sci. Technol., 40, 6934–6937, 2006.

Yttri, K. E., Dye, C., and Kiss, G.: Ambient aerosol concentrations of sugars and sugar-alcohols at four different sites in Norway, Atmos. Chem. Phys., 7, 4267–4279, doi:10.5194/acp-7-4267-2007, 2007.

Zdráhal, Z., Oliveira, J., Vermeylen, R., Claeys, M., and Maenhaut, W.: Improved method for quantifying levoglucosan and related monosaccharide anhydrides in atmospheric aerosols and application to samples from urban and tropical locations, Environ. Sci. Technol., 36, 747–753, 2002.

4.5. Підсумки розділу 4.

У рамках проведених досліджень розроблено та випробувано ГХ/МС методику для визначення мас-спектрометричних маркерів біологічно активних органічних компонентів атмосферних аерозолів, зокрема левоглюкозану та інших моносахаридних ангідридів, які завдяки своїм молекулярно-структурним та фізико-хімічним властивостям активно взаємодіють з іншими компонентами в атмосфері, включаючи воду та інші водорозчинні органічні сполуки. Розроблена ГХ/МС методика підтвердила свою практичну цінність завдяки використанню в масштабних міжнародних біосферних дослідженнях зразків атмосферних аерозолів із тропічних лісів Амазонії для встановлення молекулярного складу та молекулярно-фізичних процесів в атмосферних аерозолях, включаючи вплив продуктів горіння біомаси на атмосферні процеси, стан живих організмів та біосферу в цілому. Основні підсумки проведених досліджень наведено нижче.

1. Уперше для визначення та дослідження ролі в атмосферних аерозолях органічної сполуки левоглюкозан та ряду інших моносахаридних ангідридів, що вважаються найважливішими атмосферними продуктами горіння біомаси, розроблено та валідовано методику на основі методу ГХ/МС з іонною пасткою. Ця методика базується на екстракції левоглюкозану та споріднених сполук із кварцових волоконних фільтрів (які використовуються для збирання частинок атмосферних аерозолів) за допомогою суміші дихлорметану з метанолом (80:20) та подальшому триметилсилілюванню екстрагованих сполук. Отриманий екстракт досліджувався методом мас-спектрометрії, зокрема вивчено поведінку піку з m/z 217, обраного у якості мас-спектрометричного маркеру левоглюкозану та інших моносахаридних ангідридів. Для кількісного аналізу вмісту левоглюкозану в аерозолях застосовано підхід внутрішнього стандартного калібрування з використанням спорідненої за структурою сполуки метил-β-L-арабінопіранозид. Розроблена ГХ/МС методика була успішно апробована в дослідженні урбаністичних

аерозолів PM_{10} (з розміром частинок менше 10 мкм), що були зібрані в районі м. Гент (Бельгія).

2. Уперше завдяки застосуванню розробленої ГХ/МС методики кількісно визначено ряд сахаридів: арабітол, маннитол, глюкозу, фруктозу, інозитол та цукрозу в аерозольних зразках з урбаністичних районів. Описано роль визначених полярних органічних сахаридів як центрів нуклеації для конденсації води в атмосфері та формування біологічно-активних вторинних органічних аерозолів завдяки взаємодії цих полярних водорозчинних сполук із молекулами води та іншими полярними компонентами атмосфери. Встановлено, що протягом зимового сезону в атмосферних аерозолях превалювали ангідриди полісахаридів (левоглюкозан та ін.), які можна розглядати як індикатори активного спалювання біомаси (деревини) при опаленні (антропогенний вплив на довкілля). В теплому літньому сезоні в складі аерозолів превалювали інші сахариди, які мають біогенне рослинне походження (глюкоза, фруктоза, цукроза та ін.).
4. Уперше завдяки детальному аналізу хромато-мас-спектрів зразків аерозолів, зібраних у районах тропічних лісів Амазонії (Бразилія) в рамках міжнародного біосферного експерименту LBA-CLAIRE (Cooperative Large-Scale Biospere-Atmosphere Experiment in Amazonia Airbone Regional Experiment), у складі природних аерозолів ідентифіковано компоненти, що раніше не спостерігалися в аерозольних зразках, а саме – полярні органічні сполуки 2-метилтреїтол та 2-метилеритритол, які є діастереоізомерами 2-метилтетролу. Запропоновано молекулярний механізм утворення цих поліолів у ході процесів фотоокислення ізопрену, що ініціюються радикалом ОН. Винайдені 2-метилтетроли мають низький тиск насиченої пари та є гігроскопічними речовинами, що дозволяє їм конденсуватися на вже існуючих аерозольних частинках та вносити значний вклад у формування вторинних органічних аерозолів із біогенних джерел, зумовлюючи здатність аерозольних частинок служити ядрами конденсації води та хмароутворення. Сформовані вторинні органічні аерозолі характеризуються значною

біологічною активністю, а молекулярно-фізичні процеси за їхньою участі мають вагомий вплив на рослинність, здоров'я людей і тварин та кліматичні явища.

5. У рамках масштабного міжнародного біосферного експерименту LBA-SMOCC (Large-Scale Biosphere Atmosphere Experiment in Amazonia – Smoke Aerosols, Clouds, Rainfall, and Climate: Aerosols From Biomass Burning Perturb Global and Regional Climate) при дослідженні зразків атмосферних аерозолів, зібраних у Рондонії (Бразилія), розроблену ГХ/МС методику в комплексі з іншими аналітичними методами було застосовано для детального вивчення особливостей молекулярного складу субмікронних аерозольних часток у залежності від біологічно значущих біосферних процесів, зокрема горіння біомаси (biomass burning). Встановлено, що в період найбільш інтенсивного горіння біомаси (сухий кліматичний сезон), склад аерозолів характеризувався високою концентрацією субмікронних частинок (зокрема і наночасток), збагачених на вуглець та водорозчинні органічні сполуки (water-soluble organic compounds, WSOC). Завдяки аналізу мас-спектрометричних маркерів органічних сполук, що входять до складу микро та наночастинок аерозолів, методом ГХ/МС та рідинної хроматографії вдалося ідентифікувати до 11% WSOC молекулярного складу зразків аерозолів, що досліджувалися. Встановлено, що основними серед ідентифікованих біологічно активних органічних компонентів мікро та наночастинок аерозолів є карбонові кислоти та полігідроксиловані сполуки, що містять складові як пірогенного, так і біогенного походження. Сполуки пірогенного походження включали безводні сахара, ароматичні кислоти та альдегіди, тоді як біогенні сполуки складалися з сахарів, цукрових спиртів, 2-метилтетролів та яблучної кислоти.
6. Уперше завдяки аналізу мас-спектрометричних маркерів, виявлених методом ГХ/МС, визначено джерела походження, молекулярні процеси, часові варіації кількості основних органічних компонентів вуглецевмісних аерозолів, які були зібрані в басейні ріки Амазонки (Рондонія, Бразилія) в рамках біосферного експерименту LBA-SMOCC. Встановлено, що

основними полярними органічними сполуками в досліджених аерозолях був левоглюкозан, яблучна кислота, ізопрен, причому левоглюкозан був домінуючим ідентифікованим органічним компонентом, який має значний вплив на біологічно важливі молекулярно-фізичні процеси в аерозолях.

7. Розроблена ГХ/МС методика для вивчення органічних біологічно активних молекул та їхніх нековалентних комплексів у складі частинок атмосферних аерозолів має значні перспективи практичного використання для подальшого пошуку маркерів біологічно та кліматично важливих молекулярно-фізичних процесів у довкіллі з метою прогнозування впливу атмосферних аерозолів на здоров'я людей і тварин та стан біосфери в цілому.

ВИСНОВКИ

У дисертаційній роботі вирішено актуальну проблему молекулярної біофізики для досліджених біологічно активних речовин (представників ряду груп ліків, а також низки органічних сполук із довкілля), що полягає у визначенні молекулярно-фізичних механізмів біологічно значущих процесів за участю цих речовин шляхом аналізу мас-спектрометричних маркерів цих біологічно активних сполук та їхніх міжмолекулярних нековалентних комплексів із біомолекулами та з компонентами оточуючого середовища.

На основі отриманих результатів зроблено наступні головні висновки:

1. Уперше в модельних системах *in vitro* визначені мас-спектрометричні маркери формування стабільних нековалентних комплексів молекул протималярійних препаратів артемізинінового ряду та хініну з їхньою потенційною молекулярною мішенню – Fe(III)-гемом. Експериментально оцінена стабільність таких комплексів та знайдено, що дигідроартемізинін (активний метаболіт артемізинінових похідних *in vivo)* єдиний з досліджених агентів формує високостабільний комплекс із гемом, в якому протон заміщений на іон Na^+. Нековалентне комплексоутворення препаратів артемізинінового ряду з гемом запропоновано в якості молекулярно-фізичного механізму, пов’язаного з протималярійною активністю цих ліків.
2. Уперше експериментально показано формування в полярному середовищі стабільних нековалентних асоціатів молекул артемізиніну та дигідроартемізиніну з азотистими основами нуклеїнових кислот (аденіном, цитозином та метилтиміном) за рахунок водневих зв’язків та сил Ван-дер-Ваальса. Утворення таких асоціатів, які можуть обмежувати функціональну активність ДНК та РНК пухлинних клітин, запропоновано в якості молекулярно-фізичної основи показаної в клінічних дослідженнях протипухлинної дії артемізинінових препаратів.
3. У рамках вивчення *in vitro* міжмолекулярної взаємодії противірусного агенту тилорон із нуклеозидами (аденозином, уридином, та тимідином) вперше встановлено вибіркове комплексоутворення тилорону з уридином, що

пропонується в якості молекулярно-фізичного механізму, який визначає противірусну активність агенту. Отримані результати вказують на РНК як найбільш ймовірну біомолекулу-мішень противірусної дії тилорону, а уридин розглядається як потенційний центр зв'язування препарату з РНК.

4. Уперше експериментально показано утворення в розчині стабільних нековалентних комплексів молекул антибіотика циклосерин із потенційною біомолекулою-мішенню – N-ацетил-D-глюкозаміном, що запропоновано розглядати в якості молекулярно-фізичної складової процесу пригнічення формування клітинної стінки бактерій, пов'язаного з протибактеріальною дією препарату.
5. Уперше в рамках *in vitro* вивчення молекулярно-фізичних механізмів дії винайденого в Україні кардіопротекторного агенту флокалін (що є активатором АТФ-чутливих калієвих мембранних каналів) експериментально визначено селективне формування нековалентних комплексів флокаліну з протонованими амінокислотами лізин та треонін. Стабільність комплексів за даними квантово-механічних розрахунків забезпечується переважно електростатичними взаємодіями між протонованими аміногрупами цих амінокислот та азотом нітрильної групи флокаліну. Нековалентне комплексоутворення між флокаліном та залишками лізину та треоніну в складі регуляторних субодиниць (рецепторів сульфонілсечовини) АТФ-чутливих калієвих мембранних каналів пропонується в якості молекулярно-фізичного механізму, що визначає дію лікарського агенту на ці канали.
6. Базуючись на результатах комплексного експериментально-теоретичного дослідження, виявлено явище міжмолекулярної конкуренції між протималярійними препаратами артемізинінового ряду та лікарськими агентами аспірин і вітамін С за нековалентне зв'язування з мембранними фосфоліпідами (на прикладі дипальмітоїлфосфатидилхоліну). Також показано формування стабільних парних асоціатів між молекулами цих препаратів різних груп у модельних системах *in vitro*. Визначені конкурентні

процеси нековалентного комплексоутворення вперше запропоновано в якості молекулярно-фізичних механізмів ймовірної модифікації функціональної активності артемізинінових агентів при їхньому одночасному застосуванні з аспірином (або вітаміном С) вже на стадії проникнення ліків через клітинні мембрани.

7. Уперше експериментально показано формування стабільних асоціатів дикатіонів протиінфекційних бісчетвертинних амонієвих сполук (декаметоксин, етоній та тіоній) із молекулами аспірину та конкуренцію лікарських сполук різних груп за зв'язування з дипальмітоїлфосфатидилхоліном у полярному середовищі. Виявлено, що нековалентні комплекси з аспірином *in vitro* формує також антибіотик циклосерин. Встановлені міжмолекулярні процеси комплексоутворення запропоновано розглядати як молекулярні механізми ймовірної зміни активності досліджених протиінфекційних ліків та аспірину при одночасному використанні.
8. Уперше ідентифіковано мас-спектрометричні маркери молекулярно-структурної стабільності протиінфекційних агентів декаметоксин та етоній в умовах мас-спектрометричного експерименту з ІЕР та МАЛДІ. Показана роль взаємодії з іонами сольватного оточення для збереження структурної стабільності дикатіонів цих сполук та їхньої функціональної активності.
9. Уперше розрахунковим методом визначено структуру гідратного комплексу дикатіону декаметоксину з 36 молекулами води, що моделює першу гідратну оболонку дикатіону цієї лікарської речовини. Встановлено, що структура дикатіону в гідратному оточенні близька до його найбільш енергетично вигідної структури у вакуумному наближенні та відповідає витягнутій конформації вуглеводневого ланцюга між четвертинними азотами декаметоксину.
10. Оптимізовано методику мас-спектрометрії з ІЕР задля ефективної реєстрації мас-спектрометричних маркерів формування високомолекулярних нековалентних комплексів протиінфекційних бісчетвертинних амонієвих

сполук та рамноліпідів з мембранними фосфоліпідами. Цю методику рекомендовано для практичного використання з метою скринінгу нових потенційних лікарських сполук серед четвертинних амонієвих агентів та інших речовин, протибактеріальна дія яких пов'язана з мембранотропним ефектом.

11. Уперше розроблено та апробовано методику на основі методу ГХ/МС для визначення в частинках атмосферних аерозолів органічної сполуки левоглюкозан та ряду інших моносахаридних ангідридів, які завдяки їхнім міжмолекулярним взаємодіям із водою та іншими полярними молекулами відіграють важливу роль у молекулярно-фізичних процесах в довкіллі. При розробці методики визначено мас-спектрометричний маркер (характеристичний пік) левоглюкозану та споріднених сполук.
12. Застосування ГХ/МС методики для досліджень зразків атмосферних аерозолів, зібраних у рамках масштабних міжнародних біосферних експериментів LBA-CLAIRE та LBA-SMOCC, дозволило комплексно проаналізувати особливості молекулярного складу та міжмолекулярні взаємодії водорозчинних органічних компонентів аерозолів та вперше ідентифікувати в складі аерозольних частинок органічні полярні сполуки 2-метилтреїол та 2-метилеритритол. Показана роль цих поліолів як центрів агрегації молекул води та формування частинок вторинних органічних аерозолів, які значно впливають на біосферні процеси та здоров'я людей.

СПИСОК ВИКОРИСТАНИХ ДЖЕРЕЛ

1. Pashynska V. A., Kosevich M. V., Van den Heuvel H., Claeys M. Characterization of noncovalent complexes of antimalarial agents of the artemisinin type and Fe(III)-heme by electrospray ionization mass spectrometry and collisional activation tandem mass spectrometry. *J. Am. Soc. Mass Spectrom.* 2004. Vol. 15. P. 1181-1190. DOI: https://doi.org/10.1016/j.jasms.2004.04.030
2. Pashynska V. A. Mass spectrometric study of intermolecular interactions between the artemisin-type agents and nucleobases. *Біофізичний вісник*. 2009. Т. 22(1). С. 20-28.
3. Pashynska V. A., Kosevich M. V., Van den Heuvel H., Cuyckens F., Claeys M. Study of non-covalent complexes formation between the bisquaternary ammonium antimicrobial agent decamethoxinum and membrane phospholipids by elecrtospray ionization and collision-induced dissociation mass spectrometry. *Вісник харківського національного університету ім. Каразіна №637. Біофізичний вісник*. 2004. Т. 1-2 (14). С. 123-130.
4. Pashynska V., Kosevich M., Stepanian S., Adamowicz L. Noncovalent complexes of tetramethylammonium with chlorine anion and 2,5-dihydroxybenzoic acid as models of the interaction of quaternary ammonium biologically active compounds with their molecular targets. A theoretical study. *Journal of Molecular Structure: THEOCHEM* . 2007. Vol. 815. P.55-62. DOI: https://doi.org/10.1016/j.theochem.2007.03.019
5. Pashynska V., Boryak O., Kosevich M., Stepanian S., Adamowicz L. Competition between counterions and active protein sites to bind bisquaternary ammonium groups. A combined mass spectrometry and quantum chemistry model study. *Eur. Phys. J. D.* 2010. Vol. 58. P.287-296. DOI: https://doi.org/10.1140/epjd/e2010-00125-5
6. Pashynska V. A. Mass spectrometric study of rhamnolipid biosurfactants and their interactions with cell membrane phospholipids. *Biopolymers and Cell.* 2009. Vol. 25, N 6. P. 504-508. DOI: http://dx.doi.org/10.7124/bc.0007FE

7. Pashynska V. A.,. Zholobak N. M, Kosevich M. V., Gomory A., Holubiev P. K., Marynin A. I. Study of intermolecular interactions of antiviral agent tilorone with RNA and nucleosides. *Біофізичний вісник.* 2018. Т. 39(1). С. 15-26. DOI: https://doi.org/10.26565/2075-3810-2018-39-02
8. Pashynska V., Stepanian S., Gomory A., Vekey K., Adamowicz L. New cardioprotective agent flokalin and its supramolecular complexes with target amino acids: An integrated mass-spectrometry and quantum-chemical study. *J. Mol. Struc.* 2017. Vol. 1146. P. 441-449. DOI: https://doi.org/10.1016/j.molstruc.2017.06.007
9. Pashynska V., Stepanian S., Gomory A., Vekey K., Adamowicz L. Competing intermolecular interactions of artemisinin-type agents and aspirin with membrane phospholipids: Combined model mass spectrometry and quantum-chemical study. *Chem. Phys.* 2015. Vol. 455. P. 81-87. DOI: https://doi.org/10.1016/j.chemphys.2015.04.014
10. Pashynska V., Stepanian S., Gömöry Á., Adamowicz L. What are molecular effects of co-administering vitamin C with artemisinin-type antimalarials? A model mass spectrometry and quantum chemical study. *J. Mol. Struc.* 2021. Vol. 1232. P. 130039. DOI: https://doi.org/10.1016/j.molstruc.2021.130039
11. Pashynska V. A., Kosevich M. V., Gomory A., Vekey K. Model mass spectrometric study of competitive interactions of antimicrobial bisquaternary ammonium drugs and aspirin with membrane phospholipids. *Biopolymers and Cell.* 2013. Vol. 29(2). P. 157-162. DOI: http://dx.doi.org/10.7124/bc.000814
12. Kasian N. A., Pashynska V. A., Vashchenko O. V., Krasnikova A. O., Gomory A., Kosevich M. V., Lisetski L. N. Probing of the combined effect of bisquaternary ammonium antimicrobial agents and acetylsalicylic acid on model phospholipid membranes: differential scanning calorimetry and mass spectrometry studies. *Molecular BioSystems.* 2014. Vol.10. P. 3155-3162. DOI: 10.1039/c4mb00420e
13. Pashynska V. A., Kosevich M. V., Gomory A. Mass spectrometry study of noncovalent complexes formation of antibiotic cycloserine with N-acetyl-D-

glucosamine and ascorbic acid. *Біофізичний вісник.* 2020. Vol. 43. P. 103-110. DOI: https://doi.org/10.26565/2075-3810-2020-43-11

14. Pashynska V. A., Kosevich M. V., Van den Heuvel H., Claeys M. The effect of cone voltage on electrospray mass spectra of the bisquaternary ammonium salt decamethoxinum. *Rapid Commun. Mass Spectrom.* 2006. Vol. 20(5). P. 755-763.
15. Пашинская В. А., Косевич М. В., Степаньян С. Г. Квантовомеханическое исследование структуры гидратированного бисчетвертичного аммониевого соединения декаметоксина. *Вісн. Харк. Ун-ту N 49. Біофізичний вісник*. 2000. Т. 2(7). С. 29-34.
16. Pashynska V. A., Kosevich M. V., Gomory A., Vekey K., Claeys M., Chagovets V. V., Pokrovskiy V. A. Variable Electrospray Ionization and Matrix-Assisted Laser Desorption/Ionization Mass Spectra of the Bisquaternery Ammonium Salt Ethonium. *Mass Spectrometry & Purification Techniques*. 2015. Vol. 1:103. P. 1-9. DOI: 10.4172/2469-9861.1000103
17. Kosevich M. V., Boryak O. A., Chagovets V. V., Pashynska V. A., Orlov V. V., Stepanian S. G., Shelkovsky V. S.“Wet chemistry” and crystallochemistry reasons for acidic matrix suppression by quaternary ammonium salts under matrix-assisted laser desorption/ionization conditions. *Rapid Commun. Mass Spectrom.* 2007. Vol. 21(11). P. 1813-1819. DOI: https://doi.org/10.1002/rcm.3020
18. Kosevich M.V., Pashinskaya V. A., Boryak O. A., Shelkovsky V. S. Low temperature fast atom bombardment mass spectra of frozen nitric acid-water solution. *J. Mass Spectrom.* 1999. Vol. 34. P.1303-1311.
19. Pashynska V., Vermeylen R., Vas G., Maenhaut W., Claeys M. Development of a gas chromatography/ion trap mass spectrometry method for determination of levoglucosan and saccharidic compounds in atmospheric aerosols. Application to urban aerosols. *J. Mass Spectrom.* 2002. Vol. 37. P.1249-1257. DOI: https://doi.org/10.1002/jms.391
20. Claeys M., Graham B., Vas G.,Wang W.,Vermeylen R., Pashynska V., Cafmeyer J., Guyon P., Andreae M., Artaxo P., Maenhaut W. Formation of Secondary

Organic Aerosols Through Photooxidation of Isoprene. *Science*. 2004. Vol. 303. P. 1173-1176. DOI: 10.1126/science.1092805

21. Decesari S., Fuzzi S., Facchini M.C., Mircea M., Emblico L., Cavalli F., Maenhaut W., Chi X., Schkolnik G., Falkovich A., Rudich Y., Claeys M., Pashynska V., Vas G., Kourtchev I., Vermeylen R., Hoffer A., Andreae M.O., Tagliavini E., Moretti F., Artaxo P. Characterization of the organic composition of aerosols from Rondônia, Brazil, during the LBA-SMOCC 2002 experiment and its representation through model compounds. *Atmos. Chem. Phys.* 2006. Vol. 6. P. 375-402. DOI: https://doi.org/10.5194/acp-6-375-2006
22. Claeys M., Kourtchev I., Pashynska V., Vas G., Vermeylen R., Wang W., Cafmeyer J., Chi X., Artaxo P., Andreao M.O., Maenhaut W. Polar organic marker compounds in atmospheric aerosols during the LBA-SMOCC 2002 biomass burning experiment in Rondonia, Brasil: sources and source processes, time series, diel variations and size distributions. *Atmos. Chem.Phys.* 2010. Vol.10. P. 9319-9331. DOI: https://doi.org/10.5194/acp-10-9319-2010
23. Pashynska V. A. Mass spectrometric markers of modulation effects on molecular level under drugs co-administering: development of mass spectrometry approach to nanobiocomplexes study. *7-th International Conference Nanobiophysics: Fundamental and Applied Aspects*: Conference Program and Book of Abstracts, Kharkiv, Ukraine, October 4-8, 2021. Kharkiv, 2021. P. 75.
24. Pashynska V., Stepanian S., Kosevich M., Gomory A. Nanobiocomplexes of ascorbic acid with antimalarial or antituberculosis drugs molecules: study of molecular mechanisms of the drugs activity modulation. *6-th International Conference Nanobiophysics: Fundamental and Applied Aspects*: Book of Abstracts, Kyiv, Ukraine, October 1-4, 2019. Kyiv, 2019. P. 69.
25. Pashynska V., Kosevich M., Gomory A. Mass spectrometry study of nanobiocomplexes formation between antibiotic cycloserine and N-acetylglucosamine. *XV-th International Conference on Molecular Spectroscopy: "From molecules to molecular materials, biological molecular systems and*

nanostructures": Programme. Abstracts. List of authors, Wroclaw-Wojanow, Poland, September 15-19, 2019. Wroclaw-Wojanow, 2019. P. 128.

26. Pashynska V., Stepanian S., Kosevich M., Gomory A., Vekey K. Model mass spectrometry and quantum chemical study of antimalarial artemisinin-type agents interactions with ascorbic acid and membrane phospholipids. *37-th Informal Meeting on Mass Spectrometry*: Book of abstracts and program, Fiera di Primiero, Italy, 5-8 May 2019. Fiera di Primiero, 2019. P. 96-97.
27. Pashynska V., Kosevich M., Gomory A., Vekey K. Mechanistic study of noncovalent complexes of antiviral and antibacterial agents with targeting biomolecules by electrospray ionization mass spectrometry. *36-th Informal Meeting on Mass Spectrometry*: Book of abstracts and program, Koszeg, Hungary, 6-9 May, 2018. Koszeg, 2018. P. 75.
28. Pashynska V. A., Kosevich M. V., Gomory A., Vekey K., Zholobak N. M. Mechanistic study of nanobiocomplexes of antiviral agent tilorone with nucleosides by electrospray ionization mass spectrometry. *5-th International Conference Nanobiophysics: Fundamental and Applied Aspects*: Book of Abstracts, Kharkiv, Ukraine, October 2-5, 2017. Kharkiv, 2017. P. 90.
29. Pashynska V., Kosevich M., Stepanian S., Gomory A., Vekey K. Mechanistic model study of intermolecular interactions of cardioprotector flokalin and amino acids by electrospray ionization mass spectrometry and quantum chemical calculations. *34-th Informal Meeting on Mass Spectrometry*: Book of Abstracts, Fiera di Primiera, Italy, 15-18 May, 2016. Fiera di Primiera, 2016. P. 130.
30. Pashynska V., Stepanian S., Kosevich M., Gomory A., Vekey K. Combined model mass spectrometric and quantum chemical study of arthemisinin-type agents and aspirin interactions with membrane phospholipids. *33-rd Informal Meeting on Mass Spectrometry*: Book of Abstracts, Szczyrk, Poland, 10-13 May, 2015. Szczyrk, 2015. P. 76.
31. Пашинська В. А., Косевич М. В., Гоморі А. Мас-спектрометричне дослідження формування нековалентних комплексів антибіотика циклосерина з N-ацетил-D-глюкозаміном та аскорбіновою кислотою. *VIII*

з'їзд Українського біофізичного товариства: Матеріали VIII з'їзду Українського біофізичного товариства, Київ-Луцьк, 12-15 листопада 2019. Київ, 2019. Стор.27.

32. Pashynska V. A., Kosevich M. V., Gomory A., Vekey K. Mass spectrometry based approach in the study of nanobiocomplexes of chemotherapeutical drugs with the targeting biological molecules. *3-rd International Conference Nanobiophysics: Fundamental and applied Aspects*: Book of Abstracts, Kharkov, Ukraine, October 7-10, 2013. Kharkov, 2013. P. 89.
33. Pashynska V., Kosevich M., Vashchenko O., Lisetski L., Gomory A., Vekey K. Mass spectrometry as an efficient method of revealing the membranotropic antimicrobial drugs activity modulation by organic acids. *30-th Informal meeting on mass spectrometry*: Book of abstracts, Olomouc, Czech Republic, 29 April-3 May 2012. Olomouc, 2012. P. 118.
34. Pashynska V. A., Kosevich M. V., Gomory A. Mass spectrometry sensing of nanoclusters composed of membrane phospholipids and antimicrobial agents . *2-nd Intern. Conf. "Nanobiophysics: Fundamental and Applied Aspects"*: Book of Abstracts, Kyiv, Ukraine, 6-9 October 2011. Kyiv, 2011. P. 105.
35. Pashynska V. Electrospray Mass Spectrometry Study of Rhamnolipid Biosurfactants and Their Interactions with Membrane Phospholipids. *27-th Informal Meeting on mass spectrometry*: Book of Abstracts, Retz, Austria, 3-6 May, 2009. Retz, 2009.P. 36.
36. Pashynska V. A., Kosevich M. V., Boryak O. A., Stepanian S. G. Stability of multi-component complexes of tetramethylammonium with biologically significant counterions by the FAB mass spectrometry and quantum chemical data. *26-th Informal Meeting on Mass Spectrometry*: Book of abstracts, Fiera di Primiero, Italy, 4 -8 May 2008. Fiera di Primiero, 2008. P. 123-124.
37. Pashynska V. A., Kosevich M. V., Boryak O. A., Stepanian S. G. Model mass spectrometry and quantum chemical study of competition between counterions and active protein sites for a binding of quaternary ammonium groups. *25-th*

Informal Meeting on Mass Spectrometry: Book of abstracts, Nyiregyhaza-Sosto, Hungary, 6-10 May 2007. Nyiregyhaza-Sosto, 2007. P. 97.

38. Pashynska V. A., Kosevich M. V., Stepanian S. G., Chagovets V. V., Pokrovsky V. A., Osaulenko V. L. Modelling of noncovalent interactions of bisquaternary antimicrobial agents with protein active groups by combined MALDI mass spectrometry and quantum-chemical study. *IV з'їзд Українського біофізичного товариства:* Тези доповідей, Донецьк, Україна, 19-21 грудня 2006. Донецьк, 2006. С. 126-128.
39. Pashynska V. A., Kosevich M. V., Van den Heuvel H., Claeys M. Comparative analysis of in-source CID and MS/MS CID under ESI mass spectrometry by the example of the bisquaternary ammonium agent decamethoxinum. *24-th Informal Meeting on Mass Spectrometry*: Book of Abstracts, Uston, Poland, 14-18 May 2006. Uston, 2006. P. 98
40. Pashynska V. A., Kosevich M. V., Chagovets V. V., Shelkovsky V. S., Osaulenko V. L., Porkovskiy V. L. Combined MALDI mass spectrometric and quantum chemical study of antimicrobial agent decamethoxinum in 2,5-dihydroxybenzoic acid. *23-rd Informal Meeting on Mass Spectrometry:* Book of Abstracts, Fiera di Primiero, Italy, 15-19 May 2005. Fiera di Primiero, 2005. P. 114-115.
41. Kosevich M., Pashynska V., Heuvel H., Claeys M. Electrospray mass spectrometry study of the bisquaternary ammonium compound decamethoxinum at different skimmer-nozzle potentials. *21-st Informal Meeting on Mass Spectrometry*: Book of Abstracts, Antwerp, Belgium, 11-15 May, 2003. Antwerp, 2003. P. 107.
42. Pashynska V., Kosevich M., Heuvel H., Claeys M. Study of formation and characteristics of non-covalent complexes between heme and antimalarial agents of the artemisinin type by electrospray ionization mass spectrometry. *21-st Informal Meeting on Mass Spectrometry*: Book of Abstracts, Antwerp, Belgium, 11-15 May, 2003. Antwerp, 2003. P. 148.

43. Pashynska V. A., Vashchenko O. V., Kosevich M. V., Boryak O. A., Kasian N. A., Lisetski L. N. Model investigation on combined effect of quaternary ammonium compounds and an organic acid on phospholipids membranes. *V з'їзд Українського біофізичного товариства*: Тези доповідей, Луцьк, 22-25 червня 2011. Луцьк, 2011. Стор.14.
44. Pashynska V., Vermeylen R., Vas G., Claeys M., Maenhaut W. Development of a gas chromatography/ion trap mass spectrometry method for determination of levoglucosan and related saccharidic compounds in atmospheric aerosols. *20-th Informal Meeting on Mass Spectrometry*: Proceedings of the conference, Primiero, Italy, 12-14 May, 2002, P.103-104.
45. Pashynska V. ESI and CID mass spectrometry study of non-covalent complexes of a bisquaternary ammonium antimicrobial agent decamethoxinum with a phospholipids dipalmitoylphosphatidylcholine, related to the molecular mechanism of the drug action. *Molecules of Biological Interest in the Gas Phase. Optical Spectroscopy, Mass Spectrometry and Computational Chemistry*: Book of Abstracts, Exeter, United Kingdom, 13-18 April 2004. Exeter, 2004. P.53.
46. Lucio M., Lima J.L.F.C., Reis S. Drug-membrane interactions: significance for medicinal chemistry. *Curr. Med. Chem*. 2010. Vol. 7. P. 1795-1809. DOI: 10.2174/092986710791111233
47. Padmanaban G., Rangarajan P. N. Heme Metabolism of Plasmodium is a Major Antimalarial Target. *Biochem. Biophys. Res. Commun.* 2000**.** Vol. 268. P. 665–668. DOI: 10.1006/bbrc.1999.1892
48. Yin V., Lai Szu-H., Caniels T. G., Brouwer P. J. M., Brinkkemper M., Aldon Y., Liu H., Yuan M., Wilson I. A., Sanders R. W., van Gils M. J., Heck A. J. R. Probing Affinity, Avidity, Anticooperativity, and Competition in Antibody and Receptor Binding to the SARS-CoV-2 Spike by Single Particle Mass Analyses. *ACS Cent. Sci.* 2021. Vol. 7. P. 1863−1873. DOI: https://doi.org/10.1021/acscentsci.1c00804

49. Hou G.-L, Lin W., Wang X.-B. Direct observation of hierarchic molecular interactions critical to biogenic aerosol formation. *Commun. Chem.* 2018. Vol. 1:37. P. 1-8. DOI: 10.1038/s42004-018-0038-7
50. Zhang R., Wang G., Guo S., Zamora M.L., Ying Q., Lin Y., Wang W., Hu M., Wang Y. Formation of urban fine particulate matter. *Chem. Rev.* 2015. Vol. 115. P. 3803–3855. DOI: https://doi.org/10.1021/acs.chemrev.5b00067
51. Mbareche H.; Morawska L.; Duchaine C. On the interpretation of bioaerosol exposure measurements and impacts on health. *J. Air Waste Manag. Assoc*. 2019. Vol. 69. P. 789–804. DOI: https://doi.org/10.1080/10962247.2019.1587552
52. Alali H., Ai Y., Pan Y.-L., Videen G., Wang C. A collection of molecular fingerprints of single aerosol particles in air for potential identification and detection using optical trappin-Raman Spectroscopy. *Molecules*. 2022. Vol. 27:5966. P. 1-23. DOI: https:// doi.org/10.3390/molecules27185966
53. Edited by Cole R.- Hoboken , in: Electrospray and MALDI Mass spectrometry:fundamentals, instrumentation, practicalities, and Biological Applications, 2ndedition, John Wiley & Sons, Inc., New Jersey, 2010, p. 1008 p.
54. Tamara S., den Boer M. A., Heck A. J. R. High-resolution native mass spectrometry. *Chem. Rev.* 2021. DOI: 10.1021/acs.chemrev.1c00212
55. Loo J. A. Electrospray ionization mass spectrometry: a technology for studying non-covalent macromolecular complexes. *Int. J. Mass Spectrom*. 2000. Vol. 200 (1-3). P. 175-186 N. DOI: 10.1016/S1387-3806(0 0)0 0298-0 .
56. Wyttenbach Th., Bowers M.T. Intermolecular interactions in biomolecular systems examined by mass spectrometry. Annu. Rev. Phys. Chem. 2007. Vol. 58. P. 511-533. DOI: 10.1146/annurev.physchem.58.032806.104515 .
57. McCullough B. J., Gaskell S. J. Using Electrospray Ionization Mass Spectrometry to Study Non-Covalent Interactions. *Comb. Chem. High Throughput Screen*. 2009. Vol. 12. P. 203-211. DOI: 10.2174/138620709787315463
58. Campbell D. I., Ferreira C. R., Eberlin L. S., Cooks R. G. Improved spatial resolution in the imaging of biological tissue using desorption electrospray ionization. *Analytical and Bioanalytical Chemistry.* 2012. Vol. 404. P. 389-398.

DOI: 10.1007/s00216-012-6173-6

59. Gavriilidou A.F.M., Sokratous K., Yen H-Y., De Colibus L. High-throughput native mass spectrometry screening in drug discovery. *Front. Mol. Biosci*. 2022. Vol. 9:837901. P. 1-15. DOI: 10.3389/fmolb.2022.837901
60. Guvench O., MacKerell A. D. Computational evaluation of protein-small molecule binding. *Curr. Opin. Struct. Biol*. 2009. Vol. 19. P. 56-61. DOI:
61. Durdagi S., Zhao C., Cuervo J. E., Noskov S. Y. Atomistic models for free energy evaluation of drug binding to membrane proteins. *Curr. Med. Chem*. 2011. Vol.18. P. 2601-2611. DOI:
62. Li A., Muddana H. S., Gilson M. K. Quantum mechanical calculation of noncovalent interactions: A large-scale evaluation of PMx, DFT and SAPT approaches. *J. Chem. Theory Comput.* 2014. Vol. 10: 4. P. 1563–1575. DOI: https://doi.org/10.1021/ct401111c
63. Sofinska K., Wilkosz N., Szymonski M., Lipiex E. Molecular spectroscopic markers of DNA damage. *Molecules.* 2020. Vol. 25: 3. P. 561. DOI: https://doi.org/10.3390/molecules25030561
64. Jakubek R. S., Handen J., White S. E., Asher S. A., Lednev I. K. Ultaviolet resonance Raman spectroscopic markers for protein structure and dynamics. *Trends in Analyical Chemistry*. 2018. Vol. 103. P. 223-229. DOI: 10.1016/j.trac.2017.12.002
65. Xiao L., Shelake S., Ozerova M., Balss K. M., Amin K., Tsai A. Spectral markers for T cell death and apoptosis – A pilot study on cell therapy drug product characretization using Raman spectroscopy. *Journal of Pharmaceutical Sceinces.* 2021. Vol. 110: 12. P. 3786-3793. DOI: https://doi.org/10.1016/j.xphs.2021.08.005
66. Wilkosz N., Czaja M., Seweryn S., Skirlinska-Nosek K., Szymonski M., Lipiex E., Sofinska K. Molecular Spectroscopic Markers of Abnormal Protein Aggregation. *Molecules.* 2020. Vol. 25: 11. P. 2498. DOI: https://doi.org/10.3390/molecules25112498

67. Гнатюк О.В. Спектроскопічні маркери взаємодії біологічних макромолекул, влітин та тканин з протипухлинними препаратами та наноструктурами. Дисертація на здобуття наукового ступеня доктора фіз.-мат наук зі спеціальності 03.00.02 біофізика (фізико-математичні науки), Харків .2021. http://rbecs.karazin.ua/wp-content/uploads/2018/dis/dis_Gnatiuk.pdf
68. Ващенко О. В. Індивідуальні та спільні взаємодії компонентів лікарських препаратів з модельними ліпідними мембранами. Дисертація на здобуття наукового ступеня доктора фіз.-мат наук зі спеціальності 03.00.02 біофізика (фізико-математичні науки), Харків .2019. http://rbecs.karazin.ua/wp-content/uploads/2018/dis/dis_Vashchenko.pdf

ДОДАТОК

СПИСОК ПУБЛІКАЦІЙ ЗДОБУВАЧА ЗА ТЕМОЮ ДИСЕРТАЦІЇ

Основні наукові результати дисертації опубліковано в статтях у провідних фахових наукових виданнях[1-22], віднесених до першого і другого квартилів (Q1 і Q2) (13 статей) та третього квартилю (Q3) (3 статті) відповідно до класифікації SCImago Journal & Country Rank, у наукових періодичних виданнях, включених до Переліку наукових фахових видань України (5 статей), та у закордонних фахових наукових виданнях (1 стаття).

Статті, в яких опубліковані основні наукові результати дисертації

1. Pashynska V. A., Kosevich M. V., Van den Heuvel H., Claeys M. Characterization of noncovalent complexes of antimalarial agents of the artemisinin type and Fe(III)-heme by electrospray ionization mass spectrometry and collisional activation tandem mass spectrometry. *J. Am. Soc. Mass Spectrom.* 2004. Vol. 15. P. 1181-1190. DOI: https://doi.org/10.1016/j.jasms.2004.04.030
2. Pashynska V. A. Mass spectrometric study of intermolecular interactions between the artemisinin-type agents and nucleobases. *Біофізичний вісник*. 2009. Т. 22(1). С. 20-28.
3. Pashynska V. A., Kosevich M. V., Van den Heuvel H., Cuyckens F., Claeys M. Study of non-covalent complexes formation between the bisquaternary ammonium antimicrobial agent decamethoxinum and membrane phospholipids by elecrtospray ionization and collision-induced dissociation mass spectrometry. *Вісник харківського національного університету ім. Каразіна №637. Біофізичний вісник*. 2004. Т. 1-2 (14). С. 123-130.
4. Pashynska V., Kosevich M., Stepanian S., Adamowicz L. Noncovalent complexes of tetramethylammonium with chlorine anion and 2,5-dihydroxybenzoic acid as models of the interaction of quaternary ammonium biologically active compounds with their molecular targets. A theoretical study. *Journal of Molecular Structure: THEOCHEM* . 2007. Vol. 815. P.55-62. DOI: https://doi.org/10.1016/j.theochem.2007.03.019

5. Pashynska V., Boryak O., Kosevich M., Stepanian S., Adamowicz L. Competition between counterions and active protein sites to bind bisquaternary ammonium groups. A combined mass spectrometry and quantum chemistry model study. *Eur. Phys. J. D.* 2010. Vol. 58. P.287-296. DOI: https://doi.org/10.1140/epjd/e2010-00125-5

6. Pashynska V. A. Mass spectrometric study of rhamnolipid biosurfactants and their interactions with cell membrane phospholipids. *Biopolymers and Cell.* 2009. Vol. 25, N 6. P. 504-508. DOI: http://dx.doi.org/10.7124/bc.0007FE
7. Pashynska V. A.,. Zholobak N. M, Kosevich M. V., Gomory A., Holubiev P. K., Marynin A. I. Study of intermolecular interactions of antiviral agent tilorone with RNA and nucleosides. *Біофізичний вісник.* 2018. Т. 39(1). С. 15-26. DOI: https://doi.org/10.26565/2075-3810-2018-39-02
8. Pashynska V., Stepanian S., Gomory A., Vekey K., Adamowicz L. New cardioprotective agent flokalin and its supramolecular complexes with target amino acids: An integrated mass-spectrometry and quantum-chemical study. *J. Mol. Struc.* 2017. Vol. 1146. P. 441-449. DOI: https://doi.org/10.1016/j.molstruc.2017.06.007
9. Pashynska V., Stepanian S., Gomory A., Vekey K., Adamowicz L. Competing intermolecular interactions of artemisinin-type agents and aspirin with membrane phospholipids: Combined model mass spectrometry and quantum-chemical study. *Chem. Phys.* 2015. Vol. 455. P. 81-87. DOI: https://doi.org/10.1016/j.chemphys.2015.04.014
10. Pashynska V., Stepanian S., Gömöry Á., Adamowicz L. What are molecular effects of co-administering vitamin C with artemisinin-type antimalarials? A model mass spectrometry and quantum chemical study. *J. Mol. Struc.* 2021. Vol. 1232. P. 130039. DOI: https://doi.org/10.1016/j.molstruc.2021.130039
11. Pashynska V. A., Kosevich M. V., Gomory A., Vekey K. Model mass spectrometric study of competitive interactions of antimicrobial bisquaternary ammonium drugs and aspirin with membrane phospholipids. *Biopolymers and Cell.* 2013. Vol. 29(2). P. 157-162. DOI: http://dx.doi.org/10.7124/bc.000814

12. Kasian N. A., Pashynska V. A., Vashchenko O. V., Krasnikova A. O., Gomory A., Kosevich M. V., Lisetski L. N. Probing of the combined effect of bisquaternary ammonium antimicrobial agents and acetylsalicylic acid on model phospholipid membranes: differential scanning calorimetry and mass spectrometry studies. *Molecular BioSystems.* 2014. Vol.10. P. 3155-3162. DOI: 10.1039/c4mb00420e

13. Pashynska V. A., Kosevich M. V., Gomory A. Mass spectrometry study of noncovalent complexes formation of antibiotic cycloserine with N-acetyl-D-glucosamine and ascorbic acid. *Біофізичний вісник.* 2020. Vol. 43. P. 103-110. DOI: https://doi.org/10.26565/2075-3810-2020-43-11

14. Pashynska V. A., Kosevich M. V., Van den Heuvel H., Claeys M. The effect of cone voltage on electrospray mass spectra of the bisquaternary ammonium salt decamethoxinum. *Rapid Commun. Mass Spectrom.* 2006. Vol. 20(5). P. 755-763.

15. Пашинская В. А., Косевич М. В., Степаньян С. Г. Квантовомеханическое исследование структуры гидратированного бисчетвертичного аммониевого соединения декаметоксина. *Вісн. Харк. Ун-ту N 49. Біофізичний вісник*. 2000. Т. 2(7). С. 29-34.

16. Pashynska V. A., Kosevich M. V., Gomory A., Vekey K., Claeys M., Chagovets V. V., Pokrovskiy V. A. Variable Electrospray Ionization and Matrix-Assisted Laser Desorption/Ionization Mass Spectra of the Bisquaternery Ammonium Salt Ethonium. *Mass Spectrometry & Purification Techniques*. 2015. Vol. 1:103. P. 1-9. DOI: 10.4172/2469-9861.1000103

17. Kosevich M. V., Boryak O. A., Chagovets V. V., Pashynska V. A., Orlov V. V., Stepanian S. G., Shelkovsky V. S. "Wet chemistry" and crystallochemistry reasons for acidic matrix suppression by quaternary ammonium salts under matrix-assisted laser desorption/ionization conditions. *Rapid Commun. Mass Spectrom.* 2007. Vol. 21(11). P. 1813-1819. DOI: https://doi.org/10.1002/rcm.3020

18. Vashchenko O. V., Pashynska V. A., Kosevich M. V., Panikarskaya V. D., Lisetski L. N. Modulation of bisquaternary ammonium agents affect on model biomembranes by complex formation with an organic anion. *Biopolymers and Cell*. 2010. Vol. 26, N 6. P. 472-477. DOI: http://dx.doi.org/10.7124/bc.000176

19. Pashynska V., Vermeylen R., Vas G., Maenhaut W., Claeys M. Development of a gas chromatography/ion trap mass spectrometry method for determination of levoglucosan and saccharidic compounds in atmospheric aerosols. Application to urban aerosols. *J. Mass Spectrom.* 2002. Vol. 37. P.1249-1257. DOI: https://doi.org/10.1002/jms.391

20. Claeys M., Graham B., Vas G., Wang W., Vermeylen R., Pashynska V., Cafmeyer J., Guyon P., Andreae M., Artaxo P., Maenhaut W. Formation of secondary organic aerosols through photooxidation of isoprene. *Science*. 2004. Vol. 303. P. 1173-1176. DOI: 10.1126/science.1092805

21. Decesari S., Fuzzi S., Facchini M.C., Mircea M., Emblico L., Cavalli F., Maenhaut W., Chi X., Schkolnik G., Falkovich A., Rudich Y., Claeys M., Pashynska V., Vas G., Kourtchev I., Vermeylen R., Hoffer A., Andreae M.O., Tagliavini E., Moretti F., Artaxo P. Characterization of the organic composition of aerosols from Rondônia, Brazil, during the LBA-SMOCC 2002 experiment and its representation through model compounds. *Atmos. Chem. Phys.* 2006. Vol. 6. P. 375-402. DOI: https://doi.org/10.5194/acp-6-375-2006

22. Claeys M., Kourtchev I., Pashynska V., Vas G., Vermeylen R., Wang W., Cafmeyer J., Chi X., Artaxo P., Andreao M.O., Maenhaut W. Polar organic marker compounds in atmospheric aerosols during the LBA-SMOCC 2002 biomass burning experiment in Rondônia, Brasil: sources and source processes, time series, diel variations and size distributions. *Atmos. Chem.Phys.* 2010. Vol.10. P. 9319-9331. DOI: https://doi.org/10.5194/acp-10-9319-2010

Наукові праці, які засвідчують апробацію матеріалів дисертації: тези наукових доповідей

23. Pashynska V. A. Mass spectrometric markers of modulation effects on molecular level under drugs co-administering: development of mass spectrometry approach to nanobiocomplexes study. *7-th International Conference Nanobiophysics: Fundamental and Applied Aspects*: Conference Program and Book of Abstracts, Kharkiv, Ukraine, October 4-8, 2021. Kharkiv, 2021. P. 75.

24. Pashynska V., Stepanian S., Kosevich M., Gomory A. Nanobiocomplexes of ascorbic acid with antimalarial or antituberculosis drugs molecules: study of molecular mechanisms of the drugs activity modulation. *6-th International Conference Nanobiophysics: Fundamental and Applied Aspects*: Book of Abstracts, Kyiv, Ukraine, October 1-4, 2019. Kyiv, 2019. P. 69.

25. Pashynska V., Kosevich M., Gomory A. Mass spectrometry study of nanobiocomplexes formation between antibiotic cycloserine and N-acetylglucosamine. *XV-th International Conference on Molecular Spectroscopy: "From molecules to molecular materials, biological molecular systems and nanostructures"*: Programme. Abstracts. List of authors, Wroclaw-Wojanow, Poland, September 15-19, 2019. Wroclaw-Wojanow, 2019. P. 128.

26. Pashynska V., Stepanian S., Kosevich M., Gomory A., Vekey K. Model mass spectrometry and quantum chemical study of antimalarial artemisinin-type agents interactions with ascorbic acid and membrane phospholipids. *37-th Informal Meeting on Mass Spectrometry*: Book of abstracts and program, Fiera di Primiero, Italy, 5-8 May 2019. Fiera di Primiero, 2019. P. 96-97.

27. Pashynska V., Kosevich M., Gomory A., Vekey K. Mechanistic study of noncovalent complexes of antiviral and antibacterial agents with targeting biomolecules by electrospray ionization mass spectrometry. *36-th Informal Meeting on Mass Spectrometry*: Book of abstracts and program, Koszeg, Hungary, 6-9 May, 2018. Koszeg, 2018. P. 75.

28. Pashynska V. A., Kosevich M. V., Gomory A., Vekey K., Zholobak N. M. Mechanistic study of nanobiocomplexes of antiviral agent tilorone with nucleosides by electrospray ionization mass spectrometry. *5-th International Conference Nanobiophysics: Fundamental and Applied Aspects*: Book of Abstracts, Kharkiv, Ukraine, October 2-5, 2017. Kharkiv, 2017. P. 90.

29. Pashynska V., Kosevich M., Stepanian S., Gomory A., Vekey K. Mechanistic model study of intermolecular interactions of cardioprotector flokalin and amino acids by electrospray ionization mass spectrometry and quantum chemical

calculations. *34-th Informal Meeting on Mass Spectrometry*: Book of Abstracts, Fiera di Primiera, Italy, 15-18 May, 2016. Fiera di Primiera, 2016. P. 130.

30. Pashynska V., Stepanian S., Kosevich M., Gomory A., Vekey K. Combined model mass spectrometric and quantum chemical study of arthemisinin-type agents and aspirin interactions with membrane phospholipids. *33-rd Informal Meeting on Mass Spectrometry*: Book of Abstracts, Szczyrk, Poland, 10-13 May, 2015. Szczyrk, 2015. P. 76.

31. Пашинська В. А., Косевич М. В., Гоморі А. Мас-спектрометричне дослідження формування нековалентних комплексів антибіотика циклосерина з N-ацетил-D-глюкозаміном та аскорбіновою кислотою. *VIII з'їзд Українського біофізичного товариства:* Матеріали VIII з'їзду Українського біофізичного товариства, Київ-Луцьк, 12-15 листопада 2019. Київ, 2019. Стор.27.

32. Pashynska V. A., Kosevich M. V., Gomory A., Vekey K. Mass spectrometry based approach in the study of nanobiocomplexes of chemotherapeutical drugs with the targeting biological molecules. *3-rd International Conference Nanobiophysics: Fundamental and applied Aspects*: Book of Abstracts, Kharkov, Ukraine, October 7-10, 2013. Kharkov, 2013. P. 89.

33. Pashynska V., Kosevich M., Vashchenko O., Lisetski L., Gomory A., Vekey K. Mass spectrometry as an efficient method of revealing the membranotropic antimicrobial drugs activity modulation by organic acids. *30-th Informal meeting on mass spectrometry*: Book of abstracts, Olomouc, Czech Republic, 29 April-3 May 2012. Olomouc, 2012. P. 118.

34. Pashynska V. A., Kosevich M. V., Gomory A. Mass spectrometry sensing of nanoclusters composed of membrane phospholipids and antimicrobial agents . *2-nd Intern. Conf. "Nanobiophysics: Fundamental and Applied Aspects"*: Book of Abstracts, Kyiv, Ukraine, 6-9 October 2011. Kyiv, 2011. P. 105.

35. Pashynska V. Electrospray Mass Spectrometry Study of Rhamnolipid Biosurfactants and Their Interactions with Membrane Phospholipids. *27-th*

Informal Meeting on mass spectrometry: Book of Abstracts, Retz, Austria, 3-6 May, 2009. Retz, 2009.P. 36.

36. Pashynska V. A., Kosevich M. V., Boryak O. A., Stepanian S. G. Stability of multi-component complexes of tetramethylammonium with biologically significant counterions by the FAB mass spectrometry and quantum chemical data. *26-th Informal Meeting on Mass Spectrometry*: Book of abstracts, Fiera di Primiero, Italy, 4 -8 May 2008. Fiera di Primiero, 2008. P. 123-124.
37. Pashynska V. A., Kosevich M. V., Boryak O. A., Stepanian S. G. Model mass spectrometry and quantum chemical study of competition between counterions and active protein sites for a binding of quaternary ammonium groups. *25-th Informal Meeting on Mass Spectrometry*: Book of abstracts, Nyiregyhaza-Sosto, Hungary, 6-10 May 2007. Nyiregyhaza-Sosto, 2007. P. 97.
38. Pashynska V. A., Kosevich M. V., Stepanian S. G., Chagovets V. V., Pokrovsky V. A., Osaulenko V. L. Modelling of noncovalent interactions of bisquaternary antimicrobial agents with protein active groups by combined MALDI mass spectrometry and quantum-chemical study. *IV з'їзд Українського біофізичного товариства:* Тези доповідей, Донецьк, Україна, 19-21 грудня 2006. Донецьк, 2006. С. 126-128.
39. Pashynska V. A., Kosevich M. V., Van den Heuvel H., Claeys M. Comparative analysis of in-source CID and MS/MS CID under ESI mass spectrometry by the example of the bisquaternary ammonium agent decamethoxinum. *24-th Informal Meeting on Mass Spectrometry*: Book of Abstracts, Uston, Poland, 14-18 May 2006. Uston, 2006. P. 98
40. Pashynska V. A., Kosevich M. V., Chagovets V. V., Shelkovsky V. S., Osaulenko V. L., Porkovskiy V. L. Combined MALDI mass spectrometric and quantum chemical study of antimicrobial agent decamethoxinum in 2,5-dihydroxybenzoic acid. *23-rd Informal Meeting on Mass Spectrometry:* Book of Abstracts, Fiera di Primiero, Italy, 15-19 May 2005. Fiera di Primiero, 2005. P. 114-115.

41. Kosevich M., Pashynska V., Heuvel H., Claeys M. Electrospray mass spectrometry study of the bisquaternary ammonium compound decamethoxinum at different skimmer-nozzle potentials. *21-st Informal Meeting on Mass Spectrometry*: Book of Abstracts, Antwerp, Belgium, 11-15 May, 2003. Antwerp, 2003. P. 107.

42. Pashynska V., Kosevich M., Heuvel H., Claeys M. Study of formation and characteristics of non-covalent complexes between heme and antimalarial agents of the artemisinin type by electrospray ionization mass spectrometry. *21-st Informal Meeting on Mass Spectrometry*: Book of Abstracts, Antwerp, Belgium, 11-15 May, 2003. Antwerp, 2003. P. 148.

43. Pashynska V. A., Vashchenko O. V., Kosevich M. V., Boryak O. A., Kasian N. A., Lisetski L. N. Model investigation on combined effect of quaternary ammonium compounds and an organic acid on phospholipids membranes. *V з'їзд Українського біофізичного товариства*: Тези доповідей, Луцьк, 22-25 червня 2011. Луцьк, 2011. Стор.14.

44. Pashynska V., Vermeylen R., Vas G., Claeys M., Maenhaut W. Development of a gas chromatography/ion trap mass spectrometry method for determination of levoglucosan and related saccharidic compounds in atmospheric aerosols. *20-th Informal Meeting on Mass Spectrometry*: Proceedings of the conference, Primiero, Italy, 12-14 May, 2002, P.103-104.

45. Pashynska V. ESI and CID mass spectrometry study of non-covalent complexes of a bisquaternary ammonium antimicrobial agent decamethoxinum with a phospholipids dipalmitoylphosphatidylcholine, related to the molecular mechanism of the drug action. *Molecules of Biological Interest in the Gas Phase. Optical Spectroscopy, Mass Spectrometry and Computational Chemistry*: Book of Abstracts, Exeter, United Kingdom, 13-18 April 2004. Exeter, 2004. P.53.